Review

Chiral Monophosphines as Ligands for Asymmetric Organometallic Catalysis#

Franz LAGASSE and Henri B. KAGAN*

Institut de Chimie Moléculaire d'Orsay, Laboratoire de Synthèse Asymétrique,[1] *Université Paris-Sud 91405 Orsay, France.* Received January 14, 2000

Chelating chiral diphosphines are often used as ligands of organometallic complexes. However monophosphines, or more generally ligands with one phosphorus linked to one or several heteroatom, may also be useful. This review gives the main results obtained in that area, by considering the classes of monodentate chiral ligands bearing one P(III) atom and involved in asymmetric catalysis with organometallic complexes.

Key words chiral monophosphines; organometallic catalysis; enantioselectivity; monodentate ligand

1. Introduction

The usefulness of triphenylphosphine as ligand of rhodium or ruthenium for the elaboration of complexes active in homogeneous catalysis was pioneered by Wilkinson *et al.*[2] This gave later a basis for the elaboration of asymmetric catalysts. Homogeneous asymmetric hydrogenation started with modest results (ee<15%) in 1968 using chiral monophosphine **1a** (mppp) (Fig. 1) as ligand.[3,4] Neomenthyldiphenylphosphine **6** (nmdpp) and menthyldiphenylphosphine **7** (mdpp) were prepared in 1971 by Morrison *et al*,[5] giving up to 61% ee in some cases. Knowles *et al.* also published in 1972 some interesting results (ee<90%) with chiral phosphines **2a** (pamp) and **4** (camp).[6] At the same time alkyldimenthylphosphines **10** were used by Wilke, Bogdanovic *et al.* as ligand of nickel complexes in the catalysis of alkene codimerization and alkene-1,3-dienes codimerization.[7,8]

In 1971—1972 we demonstrated that a chelating chiral C_2-symmetric diphosphine (diop) without asymmetric phosphorus atoms was an excellent enantioselective catalyst (ee <88%).[9,10] Since that time C_2-symmetric diphosphines have been widely and successfully investigated, releasing chiral monophosphines in the darkness. A multitude of chelating diphosphines are presently known (of C_1 or C_2-symmetry), some of them are patented because of industrial applications. This area has been often reviewed since the early developments, see for example in chronological order refs.[11—17]

By contrast to chiral diphosphines, the field of chiral monophosphines remained stagnant for a long time. However there were in literature some indications that more consideration should be given to this family of compounds, as outlined in the following section.

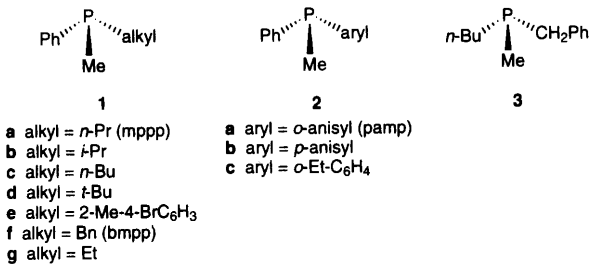

1

a alkyl = *n*-Pr (mppp)
b alkyl = *i*-Pr
c alkyl = *n*-Bu
d alkyl = *t*-Bu
e alkyl = 2-Me-4-BrC_6H_3
f alkyl = Bn (bmpp)
g alkyl = Et

2

a aryl = *o*-anisyl (pamp)
b aryl = *p*-anisyl
c aryl = *o*-Et-C_6H_4

3

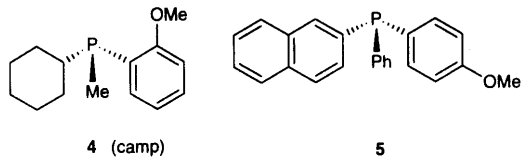

4 (camp)

5

Fig. 1. List of Phosphines Where Phosphorus is the Sole Source of Chirality

2. Potential Interest of Chiral Monophosphines in Asymmetric Catalysis

It is obvious that chelating diphosphines are especially well fitted for catalytic species involving a transition metal bond to two phosphorus (at least in the stereodetermining step). This condition is fulfilled with the Wilkinson catalyst for hydrogenation. Of course monophosphines may also play a useful role, if two equivalents of phosphines are available for the metallic center, although a cis-trans mixture of complexes may be generated on square planar systems.[20]

One also may expect a specific use of monophosphines when the catalytic complexes only accomodate one phosphine or if a monodentate ligand is required for the generation of a catalytically active species.

Monophosphines, and more generally phosphorus derivatives where phosphorus is connected to one or several heteroatoms, may be of interest in asymmetric catalysis, even in the absence of chelate effects. In this review we shall only consider monodentate phosphine ligands. The case involving chelation by an additional heteroatom such as nitrogen has already been reviewed.[22]

3. Structural Classification of Chiral Monophosphines and Analogues

The phosphorus ligands may be classified according to the nature of the substituents attached to the phosphorus atom. The usual case is that of *phosphines*, where there are three P–C bonds. The main chiral monophosphines of potential interest for asymmetric catalysis are listed in Figs. 1—4. In Fig. 1 are placed the phosphines having an asymmetric phosphorus center as sole source of chirality. The monophosphines involving a chiral unit connected to phosphorus (which may be or not a stereogenic center) are in Figs. 2, 3. In Fig. 4 are indicated some examples of phosphines with axial or planar chirality.

Phosphinites, *phosphonites*, *phosphites*, *phosphinamides* and *phosphinimides* are phosphorus compounds with at least one P–O or P–N single bond. These compounds are outside

* To whom correspondence should be addressed.
\# Dedicated to Professor Günther Wulff for his 65th birthday.

© 2000 Pharmaceutical Society of Japan

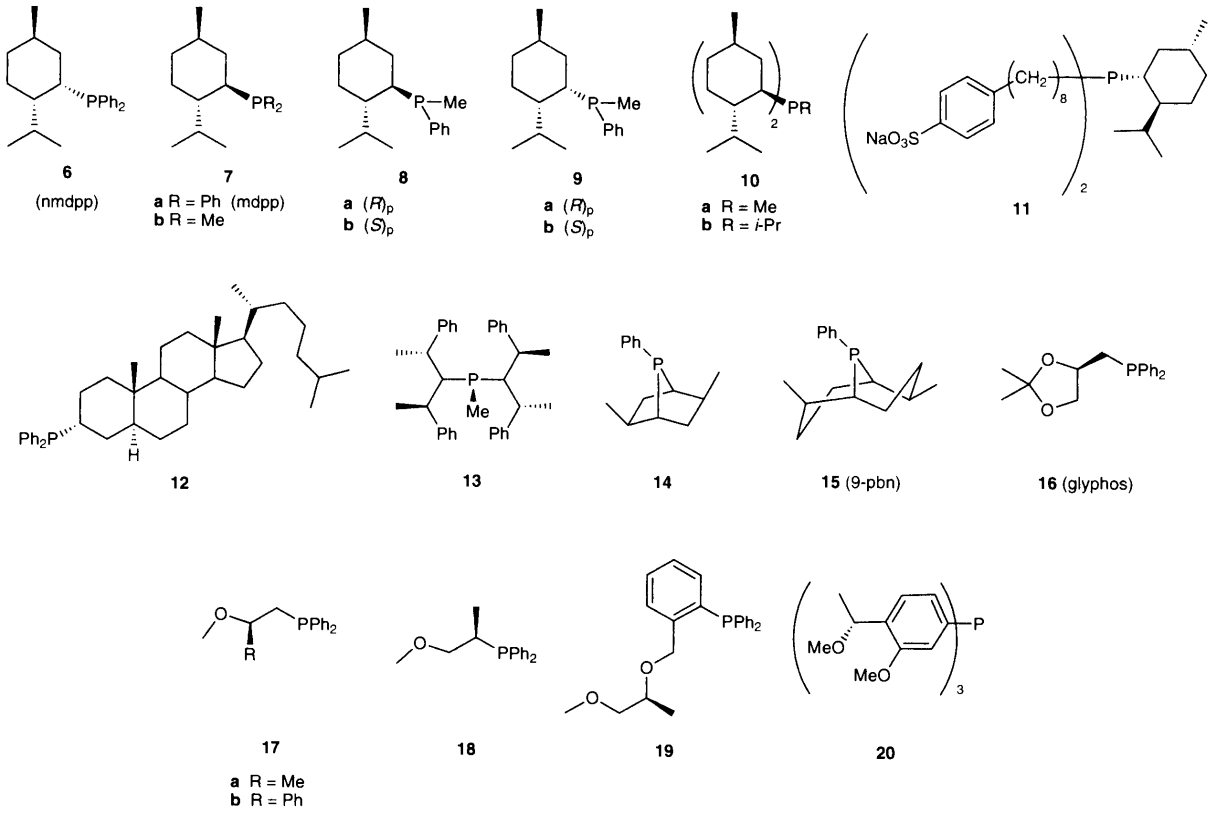

Fig. 2. List of Phosphines with Asymmetric Centers

of the scope of the present article, and will be reviewed elsewhere.[23]

The preparation of various classes of phosphines will not be detailed here. The general approaches are the resolution of phosphine oxides by a chiral acid such as tartaric acid. Asymmetric syntheses of phosphines (asymmetric at P) from chiral phosphinates by nucleophilic displacement are very efficient.[24] Enantiopure phosphinates are easily obtained from chiral oxazaphospholidines or oxathiaphospholidines.[25,26] The preparation of phosphorus ligands where phosphorus is not a stereogenic center does not present difficulty. One widely used reaction is the nucleophilic displacement of a halide or tosylate by a phosphide such as $LiPPh_2$.

Henri, B. Kagan was born in Boulogne-Billancourt, France in December 1930. He graduated from Sorbonne and Ecole Nationale Supérieur de Chimie de Paris in July 1954. He got a PhD in College de France (1960, Paris) under the supervision of Dr J. Jacques. After his PhD he became research associate with professor A. Horeau in College of France. In 1965 he was research associate at University of Texas, Austin (Pr T. Mabry). In 1967 he became assistant professor in University of Paris-South and full professor in 1973. He is member of the french Academy of Sciences. He was the supervisor of 60 PhD and 60 postdoctoral fellows, including several from Japan.

Henri B. Kagan

Franz Lagasse

Franz Lagasse was born in Boulogne Billancourt (France) in 1970. He received his diploma of organic chemistry in 1996. He studied the use of chiral acetals and aminals in asymmetric synthesis under the supervision of Prof. A. Alexakis from University of Pierre et Marie Curie (France). In 1997, he worked at the Research Institute of the pharmaceutical compagny Servier. Then, he joined the group of Prof. H. B. Kagan. His PhD thesis is focused on the synthesis of new ligands for organometallic asymmetric catalysis.

4. Use of Chiral Monophosphines in Asymmetric Organometallic Catalysis

4.1. Asymmetric Hydrogenation. Hydrogenation of C=C Double Bonds The first examples of asymmetric hydrogenation were simultaneously described in 1968 by Horner *et al.*[3] and Knowles *et al.*[4] The rhodium complexes were prepared *in situ* from [Rh(1,5-hexadiene)Cl]$_2$ by addition of two equivalents (by respect to rhodium) of phosphine **1a** or from $RhCl_3L_3$ (L=**1a**) by treatment with hydrogen (20 atm) in the presence of NEt_3. The reduction of some styrene derivatives gave ee's not higher than 20% (Fig. 5). The study of the family of phosphines **1a**—**1e** showed that **1b** provided the highest ee (19% ee).[3b] 2-Methoxystyrene also gave low ee's (<15%) in asymmetric hydrogenation using ligands **1a**, **1b**.[3b] Morrison *et al.* studied in 1971 rhodium catalysts involving neomenthyl- or menthyldiphenylphosphines **6** and **7a**, some results for hydrogenation of conjugated acids **37** are indicated in Fig. 5.[5a] In 1972 it was shown that some phosphines with an asymmetric phosphorus may lead to high enantioselectivities in hydrogenation when one of the groups connected to phosphorus is an *ortho*-anisyl ring.[27] Various α-acylaminoacrylic acids **39**, **41** were transformed into *N*-acylaminoacids (**40**, **42**) with ee's up to 90%. Some examples are given in Fig. 5. The rhodium catalyst was prepared in smooth conditions from [Rh(1,5-hexadiene)Cl]$_2$ or in more severe conditions from $RhCl_3,3H_2O$ and addition of two equivalents of chiral ligands. The authors established that two monophosphines L* are needed for one rhodium. The monoligand complex gave slow hydrogenation and low ee, addition *in situ* of another equivalent of ligand gave high ee and fast rates. Addition of one equivalent of Me_2PhP to the monoligand complex gave fast rates but only one half of the ee. Finally isolation of crystalline [Rh(cod)Cl(**2a**)$_2$] and [Rh(cod)(**2a**)$_2$]$^+$ $(C_6H_5)_4B^-$ is also a nice confirmation of the 1 : 2 stoichiometry for the Rh/L* complex. The asymmetric hydrogenation of *N*-acetyldehydrophenylalanine **41** (R^1=Me) has been studied in great details with the rhodium/camp **4** complex. The replacement of the *ortho*-anisyl group in camp **4** by a 2-Me-4-Br-C_6H_3 group (**1e**) decreased only moderately the enantioselectivity. The methoxy group is then useful mainly for steric reasons, and does not act as a permanent chelating group (see a recent report of Imamoto *et al.* on the influence of the *ortho*-anisyl group in asymmetric hydrogenation[27]). A conjugated ketone, piperitenone **45** (Fig. 5), has been hydrogenated to pulegone (ee<38%) as the major product.[28a] The catalyst was [Rh(cod)(camp)$_2$]$^+BF_4$- and the reaction was performed in DMF or methanol.

Diastereomeric P-chiral phosphines involving a menthyl or neomenthyl fragment (**8**, **9**) were used in Hoffman-La Roche to prepare rhodium catalysts for hydrogenation.[29] For example Geranic acid (with nmdpp **6**) and *N*-acetyl 6-methyl-dehydrotryptophane (with **9b**) led to products of ee's up to 70% and 37% respectively.

Ferrocenylphosphine **31** gave a quite active and enantioselective rhodium catalyst for asymmetric hydrogenation of *N*-acetyldehydrophenylalanine (87% ee).[30] It has not been established if the ligand (2 equiv. by respect to Rh) acts as monodentate or if one of the oxygens of the vicinal cyclic acetal interacts with rhodium.

Monophosphines where the phosphorus atom is part of a saturated ring have been investigated recently in asymmetric hydrogenation.

The *trans*-2,5-dimethyl-1-phenylphospholane **23a** provided 60% ee in the Rh-catalyzed hydrogenation of the methyl ester of *N*-acetyl-dehydrophenylalanine and 65% ee in the reduction of dimethyl itaconate.[31] Improved enantioselectivity (*N*-acetyl phenylalanine of 82% ee) was obtained with the *trans*-1,2,5-triphenyl analog **23b**.[32a] A careful control of experimental conditions allowed even to reach 92% ee.[32b] Phosphiranes **21a** and **21b** have been used to prepare the corresponding cationic rhodium complexes. X-ray crystallography of [Rh (cod)(**21a**)2]$^+$ PF_6^- showed a significant deviation from the square planar coordination around rhodium, due to steric interactions between the two ligands in *cis* relationship.[33] Hydrogenation of *N*-acetyl dehydrophenylalanine **41** (R=Me) provided up to 76% ee (see Fig. 5). The authors did not eliminate the possibility that the actual catalyst involved a phosphine deriving from the phosphiranes by an *in situ* hydrogenolytic ring opening. Itaconic acid was hydrogenated into 2-methyl succinic acid (26% ee) in the presence of a rhodium complex containing **21b** as ligand. The phosphetanes **22** were also checked as ligand of rhodium or iridium in asymmetric hydrogenation.[34] Phosphetane **22b** is a poor ligand for rhodium and gave 40% ee in the hydrogenation of the methyl ester of *N*-acetyldehydrophenylalanine.

Hydrogenation of C=O Double Bonds Camp **4** was screened in 1975 at Monsanto as ligand of rhodium catalysts for hydrogenation of ketones.[28b] Methyl acetylacetate has been transformed into methyl β-hydroxybutyrate with 71% ee. Complex [Rh(nbd)(**1f**)$_2$]$^+$ ClO_4^- has a low catalytic activity at room temperature under 1 atm hydrogen for hydrogenation of acetophenone (8% ee) and butan-2-one (2% ee).[35] Negligible ee's (<1%) were given by catalyst [Rh(nbd)-(**1g**)$_2$]$^+$ PF_6^- in hydrogenation of the same ketones.[36]

One carbonyl group of a cyclopentanetrione has been reduced into an α-ketol which is an intermediate of total synthesis of prostaglandin E_1 in the presence of a Rh/camp catalyst.[37] Unfortunately the enantioselectivity is low, the product (68% ee) was recovered after crystallization.

Since the early time of asymmetric hydrogenation there were no major improvements in enantioselectivities using rhodium/monophosphine complexes in the asymmetric hydrogenation of C=C or C=O double bonds. However 1,2,5-triphenylphospholane **23b** has been found recently to catalyze asymmetric hydrogenation of **41** with the same level of enantioselectivity than camp.[32] This leaves good hope that a suitable tuning of the structure of phospholanes will lead to excellent ligands for asymmetric hydrogenation.

4.2. Alkene Codimerization and Related Processes Asymmetric codimerization of olefins or conjugated dienes was quite successful already in the early seventies. Wilke, Bogdanovic *et al.* developed the use of a family of chiral nickel complexes with one equivalent of alkyldimenthylphosphines **10** by respect to nickel.[7,8,38] The chemistry which was developed at the Max–Planck-Institut in Mülheim in early seventies used alkyl phosphines prepared from terpenes. Some examples of reaction are listed in Fig. 6. The phosphine giving the highest enantioselectivity was dimenthyl isopropyl phosphine **10b**. *Exo*-2-vinylnorbornane (80% ee) and *exo*-2-vinylnorbornene (77% ee) were obtained for reactions performed at −97 °C and −65 °C respectively (Fig. 6). A crystalline complex formed from methyl(π-1-methyl-2-

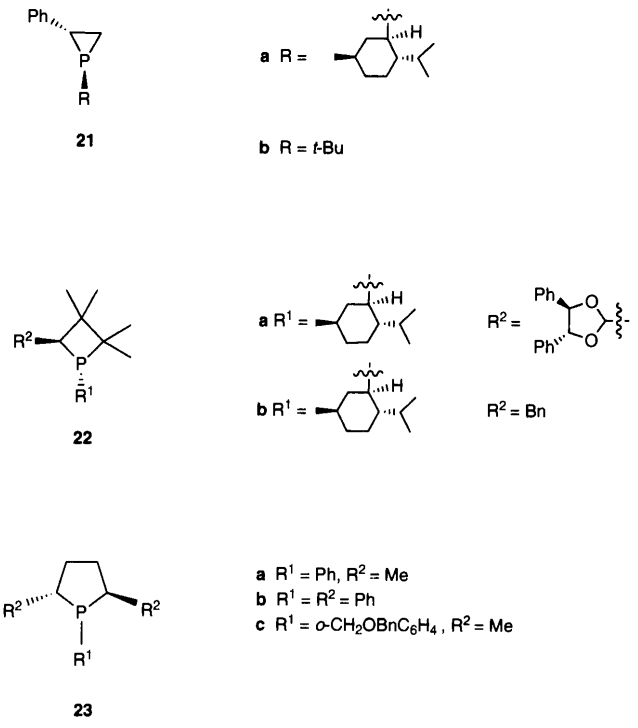

Fig. 3. List of Phosphines Included in a Ring with Asymmetric Centers

butenyl)nickel and (−)-dimenthyl methyl phosphine **10a**. The X-ray crystallographic structure showed a square planar coordination with **10a** coordinated to Ni, the isopropyl group of one menthyl being located close to the nickel above the coordination plane. The authors assumed that the catalytic cycle involves a square planar hydride nickel complex, with the alkene coordinated *cis* to the hydride and *trans* to the phosphine. This later introduces a steric control in the insertion reaction and gives the asymmetric induction.

RajanBabu *et al.* reinvestigated hydrovinylation reactions with nickel catalysts.[39] They found a synergistic effect between counteranions and hemilabile coordination of a chiral monophosphine. Both yields and ee's were highly dependent of the suitable combination of these parameters. The authors selected mop **25a** and analogues as the chiral monophosphines. Mop has been previously devised by Hayashi *et al.*[40] Some results (ee's up to 80%) are indicated in Fig. 6. Phospholanes **23** also led to some asymmetric induction (ee's up to 50%) in the hydrovinylation of styrene (Fig. 6).[39]

An interesting intramolecular C–H/olefins coupling in a 1,5-diene has been described by Murai *et al.*, with a catalyst $[RhCl(cyclooctene)_2]_2$/L* where L* is the ferrocenylphosphine **30**.[41] Some details are given in Fig. 7. The reaction was strongly inhibited by bidentate diphosphines.

4.3. Allylic Substitution Hayashi *et al.* pioneered the

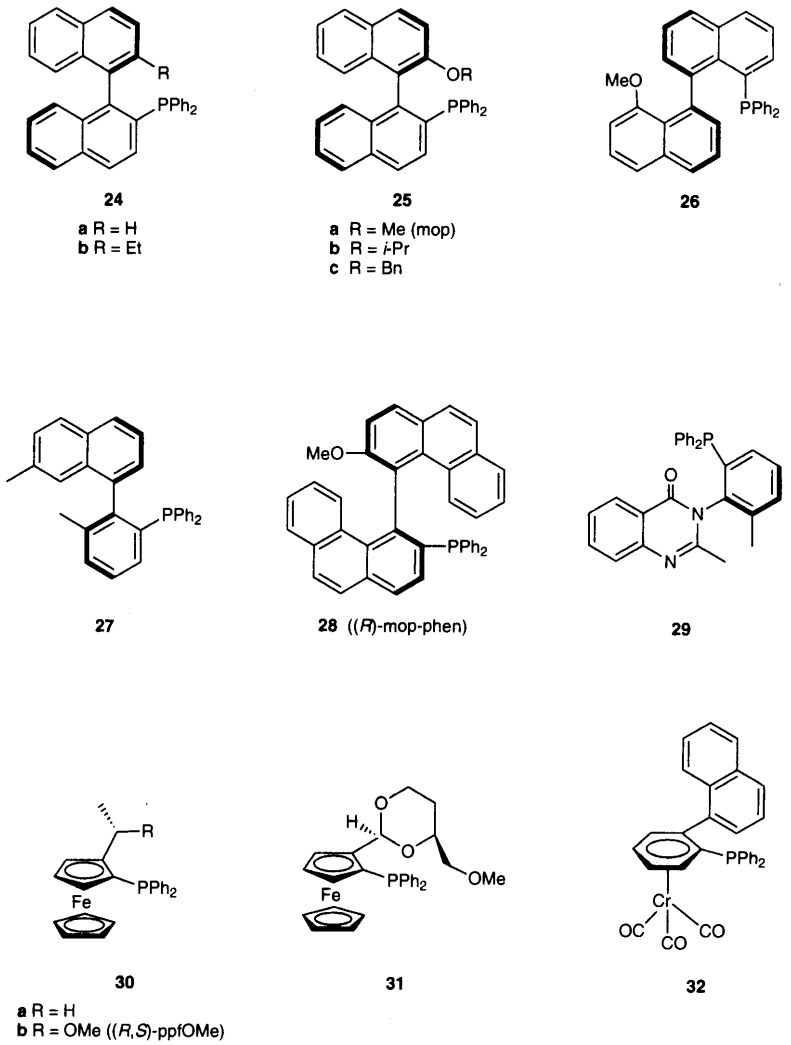

Fig. 4. List of Phosphines with Axial or Planar Chirality

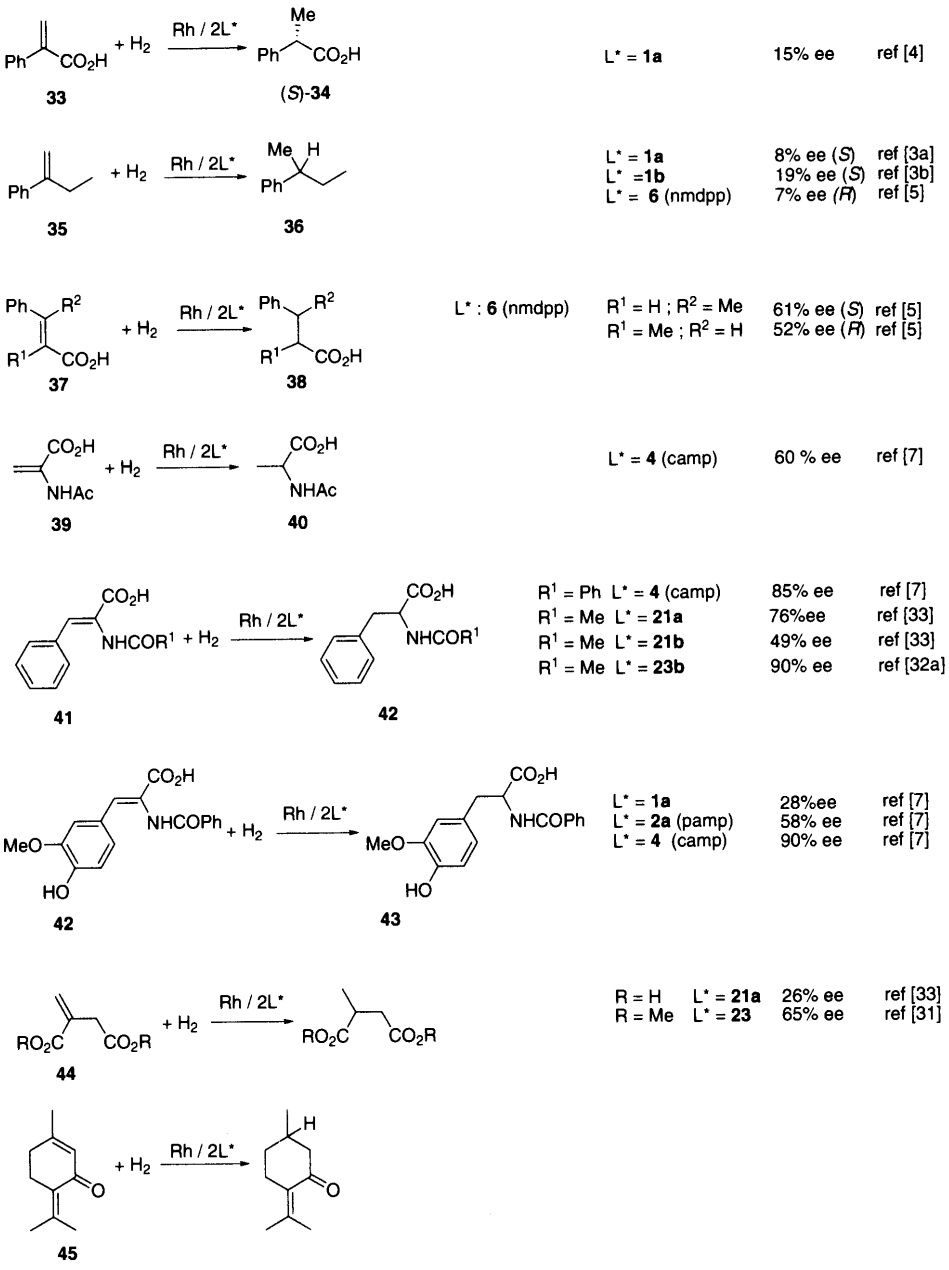

Fig. 5. Asymmetric Hydrogenation Reactions

use of chiral monophosphines. They prepared a large variety of 2-(diphenylphosphino)-2′-alkoxy-1,1′-binaphthyls (mops **25**)[40a] as well as 1-[2-(diphenylphosphino)-ferrocenyl]alkyl methyl ether ppfOMe **30b**.[40b] Palladium-mop complexes were useful in catalytic asymmetric reduction of allylic esters with formic acid.[42] Excellent yields and ee's (up to 85%) were obtained at room temperature with 1% catalyst (Fig. 8). The phenanthrene analog **28** of mop is also efficient. By contrast reduction is very slow and not regioselective with chelating diphosphines as binap. The reaction involves a π-allylpalladium intermediate. The X-ray crystal structure of [PdCl(η^3-1,1-dimethylallyl)mop] showed that the naphthyl ring substituted with a methoxy group lies above palladium, the methoxy group being not coordinated to the metal. However the monodentate character of mop **25a** has been recently questioned by Kocovsky *et al.*[43] These authors have been able to get the X-ray crystal structure of [(mop)Pd(η^3-C_3H_5)]$^+$ TfO$^-$ where a η^2 coordination of the phosphine has been observed thanks to a P, C_σ ligation. The C-bonding involves C_1 position vicinal to the methoxy group. This unusual coordination could be of importance in some part of the catalytic cycle.

8-MeO-mop **26** has been recently synthesized by Fuji *et al.*[44] This new monodentate ligand provided excellent results in asymmetric reduction of allylic esters (Fig. 8).

The ferrocenylphosphine **31** bearing a cyclic acetal gave a moderate enantioselectivity in the allylic substitution on **46** (65% ee when benzylamine is the nucleophile).[30]

Fiaud *et al.* have studied the substitution reaction of cyclohex-2-enyl acetate with sodium dimethyl malonate or phenylzinc catalyzed by a palladium/phospholane **23b** complex.[45b] Unfortunately the product was only of 10% ee. Good results have been obtained by Marinetti *et al.* in the allylic substitution catalyzed by a palladium/phosphetane **22a** complex (Fig. 8).[46] A X-ray crystal structure of (η^3-C_3H_5)PdCl (**22a**) complex shows the monodentate character of the lig-

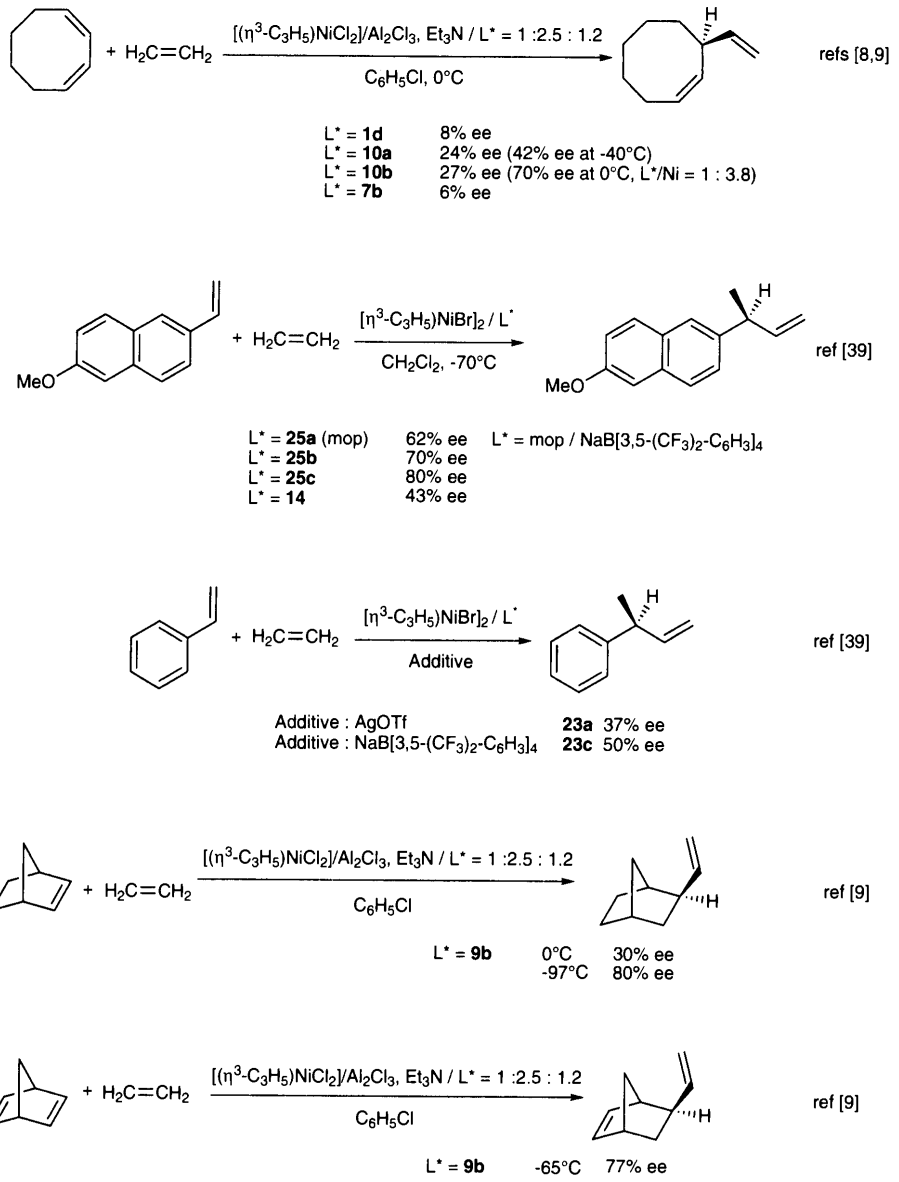

Fig. 6. Alkene Codimerization Reactions

and without coordination to Pd of one of its oxygens.

A new promissing chiral monophosphine with planar chirality **32** has been prepared by Nelson and Hifliker.[47] It gave a Pd(II) complex which catalyzed the alkylation of 1-phenylcinnamyl acetate **46** by the anion of dimethyl malonate (92% ee). The X-ray crystal structure of Pd(η^3-C_3H_5)(**32**)Br shows that the naphthyl ring shields the top side of the square planar Pd(II) metal.

The crowded trialkylphosphine **13** has been synthesized by Knochel *et al.*[48] The corresponding Pd(II) complex catalyzed the allylic alkylation of **46** by the anion of dimethyl malonate with 73% ee.

Some rigid chiral phosphines have been recently synthesized and are useful in palladium-catalyzed asymmetric allylic substitution. For example 9-pbn **15** gave 95% ee in the substitution reaction on **46** (Fig. 8).[49] This ligand is also very efficient (90—95% ee) in asymmetric substitution of **46** by various primary and secondary amines.[50] Monophosphine **14** with a rigid fused bicyclic [2.2.1] ring is excellent for asymmetric alkylation of **46** (Fig. 8).[51] A monodentate atropoisomeric quinazolinone phosphine ligand **29** has been screened in the allylic substitution on **46**, the product was obtained in 52% ee.[52] A propeller-shapped C_3-symmetric triaryl phosphine **20** is efficient in the palladium-catalyzed substitution of *O*-benzoyl-cyclopentene-3-ol by phtalimide, leading to a product of 82% ee.[53]

In conclusion many structural types of chiral monophosphines L* may generate enantioselective palladium catalysts of stoichiometry Pd/L*=1 : 2. A fine tuning of the structure of these ligands is possible and should give rise to useful developments.

The catalytic asymmetric reactions of π-allylpalladium complexes coordinated with achiral monophosphine has been recently reviewed.[54]

4.4. Cross-coupling Reactions Asymmetric C–C bond formation involving a Grignard cross-coupling has been widely studied by Hayashi and Kumada[40b] when the Grignard reagent derives from a secondary halide such as 1-phenylethylmagnesium chloride **47** (Fig. 9). The reagent stays in racemic composition because of its fast *in situ* racemisation compared to the reaction rate. The coupling reaction with vinyl bromide is catalyzed by the complex gener-

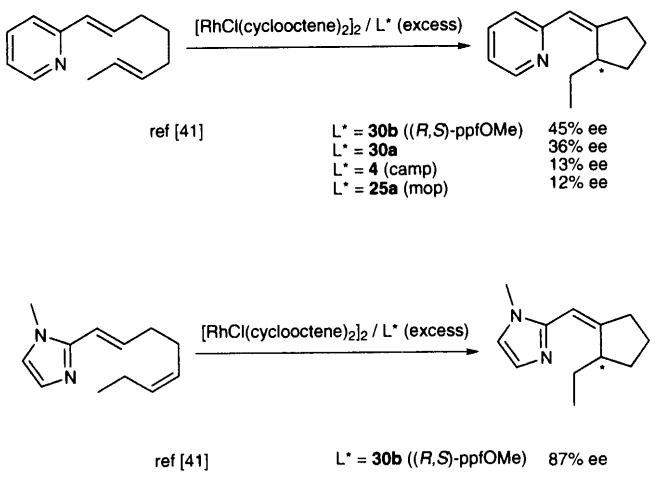

Fig. 7. Intramolecular C-H/Olefins Coupling Reactions

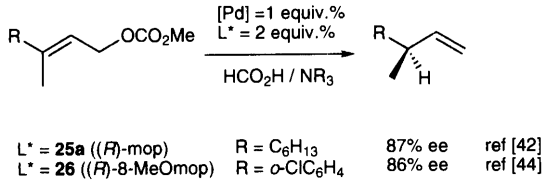

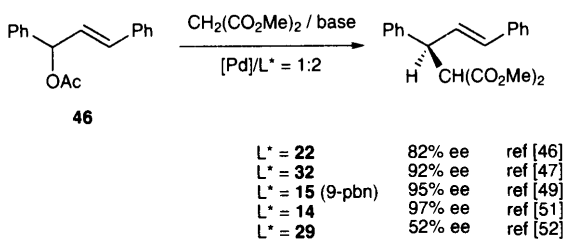

Fig. 8. Allylic Substitution Reactions

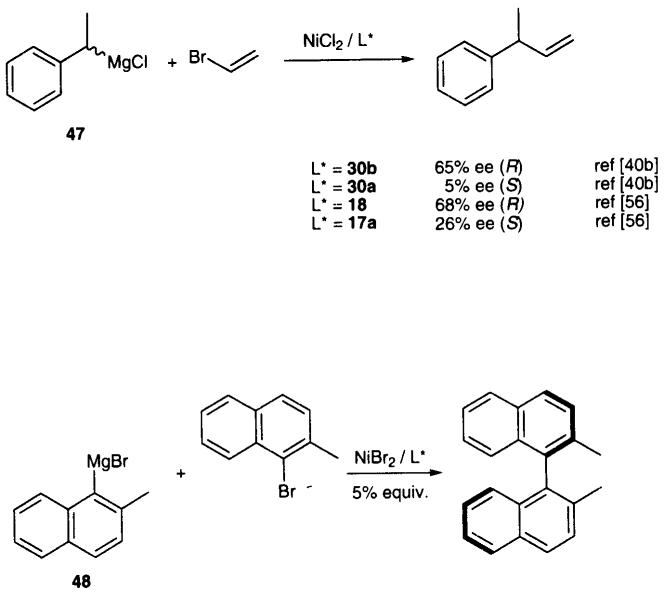

Fig. 9. Cross-Coupling Reactions

ated from $NiCl_2$ and various types of phosphines. High enantioselectivities were given by aminoferrocenylphosphines, however nitrogen which plays a key role for coordination with magnesium atom is not compulsory in order to observe some asymmetric induction (almost up to 60% ee, Fig. 9).

The C–C bond formation between two aryl systems may generate atropoisomerism. A new type of asymmetric catalysis has been developed by Hayashi *et al.* by reaction between an aromatic halide and an aromatic Grignard reagent (Fig. 8).[55] The catalyst was the combination between $NiCl_2$ and 3 equiv. of ferrocenylphosphine **30b** (ppfOMe). By this way 2,2′-dimethyl-1,1′-binaphthyl was produced with up to 95% ee (Fig. 9). The methoxy is essential for high enantioselectivity (phosphine **30a** gave a racemic product), presumably by acting as coordinating group to the Grignard reagent. Diphosphines were inefficient in this process. Several Nickel/alkoxy phosphines (**16**—**19**) catalysts have been investigated by Brunner *et al.* in the coupling reactions involving Grignard reagents **47** and **48**.[56] Some results are indicated in Fig. 9.

4.5. Hydroformylation Asymmetric hydroformylation and related processes developed mainly by the use of bidentate phosphorus ligands (review: ref. 57). The main problem is to combine a high enantioselectivity to a high regioselectivity. There are only a few examples involving a monodentate phosphine. Rhodium complexes with chiral ligands are frequently use. In the hydroformylation of styrene (Fig. 10) Nmdpp **1a** or bmpp **1f** have been reported to give some asymmetric induction (up to 20% ee) in hydroformylation of styrene.[58,59] By decreasing the temperature to 60 °C 50% ee could be reached with **1f**.[60] In the same reaction water-soluble phosphine **11** or dicol **12** provided negligible ee's[61,62] while a P-Phenylphosphepine (based on the 1,1′-binaphthyl skeleton) achieved 20% ee.[63] **1a** (mppp) has been studied at the BASF company.[64] A catalyst prepared from $[RhCl(cod)]_2$ and **1a** allowed to isolate hydratropaldehyde from styrene (at 200 bar) in 40% ee.

Asymmetric carboesterification usually gives higher enantioselectivity than the corresponding hydrocarbonylations. In Fig. 10 are indicated a few examples of carbomethoxycarbonylation in methanol catalyzed by the nmdp **6**/$Pd(dba)_2$ combination. Enantioselectivities up to 50% ee were reached.[65]

4.6. Hydrosilylation. Hydrosilylation of C=C Double Bonds In 1971—1972 were reported the first examples of asymmetric hydrosilylation of olefins in the presence of some platinum (II) complexes (Fig. 11).[66,67] The ligands were bmpp **1f**, nmdpp **6** and mdpp **7**, the enantiomeric excess of the product was not higher than 5%. Later palladium complexes afforded higher although moderate enantioselectivities, needing diphosphines as ligands. A breakthrough occured in 1991 with the introduction by Hayashi *et al.* in hydrosilylation of the chiral monophosphine mop **25a** as ligand of palladium catalysts.[68] Monodentate phosphine ligands generate a palladium catalyst which is more active than the similar complex with a diphosphine. The reason is the initial oxidative addition of the H–Si bond of $HSiCl_3$ on a Pd(0) center, which needs to be followed by an activation of olefin by coordination on an empty site. This cannot occurs in the

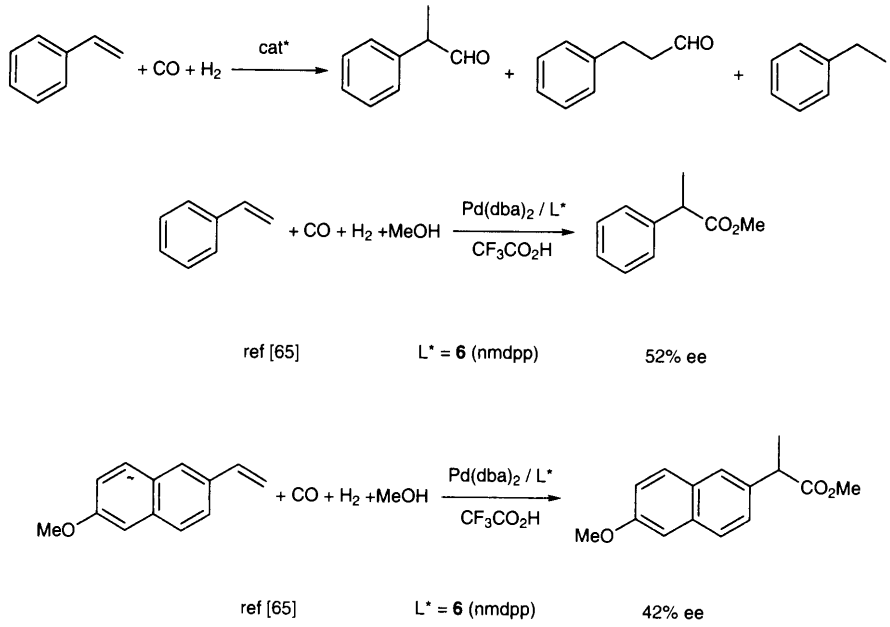

Fig. 10. Hydroformylation Reactions

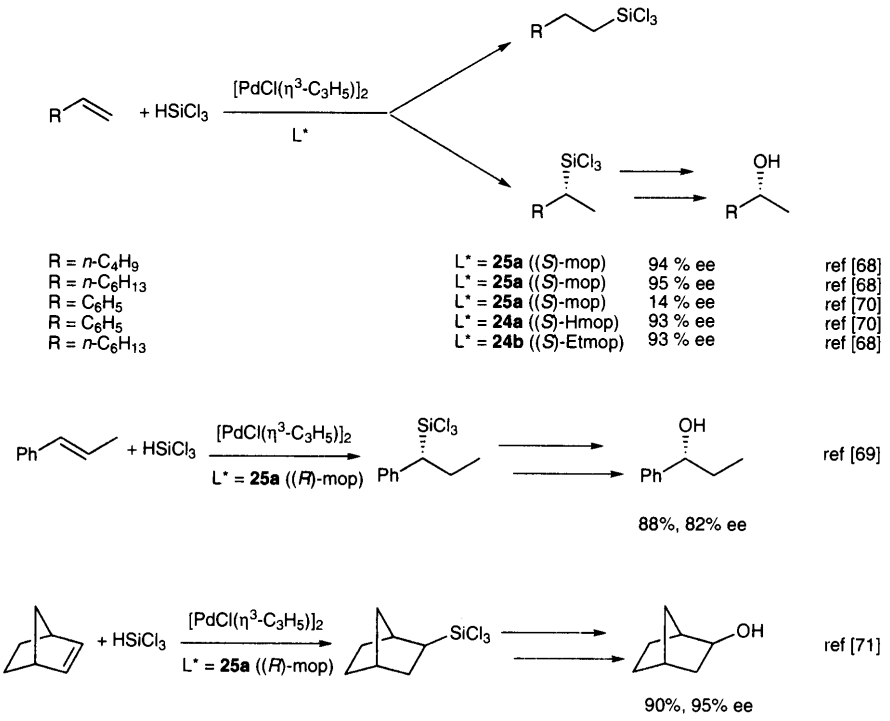

Fig. 11. Asymmetric Hydrosilylation Reactions of C=C Double Bonds

presence of a resident chelating diphosphine, while a monophosphine allows the formation of a square-planar intermediate $HPd(SiCl_3)(L^*)(RCH{=}CH_2)$. Reactions could be runned at 40 °C with 0.1% equiv. of catalyst. The products are easily transformed by a two-step procedure into the corresponding alkanol, with retention of configuration. Some representative results on alkenes are listed in Fig. 11. It is interesting to point out that mop **25a** and **24b** gave almost the same enantioselectivity (95% ee (*R*) and 93% ee (*R*) respectively) in the reaction on 1-octene. This a good evidence here that the methoxy group of mop is not acting as a coordinating group. This chemistry was successfully extended to 1-arylalkenes and to norbornene (Fig. 11).[69—71] It was found that a mop analog **24a** where the methoxy group is missing (H-mop) is superior to the usual mop ligand **25a** (MeO-mop) in the hydrosilylation of styrene (Fig. 11). Finally a phenanthrene analog **28** of mop has been found useful in hydrosilylation of cyclic-1,3-dienes.[72]

Hydrosilylation of C=O Double Bonds Catalytic asymmetric hydrosilylation of ketones was first reported in 1972 with the use of catalysts of the type $[L^*PtCl_2]_2$, where L* stands for a monophosphine (bmpp **1f** or mppp **1a**).[73] Dichloromethylsilane reacts on alkyl phenyl ketones to give after hydrolysis the corresponding alcohols with a modest enantioselectivity (ee<20%). It was soon discovered by Ojima *et al.* that rhodium catalysts such as $[(bmpp)_2RhCl$-

(solvent)] and the proper choice of a silane transformed some ketones or α-ketoesters into alcohols of enantioselectivities up to 60% ee.[74—76] A ferrocenylphosphine **30a** gave a low enantioselectivity (5% ee) in the reaction of trimethylsilane on propiophenone.[77] Usually the highest ee's were obtained with silanes bearing a phenyl group connected to silicon. Some selected examples are listed in Fig. 12. A survey of the catalytic asymmetric silylation of ketones including many data on the use of monophosphines as ligands as well as mechanistic discussions (assuming a *trans* relationship between the two monophosphines[78]) can be found in a review published in 1977.[79]

Since the late seventies there were no much research in that area since diop and other bidentate ligands gave superior results. Moreover chiral nitrogen ligands became of growing importance[80] However there is still a good potential for the exploration of catalytic properties of the many new monophosphines which were subsequently synthesized. They were no reports concerning hydrosilylation of imines.

4.7. Hydroacylation In this section is reported an unusual reaction which, formally, is the addition of a C–H bond of an aromatic ring on an alkene. The only case of such an enantioeselective process has been described by Brunner *et al.*[81] It involved the reaction between iodobenzene and norbornene in the presence of formic acid and an amine. When glyphos **16** was the ligand of the palladium catalyst, *exo*-5-norbornane (10% ee) was produced. A bidentate ligand such as norphos gave around 35% ee.

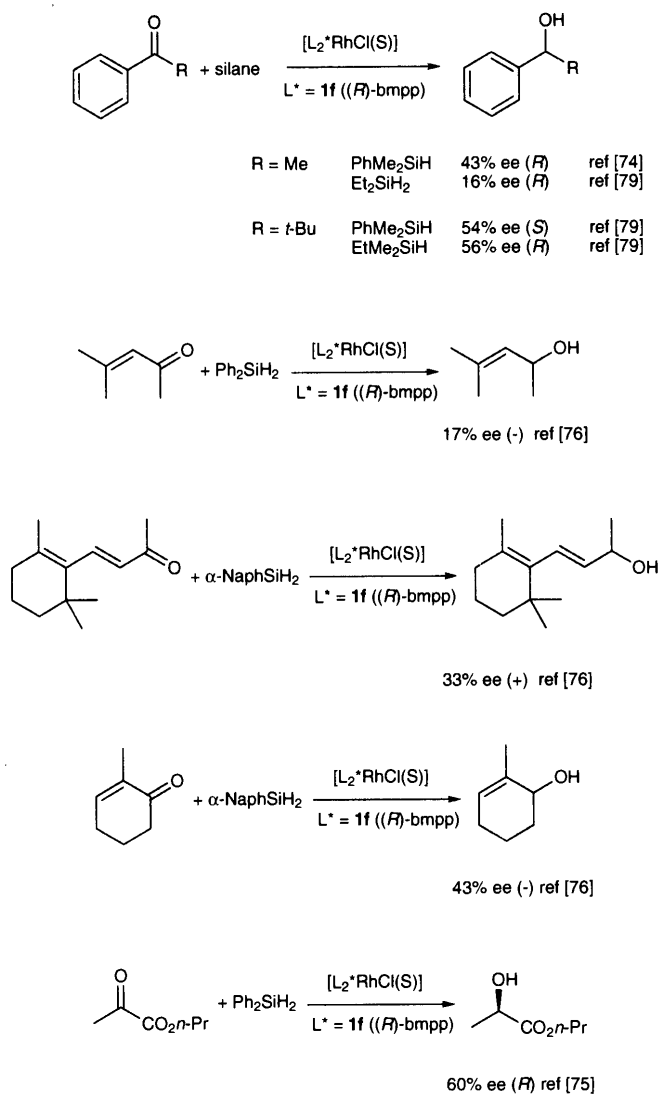

Fig. 12. Asymmetric Hydrosilylation Reactions of C=O Double Bonds

5. Conclusion

Monodentate chiral phosphines of various types are presently known and found some application in organometallic catalysis. The structural diversity is well evidenced by inspection of the structures reported in Figs. 1—4.

Monodentate chiral phosphines were for a long time neglected, because bidentate diphosphines were very successful in asymmetric hydrogenation and for some other reactions, as explained in the introduction of the present article. However one may consider that they are some good indications that suitable monodentate chiral phosphines should play a useful role in the future. They are already the ligands of choice for controlling asymmetric hydrosilylation of carbon carbon double bonds.[80b] They also gave excellent results in cross-coupling reactions and allylic substitutions. We can expect that they will play a role of increasing importance in many aspects of organometallic catalysis. We hope that this review will encourage practitioners of asymmetric catalysis to consider the potential interest of chiral monodentate phosphines and to investigate this area which has been quite neglected till now.[82]

References and Notes

1) Part of Laboratoire de Catalyse Moléculaire, UPRESA 8075.
2) Osborn J. A., Jardine F. J., Young J. F., Wilkinson G., *J. Chem. Soc.*, **1966**, 1711—1732.
3) *a*) Horner L., Siegel H., Büthe H., *Angew. Chem. Int. Ed. Engl.*, **7**, 942 (1968); *b*) Horner L., Siegel H., *Phosphorus*, **1**, 209—216 (1972).
4) Knowles W. S., Sabacky M. J., *J. Chem. Soc. Chem. Commun.*, **1968**, 1445.
5) Morrison J. D., Burnett R. E., Aguiar A. M., Morrow C. J., Philipps C., *J. Am. Chem. Soc.*, **93**, 1301—1303 (1971).
6) Morrison J. D. Masler W. F., *J. Org. Chem.*, **39**, 270—272 (1974).
7) Knowles W. S., Sabacky M. J., Vineyard B. D., *J. Chem. Soc. Chem. Commun.*, **1972**, 10—11.
8) Bogdanovic B., Henc B., Meister B., Pauling H., Wilke G., *Angew. Chem. Int. Ed. Engl.*, **11**, 1023—1024 (1972).
9) Bogdanovic B., *Angew. Chem. Int. Ed. Engl.*, **12**, 954—964 (1973).
10) Dang T. P., Kagan H. B., *J. Chem. Soc. Chem. Commun.*, **1971**, 481.
11) Kagan H. B., Dang T. P., *J. Am. Chem. Soc.*, **94**, 6429—6433 (1972).
12) Kagan H. B., Asymmetric catalysis by organometallic catalyst, in "Comprehensive Organometallic Chemistry," Wilkinson G. and Eds, (1982).
13) Morrison H. S. (Ed.), Asymmetric Reactions, Vol. 5, Asymmetric Catalysis Academic Press: New York, 1985.
14) Bosnich, B. Ed., Asymmetric Catalysis, NATO ASI Series, Martinus Nijhoff Publishers, Dordrecht, 1986.
15) Brunner H. in *Topics in Stereochem.*, **18**, 129—247 (1988).
16) Brunner H., Zettlmeier W., Handbook of Enantioselective Catalysis, Vol. I and II, VCH, 1993.
17) Ojima I. (Ed.), Catalytic Asymmetric Synthesis, VCH, Weinheim, 1993.
18) Noyori, R., Asymmetric Catalysis in Organic Synthesis, J. Wiley and Sons, New York, 1994.
19) Pietrusiewicz K. M., Zablocka M., *Chem. Rev.*, **94**, 1375—1411 (1994).
20) However Brown *et al.* established by ^{31}P nmr that complex [Rh $(MeOH)_2(\mathbf{8})_2]^+$ exists in solution with the two monophosphines in *cis* position.[21] X-ray crystal structure of several complexes of the type [Rh(chelating diene)$(L^*)_2]^+$ X^- where L* is a chiral monophosphine have been published (see in the text). See ref. 30 for a discussion on the importance of the relative configuration (*cis* or *trans*) of the two chiral monophosphines at the various steps of the catalytic cycle.

21) Brown J. M, Chaloner P. A., Nicholson P. N., *J. Chem. Soc. Chem. Commun.*, **1978**, 646—647.
22) Togni A., Venanzi L., *Angew. Chem. Int. Ed. Engl.*, **33**, 497—521 (1994).
23) Lagasse F., Kagan H. B., manuscript in preparation.
24) Korpium O., Lewis R. A., Chickos J., Mislow K., *J. Am. Chem. Soc.*, **90**, 4842—4846 (1968).
25) Jugé S., Genêt J.-P., *Tetrahedron Lett.*, **30**, 2783—2766 (1989).
26) Corey E. J., Chen Z., Tanoury G. J., *J. Am. Chem. Soc.*, **115**, 11000—11001 (1993).
27) Imamoto T., Watanabe J., Wada Y., Masuda H., Yamada H., Tsuruta H., Matsukawa S., Yamaguchi K., *J. Am. Chem. Soc.*, **120**, 1635—1636 (1998).
28) *a*) Solodar J., *J. Org. Chem.*, **43**, 1787—1789 (1978); *b*) Solodar J., *ChemTech*, 421 (1975).
29) Valentine D., Johnson K. K., Prister W., Sun, R. C., Toth, K., Saucy G., *J. Org. Chem.*, **45**, 3698—3703 (1980).
30) Riant O., Samuel O., Flessner T., Taudien S., Kagan H. B., *J. Org. Chem.*, **62**, 6733—6745 (1997).
31) Burk M. J., Feaster, J. E., Harlow R. L., *Tetrahedron: Asymmetry*, **2**, 569—592 (1991).
32) *a*) Guillen F., Fiaud J.-C., *Tetrahedron Lett.*, **40**, 2939—2942 (1999); *b*) Guillen F., PhD thesis, Université Paris-Sud, 1999.
33) Marinetti A., Mathey F., Ricard L, *Organometallics*, **12**, 1207—1212 (1993).
34) Marinetti A., Ricard L, *Organometallics*, **13**, 3956—3962 (1994).
35) Bonvicini P., Levi A., Modena G., Scorrano G., *J. Chem. Soc. Chem. Commun.*, **1972**, 1188—1189.
36) Tanaka M., Watanabe Y., Mitsudo T., Iwane H., Takegami Y., *Chem. Lett.*, **1973**, 239—240.
37) Sih C. J., Heather J. B., Peruzotti G. P., Price P., Sood R., Lee L. F. H., *J. Am. Chem. Soc.*, **95**, 1676—1677 (1973).
38) Wilke G., Angew. *Chem. Int. Ed. Engl.*, **27**, 185—206 (1988).
39) Nandi M., Jin J., RajanBabu T. V., *J. Am. Chem. Soc.*, **121**, 9899—9900 (1999).
40) *a*) Uozumi Y., Tanahashi A., Lee S.-Y., Hayashi T., *J. Org. Chem.*, **58**, 1945— 1948 (1993); *b*) Hayashi T., Konishi M., Fukushima M., Mise T., Kagotani M., Tajika M., Kumada M., *J. Am. Chem. Soc.*, **104**, 180—186 (1982).
41) Fuji N., Kakiuchi F., Yamada A., Chatani N., Murai S., *Chem. Lett.*, **1997**, 425—425.
42) Hayashi T., Iwamura H., Naito M., Matsumoto Y., Uozumi Y., Miki M., Yanagi K., *J. Am. Chem. Soc.*, **116**, 775—776 (1994).
43) Kocovsky P., Vyskocil S., Cisarova I., Sjbal J., Tislerova I., Smrcina M., Lloyd-Jones G. C., Stephen S. C., Butts C. P., Murray M., Langer V., *J. Am. Chem. Soc.*, **121**, 7114—7115 (1999).
44) Fuji K., Sakurai M., Kinoshita T., Kawabata T., *Tetrahedron Lett.*, **39**, 6323—6326 (1998).
45) *a*) Fiaud J.-C., Aribi-Zouioueche L., *J. Organomet. Chem.*, **295**, 383—387 (1985); *b*) Fiaud J.-F., Legros J.-Y., *Tetrahedron Lett.*, **32**, 5089—5092 (1991).
46) Marinetti A., Kruger V., Ricard L., *J. Organomet. Chem.*, **529**, 465—472 (1997).
47) Nelson S. G., Hilfiker M. A., *Org. Lett.*, **1**, 1379—1382 (1999).
48) Graf C.-D., Malan C., Harms K., Knochel P., *J. Org. Chem.*, **64**, 5581—5588 (1999).
49) Hamada Y., Seto N., Ohmori H., Hatano K., *Tetrahedron Lett.*, **37**, 7565—7568 (1996).
50) Hamada Y., Seto N., Takayanagi Y., Nakano T., Hara O., *Tetrahedron Lett.*, **40**, 7791—7794 (1999).
51) Chen Z., Jiang Q., Zhu G., Xia D., Cao P., Gua C., Zhang X., *J. Org. Chem.*, **62**, 4521—4523 (1997).
52) Dai X., Virgil S., *Tetrahedron Lett.*, **40**, 1245—1248 (1999).
53) Powell M. T., Porte A. M., Burgess K., *J. Chem. Soc. Chem. Commun.*, **1998**, 2161—2162.
54) Hayashi T., *J. Organomet. Chem.*, **576**, 195—202 (1999).
55) Hayashi T., Hayashizaki K., Kiyoi T., Ito Y., *J. Am. Chem. Soc.*, **110**, 8153—8156 (1988).
56) Terfort A., Brunner H., *J. Chem. Soc. Perkin Trans 1*, **1996**, 1467—1479.
57) Agbossou F., Carpentier J.-F., Mortreux A., *Chem. Rev.*, **95**, 2485—2506 (1995).
58) Tanaka M., Watanabe Y., Mitsudo T., Yamamoto K., Takegami Y., *Chem. Lett.*, **1972**, 483—485.
59) Ogata I., Ikeda Y., *Chem. Lett.*, **1972**, 487—488.
60) Tanaka M., Watanabe Y., Mitsudo T., Takegami Y., *Bull. Chem. Soc. Jpn.*, **47**, 1698—1703 (1974).
61) Bartik T., Ding H., Bartik B., Hanson B. E., *J. Mol. Cat., Chemical*, **98**, 117—122 (1995).
62) Gladiali D. S., Faedda G., Marchetti M., Botteghi C., *J. Organomet. Chem.*, **244**, 289—302 (1983).
63) Gladiali S., Dore A., Fabbri D., De Lucchi O., Manassero M., *Tetrahedron: Asymmetry*, **5**, 511—514 (1994).
64) Siegel H., Himmele W., *Angew. Chem. Int. Ed. Engl.*, **19**, 178—183 (1980).
65) Cometti G., Chiusoli G. P., *J. Organomet. Chem.*, **236**, C31—C32 (1982).
66) Yamamoto K., Hayashi T., Kumada M., *J. Am. Chem. Soc.*, **93**, 5301—5302 (1971).
67) Kiso Y., Yamamoto K., Tamao K., Kumada K., *J. Am. Chem. Soc.*, **94**, 4373—4374 (1972).
68) Uozumi Y., Hayashi T., *J. Am. Chem. Soc.*, **113**, 9887—9898 (1991).
69) Uozumi Y., Kitayama K., Hayashi T., *Tetrahedron: Asymmetry*, **4**, 2419—2422 (1993).
70) Kitayama K., Uozumi Y., Hayashi T., *J. Chem. Soc. Chem. Commun.*, **1995**, 1533—1534.
71) Uozumi Y., Lee S. Y., Hayashi T., *Tetrahedron Lett.*, **33**, 7185—7188 (1992).
72) Kitayama K., Tsuji H., Uozumi Y., Hayashi T., *Tetrahedron Lett.*, **37**, 4169—4172 (1996).
73) Yamamoto K, Hayashi T., Kumada M., *J. Organomet. Chem.*, **46**, C65—C67 (1972).
74) Ojima I., Kogure T., Nagai Y., *Chem. Lett.*, **1973**, 541—544.
75) Ojima I., Kogure T., Nagai Y., *Tetrahedron Lett.*, **15**, 1889—1892 (1974).
76) Ojima I., Kogure T., Nagai Y., *Chem. Lett.*, **1975**, 985—988.
77) Hayashi T., Yamamoto K., Kumada M., *Tetrahedron Lett.*, **15**, 4405—4408 (1974).
78) Ojima I., Kogure T., Kumagai M., Horiuchi S., Sato T., *J. Organomet. Chem.*, **122**, 83—97 (1976).
79) Ojima I., Yamamoto K., Kumada M., Asymmetric hydrosilylation by means of homogeneous catalysts with chiral ligands in "Aspects of Homogeneous Catalysis," Ugo R., Ed, Reidel D. Publishing Co, **3**, 185—228 (1977).
80) *a*) Review on asymmetric hydrosilylation: Brunner H. in Catalytic Asymmetric Synthesis, Ojima I. Ed, 303—321, VCH (1993); *b*) Recent review on asymmetric hydrosilylation of C=C double bonds: Hayashi T., in *Comprehensive Asymmetric Catalysis*, Jacobsen E. N., Pfaltz A., Yamamoto H. Eds, 1, Chapter **7**, 319—333, Springer, 1999.
81) Brunner H., Kramler K., *Synthesis*, **1991**, 1121—1124.
82) Apart asymmetric organometallic catalysis, chiral monophosphines have found several applications as catalysts in some organic transformations. For example Vedejs *et al.* reported that a bicyclic monophosphine was an excellent enantioselective catalyst in some kinetic resolutions.[83]
Zhang *et al.* discovered an asymmetric synthesis of substituted cyclopentenes starting from some 2,3-butadienolates with electron-deficient olefins, using **14** as catalyst.[84]
83) Vedejs E., Daugulis O., *J. Am. Chem. Soc.*, **121**, 5813—5814 (1999).
84) Zhu G., Chen Z., Jiang Q., Xiao D., Cao P., Zhang X., *J. Am. Chem. Soc.*, **119**, 3836—3837 (1999).

High Entrapment of Insulin and Bovine Serum Albumin into Neutral and Positively-Charged Liposomes by the Remote Loading Method

Sung Hee HWANG,* Yoshie MAITANI, Kozo TAKAYAMA, and Tsuneji NAGAI

Department of Pharmaceutics, Hoshi University, Ebara 2–4–41, Shinagawa-ku, Tokyo 142–8501, Japan.
Received July 26, 1999; accepted November 3, 1999

Remote loading of insulin and bovine serum albumin (BSA) into neutral or positively-charged liposomes by incubation under a transmembrane pH gradient or non-pH gradient was investigated. Trapping efficiencies in several incubation conditions were compared with those of the conventional reverse-phase evaporation vesicle method (c-REV method). For neutral liposomes, insulin could not be effectively loaded into the liposomes by incubation, regardless of the incubation conditions. The trapping efficiency of insulin into positively-charged liposomes was higher than that of neutral liposomes, especially by the pH-gradient method. Insulin could be loaded into positively-charged liposomes about twofold more efficiently than by the pH-gradient method, compared with the c-REV method. Insulin distributed more on the surface of liposomes by the pH-gradient method than by the c-REV method. BSA showed significantly higher affinity to positively-charged liposomes than to neutral ones by various methods. However, the transmembrane pH-gradient method did not increase BSA loading into liposomes, compared with the c-REV and the non-pH-gradient methods. Our results suggest that the pH-gradient method, combining electrostatic interactions, may be useful for preparation of liposomal insulin and that the high hydrophobicity of BSA may not increase the remote loading of BSA into liposomes by the pH-gradient method.

Key words liposome; remote loading; pH gradient; insulin, serum albumin; positive charge

The use of liposomes as drug-delivery systems has been investigated for a number of potential applications in pharmaceutical formulations. A variety of procedures for the formation of liposomes have been described in the literature.[1] However, all of these methods suffer from drawbacks in terms of low trapping efficiency of drug. During the encapsulation process, proteins are exposed to mechanical stress and to organic solvents such as chloroform or isopropyl ether, which can lead to denaturation of sensitive proteins. To avoid the use of unacceptable solvents and sonication for drugs during the formation of liposomes (passive entrapment), several methods have been studied, including remote loading methods which load drug molecules into preformed liposomes using pH gradients and potential differences across liposomal membranes. Weak bases like doxorubicin[2,3] and vincristine[4] have been successfully loaded into preformed liposomes *via* the pH gradient method. Chakrabarti *et al.*[5] reported that short modified peptides can be efficiently accumulated in large unilamellar vesicle (LUV) *via* pH gradients (inside acidic). The electrostatic interaction can also be used to carry molecules such as DNA.[6]

High molecular weight may be a drawback for remote loading of peptides into liposomes. Insulin and bovine serum albumin (BSA) were selected as peptide drug models because they have different molecular weights and have been studied in terms of interaction with liposomes. Many studies on insulin encapsulated in liposomes have been carried out to examine the potency of orally administered liposomes[7,8] and the aggregation of liposomes in their preparation. The interaction of serum albumin with liposomes has been studied due to the possibility of destabilization of liposomes in the blood stream.[9] Liposomal serum albumin has been studied for the immunoadjuvant effect.[10,11] In most of these reports, the preparation method for the liposomal formulation has been based on passive entrapment. To our knowledge, the remote loading of large peptide molecules into liposomes has never been investigated.

Recently, we reported that diclofenac sodium could be loaded into neutral reverse-phase evaporation vesicles (REV), but that insulin could not be loaded into them, however fluorescein isothiocyanate labeled insulin can be loaded by the pH-gradient method.[12]

In this study, remote loading of peptides into liposomes by incubation under various conditions, including the pH-gradient and the non-pH-gradient methods was investigated, using neutral and positively-charged liposomes.

Experimental

Materials Dipalmitoylphosphatidylcholine (DPPC) was purchased from NOF Co., Ltd. (Tokyo, Japan). Bovine pancreas insulin (crystalline, zinc content approx. 0.5%), BSA and stearylamine (SA) were purchased from Sigma Chemical Co. (St. Louis, MO, U.S.A.). Cholesterol (Ch) and *N*-2-hydroxyethylpiperazine-*N'*-2-ethanesulfonic acid (HEPES) were obtained from Tokyo Kasei Kogyo (Tokyo, Japan). All other chemicals were from Wako Pure Chemical Industries, Ltd. (Osaka, Japan), and were analytical grade.

Preparation of Preformed Liposomes and Conventional Liposomes The preformed neutral and positively-charged liposomes (empty liposomes) were prepared according to the conventional reverse-phase evaporation vesicle method (c-REV method),[13] as described previously.[14] Insulin and BSA were loaded into the empty liposomes by incubation under pH gradient or non-pH gradient conditions. Briefly, DPPC/Ch (7 : 2, molar ratio) and DPPC/Ch/SA (6 : 2 : 1, molar ratio) for neutral liposomes and for positively-charged liposomes, respectively, were dissolved in chloroform and dried in an evaporator. The dried lipid film was redissolved in chloroform and mixed with a 10 fold dilution of phosphate-buffered saline (1/10 PBS, pH 7.4) or citric acid buffer solution (CBS, 300 mmol/l citric acid, pH 4.0) for empty liposomes. Each mixture was mixed by vortexing, followed by sonication in a bath-type sonicater (Honda Electronics, Tokyo, Japan) to give a homogeneous w/o emulsion. Each emulsion was then placed on a rotary evaporator and the organic solvent was removed to obtain liposome suspension. The suspension was extruded through polycarbonate membranes (Nuclepore, Costar Scientific Corporation, U.S.A.) with pore sizes of 0.4 and 0.2 μm at about 60 °C.

Conventional liposomes as reference were prepared by the c-REV method as described above except using 1/10 PBS containing each peptide drug instead of only buffer solution as the aqueous phase.

Incubation of Empty Liposomes with Peptide Drugs Liposomes pre-

* To whom correspondence should be addressed.

© 2000 Pharmaceutical Society of Japan

formed in 1/10 PBS (pH 7.4) were incubated with insulin or BSA in 1/10 PBS at 25 °C for 1 h (non-pH-gradient method). Liposomes preformed in CBS (inside pH 4.0) were washed with HEPES buffer saline (HBS, 20 mmol/l HEPES and 150 mmol/l sodium chloride, pH 7.5), or CBS (pH 2.5 or pH 5.5) by ultracentrifugation (100000×***g***, 4 °C, 1 h) to create a pH gradient across the liposomal membrane, and then were incubated with insulin or BSA in an external aqueous phase solution at 25 °C for 1 h (pH-gradient method).

Determination of DPPC, Insulin and BSA Concentrations and Insulin Activity Liposomes loaded with drug by the c-REV, pH-gradient or non-pH-gradient methods, were separated from free drug by ultracentrifugation (100000×***g***, 1 h) at 4 °C. The process was repeated three times by making a suspension of the precipitate in each buffer solution. In the case of positively-charged liposomes, liposomal insulin was also washed with 0.1 mol/l hydrochloric acid, HBS, or 1/10 PBS in order to remove insulin bound to the surface of the liposomal membrane. The concentration of DPPC in liposome suspension was determined by enzymatic assays (Phospholipid B Test Wako, Wako Pure Chemical Industries, Ltd., Osaka, Japan).[14] Insulin concentration was determined by HPLC, as previously reported.[15] The HPLC system consisted of a Shimadzu LC-10AS liquid chromatograph, SPD-10AV UV-VIS detector, SCL-10A system controller, SIL-10A autoinjector and C-R6A chromatopac. The concentration of BSA was determined by measurement of protein using bicinchoninic acid (BCA Protein Assay Reagent, Pierce, IL, U.S.A.).[16] The insulin activity was measured by enzymatic immunoassay (IMx Insulin, Dainabot Co., Ltd., Tokyo, Japan). The insulin activity adsorbed on liposomes was determined by measuring the insulin activity of liposome-loaded insulin (insulin 0.02 μmol/l) in 1 ml of PBS containing 0.001% methyl cellulose without further treatment. Total recovered liposomal insulin activity was measured after disruption of the liposomes by adding 10% Triton X-100.

Calculation of Trapping Efficiency From the amount of DPPC and drug determined before and after separation of liposomal drug from free drug, the trapping efficiencies were calculated according to the following equation:

$$\text{trapping efficiency (T. E.)}(\%)=\frac{M_{drug}{}^{a}M_{total\ lipid}{}^{b}}{M_{drug}{}^{b}M_{total\ lipid}{}^{a}}\times 100 \quad (1)$$

where $M_{drug}{}^{b}$ and $M_{drug}{}^{a}$ are the amount of drug in the liposome suspension, and $M_{total\ lipid}{}^{b}$ and $M_{total\ lipid}{}^{a}$ are the amount of total lipid in liposome suspension calculated from the amount of DPPC determined before and after separation from free drug, respectively.

Determination of ζ-Potential and Size Distribution of Liposomes The size distribution and ζ-potential of liposomes were determined using a light scattering instrument (Model ELS-800, Otsuka Electronics Co., Ltd., Japan) by a dynamic laser light scattering method and a electrophoretic light scattering method, respectively. The ζ-potentials of positively-charged empty liposomes, produced by the c-REV and pH-gradient methods, and neutral empty liposomes prepared by the c-REV method, were 27.0±2.6, 27.3±1.2 and −2.8±0.9 mV in 1/20 PBS (pH 7.4) at 25 °C, respectively. The ζ-potentials of positively-charged liposomes loaded with insulin by the c-REV and pH-gradient methods were 8.3±3.1 and −5.0±1.2 mV, respectively.

Release of Insulin from Liposomes The released amount of insulin from positively-charged liposomes prepared by the c-REV and pH-gradient methods, were measured in pH 7.4 PBS. The liposomal suspension was added to PBS solution containing 0.001% methyl cellulose and incubated at 37 °C. The final total lipid and insulin concentrations were adjusted to 15—20 mmol/l and 20—30 μmol/l, respectively. An aliquot of sample was taken at appropriate intervals for 6 h. Each sample was centrifuged for 10 min at 5000 rpm and the insulin concentration in the supernatant was measured with the HPLC system. The total liposomal insulin concentration was determined after disruption of the liposomes, achieved by adding 10% Triton X-100.

Statistical Analysis The statistical significance of the results was evaluated by Student's *t*-test. A p value less than 0.01 was considered significant.

Results

Loading of Insulin into Liposomes In the case of the non-pH-gradient method, neutral liposomes precipitated with insulin in 1/10 PBS. The insulin recoveries associated with liposomes after ultracentrifugation (4 °C, 100000×***g***, 1 h) were 73.3±4.9, 67.6±12.4, 36.4±1.4 and 5.7±1.2% at incubation temperatures of 4, 25, 37, and 60 °C, respectively. These values inversely correspond to the solubility of insulin in 1/10 PBS at each temperature (2.0±0.0, 3.0±0.0, 42.0±1.0, and 140.0±1.0 nmol/l at 4, 25, 37, and 60 °C, respectively). The lower solubility of insulin in 1/10 PBS at the lower temperature resulted in higher recovery of insulin associated with liposomes. After washing the pellets with 0.1 mol/l hydrochloric acid (acid), the insulin associated with liposomes was not detected by HPLC, although the size of liposomes was not changed significantly before and after incubation (345.9±74.8 and 473.2±114.3 nm, respectively).

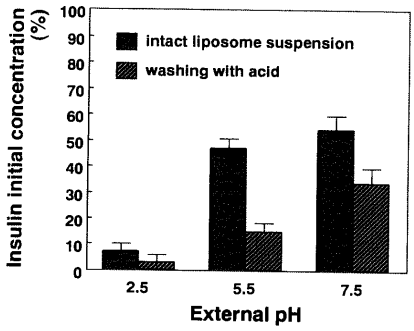

Fig. 1. Effects of External pH on Association of Insulin with Positively-Charged Liposomes *via* pH Gradient at 25 °C before and after Washing with 0.1 mol/l Hydrochloric Acid

Each value represents the mean±S.D. (n=3). The concentrations of total lipid and insulin in the incubation media were 10 mmol/l and 0.08 mmol/l, respectively. The internal pH of liposomes was 4.0.

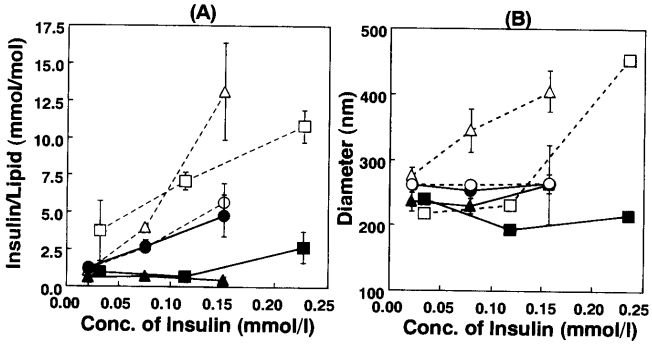

Fig. 2. Effect of Concentration of Insulin on Association of Insulin with Positively-Charged Liposomes (A) and Size Change of Liposomes (B) by Various Methods after Washing with HBS or 1/10 PBS (----, Open Symbol) and 0.1 mmol/l Hydrochloric Acid Solution (—, Closed Symbol)

Method: □, ■, c-REV; △, ▲, non-pH-gradient; ○, ●, pH-gradient. Each value represents the mean±S.D. (n=3). The concentrations of total lipid in the incubation media were 10 mmol/l, except for the c-REV method (30 mmol/l).

In the case of positively-charged liposomes prepared by the pH-gradient method, the percentage of insulin associated with the positively-charged liposomes was different according to the external pH (Fig. 1), even though the size of the liposomes was not changed before and after incubation (256.9±77.5 and 258.8±81.0 nm, respectively).

The ratio of associated millimoles of insulin to moles of lipid, and the size distribution of positively-charged liposomes *vs.* initial concentration of insulin, by the various methods after washing, are shown in Fig. 2(A) and (B). After washing with 1/10 PBS and acid, the ratios of associated insulin (mmol) to lipid (mol), prepared by the c-REV method, into positively-charged liposomes were 1.67—11.35 and 0.49—3.89, respectively (Fig. 2(A)), and those by the non-

pH-gradient method were 0.92—16.55 and 0.15—1.20, respectively. After washing with acid in these two methods, the size of liposomes decreased (Fig. 2(B)). After washing with HBS and acid, ratios by the pH-gradient method were 0.98—6.95 and 1.00—5.54, respectively (Fig. 2(A)). These values and the size of the liposomes were not changed before and after washing with HBS and acid (Fig. 2(B)). The insulin activity adsorbed to positively-charged liposomes prepared by the c-REV and pH-gradient methods, after washing with acid, were 1.9±0.2, and 17.6±1.7% of the total amount of liposomal insulin, respectively. The pH-gradient methods showed the highest loading of insulin into positively-charged liposomes after washing with acid, depending on the concentration of insulin. We used liposomes loaded with insulin prepared by various methods after washing with acid, in further experiments.

Release of Insulin from Liposomes The release profiles of insulin from positively-charged liposomes prepared by the c-REV and pH-gradient methods, are shown in Fig. 3. Released amounts of insulin from c-REV and pH-gradient liposomes were 3.0±0.3 and 31.9±15.7% at 6 h, respectively.

Loading of BSA into Liposomes In the case of neutral and positively-charged liposomes, amounts of BSA associated with liposomes (mmol BSA per mol of lipid) were not significantly different between the c-REV method (0.214, 0.233, respectively), the non-pH-gradient method (0.186, 0.340) and the pH-gradient method (0.195, 0.310) for a low concentration (7.6 μmol/l) of BSA (Table 1). BSA showed significantly higher affinity to positively-charged liposomes than neutral ones at the higher concentration (37.9 μmol/l) of BSA, except for liposomes prepared by the c-REV methods.

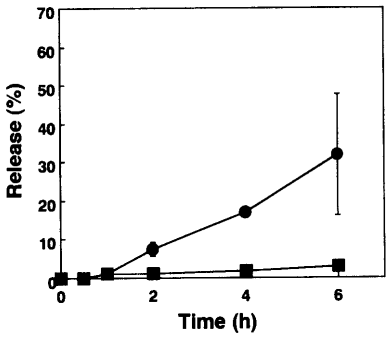

Fig. 3. Release Profiles of Insulin from Positively-Charged Liposomes in PBS at pH 7.4 and 37 °C

Method: ■, c-REV; ●, pH-gradient. Each value represents the mean ±S. E. (n=3).

The size of neutral and positively-charged liposomes was not changed after incubation (Table 2).

Table 3 shows the molar ratio of insulin and BSA associated with liposomes to total lipid and trapping efficiency into liposomes.

Discussion

Loading of Insulin into Liposomes Remote loading of peptides by incubation has various advantages, such as improved drug loading and prevention of drug inactivation during the preparation. The curvature and composition of liposomes influence insulin binding,[17] thus we selected REV liposomes, large unilamellar vesicles, instead of small unil-

Table 1. Amount of BSA Associated with Liposomes by Various Methods

Liposome	Method	BSA/lipid (mmol/mol) L	BSA/lipid (mmol/mol) H
Neutral	c-REV	0.214±0.039	0.242±0.009 [a)]
	Non-pH-gradient	0.186±0.013 [b)]	0.207±0.019 [a)]
	pH-gradient	0.195±0.002 [b)]	0.208±0.006 [a)]
Positively -charged	c-REV	0.233±0.080	0.279±0.023
	Non-pH-gradient	0.340±0.005	0.495±0.105
	pH-gradient	0.310±0.054	0.256±0.009

The concentrations of total lipid were approximately 30, 15 and 15 mmol/l by the c-REV, the non-pH-gradient and the pH-gradient methods, respectively. The concentrations of BSA were approximately 7.6 μmol/l (L) and 37.9 μmol/l (H), respectively. Each value represents the mean±S.D. (n=3). *a*) p<0.01, *b*) p<0.001, significantly different.

Table 2. The Size Distribution of BSA Liposomes Prepared by Various Methods

Liposome	Method	Diameter (nm) L	Diameter (nm) H
Neutral	c-REV	289.9±36.4	255.1± 7.2
	Non-pH-gradient	326.5±63.0	357.1±33.3
	pH-gradient	245.1± 7.6	236.7±15.1
Positively -charged	c-REV	259.2±65.8	225.4± 6.1
	Non-pH-gradient	233.3± 4.5	224.8± 5.8
	pH-gradient	285.7±32.2	293.2±20.4

The concentrations of total lipid were approximately 30, 15 and 15 mmol/l by the c-REV, the non-pH-gradient and the pH-gradient methods, respectively. The concentrations of BSA were approximately 7.6 μmol/l (L) and 37.9 μmol/l (H), respectively. Each value represents the mean±S.D. (n=3−6). The liposomes size was 365.6±142.2 and 278.2±77.4 nm for neutral and positively-charged liposomes before incubation, respectively.

Table 3. The Molar Ratio of Insulin and BSA Associated with Liposomes to Total Lipid and Trapping Efficiency (T.E.) into Liposomes by Various Methods

Liposome	Method	Insulin: Insulin/lipid (mmol/mol)	Insulin: T.E. (%)	BSA: BSA/lipid (mmol/mol)	BSA: T.E. (%)
Neutral	c-REV	0.270—0.598[a)]	5—15	0.242[b)]±0.009 [c)]	19.17±0.73 [d)] [d)]
	Non-pH-gradient	n.d.[e)]	n.d.[e)]	0.207[f)]±0.019 [c)]	8.19±0.75 [c)]
	pH-gradient	n.d.[e)]	n.d.[e)]	0.208[f)]±0.006 [c)]	8.24±0.23 [d)]
Positively -charged	c-REV	0.679[g)]±0.167	15.6±3.8	0.279[b)]±0.023	23.55±1.95 [d)]
	Non-pH-gradient	0.664[h)]±0.091 [c)] [c)]	8.6±0.9 [c)] [c)]	0.495[f)]±0.105	20.89±4.44
	pH-gradient	2.684[h)]±0.422	33.7±5.3	0.256[f)]±0.009	10.82±0.37

Conc. in preparation: *a*) insulin: approximately 0.13—0.14 mmol/l, lipid: 30 mmol/l from ref.[12] Insulin: *g*) 0.12 mmol/l, *h*) 0.08 mmol/l. Lipid: *g*) 30 mmol/l, *h*) 10 mmol/l., BSA: *b*, *f*) 37.9 μmol/l (Table 1, H). Lipid: *b*) 30 mmol/l, *f*) 15 mmol/l. Incubation by the non-pH-gradient and pH gradient methods: 1 h at 25°C. Each value represents the mean±S.D. (n=3). *c*) p<0.01, *d*) p<0.001, significantly different. *e*) n.d.: not detected.

amellar vesicles (SUV), to observe not adsorption but loading of insulin. Insulin precipitated in neutral pH solution by polymerization, and could not be loaded into neutral liposomes. From these results, the amount of insulin associated with liposome after washing with acid was considered to be the amount of trapped insulin, because the solubility of insulin is much higher under acidic conditions than at neutral pH.

For enhanced remote loading of insulin, we selected the pH-gradient method since insulin is an amphoteric molecule and its charge is changed according to the pH of the solution. The pH-gradient method (inside pH 4.0, outside pH 7.5) was effective for remote loading of basic molecules such as doxorubicin,[2,3] and the calcium acetate gradient (inside basic) method was effective for remote loading of acidic molecules such as diclofenac sodium into liposomes.[12]

Insulin was entrapped into neutral liposomes at 0.27—0.60 of the ratio of entrapped mmol insulin to mol lipid (5—15% as trapping efficiency), obtained by the c-REV method,[12] but it was not loaded into liposomes by the non-pH- and pH-gradient methods (Table 3). At neutral pH, insulin may be negatively charged since its isoelectric point is about pH 5.5. Due to electrostatic forces, it is expected that negatively-charged drug molecules can be bound to positively-charged liposomes more efficiently than neutral or negatively-charged liposomes.

On the basis of these considerations, the non-pH gradient method was applied to load insulin into positively-charged liposomes. 8.3—148.9 μg insulin to μmol DPPC (equivalent to 0.92—16.55 mmol insulin/mol total lipid) was associated with positively-charged liposomes containing 11% molar fraction of SA at 25 °C before washing with acid, although most molecules adsorbed on the liposomes were removed after washing (Fig. 2(A), non-pH gradient method). These values correspond to the following reports.[17,18] Wiessner and Hwang[17] reported that insulin was tightly adsorbed on small unilamellar liposomes containing a 5% molar fraction of SA (64.7 μg insulin per μmol DPPC, equivalent to approximately 10.3 mmol insulin/mol total lipid at 21 °C). Kato *et al.*[18] reported that insulin can be easily adsorbed onto positively-charged liposomes after incubation.

In the pH-gradient method using positively-charged liposomes, the insulin loading was different according to the external pH (Fig. 1). Only trace amounts of insulin were associated with positively-charged liposomes at an external pH of 2.5. Under these conditions, both insulin and the liposomes may be positively charged, resulting in electrostatic repulsion, and no drug loading and little binding of insulin to the liposomal surface (Fig. 1). At an external pH of 7.5, the highest loading of insulin after washing with acid was observed. At pH 7.5 liposomes containing SA are positively charged (ζ-potential, 27.3±1.2 mV at pH 7.4), and the acidic groups of insulin may be negatively charged. Therefore, the negatively-charged acidic groups of insulin may interact with the positively-charged SA in liposomes by electrostatic attraction.

From these results and the paper reported by Wiessner and Hwang,[17] it is suggested that electrostatic interactions aid the loading of insulin into liposomes, because electrostatic forces are generally stronger than hydrophobic forces. The size of positively-charged liposomes increased at high concentrations of insulin (Fig. 2(B)), which showed a stronger interaction of insulin with liposomal membranes, compared with neutral liposomes. The difference between the non-pH-gradient and pH-gradient method in loading of insulin into positively-charged liposomes may support the idea that insulin was loaded into liposomes in response to a transmembrane pH gradient by the pH-gradient method, in a form which can not be removed by washing with acid, although we cannot explain the accurate mechanism in detail.

Comparison of Liposomal Insulins Prepared by the c-REV and pH-Gradient Methods The release profile was studied to compare the distribution of insulin in c-REV liposomes and pH-gradient liposomes. Only positively-charged liposomes were selected, because of the higher insulin trapping efficiency. Spontaneous dissociation of insulin from the liposomes was not observed. About 32% of the original insulin was released from the pH-gradient liposomes by incubation in PBS (pH 7.4) for 6 h at 37 °C (Fig. 3), whereas only about 3% from the c-REV liposomes.

The change of the ζ-potential of the positively-charged liposomes supports the higher adsorption of insulin on the surface of pH-gradient liposomes than c-REV liposomes. The ζ-potentials of positively-charged empty liposomes, obtained by the c-REV and pH-gradient methods were 27.0±2.6 and 27.3±1.2 mV at pH 7.4, respectively. The ζ-potentials of c-REV and pH-gradient liposomes with loaded insulin were 8.3±3.1 and −5.0±1.2 mV at pH 7.4, respectively. In the latter case, the larger shift of the ζ-potential to negative values represents the higher adsorption of insulin to liposomes since insulin may be charged negatively at neutral pH.

The adsorbed insulin activity of positively-charged liposomes obtained by the c-REV and pH-gradient methods, were 1.9±0.2, and 17.6±1.7% of the total amount of liposomal insulin, respectively. These results correspond well to the results of the ζ-potentials of liposomes.

From the results of the release profiles, ζ-potential and the adsorbed insulin activity, it can be suggested that insulin distributes more at the surface of the liposomes prepared by the pH-gradient method, than those obtained by the REV method.

Loading of BSA into Liposomes Two concentrations of BSA (7.6 and 37.9 μmol/l) were selected, since Law *et al.*[19] showed saturation in adsorption to liposomes at a BSA concentration of approximately 24.2 μmol/l at 37 °C. However, 0.186 and 0.207 mmol BSA/mol lipid (Table 1, non-pH gradient method) was associated with neutral liposomes at 7.6 and 37.9 μmol/l BSA concentrations after 1 h incubation at 25 °C. From the result that the amount of BSA loaded into liposomes was not significantly increased (Table 1), it is suggested that the binding sites on the liposomes may be limited and a constant amount of BSA may bind with liposomes. From these results, binding appears to be saturated at a low concentration of BSA. The size of liposomes did not increase after incubation (Table 2), different from the case of insulin.

BSA showed significantly higher association affinity for positively-charged liposomes than neutral ones (Table 1). BSA may interact more with positively-charged liposomes than neutral ones, by electrostatic interaction. Because the isoelectric point of BSA is 4.2—4.8, many parts of BSA may be negatively-charged at experimental neutral pH.

The adsorption of serum albumin to liposomes at 37 °C

has been reported,[19—21] in order to investigate the behavior of liposomes in plasma. Law *et al.*[19] suggested that the adsorption of BSA to the phospholipid bilayers of liposomes may be driven by hydrophobic effects, despite the charge characteristics of phosphatidylcholine liposomes incubated with BSA at a high concentration (6.8 mmol/l).[19] BSA molecules might adsorb onto the liposome surface by the charge effect for charged surfaces, and by van der Waals forces, ion-dipole forces and hydrogen bonds, for neutral surfaces, as in the case of insulin. The pH-gradient method did not increase the ratio of BSA associated with lipid in neutral and positively-charged liposomes (Table 3). It seems that the electrostatic interaction increases to entrap BSA, but is weaker than hydrophobic interaction of BSA and liposomes.

It is suggested that the loading of BSA into liposomes may be mainly due to hydrophobic interactions, with only a relatively weak influence from electrostatic interactions.

Comparison of Insulin and BSA Loading into Liposomes Trapping efficiencies of insulin and BSA for positively-charged liposomes were significantly higher than those for neutral liposomes (Table 3). In positively-charged liposomes, the pH-gradient method is significantly effective for loading insulin, but not for BSA, compared to the c-REV and non-pH-gradient methods. To explain this difference between BSA and insulin, we suggest that the affinity of insulin for liposomes can be changed by altering pH,[17,22] whereas the affinity of BSA is not changed because of its high hydrophobicity.[19] With the pH-gradient method, pH-dependency of affinity of BSA molecules for liposomes is required, as the molecules may penetrate the liposomal membrane in a non-ionized form with high affinity to lipid, and then may be accumulated in liposomes in an ionized form, with low affinity to lipid. Furthermore, the interaction of liposomes with serum proteins *in vitro* has been shown to enhance the leakage of solutes or probe molecules from liposomes.[23,24] Partial penetration of large molecular weight BSA into the liposomal membrane might cause leakage of citric acid molecules from liposomes, resulting in no transmembrane pH gradient.

Electrostatic interactions may be important to attract a drug at the surface of liposome and appropriate hydrophobic interaction may be effective for penetration of high molecular weight drugs into liposomal membranes. In the case of BSA, remote loading by the pH-gradient method may not be effective due to its high hydrophobicity and no change in its affinity for liposomes at different pH.

Conclusions

The present work has demonstrated remote loading of peptide molecules into preformed liposomes by incubation. Insulin could be loaded into positively-charged liposomes with about twofold better efficiency by the pH-gradient method, compared with the conventional REV method. BSA could be loaded equally into neutral and positively-charged liposomes by incubation, regardless of the loading method. Our results suggest that the pH-gradient method, combining electrostatic interaction, may be useful for preparation of liposomal insulin and that the high hydrophobicity of BSA may interfere with remote loading of BSA into liposomes by the pH-gradient method.

Acknowledgements We would like to thank Ms Takako Morimoto and Ms Yoko Kawachi for their assistance in the experimental work.

This work was supported by the Ministry of Education, Science, Sports, and Culture of Japan.

References

1) Mayer L. D., Madden T. D., Bally M. B., Cullis P. R., "Liposome Technology," Vol. II, 2nd ed., ed. by Gregoriadis G., CRS Press., Inc., Chapter 2, pp. 27—44 (1993).
2) Mayer L. D., Bally M. B., Cullis P. R., *Biochim. Biophys. Acta*, **857**, 123—126 (1986).
3) Harrigan P. R., Wong K. F., Redelmeier T. E., Wheeler J. J., Cullis P. R., *Biochim. Biophys. Acta*, **1149**, 329—338 (1993).
4) Mayer L. D., Bally M. B., Loughrey H., Masin D., Cullis P. R., *Cancer Res.*, **50**, 575—579 (1990).
5) Chakrabarti A. C., Clark-Lewis I., Harrigan P. R., Cullis P. R., *Biophys. J. Biophys. Soc.*, **61**, 228—234 (1992).
6) Felgner P. L., Gadek T. R., Holm M., Roman R., Chan H. W., Wenz M., Northrop J. P., Ringold G. M., Danielsen M., *Proc. Natl. Acad. Sci. U.S.A.*, **84**, 7413—7417 (1987).
7) Patel H. M., Ryman B. E., *FEBS Lett.*, **62**, 60—63 (1976).
8) Muramatsu K., Maitani Y., Nagai T., *Biol. Pharm. Bull.*, **19**, 1055—1058 (1996).
9) Panagi Z., Avgoustakis K., Evangelatos G., Ithakissios D. S., *Int. J. Pharm.*, **176**, 203—207 (1999).
10) Shek P. N., Yung B. Y., Stanacev N. Z., *Immunology*, **49**, 37—44 (1983).
11) Yung B., Shek P. N., Stanacev N. Z., *Chem. Phys. Lipids*, **37**, 283—295 (1985).
12) Hwang S. H., Maitani Y., Qi X. R., Takayama K., Nagai T., *Int. J. Pharm.*, **179**, 85—95 (1999).
13) Szoka F. J., Papahadjopouls D., *Proc. Natl. Acad. Sci. U.S.A.*, **75**, 4194—4198 (1978).
14) Qi X. R., Maitani Y., Shimoda N., Sakaguchi K., Nagai T., *Chem. Pharm. Bull.*, **43**, 295—299 (1995).
15) Nakazawa H., Nagase M., *Yakugaku Zasshi*, **106**, 398—405 (1986).
16) Smith P. K., Krohn R. I., Hermanson G. T., Mallia A. K., Gartner F. H., Provenzano M. D., Fujimoto E. K., Goeke N. M., Olson B. J., Klenk D. C., *Anal Biochem.*, **150**, 76—85 (1985).
17) Wiessner J. H., Hwang K. J., *Biochim. Biophys. Acta*, **689**, 490—498 (1982).
18) Kato Y., Hosokawa T., Hayakawa E., Ito K., *Biol. Pharm. Bull.*, **16**, 457—461 (1993).
19) Law S. L., Lo W. Y., Pai S. H., Teh G. W., Kou F. Y., *Int. J. Pharm.*, **32**, 237—241 (1986).
20) Hoekstra D., Scherphof G., *Biochim. Biophys. Acta*, **551**, 109—121 (1979).
21) Law S. L., Lo W. Y., Pai S. H., Teh G. W., *Int. J. Pharm.*, **43**, 257—260 (1988).
22) Farias R. N., Lopez Vinals A. E., Posse E., Morero D., *Biochem. J.*, **264**, 285—287 (1989).
23) Zborwski J., Roerdink F., Scherphof G., *Biochim. Biophys. Acta*, **497**, 183—191 (1977).
24) Matsumura H., Dimitrova M., *Colloids Surf., B*, **6**, 165—172 (1996).

Characterization of the Activity of L-Ascorbic Acid 2-[3,4-Dihydro-2,5,7,8-tetramethyl-2-(4,8,12-trimethyltridecyl)-2*H*-1-benzopyran-6-yl-hydrogen Phosphate] Potassium Salt in Hydroxyl Radical Elimination

Takashi TOMITA, Midori KASHIMA, and Yasuhisa TSUJIMOTO*

Department of Endodontics, Nihon University School of Dentistry at Matsudo, 870–1 Sakaecho, Nishi-2, Matsudo, Chiba 271–8587, Japan. Received August 19, 1999; accepted November 18, 1999

The effect of L-ascorbic acid 2-[3,4-dihydro-2,5,7,8-tetramethyl-2-(4,8,12- trimethyltridecyl)-2*H*-1-benzopyran-6-yl-hydrogen phosphate] potassium salt (EPC-K_1) on hydroxyl radical (·OH) elimination was studied using electron spin resonance (ESR) and spectrophotometric experiments. The addition of EPC-K_1 and ·OH scavengers eliminated the ·OH generated from Cu^{2+}/H_2O_2, Fe^{2+}/H_2O_2 and H_2O_2/UV-irradiation reaction systems. However, in competitive reactions using different concentrations of a spin-trap agent, the addition of the ·OH scavenger altered the IC_{50} values, whereas the addition of EPC-K_1 and a metal chelater did not change the value in the Cu^{2+}/H_2O_2 and Fe^{2+}/H_2O_2 reaction systems. The addition of EPC-K_1 and metal chelater changed the ESR signal for free Cu^{2+}. The spectrophotometric experiments confirmed that the addition of EPC-K_1 and metal chelater altered the absorption spectra due to $CuCl_2$ and $FeSO_4$, whereas the ·OH scavenger did not alter the spectra.

Therefore, it was demonstrated that EPC-K_1 has the ability both to scavenge ·OH directly and to inhibit the generation of ·OH by the chelation of Cu^{2+} and Fe^{2+}.

Key words ESR; hydroxyl radical; scavenging; L-ascorbic acid 2-[3,4-dihydro-2,5,7,8-tetramethyl-2-(4,8,12-trimethyltridecyl)-2*H*-1-benzopyran-6-yl-hydrogen phosphate] potassium salt

The hydroxyl radical (·OH) generated in human tissue occasionally exerts unfavorable biological actions, such as lipid peroxidation and ischemia-reperfusion injury. It also plays an important role in tissue injury at inflammation sites in various diseases, including oral diseases.[1,2] It is well known that vitamin C and vitamin E have antioxidant effects and ·OH scavenging ability. Recently, L-ascorbic acid 2-[3,4-dihydro-2,5,7,8-tetramethyl-2-(4,8,12-trimethyltridecyl)-2*H*-1-benzopyran-6-yl-hydrogen phosphate] potassium salt (EPC-K_1), a conjugation of vitamin C and vitamin E that is water-soluble and stable at room temperature, was developed as an ·OH scavenger and antioxidant agent. Kuribayashi *et al.*[3] reported that EPC-K_1 inhibited lipid peroxidation and phospholipase A_2 activity in rat brain homogenates and human plasma, and suggested that these properties of EPC-K_1 might be useful in the treatment of ischemia-reperfusion. Yagi *et al.*[4] reported that the intravenous administration of EPC-K_1 had a strong protective effect on warm ischemic damage to liver grafts and recipient survival in swine. Previous studies also showed that EPC-K_1 had ·OH scavenging and anti-lipid peroxidation properties.[5—11] Recently, Anzai *et al.*[12] reported that EPC-K_1 has potent ·OH scavenging and iron chelating activity, and very weak reducing activity, and that these activities may work together to scavenge and reduce the ·OH, which may make EPC-K_1 beneficial *in vivo* by offering protection against ·OH-related damage. In this study, we examined the ability of EPC-K_1 in detail.

Experimental

Materials EPC-K_1 was kindly provided by Dr. Kazumi Ogata, Senju Pharmaceutical (Japan). The chemical agents used for the generation of ·OH were $CuCl_2$, $FeSO_4$ and H_2O_2. Ethylenediamine-*N,N,N',N'*-tetraacetic acid (EDTA) and diethylenetriamine-*N,N,N',N'',N''*-pentaacetic acid (DETAPAC) were used for metal chelation, and dimethyl sulfoxide (DMSO) and ethanol were used as agents that scavenge ·OH. All of these chemicals were obtained from Wako Pure Chemical Co. (Japan). 5,5-Dimethyl-1-pyrroline-*N*-oxide (DMPO), which is a trapping agent for radicals, was obtained from Dojin Chemicals (Japan).

Effects of EPC-K_1 on ·OH Elimination The amounts of ·OH generated from the $CuCl_2+H_2O_2$ (Cu^{2+}/H_2O_2) and $FeSO_4+H_2O_2$ (Fe^{2+}/H_2O_2) reaction systems were measured using the electron spin resonance (ESR) spin-trapping method.[11,13,14] The ·OH eliminating ability of EPC-K_1 was analyzed by adding EPC-K_1 and an ·OH scavenging agent to these reaction systems, then allowing them to react competitively with DMPO, the spin-trapping agent. The final concentration of DMPO in 200 μl of the Cu^{2+}/H_2O_2 reaction mixture (1 mM $CuCl_2$/100 mM H_2O_2) was adjusted to either 89.0 or 8.9 mM for this experiment. Various concentrations of EPC-K_1 and DMSO were added to the reaction mixture. In the Fe^{2+}/H_2O_2 reaction system, the reaction mixture comprised 1.0 mM $FeSO_4$ solution and 100 mM H_2O_2, along with 0.8 mM DETAPAC in 200 μl. The reaction was started by adding the H_2O_2, and the ·OH generated was measured with ESR after 50 s. Further, the amount of ·OH generated from the reaction system after irradiation of 1 M H_2O_2 with ultraviolet light (UV, 254 nm) for 45 s was measured according to the method of Ueda *et al.*[15] The quantity of ·OH was normalized relative to the standard signal intensity of the manganese oxide marker as ·OH relative intensity = ·OH signal intensity (first peak)/Mn^{2+} marker intensity.[11] The ESR spectra were measured using a JEOL JES FR-80 Radical Bio Sensor. The measurement conditions were as follows: microwave power, 8 mW; magnetic field, 335.4±5 mT; sweep time, 2 min; modulation frequency, 100 kHz; and time constant, 0.3 s or 0.1 s (UV experiment).

Measurement of the ESR Signal for Cu^{2+} Since the ESR signals of EDTA-chelated Cu^{2+} and free Cu^{2+} are known to be different, in this experiment the influence of EPC-K_1 on Cu^{2+} was studied using ESR at a temperature of 77 K. For measurement of the free Cu^{2+} ESR signal, the final concentration of $CuCl_2$ was adjusted to 1 mM. Several concentrations of EDTA, DMSO and/or EPC-K_1 solutions were mixed with $CuCl_2$, then their ESR signals were measured.

The measurement conditions were as follows: microwave power, 1.0 mW; magnetic field, 300.0±100 mT; sweep time, 2 min; modulation frequency, 100 kHz; and time constant, 0.1 s. The coordinate bond of Cu^{2+} and EPC-K_1 was assessed from the ESR parameters obtained from the ESR signal. Fe^{2+} could not be measured as the diamagnetic.

Measurement of the Absorption Spectra of Cu and Fe The influence of EPC-K_1, DMSO and EDTA on the absorption spectra of $CuCl_2$ and $FeSO_4$ was studied. The final concentration of $CuCl_2$ or $FeSO_4$ was 1 mM in the total amount of 1200 μl. Alterations to the absorption spectrum were observed using a Shimadzu spectrophotometer UV-2200 over a 50 s period. The absorption range of Cu and Fe (from $CuCl_2$ and $FeSO_4$) was 202.4—327.4 nm and 208.4—511.0 nm, respectively. The influences of EPC-K_1, DMSO and EDTA (changes in $CuCl_2$ and $FeSO_4$ orientation) were determined in terms of the changes in instinct absorbance.

* To whom correspondence should be addressed.

© 2000 Pharmaceutical Society of Japan

Table 1. IC_{50} (M) for Samples on Each Reaction System

	Cu^{2+}/H_2O_2 reaction system		Fe^{2+}/H_2O_2 reaction system		H_2O_2/UV-irradiation reaction system	
	DMPO 89.0 mM	DMPO 8.9 mM	DMPO 89.0 mM	DMPO 8.9 mM	DMPO 89.0 mM	
DMSO	8.9×10^{-2}	4.1×10^{-3}	1.0×10^{-2}	5.1×10^{-4}	DMSO	2.3×10^{-3}
EDTA	5.6×10^{-5}	5.6×10^{-5}	1.4×10^{-3}	1.4×10^{-3}	Ethanol	1.2×10^{-2}
EPC-K_1	2.7×10^{-4}	1.2×10^{-4}	5.9×10^{-4}	4.0×10^{-4}	EPC-K_1	2.8×10^{-2}

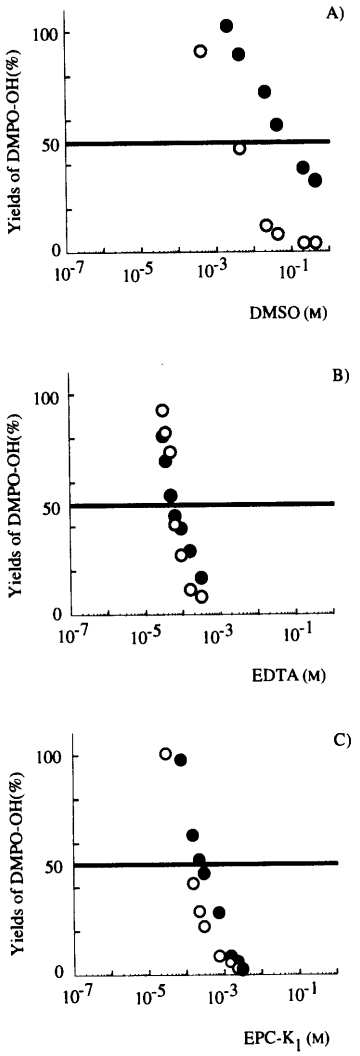

Fig. 1. Elimination Modes of ·OH (%) by Adding Samples to the Cu^{2+}/H_2O_2 Reaction System

A) DMSO, B) EDTA, C) EPC-K_1. ●: 89.0 mM DMPO, ○: 8.9 mM DMPO. A hundred percent yield was given before the addition of sample.

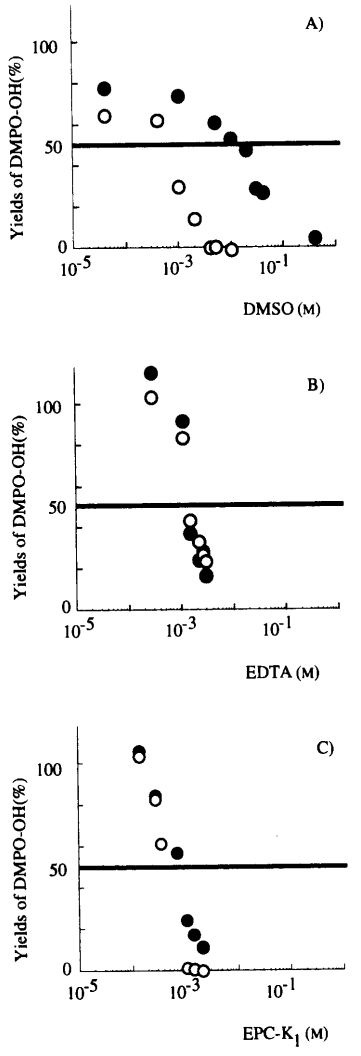

Fig. 2. Elimination Modes of ·OH (%) by Adding Samples to the Fe^{2+}/H_2O_2 Reaction System

A) DMSO, B) EDTA, C) EPC-K_1. ●: 89.0 mM DMPO, ○: 8.9 mM DMPO. A hundred percent yield was given before the addition of sample.

Results

Elimination of ·OH Generated from the Cu^{2+}/H_2O_2 Reaction System The ·OH (DMPO–OH) was detected when DMPO was added to the reaction mixture. This adduct was confirmed as ·OH because the hyperfine coupling constant was consistent with that given in a previous report ($aN=aH=1.49$ mT).[16] Additions of EPC-K_1, DMSO and EDTA to the Cu^{2+}/H_2O_2 reaction system reduced the concentration of ·OH (Fig. 1). Changing the DMPO concentration altered the DMPO–OH level, showing that these agents are involved in a competitive reaction. When different concentrations of DMPO were used, the sigmoid curve was shifted laterally with the addition of DMSO, slightly with EPC-K_1, but not with EDTA. The IC_{50} (Table 1) was determined from the regression line obtained by the least-squares method, shown in Fig. 1. Remarkable change in IC_{50} values for EPC-K_1 or EDTA was observed by adding different concentrations of DMPO. However, the IC_{50} of DMSO varied with different concentrations of DMPO.

Elimination of ·OH Generated from the Fe^{2+}/H_2O_2 Reaction System When EPC-K_1, DMSO and EDTA were added to the Fe^{2+}/H_2O_2 reaction system, the levels of DMPO–OH adducts were reduced in a concentration-dependent manner (Fig. 2). The sigmoid curve shifted laterally with the addition of DMSO, but similar shifts were not observed with EPC-K_1 and EDTA. The IC_{50} values of EPC-K_1,

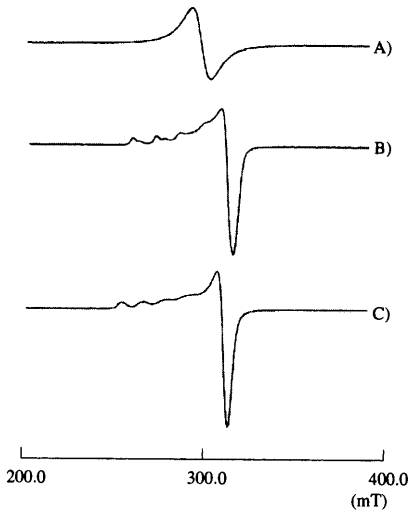

Fig. 3. ESR Signals from $CuCl_2$ with/without Each Solution

A) 1 mM $CuCl_2$, B) 1 mM $CuCl_2$+7.5 mM EDTA, C) 1 mM $CuCl_2$+7.5 mM EPC-K_1.

DMSO and EDTA are shown in Table 1. However, the IC_{50} of DMSO varied with different concentrations of DMPO.

Interaction between Cu^{2+} or Fe^{2+} and EPC-K_1 To confirm whether EPC-K_1 acted on the ·OH generation system or on generated ·OH, we examined changes in the ESR signals for Cu^{2+} and changes in the absorption spectra of Cu^{2+} and Fe^{2+}. The alteration of the ESR signal for Cu^{2+} is shown in Fig. 3. The ESR signal obtained after the addition of EDTA was shifted to a higher field compared with the control. This shift in the signal indicated the chelation of EDTA with Cu^{2+}. In the EPC-K_1 experiment, the ESR signal for Cu^{2+} also changed, like EDTA, indicating EPC-K_1 also possessive chelating activity with Cu^{2+}. The effects of EPC-K_1, EDTA and DMSO on the absorption spectra of $CuCl_2$ and $FeSO_4$ are shown in Fig. 4. The absorption spectra obtained by reacting $CuCl_2$ and $FeSO_4$ with EDTA shifted to the long-wavelength side compared with the spectrum of EDTA alone. The absorption spectra slightly shifted when EPC-K_1 was added to $CuCl_2$ and $FeSO_4$. By contrast, no changes were seen with the addition of DMSO.

Elimination of ·OH Generated from the H_2O_2/UV-Irradiation Reaction System The ·OH generated from the H_2O_2/UV-irradiation reaction system was confirmed by the ESR spin-trapping method. When the ·OH scavenger, DMSO or ethanol, was added to the reaction system, the amounts of ·OH were decreased and new signals were observed (Fig. 5). The amount of ·OH also decreased with the addition of EPC-K_1. The level of DMPO-OH adducts was reduced in a concentration-dependent manner (Fig. 6). The IC_{50} values are shown in Table 1.

Discussion

It was reported that EPC-K_1 was composed of ascorbate and vitamin E, joined by a phosphodiester linkage, and had potent ·OH scavenging ability and anti-lipid peroxidation ability.[5—11] Recently, Anzai *et al.*[12] reported the potency of EPC-K_1 using the ESR spin-trapping method and other methods. They have reported that ·OH generated by the Fenton reaction (Fe^{2+}/H_2O_2) or by the UV irradiation of H_2O_2 was quenched efficiently and dose-dependently by EPC-K_1. The spectrophotometric change of the mixture of EPC-K_1 and

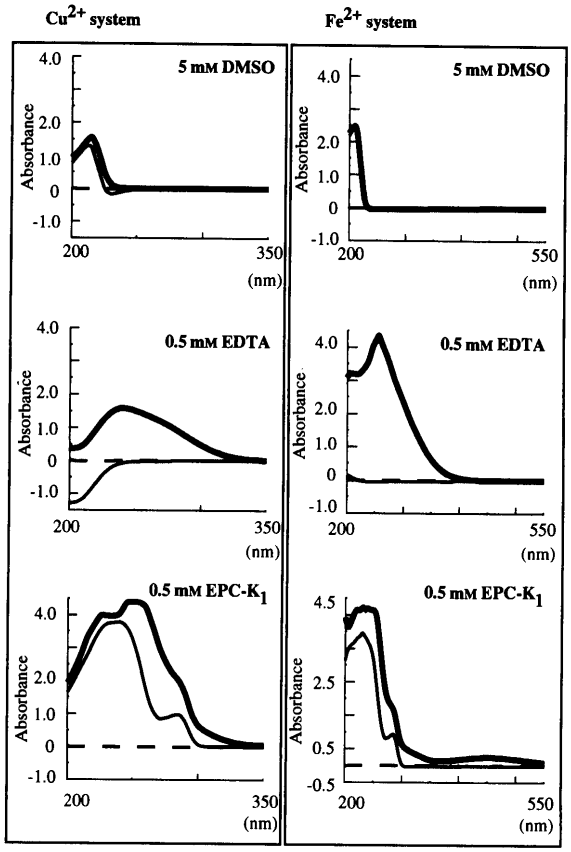

Fig. 4. Spectrum Analyses

---- 1 mM $CuCl_2$ or 1 mM $FeSO_4$, — sample alone, — 1 mM $CuCl_2$ or 1 mM $FeSO_4$+sample.

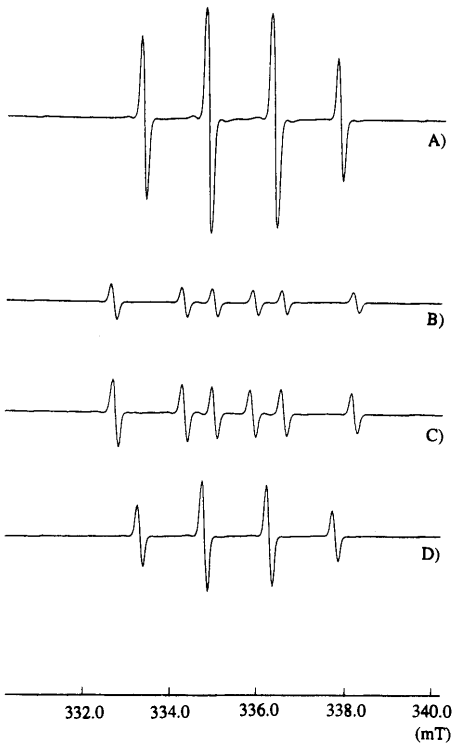

Fig. 5. ·OH Signals from the 1 M H_2O_2/UV-Irradiation Reaction System with/without Each Solution

A) 1 M H_2O_2/UV, B) 1 M H_2O_2/UV+3.5 M DMSO, C) 1 M H_2O_2/UV+4.3 M ethanol, D) 1 M H_2O_2/UV+6.25 mM EPC-K_1. 89.0 mM DMPO was used in this experiment.

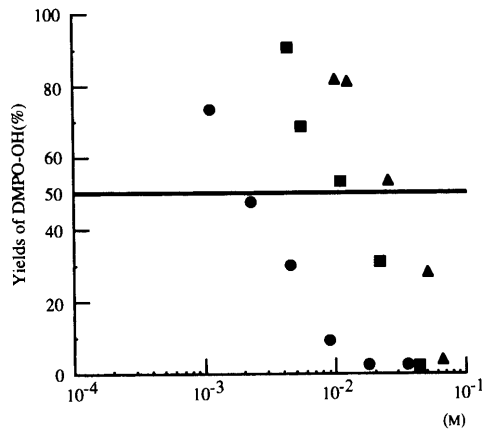

Fig. 6. Elimination Modes of ·OH (%) by Adding Samples to the H_2O_2/UV-Irradiation Reaction System with 89.0 mM DMPO
●: DMSO, ■: ethanol, ▲: EPC-K_1.

iron in water suggested that EPC-K_1 chelated the iron. As EPC-K_1 did not inhibit the peroxidation of linoleic acids caused by the reaction with an alkylperoxyl radical, EPC-K_1 did not have changing potency against the alkylperoxyl radical.[12]

In previous studies, we reported[7—9] that the ·OH was generated from the Cu^{2+}/H_2O_2 reaction system. However, details of the mechanism of action of EPC-K_1 with regard to Cu^{2+}/H_2O_2 have not been clarified. Therefore, we examined the potency of EPC-K_1 on the reaction systems of both Cu^{2+}/H_2O_2 and Fe^{2+}/H_2O_2. Further, Anzai *et al.*[12] did not examine the competitive reaction using different concentrations of spin-trap agent in the ESR experiment. In the present experiment, we examined the ability of EPC-K_1 to eliminate the ·OH generated from three reaction systems: Cu^{2+}/H_2O_2, Fe^{2+}/H_2O_2, and H_2O_2/UV-irradiation, by using ESR and the absorption spectra.

There are two possible mechanisms for the antioxidant action: inhibiting the generation of ·OH, or scavenging the generated ·OH. In the former action, the antioxidant may bind with transition metal ions that react with H_2O_2 and generate ·OH. The metal complex thus formed cannot further react with H_2O_2 to generate ·OH. In the latter, the lipid peroxidation induced by ·OH is protected by direct scavenging of ·OH. Namely, ·OH extracts a H atom from the lipid (LH), then the lipid radical (·L) generated becomes a lipid peroxy radical (·LOO) under the presence of O_2. Further, the peroxy radical thus formed extracts H atom from the lipid to become hydroperoxide (LOOH) in the reaction of lipid peroxidation.[17]

In the ESR spin-trapping method, the IC_{50} was not remarkable affected by the addition of EPC-K_1 or EDTA using different concentrations of DMPO in either the Cu^{2+}/H_2O_2 or Fe^{2+}/H_2O_2 reaction system. The IC_{50} was, however, changed by the addition of the ·OH scavenger, DMSO. The absorption spectra were altered by the addition of EPC-K_1 or EDTA, but not by the addition of DMSO. In addition, the ESR signal of Cu^{2+} was altered by the addition of EPC-K_1 or EDTA. These results suggest that EPC-K_1 and EDTA may inhibit ·OH generation by binding with the Cu^{2+} and Fe^{2+}. The complexes thus formed are considered to be unable to react with H_2O_2 to generate ·OH.

The concentration of ·OH generated from the H_2O_2/UV-irradiation reaction system was decreased by the addition of ·OH scavengers, DMSO and ethanol. The concentration of the ·OH generated from the UV irradiation reaction system was also decreased by the addition of EPC-K_1. In a pilot study, we confirmed that EPC-K_1 did not generate any radicals with UV irradiation (data not shown). These results suggest that EPC-K_1 also has a direct scavenging ability for ·OH. Our results agreed with the report of Anzai *et al.*[12]

In conclusion, we confirmed that EPC-K_1 has the ability to inhibit the generation of ·OH from the Cu^{2+}/H_2O_2 reaction system. We also reconfirmed the report of Anzai *et al.*[12] which stated that EPC-K_1 has the ability to inhibit the generation of ·OH from Fe^{2+}/H_2O_2 reaction system and to scavenge of ·OH generated from the H_2O_2/UV-irradiation reaction system. This report demonstrated that EPC-K_1 has two actions, namely, inhibiting the generation of ·OH by the chelation of both Cu^{2+} and Fe^{2+}, and scavenging ·OH directly.

These results suggest that EPC-K_1 might be effective for the treatment of various diseases in oral tissue. Studies for such application are currently under investigation in our group.

References

1) Bartold P. M., Wiebkin O. W., Thonard J. C., *J. Periodontal Res.*, **19**, 390—400 (1984).
2) Takeichi O., Saito I., Hayashi M., Tsurumachi T., Saito T., *J. Endodont.*, **24**, 157—160 (1998).
3) Kuribayashi Y., Yoshida K., Sakaue T., Okumura A., *Arzneim.-Forsch./Drug Res.*, **42**, 1072—1074 (1992).
4) Yagi T., Sakagami K., Nakagawa H., Takaishi Y., Orita K., *Transplant Int.*, **5**, 420—423 (1992).
5) Mori A., Edamatsu R., Kohno M., Ohmori S., *Neurosciences*, **15**, 371—376 (1989).
6) Shiozawa A., Kimura K., Hashizume H., Tsujimoto Y., Yamazaki M., *Jpn. J. Conserv. Dent.*, **39**, 1171—1177 (1996).
7) Miura T., Tsujimoto Y., *Nihon Univ. J. Oral Sci.*, **23**, 103—110 (1997).
8) Yamamoto H., Kimura K., Tsujimoto Y., Yamazaki M., *Jpn. J. Conserv. Dent.*, **40**, 1247—1254 (1997).
9) Yamamoto H., *Nihon Univ. J. Oral Sci.*, **24**, 29—37 (1998).
10) Noda Y., Anzai K., Mori A., Kohno M., Shinmei M., Packer L., *Biochem. Mol. Biol. Int.*, **42**, 35—44 (1997).
11) Tsujimoto Y., Saitoh K., Kashima M., Shiozawa A., Kozuka M., Hashizume H., Kimura K., Yamazaki M., Fujii A., *Gen. Pharmacol.*, **31**, 405—408 (1998).
12) Anzai K., Miura Y., Ueda J., Ozawa T., Noda Y., Mori A., Packer L., *Research Commun. Biochem. Cell Mol. Biol.*, **2**, 129—138 (1998).
13) Tanigawa T., *J. Kyoto Pref. Univ. Med.*, **99**, 133—143 (1990).
14) Kohno M., Yamada M., Mitsuta K., Mizuta K., Yoshikawa T., *Bull. Chem. Soc. Jpn.*, **64**, 1447—1453 (1991).
15) Ueda J., Saito N., Shimazu Y., Ozawa T., *Arch. Biochem. Biophys.*, **333**, 377—384 (1996).
16) Buettner G. R., *Free Radical Biol. Med.*, **3**, 259—303 (1987).
17) Livrea M. A., Tesoriere L., *Meth. Enzymol.*, **234**, 401—410 (1994).

Chemical Constituents of *Micromelum minutum*. Isolation and Structural Elucidation of New Coumarins[1)]

Chihiro ITO,*[,a] Takashi OTSUKA,[a] Nijsiri RUANGRUNGSI,[b] and Hiroshi FURUKAWA[a]

Faculty of Pharmacy, Meijo University,[a] Tempaku, Nagoya 468–8503, Japan and Faculty of Pharmaceutical Sciences, Chulalongkorn University,[b] Bangkok 10330, Thailand. Received August 24, 1999; accepted November 9, 1999

The chemical constituents of an acetone extract of the stems of *Micromelum minutum* WIGHT *et* ARN (Rutaceae), collected at Nakorn-Rachasima province in Thailand, were studied. Six new coumarins, named micromarin-A (1), -B (2), -C (3), -F (4), -G (5), and -H (6), were isolated along with six known coumarins, and their structures were elucidated by chemical and spectroscopic methods.

Key words coumarin; micromarin; *Micromelum minutum*; Rutaceae; isovalerate

Micromelum minutum (Rutaceae) is used for the treatment of fever and giddiness and as a poultice for ringworm and ague in Malaysia.[2)] Also it is used in the traditional folk medicine of Fiji.[2)] Some coumarins,[3—9)] a flavanone,[9)] a quinolone alkaloid,[5)] and a carbazole alkaloid[9)] have been reported as constituents of plants of the *genus Micromelum*. In our search for anti-tumor promoters from medicinal plants, an acetone extract of the stems of *M. minutum* WIGHT *et* ARN (Rutaceae), collected in Nakorn-Rachasima province in Thailand, was found to exhibit anti-tumor-promoting activity. This paper describes the isolation and structural elucidation of six new coumarins named micromarin-A (**1**), -B (**2**), -C (**3**), -F (**4**), -G (**5**), and -H (**6**) from the stems of *M. minutum*.

An acetone extract of stems of the plant was chromatographed on silica-gel, eluting with hexane-acetone, followed by repeated preparative TLC to afford six new coumarins along with six known ones.

Structure of Micromarin-A (1) Micromarin-A (**1**), $[\alpha]_D$ +3.44° ($CHCl_3$), was obtained as a colorless powder. The molecular formula $C_{20}H_{22}O_6$ was established by analysis of high resolution (HR)-MS. The UV spectrum [λ_{max} (log ε): 209 (4.82), 256 (4.14), 267 (4.03), 321 (4.60) nm], IR band [ν_{max} 1732, 1606 cm^{-1}], and ^{1}H-NMR spectra [δ 3.96 (3H, s, OCH_3), 7.62 (1H, d, J=9.5 Hz), 6.26 (1H, d, J=9.5 Hz), 7.43 (1H, d, J=8.4 Hz), and 6.87 (1H, d, J=8.4 Hz)], coupled with a nuclear Overhauser effect (NOE) enhancement between the 7-OCH_3 (δ 3.96) and H-6 (δ 6.87), indicated the presence of a 7-methoxy-8-substituted coumarin nucleus in this molecule.[10)] The existence of an isovaleryloxy group in the molecule was confirmed by EI-MS [*m/z* 257 ($M-\cdot OCOCH_2CH(CH_3)_2)^+$] and ^{1}H-NMR spectrum [δ 2.25 (2H, d, J=7.3 Hz), 2.13 (1H, m), 0.95 (6H, d, J=6.7 Hz)]. Furthermore, in the ^{1}H-NMR spectrum, AB-type signals at δ 4.78 and 4.72 (each 1H, d) having a geminal coupling constant (J=13.2 Hz), two methine proton signals at δ 4.03 and 4.05 (each 1H, d, J=2.2 Hz), and two 1H-singlets at δ 5.54 and 5.37 assignable to methylene protons attached to an ester moiety, vicinal methines of an epoxide, and an *exo*-methylene group, respectively, were observed, indicating the presence of the partial structure [–C(H)(O)–C(H)–C(=CH_2)–CH_2–O–]. *trans*-Orientation of the epoxide ring was proposed from the value of the coupling constant (J=2.2 Hz) of two vicinal protons, the same as that in the case of phebalosin.[11,12)]

Finally, connectivities of these structural units were established from the results of analyses of the ^{1}H-detected heteronuclear multiple bond connectivity (HMBC) spectrum shown by arrows in Fig. 1. The significant C–H long-range correlations for structure determination are described below. A carbon signal at δ_C 161.81 (C-7) showed three-bond correlations with proton signals at δ_H 7.43 (H-5), 3.96 (7-OCH_3), and 4.03 (H-1′), indicating the presence of a side-chain at C-8 on the coumarin nucleus. One of the carbonyl carbons at δ_C 172.69 (C-1″) showed three-bond correlations with the methylene protons at δ_H 4.72 and 4.78 (H-5′) on the side-chain which correlated with the methine carbon at δ_C 58.07 (C-2′) on the epoxide. The *exo*-methylene carbon at δ_C 115.84 (C-4′) correlated with the methine proton at δ_H 4.05 (H-2′) and the methylene protons at δ_H 4.72 and 4.78 (H-5′). On the basis of the foregoing spectral data, structure **1** was assigned for micromarin-A.

Structures of Micromarin-B (2) and -C (3) These new coumarins were isolated as pale yellow oils, $[\alpha]_D$ −1.64° ($CHCl_3$) and $[\alpha]_D$ −8.11° ($CHCl_3$), respectively, and had the same molecular formula $C_{20}H_{24}O_7$ based on the HR-FAB-MS spectra of both compounds. The UV and IR spectra of these compounds closely resemble each other. In the ^{1}H-NMR spectra, both compounds showed characteristic signals assignable to a 7-methoxy-8-substituted coumarin nucleus and an isovaleryloxy group (Table 1). Moreover, the presence of an *exo*-methylene group [δ 5.02 (2H, br s); δ 5.34 (1H, br s), 5.33 (1H, br s)], two adjacent methines [δ 5.32, 4.65 (each 1H, d, J=8.4 Hz); δ 5.43 (1H, dd, J=8.1, 11.0 Hz), 4.64 (1H, dd, J=8.1, 6.6 Hz)] attached to a hydroxyl group [δ 3.79, 3.32 (each 1H, br); δ 3.68 (1H, d, J=11.0 Hz), 2.41 (1H, d, J=6.6 Hz)], and an allylic methylene [δ 4.57 (2H, br s); δ 4.77 (1H, d, J=13.2 Hz), 4.80 (1H, d, J=13.2 Hz)] bearing an ester group were suggested in each of the coumarins. These spectral data clearly show that both coumarins have the partial structure [–CH(OH)–CH(OH)–C(=CH_2)–CH_2–O–]. These spectral data and analyses of HMBC spectrum (see Experimental) suggested that these coumarins were diastereoisomeric isomers of each other involving their two oxygenated carbons. In order to confirm the structure of these coumarins, treatment of micromarin-A (**1**) with 1 N H_2SO_4 in dioxane at room temperature gave two glycols **2′** and **3′**. One (**2′**) of them was found to be identical with natural **2** and the other with natural **3** by IR, ^{1}H-NMR, and co-TLC comparisons. Furthermore, treatment of these glycols

* To whom correspondence should be addressed.

© 2000 Pharmaceutical Society of Japan

***Micromelum minutum* Wight et Arn**

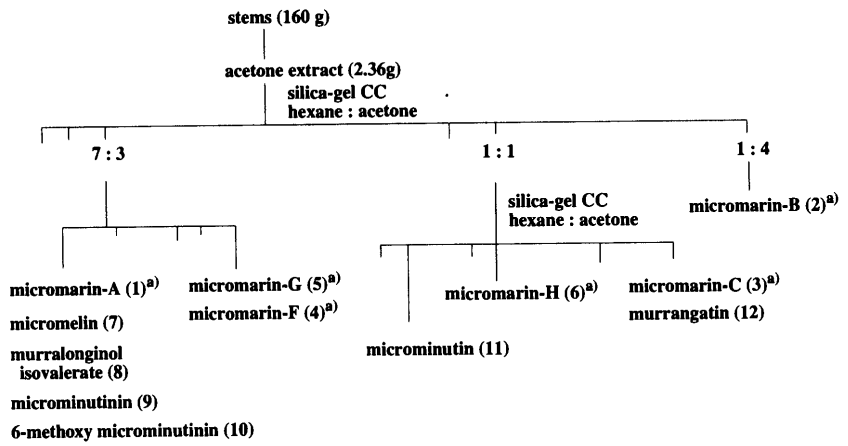

Silica-gel CC and Preparative TLC were carried out with appropriate combinations of hexane, benzene, iso-Pr_2O, Et_2O, EtOAc, acetone, $CHCl_3$, CH_2Cl_2, and MeOH. a) New compounds.

Chart 1

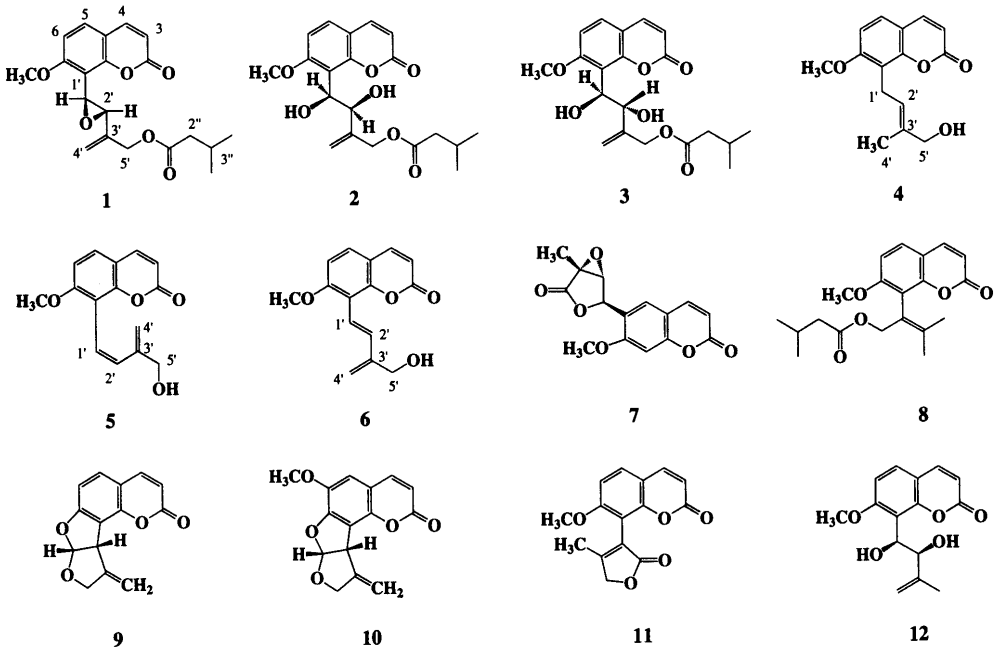

Chart 2

with acetone in the presence of a catalytic amount of toluene-*p*-sulphonic acid (*p*-TsOH) gave the corresponding acetonides, (**2a**) and (**3a**), respectively. For the reciprocal differential NOEs between H-1′ (δ 6.13) and H-2′ (δ 5.13) in micromarin-C acetonide (**3a**), 13 and 11% enhancements were observed. On the other hand, in the case of micromarin-B acetonide (**2a**), no NOE enhancement was observed, neither by irradiation of H-1′ at δ 5.57 nor of H-2′ at δ 5.21. Since this spectral evidence shows clearly that the vicinal protons adjacent to the oxygen atoms of the acetonide ring in the micromarin-C acetonide (**3a**) molecule should be *cis*, the structure of micromarin-C must be in the *erythro* form (**3**). Thus, micromarin-B should be in the *threo* form (**2**). The absolute stereochemistry of these coumarins remains undetermined.

Structure of Micromarin-F (4) Micromarin-F (**4**) was obtained as a colorless oil, $C_{15}H_{16}O_4$. The 7-methoxy-8-substituted coumarin nucleus in this compound was also confirmed by the typical UV bands (see Experimental), and two pairs of AB-type doublets [δ 7.62 (H-4), 6.24 (H-3) (each 1H, d, J=9.5 Hz) and δ 7.31 (H-5), 6.84 (H-6) (each 1H, d, J=8.4 Hz)] and a 3H-singlet at δ 3.92 (7-OCH_3) in the ^{1}H-NMR spectrum.[10] The remaining ^{1}H-NMR signals at δ 3.60 (2H, d, J=7.0 Hz), 5.50 (1H, m), 1.89 (3H, s), and 3.99 (2H, s) and mass fragment peaks at *m/z* 229 $(M-\cdot CH_2\text{–}OH)^+$ and 175 $(M-\cdot CH_2\text{–}CH{=}C(CH_3)\text{–}CH_2\text{–}OH)^+$ suggested the presence of [–CH_2–CH=C(CH_3)–CH_2–OH] in the side-chain. Based on these spectral data, coupled with the appearance of NOE enhancement between the benzyl proton signal (H-1′, δ 3.60) and a vinyl methyl proton signal (H-4′, δ 1.89), and the results of the HMBC experiment (see Experimental), the structure of micromarin-F was concluded to be **4**.

Table 1. ^{1}H-NMR Data for the New Coumarins in $CDCl_3$

	1	2	3	4	5	6
H-3	6.26 (d, 9.5)	6.25 (d, 9.5)	6.27 (d, 9.5)	6.24 (d, 9.5)	6.24 (d, 9.5)	6.28 (d, 9.5)
H-4	7.62 (d, 9.5)	7.62 (d, 9.5)	7.64 (d, 9.5)	7.62 (d, 9.5)	7.65 (d, 9.5)	7.63 (d, 9.5)
H-5	7.43 (d, 8.4)	7.41 (d, 8.8)	7.42 (d, 8.8)	7.31 (d, 8.4)	7.37 (d, 8.4)	7.32 (d, 8.4)
H-6	6.87 (d, 8.4)	6.88 (d, 8.8)	6.90 (d, 8.8)	6.84 (d, 8.4)	6.88 (d, 8.4)	6.87 (d, 8.4)
7-OCH_3	3.96 (3H)	3.95 (3H)	3.97 (3H)	3.92 (3H)	3.95 (3H)	3.97 (3H)
H-1′	4.03 (d, 2.2)	5.32 (br d, 8.4)	5.43 (dd, 11.0, 8.1)	3.60 (2H, d, 7.0)	6.42 (d, 12.2)	7.44 (d, 17.1)
H-2′	4.05 (d, 2.2)	4.65 (d, 8.4)	4.64 (dd, 6.6, 8.1)	5.50 (m)	6.41 (d, 12.2)	7.00 (d, 17.1)
H-4′	5.54 (br)	5.02 (2H, br)	5.34 (br)	1.89 (3H)	4.87 (d, 1.7)	5.41 (d, 1.5)
	5.37 (br)		5.33 (br)		4.72 (d, 1.7)	5.36 (d, 1.5)
H-5′	4.78 (d, 13.2)	4.57 (2H, br)	4.80 (d, 13.2)	3.99 (2H)	4.22 (2H)	4.53 (2H)
	4.72 (d, 13.2)		4.77 (d, 13.2)			
Others	2.25 (2H, d, 7.3, H-2″)	2.19 (2H, d, 7.3, H-2″)	2.28 (2H, d, 7.3, H-2″)			
	2.13 (m, H-3″)	2.07 (m, H-3″)	2.14 (m, H-3″)			
	0.95	0.93	0.98			
	(6H, d, 6.7, 3″-CH_3)	(6H, d, 6.7, 3″-CH_3)	(6H, d, 6.7, 3″-CH_3)			
		3.79 (br, 11-OH)	3.68 (d, 11.0, 11-OH)			
		3.32 (br, 12-OH)	2.41 (d, 6.6, 12-OH)			

Values in (δ) ppm. The coupling constants (J) in parentheses are in Hz. All signals correspond to 1H, and were observed as a singlet, unless otherwise stated.

Table 2. ^{13}C-NMR Data for the New Coumarins in $CDCl_3$

	1	2	3	4
C-2	160.14 (s)	159.90 (s)	160.01 (s)	161.28 (s)
C-3	113.50 (d)	113.45 (d)	113.54 (d)	113.03 (d)
C-4	143.32 (d)	143.61 (d)	143.65 (d)	145.96 (d)
C-4a	112.85 (s)	113.13 (s)	113.25 (s)	112.98 (s)
C-5	129.10 (d)	128.78 (d)	128.60 (d)	127.23 (d)
C-6	107.55 (d)	107.78 (d)	107.87 (d)	107.31 (d)
C-7	161.81 (s)	160.09 (s)	160.37 (s)	160.22 (s)
7-OCH_3	56.31 (q)	56.28 (q)	56.35 (q)	56.05 (q)
C-8	112.02 (s)	115.41 (s)	116.11 (s)	117.12 (s)
C-8a	153.97 (s)	152.88 (s)	153.25 (s)	152.87 (s)
C-1′	53.01 (d)	70.24 (d)	69.15 (d)	21.46 (d)
C-2′	58.07 (d)	75.90 (d)	75.89 (d)	122.50 (d)
C-3′	140.27 (s)	142.60 (s)	144.08 (s)	135.75 (s)
C-4′	115.84 (t)	115.17 (t)	116.59 (t)	13.83 (q)
C-5′	63.19 (t)	63.39 (t)	64.34 (t)	68.75 (t)
C-1″	172.69 (s)	172.68 (s)	172.97 (s)	
C-2″	43.34 (t)	43.26 (t)	43.33 (t)	
C-3″	25.65 (d)	25.64 (d)	25.67 (d)	
3″-CH_3	22.38 (q×2)	22.36 (q×2)	22.42 (q ×2)	

Values in (δ) ppm.

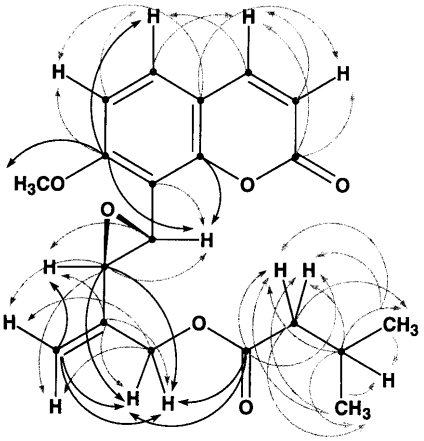

Fig. 1. C–H Long-Range Correlations in the HMBC Spectrum of Micromarin-A (**1**) in $CDCl_3$

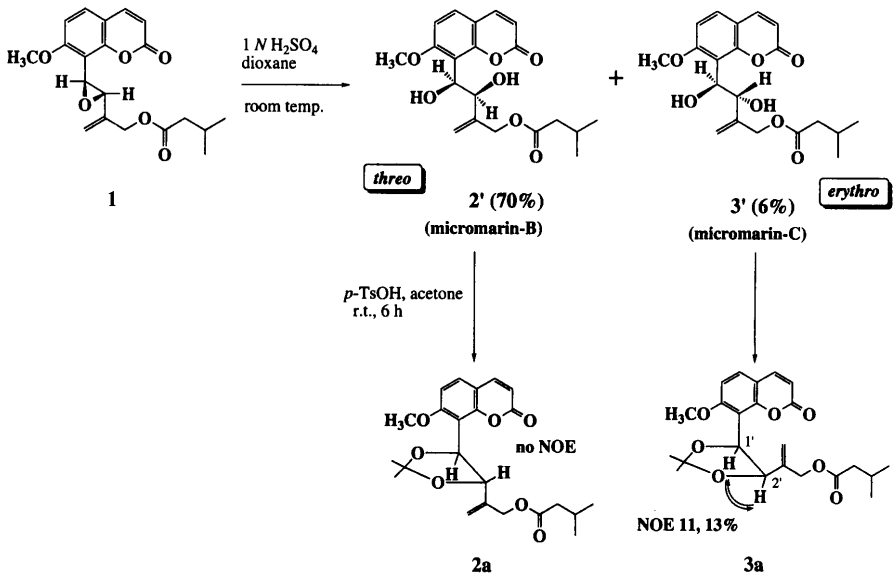

Chart 3

Structure of Micromarin-G (5) Micromarin-G (**5**) was obtained as a colorless oil, $C_{15}H_{14}O_4$. The presence of a 7-methoxy-8-substituted coumarin nucleus was also suggested by the UV, IR, and ^{1}H-NMR spectra (see Table 1 and Experimental). In the ^{1}H-NMR spectrum, there were signals assignable to a *Z*-oriented disubstituted double bond [δ 6.42 (H-1′), 6.41 (H-2′) (each 1H, d, J=12.2 Hz)], an *exo*-methylene group [δ 4.87, 4.72 (each 1H, d, J=1.7 Hz, H-4′)], and a methylene [δ 4.22 (2H, s, H-5′)] adjacent to a hydroxyl group. Based on the aforementioned results, together with mass fragment ions at *m/z* 227 $(M-\cdot CH_2\text{–}OH)^+$ and 175 $(M-\cdot CH{=}CH(=CH_2)\text{–}CH_2\text{–}OH)^+$ in the EI-MS, the structure of micromarin-G was concluded to be **5**.

Structure of Micromarin-H (6) Micromarin-H (**6**) was obtained as a pale yellow oil. The molecular formula $C_{15}H_{14}O_4$ was found to be the same as that of **5** by HR-MS. The presence of the side-chain [(*E*)–CH=CH–C(=CH_2)–CH_2OH] at C-8 was suggested by the following spectral data: observations of 1) *exo*-methylene proton signals [δ 5.41, 5.36 (each 1H, d, J=1.5 Hz, H-4′)] and a 2H-singlet [δ 4.53 (H-5′)] adjacent to a hydroxyl group, 2) AB-type signals at δ 7.44 and 7.00 (each 1H, d) having a large coupling constant (J=17.1 Hz) in the ^{1}H-NMR spectrum, 3) mass fragment ions at *m/z* 227 $(M-\cdot CH_2\text{–}OH)^+$ and 175 $(M-\cdot CH{=}CH(=CH_2)\text{–}CH_2\text{–}OH)^+$ in the EI-MS. Based on these results, we assigned the structure **6** to micromarin-H.

Known coumarins isolated from the same plant material were characterised as micromelin (**7**),[5,7,8] murralonginol isovalerate (**8**),[11,12] microminutinin (**9**),[3] 6-methoxymicrominutinin (**10**),[3] microminutin (**11**),[5] and murrangatin (**12**)[11,12] by comparisons of ^{1}H-NMR and IR spectra with spectroscopic data reported in the literature.[3,5,7,8,11,12]

Experimental

^{1}H- and ^{13}C-NMR, H–H correlation spectroscopy (COSY), NOE, and HMBC (J=8 Hz) spectra were recorded on an A-400 or A-600 (JEOL) spectrometer in $CDCl_3$, unless otherwise stated. Chemical shifts are shown in δ values (ppm) with tetramethylsilane (TMS) as an internal reference. MS were recorded on an M-80 (Hitachi), HX-110 (JEOL), or JMS-700 (JEOL) spectrometer having a direct inlet system. UV spectra were recorded on a V-550 UV/VIS spectrophotometer (JASCO) in MeOH, IR spectra on a FT/IR-230 (JASCO) in $CHCl_3$, and optical rotations on a DIP-370 (JASCO) in $CHCl_3$ at 25 °C. Preparative TLC was carried out on Kieselgel 60 F_{254} (Merck).

Plant Material Stems of *Micromelum minutum* WIGHT *et* ARN (Rutaceae) were collected in Nakorn-Rachasima province, Thailand, in April, 1996. Voucher specimens have been deposited in the herbarium of the Faculty of Pharmaceutical Sciences, Chulalongkorn University. The plant materials were identified by Dr. Nijsiri Ruangrungsi and compared with herbarium specimens at the Royal Forest Department, Ministry of Agriculture and Cooperative, Bangkok.

Extraction and Isolation Dried stems of the plant (160 g) were extracted with acetone at room temperature. The acetone extract (2.36 g) was subjected to silica-gel column chromatography eluting with hexane and hexane–acetone (7 : 3, 3 : 2, 1 : 1, 1 : 4), successively, to give 6 fractions. Each fraction was further subjected to silica-gel column chromatography and preparative TLC with appropriate combinations of hexane, CH_2Cl_2, iso-Pr_2O, benzene, $CHCl_3$, EtOAc, acetone, and MeOH as developing solvents to give six new coumarins along with six known coumarins, as stated below. The hexane–acetone (7 : 3) eluate gave micromarin-A (**1**) (57.9 mg), micromelin (**7**) (28.8 mg), murralonginol isovalerate (**8**) (0.4 mg), microminutinin (**9**) (471.9 mg), 6-methoxymicrominutinin (**10**) (9.7 mg), micromarin-F (**4**) (10.7 mg), and micromarin-G (**5**) (1.1 mg). The hexane–acetone (1 : 1) eluate gave microminutin (**11**) (105.1 mg), micromarin-H (**6**) (1.0 mg), micromarin-C (**3**) (1.2 mg), and murrangatin (**12**) (0.5 mg). The hexane–acetone (1 : 4) eluate gave micromarin-B (**2**) (7.5 mg).

Micromarin-A (**1**); Colorless powder. $[\alpha]_D$ +3.44° (c=0.16, $CHCl_3$). UV λ_{max} (log ε) nm: 209 (4.82), 256 (4.14), 267 (4.03), 321 (4.60). IR ν_{max} cm^{-1}: 1732, 1606. EI-MS *m/z* (%): 358 (M^+, 5), 274 (41), 257 (40), 256 (78), 245 (23), 229 (33), 213 (38), 211 (29), 205 (31), 203 (33), 190 (100), 185 (57), 175 (15). HR-MS Calcd for $C_{20}H_{22}O_6$: 358.1414. Found: 358.1385. Differential NOE: irradiation at δ 3.96 (7-OCH_3) gave 15% enhancement at δ 6.87 (H-6).

Micromarin-B (**2**); Pale yellow oil. $[\alpha]_D$ −1.64° (c=0.22, $CHCl_3$). UV λ_{max} (log ε) nm: 207 (4.74), 247 (3.95), 258 (3.93), 322 (4.42). IR ν_{max} cm^{-1}: 3545 (br), 1732, 1606. EI-MS *m/z* (%): 257 (52), 206 (100), 205 (99), 189 (11), 175 (27). FAB-MS *m/z*: 377 $(M+H)^+$. HR-FAB-MS Calcd for $C_{20}H_{25}O_7$: 377.1600. Found: 377.1591. Differential NOE: irradiation at δ 3.95 (7-OCH_3) gave 26% enhancement at δ 6.88 (H-6). HMBC C–H correlations: C-2→H-3, H-4; C-4→H-5; C-4a→H-3, H-6; C-5→H-4; C-7→H-5, H-6, 7-OCH_3; C-8→H-6, H-2′; C-8a→H-4, H-5; C-1′→H-2′; C-2′→H-4′, H-5′; C-3′→H-2′, H-4′, H-5′; C-4′→H-5′; C-5′→H-2′, H-4′; C-1″→H-5′, H-2″; C-2″→H-3″, 3″-CH_3; C-3″→H-2″, 3″-CH_3; 3″-CH_3→H-2″, H-3″.

Micromarin-C (**3**); Pale yellow oil. $[\alpha]_D$: −8.11° (c=0.09, $CHCl_3$). UV λ_{max} nm: 205, 248, 257, 321. IR ν_{max} cm^{-1}: 3568 (br), 1732, 1608. EI-MS *m/z* (%): 257 (3), 205 (100), 190 (7), 175 (13). FAB-MS *m/z*: 377 $(M+H)^+$. HR-FAB-MS Calcd for $C_{20}H_{25}O_7$: 377.1600. Found: 377.1580. Differential NOE: irradiation at δ 3.97 (7-OCH_3) gave 19% enhancement at δ 6.90 (H-6). HMBC C-H correlations: C-2→H-3, H-4; C-4→H-5; C-4a→H-3, H-6; C-5→H-4; C-7→H-5, H-6, H-1′, 7-OCH_3; C-8→H-6, H-1′, H-2′; C-8a→H-4, H-5, H-1′; C-1′→H-2′, 1′-OH, 2′-OH; C-2′→H-1′, 2′-OH, H-4′, H-5′; C-3′→H-2′, 2′-OH, H-4′, H-5′; C-4′→H-5′; C-5′→H-2′, H-4′; C-1″→H-5′, H-2″; C-2″→H-3″, 3″-CH_3; C-3″→H-2″, 3″-CH_3; 3″-CH_3→H-2″, H-3″.

Treatment of Micromarin-A (1) with 1 N H_2SO_4 A solution of micromarin-A (**1**) (9.8 mg) in dioxane (2.5 ml) and 1 N H_2SO_4 (2.5 ml) was stirred for 1.5 h at room temperature. The reaction mixture was treated in the usual manner and the residue was subjected to preparative TLC (MeOH–$CHCl_3$, 1 : 49) to yield glycols **2′** (7.2 mg) and **3′** (0.6 mg). Glycols **2′** and **3′** were found to be identical with natural **2** and **3**, respectively, by IR, ^{1}H-NMR, and co-TLC comparisons.

Micromarin-B Acetonide (2a) A solution of micromarin-B (**2**) (2.1 mg) in acetone (1.0 ml) and a catalytic amount of *p*-TsOH were stirred for 20 min at room temperature. The mixture was then neutralized with Et_3N and the solvent was evaporated under reduced pressure. The residue was subjected to silica-gel preparative TLC (MeOH–$CHCl_3$, 1 : 49) to yield compound (**2a**) (2.0 mg) as a colorless oil. UV λ_{max} nm: 206, 219 (sh), 249, 258, 321. IR ν_{max} cm^{-1}: 1732, 1608. EI-MS *m/z* (%): 416 (M^+, 1), 401 (3), 257 (24), 246 (47), 212 (17), 205 (22), 189 (27), 160 (21), 127 (26), 110 (100). ^{1}H-NMR δ: 7.61 (1H, d, J=9.5 Hz, H-4), 7.42 (1H, d, J=8.4 Hz, H-5), 6.88 (1H, d, J=8.4 Hz, H-6), 6.27 (1H, d, J=9.5 Hz, H-3), 5.57 (1H, d, J=8.8 Hz, H-1′), 5.31 (1H, s, H-4′), 5.21 (1H, d, J=8.8 Hz, H-2′), 5.19 (1H, s, H-4′), 4.56 (1H, d, J=13.9 Hz, H-5′), 4.54 (1H, d, J=13.9 Hz, H-5′), 3.93 (3H, s, 7-OCH_3), 2.06 (2H, d, J=7.3 Hz, H-2″), 2.00 (1H, m, H-3″), 1.71 (3H, s, CH_3), 1.54 (3H, s, CH_3). 0.88 (6H, d, J=6.6 Hz, 3″-CH_3).

Micromarin-C Acetonide (3a) Micromarin-C (**3**) (0.6 mg) was treated with acetone and *p*-TsOH under the same conditions as for **2** to yield compound (**3a**) (0.5 mg) as a colorless oil. UV λ_{max} (log ε) nm: 204, 224 (sh), 249, 259, 321. IR ν_{max} cm^{-1}: 1732, 1606. EI-MS *m/z* (%): 416 (M^+, 1), 401 (3), 258 (3), 246 (53), 212 (19), 205 (28), 189, (34), 160 (26), 127 (36), 110 (100). ^{1}H-NMR δ: 7.56 (1H, d, J=9.5 Hz, H-4), 7.35 (1H, d, J=8.4 Hz, H-5), 6.80 (1H, d, J=8.4 Hz, H-6), 6.22 (1H, d, J=9.5 Hz, H-3), 6.13 (1H, d, J=8.8 Hz, H-1′), 5.41 (1H, br s, H-4′), 5.13 (1H, d, J=8.4 Hz, H-2′), 4.95 (1H, s, H-4′), 4.19 (1H, d, J=13.2 Hz, H-5′), 4.11 (1H, d, J=13.2 Hz, H-5′), 3.88 (3H, s, 7-OCH_3), 2.11 (2H, d, J=7.3 Hz, H-2″), 2.01 (1H, m, H-3″), 1.81 (3H, s, CH_3), 1.50 (3H, s, CH_3), 0.89 (6H, d, J=6.6 Hz, 3″-CH_3). Differential NOE: irradiation at δ 6.13 (H-1′) gave 13% enhancement at δ 5.13 (H-2′); irradiation at δ 5.13 (H-2′) gave 11% enhancement at δ 6.13 (H-1′).

Micromarin-F (**4**); Colorless oil. UV λ_{max} (log ε) nm: 206 (4.61), 220 (sh) (4.09), 249 (3.68), 257 (3.72), 322 (4.18). IR ν_{max} cm^{-1}: 3535 (br), 1720, 1608. EI-MS *m/z* (%): 260 (M^+, 27), 242 (17), 229 (12), 211 (24), 190 (58), 175 (19), 167 (69), 151 (100). HR-MS Calcd for $C_{15}H_{16}O_4$: 260.1047. Found: 260.1030. Differential NOE: irradiation at δ 3.92 (7-OCH_3) gave 15% enhancement at δ 6.84 (H-6); irradiation at δ 3.99 (H-5′) gave 9% enhancement at δ 5.50 (H-2′) and 4% enhancement at δ 1.89 (H-4′); irradiation at δ 3.60 (H-1′) gave 7% enhancement at δ 5.50 (H-2′) and 8% enhancement at δ 1.89 (H-4′); irradiation at δ 1.89 (H-4′) gave 4% enhancement at δ 3.60 (H-1′) and 4% enhancement at δ 3.99 (H-5′). HMBC C–H correlations: C-2→H-3, H-4; C-3→H-4; C-4→H-5; C-4a→H-3, H-6; C-5→H-4; C-7→H-5, H-1′, 7-OCH_3; C-8→H-6, H-1′, H-2′; C-8a→H-4, H-5, H-1′; C-1′→H-2′; C-2′→H-1′, H-4′, H-5′; C-3′→H-1′, H-4′, H-5′; C-4′→H-2′, H-5′; C-5′→H-2′, H-4′.

Micromarin-G (**5**); Colorless oil. UV λ_{max} nm: 205, 264, 276, 315. IR ν_{max} cm^{-1}: 3508 (br), 1724, 1601. EI-MS *m/z* (%): 258 (M^+, 100), 227 (23), 226 (40), 213 (25), 197 (46), 185 (25), 175 (16). HR-MS Calcd for $C_{15}H_{14}O_4$: 258.0891. Found: 258.0902. Differential NOE: irradiation at δ 3.95 (7-OCH_3) gave 10% enhancement at δ 6.88 (H-6).

Micromarin-H (**6**); Pale yellow oil. UV λ_{max} nm: 205, 259, 274, 301, 315. IR ν_{max} cm^{-1}: 3534 (br), 1722, 1599. EI-MS *m/z* (%): 258 (M^+, 100), 227 (19), 222 (30), 213 (24), 197 (34), 185 (24), 175 (17). HR-MS Calcd for $C_{15}H_{14}O_4$: 258.0891. Found: 258.0909. Differential NOE: irradiation at δ 3.97 (7-OCH_3) gave 17% enhancement at δ 6.87 (H-6).

Acknowledgements This work was partly supported by Grants-in-Aid for Scientific Research (No. 09672173, H.F.) and the High-Tech Research Center Project from the Japan Society for the Promotion of Science and the Ministry of Education, Science, Sports and Culture of Japan, respectively.

References and Notes

1) Part of this paper was presented at the 117th Annual Meeting of the Pharmaceutical Society of Japan, Tokyo, March 1997 and the 21st IUPAC International Symposium on the Chemistry of Natural Products, Beijing, China, October 1998.
2) Croft K. D., Toia R. F., *Planta Med.*, **55**, 401 (1989) and references cited therein.
3) Rahmani M., Taufiq-Yap Y. H., Ismail H. B. M., Sukari A., Waterman P. G., *Phytochemistry*, **37**, 561—564 (1994).
4) Banerji J., Das A. K., Das B., *Heterocycles*, **26**, 2871—2875 (1987).
5) Tantivatana P., Ruangrungsi N., Vaisiriroj V., Lankin D. C., Bhacca N. S., Borris R. P., Cordell G. A., Johnson L. F., *J. Org. Chem.*, **48**, 268—270 (1983).
6) Das S., Baruah R. H., Sharma R. P., Barua J. N., Kulanthaivel P., Herz W., *Phytochemistry*, **23**, 2317—2321 (1984).
7) Lamberton J. A., Price J. R., Redcliffe A. H., *Aust J. Chem.*, **20**, 973—979 (1967).
8) Cassady J. M., Ojima N., Chang C.-J., McLaughlin J. L., *J. Nat. Prod.*, **42**, 274—277 (1979).
9) Bowen I. H., Christopher Perera K. P. W., *Phytochemistry*, **21**, 433—437 (1982).
10) Murray R. D. H., Mendez J., Brown S. A., "The Natural Coumarins. Occurrence, Chemistry and Biochemistry," John Wiley & Sons Ltd., New York, 1982, pp. 27—51.
11) Ito C., Furukawa H., *Chem. Pharm. Bull.*, **35**, 4277—4285 (1987).
12) Ito C., Furukawa H., Ishii H., Ishikawa T., Haginiwa J., *J. Chem. Soc., Perkin Trans 1*, **1990**, 2047—2055.

Chemical Constituents of *Avicennia alba*. Isolation and Structural Elucidation of New Naphthoquinones and Their Analogues[1)]

Chihiro ITO,*[,a] Shinya KATSUNO,[a] Yuichi KONDO,[a] Hugh T.-W. TAN,[b] and Hiroshi FURUKAWA[a]

Faculty of Pharmacy, Meijo University,[a] Tempaku, Nagoya 468–8503, Japan and Department of Botany,[b] National University of Singapore, 10 Kent Ridge Crescent, Singapore 0511.

Received August 30, 1999; accepted November 9, 1999

Three new naphthoquinones and their analogues, named avicequinone-A (1), -B (2), -C (3), and avicenol-A (4), -B (5), -C (6), respectively, were isolated from the stem bark of *Avicennia alba* (Avicenniaceae) collected in Singapore, and their structures were elucidated by means of spectral methods.

Gillan and co-workers have proposed that the structures of the new phytoalexins isolated from *Avicennia marina* are 1,2-naphthoquinones 8 and 9. Our synthetic and spectrometric studies showed that these structures should be revised respectively to 1,4-naphthoquinones 2 and 3, named avicequinone-B and -C by us.

Key words *Avicennia alba*; naphthoquinone; phytoalexin; avicequinone; avicenol; Avicenniaceae

Avicennia alba BLUME, belonging to the family Avicenniaceae,[2)] is known to be a type of mangrove tree and grows in the tidal forests at the mouth of rivers. This species is found far away from salt water, unlike other species, *e.g. A. marina* which grows on the shore of very saline seas.[3)] Some species of this genus are found in the tropics and their chemical constituents have been studied.[4—10)]

This paper is the first study of constituents of *A. alba* and describes the isolation and structural elucidation of three new naphthoquinones and their analogues along with a known naphthoquinone from the stem bark of this plant.

Results and Discussion

The acetone extract of the stem bark of the plant was fractionated by a combination of silica-gel column chromatography and preparative TLC to give new 1,4-naphthoquinones and their analogues along with a known naphthoquinone.

Structures of Avicequinones The presence of a 1,4-naphthoquinone nucleus with no substituent on the aromatic ring in avicequinone-A (**1**), -B (**2**), and -C (**3**) was suggested by the following UV, IR, ^{1}H- (Table 1), and ^{13}C-NMR (Table 2) spectral data: 1) One or two strong and sharp UV bands at 244—251 nm, a medium intensity band at 286—292 nm, a broad band at 334—336 nm, and a shoulder band at 374—380 nm; 2) Strong IR bands at 1672—1685 cm^{-1} and 1587—1595 cm^{-1}; 3) Two typical carbonyl carbon signals at δ_C 173.27—178.14 and 180.54—182.65 ppm in the ^{13}C-NMR spectrum; 4) Four contiguous aromatic proton signals at δ_H 8.08—8.24 (2H) and 7.71—7.77 (2H) assignable to two deshielded protons (H-5, H-8) *peri*-located to the carbonyl groups and other two aromatic protons (H-6, H-7), respectively; 5) Three-bond C–H long-range correlations in the ^{1}H-detected heteronuclear multiple bond connectivity (HMBC) spectrum between carbonyl carbons (C-4, C-1) and deshielded protons (H-5, H-8). The structure of the remaining parts of these compounds will be dicussed below.

Structure of Avicequinone-A (1) Avicequinone-A (**1**) was obtained as a yellow oil, $[\alpha]_D$ +35° ($CHCl_3$). The high-

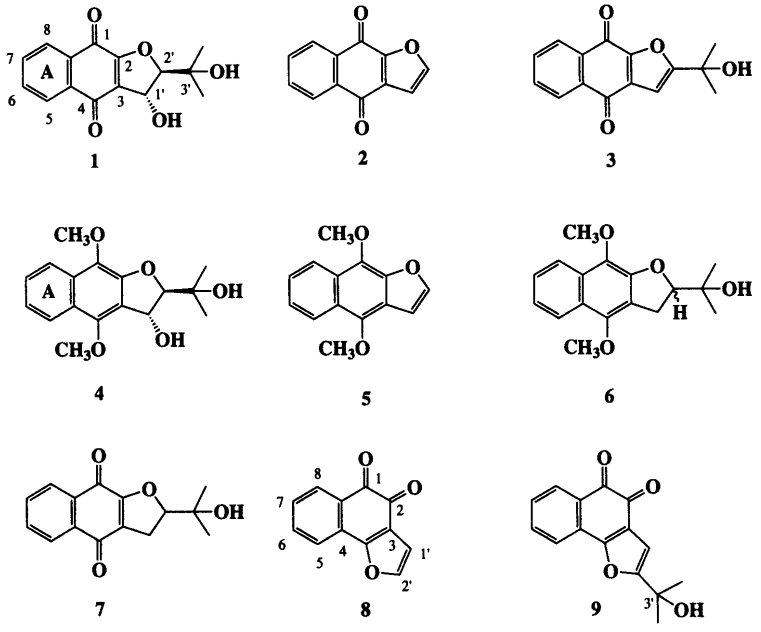

Chart 1

* To whom correspondence should be addressed.

© 2000 Pharmaceutical Society of Japan

Table 1. ^{1}H-NMR Data for the New Naphthoquinones and Their Analogues in $CDCl_3$

	1	2	3	4	5	6
5	8.08 (dd, 7.7, 1.5)	8.21 (m)	8.14 (m)	8.04 (br d, 8.4)	8.24 (d, 8.4)	8.02 (br d, 8.4)
6	7.76 (dt, 1.5, 7.7)	7.77 (m)	7.73 (m)	7.46 (br t, 8.4)	7.47 (t, 8.4)	7.41 (br t, 8.4)
7	7.71 (dt, 1.5, 7.7)	7.77 (m)	7.73 (m)	7.33 (br t, 8.4)	7.45 (t, 8.4)	7.31 (br t, 8.4)
8	8.10 (dd, 7.7, 1.5)	8.24 (m)	8.18 (m)	8.04 (br d, 8.4)	8.27 (d, 8.4)	8.00 (br d, 8.4)
1′	5.62 (d, 5.1)	7.01 (d, 1.5)	6.80 (s)	4.44 (d, 4.0)	7.04 (d, 2.2)	3.38 (2H, d, 8.4)
2′	4.54 (d, 5.1)	7.78 (d, 1.5)		5.69 (d, 4.0)	7.64 (d, 2.2)	4.71 (t, 8.4)
3′-CH_3	1.35 (3H, s)		1.67 (6H, s)	1.33 (3H, s)	-	1.26 (3H, s)
	1.44 (3H, s)			1.35 (3H, s)		1.39 (3H, s)
Others	3.04 (br s, OH)			4.03 (3H, s, 1′-OCH_3)	4.27 (3H, s, 1′-OCH_3)	3.96 (3H, s, 1′-OCH_3)
	1.85 (br s, OH)			4.12 (3H, s, 4′-OCH_3)	4.17 (3H, s, 4′-OCH_3)	4.01 (3H, s, 4′-OCH_3)
						1.90 (br s, OH)

Values in (δ) ppm. The coupling constants (J) in parentheses are in Hz. All signals correspond to 1H, and were observed as a singlet, unless otherwise stated.

Table 2. ^{13}C-NMR Data for the New Naphthoquinones and Their Analogues in $CDCl_3$

	1	2	3	4	5	6
C-1	178.14 (s)	173.59 (s)	173.27 (s)	148.70 (s)	134.43 (s)	147.54 (s)
C-2	160.61 (s)	152.69 (s)	151.60 (s)	147.18 (s)	143.72 (s)	147.24 (s)
C-3	124.84 (s)	130.46 (s)	131.24 (s)	119.93 (s)	119.09 (s)	118.53 (s)
C-4	182.65 (s)	180.54 (s)	180.71 (s)	132.34 (s)	143.27 (s)	132.19 (s)
C-4a	132.86 (s)	133.20 (s)	132.89 (s)	130.43 (s)	125.12 (s)	129.27 (s)
C-5	126.13 (d)	127.05 (d)	126.83 (d)	121.20 (d)	121.87 (d)	120.99 (d)
C-6	134.56 (d)	133.94 (d)	133.86 (d)	126.71 (d)	123.87 (d)	125.82 (d)
C-7	133.35 (d)	133.86 (d)	133.68 (d)	123.53 (d)	124.78 (d)	123.32 (d)
C-8	126.65 (d)	126.93 (d)	126.75 (d)	122.27 (d)	121.74 (d)	121.71 (d)
C-8a	131.75 (s)	132.43 (s)	132.38 (s)	123.96 (s)	123.62 (s)	124.08 (s)
C-1′	71.94 (d)	108.64 (d)	102.55 (d)	71.87 (d)	104.34 (d)	28.81 (t)
C-2′	98.48 (d)	148.59 (d)	168.14 (s)	97.24 (d)	145.60 (d)	90.25 (d)
C-3′	71.07 (s)		69.27 (s)	71.39 (s)		71.73 (s)
3′-CH_3	25.81 (q)		28.67 (q×2)	24.93 (q)		24.32 (q)
	24.46 (q)			25.70 (q)		26.06 (q)
Other				60.68 (1′-OCH_3)	61.24 (1′-OCH_3)	60.32 (1′-OCH_3)
				61.15 (4′-OCH_3)	61.47 (4′-OCH_3)	60.55 (4′-OCH_3)

Values in (δ) ppm.

resolution (HR)-MS spectrum of avicequinone-A showed a molecular ion at *m/z* 274.0847, corresponding to the formula $C_{15}H_{14}O_5$. The presence of a 1-hydroxy-1-methylethyl side-chain in the molecule was prompted by the observation of two 3H singlets at δ_H 1.35 and 1.44 due to methyls attached to a quarternary carbon linked to an oxygen atom in the ^{1}H-NMR spectrum, the ^{13}C-NMR signal at δ_C 71.07 (C-3′), and a significant mass fragment ion at *m/z* 216 $(M-59+\cdot H)^+$ with the loss of C_3H_7O followed by $\cdot$H transfer in the EI-MS. The remaining two protons appeared as AB-type doublets (J=5.1 Hz) at δ_H 4.54 (H-2′) and 5.62 (H-1′) and were assigned to vicinal methine protons, both attached to oxygen-bearing carbons, on the basis of their chemical shifts. Furthermore, in the HMBC spectrum of **1**, as shown by arrows in Fig. 1, these two methine protons [δ_H 5.62 (H-1′), 4.54 (H-2′)] showed three-bond correlations with the sp^2 carbon (δ_C 160.61, C-2) linked both with a carbonyl group and an oxygen atom, suggesting the presence of a vicinal methine unit fused to the naphthoquinone nucleus as a dihydrofuran ring. The location of the side-chain at C-2′ was revealed by the three-bond correlations between two methyl protons (δ_H 1.35, 1.44) and the carbon at δ_C 98.48 (C-2′) with a proton at δ_H 4.54, indicating a hydroxyl group attached to the remaining site (C-1′). *trans*-Orientation of these moieties on the dihydrofuran ring was proposed from the coupling constants (J=5.1 Hz) of the AB-type doublets[11] and no nuclear Overhauser effect (NOE) enhancement between these two methine proton signals. Based on these results, the structure of avicequinone-A was concluded to be **1**, corresponding to the hydroxy derivative of stenocarpoquinone-B (**7**) isolated from *Stenocarpus salignus*,[12] leaving the absolute stereochemistry undetermined.

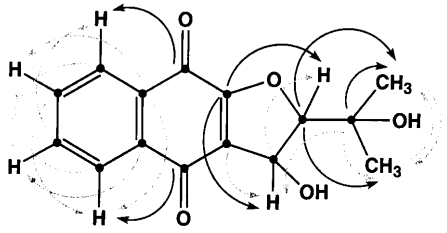

Fig. 1. C–H Long-Range Correlations in the HMBC Spectrum of Avicequinone-A (**1**) in $CDCl_3$

Structure of Avicequinone-B (2) The molecular formula $C_{12}H_6O_3$ was established by HR-MS. In the ^{1}H- and ^{13}C-NMR spectra, only AB-type olefinic protons at δ_H 7.78, 7.01 (each 1H, d, J=1.5 Hz) and sp^2 carbon signals at δ_C 148.59, 108.64 were observed, in addition to signals due to the 1,4-naphthoquinone skeleton. Based on the J-value (1.5 Hz) of the AB-type signals and the appearance of three-bond C–H long-range correlations between C-2 and C-3 carbons

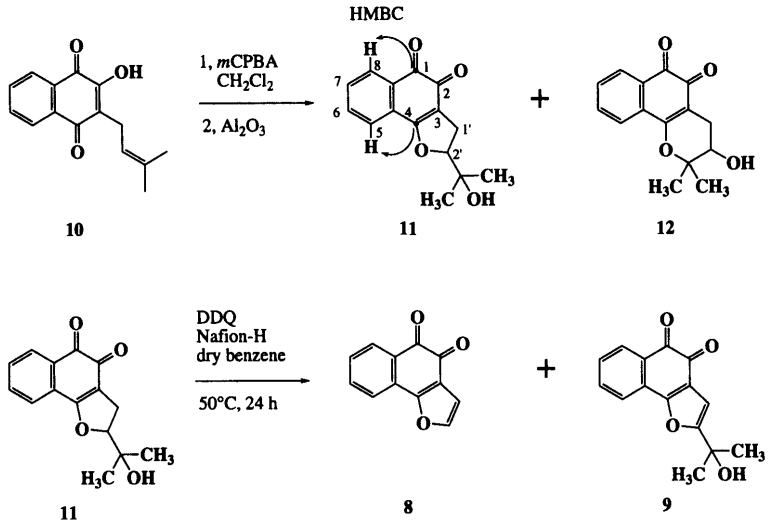

Chart 2

Table 3. ^{1}H-NMR Data for Phytoalexins and the Corresponding Naphthoquinones in MeOD-d_4

	Phytoalexin (**8′**)	**8**	**2**	Phytoalexin (**9′**)	**9**	**3**
5	8.22 (m)	8.05 (br d, 7.7)	8.18 (m)	8.21 (m)	8.00 (br d, 7.7)	8.11 (m)
6	7.85 (m)	7.53 (br t, 7.7)	7.82 (m)	7.86 (m)	7.49 (br t, 7.7)	7.78 (m)
7	7.85 (m)	7.73 (br t, 7.7)	7.82 (m)	7.86 (m)	7.70 (br t, 7.7)	7.78 (m)
8	8.22 (m)	7.79 (br d, 7.7)	8.18 (m)	8.21 (m)	7.76 (br d, 7.7)	8.11 (m)
1′	7.08 (d, 1.6)	6.90 (d, 1.8)	7.05 (d, 1.5)	6.90 (s)	6.65 (s)	6.82 (s)
2′	8.06 (d, 1.6)	7.75 (d, 1.8)	8.03 (d, 1.5)			
3′-CH_3				1.66 (6H, s)	1.63 (6H, s)	1.64 (6H, s)

Values in (δ) ppm. The coupling constants (J) in parentheses are in Hz. All signals correspond to 1H, and were observed as a singlet, unless otherwise stated.

(δ_C 152.69 and 130.46, respectively) on the 1,4-naphthoquinone nucleus and these olefinic protons (δ_H 7.78 and 7.01) in the HMBC spectrum, the structure of avicequinone-B was proposed as **2**. Although synthesis of this compound has already been reported by Tanaka and co-workers,[13] this is its first isolation from a natural source.

Structure of Avicequinone-C (3) The molecular formula, $C_{15}H_{12}O_4$, with a difference of C_3H_6O compared with that of **2**, was determined by HR-MS. The ^{1}H-NMR spectrum of this compound was similar to that of **2**, except for the appearance of a 6H singlet at δ_H 1.67, due to two methyls, and a 1H sharp singlet at δ_H 6.80, instead of the AB-type olefinic proton signals in the spectrum of **2**. The presence of a 1-hydroxy-1-methylethyl side-chain in the molecule was prompted by the observation of a quarternary cabon signal at δ_C 69.27 (C-3′) assignable to an oxygen-bearing carbon in the ^{13}C-NMR spectrum, a 6H singlet (δ_H 1.67) in the ^{1}H-NMR spectrum, and a base fragment ion at *m/z* 241 produced by loss of a methyl radical from the molecular ion. The location of the side-chain at C-2′ was suggested by the chemical shifts of a sharp singlet at δ_H 6.80 (H-1′, not H-2′) and the carbon (δ_C 102.55, C-1′) with this proton. On the basis of these spectral data, we proposed structure **3** for avicequinone-C.

Gillan and co-workers reported the isolation of phytoalexins for fungus belonging to the genus *Phytophthora*[14] from *Avicennia marina*, and proposed their structures to be 1,2-naphthoquinones (naphtho[1,2-*b*]furan-4,5-diones) (**8**) and (**9**). Strangely, we found that the ^{1}H-NMR data of the phytoalexins assigned to 1,2-naphthoquinones reported in the literature[14] showed close similarity to that of **2** and **3**, determined as 1,4-naphthoquinones by us, as shown in Table 3. To clarify this discrepancy, synthesis of the 1,2-naphthoquinones (**8**) and (**9**) proposed by Gillan and co-workers was carried out as outlined in Chart 2.

Lapachol (**10**), which is commercially available, was treated with *m*-chloroperbenzoic acid (*m*CPBA) in CH_2Cl_2 followed by treatment with Al_2O_3 to give two cyclization products, dihydrofuran **11** and dihydropyran **12** in a ratio of 1 : 1.[12,15]

The *ortho*-quinoid structure of **11** was confirmed by the HMBC spectrum. Of the two carbonyl carbons of **11**, C-1 at δ_C 180.93 showed a three-bond long-range correlation with a lower field aromatic proton at δ_H 8.04 (H-8), and the other carbonyl carbon at δ_C 175.26 (C-2) had no correlation with any aromatic protons. Instead, the sp^2 carbon (C-4) with an oxygen atom at δ_C 169.73 showed a correlation with one of the four aromatic protons at δ_H 7.66 (H-5). Treatment of **11** with 2,3-dichloro-5,6-dicyano-1,4-benzoquinone (DDQ) in the presence of Nafion-H in dry benzene afforded the corresponding dehydro compound **9** and the dealkylation product **8**.[16]

As shown in Table 3, the ^{1}H-NMR data of the synthetic compounds were clearly different from that of the phytoalexins reported by Gillan and co-workers.[14,17] From these results, we concluded that the structures of the phytoalexins isolated from *A. marina* by Gillan and co-workers must be revised to *para*-quinoid structures **2** and **3**, named avicequinone-B and -C by us, respectively.

Structures of Avicenols Three additional new com-

pounds, avicenol-A (**4**), -B (**5**), and -C (**6**) were isolated and shown to have a 1,4-naphthoquinol chromophore, based on the similarities in their UV spectra with a high-intensity band at λ_{max} 239—246 nm and low-intensity bands with fine-structures over the range 286 to 338 nm, although a hyperchromic shift of the bands in avicenol-B was observed.

Structure of Avicenol-A (4) Avicenol-A (**4**) was obtained as a colorless oil, $[\alpha]_D$ +5.1° ($CHCl_3$). The molecular formula was established as $C_{17}H_{20}O_5$ by HR-MS. In the ^{1}H-NMR spectrum, observation of symmetrical four-spin proton signals, analyzed as an AA'BB'-type [δ_H 8.04 (2H, d, J=8.4 Hz), 7.46 (1H, t, J=8.4 Hz), 7.33 (1H, t, J=8.4 Hz)], and two 3H singlets due to methoxyls (δ_H 4.12, 4.03), together with 4 and 3% NOE enhancement of the 2H-doublet at δ_H 8.04 on irradiation of each methoxyl at δ_H 4.12 and 4.03, respectively, suggested the presence of a 1,4-dimethoxynaphthol nucleus having no substituents on the A-ring. The presence of a 2-(1-hydroxy-1-methylethyl)-3-hydroxydihydrofuran ring fused to the naphthol skeleton, as shown in formula **4**, was proposed from the ^{1}H- and ^{13}C-NMR spectral data: a) Appearance of two 3H singlets at δ_H 1.33 and 1.35, a quarternary carbon linked to an oxygen atom at δ_C 71.39, AB-type doublets at δ_H 4.44 and 5.69 (J=4.0 Hz) which bonded to carbons at δ_C 71.87 and 97.24, respectively. b) C–H long-range correlations in the HMBC spectrum of the carbons at δ_C 97.24 (C-2′) and 71.39 (C-3′) with two methyls at δ_H 1.33 (3′-CH_3) and 1.35 (3′-CH_3). Another possible 6-membered ring system (2,2-dimethyl-3,4-dihydroxypyran ring) was excluded by consideration of the typical chemical shift values of the quarternary carbon (δ_C 71.39) and the methine carbon (δ_C 97.24) linked to the side-chain. *trans*-Configuration of two substituents on the dihydrofuran ring was proposed based on the coupling constants (J=4.0 Hz) of the AB-type doublets and no NOE enhancement between the two methine doublets at δ_H 4.44 and 5.69, as in the case of **1**. Thus, the structure of avicenol-A is that depicted by formula **4**.

Structure of Avicenol-B (5) Avicenol-B (**5**) was isolated as a colorless oil, $C_{14}H_{12}O_3$. Some red-shift in the UV absorption spectrum of this compound compared with that of **4**, suggested the presence of an additional conjugated system. In the ^{1}H-NMR spectrum, lack of two methyl signals (δ_H 1.33, 1.35) in the high-field and aliphatic vicinal protons [δ_H 4.44, 5.69 (J=4.0 Hz)] adjacent to the oxygen atoms in **4**, and the appearance of two doublets at δ_H 7.04 and 7.64 (J= 2.2 Hz) coupled to each other, along with four contiguous aromatic proton signals and two methoxy signals, indicated that **5** was the structure of avicenol-B.

Structure of Avicenol-C (6) Avicenol-C (**6**) was also isolated as a colorless oil, $[\alpha]_D$ +22° ($CHCl_3$). The molecular formula $C_{17}H_{20}O_4$, a difference of an oxygen atom compared with **4**, was established by HR-MS. The ^{1}H- and ^{13}C-NMR spectra (Tables 1, 2) were very similar to those of **4**, except for the proton signals at δ_H 3.38 (2H, d, J=8.4 Hz) and 4.71 (1H, t, J=8.4 Hz) coupled to each other, instead of the two doublets at δ_H 4.44 and 5.69 (J=4.0 Hz) in **4**, and the displacement of a methine carbon signal having a hydroxyl group at δ_C 71.87 in **4** to a high-field methylene carbon signal at δ_C 28.81 in the ^{13}C-NMR spectrum of **6**. These facts together with the results of the HMBC spectrum (see Experimental) led us to conclude that **6** was the structure of avicenol-C, although the absolute stereochemistry remained undetermined.

Another naphthoquinone isolated from this plant material was characterized as stenocarpoquinone-B (**7**) by comparison of the ^{1}H-NMR and IR data with that reported in the literature.[12]

Experimental

The ^{1}H- and ^{13}C-NMR, H–H correlation spectroscopy (COSY), NOE, and HMBC (J=8 Hz) spectra were recorded on an A-400 or A-600 (JEOL) spectrometer in $CDCl_3$, unless otherwise stated. Chemical shifts are shown in δ values (ppm) with tetramethylsilane (TMS) as an internal reference. All MS were recorded under electron impact (EI) conditions using an M-80 instrument (Hitachi) having a direct inlet system. UV spectra were recorded on a UVIDEC-610C double-beam spectrophotometer (JASCO) in methanol, IR spectra on an IR-230 instrument (JASCO) in $CHCl_3$, and optical rotations on a DIP-370 instrument (JASCO) in $CHCl_3$ at 25 °C. Preparative TLC was carried out on Kieselgel 60 F_{254} (Merck).

Plant Material *A. alba* Blume (Avicenniaceae) stem bark from young trees was collected on August 1995. Dr. H.T.W. Tan identified the material using keys or by comparison with herbarium sheet specimens at the Herbarium, Department of Biological Sciences, the National University of Singapore (SINU) or the Herbarium, Botanic Gardens, Singapore (SING). A voucher specimen has been deposited at SINU.

Extraction and Isolation The dried stem bark (1.63 kg) of *A. alba* collected in Singapore was extracted with acetone. The acetone extract (9.0 g) was subjected to silica-gel column chromatography, eluting with hexane–acetone (19 : 1, 18 : 2, 17 : 3, 4 : 1, 7 : 3, 1 : 1, 1 : 2), acetone, CH_2Cl_2–MeOH (3 : 1), and MeOH, successively, to give 10 fractions. Each fraction was further subjected to silica-gel column and preparative thin-layer chromatographies with appropriate combinations of hexane, CH_2Cl_2, iso-Pr_2O, EtOAc, benzene, $CHCl_3$, acetone, and MeOH as developing solvents to give three new naphthoquinones and their analogues, along with a known naphthoquinone, as stated below. From the hexane–acetone (19 : 1) eluate: avicequinone-B (**2**) (2.6 mg) and avicenol-B (**5**) (1.6 mg). From the hexane–acetone (17 : 3) eluate: avicenol-C (**6**) (20.7 mg). From the hexane–acetone (4 : 1) eluate: avicequinone-C (**3**) (14.3 mg) and stenocarpoquinone-B (**7**) (13.8 mg). From the hexane–acetone (7 : 3) eluate: avicenol-A (**4**) (10.2 mg). From the hexane–acetone (1 : 1) eluate: avicequinone-A (**1**) (3.7 mg).

A known compound, stenocarpoquinone-B, was fully characterized by comparison of the ^{1}H-NMR and IR data with that reported in the literature.[12]

Avicequinone-A (**1**): Yellow oil. $[\alpha]_D$ +35° (c=0.108). UV λ_{max} nm: 206, 245, 251, 286, 334. IR ν_{max} cm^{-1}: 3587, 3406 (br), 1685, 1653, 1635, 1595. EI-MS *m/z* (%): 274 (M^+, 2), 241 (14), 216 (12), 198 (10), 173 (10), 146 (10). HR-MS Calcd for $C_{15}H_{14}O_5$: 274.0840. Found: 274.0847. NOE: No enhancement of any proton signal was observed on irradiation of the methine proton at δ_H 5.62 and 4.54.

Avicequinone-B (**2**): Pale yellow powder. UV λ_{max} nm: 244, 248, 286, 336. IR ν_{max} cm^{-1}: 1682, 1587. EI-MS *m/z* (%): 198 (M^+, 100), 170 (54), 142 (21), 114 (76). HR-MS Calcd for $C_{12}H_6O_3$: 198.0315. Found: 198.0277. HMBC C–H correlations: C-1→H-8; C-2→H-1′, H-2′; C-3→H-1′, H-2′; C-4→H-5; C-4a→H-6; C-5→H-7; C-6→H-8; C-7→H-5; C-8→H-6; C-8a→H-7; C-1′→H-2′; C-2′→H-1′.

Avicequinone-C (**3**): Yellow powder. UV λ_{max} nm: 249, 292, 335, 374. IR ν_{max} cm^{-1}: 3589, 3450 (br), 1672, 1595, 1537. EI-MS *m/z* (%): 256 (M^+, 12), 241 (100), 214 (18), 199 (10), 129 (10), 115 (17), 105 (22). HR-MS Calcd for $C_{15}H_{12}O_4$: 256.0734. Found: 256.0723. HMBC C–H correlations: C-1→H-8; C-2→H-1′; C-3→H-1′; C-4→H-5; C-4a→H-6; C-5→H-7; C-6→H-8; C-7→H-5; C-8→H-6; C-8a→H-7; C-2′→H-1′, 3′-CH_3; C-3′→3′-CH_3.

Reaction of Lapachol with *m*CPBA To a solution of lapachol (**10**) (30 mg) in dry CH_2Cl_2 (2 ml) was added a solution of *m*CPBA (30 mg) in CH_2Cl_2 (1 ml). After 10 min, the reaction mixture was treated with Al_2O_3 (10 mg) for 5 min. The mixture was then filtered through a short column of Al_2O_3, and eluted with MeOH. On evaporation, the combined eluates gave a crude orange oil. This was subjected to preparative TLC with iso-Pr_2O–MeOH (24 : 1) as the developing solvent to give a dihydrofuran **11** (13.1 mg) and a dihydropyran **12** (13.2 mg). Dihydropyran **12** was found to be identical to stenocarpoquinone-A[12] and dihydrofuran **11** to hydroxyiso-β-lapachone[12] by comparison of the ^{1}H-NMR, UV, and IR spectra.

Dihydrofuran **11**: Red oil. ^{1}H-NMR (400 MHz, $CDCl_3$) δ: 8.04 (1H, d,

J=7.3 Hz, H-8), 7.66 (2H, m, H-5, 6), 7.57 (1H, br t, J=7.3 Hz, H-7), 4.93 (1H, t, J=9.2 Hz, H-2′), 3.08 (2H, d, J=9.2 Hz, H-1′), 1.43 (3H, s, 3′-CH_3), 1.29 (3H, s, 3′-CH_3); ^{13}C-NMR (100 MHz, $CDCl_3$) δ: 180.93 (C-1), 175.26 (C-2), 169.73 (C-4), 134.50 (C-6), 131.93 (C-7), 130.59 (C-8a), 129.43 (C-8), 127.26 (C-4a), 124.41 (C-5), 115.96 (C-3), 93.50 (C-2′), 71.69 (C-3′), 27.40 (C-1′), 25.70 (3′-CH_3), 24.41 (3′-CH_3). HMBC C–H correlations: C-1→H-8; C-3→H-1′; C-4→H-5, H-1′; C-4a→H-6, H-8; C-5→H-7; C-6→H-8; C-8a→H-5, H-7; C-2′→3′-CH_3; C-3′→3′-CH_3; 3′-CH_3→H-2′.

Dihydropyran **12**: Red oil. ^{1}H-NMR (400 MHz, $CDCl_3$) δ: 8.03 (1H, d, J=7.7 Hz, H-8), 7.82 (1H, d, J=7.7 Hz, H-5), 7.64 (1H, t, J=7.7 Hz, H-6), 7.50 (1H, t, J=7.7 Hz, H-7), 3.93 (1H, t, J=5.1 Hz, H-2′), 3.50 (1H, br, OH), 2.80 (1H, dd, J=17.6, 5.1 Hz, H-1′), 2.62 (1H, dd, J=17.6, 5.1 Hz, H-1′), 1.51 (3H, s, 3′-CH_3), 1.45 (3H, s, 3′-CH_3); ^{13}C-NMR (100 MHz, $CDCl_3$) δ: 179.53 (C-1), 178.66 (C-2), 161.70 (C-4), 134.84 (C-6), 132.07 (C-8a), 130.82 (C-7), 129.93 (C-4a), 128.57 (C-8), 124.34 (C-5), 110.54 (C-3), 81.64 (C-3′), 68.05 (C-2′), 25.21 (3′-CH_3), 25.00 (C-1′), 21.99 (3′-CH_3).

Dehydrogenation of 11 with DDQ A mixture of **11** (10 mg), DDQ (15 mg), and Nafion-H (solid, Aldrich) (3.0 mg) in dry benzene (2 ml) was heated in an oil bath at 50 °C for 24 h. The reaction mixture was filtered, and the filtrate was evaporated to dryness. The residue was subjected to preparative TLC with hexane–acetone (7 : 3) and $CHCl_3$–MeOH (19 : 1) as developing solvents to afford 2-[2′-(2′-hydroxy)propyl]naphtho[1,2-*b*]furan-4,5-dione (**9**, 1 mg) and naphtho[1,2-*b*]furan-4,5-dione (**8**, 0.4 mg).

Naphtho[1,2-*b*]furan-4,5-dione (**8**): Red oil. UV λ_{max} nm: 214, 244, 261, 267 (sh), 327, 436. IR ν_{max} cm^{-1}: 1709, 1678, 1603. EI-MS *m/z* (%): 198 (M^+, 85), 170 (100), 142 (26). HR-MS Calcd for $C_{12}H_6O_3$: 198.0317. Found: 198.0323. ^{1}H-NMR (400 MHz, $CDCl_3$) δ: 8.10 (1H, d, J=7.7 Hz, H-8), 7.74 (1H, d, J=7.7 Hz, H-5), 7.67 (1H, t, J=7.7 Hz, H-6), 7.52 (1H, d, J=2.2 Hz, H-1′), 7.49 (1H, t, J=7.7 Hz, H-7), 6.88 (1H, d, J=2.2 Hz, H-2′); ^{13}C-NMR (100 MHz, $CDCl_3$) δ:180.51 (C-1), 174.48 (C-2), 160.58 (C-4), 145.07 (C-2′), 135.43 (C-6), 130.60 (C-8), 130.31 (C-7), 128.77 (C-8a), 128.44 (C-4a), 122.36 (C-5), 121.52 (C-3), 108.89 (C-1′).

2-[2′-(2′-Hydroxy)propyl]naphtho[1,2-*b*]furan-4,5-dione (**9**): Red oil. UV λ_{max} nm: 214, 246, 264, 272 (sh), 328, 436. IR ν_{max} cm^{-1}: 3504 (br), 1709, 1678, 1603. EI-MS *m/z* (%): 256 (M^+, 31), 241 (60), 213 (51), 199 (10), 185 (8), 170 (16), 149 (46). HR-MS Calcd for $C_{15}H_{12}O_4$: 256.0734. Found: 256.0725. ^{1}H-NMR (400 MHz, $CDCl_3$) δ: 8.09 (1H, d, J=7.7 Hz, H-8), 7.74 (1H, d, J=7.7 Hz, H-5), 7.66 (1H, t, J=7.7 Hz, H-6), 7.47 (1H, t, J=7.7 Hz, H-7), 6.68 (1H, s, H-1′), 2.17 (1H, br s, OH), 1.68 (6H, s, 3′-CH3); ^{13}C-NMR (100 MHz, $CDCl_3$) δ:180.42 (C-1), 174.48 (C-2), 163.61 (C-2′), 159.94 (C-4), 135.36 (C-6), 130.54 (C-8), 130.20 (C-7), 128.83 (C-8a), 128.41 (C-4a), 122.28 (C-5), 122.02 (C-3), 102.65 (C-1′), 68.78 (C-3′), 28.54 (3′-CH_3×2).

Avicenol-A (**4**): Colorless oil. $[\alpha]_D$ +5.1° (c=0.392). UV λ_{max} nm: 210, 239, 290, 300, 321, 335. IR ν_{max} cm^{-1}: 3587, 3429 (br), 1639. EI-MS *m/z* (%): 304 (M^+, 100), 289 (23), 286 (72), 271 (91), 253 (10), 241 (42), 232 (11), 229 (25), 217 (79), 213 (57), 211 (10), 199 (17), 189 (26), 173 (15). HR-MS Calcd for $C_{17}H_{20}O_5$: 304.1310. Found: 304.1310. NOE: Irradiation of 1-OCH_3 (δ 4.03) gave a 3% NOE at H-8 (δ 8.04); irradiation of 4-OCH_3 (δ 4.12) gave a 4% NOE at H-1′ (δ 4.44) and a 4% NOE at H-5 (δ 8.04); No enhancement of any proton signal was observed on irradiation of the methine protons at δ_H 5.69 and 4.44. HMBC C–H correlations: C-1→H-8, 1-OCH_3; C-2→H-1′; C-4→4-OCH_3; C-4a→H-6; C-5→H-7; C-7→H-5; C-8→H-6; C-8a→H-7; C-2′→3′-CH_3; C-3′→3′-CH_3.

Avicenol-B (**5**): Colorless oil. UV λ_{max} nm: 212, 246, 331, 345. IR ν_{max} cm^{-1}: 1639, 1608. EI-MS *m/z* (%): 228 (M^+, 13), 213 (28), 167 (63), 149 (100), 135 (6). HR-MS Calcd for $C_{14}H_{12}O_3$: 228.0786. Found: 228.0811. NOE: Irradiation of 1-OCH_3 (δ 4.27) gave a 2% NOE at H-8 (δ 8.27); irradiation of 4-OCH_3 (δ 4.17) gave a 3% NOE at H-1′ (δ 7.04) and 1% NOE at H-5 (δ 8.24). HMBC C–H correlations: C-1→H-8, 1-OCH_3; C-2→H-2′; C-3→H-1′, H-2′; C-4→H-5, H-1′, 4-OCH_3; C-4a→H-6; C-5→H-7; C-6→H-8; C-7→H-5; C-8→H-6; C-8a→H-7; C-1′→H-2′; C-2′→H-1′.

Avicenol-C (**6**): Colorless oil. $[\alpha]_D$ +22° (c=1.031). UV λ_{max} nm: 210, 239, 286, 297, 326, 338. IR ν_{max} cm^{-1}: 3587, 3442 (br), 1639, 1608. EI-MS *m/z* (%): 288 (M^+, 100), 273 (19), 255 (16), 229 (7), 215 (18), 213 (32), 201 (27), 199 (17), 195 (11), 187 (13), 183 (10), 173 (63), 171 (12), 157 (16), 143 (23). HR-MS Calcd for $C_{17}H_{20}O_4$: 288.1360. Found: 288.1355. NOE: Irradiation of 1-OCH_3 (δ 3.96) gave a 2% NOE at H-8 (δ 8.00); irradiation of 4-OCH_3 (δ 4.01) gave a 2% NOE at H-5 (δ 8.02). HMBC C–H correlations: C-1→H-8, 1-OCH_3; C-2→H-1′; C-3→H-1′; C-4→H-5, 4-OCH_3; C-4a→H-6, H-8; C-5→H-7; C-6→H-8; C-8→H-6; C-8a→H-5, H-7; C-2′→H-1′, 3′-CH_3; C-3′→H-1′, 3′-CH_3.

Acknowledgements We are grateful to Mr. Chua Keng Soon of the Department of Botany, National University of Singapore, for collection of the plant material. This work was partly supported by Grants-in-Aid from the Ministry of Education, Science, Sports, and Culture of Japan and the Japan Society for the Promotion of Science [High-Tech Research Center Project and H. F., No. 09672173 for Scientific Research (C), respectively].

References and Notes

1) Part of this paper was presented at the 116th and 117th Annual Meetings of the Pharmaceutical Society of Japan, Kanazawa, March 1996 and Tokyo, March 1997.
2) A different classification of this genus has been reported by several authors. Konig G., Rimpler H., Hunkler D., *Phytochemistry*, **26**, 423—427 (1987), and references cited herein.
3) "A Dictionary of the Economic Products of the Malay Peninsula," ed. by Burkill I. H., Ministry of Agriculture and Co-Operatives, Kuala Lumpur, Malaysia, 1966, pp. 274—279.
4) Fauvel M.-T., Bousquet-Melou A., Moulis C., Gleye J., Jensen S. R., *Phytochemistry*, **38**, 893—894 (1995).
5) Fauvel M. T., Taoubi K., Gleye J., Fouraste I., *Planta Med.*, **59**, 387 (1993).
6) Misra S., Choudhury A., Pal P. K., Ghosh A., *Phytochemistry*, **25**, 1083—1087 (1986).
7) Ghosh A., Misra S., Dutta A. K., Choudhury A., *Phytochemistry*, **24**, 1725—1727 (1985).
8) Konig G., Rimpler H., *Phytochemistry*, **24**, 1245—1248 (1985).
9) Wannigama G. P., Volkman J. K., Gillan F. T., Nichols P. D., Johns R. B., *Phytochemistry*, **20**, 659—666 (1981).
10) Majumdar S. G., Patra G., *J. Indian Chem. Soc.*, **56**, 111—113 (1979).
11) Hayward E. C., Tarbell D. S., Colebrook L. D., *J. Org. Chem.*, **33**, 399—402 (1968).
12) Mock J., Murphy S. T., Ritchie E., Taylor W. C., *Aust. J. Chem.*, **26**, 1121—1130 (1973).
13) Koyanagi J., Yamamoto K., Nakayam K., Tanaka A., *J. Heterocyclic Chem.*, **31**, 1303—1304 (1994).
14) Sutton D. C., Gillan F. T., Susic M., *Phytochemistry*, **24**, 2877—2879 (1985).
15) Murray R. D. H, Sutcliffe M., McCabe P. H., *Tetrahedron*, **27**, 4901—4906 (1971).
16) Mathieson J. W., Thomson R. H., *J. Chem. Soc. (C)*, **1971**, 153—160.
17) The UV data could not be compared, because sufficient data were not reported in the literature.[14]

Chem. Pharm. Bull. **48**(3) 344—348 (2000) Vol. 48, No. 3

Mechanism of C-2 Hydroxylation during the Biosynthesis of 20-Hydroxyecdysone in *Ajuga* Hairy Roots

Keiko NOMURA and Yoshinori FUJIMOTO*

Department of Chemistry and Materials Science, Tokyo Institute of Technology, Meguro, Tokyo 152–8551, Japan.

Received August 31, 1999; accepted November 11, 1999

Feeding synthetic [2β-^{2}H]- and [2α-^{2}H]-cholesterols to the hairy roots of *Ajuga reptans* var. *atropurpurea* and ^{2}H-NMR analysis of the biosynthesized 20-hydroxyecdysone revealed that hydroxylation at C-2 proceeds with retention of configuration. Feeding [2α,3α-^{2}H$_2$]cholesterol followed by ^{2}H-NMR analysis of the 2,3,22-triacetate of the resulting 20-hydroxyecdysone ruled out a mechanism which involves a partial loss of the 2α-hydrogen. The steric course of C-2 hydroxylation in *Ajuga* hairy roots is identical with that reported in the insect, *Schistocerca gregaria*.

Key words 20-hydroxyecdysone; *Ajuga reptans var. atropurpurea*; biosynthesis; hydroxylation; ecdysteroid

20-Hydroxyecdysone (**1**), a molting hormone of insects, is also distributed in the plant kingdom.[1] We previously demonstrated that the hairy roots of *Ajuga reptans* var. *atropurpurea* (Labiatae)[2] are useful for biosynthetic studies of phytoecdysteroids.[3] In this tranformed biosystem, feeding studies of ^{2}H-labeled substrates have revealed that the 3α-, 4α- and 4β-hydrogens of cholesterol are retained at their original positions after conversion to 20-hydroxyecdysone,[4] and that most of the 6-hydrogen of cholesterol migrates to the C-5 position of 20-hydroxyecdysone.[5] The metabolic fates of these hydrogens are different from those reported in the insects, *Schistocerca gregaria*[6] and *Locusta migratoria*,[7] and the fern *Polypodium vulgare*.[8] In particular, the fate of 3α-hydrogen differs markedly among these species. In contrast to the complete retention of the 3α-hydrogen of cholesterol in *Ajuga* hairy roots, the hydrogen is reported to migrate to the C-4 position of 20-hydroxyecdysone in *P. vulgare*. Further, in *S. gregaria ca.* 20% of the hydrogen is reportedly retained at positions other than the C-3 of 20-hydroxyecdysone. These differences may be correlated with the mechanism of the introduction of the adjacent C-2 hydroxy group. It is, therefore, interesting to investigate the mechanism of C-2 hydroxylation in *Ajuga* hairy roots and compare it with those of other plants and insects.

Results and Discussion

The metabolic fate of the 2β- and 2α-hydrogens of cholesterol during the biosynthesis of 20-hydroxyecdysone was followed up by feeding studies of ^{2}H-labeled substrates, [2β-^{2}H]- and [2α-^{2}H]-cholesterols (**2a**, **2b**). Compound **2a** was synthesized according to Chart 1. 6β-Hydroxy-5α-cholest-2-ene (**3**), prepared from 3,5α-cyclocholestan-6-one in two steps (heating with LiBr in *N*,*N*-dimethylformamide (DMF)[9] and reduction with $NaBH_4$), was converted to tetrahydropyranyl (THP) ether **4** which was epoxidized to give 2α,3α-epoxide **5**, stereoselectively. Reduction of **5** with $LiAlD_4$ pro-

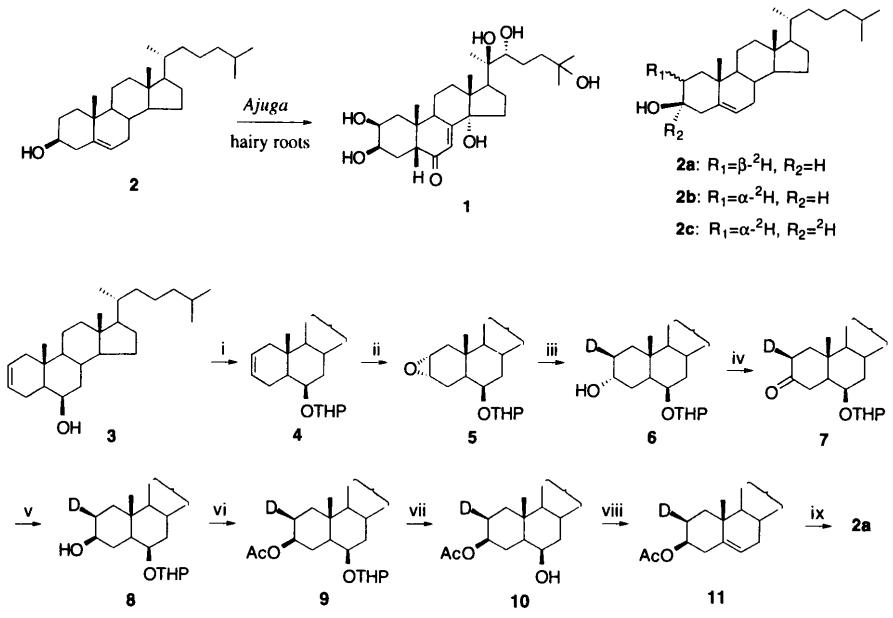

Reagents: i) DHP, *p*-TsOH, CH_2Cl_2 (83%), ii) *m*CPBA, Na_2CO_3, CH_2Cl_2 (80%), iii) $LiAlD_4$, THF (93%), iv) PCC, MS4A, NaOAc, CH_2Cl_2, v) $LiAlH_4$, THF (85% for 2 steps), vi) Ac_2O, Py (91%), vii) H^+, MeOH–THF (76%), viii) $POCl_3$, Py, ix) 5% KOH–MeOH, THF (85% for 2 steps).

Chart 1. Synthesis of [2β-^{2}H]cholesterol (**2a**)

* To whom correspondence should be addressed.

© 2000 Pharmaceutical Society of Japan

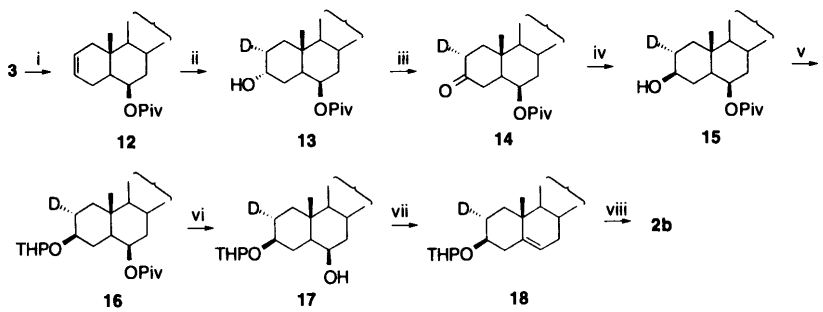

Reagents: i) PivCl, Py (74%), ii) BD_3·THF, THF (23%), iii) PCC, NaOAc, CH_2Cl_2, iv) $NaBH_4$, MeOH–THF (76% for two step), v) DHP, *p*-TsOH, CH_2Cl_2 (85%), vi) $LiAlH_4$, ether (91%), vii) $POCl_3$, Py (99%), viii) H^+, MeOH–THF (79%).

Chart 2. Synthesis of [2α-^{2}H]cholesterol (**2b**)

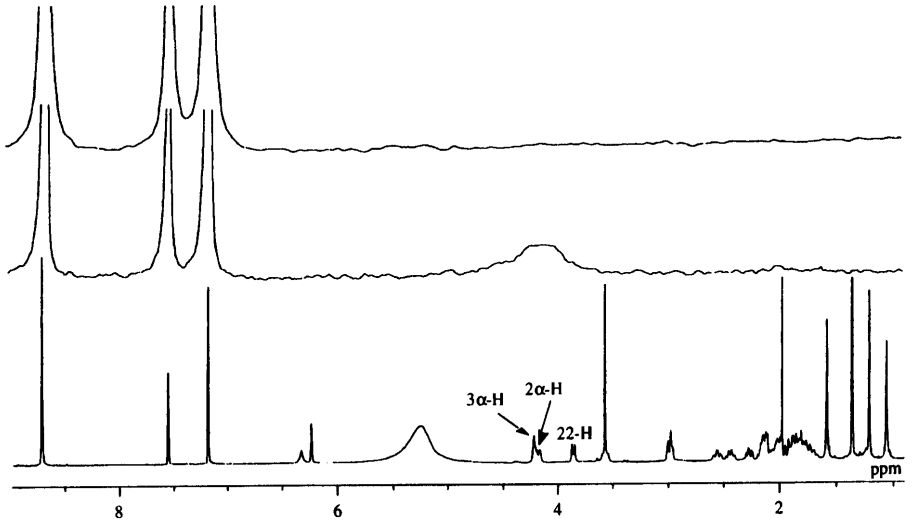

Fig. 1. ^{2}H-NMR (61 MHz, in Pyridine) Spectra of 20-Hydroxyecdysone Samples Biosynthesized from [2β-^{2}H]Cholesterol **2a** (Top) and [2α-^{2}H]Cholesterol **2b** (Middle)

^{1}H-NMR spectrum of authentic 20-hydroxyecdysone is given at the bottom.

ceeded in an axial manner to afford [2β-^{2}H]-3α-ol **6**. The 3α-alcohol **6** was converted to 3β-alcohol **8** *via* oxidation leading to 3-ketone **7** and reduction. After protecting **8** as the acetate **9**, the THP group was deprotected to give 6β-ol **10** which, upon dehydration, afforded 5-ene **11**. Hydrolysis of the acetyl group of **11** gave the desired **2a**. Compound **2a** exhibited a single signal at δ 1.50 in its ^{2}H-NMR spectrum.

[2α-^{2}H]Cholesterol (**2b**) was synthesized according to Chart 2. The same starting material **3** was converted to pivaloyl ester **12**. Hydroboration of **12** with BD_3 afforded a mixture of four isomeric alcohols, from which 3α-alcohol **13** was separated by silica-gel chromatography. The 3α-alcohol **13** was converted to 3β-alcohol **15** in an oxidation–reduction sequence *via* **14**. Compound **15** was converted to THP ether **16**, and then the pivaloyl group was removed by reduction to give 6β-ol **17**. Dehydration of **17** gave 5-ene **18**. Removal of the THP group of **18** furnished the desired **2b**. The α-orientation of the deuterium atom at the C-2 of **2b** was established at the stage of the ketone **14**. The ^{1}H-NMR spectrum of the non-labeled compound corresponding to **14** exhibited 2α-H and 2β-H signals at δ 2.33 (dt, J=13.8, 2.8 Hz) and 2.41 (td, J=13.7, 7.3 Hz), respectively, whereas that of compound **14** lacked the former signal but exhibited the latter signal at δ 2.39 (dd, J=13.7, 7.3 Hz). Compound **2b** exhibited a single signal at δ 1.83 in its ^{2}H-NMR spectrum.

With the two isomeric ^{2}H-labeled cholesterols available, experiments feeding *Ajuga* hairy roots were performed as described previously. Briefly, 100 mg of the deuteriocholesterol was administered to *Ajuga* hairy roots which had been preincubated for two weeks, followed by incubation for another two weeks. From the roots, 20-hydroxyecdysone was obtained after chromatographic separation and final purification by HPLC.

The ^{2}H-NMR spectra of the 20-hydroxyecdysones derived from **2a** and **2b** are shown in Fig. 1. The 20-hydroxyecdysone derived from **2b** displayed a deuterium signal at δ 4.15, which corresponds to the 2α-hydrogen of 20-hydroxyecdysone, whereas the 20-hydroxyecdysone derived from **2a** did not exhibit any signals in this region. The observed signal could be assigned to the deuterium at C-2 rather than C-3, since the 3α-hydrogen of cholesterol is known to be retained during the conversion to 20-hydroxyecdysone.[4] The assignment was further confirmed by ^{2}H-NMR analysis of the corresponding 2,3,22-triacetate derivative which showed a signal at δ 5.08 due to 2α-^{2}H (Fig. 2). These results indicated that the 2β-hydrogen of cholesterol is stereospecifically removed and the 2α-hydrogen is retained during 20-hydroxyecdysone biosynthesis in *Ajuga* hairy roots.

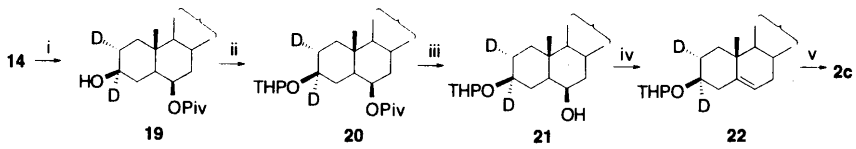

Reagents: i) $LiAlD_4$, THF (75%), ii) DHP, *p*-TsOH, CH_2Cl_2 (76%), iii) $LiAlH_4$, ether (93%), iv) $POCl_3$, Py (93%), v) H^+, MeOH–THF (86%).

Chart 3. Synthesis of [2α,3α-$^2H_2$]cholesterol (**2c**)

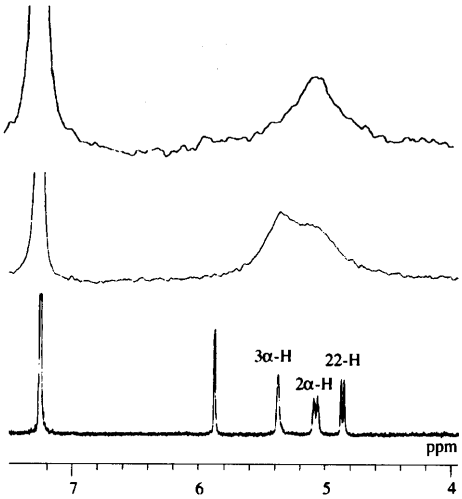

Fig. 2. ^{2}H-NMR (61 MHz, in Pyridine) Spectra of 2,3,22-Triacetate Derivatives of 20-Hydroxyecdysone Biosynthesized from [2α-^{2}H]Cholesterol **2b** (Top) and [2α,3α-$^2H_2$]Cholesterol **2c** (Middle)

^{1}H-NMR spectrum of authentic 20-hydroxyecdysone 2,3,22-triacetate is given at the bottom.

The retention of the 2α-hydrogen was shown in the above feeding studies. However, an equilibration between the 2-hydroxy compound and 2-oxo derivative, during or after the biosynthesis of 20-hydroxyecdysone, would cause partial loss of the 2α-hydrogen. Indeed, characterization of 3-oxo compounds such as 3-dehydroecdysone[10] and their possible involvement in biosynthesis[8] have been reported. In contrast, no loss of the 3α-hydrogen was reported with the plant, *Taxus baccata*.[11] A further study was, therefore, undertaken using a doubly labeled compound, [2α,3α-$^2H_2$]cholesterol (**2c**). The synthesis of **2c** is illustrated in Chart 3. Compound **14** was reduced with $LiAlD_4$ to give a [2α,3α-$^2H_2$]-derivative **19**, which was converted into **2c**, through THP ether **20**, 6-ol **21** and 5-ene **22**, in the same manner as described for the synthesis of **2b**. The ^{2}H-NMR spectrum of **2c** exhibited signals at δ 1.82 and 3.50 due to 2α-^{2}H and 3α-^{2}H, respectively.

Compound **2c** was fed to *Ajuga* hairy roots in the same manner as described above, and the resulting 20-hydroxyecdysone and its 2,3,22-triacetate derivative were analyzed by ^{2}H-NMR. The 20-hydroxyecdysone exhibited a broad ^{2}H signal at *ca.* δ 4.15 (data not shown). The ^{2}H-NMR spectrum of the triacetate is shown in Fig. 2, which displayed partially overlapping signals at δ 5.38 and 5.17 assignable to the C-3α and C-2α deuterium atoms, respectively. The intensity of the two signals was fairly simmilar. Thus, it is safe to conclude that a mechanism involving partial loss of the 2α-hydrogen does not operate in *Ajuga* hairy roots.

In conclusion, the present study has established that C-2 hydroxylation during the biosynthesis of 20-hydroxyecdysone in *Ajuga* hairy roots proceeds with retention of configuration. A possible contribution from a 2-oxo compound was ruled out. Thus, the C-2 hydroxylation is most likely to occur in a direct hydroxylation mechanism. The steric course of the C-2 hydroxylation in *Ajuga* hairy roots is identical with that reported in the insect, *S. gregaria*.[12] It is reported that the enzyme responsible for the C-2 hydroxylation of *L. migratoria* is a monooxygenase which is not a cytochrome P450.[13,14] We recently reported that the C-25 hydroxylation during the biosynthesis of 20-hydroxyecdysone in *Ajuga* hairy roots is not stereospecific, but proceeds both *via* retention and inversion mechanisms.[15]

Experimental

^{1}H-NMR spectra were obtained on a JEOL JNM-LA300 (300 MHz) or LA400 (400 MHz) spectrometer in $CDCl_3$ solutions and chemical shifts (δ) are reported in ppm downfield from tetramethylsilane (used as an internal reference). The signals for 26-H_3 and 27-H_3 (6H, d, *J*=7.5—8.1 Hz) were observed at δ 1.86—1.87 for all steroidal compounds, and these data are not described. ^{2}H-NMR spectra were recorded on a JEOL JNM-LA400 spectrometer (61 MHz for ^{2}H) in $CHCl_3$ (the signal of residual C^2HCl_3 was at δ 7.26) or in pyridine (the signal of 2-^{2}H of the solvent was at δ 7.19). HPLC was performed on a Shimadzu LC-6A instrument with an SPD-6A UV detector using a preparative octadecyl silica (ODS) column (Shimadzu STR PREP-ODS column, 25 cm×20 mm i.d.). Merck Kieselgel 60 and Merck Kieselgel F_{254} plates (20×20 cm, 0.5 mm thick) were used for column chromatography and preparative thin-layer chromatography (TLC), respectively.

5α-Cholest-2-en-6β-ol THP Ether (4) Dihydropyran (DHP) (0.44 ml, 4.88 mmol) and *p*-toluenesulfonic acid monohydrate (*p*-TsOH·H_2O) (2 mg) were added to a solution of compound **3** (940 mg, 2.44 mmol, obtained by $NaBH_4$ reduction of 5α-cholest-2-en-6-one which was prepared from 3,5α-cyclocholestan-6-one by the method of Aburatani *et al.*[9]) in dry CH_2Cl_2 (20 ml), and the reaction mixture was stirred at room temperature for 30 min. Addition of saturated $NaHCO_3$ followed by an extractive (AcOEt) work-up gave a crude product which was chromatographed on silica-gel (hexane : AcOEt=30 : 1) to give **4** (950 mg, 83%) as a colorless oil. ^{1}H-NMR δ: 0.68 (1.3H, s, 18-H_3), 0.70 (1.7H, s, 18-H_3), 0.93 (3H, d, *J*=5.4 Hz, 21-H_3), 0.96 (3H, s, 19-H_3), 3.52 (1H, d, *J*=2.0 Hz, 6′-Hax), 3.60 (0.65H, d, *J*=2.7 Hz, 6-H), 3.77 (0.35H, d, *J*=2.6 Hz, 6-H), 3.90 (1H, m, 6′-Heq), 4.60 (0.65H, t, *J*=3.3 Hz, 2′-H), 4.68 (0.35H, s, 2′-H), 5.55 (1H, m, 3-H), 5.57 (1H, m, 2-H). *Anal.* Calcd for $C_{32}H_{54}O_2$: C, 81.64; H, 11.56. Found: C, 81.85; H, 11.59.

2α,3α-Epoxy-5α-cholestan-6β-ol THP Ether (5) Na_2CO_3 (160 mg) and *m*-chloroperbenzoic acid (*m*CPBA) (492 mg, 2.00 mmol) were added to a solution of **4** (940 mg, 2.00 mmol) in dry CH_2Cl_2 (6 ml) and the reaction mixture was stirred at room temperature for 30 min. An extractive (CH_2Cl_2) work-up gave a crude product which was chromatographed on silica-gel (hexane : AcOEt=20 : 1) to give **5** (781 mg, 80%) as an amorphous solid. ^{1}H-NMR δ: 0.65 (1.3H, s, 18-H_3), 0.69 (1.7H, s, 18-H_3), 0.90 (3H, d, *J*=5.4 Hz, 21-H_3), 0.95 (3H, s, 19-H_3), 3.11 (1H, m, 3-H), 3.24 (1H, m, 2-H), 3.49 (1H, m, 6′-Hax), 3.66 (0.65H, d, *J*=2.6 Hz, 6-H), 3.83 (0.35H, d, *J*=2.6 Hz, 6-H), 3.89 (1H, m, 6′-Heq), 4.59 (1H, m, 2′-H). *Anal.* Calcd for $C_{32}H_{54}O_3$: C, 78.96; H, 11.18. Found: C, 79.05; H, 11.46.

[2β-^{2}H]-5α-Cholestane-3α,6β-diol 6-THP Ether (6) $LiAlD_4$ (80 mg, 1.91 mmol) was added to a solution of **5** (767 mg, 1.57 mmol) in dry tetrahydrofuran (THF) (15 ml) at room temperature and the reaction mixture was stirred at 60 °C for 30 min. An extractive (ether) work-up gave a crude product which was chromatographed on silica-gel (hexane : AcOEt=4 : 1) to give **6** (716 mg, 1.46 mmol, 93%) as white crystals, mp 62—64 °C (from hexane). ^{1}H-NMR δ: 0.65 (1.3H, s, 18-H_3), 0.69 (1.7H, s, 18-H_3), 0.90 (3H, d, *J*=5.4 Hz, 21-H_3), 0.95 (3H, s, 19-H_3), 3.48 (1.35H, m, 6-H, 6′-Hax), 3.62 (0.65H, d, *J*=2.6 Hz, 6-H), 3.86 (1H, m, 6′-Heq), 4.09 (1H, m, 3-H), 4.56 (0.65H,

br s, 2′-H), 4.63 (0.35H, br s, 2′-H). *Anal.* Calcd for $C_{32}H_{55}{}^2HO_3$: C, 78.47; H+^{2}H, 11.52. Found: C, 78.47; H, 11.94.

[2β-^{2}H]-5α-Cholestane-3β,6β-diol 6-THP Ether (8) NaOAc (48 mg, 0.58 mmol), pyridinium chlorochromate (PCC) (624 mg, 2.90 mmol) and molecular sieves 4A (MS4A) (powder, 6.0 g) were added to a solution of **6** (711 mg, 1.45 mmol) in dry CH_2Cl_2 (20 ml) and the reaction mixture was stirred at room temperature for 10 min. Dry ether was added and the mixture was filtered through a short column of Florisil. Concentration of the filtrate gave **7** (721 mg) as a colorless oil. ^{1}H-NMR δ: 0.70 (1.3H, s, 18-H_3), 0.72 (1.7H, s, 18-H_3), 0.90 (3H, d, J=5.4 Hz, 21-H_3), 2.71 (0.65H, dd, J=14.5 Hz, 4β-H), 2.94 (0.35H, dd, J=14.5 Hz, 4β-H), 3.51 (1.65H, m, 6-H, 6′-Hax), 3.68 (0.35H, d, J= 2.6 Hz, 6-H), 3.83 (1H, m, 6′-Heq), 4.55 (0.65H, br s, 2′-H), 4.67 (0.35H, br s, 2′-H).

$LiAlH_4$ (86 mg, 2.27 mmol) was added to a solution of **7** (721 mg) in THF (11 ml) and the reaction mixture was stirred at room temperature for 20 min. An extractive (ether) work-up gave a crude product which was chromatographed on silica-gel (hexane : AcOEt=3 : 1) to afford **8** (601 mg, 85% from **6**) as white crystals, mp 100—104 and 120—124 °C (from hexane). ^{1}H-NMR δ: 0.70 (1.3H, s, 18-H_3), 0.72 (1.7H, s, 18-H_3), 0.90 (3H, d, J=5.4 Hz, 21-H_3), 2.28 (1H, br s, 2α-H), 3.49 (1H, m, 3-H), 3.57 (0.65H, J=1.9 Hz, 6-H), 3.63 (1H, m, 6′-H), 3.70 (0.35H, d, J= 2.6 Hz, 6-H), 3.87 (1H, m, 6′-Heq), 4.59 (0.65H, br s, 2′-H), 4.69 (0.35H, br s, 2′-H). HR-FAB-MS *m/z* 472.4261 (MH^+-H_2O). Calcd for $C_{32}H_{53}{}^2HO_2$, 472.4265.

[2β-^{2}H]-5α-Cholestane-3β,6β-diol 3-Acetate (10) Ac_2O (2.0 ml) was added to a solution of **8** (601 mg, 1.22 mmol) in pyridine (2.0 ml), and the reaction mixture was stirred at room temperature overnight. Addition of ice chips and an extractive (ether) work-up gave a crude product **9** (597 mg, 91%) as an amorphous solid. ^{1}H-NMR δ: 0.70 (1.3H, s, 18-H_3), 0.72 (1.7H, s, 18-H_3), 0.90 (3H, d, J=5.4 Hz, 21-H_3), 2.04 (3H, s, Ac), 3.48 (1H, m, 6′-Hax), 3.55 (0.6H, d, J=2.0 Hz, 6-H), 3.70 (0.4H, d, J=2.6 Hz, 6-H), 3.85 (1H, m, 6′-Heq), 4.56 (0.6H, br s, 2′-H), 4.65 (0.4H, br s, 2′-H).

MeOH (5.0 ml) and a drop of 2 N HCl were added to a solution of **9** (590 mg) in THF (3.0 ml), and the reaction mixture was stirred at room temperature for 6 h. An extractive (ether) work-up gave a crude product which was chromatographed on silica-gel (hexane : AcOEt=4 : 1) to give **10** (415 mg, 76%) as white crystals, mp 140—143 °C (from MeOH) (lit.[16] 141—142 °C for non-labeled sample). ^{1}H-NMR δ: 0.69 (3H, s, 18-H_3), 0.91 (3H, d, J=6.8 Hz, 21-H_3), 1.04 (3H, s, 19-H), 2.04 (3H, s, Ac), 3.80 (1H, m, 6-H), 3.73 (1H, m, 6-H). *Anal.* Calcd for $C_{29}H_{49}{}^2HO_3$: C, 77.80; H+^{2}H, 11.26. Found: C, 77.89; H, 11.67.

[2β-^{2}H]Cholesterol (2a) $POCl_3$ (103 μl, 1.13 mmol) was added to a solution of **10** (337 mg, 0.753 mmol) in pyridine (4.0 ml), and the reaction mixture was stirred at room temperature for 3 h. An extractive (ether) work-up gave a crude product **11** (412 mg) as white crystals, mp 117—119 °C. ^{1}H-NMR δ: 0.67 (3H, s, 18-H_3), 0.91 (3H, d, J=5.4 Hz, 21-H_3), 1.02 (3H, s, 19-H_3), 2.17 (1H, d, J=8.6 Hz, 4β-H), 5.37 (1H, d, J=5.3 Hz, 6-H).

5% MeOH/KOH (4.0 ml) was added to a solution of **11** (412 mg) in THF (2.0 ml), and the mixture was stirred at room temperature overnight. An extractive (ether) work-up gave a crude product which was chromatographed on silica-gel (hexane : AcOEt=3 : 1) and then recrystallized from MeOH to give **2a** (220 mg, 75% from **10**) as white crystals, mp 149—152.5 °C. ^{1}H-NMR δ: 0.68 (3H, s, 18-H_3), 0.91 (3H, d, J=6.6 Hz, 21-H_3), 1.00 (3H, s, 19-H_3), 3.53 (1H, m, 3-H), 5.35 (1H, m, 6-H). ^{2}H-NMR δ: 1.51 (2β-^{2}H). *Anal.* Calcd for $C_{27}H_{45}{}^2HO$: C, 83.65; H+^{2}H, 11.96. Found: C, 83.45; H, 12.30.

5α-Cholest-2-en-6β-ol Pivaloate (12) Pivaloyl chloride (6.6 ml, 54.7 mmol) was added to a solution of **3** (3.02 g, 7.81 mmol) in pyridine (10 ml) at 0 °C, and the reaction mixture was stirred at 60 °C over night. An extractive (ether) work-up gave a crude product which was chromatographed on silica-gel (hexane : AcOEt=20 : 1) to give **12** (2.71 g, 74%) as white crystals, mp 78—78.5 °C (from MeOH). ^{1}H-NMR δ: 0.67 (3H, s, 18-H_3), 0.91 (3H, d, J=6.6 Hz, 21-H_3), 0.98 (3H, s, 19-H_3), 1.21 (9H, s, pivaloyl), 4.96 (1H, m, 6-H), 5.60 (2H, m, 2-H, 3-H). *Anal.* Calcd for $C_{32}H_{54}O_2$: C, 81.64; H+^{2}H, 11.56. Found: C, 81.39; H, 11.64.

[2α-^{2}H]-6β-Pivaloyloxy-5α-cholestan-3α-ol (13) $BF_3 \cdot Et_2O$ (0.74 ml, 6.01 mmol) was added to a solution of **12** (2.49 mg, 5.28 mmol) and $NaBD_4$ (188 mg, 4.49 mmol) in THF (20 ml) dropwise at 0 °C, and the reaction mixture was stirred at room temperature for 30 min. Water (2.0 ml), 3 N NaOH (2.0 ml) and 30% H_2O_2 (2.0 ml) was added and the mixture was stirred for 30 min. An extractive (AcOEt) work-up gave a crude product which was chromatographed on silica-gel (hexane : AcOEt=6 : 1) to give **13** (584 mg, 23%) as an amorphous solid. ^{1}H-NMR δ: 0.68 (3H, s, 18-H_3), 0.90 (3H, d, J=6.4 Hz, 21-H_3), 1.01 (3H, s, 19-H_3), 1.20 (9H, s, pivaloyl), 4.12 (1H, s, 3-H), 4.84 (1H, d, J=2.4 Hz, 6-H). *Anal.* Calcd for $C_{32}H_{55}{}^2HO_3$: C, 78.47; H+^{2}H, 11.52. Found: C, 78.49; H, 11.72.

The hydroboration–oxidation reaction using $NaBH_4$ in place of $NaBD_4$ afforded four non-labeled products in order of increasing polarity in the ratio of 51 : 11 : 12 : 26; 5α-cholestane-2β,6β-diol 6-pivaloyl ester, ^{1}H-NMR δ: 0.67 (3H, s, 18-H_3), 0.91 (3H, d, J=6.4 Hz, 21-H_3), 1.20 (9H, s, pivaloyl), 1.25 (3H, s, 19-H_3), 4.14 (1H, s, 2-H), 4.94 (1H, d, J=2.9 Hz, 6-H); 5α-cholestane-3α,6β-diol 6-pivaloyl ester, ^{1}H-NMR δ: 0.67 (3H, s, 18-H_3), 0.91 (3H, d, J=6.3 Hz, 21-H_3), 1.01 (3H, s, 19-H_3), 1.20 (9H, s, pivaloyl), 4.12 (1H, s, 3-H), 4.84 (1H, d, J=2.0 Hz, 6-H); 5α-cholestane-2α,6β-diol 6-pivaloyl ester, ^{1}H-NMR δ: 0.67 (3H, s, 18-H_3), 0.91 (3H, d, J=6.3 Hz, 21-H_3), 1.02 (3H, s, 19-H_3), 1.19 (9H, s, pivaloyl), 3.80 (1H, m, 2-H), 4.95 (1H, d, J=2.5 Hz, 6-H); 5α-cholestane-3β-,6β-diol 6-pivaloyl ester, ^{1}H-NMR δ: 0.67 (3H, s, 18-H_3), 0.91 (3H, d, J=6.4 Hz, 21-H_3), 1.05 (3H, s, 19-H_3), 1.20 (9H, s, pivaloyl), 3.64 (1H, m, 3-H), 4.89 (1H, d, J=2.4 Hz, 6-H).

[2α-^{2}H]-6β-Pivaloyloxy-5α-cholestan-3β-ol (15) Oxidation of **13** (584 mg, 1.19 mmol) in the same manner as described for **6** gave **14** (567 mg, 97%), after filtration through Florisil and concentration, as white crystals, mp 118—119 °C. ^{1}H-NMR δ: 0.70 (3H, s, 18-H_3), 0.91 (3H, d, J=6.8 Hz, 21-H_3), 1.21 (9H, s, pivaloyl), 1.22 (3H, s, 19-H_3), 2.11 (1H, d, J=15.6 Hz, 4-H), 2.10 (1H, d, J=14.7 Hz, 4-H), 2.39 (1H, dd, J=13.3, 6.9 Hz, 2β-H), 4.84 (1H, d, J=2.0 Hz, 6-H).

MeOH (10 ml) and $NaBH_4$ (60 mg, 1.59 mmol) were added to a solution of **14** (567 mg, 1.16 mmol) in THF (5.0 ml), and the reaction mixture was stirred at room temperature for 30 min. An extractive (ether) work-up gave a crude product which was chromatographed on silica-gel (hexane : AcOEt=7 : 1) to give **15** (445 mg, 76% from **13**) as an amorphous solid. ^{1}H-NMR δ: 0.69 (3H, s, 18-H_3), 0.91 (3H, d, J=6.8 Hz, 21-H_3), 1.04 (3H, s, 19-H_3), 1.20 (9H, s, pivaloyl), 2.00 (1H, dt, J=12.5, 2.1 Hz, 4-H), 3.65 (1H, m, 3-H), 4.89 (1H, d, J=2.9 Hz, 6-H). *Anal.* Calcd for $C_{32}H_{55}{}^2HO_3$: C, 78.47; H+^{2}H, 11.52. Found: C, 78.25; H, 11.82.

[2α-^{2}H]-6β-Pivaloyloxy-5α-cholestan-3β-ol THP Ether (16) DHP (165 μl, 1.76 mmol) and *p*-TsOH·H_2O (1.6 mg) were added to a solution of **15** (433 mg, 0.883 mmol) in dry CH_2Cl_2 (2.0 ml) and the reaction mixture was stirred at room temperature for 1 h. An extractive work-up (ether) gave a crude product which was chromatographed on silica-gel (hexane : AcOEt=7 : 1) to afford **16** (428 mg, 85%) as an amorphous solid. ^{1}H-NMR δ: 0.67 (3H, s, 18-H_3), 0.91 (3H, d, J=6.8 Hz, 21-H_3), 1.05 (3H, s, 19-H), 1.20 (9H, s, pivaloyl), 3.49 (1H, m, 6′-Hax), 3.62 (1H, m, 3-H), 3.89 (1H, m, 6′-Heq), 4.71 (1H, m, 2′-H), 4.89 (1-H, m, 6-H). *Anal.* Calcd for $C_{37}H_{63}{}^2HO_4$: C, 77.43; H+^{2}H, 11.42. Found: C, 77.36; H, 11.71.

[2α-^{2}H]-5α-Cholestane-3β,6β-diol 3-THP Ether (17) $LiAlH_4$ (20 mg, 0.527 mmol) was added to a solution of **16** (421 mg, 0.733 mmol) in dry ether (10 ml) and the reaction mixture was stirred at room temperature for 30 min. An extractive (ether) work-up gave a crude product which was chromatographed on silica-gel (hexane : AcOEt=7 : 1) and recrystallized from MeOH to afford **17** (325 mg, 91%) as white crystals, mp 150—152 °C. ^{1}H-NMR δ: 0.68 (3H, s, 18-H_3), 0.90 (3H, d, J=6.3 Hz, 21-H_3), 1.03 (3H, s, 19-H_3), 3.50 (1H, m, 6′-Hax), 3.65 (1H, m, 3-H), 3.79 (1H, d, J=2.2 Hz, 6-H), 3.93 (1H, m, 6′-H), 4.75 (1H, m, 2′-H). *Anal.* Calcd for $C_{32}H_{55}{}^2HO_3$: C, 78.47; H+^{2}H, 11.73. Found: C, 78.30; H, 11.88.

[2α-^{2}H]Cholest-5-en-3β-ol THP Ether (18) Dehydration of **17** (325 mg, 0.664 mmol) in the same manner as described for **10** gave a crude product which, upon recrystallization from MeOH, afforded **18** (309 mg, 99%) as white crystals, mp 150—153 °C. ^{1}H-NMR δ: 0.68 (3H, s, 18-H_3), 0.91 (3H, d, J=7.1 Hz, 21-H_3), 1.01 (3H, s, 19-H_3), 3.50 (2H, m, 3-H, 6′-Hax), 3.91 (1H, m, 6′-H), 4.72 (1H, br s, 2′-H), 5.35 (1H, s, 6-H). *Anal.* Calcd for $C_{32}H_{53}{}^2HO_2$: C, 81.47; H+^{2}H, 11.54. Found: C, 81.57; H, 11.94.

[2α-^{2}H]Cholesterol (2b) 2 N HCl (100 μl) was added to a solution of **18** (306 mg, 0.649 mmol) in THF (7.0 ml) and MeOH (5.0 ml), and the reaction mixture was stirred at room temperature for 30 min. An extractive (ether) work-up and recrystallization of the crude product from MeOH gave **2b** (197 mg, 79%) as white crystals, mp 148—151 °C. ^{1}H-NMR δ: 0.68 (3H, s, 18-H_3), 0.91 (3H, d, J=6.6 Hz, 21-H_3), 1.01 (3H, s, 19-H_3), 3.51 (1H, m, 3-H), 5.35 (1-H, m, 6-H). ^{2}H-NMR δ: 1.83 (2α-^{2}H). *Anal.* Calcd for $C_{27}H_{45}{}^2HO$: C, 83.65; H+^{2}H, 11.96. Found: C, 83.35; H, 12.17.

[2α,3α-$^2H_2$]-6β-Pivaloyloxy-5α-cholestan-3β-ol (19) $LiAlD_4$ (32 mg, 0.772 mmol) was added to a solution of **14** (678 mg, 1.39 mmol) in THF (10 ml), and the reaction mixture was stirred at room temperature for 30 min. An extractive (ether) work-up gave a crude product which was chromatographed on silica-gel (hexane : AcOEt=7 : 1) to give **19** (437 mg, 75%) as an amorphous solid. ^{1}H-NMR δ: 0.69 (3H, s, 18-H_3), 0.91 (3H, d, J=6.8 Hz, 21-H_3), 1.04 (3H, s, 19-H_3), 1.20 (9H, s, pivaloyl), 2.00 (1H, dt, J=12.5, 2.1 Hz, 4-H), 4.89 (1H, d, J=2.9 Hz, 6-H). *Anal.* Calcd for $C_{32}H_{54}{}^2H_2O_3$: C, 78.31; H+^{2}H, 11.50. Found: C, 78.24; H, 12.94.

[2α,3α-$^2H_2$]-6β-Pivaloyloxy-5α-cholestan-3β-ol THP Ether (20) Pro-

tection of **19** (503 mg, 1.02 mmol) in the same manner as described for **15** gave, after silica-gel chromatography, **20** (443 mg, 76%) as an amorphous solid. ^{1}H-NMR δ: 0.67 (3H, s, 18-H$_3$), 0.90 (3H, d, J=6.8 Hz, 21-H$_3$), 1.04 (3H, s, 19-H$_3$), 1.20 (9H, s, pivaloyl), 3.49 (1H, m, 6′-Hax), 3.89 (1H, m, 6′-Heq), 4.71 (1H, m, 2′-H), 4.89 (1-H, m, 6-H). *Anal.* Calcd for $C_{37}H_{62}{}^2H_2O_4$: C, 77.30; H+^{2}H, 11.22. Found: C, 77.20; H, 11.64.

[2α,3α-$^2H_2$]-5α-Cholestane-3β,6β-diol 3-THP Ether (21) Reduction of **20** (443 mg, 0.772 mmol) in the same manner as described for **16** gave, after silica-gel chromatography, **21** (350 mg, 93%) as white crystals, mp 149—151.5 °C (from MeOH). ^{1}H-NMR δ: 0.68 (3H, s, 18-H$_3$), 0.90 (3H, d, J=6.3 Hz, 21-H$_3$), 1.03 (3H, s, 19-H$_3$), 3.50 (1H, m, 6′-Hax), 3.79 (1H, br s, 6-H), 3.93 (1H, m, 6′-Heq), 4.75 (1H, m, 2′-H). HR-FAB-MS *m/z* 491.4454 (MH$^+$). Calcd for $C_{32}H_{55}{}^2H_2O_3$; 491.4433.

[2α,3α-$^2H_2$]Cholest-5-en-3β-ol THP Ether (22) Dehydration of **21** (299 mg, 0.609 mmol) in the same manner as described for **17** gave, after recrystallization from MeOH, **22** (268 mg, 93%) as white crystals, mp 149—151.5 °C. ^{1}H-NMR δ: 0.68 (3H, s, 18-H$_3$), 0.91 (3H, d, J=7.1 Hz, 21-H$_3$), 1.01 (3H, s, 19-H$_3$), 3.50 (1H, m, 6′-Hax), 3.91 (1H, m, 6′-H), 5.35 (1H, s, 6-H). *Anal.* Calcd for $C_{32}H_{52}{}^2H_2O_2$: C, 81.29; H+^{2}H, 11.51. Found: C, 81.37; H, 12.00.

[2α,3α-$^2H_2$]Cholesterol (2c) Deprotection of **22** (268 mg, 0.566 mmol) in the same manner as described for **18** gave, after recrystallization from MeOH, **2c** (190 mg, 86%) as white crystals, mp 149.5—151 °C. ^{1}H-NMR δ: 0.68 (3H, s, 18-H$_3$), 0.91 (3H, d, J=6.6 Hz, 21-H$_3$), 1.01 (3H, s, 19-H$_3$), 5.35 (1-H, m, 6-H). ^{2}H-NMR δ: 1.82 (2α-^{2}H), 3.50 (3α-^{2}H). *Anal.* Calcd for $C_{27}H_{44}{}^2H_2O$: C, 83.44; H+^{2}H, 11.93. Found: C, 83.69; H, 12.23.

Incubation with the Hairy Roots of *Ajuga reptans* var. *atropurpurea* The hairy roots, maintained in solid Murashige–Skoog (MS) medium, were transferred sterilely into four 500 ml flasks each containing 250 ml liquid MS medium and preincubated on a rotary shaker (80 rpm) at 25 °C in the dark as described previously.[3] On day 14, the labeled sterol (100 mg of **2a**, **2b** or **2c**), dissolved in acetone (1 ml) and Tween 80 (1 ml), was added to the four flasks through a sterile membrane filter. Incubation was continued for another 14 and the roots were harvested. The roots (*ca.* 110 g wet wt) were mixed with sea sand and $CHCl_3$–MeOH and ground in a mortar with a pestle. The mixture was sonicated in $CHCl_3$–MeOH (1 : 1, 300 ml) for 1 h and filtered. The residue of the tissues was sonicated once again in the same solvent. The combined filtrate was concentrated *in vacuo*. The residue was dissolved in *n*-BuOH, washed with brine, and concentrated to dryness. The residue was taken up in $CHCl_3$–MeOH (1 : 1, 20 ml) and the soluble part was concentrated. Chromatography of the residue on silica-gel using a $CHCl_3$–MeOH gradient system give the ecdysteroid fraction (eluted with $CHCl_3$–MeOH, 7 : 1—4 : 1). This (*ca.* 60 mg) was further separated by preparative-TLC (developed twice with $CHCl_3$: MeOH = 7 : 1), and finally by HPLC (solvent, water–MeOH 1 : 1; flow rate, 6.0 ml/min; detector, 243 nm; retention time 21.3 min) to give 20-hydroxyecdysone (6.0 mg from **2a**, 4.1 mg from **2b** and 5.0 mg from **2c**).

Acknowledgments We are grateful to Dr. T. Matsumoto, Daicel Chemical Industries Ltd., for providing *Ajuga* hairy root cultures. This work was partially supported by a Grant-in-Aid for Scientific Research on Priority Areas from the Ministry of Education, Science, Sports and Culture.

References

1) Lafont R., Horn D. H. S., "Ecdysone," ed. by Koolman J., Thieme Med. Publ., New York, 1989, pp. 39—64.
2) Matsumoto T., Tanaka N., *Agric. Biol. Chem.*, **55**, 1019—1025 (1991).
3) Nagakari M., Kushiro T., Matsumoto T., Tanaka N., Kakinuma K., Fujimoto Y., *Phytochemistry*, **36**, 907—910 (1994).
4) Nagakari T., Kushiro T., Yagi T., Tanaka N., Matsumoto Y., Kakinuma K., Fujimoto Y., *J. Chem. Soc., Chem. Commun.*, **1994**, 1761—1762.
5) Fujimoto Y., Kushiro T., Nakamura K., *Tetrahedron Lett.*, **38**, 2697—2700 (1997).
6) Davies T. G., Dinan L. N., Lockley W. J. S., Rees H. H., Goodwin T.W., *Biochem. J.*, **194**, 53—62 (1981).
7) Fujimoto Y., Hiramoto M., Kakinuma K., Ikekawa N., *Steroids*, **53**, 477—485 (1989).
8) Davies T. G., Lockley W. J. S., Boid R., Rees H. H., Goodwin T. W., *Biochem. J.*, **190**, 537—544 (1980).
9) Aburatani M, Takeuchi T, Mori K., *Synthesis*, **1987**, 181—183.
10) Warren J. T., Sakurai S., Rountree D. B., Gilbert L. I., Lee S.-S., Nakanishi K., *Proc. Natl. Acad. Sci. U.S.A.*, **85**, 958—962 (1988).
11) Lloyd-Jones J. G., Rees, H. H., Goodwin, T. W., *Phytochemistry*, **12**, 569—572 (1973).
12) Greenwood D. R., Dinan L. N., Rees H. H., *Biochem. J.*, **217**, 783—789 (1984).
13) Kappler C., Kabbouh M., Durst F., Hoffmann J. A., *Insect Biochem.*, **16**, 25—32 (1986).
14) Kabbouh M., Kappler C., Hetru C., Durst F., *Insect Biochem.*, **17**, 1155—1161 (1987).
15) Nakagawa T., Hara N., Fujimoto Y., *Tetrahedron Lett.*, **38**, 2701—2704 (1997).
16) Barton D. H. R., Hesse R. H., Pedret M. M., Smith L. C., *J. Chem. Soc., Perkin 1*, **1979**, 1159—1165.

Structure-Specificity Relationship of Cardiac Glycosides as a Substrate for Glucohydrolase II

Yukimasa TERADA,*,[a] Rumi MISOI,[a] Naoharu WATANABE,[b] Martin HORNBERGER,[c] and Wolfgang KREIS[c]

Faculty of Pharmacy, Meijo University,[a] Yagotoyama, Tenpaku, Nagoya 468–8503, Japan, Department of Applied Biological Chemistry, Shizuoka University,[b] Ohya, Shizuoka 422–8529, Japan, and Lehrstuhl für Pharmazeutische Biologie, Friedrich-Alexander-Universität,[c] Staudstraße 5, 91058 Erlangen, Germany.

Received September 6, 1999; accepted November 25, 1999

Cardenolide glucohydrolase II (CGH II) is a cardenolide-specific glucohydrolase obtained from *Digitalis lanata* leaves. We investigated the structure–specificity relationship of several cardenolide disaccharides as a substrate for CGH II. Conformation analysis of the substrates was performed using molecular mechanics calculations. The sugar chain conformation of two inert glycosides was significantly different from that of the other glycosides. The other two glycosides, which were weak substrates of CGH II, were suggested to have an intramolecular hydrogen bond between the sugar groups. It was deduced that this hydrogen bond restricts the conformational change of the sugar chain and prevents the glycosides from enzymatic recognition.

Key words cardenolide glucohydrolase II (CGH II); cardiac glycoside; structure–specificity relationship; conformation analysis; molecular mechanics

The leaves of *Digitalis lanata* contain large amounts of cardiac glycosides, most of which belong to a group termed primary glycosides. The common feature of these glycosides is a terminal glucose residue at the end of the sugar side chain.[1] During the isolation of primary cardiac glycosides, enzymatic hydrolysis may occur that leads to the so-called secondary glycosides.

Stoll *et al.*[2] reported the enzyme activities in *Digitalis* leaves capable of hydrolyzing primary glycosides to their corresponding secondary glycosides. Since then, two cardenolide-specific glucohydrolases termed cardenolide glucohydrolase I (CGH I) and cardenolide glucohydrolase II (CGH II) have been isolated from various *Digitalis* species. CGH I characteristically hydrolyzes cardenolide tetrasaccharides,[3] whereas CGH II is specific for the cardenolide disaccharides.[4] Glucoevatromonoside (**1**) is the main substrate of CGH II and the velocity of the deglucosylation decreases by the substitution of the inner sugar (digitoxose) with glucose (**2**), glucomethylose (**3**), fucose (**5**), and digitalose (**6**) (for structural formulas, see Fig. 1 and Table 1).

In this paper, the substrate selectivity of CGH II is discussed in connection with the sugar chain conformation of the cardiac glycosides. The Search-Compare routine of the Insight II program package[5] was used to scan all possible conformations of the genin–sugar and sugar–sugar linkages. It was inferred that an intramolecular hydrogen bond restricts the rotation of the sugar–sugar linkage and this may hinder the conformational change relevant to the enzymatic recognition.

Experimental

The cardenolide disaccharides are hydrolyzed as substrates for CGH II releasing the terminal glucose. The molecular structures of the substrates studied in this work are shown in Fig. 1 and Table 1. The relative velocity of the deglucosylation is shown in Table 1, and the detailed kinetic constants of the catalytic deglucosylation by CGH II will be reported by Hornberger and Kreis[4].

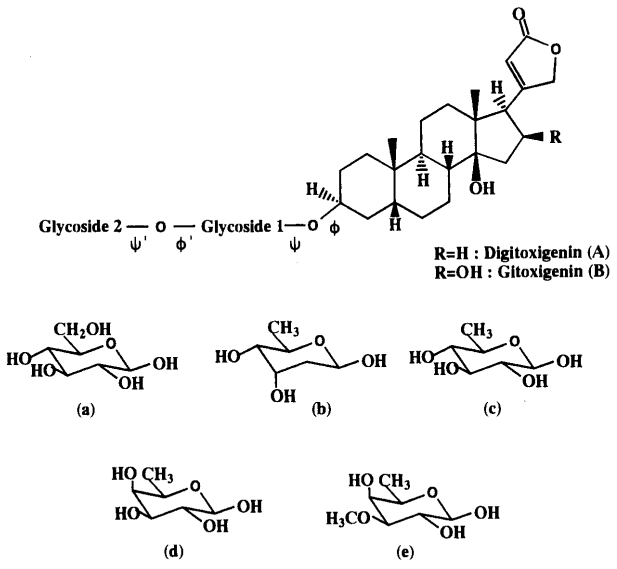

Fig. 1. Chemical Structures of the Cardenolide Genins and Sugars Occurring in the Cardiac Glycosides in the Text

(a) β-D-glucose, (b) β-D-digitoxose, (c) β-D-glucomethylose, (d) β-D-fucose and (e) β-D-digitalose.

Table 1. Structure and Deglucosylation Velocity of the Cardiac Glycosides

Compound	Genin[a]	Glycoside 1	Glycoside 2	Velocity at 1 mM substrate (%)[b]
Glucoevatromonoside (**1**)	A	β-D-digitoxose	β-D-glucose	100
Cellobioside (**2**)	A	β-D-glucose	β-D-glucose	52
Glucodigimethyloside (**3**)	A	β-D-glucomethylose	β-D-glucose	38
Glucogitroside (**4**)	B	β-D-digitoxose	β-D-glucose	33
Glucodigifucoside (**5**)	A	β-D-fucose	β-D-glucose	0
Glucodigitaloside (**6**)	A	β-D-digitalose	β-D-glucose	0

a) See Fig. 1. *b*) Substrate preferences of CGH II (see ref. 4).

* To whom correspondence should be addressed.

© 2000 Pharmaceutical Society of Japan

Table 2. The Calculated Energy and the Geometry of the Conformations within 1.8 kcal/mol of the Global Minimum

Compound		Relative energy (kcal mol^{-1})	Dihedral angle (°)[a]				H···O Distance[b] (Å)
			ϕ	Ψ	ϕ'	Ψ'	
Glucoevatromonoside (**1**)	1	0.00	−89	172	103	170	3.40
	2	0.00	−89	172	102	170	3.37
	3	0.00	−89	172	75	153	2.42
	4	0.05	−89	172	101	169	3.32
	5	0.44	−131	177	103	170	3.41
	6	0.44	−131	177	103	170	3.39
	7	0.44	−131	177	103	170	3.38
	8	0.44	−131	177	75	153	2.42
	9	0.44	−124	176	103	170	3.41
	10	0.80	−89	172	88	98	3.19
	11	0.91	−145	−169	123	179	4.03
	12	1.24	−131	177	88	98	3.19
	13	1.24	−130	177	88	98	3.19
	14	1.24	−132	177	89	97	3.20
	15	1.25	−145	−180	118	−77	4.58
	16	1.26	−130	176	88	100	3.15
	17	1.58	−89	172	114	−74	4.52
Cellobioside (**2**)	1	0.00	150	169	103	164	1.72
	2	0.93	150	169	103	164	1.72
	3	1.40	109	174	103	164	1.72
	4	1.40	108	174	103	164	1.72
	5	1.40	110	174	103	164	1.72
	6	1.40	112	174	103	164	1.72
Glucodigimethyloside (**3**)	1	0.00	−89	169	107	169	1.73
	2	0.49	−127	174	107	169	1.73
	3	0.49	−128	174	107	169	1.73
	4	0.49	−128	174	107	169	1.73
	5	0.49	−129	174	107	169	1.73
	6	0.49	−130	174	107	169	1.73
	7	1.01	−145	−170	112	178	1.73
	8	1.02	−150	95	107	169	1.78
	9	1.18	−104	−80	107	169	1.73
	10	1.54	−162	−115	107	170	1.73
Glucogitroside (**4**)	1	0.00	−89	172	103	170	3.41
	2	0.00	−89	172	103	170	3.40
	3	0.00	−89	172	102	169	3.36
	4	0.01	−89	172	75	153	2.43
	5	0.01	−89	172	75	153	2.41
	6	0.03	−89	172	105	172	3.47
	7	0.43	−131	177	103	170	3.40
	8	0.44	−131	177	75	153	2.42
	9	0.80	−89	172	88	98	3.19
	10	0.94	−145	−170	123	179	4.03
	11	1.23	−131	177	88	98	3.19
	12	1.29	−145	−180	118	−77	4.58
	13	1.58	−89	172	114	−74	4.51
Glucodigifucoside (**5**)	1	0.00	−141	−178	−99	135	3.99
	2	0.08	−139	−179	61	155	1.87
	3	0.08	−139	−179	61	155	1.87
	4	0.09	−139	−178	61	155	1.87
	5	0.14	−91	170	61	155	1.84
	6	0.58	−109	81	68	156	2.03
	7	0.99	−164	−111	−95	134	3.96
	8	1.02	−109	74	63	155	1.92
	9	1.18	−89	169	−97	137	3.95
	10	1.24	−147	94	62	155	1.85
	11	1.33	−118	−76	64	156	1.90
	12	1.67	−110	81	68	156	2.03
Glucodigitaloside (**6**)	1	0.00	−139	−179	−112	134	—
	2	0.03	−144	−174	−101	170	—
	3	0.07	−165	−109	−92	175	—
	4	0.41	−144	−176	−107	168	—
	5	0.77	−89	169	−96	175	—
	6	0.77	−166	−112	−90	175	—
	7	0.97	−132	177	−140	87	—
	8	1.10	−134	177	−95	175	—
	9	1.15	−88	168	−97	176	—
	10	1.62	−88	169	−140	87	—
	11	1.64	−113	−78	−143	89	—
	12	1.71	−117	−77	−143	89	—

a) ϕ: C4-C3-O-C1′; Ψ: C3-O-C1′-C2′; ϕ': C3′-C4′-O-C1″; Ψ': C4′-O-C1″-C2″. *b*) Non-bonding distance between the C3′-OH and the glucopyranosyl oxygen. Hydrogen bond is plausible to the underlined distance.

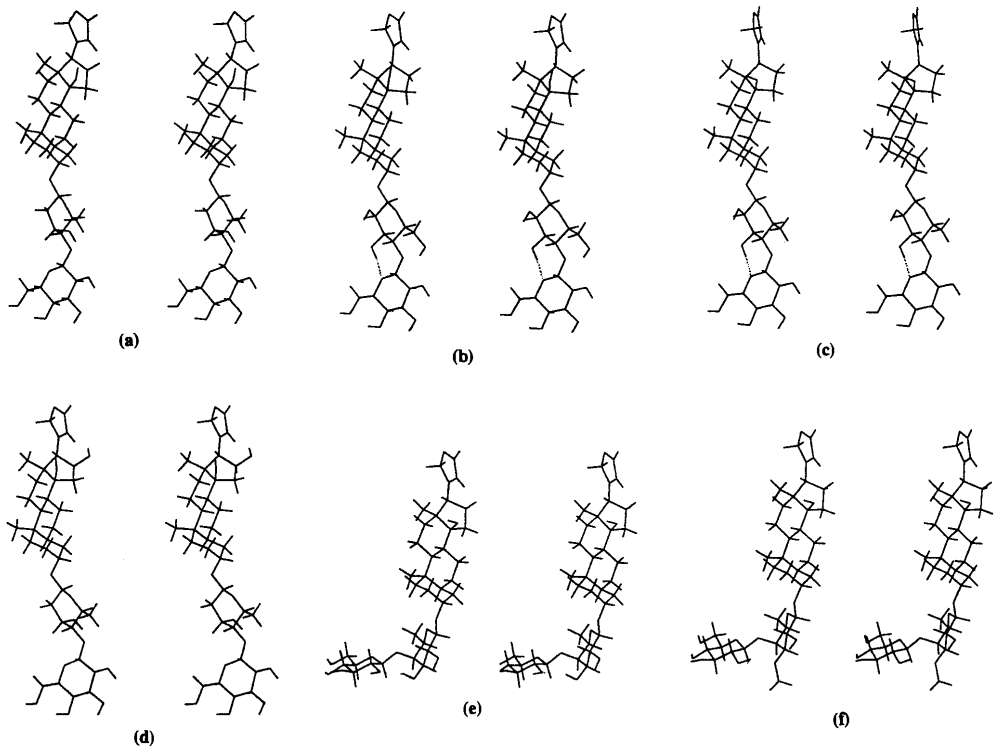

Fig. 2. Stereoview of the Most Stable Conformation of the Cardiac Glycosides

A broken line shows the possible hydrogen bond. (a) glucoevatromonoside (**1**), (b) cellobioside (**2**), (c) glucodigimethyloside (**3**), (d) glucogitoroside (**4**), (e) glucodigifucoside (**5**) and (f) glucodigitaloside (**6**).

The conformational analysis of the individual substrate was performed by using Insight II[5] and Discover[6] modeling and simulation softwares on an O2 workstation (OS: IRIX 5.2) from Silicon Graphics.

Starting coordinates were generated by using the drawing tool of Insight II,[5] and geometry optimization was carried out using the CFF91 force field of the Discover program.[6] All calculations were performed in a vacuum. In the CFF91 force field, hydrogen bonds are a natural consequence of the standard van der Waals and electrostatic parameters, thus hydrogen bond functions were not used in particular. The dielectric constant (relative permittivity) was 1.00 and the cutoff distance was 9.5 Å. The optimization was terminated when average derivatives reached less than 0.01 kcal/mol·Å or at 5000 iterations.

The three cyclohexane rings of the digitoxigenin framework were assumed to be in the chair form as reported by Allinger and Wu.[7] The orientation of the butenolide ring was not specified during the entire calculation process. The intramolecular flexibility was then completely optimized using the CFF91 force field of the Discover program. Subsequently, the four bonds, namely C3-O (ϕ), O-C1′ (Ψ), C4′-O (ϕ'), and O-C1″ (Ψ'') (Fig. 1), were rotated in increments of 60° using the Search-Compare routine. Among the numerous conformations thus generated, the conformers that had atoms within the van der Waals contact zone were automatically eliminated. In this elimination step, the van der Waals radius of all atoms was reduced by 70% of the default value in order to get sufficient conformations. Starting from these conformations, structural optimization by the CFF91 force field was again performed. During this geometry optimization, all internal coordinates including the four dihedral angles were relaxed.

Results

The four C–O bonds, which define the overall shape of the molecule, were rotated in increments of 60° and the conformers without the van der Waals contact were selected using the Search-Compare routine. After the energy minimization of these conformers, each cardiac glycoside resulted in dozens of stable conformations. However, the results include a number of similar conformations with comparable total energy and similar dihedral angles. This means that there are only a few low barriers on the potential energy hypersurface. Therefore, even when the starting conformers have a dihedral difference of more than 60°, they can converge to the same conformation overcoming energy barriers in the minimization process. In Table 2, we have listed the low energy conformations within 1.8 kcal/mol of the global minimum, since a 1.8 kcal energy difference indicates that 95% of the conformers exist in the stable form. In this table, the four dihedral angles (ϕ, Ψ, ϕ', and Ψ') and the nonbonded distance between the hydrogen atom of C3′-OH of the inner sugar and the oxygen atom of the terminal glucopyranose ring are also shown. A hydrogen bond was assumed when the H···O distance was shorter than 1.8 Å, because the distance between the electronegative atoms in the hydrogen bond is usually in the range of 2.5—2.7 Å.[8] The appearance of the most stable conformation of each compound is shown in Fig. 2.

Discussion

The overall conformation of cardiac glycosides is defined by three fragments having the ability to rotate around the four C–O bonds. One of these fragments is the digitoxigenin group that is rigid except for the rotation of the butenolide ring. The others are the sugar rings, which take the chair conformation. The mutual positions of the genin and the saccharide fragments play a crucial role with respect to the overall shape of the cardiac glycosides. When a cardenolide disaccharide reacts under the catalytic control of CGH II, the genin and the two saccharide fragments must fit into the active site of the enzyme. As glucoevatromonoside (**1**) is the best substrate for CGH II, this molecule can take the best position and orientation in the enzyme's active site. Contrarily, there must be some reason that the other less reactive compounds can not fit as well as compound **1**. The conforma-

tional analysis was thus performed on the six cardiac glycosides.

On the structure optimizing calculations, the resulting minimum energy geometry generally depends on the starting geometry.[9] Hence, all possible rotations in the starting geometry must be examined in order to reach the global minimum. Moreover, when the structure of the enzyme's active site is unknown, it is often assumed that even though the bioactive conformation is not the global minimum, they are not very different from each other. Because a compound should be more active if a smaller energy is required to attain the correct spatial relationship to the enzyme.[10]

Since compounds **5** and **6** have a β-axial 1–4 connected sugar chain, the position of the terminal glucose is significantly different from that of the other cardiac glycosides as can be seen in Fig. 2. Therefore, these glycosides can not be recognized by CGH II.

The other cardiac glycosides have an α-equatorial 1–4 connection between the sugars, therefore, they are similar in overall shape. Besides, cellobioside (**2**) and glucodigimethyloside (**3**) have a 3β-equatorial OH group on the inner sugar, and this OH group is expected to form a hydrogen bond with the pyranose oxygen of the terminal glucose. Actually, all conformations of **2** and **3** listed in Table 2 have a short H···O distance possible to form a hydrogen bond (seen also Fig. 2). On the other hand, the corresponding OH group of **1** is 3α-axial, therefore, it is too distant from the glucopyranose oxygen to form a hydrogen bond. No conformation of **1** in Table 2 has the possibility of a hydrogen bond. The terminal glucose of **1** can then easily take an essential position to form the effective complex with CGH II. Contrarily, the intramolecular hydrogen bond of **2** and **3** should restrict the movement of the terminal glucose and, therefore, should prevent the formation of the enzyme-substrate complex. Accordingly, the reaction rate must decrease.

Glucodigimethyloside (**4**) has the same sugar chain as **1**, so they can take the same conformation. Compound **4**, however, has an OH group in position 16 of the gitoxigenin framework. This OH group may cause a crucial steric hindrance to the enzyme active site. Consequently, the reaction rate of **4** must slow down.

In conclusion, the orientation of the terminal glucose with respect to the genin group must play an important role in the formation of the enzyme-substrate complex. A detailed knowledge of the properties and substrate preferences of the enzymes involved in the glycoside formation and hydrolysis will help us to understand the cardenolide pathway, its regulation and the biosynthetic relationship among the individual cardenolides.[11] Our present work contributes to the understanding of the structure and properties of the cardenolide glucohydrolase.

References and Notes

1) Wichtl M., Mangkudidjojo M., *Pharm. Zeitung*, **129**, 686—689 (1984).
2) Stoll A., Hoffmann A., Kreis W., *Hoppe-Seyler's Z. Physiol. Chem.*, **235**, 249—264 (1935).
3) May U., Kreis W., *Plant Physiol. Biochem.*, **35** (7), 523—532 (1997).
4) Hornberger M., Kreis W., *Plant Physiol. Biochem.*, in press.
5) Insight II Program Package, ver. 95.0, Biosym/MSI, San Diego, CA, U.S.A. (1995).
6) Discover Program Package, ver. 2.9.7, Biosym/MSI, San Diego, CA, U.S.A. (1995).
7) Allinger N. L., Wu F., *Tetrahedron*, **27**, 5093—5113 (1971).
8) Bowden K., "Comprehensive Medicinal Chemistry," Vol. 4, ed. by Hansch C., Pergamon Press, Oxford, 1990, pp. 220—221.
9) Burkert U., Allinger N. L., "Molecular Mechanics," ACS Monograph, **177**, 1982, pp. 59—78.
10) Pettersson I., Liljefors T., *J. Comput.-Aid. Mol. Des.*, **1**, 143—152 (1987).
11) Theurer C., Treumann H.-J., Faust T., May U., Kreis W., *Plant Cell, Tissue and Organ Culture*, **38**, 327—335 (1994).

Sesquiterpenoid Derivatives from *Ferula ferulioides*. IV[1)]

Keisuke KOJIMA,*[,a] Kimio ISAKA,[a] Purev ONDOGNII,[b] Oyun ZEVGEEGIIN,[c] Purevsuren GOMBOSURENGYIN,[c] Khishgee DAVGIIN,[c] Hajime MIZUKAMI,[a] and Yukio OGIHARA[a]

Faculty of Pharmaceutical Sciences, Nagoya City University,[a] 3–1 Tanabe-Dori, Mizuho-ku, Nagoya 467–8603, Japan, Institute of Chemistry, Mongolian Academy of Sciences,[b] Ulaanbaatar 51, Mongolia and Centre for Mongolian Traditional Medicine,[c] Ulaanbaatar 36, Mongolia. Received September 9, 1999; accepted November 9, 1999

Four novel prenyl-furocoumarin type sesquiterpenoid derivatives, 2,3-dihydro-7-hydroxy-2*S,3*R**-dimethyl-3-[4,8-dimethyl-3(*E*),7-nonadienyl]-furo[3,2-*c*]coumarin, 2,3-dihydro-7-hydroxy-2*R**,3*R**-dimethyl-3-[4,8-dimethyl-3(*E*),7-nonadienyl]-furo[3,2-*c*]coumarin, 2,3-dihydro-7-hydroxy-2*S**,3*R**-dimethyl-3-[4-methyl-5-(4-methyl-2-furyl)-3(*E*)-pentenyl]-furo[3,2-*c*]coumarin, and 2,3-dihydro-7-methoxy-2*S**,3*R**-dimethyl-3-[4,8-dimethyl-3(*E*),7-nonadienyl]-furo[3,2-*c*]coumarin were isolated from the roots of *Ferula ferulioides*. Their structures were established by detailed spectral analysis and the biosynthetic pathway leading to these prenyl-furocoumarin type sesquiterpenoids is proposed based on these structures.**

Key words *Ferula ferulioides*; Umbelliferae; sesquiterpenoid; prenyl-furocoumarin

Ferula ferulioides (STEUD.) KOROVIN (Umbelliferae) grows in Bulgan Somon, Hovd City, Mongolia, and has been used as a traditional medicine for the treatment of spasm. In previous papers,[1—3)] we reported the isolation of prenyl-acetophenone (**1**—**4**), prenyl-benzofuranone (**5**), and prenyl-benzoyl-furanone type (**6**—**8**) sesquiterpenoid derivatives from this plant. The present paper deals with the isolation and the structural elucidation of four novel prenyl-furocoumarin type sesquiterpenoid derivatives from *F. ferulioides*.

The dried and powdered roots were extracted with methanol, and removal of the solvent gave a waxy solid which was successively extracted with ethyl acetate and water. From the ethyl acetate extract, four novel prenyl-furocoumarin type sesquiterpenoids (**9**—**12**) were isolated and identified.

The molecular formula of compound **9** was determined as $C_{24}H_{30}O_4$ ($[M]^+$ at *m/z* 382.2145) by high-resolution mass spectrometry (HR-MS). The ^{1}H-NMR and ^{13}C-NMR spectra of **9** showed the presence of a 1,2,4-trisubstituted benzene ring (δ_H 6.83, 7.10, 7.53), three olefinic-methyl groups (δ_H 1.55, 1.58, 1.67; δ_C 16.0, 17.7, 25.7), two trisubstituted double bonds (δ_H 5.06, 5.10), an ester (δ_C 161.5), and two quaternary carbon signals at δ_C 105.9, 166.2 assigened to C-3a and C-9b. In addition, the characteristic absorption of a carbonyl group (ν 1701 cm^{-1}) in the IR spectrum of **9** supported the presence of a conjugated δ-lactone structure in this compound. These spectral data were similar to those of 3-alkyl-4-hydroxy coumarin derivatives.[4—6)]

The NMR signals assigned to an oxyl group at a methine (δ_H 4.89, q, J=7 Hz; δ_C 89.9) attached to a secondary methyl group (δ_H 1.45, d, J=7 Hz; δ_C 15.8) and to a tertiary methyl group (δ_H 1.29; δ_C 19.2) at C-3 revealed the presence of a dimethyldihydrofuran moiety.

We confirmed the location of coumarin, furan, and prenyl side-chains based on the heteronuclear multiple bond correlation (HMBC) spectrum, and the correlation peaks are shown in Fig. 1. The structure of the side-chain was deduced from nuclear Overhauser and exchange spectroscopy (NOESY) experiments, in which cross-peaks were observed from H-3″/H-5″ and H-7″/H-9″ pairs. This indicated an *E* configuration for the C-3″—C-4″ double bond. Compound **9** was, thus, identified as 2,3-dihydro-7-hydroxy-2,3-dimethyl-3-[4,8-dimethyl-3(*E*),7-nonadienyl]-furo[3,2-*c*]coumarin.

Compound **9** is presumably a racemate of the chiral centers, C-2 and C-3, because it exhibited an optical rotation of ±0° ($[\alpha]_D^{22}$). HPLC analysis using a chiral column produced two peaks as shown in Fig. 2, confirming that **9** is a racemic mixture.

Compound **10** had an $[M]^+$ peak at *m/z* 382.2144 ($C_{24}H_{30}O_4$) but the ^{1}H- and ^{13}C-NMR spectra of **10** were slightly different from **9**, especially $Me_{C\text{-}2}$ and $Me_{C\text{-}3}$ (**9**: δ_H 1.45, 1.29, **10**: δ_H 1.54, 1.45). The HMBC experiment suggested that the planar structure of **10** was the same as that of **9**. Therefore, **10** may be diastereomer of **9** at chiral centers

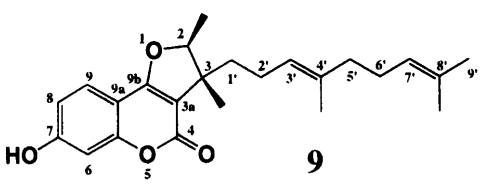

9

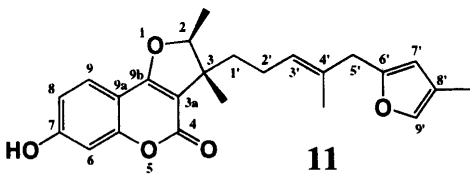

11

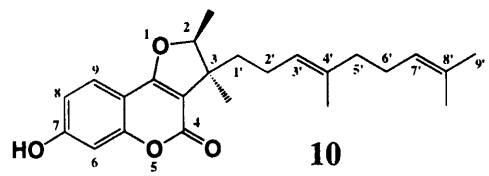

10

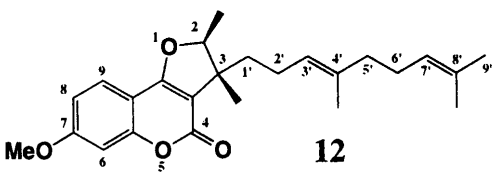

12

* To whom correspondence should be addressed.

© 2000 Pharmaceutical Society of Japan

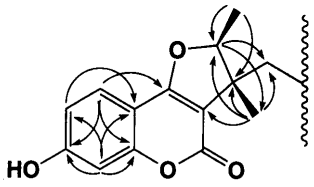

Fig. 1. HMBC Spectrum (H→C) of **9**

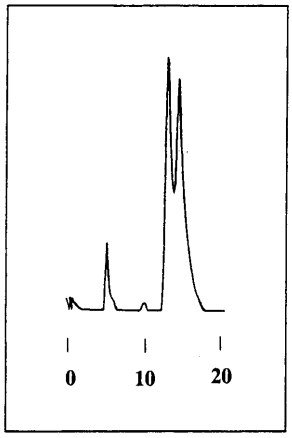

Fig. 2. HPLC Separation Using a Chiral Column
Column: Chiralcel OD, solvent: hexane/2-propanol (93 : 7), wavelength: 221 nm.

C-2, C-3. A series of NOESY experiments was carried out with **9** and **10** to identify the relative stereochemistry of the dimethyldihydrofuran moiety at C-2 and C-3. Cross-peaks were observed from the pairs: H-2/H-Me_{C-3} in **10**, but not in **9**. These nuclear Overhauser effects (NOE) indicated that the relationship between the Me_{C-2} and Me_{C-3} is *cis* in **9**, and *trans* in **10**. Thus, compounds **9** and **10** were assigned to be 2,3-dihydro-7-hydroxy-2*S**,3*R**-dimethyl-3-[4,8-dimethyl-3(*E*),7-nonadienyl]-furo[3,2-*c*]coumarin, 2,3-dihydro-7-hydroxy-2*R**,3*R**-dimethyl-3-[4,8-dimethyl-3(*E*),7-nonadienyl]-furo[3,2-*c*]coumarin, respectively.

Compound **11** had an $[M]^+$ peak at *m/z* 394.1776 ($C_{24}H_{26}O_5$). The ^{1}H- and ^{13}C-NMR spectra of **11** were similar to those of **9** except for the presence of a 4-methyl-2-furyl system (δ_H 1.97, 5.84, 7.04; δ_C 9.8, 108.8, 120.5, 137.7, 154.2) at C-5″ in place of the trisubstituted olefin present in **9**. Compound **12** had an $[M]^+$ peak at *m/z* 396.2301 ($C_{25}H_{32}O_4$). The ^{1}H- and ^{13}C-NMR spectra of **12** were similar to those of **9**, except for the presence of a methoxyl group (δ_H 3.86; δ_C 55.7) at C-7. A series of NOESY experiments with **11** and **12** indicated that their stereochemistry is the same as that of **9**. The chemical shifts of the ^{1}H- and ^{13}C-NMR spectra were very similar for compounds **9**, **11** and **12**, indicating that they have the same relative stereochemistry, *i.e.* a *cis*-relationship between the Me_{C-2} and Me_{C-3}. In contrast, the chemical shifts of these compounds were slightly different from those of **10** which have a *trans*-relationship between the Me_{C-2} and Me_{C-3}. Thus, compounds **11** and **12** were assigned to be 2,3-dihydro-7-hydroxy-2*S**,3*R**-dimethyl-3-[4-methyl-5-(4-methyl-2-furyl)-3(*E*)-pentenyl]-furo[3,2-*c*]-coumarin, 2,3-dihydro-7-methoxy-2*S**,3*R**-dimethyl-3-[4,8-dimethyl-3(*E*),7-nonadienyl]-furo[3,2-*c*]coumarin, respectively.

Like compound **9**, compounds **10**—**12** were racemates, since they were optically inactive.

To our knowledge, this is the first report of the isolation of 3-prenyl-furocoumarin type sesquiterpenoid derivatives, in which the prenyl side-chain is attached to the C-3 position of furocoumarin moiety.

In previous papers, we proposed a biosynthetic pathway leading to the sesquiterpenoid compounds **1**—**8** isolated from *F. ferulioides*.[1—3] Isolation of the compounds **9**—**12** described in this paper suggests the presence of an additional biosynthetic route arising from the hypothetical precursor C as described below (Fig. 3).

Rearrangement of the C6—C3 moiety of the intermediate C to C-2 position of the farnesyl moiety may lead to formation of a hypothetical intermediate E, which is then converted to compounds **6**—**8** by intramolecular esterification, as proposed in the previous paper. On the other hand, hydroxylation of the vinyl group of the intermediate C through hydration leads to formation of another hypothetical intermediate F, which is then converted to the third hypothetical intermediate G by intramolecular esterification. Furthermore, dehydration of G leads to compounds **9**—**12**.

Some prenylated coumarins, including furo[3,2-*c*]coumarins and pyrano[3,2-*c*]coumarins, were isolated from *Ferula communis*, which was identified as the causative agent of a severe haemorrhagic condition.[7—10] It has also been reported that the prenylated coumarins isolated from *F. communis* exhibit haemorrhagic activity.[7]

It will be interesting to examine the pharmacological activity of the sesquiterpenoid derivatives isolated from *F. ferulioides*.

Experimental

General Procedures NMR spectra were recorded on a JEOL JNM-A500 spectrometer in $CDCl_3$ with tetramethylsilane (TMS) as an internal standard. Electron impact mass spectra (EI-MS) were recorded on a JEOL JMS-DX300 spectrometer. Optical rotation was measured with a JASCO DIP-4 digital polarimeter. IR spectra were recorded on a Shimadzu FT-IR-8100 spectrometer.

Plant Material The roots of *Ferula ferulioides* (STEUD.) KOROVIN were collected in July 1996 at Bulgan Somon, Hovd City. Voucher specimens have been deposited in the Botanical Department of the Mongolian State University.

Extraction and Isolation The dried and pulverized roots of *Ferula ferulioides* (400 g) were extracted successively with methanol under reflux. After evaporation of the solvent, part of the methanol extract (40 g) was partitioned between ethyl acetate and water. The ethyl acetate layer was evaporated under reduced pressure and the residue was chromatographed on silica gel with hexane–ethyl acetate (10 : 1—1 : 1) to afford twelve fractions. Fraction 2 was subjected to RP-18 Lober chromatography (80% CH_3CN) to give **12** (10 mg); fr. 7 was subjected to RP-18 Lober chromatography (45—65% CH_3CN) to give **9** (3 mg) and **10** (3 mg); fr. 7 was subjected to RP-18 Lober chromatography (65% CH_3CN) to give **11** (3 mg).

2,3-Dihydro-7-hydroxy-2*S**,3*R**-dimethyl-3-[4,8-dimethyl-3(*E*),7-nonadienyl]-furo[3,2-*c*]coumarin (**9**): Oil, $[\alpha]_D^{23}=\pm0°$ (c=0.3, $CHCl_3$), EI-MS *m/z*: 382 $[M]^+$, 231 $[C_{13}H_{11}O_4]^+$, HR-MS *m/z*: 382.2145 $[M]^+$ (Calcd for $C_{24}H_{30}O_4$: 382.2144), IR ν_{max} ($CHCl_3$): 1701 cm^{-1}. ^{1}H-, ^{13}C-NMR: Tables 1, 2.

2,3-Dihydro-7-hydroxy-2*R**,3*R**-dimethyl-3-[4,8-dimethyl-3(*E*),7-nonadienyl]-furo[3,2-*c*]coumarin (**10**): Oil, $[\alpha]_D^{23}=\pm0°$ (c=0.3, $CHCl_3$), EI-MS *m/z*: 382 $[M]^+$, 231 $[C_{13}H_{11}O_4]^+$, HR-MS *m/z*: 382.2144 $[M]^+$ (Calcd for $C_{24}H_{30}O_4$: 382.2144), IR ν_{max} ($CHCl_3$): 1705 cm^{-1}. ^{1}H-, ^{13}C-NMR: Tables 1, 2.

2,3-Dihydro-7-hydroxy-2*S**,3*R**-dimethyl-3-[4-methyl-5-(4-methyl-2-furyl)-3(*E*)-pentenyl]-furo[3,2-*c*]coumarin (**11**): Oil, $[\alpha]_D^{23}=\pm0°$ (c=0.9, $CHCl_3$), EI-MS *m/z*: 394 $[M]^+$, 231 $[C_{13}H_{11}O_4]^+$, HR-MS *m/z*: 394.1776 $[M]^+$ (Calcd for $C_{24}H_{26}O_5$: 394.1780), IR ν_{max} ($CHCl_3$): 1701 cm^{-1}. ^{1}H-, ^{13}C-NMR: Tables 1, 2.

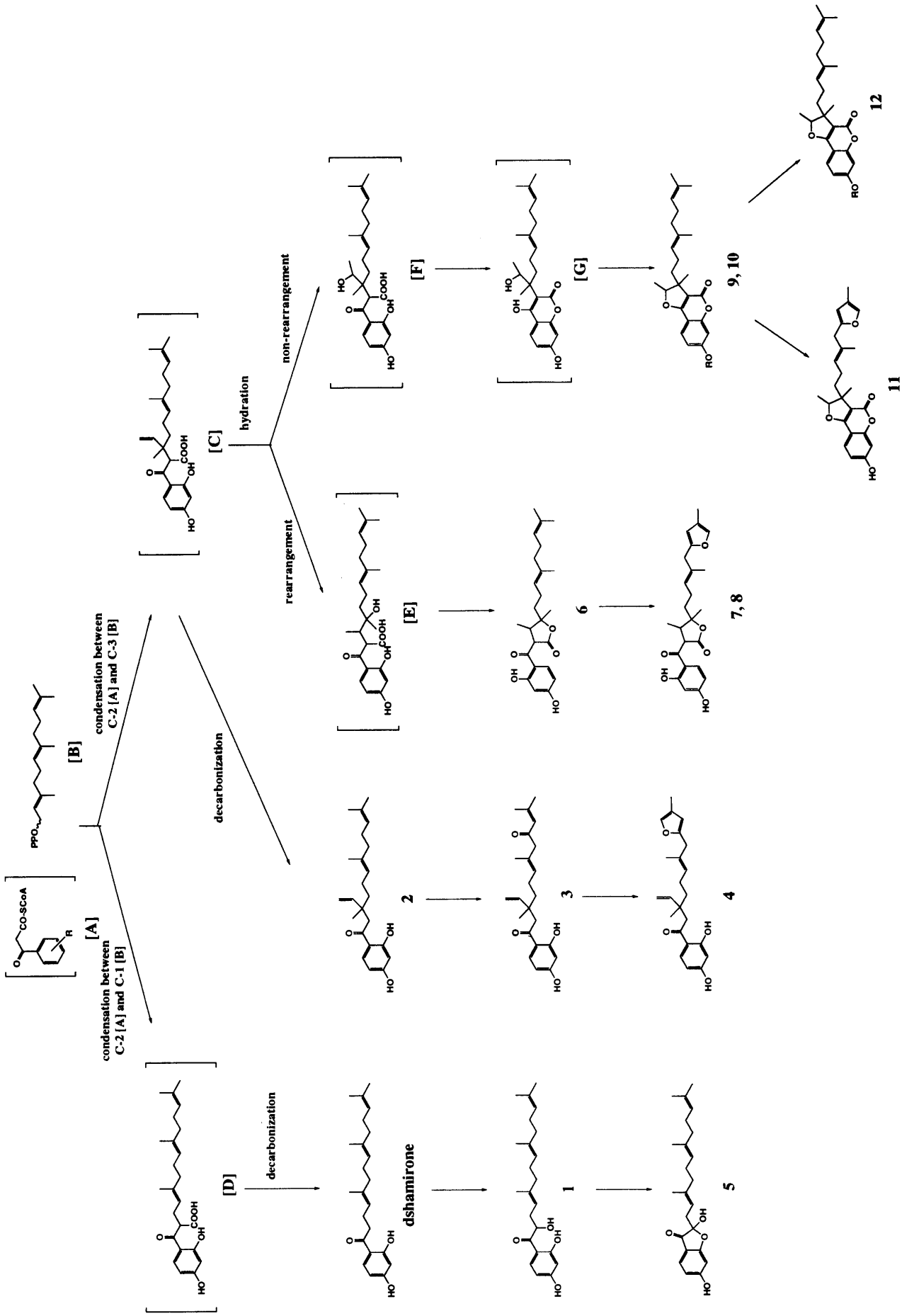

Fig. 3. Proposed Biosynthesis Pathway of the Sesquiterpenoid Derivatives in *Ferula ferulioides*

Compounds **1**—**12** and dshamirone were isolated from *F. ferulioides*. The compounds in brackets are hypothetical precursors, not isolated so far. The pairs of compounds **7**, **8** and **9**, **10** are stereoisomers.

Table 1. ^{1}H-NMR Spectral Data of Compounds **9**—**12** in $CDCl_3$

	9	**10**	**11**	**12**
2	4.89 (1H, q, J=7 Hz)	4.62 (1H, q, J=7 Hz)	4.88 (1H, d, J=6.5 Hz)	4.88 (1H, q, J=7 Hz)
6	7.10 (1H, d, J=2 Hz)	6.96 (1H, d, J=2 Hz)	7.05 (1H, d, J=2 Hz)	6.84 (1H, br s)
8	6.83 (1H, dd, J=2, 9 Hz)	6.79 (1H, dd, J=2, 9 Hz)	6.82 (1H, dd, J=2, 9 Hz)	6.83 (1H, dd, J=2, 9 Hz)
9	7.53 (1H, d, J=9 Hz)	7.53 (1H, d, J=9 Hz)	7.52 (1H, d, J=9 Hz)	7.53 (1H, d, J=9 Hz)
1′	1.72 (2H, m)	1.66 (2H, m)	1.81 (2H, m)	1.72 (2H, m)
2′	1.98 (2H, m)	1.95 (2H, m)	2.01 (2H, m)	1.92 (2H, m)
3′	5.10 (1H, t, J=7 Hz)	5.04[a]	5.19 (1H, t, J=7 Hz)	5.11 (1H, t, J=7 Hz)
5′	1.95 (2H, m)	1.91 (2H, m)	3.18 (2H, s)	1.94 (2H, m)
6′	2.02 (2H, m)	1.99 (2H, m)		2.04 (2H, m)
7′	5.06 (1H, t, J=7 Hz)	5.04[a]	5.84 (1H, br s)	5.07 (1H, t, J=7 Hz)
9′	1.67 (3H, s)	1.66 (3H, s)	7.04 (1H, br s)	1.67 (3H, s)
2Me	1.45 (3H, d, J=7 Hz)	1.54 (3H, d, J=7 Hz)	1.44 (3H, d, J=6.5 Hz)	1.45 (3H, d, J=7 Hz)
3Me	1.29 (3H, s)	1.45 (3H, s)	1.29 (3H, s)	1.29 (3H, s)
4′Me	1.55 (3H, s)	1.50 (3H, s)	1.56 (3H, s)	1.56 (3H, s)
8′Me	1.58 (3H, s)	1.57 (3H, s)	1.97 (3H, s)	1.59 (3H, s)
OMe				3.86 (3H, s)

a) Overlapped by other signals.

Table 2. ^{13}C-NMR Spectral Data of Compounds **9**—**12** in $CDCl_3$

	9	**10**	**11**	**12**
2	89.9	93.2	89.8	89.7
3	46.9	46.7	46.9	47.0
3a	105.9	106.0	105.9	106.2
4	161.5	161.5	161.2	160.6
5a	156.7	156.8	156.7	157.0
6	103.2	103.2	103.2	100.6
7	160.5	159.8	160.2	163.2
8	113.2	112.7	113.0	112.2
9	124.3	124.2	124.1	123.7
9a	106.0	106.3	106.0	106.3
9b	166.2	166.4	166.1	165.5
1′	38.3	34.8	38.1	38.3
2′	23.4	23.4	23.5	23.4
3′	123.6	124.0	125.9	123.7
4′	135.6	135.2	132.4	135.6
5′	39.6	39.6	38.3	39.7
6′	26.6	26.7	154.2	26.7
7′	124.1	124.3	108.8	124.3
8′	131.4	131.3	120.5	131.4
9′	25.7	25.7	137.7	25.7
2Me	15.8	13.9	15.8	15.8
3Me	19.2	23.5	19.2	19.2
4′Me	16.0	16.0	15.9	16.0
8′Me	17.7	17.7	9.8	17.7
OMe				55.7

2,3-Dihydro-7-methoxy-2*S**,3*R**-dimethyl-3-[4,8-dimethyl-3(*E*),7-nonadienyl]-furo[3,2-*c*]coumarin (**12**): Oil, $[\alpha]_D^{23}=\pm 0°$ (c=0.8, $CHCl_3$), EI-MS m/z: 396 $[M]^+$, 245 $[C_{14}H_{13}O_4]^+$, HR-MS m/z: 396.2301 $[M]^+$ (Calcd for $C_{25}H_{32}O_4$: 396.2300), IR ν_{max} ($CHCl_3$): 1707 cm^{-1}. ^{1}H-, ^{13}C-NMR: Tables 1, 2.

References

1) Kojima K., Isaka K., Purev O., Oyun Z., Khishgee D., Mizukami H., Ogihara Y., *Chem. Pharm. Bull.*, **47**, 1145—1147 (1999).
2) Kojima K., Isaka K., Purev O., Jargalsaikhan G., Suran D., Mizukami H., Ogihara Y., *Chem. Pharm. Bull.*, **47**, 690—691 (1999).
3) Kojima K., Isaka K., Purev O., Jargalsaikhan G., Suran D., Mizukami H., Ogihara Y., *Chem. Pharm. Bull.*, **46**, 1781—1784 (1998).
4) Lamnaouer D., Bodo B., Martin M.-T., Molho D., *Phytochemistry*, **26**, 1613—1615 (1987).
5) Valle M. G., Appendino G., Nano G. M., Picci V., *Phytochemistry*, **26**, 253—256 (1987).
6) Teresa J. de P., Villaseco M. A., Hernandez J. M., Moran J. R., Urones J. G., Grande M., *Planta Medica*, **1986**, 458—462.
7) Appendino G., Tagliapietra S., Gariboldi P., Nano G. M., Picci V., *Phytochemistry*, **27**, 3619—3624 (1988).
8) Lamnaouer D., Fraigui O., *J. Nat. Prod.*, **54**, 576—578 (1991).
9) Miski M., Jakupovic J., *Phytochemistry*, **29**, 1995—1998 (1990).
10) Appendino G., Tagliapietra S., Nano G. M., Picci V., *Phytochemistry*, **27**, 944—946 (1988).

The Constituents of the Root and Stem of *Aristolochia heterophylla* Hemsl

Tian-Shung Wu,* Yu-Yi Chan, and Yann-Lii Leu

Department of Chemistry, National Cheng Kung University, Tainan, Taiwan 701, R. O. C.
Received September 9, 1999; accepted November 17, 1999

Seven new compounds, sodium aristolochate-VII (1), aristolactam-CIV (2), madolin-I (3), -J (4), -K (5), -L (6) and -M (7) together with 71 known compounds were isolated and characterized from the fresh root and stem of *Aristolochia heterophylla* Hemsl. Their structures were determined by spectral methods. Compound 8 was revised as aromadendrane-4β, 10β-diol by spectral data and single-crystal X-ray analysis.

Key words *Aristolochia heterophylla*; Aristolochiaceae; madolin-I—M; sesquiterpene; aromadendrane-4β, 10β-diol

Aristolochia heterophylla Hemsl (*A. shimada*) is a perennial shrub found in the thickets and forests in Mainland China and Taiwan.[1] The root and fruit of this plant have been used in traditional Chinese medicine as an expectorant, antitussive, analgesic, antiasthmatic and also for the treatment of snakebite and lung inflammation.[1] Aristolochic acids, aristolactams, terpenes and other constituents have been isolated from this species.[2—10] We report here the isolation and structural elucidation of seven new compounds, sodium aristolochate-VII (**1**), aristolactam-CIV (**2**), madolin-I (**3**), -J (**4**), -K (**5**), -L (**6**) and -M (**7**), together with 71 known compounds from a methanol extract of the root and stem of *Aristolochia heterophylla* Hemsl.

Results and Discussion

Sodium aristolochate-VII (**1**) was isolated as yellowish needles. The UV absorption bands at 222, 264, 310, 367 and 372 nm suggested it is an aristolochic acid derivative.[11] The IR spectrum showed the presence of a carboxylic salt and a nitro group at 1544, 1514 and 1392 cm^{-1}.[12] In the ^{1}H-NMR spectrum of **1**, two methoxyl signals appeared at δ 3.98 and 4.00 (each 3H, s). In the aromatic region, two singlet signals at δ 7.71 and 8.41 were ascribed to H-2 and H-9, respectively. A methylenedioxy group was indicated based on the singlet at δ 6.46. AB type signals at δ 8.80 and 7.74 (each 1H, d, J=9.5 Hz) were assigned to H-5 and H-6, respectively. The signal of H-5 appeared at a relatively lower field, at δ 8.80, due to the deshielding effect of the A ring. Compound **1** was dissolved in 5% HCl, applied to a Sephadex LH-20 column and eluted successively with H_2O and MeOH. The residue obtained from the H_2O fraction was confirmed to be a sodium ion by atomic absorption spectroscopy. The MeOH eluted fraction involved methylation with excess CH_2N_2 to afford **1a**, which was identified as aristolochic acid-VII methyl ester.[13] Thus, compound **1** was assigned as sodium aristolochate-VII.

Aristolactam-CIV (**2**) was obtained as yellowish needles. The mass spectrum showed a molecular ion peak at m/z 325.0956, implying the molecular formula $C_{18}H_{15}NO_5$. The UV absorption bands at 207, 239, 253, 281, 293, 316 and 399 nm suggested a phenanthrene derivative.[11] The IR spectrum revealed a lactamic carbonyl based on the absorption band at 1705 cm^{-1}. In the ^{1}H-NMR spectrum, two methoxyl and one hydroxymethyl groups appeared at δ 3.98, 4.02 (each 3H, s) and 5.27 (2H, s), respectively. The aromatic region of the spectrum showed an ABX pattern at δ 7.22 (1H, dd, J=8.0, 2.0 Hz), 7.78 (1H, d, J=8.0 Hz) and 8.66 (1H, d, J=2.0 Hz) attributable to H-7, H-8 and H-5, respectively. One singlet at δ 7.11 (1H, s) was assigned to H-9. The nuclear overhauser and exchange spectroscopy (NOESY) experiment (Fig. 1) showed that both the methoxy groups had correlations with H-5, indicating that the methoxy groups are located at C-4 and C-6. In addition, evidence for the location of the hydroxymethyl group in aristolactam-CIV was mainly inferred from the results of literature which showed that hydroxymethyl or carbonyl groups were substituted at C-2, only.[14—18] On the basis of the above results, the structure of aristolactam-CIV was established as **2**.

Madolin-I (**3**) was isolated as an optically active oil, and its molecular formula, $C_{15}H_{18}O_3$ (M^+ at m/z 246.1258), indicated seven degrees of unsaturated ration. The presence of α,β-unsaturated γ-lactone was inferred by the IR band at 1751 cm^{-1}, the ^{13}C-NMR spectra at δ 174.3 (s), 150.4 (d), 132.5 (s), 82.7 (d) and the ^{1}H-NMR spectra at δ 6.88 (1H, s), 4.94 (1H, s). The ^{1}H-NMR and the heteronuclear multiple quantum coherence (HMQC) spectra displayed two terminal methylene groups at δ 5.73 (1H, d, J=1.4 Hz), 5.57 (1H, d, J=2.3 Hz), 4.84 (1H, s) and 4.75 (1H, s), as well as one olefinic methyl group at δ 1.76 (3H, s). The presence of a bicyclic skeleton in the molecule can be deduced based on the unsaturation values and its evident unsaturated groups (two terminal methylene, an α,β-unsaturated γ-lactone and one carbonyl signal at δ 206.8 in the ^{13}C-NMR spectrum). The correlation spectroscopy (COSY) and HMQC spectra readily established the presence of one CH_2=C–CH_2CH_2CH– and one –CH_2CH_2– partial structure. The above fragments could be arranged as shown in formula **3** on the basis of the heteronuclear multiple bond coherence (HMBC) experiment (Fig. 2). On the other hand , the configurations of H-6 and H-7 were determined to be **3** based on the cross peak between H-7 (δ 2.32) with H-6 (δ 4.94) and H-3α (δ 2.65); and between H-3β (δ 2.48) with H-13 (δ 1.76) and H-12 (δ 4.75, 4.84) in the NOESY experiment (Fig. 1), together with the comparison of aristolactone **3a**.[19] Based on the above analysis, structure **3** was assigned for madolin-I.

Madolin-J (**4**) was isolated as a colorless oil. The high resolution mass spectrum (HR-MS) showed a $[M]^+$ at m/z 232.1463, corresponding to the molecular formula $C_{15}H_{20}O_2$ and six degrees of unsaturation. The IR absorption band at 1789 cm^{-1} and the signal at δ 179.2 (s) in the ^{13}C-NMR spectrum suggested the existence of a γ-lactone. The ^{1}H-NMR and ^{13}C-NMR spectra of **4** indicated the presence of

* To whom correspondence should be addressed.

© 2000 Pharmaceutical Society of Japan

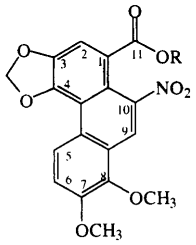

1 R=Na
1a R=CH_3

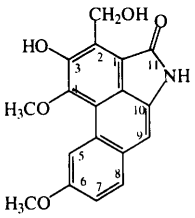

2

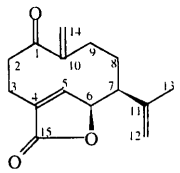

3

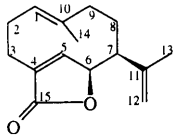

3a

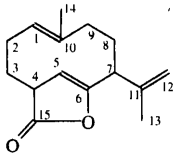

4

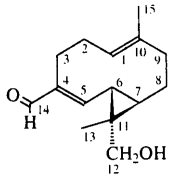

5

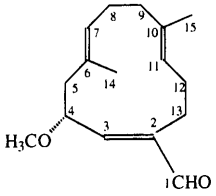

6

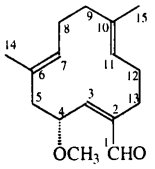

7

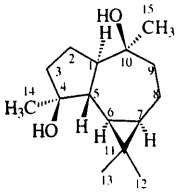

8

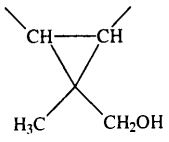

A

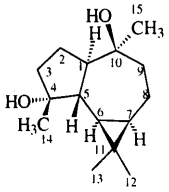

8a

two sets of trisubstituted double bonds (δ_H: 5.20, δ_C: 156.0, 109.1; δ_H: 5.16, δ_C: 131.8, 126.9) and one terminal methylene group (δ_H: 4.82, 4.80, δ_C: 144.9, 111.4). The presence of these three double bonds and one γ-lactone indicated a bicyclic structure for **4**. The COSY and HMQC spectra established the presence of –O–C=CH–CH–CH_2–CH_2–CH=C–CH_3, CH_2=C–CH_3 and –CH–CH_2–CH_2– partial structures. The connection of the partial structures was clarified by means of a HMBC experiment, as shown in Fig. 2. Based on the above information, structure **4** was established for madolin-J.

Madolin-K (**5**), a colorless oil with a molecular formula of $C_{15}H_{22}O_2$ (M^+ at *m/z* 234.1630) indicated five degrees of unsaturation. Compound **5** was revealed by the following spectroscopic evidence to be a bicyclic sesquiterpenoid which contained a formyl group conjugated with a trisubstituted double bond [λ_{max} 260 nm; ν_{max} 1676 cm^{-1}; δ_H: 6.29 (1H, d, J=9.6 Hz) and 9.28 (1H, s); δ_C: 194.3 (d), 154.2 (d) and 143.7 (s)] as well as another trisubstituted double bond bearing a methyl group [δ_H: 1.25 (3H, s) and 5.07 (1H, dd, J= 11.2, 5.2 Hz); δ_C: 134.5 (s) and 124.5 (d)]. In addition, the ^{1}H- and ^{13}C-NMR signals showed the presence of a partial structure A [δ_H: 1.07 (1H, m), 1.28 (3H, s), 1.65 (1H, dd, J= 9.6, 9.6 Hz), 3.42 (1H, d, J=11.0 Hz) and 3.51 (1H, d, J= 11.0 Hz); δ_C: 72.1 (t), 33.9 (d), 27.3 (s), 26.4 (d), 11.6 (q)], which was also supported by a long range correlation of H-12 and H-13 to C-6 and C-7 in the HMBC spectrum (Fig. 2). In order to confirm the structure of **5**, two-dimensional (2D) shift COSY and long range ^{13}C–^{1}H correlation in the HMBC experiment were conducted. The above spectral evidence disclosed the plane structure of madolin-K. The 9.6 Hz coupling constant and nuclear Overhauser effect (NOE) between H-6 and H-7 indicated a *cis* configuration of a cyclopropane moiety.[20] On the other hand, the configuration of C-11 was determined to be **5** due to a cross peak between H-6 (δ 1.65) with H-12 (δ 3.42) in the NOESY experiment (Fig. 1). On the basis of above results, structure **5** was assigned for madolin-K.

Madolin-L (**6**) was obtained as an optically active colorless oil, and the molecular formula was determined to be $C_{16}H_{24}O_2$ by HRMS (M^+, *m/z* 248.1785). The IR spectrum showed an α,β-unsaturated carbonyl band at 1692 cm^{-1}. The ^{1}H-NMR spectrum of madolin-L displayed three signals of olefinic protons at δ 6.16 (d, J=11.0 Hz), 4.98 (t, J=7.7 Hz) and 4.74 (t, J=7.4 Hz). The ^{13}C-NMR spectrum of **6** also showed six signals of olefinic carbons. Obviously, two of the double bonds are substituted by a methyl group, which showed a correlation in the COSY spectrum with olefinic

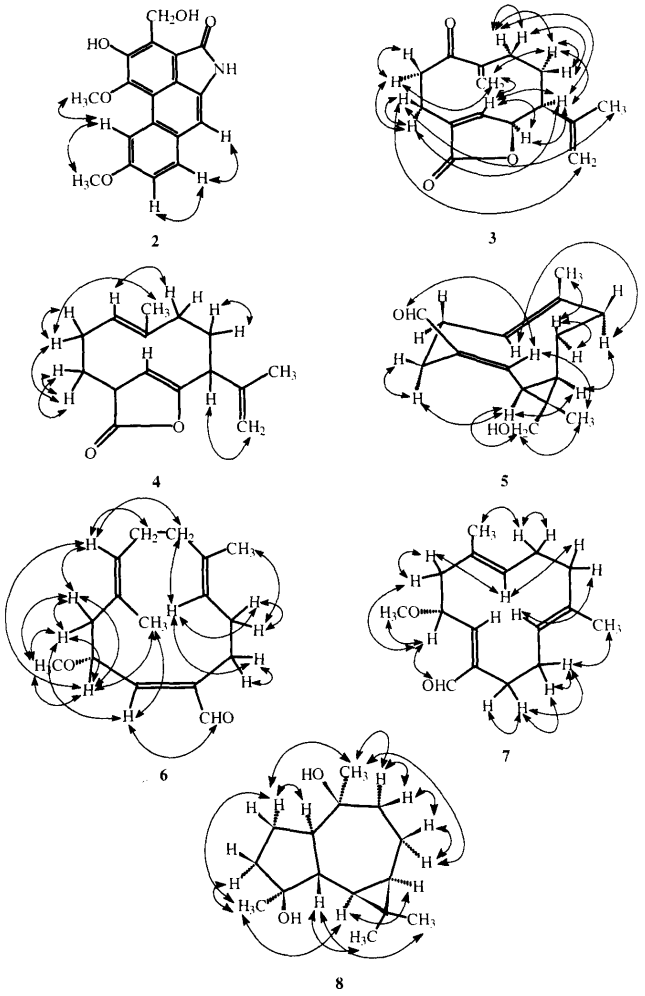

Fig. 1. NOESY Correlations of **2**—**8**

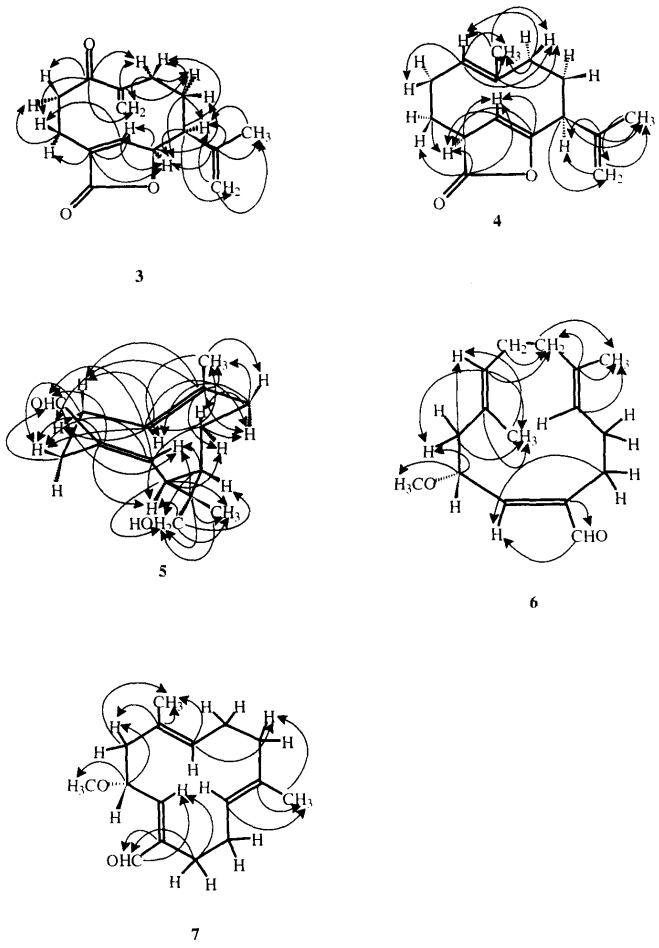

Fig. 2. HMBC Correlations of **3**—**7**

protons at δ 4.98 and 4.74, respectively. In addition, the presence of one methoxyl, two methylene groups and two partial structures, $-CH_2-CH(-O-)-CH=C-CHO$ and $-CH=C-CH_2CH_2-$ in **6**, were solved by COSY and HMQC spectra. The connections of the partial structures were established by HMBC experiment (Fig. 2). The NOESY experiment of **6** (Fig. 1) showed that all of the $\Delta^{2,3}$, $\Delta^{6,7}$ and $\Delta^{10,11}$ double bonds had *E* configurations, and the optical rotation of **6** indicated that the stereochemistry of the methoxyl group at C-4 is *R*.[7] Based on the above analyses, madolin-L has structure **6**.

Madolin-M (**7**) was isolated as an optically active oil and was determined to have the molecular formula $C_{16}H_{24}O_2$. It exhibited spectral data similar to madolin-L (**6**). The striking differences included three signals for more deshielded H-1, H-4, H-13 and two signals for shielded H-3 and H-13. The structure was assigned using the COSY, HMQC, HMBC (Fig. 2) and NOESY (Fig. 1) experiments, as shown for **7**. The *Z* configuration of $\Delta^{2,3}$ was supported by a clear correlation between the aldehyde (δ 10.05) and H-4 (δ 4.70) in the NOESY experiment. In addition, the *R* configuration at C-4 was determined by the negative optical rotation.[7] From the above results, the structure of madolin-M was assigned as **7**.

Aromadendrane-4β, 10β-diol (**8**) was isolated as optically active colorless prisms, mp 136—137 °C, with a molecular formula of $C_{15}H_{26}O_2$, which was confirmed by mass spectrometry. The IR absorption band at 3396 cm^{-1} showed the presence of a hydroxyl group in the molecular structure. The NMR spectra (^1H, ^{13}C, COSY, HMQC, HMBC) analyses indicated compound **8** presented four tertiary methyls, four methylenes, four methines and three quaternary carbons (including two bearing oxygen tertiary carbons). According to the above data, the structure of **8** is similar to aromadendrane-4α, 10β-diol (**8a**), which was isolated from *Brasilia sickii* by Bohlmann *et al.*[20] However, a single-crystal X-ray analysis (Fig. 3) and NOESY experiment (Fig. 1) indicated that the relative stereochemistry of the hydroxyl group at C-4

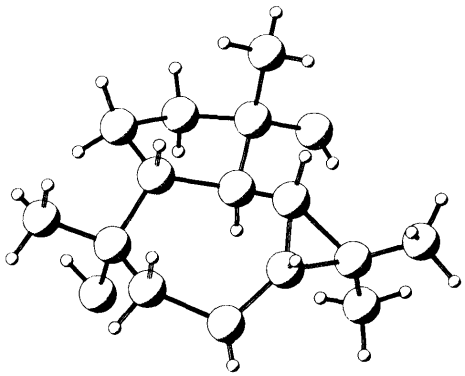

Fig. 3. X-Ray Structure of **8**

and C-10 both had β-orientations, respectively. Consequently, the structure of **8** was suggested to be aromadendrane-4β, 10β-diol.

The known compounds aristofolin-B (**9**),[21] aristolide-A (**10**),[9] -B (**11**),[9] borneol (**12**),[22] morindaparvin-A (**13**),[21] *N-trans*-feruloyltyramine (**14**),[23] *N-cis*-feruloyltyramine (**15**),[23] allantoin (**16**),[23] isorhamnetin-3-*O*-robinobioside (**17**),[23] sodium aristolochate-I (**18**),[12] -II (**19**),[24] -C (**20**),[12] -IVa (**21**),[24] sodium 7-hydroxylaristolochate-A (**22**),[12] aristolochic acid-II (**23**),[23] -C (**24**),[23] -IVa (**25**),[23] methyl aristolochate (**26**),[21] aristolochic acid II methyl ester (**27**),[23] methyl isovanillate (**28**),[25] methyl vanillate (**29**),[23] methyl 22-feruloyloxydocosanoate (**30**),[26] vanillin (**31**),[14] vanillic acid (**32**),[14] ferulic acid (**33**),[14] syringic acid (**34**),[27] methyl 3,4-dihydroxybenzoate (**35**),[28] picrorhizin (**36**),[29] methyl paraben (**37**),[23] methyl aristolate (**38**),[13] cuminyl alcohol (**39**),[30] aristolic acid (**40**),[13] 4,5-dioxodehydroasimilobine (**41**),[13] cepharadione-A (**42**),[23] aristolactam-BII (**43**),[13] -AII (**44**),[13] -AIIIa (**45**),[14] -IIIa (**46**),[14] 9-methoxyaristolactam-I (**47**),[23] aristolactam (**48**),[23] piperolactam-A (**49**),[31] aristolactam-C-*N*-β-D-glucoside (**50**),[23] aristolactam-*N*-β-D-glucoside (**51**),[23] cepharanone-A-*N*-β-D-glucoside (**52**),[23] *trans*-feruloyl esters (**53**),[23] *cis*-feruloyl esters (**54**),[23] β-sitosterol (**55**),[13] stigmasterol (**56**),[24] β-sitosterylglucoside (**57**),[13] stigmast-4-en-3,6-dione (**58**),[24] aristophyllide-A (**59**),[8] -B (**60**),[8] -C (**61**),[8] -D (**62**),[8] aristoloterpenate-I (**63**),[7] -II (**64**),[7] -III (**65**),[7] -IV (**66**),[7] madolin-A (**67**),[19] -B (**68**),[19] -E (**69**),[19] -F (**70**),[10] -G (**71**),[10] -H (**72**),[10] versicolactone-B (**73**),[32] aristolactone (**74**),[19] versicolactone-C (**75**),[32] manshurolide (**76**),[19] versicolactone-D (**77**),[33] and 1,10-epoxylepidozenal (**78**)[34] were also isolated. Their structures were elucidated by comparison of their spectroscopic data (UV, IR, NMR, mass spectrometry) with values in the literature.

Experimental

General Procedures Melting points (Yanagimoto apparatus) are uncorrected. Optical rotations were recorded on a Jasco DIP-370 digital polarimeter. UV spectra of the MeOH solution were obtained on a Hitachi UV-3210 spectrophotometer. The IR spectra of the KBr of discs were recorded on a Shimadzu FT-IR DR-8011 spectrophotometer. Mass and HR mass spectra were measured on a VG-70-250S spectrometer having a direct inlet system. ^{1}H-NMR and ^{13}C-NMR spectra were determined on Bruker AMX-400 and Varian Unity plus 400 spectrometers. Chemical shifts are shown in δ values (ppm) with tetramethylsilane (TMS) as an internal standard.

Plant Material *Aristolochia heterophylla* Hemsl was collected from Tsueg Feng , Nantou Hsien, Taiwan, in May, 1992 and verified by Prof. C.-S. Kuoh. A voucher specimen is deposited in the Herbarium of National Cheng Kung University, Taiwan.

Extraction and Isolation The fresh root and stem (4.5 kg) of *Aristolochia heterophylla* Hemsl were extracted with MeOH (×5) at room temperature and concentrated under reduced pressure into a brown syrup. To the distilled MeOH was added H_2O, followed by partitioning with Et_2O. The MeOH extract was partitioned successively between H_2O and $CHCl_3$, then *n*-BuOH. The Et_2O layer was chromatographed directly on silica gel and eluted with *n*-hexane–iso-Pr_2O (9 : 1) to afford **6** (4 mg), **7** (2 mg), **12** (28 mg), **67** (4 mg), **68** (10 mg) and **78** (1 mg). The $CHCl_3$ extract was filtered to give **18** (135 mg) and the filtrate was subjected to chromatography on a silica gel column and eluted with gradients of $CHCl_3$–MeOH (99 : 1) to afford 7 fractions. Fraction 2 was rechromatographed on silica gel and eluted with *n*-hexane–EtOAc (19 : 1) to give **4** (12 mg), **8** (24 mg), **26** (22 mg), **38** (6 mg), **53** (5 mg), **54** (3 mg), **58** (180 mg), **59** (9 mg), **60** (3 mg), **61** (7 mg), **62** (1 mg), **63** (15 mg), **64** (2 mg), **65** (4 mg), **66** (1 mg), **69** (8 mg), **72** (16 mg), **76** (230 mg) and **77** (12 mg). Fractions 3 and 4 were combined and underwent chromatography on silica gel using *n*-hexane–EtOAc (19 : 1) as an eluent to afford **4** (12 mg), **10** (2 mg), **11** (5 mg), **13** (2 mg), **27** (2 mg), **28** (1 mg), **29** (2 mg), **30** (6 mg), **31** (7 mg), **39** (1 mg), **48** (5 mg), **55** (532 mg), **56** (267 mg), **70** (4 mg), **71** (2 mg) and **74** (565 mg), successively. Fractions 5 and 6 were also combined and separated by chromatography on silica gel using $CHCl_3$–Me_2CO (12 : 1) as an eluent to give **3** (12 mg), **42** (3 mg), **43** (1 mg), **47** (12 mg), **49** (26 mg) and **73** (375 mg). Fraction 7 underwent chromatography on silica gel and was eluted with a gradient of $CHCl_3$–MeOH (19 : 1) to give **2** (1 mg), **14** (7 mg), **15** (9 mg), **40** (220 mg), **41** (31 mg), **44** (26 mg), **57** (12 mg) and **75** (5 mg). The *n*-BuOH layer underwent chromatography on Diaion HP-20 and was eluted with a gradient of H_2O–MeOH to give 9 fractions. Fraction 1 was filtered to give **16** (7 g). Fractions 4 and 5 were combined and chromatographed on Sephadex LH-20 using a gradient of H_2O–MeOH to afford **34** (3 mg), **35** (7 mg) and **37** (2 mg). Fraction 6 also underwent chromatography on Sephadex LH-20 and was eluted with a gradient of H_2O–MeOH to give **17** (510 mg), **36** (5 mg) and **50** (34 mg). Fraction 7 was separated by chromatography on silica gel using $CHCl_3$–MeOH–H_2O (3 : 1 : 0.1) as an eluent to obtain **45** (9 mg) and **52** (36 mg), respectively. Fraction 8 was rechromatographed on silica gel and eluted with $CHCl_3$–MeOH–H_2O (5 : 1 : 0.1) to give **20** (3 mg), **21** (4 mg), **25** (14 mg), **46** (7 mg) and **51** (43 mg). Fraction 9 was also separated by chromatography on silica gel using $CHCl_3$–MeOH–H_2O (5 : 1 : 0.1) to give **1** (2 mg), **9** (5 mg), **19** (12 mg), **22** (2 mg), **23** (2 mg), **24** (4 mg), **32** (4 mg) and **33** (4 mg), successively.

Sodium Aristolochate-VII (**1**): Yellowish needles. mp: >280 °C. UV λ_{max}^{MeOH} nm: 222, 264, 310, 367, 372. IR ν_{max}^{KBr} cm^{-1}: 1544 (C=O), 1514, 1392, 1286, 1253, 1087, 1035, 939 (OCH_2O). ^{1}H-NMR (DMSO-d_6, 200 MHz) δ: 3.98 (3H, s, OCH_3), 4.00 (3H, s, OCH_3), 6.46 (2H, s, OCH_2O), 7.71 (1H, s, H-2), 7.74 (1H, d, J=9.5 Hz, H-6), 8.41 (1H, s, H-9), 8.80 (1H, d, J=9.5 Hz, H-5).

Acidification of 1 Compound **1** was dissolved in 1 ml 5% $HCl_{(aq)}$, applied to a Sephadex LH-20 column and eluted successively with H_2O and MeOH. The residue obtained from the H_2O fraction was confirmed to be a sodium ion by atomic absorption spectroscopy. The MeOH eluted fraction was concentrated and the residue was dissoved in 1 ml MeOH, then excess CH_2N_2 ether solution was added to afford **1a**, which was identified as aristolochic acid-VII methyl ester by the ^{1}H-NMR and IR spectra.

Aristolactam-CIV (**2**): Yellowish needles. mp: 206—207 °C. HR-FAB-MS: Calcd for $C_{18}H_{15}O_5$, *m/z*: 325.0950 [M$^+$]. Found: 325.0956. UV λ_{max}^{MeOH} nm (log ε): 207 (4.54), 239 (4.56), 253 (4.47), 281 (4.33), 293 (4.34), 316 (sh, 4.09), 399 (3.63). IR ν_{max}^{KBr} cm^{-1}: 3202, 1705 (C=O), 1618, 1504, 1421, 1350, 1296. FAB-MS *m/z* (rel. int.): 326 ([M$^+$]+1, 3), 325 ([M$^+$], 4), 307 (17), 289 (12), 176 (24), 15 (24), 154 (100), 152 (13), 139 (15), 138 (30), 137 (52), 136 (77), 120 (13), 107 (28), 105 (11), 91 (10). ^{1}H-NMR (CD_3OD-d_4, 400 MHz) δ: 3.98 (3H, s, OCH_3), 4.02 (3H, s, OCH_3), 5.25 (2H, s, OCH_2OH), 7.11 (1H, s, H-9), 7.22 (1H, dd, J=8.0, 2.0 Hz, H-7), 7.78 (1H, d, J=8.0 Hz, H-8), 8.66 (1H, d, J=2.0 Hz, H-5).

Madolin-I (**3**): Colorless oil. $[\alpha]_D$ +141.3° (c=0.07, $CHCl_3$). HR-EI-MS: Calcd for $C_{15}H_{18}O_3$, *m/z*: 246.1255 [M$^+$]. Found: 246.1258. UV λ_{max}^{MeOH} (log ε) nm: 213 (4.05). IR ν_{max}^{KBr} cm^{-1}: 2925, 2860, 1751, 1679, 1453, 1064, 935. EI-MS *m/z* (rel. int.): 246 ([M$^+$], 9), 203 (19), 150 (30), 149 (19), 138 (16), 135 (57), 121 (13), 117 (15), 108 (42), 107 (36), 105 (14), 95 (46), 93 (33), 91 (50), 81 (25), 79 (39), 77 (39), 53 (100). ^{1}H-NMR ($CDCl_3$, 400 MHz) δ: 1.49 (1H, ddd, J=15.2, 11.1, 9.6 Hz, H-8), 1.76 (3H, s, 13-CH_3), 1.77 (1H, m, H-8), 1.87 (1H, dd, J=15.9, 9.6 Hz, H-9), 2.32 (1H, dd, J=11.1, 2.1 Hz, H-7), 2.46 (1H, dd, J=15.9, 7.2 Hz, H-9), 2.48 (1H, ddd, J=12.0, 10.4, 2.6 Hz, H-3), 2.51 (1H, dd, J=17.0, 2.6 Hz, H-2), 2.65 (1H, dd, J=12.0, 3.1 Hz, H-3), 3.39 (1H, ddd, J=17.0, 10.4, 3.1 Hz, H-2), 4.75 (1H, s, H-12), 4.84 (1H, s, H-12), 4.94 (1H, s, H-6), 5.57 (1H, d, J=2.3 Hz, H-14), 5.73 (1H, d, J=1.4 Hz, H-14), 6.88 (1H, s, H-5). ^{13}C-NMR ($CDCl_3$, 100 MHz) δ: 21.3 (C-13), 23.3 (C-3), 27.5 (C-8), 28.0 (C-9), 37.6 (C-2), 52.2 (C-7), 82.7 (C-6), 112.2 (C-12), 124.4 (C-14), 132.5 (C-4), 147.7 (C-11), 150.4 (C-5), 152.2 (C-10), 174.4 (C-15), 206.8 (C-1).

Madolin-J (**4**): Colorless oil. $[\alpha]_D$ +140.3° (c=0.12, $CHCl_3$). HR-EI-MS: Calcd for $C_{15}H_{20}O_2$, *m/z*: 232.1463 [M$^+$]. Found: 232.1463. IR ν_{max}^{KBr} cm^{-1}: 3089, 2923, 2854, 1789, 1645, 1446, 1120, 977, 927. EI-MS *m/z* (rel. int.): 232 ([M$^+$], 48), 217 (7), 204 (11), 189 (10), 177 (14), 162 (11), 149 (14), 138 (26), 120 (27), 107 (57), 93 (48), 79 (49), 67 (100). ^{1}H-NMR ($CDCl_3$, 400 MHz) δ: 1.48 (1H, m, H-8), 1.70 (3H, s, H-14), 1.72 (3H, s, H-13), 1.75 (1H, ddd, J=14.0, 5.4, 2.0 Hz, H-3), 1.95 (1H, dddd, J=14.0, 12.3, 12.3, 2.0 Hz, H-8), 2.06 (1H, m, H-2), 2.13 (1H, dddd, J=14.0, 6.9, 6.9, 2.0 Hz, H-3), 2.20 (1H, ddd, J=12.3, 12.3, 2.0 Hz, H-9), 2.52 (1H, m, H-9), 2.56 (1H, dddd, J=12.2, 12.2, 6.9, 5.4 Hz, H-2), 3.03 (1H, dd, J=12.3, 3.6 Hz, H-7), 3.30 (1H, ddd, J=6.9, 2.0, 2.0 Hz, H-4), 4.80 (1H, s, H-12), 4.82 (1H, s, H-12), 5.16 (1H, d, J=12.2 Hz, H-1), 5.20 (1H, d, J=2.0 Hz, H-5). ^{13}C-NMR ($CDCl_3$, 100 MHz) δ: 14.9 (C-14), 21.5 (C-13), 22.7 (C-8), 25.2 (C-2), 26.0 (C-3), 40.5 (C-9), 44.0 (C-4), 48.3 (C-7), 109.1 (C-5), 111.4 (C-12), 126.9 (C-1), 131.8 (C-10), 144.9 (C-11), 156.0 (C-6), 179.2 (C-15).

Madolin-K (**5**): Colorless oil. $[\alpha]_D$ +128.0° (c=0.13, $CHCl_3$). HR-EI-MS: Calcd for $C_{15}H_{22}O_2$, *m/z*: 234.1619 [M^+]. Found: 234.1620. UV λ_{max}^{MeOH} (log ε) nm: 260 (3.92). IR ν_{max}^{KBr} cm^{-1}: 2925, 2858, 1676, 1625, 1515, 1471, 1217. EI-MS *m/z* (rel. int.): 234 ([M^+], 14), 216 (47), 201 (11), 187 (30), 175 (21), 161 (23), 146 (71), 134 (40), 119 (34), 107 (92), 91 (100). ^{1}H-NMR ($CDCl_3$, 400 MHz) δ: 0.90 (1H, m, H-8), 1.07 (1H, m, H-7), 1.25 (3H, s, 15-CH_3), 1.28 (3H, s, 13-CH_3), 1.65 (1H, dd, J=9.6, 9.6 Hz, H-6), 1.85 (1H, dddd, J=11.4, 5.0, 2.4, 2.4 Hz, H-8), 1.99 (1H, dd, J=12.2, 4.5 Hz, H-3), 2.07 (1H, ddd, J=12.5, 12.5, 2.4 Hz, H-9), 2.12 (1H, m, H-2), 2.15 (1H, m, H-9), 2.20 (1H, m, H-2), 2.77 (1H, ddd, J=12.2, 3.4, 3.4 Hz, H-3), 3.42 (1H, d, J=11.0 Hz, H-12), 3.51 (1H, d, J=11.0 Hz, H-12), 5.07 (1H, dd, J=11.2, 5.2 Hz, H-1), 6.29 (1H, d, J=9.6 Hz, H-5), 9.28 (1H, d, J=0.8 Hz, CHO). ^{13}C-NMR ($CDCl_3$, 100 MHz) δ: 11.6 (C-13), 17.3 (C-15), 23.3 (C-8), 23.6 (C-3), 26.4 (C-6), 27.3 (C-11), 27.7 (C-2), 33.9 (C-7), 39.7 (C-9), 72.1 (C-12), 124.5 (C-1), 134.5 (C-10), 143.7 (C-4), 154.2 (C-5), 194.3 (C-14).

Madolin-L (**6**): Colorless oil. $[\alpha]_D$ −88.5° (c=0.05, $CHCl_3$). HR-EI-MS: Calcd for $C_{16}H_{24}O_2$, *m/z*: 248.1776 [M^+]. Found: 248.1785. UV λ_{max}^{MeOH} (log ε) nm: 223 (3.69). IR ν_{max}^{KBr} cm^{-1}: 2924, 2855, 1692, 1462, 1093. EI-MS *m/z* (rel. int.): 248 ([M^+],19), 216 (13), 161 (11), 151 (23), 136 (29), 121 (32), 112 (100), 105 (24), 91 (40). ^{1}H-NMR ($CDCl_3$, 400 MHz) δ: 1.38 (3H, s, H-15), 1.60 (3H, s, H-14), 2.02 (2H,t , J=5.7 Hz, H-9), 2.11 (2H, m, H-8), 2.13 (1H, m, H-12), 2.15 (1H, dd, J=10.0, 10.0 Hz, H-13), 2.19 (1H, dd, J=11.0, 11.0 Hz, H-5), 2.38 (1H, m, H-12), 2.58 (1H, m, H-13), 2.62 (1H, dd, J=11.0, 3.8 Hz, H-5), 3.21 (3H, s, OCH_3), 4.04 (1H, ddd, J=11.0, 11.0, 3.8 Hz, H-4), 4.74 (1H, t, J=7.4 Hz, H-11), 4.98 (1H, t, J=7.7 Hz, H-7), 6.16 (1H, d, J=11.0 Hz, H-3), 9.47 (1H, s, H-1). ^{13}C-NMR ($CDCl_3$, 100 MHz) δ: 15.4 (C-15), 18.6 (C-14), 24.9 (C-8), 25.0 (C-12), 25.4 (C-13), 38.4 (C-9), 44.9 (C-5), 56.1 (OCH_3), 77.0 (C-4), 125.2 (C-11), 128.5 (C-7), 129.8 (C-6), 133.8 (C-10), 145.2 (C-2), 152.8 (C-3), 195.7 (C-1).

Madolin-M (**7**): Colorless oil. $[\alpha]_D$ −23.2° (c=0.03, $CHCl_3$). HR-EI-MS: Calcd for $C_{16}H_{24}O_2$, *m/z*: 248.1776 [M^+]. Found: 248.1781. UV λ_{max}^{MeOH} (log ε) nm: 227 (3.70). IR ν_{max}^{KBr} cm^{-1}: 2924, 2852, 1680, 1454, 1094. EI-MS *m/z* (rel. int.): 248 ([M^+], 14), 216 (29), 151 (15), 136 (21), 121 (27), 112 (100), 105 (17), 93 (28). ^{1}H-NMR ($CDCl_3$, 400 MHz) δ: 1.31 (3H, s, H-15), 1.52 (3H, s, H-14), 1.79 (1H, ddd, J=12.8, 12.8, 3.6 Hz, H-13), 1.96 (1H, m, H-8), 2.00 (1H, m, H-9), 2.04 (1H, m, H-12), 2.16 (1H, dd, J=10.8, 10.8 Hz, H-5), 2.18 (1H, m, H-9), 2.28 (1H, m, H-8), 2.38 (1H, m, H-12), 2.56 (1H, br d, J=10.8 Hz, H-5), 2.83 (1H, ddd, J=12.8, 3.6, 3.6 Hz, H-13), 3.29 (3H, s, OCH_3), 4.70 (1H, ddd, J=10.8, 10.8, 4.4 Hz, H-4), 4.80 (1H, d, J=11.2 Hz, H-11), 4.96 (1H, d, J=10.8 Hz, H-7), 5.92 (1H, d, J=10.8 Hz, H-3), 10.05 (1H, s, H-1). ^{13}C-NMR ($CDCl_3$, 100 MHz) δ: 14.9 (C-15), 16.1 (C-14), 25.0 (C-8), 25.8 (C-12), 31.8 (C-13), 39.6 (C-9), 46.2 (C-5), 56.4 (OCH_3), 72.2 (C-4), 125.0 (C-11), 129.0 (C-6), 129.9 (C-7), 135.1 (C-10), 142.3 (C-2), 149.4 (C-3), 190.7 (C-1).

Aromadendrane-4β,10β-diol (**8**): Colorless prisms. mp: 136—137 °C. $[\alpha]_D$ −20.2° (c=0.24, $CHCl_3$). IR ν_{max}^{KBr} cm^{-1}: 3396, 2924, 2862, 1456, 1375, 1109. EI-MS *m/z* (rel. int.): 238 ([M^+], 6), 220 (39), 205 (38), 162 (100), 147 (47), 121 (63), 119 (55), 107 (66), 95 (60), 93 (77). ^{1}H-NMR ($CDCl_3$, 400 MHz) δ: 0.40 (1H, ddd, J=10.7, 9.6 Hz, H-6), 0.62 (1H, ddd, J=11.0, 9.6, 6.0 Hz, H-7), 0.88 (1H, m, H-8), 1.01 (6H, s, H-12, H-13), 1.15 (3H, s, H-15), 1.18 (1H, dd, J=10.7, 10.7 Hz, H-5), 1.23 (3H, s, H-14), 1.50—1.90 (8H, m, H-1, 2, 3, 8, 9). ^{13}C-NMR ($CDCl_3$, 100 MHz) δ: 16.4 (C-13), 19.5 (C-11), 20.1 (C-8), 20.3 (C-15), 23.8 (C-2), 24.4 (C-14), 26.6 (C-7), 28.3 (C-6), 28.6 (C-12), 41.1 (C-3), 44.4 (C-9), 48.4 (C-5), 56.4 (C-1), 75.0 (C-10), 80.3 (C-4). Crystal data: monoclinic, space group $P2_12_12_1$: a=10.726 (5), b=16.0817 (18), c=16.7487 (19) Å, U=2888.9 (15) Å^3, Z=4, Dc= 0.548 mg m^{-3}, μ (MoK_α radiation, λ=0.70930 Å) crystal dimensions: 0.48×0.31×0.34 mm. Intensity data (+h, +k, +l, $2\theta_{max}$=44.9°) were recorded on a Nonius diffractometer. The crystal structure was solved by a direct method. Full-Matrix Least-Squares refinement of atomic parameters (anisotropic C, O; isotopic H) converged at R=0.015 (R_w=0.090) over 1566 reflections with I>2.5σ (I).

Acknowledgments We thank the National Science Council, R. O. C. (NSC grant 86-2113-M-006-008), for support of this research. We also thank Professor C. S. Kuoh for plant identification.

Reference and Notes

1) Jiangsu New Medicine College, in "Encyclopedia of Chinese Materia Medica," Vol. 1, Shanghai Science and Technology Press, Shanghai, 1977, p. 294.
2) Chen H., Jin R., Xu L. *Zhongguo Zhongyao Zazhi*, **19**, 323—324 (1994).
3) Mizuno M., Oka M., Tanaka T., Yamamoto H., Iinuma M., Murata H., *Chem. Pharm. Bull.*, **39**, 1310—1311 (1991).
4) Zhang H., Wang C., Xie C., *Tianran Chanwu Yanjiu Yu Kaifa*, **8**, 17—21 (1996).
5) Tian B., Zou W., Huang S., Tan T., Lu L., *Zhongcaoyao*, **13**, 10—12 (1982).
6) Ho M., Li X., Lo J., Liu J., *Zhongcaoyao*, **14**, 158 (1983).
7) Wu T. S., Chan Y. Y., Leu Y. L., Chen Z. T., *J. Nat. Prod.*, **62**, 415—418 (1999).
8) Wu T. S., Chan Y. Y., Leu Y. L., Wu P. L., Li C. Y., Mori Y., *J. Nat. Prod.*, **62**, 348—351 (1999).
9) Wu T. S., Chan Y. Y., Leu Y. L., *Chem. Pharm. Bull.*, **46**, 370—372 (1998).
10) Chan Y. Y., Leu Y. L., Wu T. S., *Tetrahedron Lett.*, **39**, 8145—8148 (1998).
11) Chen Z. L., Zhu D. Y., (1987) "The Alkaloids," Vol. 31, ed. by Brossi A., Academic Press, Orlando, America, p. 29.
12) Leu Y. L., Chan Y. Y., Wu T. S., *Phytochemistry*, **48**, 743—745 (1998).
13) Wu T. S., Leu Y. L., Chan Y. Y., *Chem. Pharm. Bull.*, **47**, 571—573 (1999).
14) Wu T. S., Leu Y. L., Chan Y. Y., *Chem. Pharm. Bull.*, **46**, 1624—1626 (1998).
15) Priestap H. A., *Phytochemistry*, **24**, 3035—3039 (1985); *idem*, *ibid.*, **26**, 519—529 (1987).
16) Talapatra S. K., Basu D., Chattopadhyay P., Talapatra B., *Phytochemistry*, **27**, 903—906 (1988).
17) Lin W. H., Fu H. Z., Hano Y,. Nomura T., *J. Chin. Pharm. Sci.*, **6**, 8—13 (1997).
18) Bulgakov V. P., Xzhuravlev Y. N., Radchenko S. V., Fedoreyev S. A., Denisenko V. A., Veselova M., Kalesh N. I., Alshevskaya E. K., *Fitoterapia*, **67**, 238—240 (1996).
19) Wu T. S., Chan Y. Y., Leu Y. L., *J. Nat. Prod.*, **61**, 511—514 (1998).
20) Bohlmann F., Grenz M., Jakupovic J., King R. M., Robinson H., *Phytochemistry*, **22**, 1213—1218 (1983).
21) Wu T. S., Leu Y. L., Chan Y. Y., *Chem. Pharm. Bull.*, **46**, 1301—1302 (1998).
22) Poucher C. J., Behnke J., "The Aldrich Library of ^{13}C and ^{1}H FT NMR Spectra," Aldrich Chemical Company, America, 1993, edit.I, 1, 251A.
23) Wu T. S., Ou L. F., Teng C. M., *Phytochemistry*, **36**, 1063—1068 (1994).
24) Chang C. Y., Leu Y. L., Chan Y. Y., Wu T. S., *J. Chin. Chem. Soc.*, **45**, 93—97 (1998).
25) Huber E. W., Kane J. M., *J. Heterocycle Chem.*, **27**, 1957—1961 (1990).
26) Guillemonat A., *Bull. Soc. Chim. Fr.*, **1963**, 142.
27) Xu L. Z., Sun N. J., *Yaoxue Xuebao*, **19**, 48—55 (1984).
28) Asakawa Y., Toyota M., Takemoto T., Mues R., *Phytochemistry*, **20**, 2695—2699 (1981).
29) Spencer P. A., Tanaka A., Towers G. H. N., *Phytochemistry*, **29**, 3785—3788 (1990).
30) Mateo C., Sanz J., Calderon J., *Phytochemistry*, **23**, 319—322 (1984).
31) Sanjay J. D., Bharathi R. P., Newand B. M., *Phytochemistry*, **27**, 1511—1515 (1988).
32) Zhang J., He L. X., *Yaoxue Xuebao*, **21**, 273—278 (1986).
33) Xue H. Z., Zhang J., He L. X., He C. H., Zheng Q. T., Feng R., *Yaoxue Xuebao*, **24**, 917—922 (1989).
34) Zheng G. C., Ichikawa A., Ishitsuka M. O., Kusumi T., Yamamoto H., Kakisawa H., *J. Org. Chem.*, **55**, 3677—3679 (1990).

Steroidal Oligoglycosides from the Seeds of *Allium tuberosum*

Tsuyoshi IKEDA, Hidetsugu TSUMAGARI, and Toshihiro NOHARA*

Faculty of Pharmaceutical Sciences, Kumamoto University, 5–1 Oe-honmachi, Kumamoto 862–0973, Japan.
Received September 24, 1999; accepted November 12, 1999

Three new spirostanol steroidal oligoglycosides, together with a known oligoglycoside, were obtained from the seeds of *Allium tuberosum* after enzymatic hydrolysis of furostanol saponin fraction by β-glucosidase. On the basis of spectroscopic analysis, the structure of new spirostanol oligoglycosides were elucidated as (25*S*)-spirost-5-ene-2α,3β-diol 3-*O*-α-L-rhamnopyranosyl-(1→4)-[α-L-rhamnopyranosyl-(1→2)]-β-D-glucopyranoside, (25*S*)-spirostane-3β,5β,6α-triol 3-*O*-α-L-rhamnopyranosyl-(1→4)-β-D-glucopyranoside, and (25*S*)-5β-spirostane-3β,6α-diol 3-*O*-α-L-rhamnopyranosyl-(1→4)-β-D-glucopyranoside.

Key words *Allium tuberosum*; steroidal oligoglycoside; spirostanol; furostanol; Liliaceae; β-chacotriose

Our survey of the anti-herpes[1] and cytotoxic[2] active compounds among solanaceous plants has produced an interim result that the spirostanol glycoside is more effective than the coexisting furostanol, salasodane, or nuatigenin glycosides. Therefore, in order to obtain more detailed information about the relationship between structures and bioactivities, we studied the constituents of the seeds of *Allium tuberosum* (Liliaceae), which is a plant material known to include two spirostanol glycosides.[3] *A. tuberosum* is widely distributed in Asia and is cultivated as a foodstuff. The seeds of *A. tuberosum* are used as a tonic in China.[4] This paper deals with the isolation and structural elucidation of three new spirostanol steroidal saponins, together with a known saponin, on the basis of spectroscopic analysis.

The methanolic extract of the seeds (285.8 g) of *A. tuberosum* was partitioned between hexane and 80% MeOH. The 80% MeOH fraction was subjected to Diaion HP-20 and octadecylsilanized (ODS) silica gel column chromatographies to provide a furostanol saponin fraction. The furostanol saponin fraction was too complicated to separate, and the furostanol type steroidal saponins tended to be less active than the corresponding spirostanol type saponins for cytotoxicity.[2] Thus, we converted the furostanol saponin fraction to the corresponding spirostanol saponin by enzymatic hydrolysis with β-glucosidase. The obtained spirostanol saponin fraction was further purified on Chromatorex ODS and silica gel column chromatographies to give compounds **1** (31.2 mg), **2** (16.6 mg), **3** (5.0 mg), and **4** (2.7 mg).

Compound **1** was isolated as an amorphous powder, $[\alpha]_D$ −78.4° (MeOH). It showed a quasi-molecular ion peak of $[M-H]^-$ at *m/z* 885, and fragment ion peaks due to [M−H−deoxy-pentose]$^-$ at *m/z* 739 and [M−H−2×deoxy-pentose]$^-$ at *m/z* 593 in the negative FAB-MS. The high-resolution (HR) FAB-MS gave a $[M+Na]^+$ ion at *m/z* 909.4836, which corresponds to the composition $C_{45}H_{74}O_{17}Na$. The ^{1}H-NMR spectrum in pyridine-d_5 displayed signals due to four steroidal methyl groups at δ 0.80, 0.89 (each 3H, s), 1.08 (3H, d, *J*=6.7 Hz), 1.14 (3H, d, *J*=6.7 Hz), two secondary

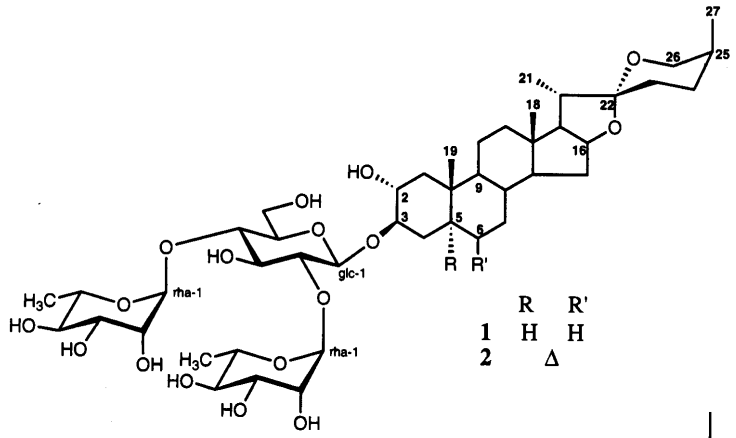

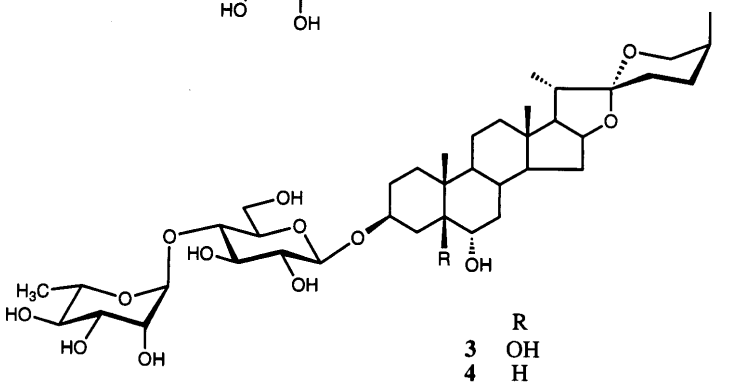

* To whom correspondence should be addressed.

© 2000 Pharmaceutical Society of Japan

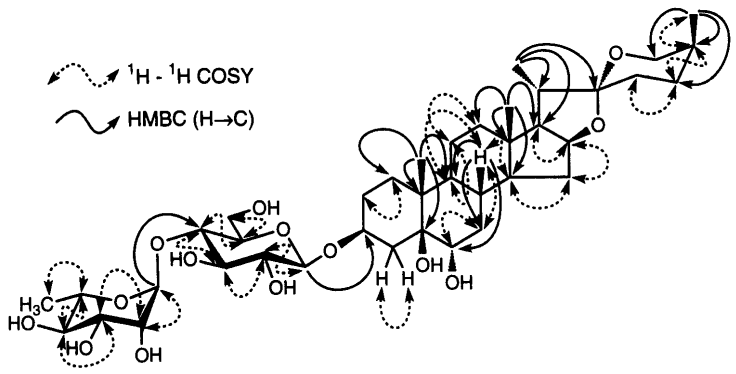

Fig. 1. ^{1}H–^{1}H COSY and HMBC Observed for **3**

methyl groups of 6-deoxypentose at δ 1.62 (3H, d, J=6.0 Hz) and 1.68 (3H, d, J=6.1 Hz), and three anomeric protons at δ 5.00 (1H, d, J=7.0 Hz), 5.81 (1H, br s) and 6.34 (1H, br s). In the ^{13}C-NMR spectrum, signals due to an aglycone part of **1** were superimposed on those of neogitogenin,[5] and signals due to the sugar moiety was assigned as α-L-rhamnopyranosy-(1→4)-[α-L-rhamnopyranosyl-(1→2)]-β-D-glucopyranose (β-chacotriose)[6] (Table 1). Thus, the structure of **1** was determined to be β-chacotriosyl neogitogenin. This compound was identified to be tuberoside D, which was recently obtained from the title plant as a genuine saponin.[3]

Compound **2** was isolated as an amorphous powder, $[\alpha]_D$ −94.2° (MeOH). It showed a quasi-molecular ion peak of $[M-H]^-$ at *m/z* 883 and fragment ion peaks due to [M−H−deoxy-pentose]$^-$ at *m/z* 737 and [M−H−2×deoxy-pentose]$^-$ at *m/z* 591 in the negative FAB-MS. The HR-FAB-MS gave a $[M+Na]^+$ ion at *m/z* 907.4679, which corresponds to the composition $C_{45}H_{72}O_{17}Na$. It suggested that the molecular ion of **2** was smaller by 2 mass units than that of **1**. When the ^{1}H- and ^{13}C-NMR spectra of **2** were compared with those of **1**, signals ascribable to the sugar moiety and the C, D, E, and F rings of the aglycone were identical. On the other hand, an olefinic proton signal appeared at δ 5.34 (1H, br s) and the signal of H_3-19 was shifted by +0.19 ppm. In the ^{13}C-NMR spectrum of **2**, trisubstituted double bond carbon signals appeared at δ 122.0 (d) and 140.0 (s) (Table 1). When the ^{13}C-NMR data of the aglycone part of **2** was compared with that of yuccagenin [(25*R*)-spirost-5-ene-2α,3β-diol],[7] it was identical except for the signals due to the F ring. Thus, the aglycone part of **2** was identified as (25*S*)-spirost-5-ene-2α,3β-diol, lilagenin.[8] The structure of **2** was therefore determined to be β-chacotriosyl lilagenin. This is the first time the ^{1}H- and ^{13}C-NMR data of lilagenin has been presented.

Compound **3** was isolated as an amorphous powder, $[\alpha]_D$ −61.1° (MeOH). It showed a quasi-molecular ion peak due to $[M-H]^-$ at *m/z* 755 and fragment ion peaks due to [M−H−deoxy-pentose]$^-$ at *m/z* 609 and [M−H−deoxy-pentose-hexose]$^-$ at *m/z* 447 in the negative FAB-MS. The HR-FAB-MS gave a $[M+Na]^+$ ion at *m/z* 779.4178, which corresponds to the composition $C_{39}H_{64}O_{14}Na$. These data suggest that **3** is a steroidal glycoside with a terminal methylpentosyl moiety and an inner hexosyl moiety. The ^{1}H-NMR spectrum displayed signals due to four steroidal methyl groups at δ 0.83, 1.15 (each 3H, s), 1.08 (3H, d, J=7.3 Hz), 1.16 (3H, d, J=6.7 Hz), one secondary methyl group of 6-deoxypentose at δ 1.71 (3H, d, J=6.1 Hz), and two anomeric protons at δ 5.00 (1H, d, J=7.9 Hz) and 5.88 (1H, br s). When the ^{13}C-NMR spectrum of **3** was compared with that of **1**, the carbon signals appearing from the D, E, F rings on the aglycone were identical (Table 1). This suggested that **3** is a 25*S*-spirostane skeleton. On the other hand, two hydroxyl methine carbon signals appeared at δ 66.1 and 79.2, and one hydroxy-bearing quaternary carbon signal was observed at δ 73.0. When the ^{13}C-NMR data of the sugar part of **3** was compared with that of **1**, the presence of a de-rhamnosyl chacotriosyl moiety was deduced for the sugar moiety of **3**. To determine the location of the hydroxyl group on the aglycone part and the glycosidic linkage, the ^{1}H–^{1}H shift correlation spectroscopy (COSY), heteronuclear multiple quantum coherence (HMQC) and heteronuclear multiple bond correlation (HMBC) experiments were made in order to assign the respective proton and carbon signals, as shown in Fig. 1. In the sugar moiety, the rhamnosyl H-1 at δ 5.88 correlated with the glucosyl C-4 at δ 78.5 in the HMBC, so the sugar moiety of **3** was disclosed to be an α-L-rhamnopyranosyl-(1→4)-β-D-glucopyranoside. Furthermore, the glucosyl H-1 at δ 5.00 correlated with the aglycone carbon signal at δ 79.2, in which the carbon was correlated to the proton signal at δ 4.63 (1H, br s, W_H=7.6 Hz) in the HMQC. Moreover, the H_3-19 (δ 1.15) and carbon signals [δ 73.0 (s), δ 42.5 (d), δ 35.9 (t)] were correlated in the HMBC, so that the hydroxy bearing quaternary carbon (δ 73.0) was deduced to be attached at C-5 or C-9. On the other hand, the hydroxyl methine carbon signal appeared at δ 66.1 corresponded to the proton signal at δ 4.04 (1H, br d, J=12.2 Hz) in the HMQC. Starting from the proton signal at δ 4.04, the ^{1}H–^{1}H COSY and HMQC measurements revealed a sequence of connectivities through respective signals at δ 4.04 [δ 66.1 (d)]→δ 2.25, 1.82 [δ 35.6 (t)]→δ 2.12 [δ 34.7 (d)]→δ 1.90 [δ 42.5 (d)]. Thus, the location of the hydroxyl groups were assigned to C-5 (δ 73.0) and C-6 (δ 66.1). A nuclear Overhauser exchange spectroscopy (NOESY) between H-7β (δ 2.25) and both H-6 (δ 4.04) and H-8 (δ 2.12) indicated a 6α hydroxy group (Fig. 2). And the correlation between H-9 (δ 1.90) and H-2α (δ 1.45), and 4α (δ 1.58) suggested an A/B *cis* ring configuration. When the ^{1}H-NMR spectrum of **3** measured in pyridine-d_5 was compared with that of methanol-d_4, the H_3-19 signal was shifted by +0.19 ppm owing to the anisotropic effect of pyridine. This observation also suggested a 5β hydroxyl group. A small W_H value of the H-3 proton at δ 4.63 (1H, br s, W_H=7.6 Hz) suggested a 3β axial hydroxyl group.

Thus, the structure of **3** was determined to be a (25*S*)-

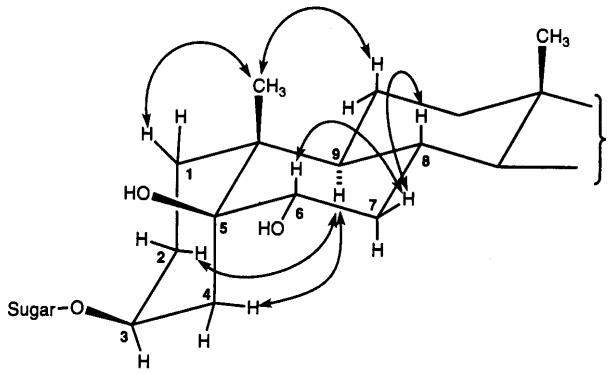

Fig. 2. NOEs Observed for **3** (NOESY)

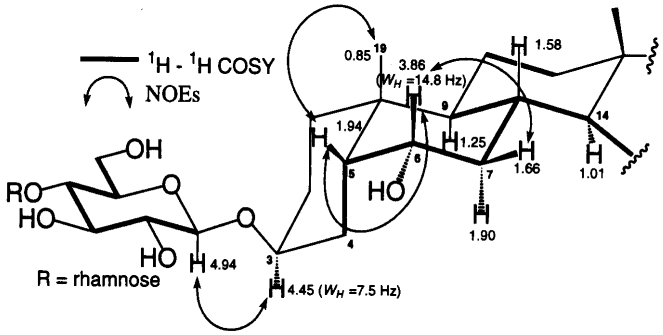

Fig. 3. ^{1}H–^{1}H COSY and NOEs Correlations Observed for **4**

Table 1. ^{13}C-NMR Data for **1**—**4** in Pyridine-d_5

	1	2	3	4		1	2	3	4
C- 1	45.8	45.9	35.9	30.0	glc-1	100.9	101.1	101.9	104.0
- 2	70.4	70.2	29.1	26.7	-2	78.8	78.6	74.9	75.0
- 3	85.0	85.2	79.2	80.1	-3	77.1	77.1	76.8	76.6
- 4	33.4	37.2	35.1	31.7	-4	78.0	77.9	78.5	78.3
- 5	44.6	140.0	73.0	36.4	-5	77.8	77.6	77.5	77.4
- 6	28.1	122.0	66.1	66.9	-6	61.2	61.7	61.2	61.4
- 7	32.1	32.2	35.6	40.5					
- 8	34.6	31.2	34.7	35.6	rha-1	102.9	101.9	102.8	103.0
- 9	54.4	50.2	42.5	41.4	-2	72.5	72.8	72.6	72.6
-10	36.9	37.9	43.1	36.9	-3	72.7	72.5	72.8	72.8
-11	21.4	21.2	21.8	21.4	-4	73.9	74.1	74.0	74.0
-12	40.1	39.8	40.1	40.2	-5	70.6	70.4	70.4	70.5
-13	40.8	40.4	40.6	40.8	-6	18.5	18.5	18.5	18.6
-14	56.4	56.5	56.4	56.4					
-15	32.3	32.3	32.2	32.1	rha'-1	102.1	102.9		
-16	81.2	81.2	81.2	81.3	-2	72.4	72.7		
-17	62.8	62.7	62.9	63.0	-3	72.7	72.4		
-18	16.6	20.4	16.5	16.6	-4	74.1	73.9		
-19	13.5	14.2	17.6	23.8	-5	69.5	69.5		
-20	42.5	42.4	44.7	42.5	-6	18.5	18.5		
-21	14.9	14.9	14.9	14.9					
-22	109.7	109.7	109.8	109.7					
-23	26.2	26.2	26.4	26.2					
-24	26.4	26.4	26.2	26.4					
-25	27.5	27.5	27.6	27.6					
-26	65.1	65.1	65.1	65.1					
-27	16.3	16.3	16.3	16.3					

spirostane-3β,5β,6α-triol 3-*O*-α-L-rhamnopyranosyl-(1→4)-β-D-glucopyranoside.

Compound **4** was isolated as an amorphous powder, $[\alpha]_D$ −60.3° (MeOH). It showed a quasi-molecular ion peak due to $[M-H]^-$ at *m/z* 739 and fragment ion peaks due to $[M-H-$deoxy-pentose$]^-$ at *m/z* 593 and $[M-H-$deoxy-pentose-hexose$]^-$ at *m/z* 431 in the negative FAB-MS. The HR-FAB-MS gave a $[M+Na]^+$ ion at *m/z* 763.4249, which corresponds to the composition $C_{39}H_{64}O_{13}Na$. When the ^{1}H- and ^{13}C-NMR spectra of **4** were compared with that of **3**, signals due to the sugar moiety and signals due to the D, E and F rings on the aglycone were identical. On the other hand, signals due to two hydroxyl methine protons were observed at δ 3.86 and 4.45, and the H_3-19 proton signal was shifted −0.30 ppm in **4**. In the ^{13}C-NMR spectrum of the aglycone moiety, three oxygen-bearing methine carbon signals appeared at δ 66.9, 80.1 and 81.3, the latter two of which were assigned as C-3 and C-16, respectively, by comparing their chemical shifts with those of **3** (Table 1). The ^{1}H–^{1}H COSY and HMQC data (Fig. 3) disclosed a sequence of connectivities through the respective signals at δ 1.25 [δ 41.4 (d)]→δ 1.58 [δ 35.6 (d)]→δ 1.66, 1.90 [δ 40.5 (t)]→δ 3.86 [δ 66.9 (d)]→δ 1.94 [δ 36.4 (d)]→δ 1.85, 1.96 [δ 31.7 (t)]. Thus, the location of the oxygen-bearing methine carbon at δ 66.9 was assigned as C-6. The NOESY between H-5 (δ 1.94) and H_3-19 (δ 0.85) indicated the presence of a 5β hydrogen, per the A/B *cis* ring configuration (Fig. 3). The correlation between H-6 (δ 3.86) and H-5, 7β (δ 1.66) indicated the presence of a 6α hydroxy group. A large W_H value (14.8 Hz) of the H-6 proton also suggested a 6α equatorial hydroxyl group. A small W_H value of the H-3 proton at δ 4.45 (1H, br s, W_H=7.5 Hz) suggested a 3β axial hydroxyl group. Furthermore, the W_H values of H-3 and H-6 were identical to (25*R*)-5β-spirostane-3β,6α-diol, ruizgenin.[7] Thus, the structure of **4** was determined to be a (25*S*)-5β-spirostane-3β,6α-diol (25*epi*-ruizgenin) 3-*O*-α-L-rhamnopyranosyl-(1→4)-β-D-glucopyranoside.

Although compounds **1**, **2**, **3**, and **4** consisted as furostanol glycosides in the authentic sample, compounds **2**, **3**, and **4** were regarded as new spirostanol oligoglycosides. Compounds **1** and **2** were chacotriosyl neogitogenin and lilagenin, respectively. In our research of cytotoxic steroidal oligoglycosides, the chacotriosyl spirostanol oligoglycosides were effective.[2,9] It seems worth subjecting **1** and **2** to tests for cytotoxicity against human cancer cell lines. Compounds **3** and **4** had an A/B *cis* ring configuration. There were fewer examples of this than the A/B *trans* ring configuration. The obtained oligoglycosides have a variety of A/B ring functions. Thus, these compounds (**1**—**4**) are useful for studying the structure–bioactivity relationship of A/B ring functions.

Work is in progress to use these oligoglycosides to study cytotoxicity against human cancer cell lines and anti-herpes simplex virus type 1 (HSV-1) activity.

Experimental

Optical rotations were measured on a JASCO DIP-360 automatic digital polarimeter. The NMR spectra were recorded at 500 MHz for ^{1}H and 125 MHz for ^{13}C on a JEOL α-500 spectrometer and chemical shifts were given on a δ (ppm) scale with tetramethylsilane as the internal standard. Standard pulse sequences were employed for the distortionless enhancement by polarization transfer (DEPT), HMQC, and HMBC experiments. NOESY spectra were measured with mixing times of 600 ms. The FAB-MS were measured with a JEOL DX-300 and/or SX102A spectrometer. The HR-FAB-MS were measured with a JEOL DX-303 HF spectrometer and taken in a glycerol, triethylene glycol and *m*-nitrobenzyl alcohol matrix. GLC was performed on a HP5890A gas chromatograph with a flame ionization detector. TLC was performed on precoated Kieselgel 60 F_{254} plates (Merck). Column chromatography was carried out on Kieselgel 60 (70—230 mesh, 230—400

mesh), Diaion HP-20 (Mitsubishi Chemical, Ind.), Sephadex LH-20 (Pharmacia), and Chromatorex ODS-DU 3050MT (Fuji Silysia). β-Glucosidase from almonds was purchased from Sigma Chemical Co. (St. Louis, MO, U.S.A.).

Extraction and Isolation The seeds (285.8 g) of *Allium tuberosium* were ground and extracted with MeOH twice under reflux. The combined extract was concentrated (19.4 g) and partitioned between hexane and 80% MeOH. The 80% MeOH fraction (11.4 g) was subjected to Diaion HP-20 column chromatography using $H_2O \rightarrow$MeOH to give fractions 1 to 5. Fraction 4 (80% MeOH eluate; 656 mg) was further separated by Chromatorex ODS (50% MeOH→MeOH) to provide Ehrlich reagent (*p*-dimethylaminobenzaldehyde and hydrochloric acid)[10] positive furostanol saponin fraction (356 mg). To a solution of a part of the furostanol saponin fraction (210 mg) in acetate buffer (100 mM, pH 5.0, 4.5 ml) was added β-glucosidase (92 mg, 100 units), and the mixture was incubated at 37 °C for 18 h. The reaction mixture was heated at 80 °C for 1 min, and the precipitate was filtrated off and washed with MeOH. The filtrate and washing was combined and chromatographed on Diaion HP-20, then successively eluted with H_2O and MeOH to give a spirostanol saponin fraction (146 mg). The spirostanol saponin fraction was further purified on Chromatorex ODS (70% MeOH→MeOH) and silica gel column chromatography ($CHCl_3$: MeOH : H_2O = 8 : 2 : 0.2→7 : 3 : 0.5) to give **1** (31.2 mg), **2** (16.6 mg), **3** (5.0 mg) and **4** (2.7 mg), respectively.

Compound **1**: An amorphous powder, $[\alpha]_D^{29}$ −78.4° (*c*=0.26, MeOH). Negative FAB-MS (*m/z*) 885 $[M-H]^-$, 739 $[M-H-\text{deoxy-pentose}]^-$, 593 $[M-H-2\times\text{deoxy-pentose}]^-$. HR-FAB-MS (*m/z*) 909.4836 $[M+Na]^+$ (Calcd for $C_{45}H_{74}O_{17}Na$; 909.4824). ^{1}H-NMR (pyridine-d_5) δ: 0.80 (3H, s, H_3-18), 0.89 (3H, s, H_3-19), 1.08 (3H, d, *J*=6.7 Hz, H_3-21), 1.14 (3H, d, *J*=6.7 Hz, H_3-27), 1.62 (3H, d, *J*=6.0 Hz, rha-H_3-6), 1.68 (3H, d, *J*=6.1 Hz, rha-H_3-6), 5.00 (1H, d, *J*=7.0 Hz, glc-H-1), 5.81 (1H, br s, rha-H-1), 6.34 (1H, br s, rha-H-1). ^{13}C-NMR (pyridine-d_5) δ: Table 1.

Analysis of Sugars Respective compounds **1**—**4** (1 mg) were hydrolyzed with 2 mol/l HCl in H_2O for 4 h at 80 °C. The reaction mixture was neutralized with 2 mol/l NaOH in H_2O and extracted with $CHCl_3$. The aqueous layer was concentrated to dryness *in vacuo* to give a residue which was dissolved in dry pyridine, to which was added L-cysteine methyl ester hydrochloride.[11] The reaction mixture was heated for 2 h at 60 °C and concentrated to dryness by blowing N_2 gas. To the residue was added trimethylsilylimidazole, followed by heating for 1 h at 60 °C. The residue was extracted with hexane and H_2O, and the organic layer was analyzed by GLC; column: OV-17 (0.32 mm×30 m), detector: FID, column temperature: 230 °C, detector temperature: 270 °C, injector temperature: 270 °C, carrier gas: He (2.6 kg/cm^2). Two peaks were observed at t_R (min): 11′78″ (D-Glc) and 8′12″ (L-Rha). The standard monosaccharides were subjected to the same reaction and GLC analysis under the same condition.

Compound **2**: An amorphous powder, $[\alpha]_D^{29}$ −94.2° (*c*=0.12, MeOH). Negative FAB-MS (*m/z*) 883 $[M-H]^-$, 737 $[M-H-\text{deoxy-pentose}]^-$, 591 $[M-H-2\times\text{deoxy-pentose}]^-$. HR-FAB-MS (*m/z*) 907.4679 $[M+Na]^+$ (Calcd for $C_{45}H_{72}O_{17}Na$; 907.4667). ^{1}H-NMR (pyridine-d_5) δ: 0.81 (3H, s, H_3-18), 1.08 (3H, s, H_3-19), 1.08 (3H, d, *J*=6.7 Hz, H_3-21), 1.14 (3H, d, *J*=6.7 Hz, H_3-27), 1.63 (3H, d, *J*=6.1 Hz, rha-H_3-6), 1.69 (3H, d, *J*=6.1 Hz, rha-H_3-6), 4.98 (1H, d, *J*=7.0 Hz, glc-H-1), 5.34 (1H, br s, H-6), 5.82 (1H, s, rha-H-1), 6.39 (1H, s, rha-H-1). ^{13}C-NMR (pyridine-d_5) δ: Table 1.

Compound **3**: An amorphous powder, $[\alpha]_D^{29}$ −61.1° (*c*=0.14, MeOH). Negative FAB-MS (*m/z*) 755 $[M-H]^-$, 609 $[M-H-\text{deoxy-pentose}]^-$, 447 $[M-H-\text{deoxy-pentose-hexose}]^-$. HR-FAB-MS (*m/z*) 779.4178 $[M+Na]^+$ (Calcd for $C_{39}H_{64}O_{14}Na$; 779.4194). ^{1}H-NMR (pyridine-d_5) δ: 0.83 (3H, s, H_3-18), 1.08 (3H, d, *J*=7.3 Hz, H_3-27), 1.15 (3H, s, H_3-19), 1.16 (3H, d, *J*=6.7 Hz, H_3-21), 1.71 (3H, d, *J*=6.1 Hz, rha-H_3-6), 1.90 (1H, m, H-9), 3.38 (1H, br d, *J*=11.0 Hz, H-26), 4.04 (1H, br d, *J*=12.2 Hz, H-6), 4.07 (1H, m, H-26), 4.63 (1H, br s, W_H=7.6 Hz, H-3), 5.00 (1H, d, *J*=8.0 Hz, glc-H-1), 5.88 (1H, br s, rha-H-1). ^{13}C-NMR (pyridine-d_5) δ: Table 1.

Compound **4**: An amorphous powder, $[\alpha]_D^{30}$ −60.3° (*c*=0.27, MeOH). Negative FAB-MS (*m/z*) 739 $[M-H]^-$, 593 $[M-H-\text{deoxy-pentose}]^-$, 431 $[M-H-\text{deoxy-pentose-hexose}]^-$. HR-FAB-MS (*m/z*) 763.4249 $[M+Na]^+$ (Calcd for $C_{39}H_{64}O_{13}Na$; 763.4244). ^{1}H-NMR (pyridine-d_5) δ: 0.81 (3H, s, H_3-18), 0.85 (3H, s, H_3-19), 1.08 (3H, d, *J*=6.7 Hz, H_3-27), 1.15 (3H, d, *J*=7.3 Hz, H_3-21), 1.73 (3H, d, *J*=6.7 Hz, rha-H_3-6), 1.94 (1H, br d, *J*=6.7 Hz, H-5), 3.86 (1H, m, W_H=14.8 Hz, H-6), 4.45 (1H, m, W_H=7.5 Hz, H-3), 4.94 (1H, d, *J*=7.3 Hz, glc-H-1), 5.89 (1H, br s, rha-H-1). ^{13}C-NMR (pyridine-d_5) δ: Table 1.

Acknowledgments We are grateful to Mr. K. Takeda and Mr. T. Iriguchi of the Analytical Center of Kumamoto University for NMR and MS measurements.

References and Notes

1) Ikeda T., Ando J., Miyazono A., Zhu X.-H., Tsumagari H., Nohara T., Yokomizo K., Yueda M., *Biol. Pharm. Bull.*, accepted.
2) Nakamura T., Komori C., Lee Y., Hashimoto F., Yahara S., Nohara T., Ejima A., *Biol. Pharm. Bull.*, **19**, 564—566 (1996).
3) Sang S., Lao A., Wang H., Chen Z., *J. Nat. Prod.*, **62**, 1028—1029 (1999).
4) Koso New Medical College (ed.), "Chinese Drug Dictionary," Vol. 2, Shanghai Science and Technology Publishing Co., 1978, p. 1646.
5) Tori K., Seo S., Terui Y., Nishikawa J., Yasuda F., *Tetrahedron Lett.*, **22**, 2405—2408 (1981).
6) Agrawal P. K., Jain D. C., Gupta R. K., Thakur R. S., *Phytochemistry*, **24**, 2479—2496 (1985).
7) *a*) Vollener Yu. S., Abdullaev N. D., Gorovits M. B., Abubakirov N. K., *Khim. Prir. Soedin.*, **6**, 736—740 (1983); *b*) Blunden G., Carabot A., Cripps A. L., Jewers K., *Steroids*, **35**, 503—510 (1980).
8) *a*) Maker R. E., Turner D. L., Shabica A. C., Jones E. M., Krueger J., Surmatis J. D., *J. Am. Chem. Soc.*, **62**, 2620—2621(1940): *b*) Elks J., in "Rodd's Chemistry of Carbon Compounds," Vol. II, Coffey S. (ed.), Elsevier, Amsterdam, London, New York, 1971, pp. 1—53.
9) *a*) Hsu S.-H., Tsai T.-R., Lin C.-N., Yen M.-H., Kuo K.-W., *Biochem. Biophys. Res. Commun.*, **229**, 1—5 (1996): *b*) Chang L.-C., Tsai T.-R., Wang J.-J., Lin C.-N., Kuo K.-W., *ibid.*, **242**, 21—25 (1998).
10) Stahl E., "Dünnschich-Chromatographie," Springer-Verlag, Berlin, 1962, pp. 498—503.
11) Hara S., Okabe H., Mihashi K., *Chem. Pharm. Bull.*, **35**, 501—507 (1987).

Preparation and Characterization of Two Crystalline Forms of 4-Amino-5-chloro-2-methoxy-*N*-[(2*S*,4*S*)-1-ethyl-2-hydroxymethyl-4-pyrrolidinyl]benzamide (TKS159)

Toshiharu YANAGI,*[a,b] Jun-ichi MIZOGUCHI,[a] Tsutomu ADACHI,[a] Seiji SATO,[a] Kazuya KODAMA,[a] Kinsei ANZAI,[a] Yasushi TAKAGISHI,[a] Chiaki KAMEI,[b] Manabu FUJIWARA,[c] Takayuki MATSUSHITA,[c] Yuko YAMASHOJI,[d] and Yoshihisa INOUE[d]

Research and Development Department, Teikoku Chemical Industries Co., Ltd.,[a] 5–41 Senzo, Itami, Hyogo 664–0898, Japan, Department of Pharmacology, Faculty of Pharmaceutical Sciences, Okayama University,[b] 1–1–1 Tsushima-naka, Okayama 700–8530, Japan, Department of Materials Chemistry, Faculty of Science and Technology, Ryukoku University,[c] 1–5 Yokotani, Seta-Oe cho, Otsu, Shiga 520–2194, Japan, and Department of Molecular Chemistry, Faculty of Engineering, Osaka University,[d] 2–1 Yamadaoka, Suita, Osaka 565–0871, Japan.
Received September 24, 1999; accepted November 15, 1999

For 4-amino-5-chloro-2-methoxy-*N*-[(2*S*,4*S*)-1-ethyl-2-hydroxymethyl-4-pyrrolidinyl]benzamide (TKS159), two polymorphs, forms α and β, were prepared and characterized by means of X-ray powder diffractometry, thermal analysis, infrared spectroscopy and ^{13}C-NMR spectroscopy, both in the solution and solid phases. The X-ray powder diffraction analysis gave different patterns for forms α and β. In the thermogravimetry and differential thermal analysis profiles, form β exhibited characteristic endo- and exothermic peaks at 112.7 °C and 116.2 °C, respectively, due to the partial melting-induced phase transition to form α without accompanying weight loss, and these were followed by an additional endothermic peak at 138.2 °C due to fusion. For form α, only an endothermic peak at 137.8 °C due to fusion was observed. The IR spectroscopic analyses of forms α and β gave different absorption bands assigned to N–H and O–H stretching, N–H bending, and C=O stretching vibrations. From the data obtained by thermal analysis, form α was shown to be thermodynamically more stable than form β.

Key words TKS159; polymorph; X-ray powder diffractometry; thermal analysis; ^{13}C-NMR spectroscopy; 4-amino-5-chloro-2-methoxy-*N*-[(2*S*,4*S*)-1-ethyl-2-hydroxymethyl-4-pyrrolidinyl]benzamide

Polymorphism is a critical issue in pharmaceutical development, since physical and chemical properties are known to vary with crystalline forms.[1] Polymorphs are regarded as thermodynamically different phases, which possess different thermal properties and spectroscopic profiles. Differences in thermodynamic properties can affect the stability, solubility, and bioavailability of pharmaceuticals. Thus, the polymorphism of various pharmaceuticals, *e.g.* indomethacin,[2] fuconazole,[3] lomeridine,[4] *etc.*, has been investigated, and the choice of crystalline form of drug substance is one of the important aspects in drug development.

4-Amino-5-chloro-2-methoxy-*N*-[(2*S*,4*S*)-1-ethyl-2-hydroxymethyl-4-pyrrolidinyl]benzamide (TKS159, **1**) developed by Teikoku Chemical Industries Co., Ltd., is a potential gastroprokinetic agent,[5] and clinical study is ongoing. The chemical structure of TKS159 and atomic numbering used in this study are shown in Chart 1. The absolute configuration determined by single crystal X-ray diffraction analysis was reported in a previous paper.[6] Crystals which were obtained by recrystallization from several solvents were characterized by various spectroscopic methods, and eventually two kinds of crystalline forms were clearly distinguished. The crystalline form that was recrystallized from aqueous ethanol, water, ethyl acetate, or methyl ethyl ketone was designated as form α, while that recrystallized from acetone was designated as form β. In this paper, we will report the preparation and characterization of the two polymorphs, forms α and β, of **1**. They were characterized by means of X-ray powder diffraction analysis, thermal analysis, infrared (IR) spectroscopy and ^{13}C-NMR spectroscopy, both in the solution and solid states, and by elemental analysis.

Results and Discussion

First, the two crystalline forms were subjected to elemental analysis. The results of the elemental analysis for the two crystalline forms agreed with the calculated value without any solvents in crystals.

The X-ray powder diffraction patterns of form α and form β are shown in Fig. 1. Sharp and intense X-ray diffraction peaks of form α occured at 2θ=8.0, 13.3, 20.4, and 23.4°, as shown in Fig. 1a, while those of form β were observed at 2θ=7.5, 9.9, 15.1, 22.9, 23.9, 24.5, and 26.4°, as shown in Fig. 1b. The distinctly different patterns observed for forms α and β are taken as definitive evidence in support of the existence of polymorphs.

The thermogravimetry–differential thermal analysis (TG-DTA) thermograms of the two polymorphs are shown in Fig. 2. The single endothermic peak at 137.8 °C for form α in Fig. 2a is attributable to fusion. In contrast, form β showed closely located endo- and exothermic peaks at 112.7 and 116.2 °C, respectively, followed by an additional endothermic peak at 138.2 °C, as shown in Fig. 2b. Over the temperature range of 25—200 °C, the TG curves for both forms showed no weight loss. Since form β finally gave the same melting point as form α, the successive endo- and exothermic peaks

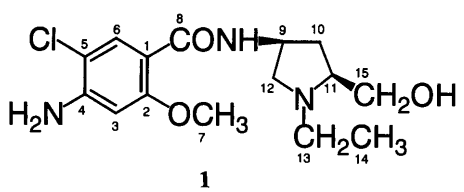

1

Chart 1

* To whom correspondence should be addressed.

© 2000 Pharmaceutical Society of Japan

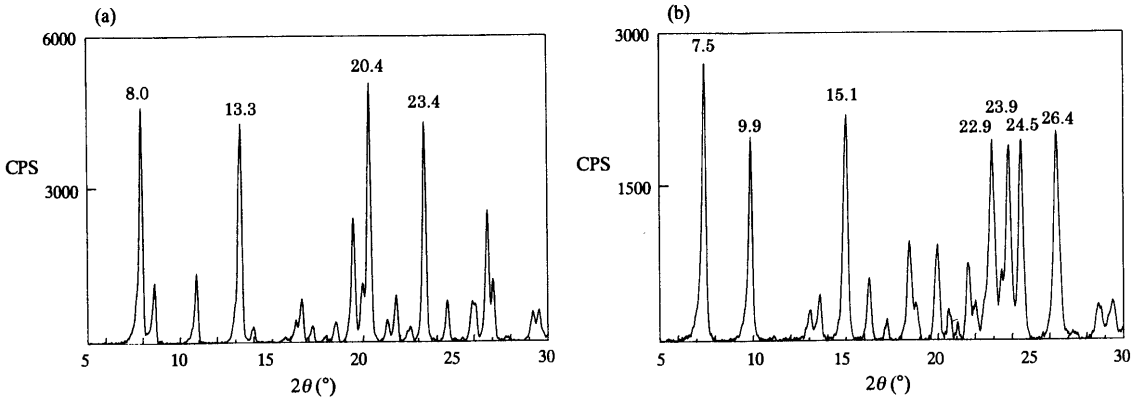

Fig. 1. X-Ray Diffraction Patterns of Forms α (a) and β (b)

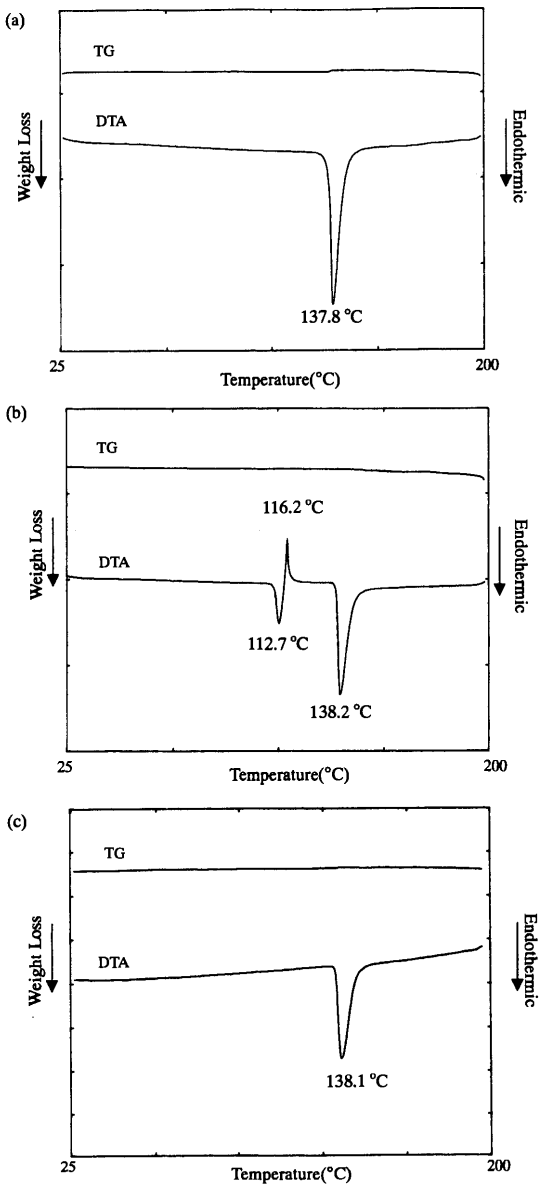

Fig. 2. TG and DTA Curves for Forms α (a) and β (b) and Form β after Heating to 120 °C (c)

peculiar to form β are most probably attributable to the phase transition from form β to α, presumably initiated by the partial melting of form β, as indicated by the endothermic peak at 112.7 °C, which is suddenly switched to an exothermic peak at 116.2 °C. A similar phenomenon has been reported for one of the polymorphic forms of indomethacin by Lin.[7] Additionally, when form β was heated to 120 °C, then cooled to room temperature, and re-heated again from 25 to 200 °C, the endo- and exothermic peaks between 110 and 120 °C completely disappeared, and only the endothermic peak at 138.1 °C appeared, as shown in Fig. 2c. This thermal profile of form β is irreversible. These observations strongly support a causative role of the phase transition.[8]

The IR spectra of forms α and β are shown in Fig. 3. Strong absorption bands due to the N–H and O–H stretching vibrations in the amino and hydroxyl groups are centered at 3421 and 3387 cm^{-1} for form α, as shown in Figs. 3a and 3d, whereas they shifted to 3453 and 3401 cm^{-1}, respectively, for form β, as shown in Figs. 3b and 3d. Absorption bands assigned to the N–H bending vibrations are centered at 1546 and 1637 cm^{-1} for form α. For form β, these shift to 1532 and 1626 cm^{-1}, respectively. The lower frequencies in the N–H and O–H stretching vibrations in the amino and hydroxyl groups, and the higher frequency in the N–H bending vibrations in the amide and amino groups are characteristic of the presence of a stronger inter- and/or intramolecular hydrogen bond.[9] For form α, the absorption band observed at 1626 cm^{-1} is characteristic of the C=O stretching vibrations in the amide group. For form β, they are same as those for form α at 1626 cm^{-1}. The absorption band assigned to the C–H bending vibrations in the aromatic group is centered at 833 cm^{-1} for form α. For form β, it shifts to 821 cm^{-1}. It is considered that the different frequencies on the C–H bending vibrations are attributable to the different conformations of forms α and β in crystals. It is also interesting to note that the IR spectrum for form β after heating to 120 °C, as shown in Fig. 3c, is practically identical to that of form α shown in Fig. 3a, for which the phase transition is responsible.

The ^{13}C-NMR spectra were obtained in $CDCl_3$ solution and in the solid state, and the results are shown in Fig. 4. Analysis of the ^{13}C-NMR spectra in the solution was facilitated by using distortionless enhancement by polarization transfer (DEPT), ^{13}C–^{1}H correlated spectroscopy (COSY), and ^{13}C–^{1}H correlated spectroscopy *via* long-range coupling (COLOC) techniques (data not shown). No peak for any solvent was observed in the ^{1}H- and ^{13}C-NMR spectra. Figs. 4b and 4c show the spectra of forms α and β, respectively. On the basis of the comparative study of the spectra obtained in

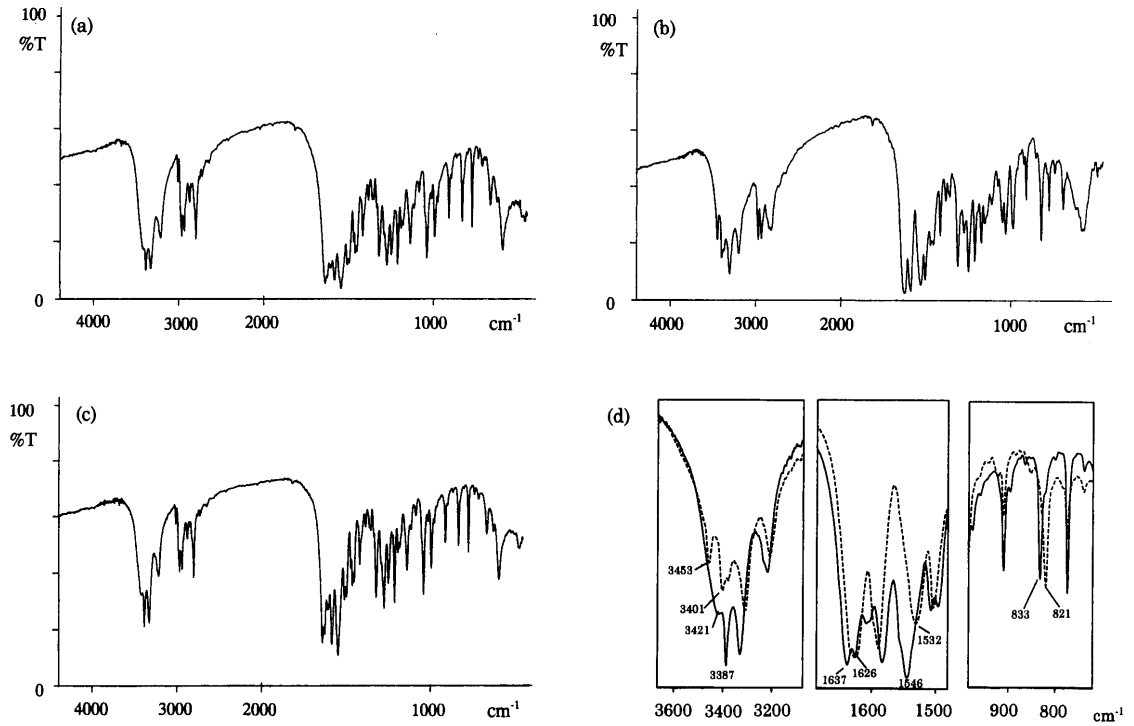

Fig. 3. IR Spectra of Form α (a), Form β (b), Form β after Heating to 120 °C (c), Overlays of Form α (—) and Form β (---) (d)

$CDCl_3$ solution and in the solid state, the principal peaks were assigned as shown in Table 1.

As can be seen from Fig. 4, notable peak broadening was observed, particularly for the signals of the aromatic C-4 and amide C-8. Since these carbons are incorporated in the hydrogen-bonding amino and amide moieties of **1**, the broadening may be attributable to the effects of the intermolecular hydrogen bonds in the crystals through the amino and carbonyl groups upon the magnetic environment of these carbons.

From comparison of the ^{13}C-NMR spectra in solution and in the solid state, further insights into the conformational differences between forms α and β can be obtained. For easier comparison, deviations in the chemical shifts obtained in the solid state from the corresponding values observed in solution are plotted for the two crystalline forms in Fig. 5. It is noted that although the deviations from the solution-phase spectrum are significant for most carbons, practically the same chemical shifts as those in solution were obtained for C-2, C-7, and C-9, which are located near the intramolecular hydrogen bond between the amide N–H and the methoxy oxgen of **1**, as shown in the X-ray crystallographic study.[6] This clearly indicates that the intramolecular hydrogen bond is not destroyed, even in $CDCl_3$ solution.[10,11] In contrast, the chemical shifts of C-4, C-10, C-14, and C-15 depend critically on the crystalline form. Since these carbons are directly involved in the intermolecular hydrogen bonding network or are located nearby in form α, the different δ values observed for form β imply some drastic changes in the hydrogen bonding structure. In this context, it is interesting to note that form β, rather than α, gives chemical shifts which are more close to those observed in solution, as can be seen from Table 1 and Fig. 5. These facts indicate that the hydrogen bonding interactions are either much weaker or absent in form β. For more detailed comparative studies on the crystal structures of forms α and β, the preparation of a single crystal of form β is currently underway.

Conclusion

Two polymorphs, forms α and β of 4-amino-5-chloro-2-methoxy-*N*-[(2*S*,4*S*)-1-ethyl-2-hydroxymethyl-4-pyrrolidinyl]benzamide (TKS159, **1**), were prepared and characterized by means of X-ray powder diffractometry, thermal analysis, IR spectroscopy, ^{13}C-NMR spectroscopy, and elemental analysis. From the data presented in this paper, particularly in thermal analysis data, form α is thermodynamically more stable than form β.

Experimental

Materials 4-Amino-5-chloro-2-methoxy-*N*-[(2*S*,4*S*)-1-ethyl-2-hydroxymethyl-4-pyrrolidinyl]benzamide (TKS159, **1**) was synthesized at Teikoku Chemical Industries Co., Ltd. (Osaka, Japan), according to the procedures reported previously.[12]

Preparation of the Polymorphs Polymorphs of **1** were prepared in the following manner.

Form α: 3.0 g of **1** was dissolved in 15 ml of a 1 : 1 mixture of water and ethanol by heating in a water bath at 85 °C for 30 min, then the clear solution obtained was allowed to stand overnight at room temperature. The resulting crystals were collected by filtration, washed with 5 ml of a 1 : 1 water–ethanol mixture, and dried *in vacuo* at 50 °C. Form α could also be obtained by recrystallization from water, ethyl acetate, or methyl ethyl ketone.

Form β: 3.0 g of **1** was dissolved in 15 ml of acetone by heating in a water bath at 60 °C for 30 min, then the clear solution obtained was allowed to stand overnight at room temperature. The resulting precipitate was collected by filtration, washed with 5 ml of acetone, and dried *in vacuo* at 50 °C.

X-Ray Powder Diffractometry X-Ray powder diffraction patterns were obtained using a Rigaku Geigerflex RAD-2C X-ray powder diffractometer under the following conditions: target, nickel filtered Cu$K\alpha$ radiation, λ= 1.5418 Å; voltage, 40 kV; current, 20 mA; receiving slit, 0.15 mm; scanning speed, 4°/min; scanning range, 5—30°/2θ.

Thermal Analysis In TG–DTA, samples of 6 mg in open aluminum pans were heated at a rate of 5 °C/min under a nitrogen purge, with an empty, open aluminum pan as the reference, in a TG–DTA apparatus (Seiko Instruments, model SSC-5000).

IR Spectroscopy IR spectra in the solid state were measured in KBr

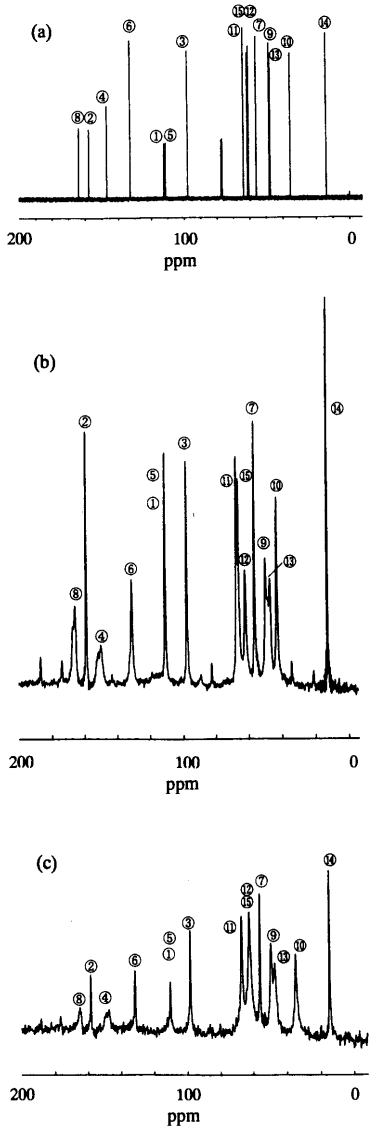

Fig. 4. ^{13}C-NMR Spectra in $CDCl_3$ Solution (a), in the Solid State for Form α (b), in the Solid State for Form β (c)

Table 1. ^{13}C Chemical Shifts of TKS159 (**1**) in $CDCl_3$ Solution and in the Solid State[a)]

No. of carbon atom	$CDCl_3$ solution[b)]	Form α	Form β	Δ ($\delta_{\beta-\alpha}$)
1	112.34	110.21	110.10	−0.11
2	157.72	158.32	158.28	−0.04
3	97.83	97.20	98.04	0.84
4	146.92	149.52	147.28	−2.24
5	111.33	110.21	110.10	−0.11
6	132.82	130.57	131.27	0.70
7	55.89	55.79	55.76	−0.03
8	163.84	165.30	164.71	−0.59
9	48.05	49.17	49.22	0.05
10	35.40	42.55	34.54	−8.01
11	63.66	66.62	66.75	0.13
12	60.50	61.41	62.06	0.65
13	47.46	46.48	46.93	0.52
14	13.89	12.60	14.54	1.94
15	61.19	65.50	62.06	−3.44

a) The chemical shifts were reported in δ values relative to tetramethylsilane (0.00 ppm) or glycine (176.03 ppm for the carbonyl). *b*) Concentration: 125 mg/ml.

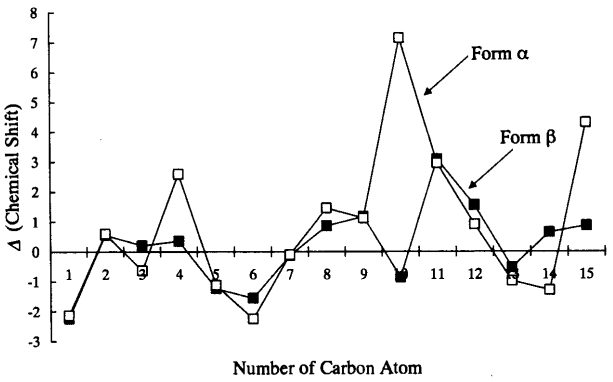

Fig. 5. Deviation in the Chemical Shift of Each Carbon in Forms α (□) and β (■) from That in $CDCl_3$ Solution

disks over a range of 4400 to 550 cm^{-1} on a Perkin-Elmer FT-IR spectrometer model 1650.

^{13}C-NMR Spectroscopy The ^{13}C-NMR spectrum in $CDCl_3$ was recorded on a Bruker AMX-400 spectrometer using tetramethylsilane as an internal standard which was referenced to 0.00 ppm. The CP/MAS (cross polarization–magic angle scanning) ^{13}C-NMR spectra were recorded on a Bruker MSL-200 instrument using the carbonyl carbon in glycine as an external standard which was referenced to 176.03 ppm.

References

1) Haleblian J. K., *J. Pharm. Sci.*, **64**, 1269—1288 (1975).
2) Yamamoto H., *Chem. Pharm. Bull.*, **16**, 17—19 (1968).
3) Gu X. J., Jiang W., *J. Pharm. Sci.*, **84**, 1438—1441 (1995).
4) Hiramatsu Y., Suzuki H., Kuchiki A., Nakagawa H., Fujii S., *J. Pharm. Sci.*, **85**, 761—766 (1996).
5) Matsuyama S., Sakiyama H., Nei K., Tanaka C., *J. Pharmacol. Exp. Ther.*, **276**, 989—995 (1996).
6) Adachi T., Mizoguchi J., Hayashi Y., Yamashoji Y., Kanehisa N., Kai Y., Inoue Y., *Acta Cryst.*, **C54**, 1527—1529 (1998).
7) Lin S., *J. Pharm. Sci.*, **81**, 572—576 (1992).
8) Grunenberg A., *Pharm. Zeit.*, **1997**, 224—231.
9) Nakanishi K., Solomon P. H., Furutachi N., "Infrared Absorption Spectroscopy", Nankodo, Tokyo, **1986**.
10) Anker L., Lauterwein J., Van de Waterbeemd H., Testa B., *Helv. Chim. Acta*, **67**, 706—716 (1984).
11) Cesario M., Pascard C., Moukhtari M. E., Jung L., *Eur. J. Med. Chem.*, **16**, 13—17 (1981).
12) Yanagi T., Kitajima A., Anzai K., Kodama K., Mizoguchi J., Fujiwara H., Sakiyama H., Kamoda O., Kamei C., *Chem. Pharm. Bull.*, **47**, 1650—1654 (1999).

Quaternary Isoquinoline Alkaloids from *Stephania cepharantha*

Takao TANAHASHI,*[,a] Yuko SU,[a] Naotaka NAGAKURA,[a] and Hidekazu NAYESHIRO[b]

Kobe Pharmaceutical University,[a] 4–19–1 Motoyamakita-machi, Higashinada-ku, Kobe 658–8558, Japan and Central Research Laboratories, Sunstar Inc.,[b] 3–1 Asahi-machi, Takatsuki, Osaka 569–1195, Japan.

Received September 24, 1999; accepted November 25, 1999

From the quaternary alkaloidal fraction of the dried tubers of *Stephania cepharantha*, two new isoquinoline alkaloids, stecepharine and tetradehydroreticuline have been isolated along with the known compounds, magnoflorine, menisperine, steponine, cyclanoline, oblongine, *cis*-*N*-methylcapaurine and 2′-*N*-methylisotetrandrine. *cis*-*N*-Methylcapaurine (=9-*O*-methylstecepharine) was isolated as a natural product for the first time. Their structures were determined on the basis of spectroscopic evidence.

Key words *Stephania cepharantha*; isoquinoline alkaloid; protoberberine *N*-metho salt; Menispermaceae; tubers

"Bai yao zi," the dried tubers of *Stephania cepharantha* HAYATA (Menispermaceae), has been used in Chinese folk medicine for the treatment of diseases such as parotiditis, gastric ulcer and leukopenia.[1—3] Previous phytochemical investigations of the plant material collected in Taiwan and Japan have revealed the presence of a large number of alkaloids including bisbenzylisoquinolines.[4] Several bisbenzylisoquinoline alkaloids have been shown to possess pharmacological activities such as vasodilator effect,[5] and our recent studies have also disclosed the effects of some members of alkaloids of this group on proliferation of cultured cells from the murine hair apparatus.[6] These intensive phytochemical and pharmacological studies were focused mainly on tertiary alkaloidal constituents, while only palmatine has so far been isolated as a quaternary base[7] because of the difficulty in isolation of quaternary alkaloids. However, good separation has recently been achieved by reverse-phase HPLC using ion-pair solvent systems.[8] This prompted us to re-examine the quaternary alkaloidal fraction of *S. cepharantha* and to isolate nine alkaloids, two of which were new. This paper deals with the isolation and structure elucidation of these new compounds and characterization of known protoberberine and bisbenzylisoquinoline alkaloids.

Separation of the quaternary alkaloidal fraction of the dried tubers of *Stephania cepharantha* afforded nine alkaloids, **1**—**9** as perchlorates. Compounds **1**—**5** were identified as magnoflorine,[8b] menisperine,[9,10] steponine,[11—13] cyclanoline,[14] and oblongine,[15] respectively by comparison of their spectral data with those described in the literature. These alkaloids have been isolated for the first time from the plant material.

Compound **6**, termed stecepharine, was isolated as a colorless amorphous powder, $[\alpha]_D$ −175°. Its high resolution secondary ion mass spectrum (HR-SI-MS) exhibited a strong peak at *m/z* 372.1826 ($[M]^+$), indicating a molecular formula of $C_{21}H_{26}NO_5$. Its ^{1}H-NMR spectrum demonstrated a singlet for aromatic proton at δ 6.50, a pair of doublets for two *ortho*-coupled protons at δ 6.68 and 6.95 (J=8.5 Hz), three signals for aromatic methoxyl groups at δ 3.80, 3.85 and 3.86, and an *N*-methyl signal at δ 3.25. The ^{1}H-NMR spectral features were comparable with those of steponine (**3**) except for the absence of an aromatic singlet and the presence of one additional methoxyl signal. High resolution electron ionization mass spectrum (HR-EI-MS) fragment ions at *m/z* 208.1007 and 150.0682, arising from A/B rings and D ring, respectively, indicated the substitution of a phenolic hydroxyl and two methoxyl groups on ring A and of a phenolic hydroxyl and a methoxyl group on ring D.[12] The placement of the methoxyl and hydroxyl groups was determined by a series of ^{1}H-detected heteronuclear multiple-bond connectivity

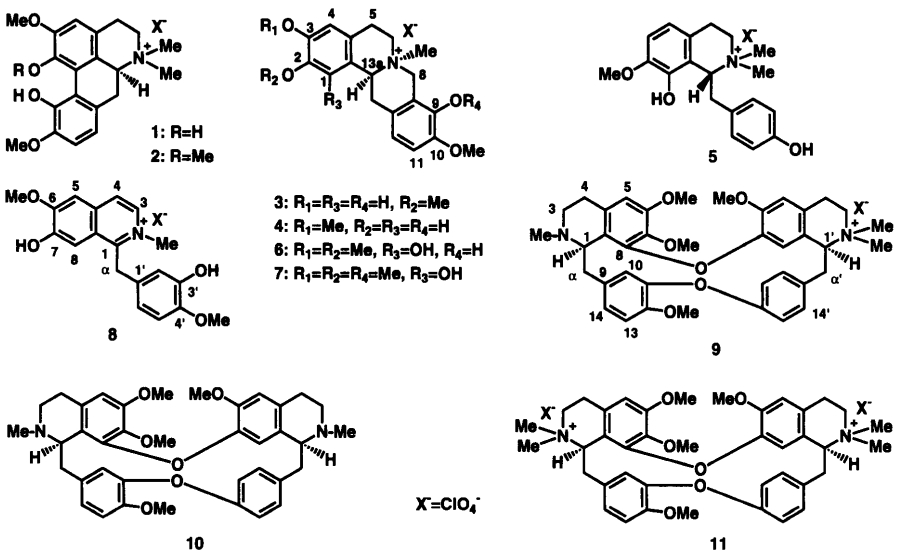

Chart 1

* To whom correspondence should be addressed.

© 2000 Pharmaceutical Society of Japan

(HMBC) and nuclear Overhauser enhancement spectroscopy (NOESY) experiments with **6**. NOESY interaction between the signal at δ 6.50 and H-5 allowed us to assign the aromatic proton signal to H-4, and thereby its correlated methoxyl signal at δ 3.85 to 3-OMe. In the HMBC spectrum, significant interactions were observed between H-4 and two aromatic carbon signals (δ 136.5, 154.9), which were associated with methoxyl groups, and between H-13a and the carbon signal at δ 148.2 bearing a hydroxyl group, suggesting the placement of a hydroxyl at C-1 and methoxyls at C-2 and C-3, respectively. The substitution pattern on ring D in **6** was suggested to be the same as in steponine (**3**) and cyclanoline (**4**) by comparison of their ^{13}C-NMR data (Table 1). The placement of the methoxyl group at C-10 was further supported by HMBC correlation between a methoxyl signal at δ 3.86 and C-10, as well as a NOESY interaction between the methoxyl group and H-11 at δ 6.95. The ^{1}H- and ^{13}C-NMR chemical shifts of *N*-methyl group (δ_H 3.25, δ_C 50.8) as well as a NOESY cross peak between the *N*-methyl group and H-13a suggested B/C-*cis* fused form.[13] The negative sign of specific optical rotation and circular dichroism (CD) curve indicated the *S* configuration of C-13a. Accordingly, the structure of the new compound was elucidated as shown.

Table 1. ^{13}C-NMR Spectral Data for **3**, **4**, **6** and **7** in CD_3OD

	3	4	6	7
C-1	111.2	111.3	148.2	148.3
C-1a	121.9	121.9	114.3	114.2
C-2	148.7	150.1	136.5	136.5
C-3	148.7	151.3	154.9	154.9
C-4	116.7	113.4	104.9	104.9
C-4a	124.2	125.4	125.1	125.0
C-5	23.9	24.2	24.4	24.4
C-6	53.4	53.4	52.3	52.3
C-8	61.2	61.2	62.3	62.2
C-8a	114.3	114.3	114.3	121.0
C-9	144.5	144.5	144.4	146.7
C-10	147.5	147.6	147.5	152.6
C-11	113.2	113.2	113.2	114.9
C-12	119.8	119.8	119.6	124.8
C-12a	123.2	123.1	123.4	123.6
C-13	35.0	35.0	33.5	33.4
C-13a	67.4	67.3	62.9	62.8
NMe	51.0	51.0	50.8	50.7
OMe	56.7	56.6	56.5	56.5
	56.7	56.7	56.7	56.5
	—	—	61.3	61.2
	—	—	—	61.3

Alkaloid **7** was also obtained as an amorphous powder. The HR-SI-MS measurement of **7** revealed the molecular formula, $C_{22}H_{28}NO_5$. The ^{1}H- and ^{13}C-NMR (Table 1) spectral features of **7** were closely similar to those of **6**, except for the presence of one additional aromatic methoxyl signal and the chemical shifts of the signals arising from the aromatic ring D. These results suggested that **7** was a 9-*O*-methyl derivative of **6**. The HR-EI-MS of **7** showed a fragment ion peak at *m/z* 164.0868, CH_2 more than the corresponding peak of **6**, which could be explained by the methylation of a phenolic hydroxyl group at C-9. The substitution pattern of ring A and B/C junction in **7** were deduced to be the same as in **6** from comparison of their ^{1}H- and ^{13}C-NMR spectral data coupled with the results of NOESY and HMBC experiments with **7**. Accordingly, compound **7** was established as 9-*O*-methylstecepharine. The alkaloid has previously been prepared from capaurine,[13] but was isolated and characterized here as a natural product for the first time.

Compound **8** was isolated as a colorless crystalline solid, mp 231—233 °C, and its HR-SI-MS established the composition $C_{19}H_{20}NO_4$. It showed UV maxima at 232, 257, 280, 318 and 367 nm. Its ^{1}H-NMR spectrum demonstrated two singlets for aromatic protons at δ 7.64 and 7.75, an aromatic ABX spin system at δ 6.46—6.86, two signals for aromatic methoxyl groups at δ 3.80 and 4.16, and also an *N*-methyl signal in the rather low field (δ 4.28) and a pair of doublets at δ 8.10 and 8.28 (J=7.0 Hz). These findings suggested that the compound is a benzylisoquinoline alkaloid with the B

Table 2. ^{13}C-NMR Spectral Data for **9**, **10** and **11** in CD_3OD

	9	10	11		9	10	11
C-1	64.9	63.4	72.1	C-1′	72.6	64.4	72.4
C-3	46.1	45.5	54.8[a)]	C-3′	55.0	46.2	54.9[a)]
C-4	24.3	24.9	24.7	C-4′	24.3	26.2	24.3
C-4a	128.3	130.5	125.7	C-4′a	126.2	129.9	126.5
C-5	107.3	107.1	107.0	C-5′	112.7	112.6	112.7
C-6	154.7	153.5	155.4	C-6′	153.1	151.3	152.8
C-7	138.6	138.4	138.9	C-7′	145.5	145.0	145.2
C-8	148.5	149.3	148.1	C-8′	121.6	121.2	121.7
C-8a	117.4	121.6	115.7	C-8′a	122.6	128.8	122.8
C-α	38.2	38.9	37.7	C-α′	37.1	37.3	37.0
C-9	133.8	136.5	133.7	C-9′	132.7	136.4	132.2
C-10	117.4	117.4	118.8	C-10′	133.8	133.5	133.7
C-11	151.3	151.0	151.0[b)]	C-11′	122.6	122.5[c)]	121.7
C-12	150.1	148.9	150.9[b)]	C-12′	157.2	155.9	158.1
C-13	113.7	113.4	114.2	C-13′	122.6	122.3[c)]	122.2
C-14	124.9	124.5	125.3	C-14′	132.1	131.5	131.8
2-NMe	42.7	43.1	51.3	2′-NMe	52.4	42.7	52.4
	—	—	55.0		52.9	—	52.8
6-OMe	56.5	56.3	56.6	6′-OMe	56.2	55.9	56.2
7-OMe	61.1	61.0	61.3				
12-OMe	56.8	56.8	56.8				

a—*c*) Assignments may be interchangeable.

ring aromatized.[16] Nuclear Overhauser effect (NOE)s observed in the NOESY spectrum of **8** demonstrated that the methoxyl groups were situated at C-6 and C-4′. Accordingly, the structure of **8** was elucidated as shown and designated tetradehydroreticuline.

Compound **9** was isolated as an amorphous powder, $C_{39}H_{45}N_2O_6$. It showed UV maxima at 232sh and 284 nm. Its ^{1}H-NMR spectral features showed analogy to those of isotetrandrine (**10**), a major tertiary alkaloid of this plant, except that **9** showed three singlets for *N*-methyl groups at δ 2.51, 3.15 and 3.46 instead of two singlets at δ 2.25 and 2.56 in **10**. These findings implied that the alkaloid was a 2-*N*- or 2′-*N*-methylated compound of **10**. This was supported by the fact that methylation of **9** with methyl iodide gave **11**, which was identified with 2,2′-*N*-dimethylisotetrandrine prepared from **10**. Two nitrogen atoms in **9** were discriminated by the two dimensional (2D)-NMR technique. HMBC interactions with H-14 and H-14′ led to the assignment of C-α and C-α', which were correlated with H_2-α and H_2-α', respectively, in the ^{1}H-detected heteronuclear multiple quantum coherence (HMQC) spectrum. HMBC cross-peaks between H_2-α', two *N*-methyl singlets at δ 3.15 and 3.46 and C-1′ as well as between H-α (δ 2.89), an *N*-methyl at δ 2.51 and C-1 confirmed the situation of an additional *N*-methyl group at 2′-nitrogen. Thus, compound **9** was determined to be 2′-*N*-methylisotetrandrine. This alkaloid has already been isolated from *Berberis oblonga*,[17] but is fully characterized here for the first time.

Experimental

The melting point was measured on a Büchi melting point apparatus and is uncorrected. UV spectra were recorded on a Shimadzu UV-240 spectrophotometer, IR spectra on a Shimadzu FT-IR-8200 spectrophotometer and CD spectra on a Shimadzu-Aviv 62 A DS CD spectrometer. Optical rotations were measured on a JASCO DIP-370 digital polarimeter. MS and HR-MS were obtained with a Hitachi M-4100 mass spectrometer. For SI-MS, glycerol was used as the matrix. All NMR spectra were recorded on a Varian VXR-500 spectrometer with tetramethylsilane as an internal standard.

Extraction and Isolation of Alkaloids Solvent extraction of the crude drug "Bai yao zi" was carried out as reported previously.[6] After extraction of the tertiary alkaloids with Et_2O and CH_2Cl_2, the remaining aq. layer was acidified with 2.5% tartaric acid and then $NaClO_4$ was added (final concentration 0.5 M). The quaternary alkaloids were extracted as ion pairs with CH_2Cl_2. The CH_2Cl_2 extract was dried over anhydrous $MgSO_4$ and concentrated *in vacuo* to leave an alkaloidal fraction (16.5 g). A part (4.31 g) of the residue was dissolved in aq. $NaHCO_3$ solution and $NaClO_4$ was added (final concentration 0.5 M) and then extracted with $C_2H_4Cl_2$. The $C_2H_4Cl_2$ layer was extracted with aq. NaOH solution, dried and concentrated to give the residue RQ-1 (561 mg). The remaining NaOH alkaline solution was acidified with HCl and extracted as ion pairs with $C_2H_4Cl_2$ after addition of $NaClO_4$. Concentration of the organic extract afforded the residue RQ-2 (2.74 g). The initial $NaHCO_3$ solution was acidified with tartaric acid and extracted with $C_2H_4Cl_2$. The $C_2H_4Cl_2$ extract was dried and concentrated *in vacuo* to leave the residue RQ-3 (624 mg). Respective residue was further purified by preparative HPLC. HPLC conditions for ion-pair chromatography were as follows. Column: Cosmosil 5C18-AR (20 mm×25 cm, Nacalai Tesque); eluent: gradient elution of (A) 50% $HClO_4$: 0.2 M $NaClO_4$ (0.2 : 1000) and (B) acetonitrile from A/B (80/20) to A/B (50/50) (linear gradient). Each fraction was worked up as described in ref. 8*b*, and gave rise to alkaloid perchlorates. RQ-1 gave **2** (30.0 mg), **3** (17.4 mg), **4** (36.9 mg), **6** (15.9 mg), **7** (11.6 mg), **9** (20.0 mg). RQ-2: **2** (17.6 mg), **3** (388 mg), **4** (82.6 mg), **5** (11.9 mg), **6** (82.6 mg), **7** (21.4 mg). RQ-3: **1** (325 mg), **3** (83.1 mg), **6** (5.4 mg), **7** (2.2 mg), **8** (16.6 mg).

Steponine (**3**) Perchlorate: $[\alpha]_D^{30}$ −151° (c=1.03, MeOH). CD λ_{max}^{MeOH} nm ($\Delta\varepsilon$): 210 (−19.8), 231i (−2.1), 241 (+0.35).

Cyclanoline (**4**) Perchlorate: $[\alpha]_D^{30}$ −131° (c=1.08, MeOH). CD λ_{max}^{MeOH} nm ($\Delta\varepsilon$): 208 (−16.5), 231i (−2.0), 242 (+0.60).

Stecepharine (**6**) Perchlorate: Colorless amorphous powder, $[\alpha]_D^{30}$ −175° (c=1.05, MeOH). CD λ_{max}^{MeOH} nm ($\Delta\varepsilon$): 211 (−24.7), 278 (−1.5). UV λ_{max}^{MeOH} nm (log ε): 230sh (4.23), 282 (3.64). IR ν_{max}^{KBr} cm^{-1}: 3431, 2941, 1622, 1595, 1506, 1465, 1442, 1364, 1294, 1250, 1198, 1085, 885, 793. ^{1}H-NMR (CD_3OD) δ: 2.95 (1H, dd, J=18.5, 11.5 Hz, H-13), 3.20 (1H, dd, J=18.5, 7.0 Hz, H-5), 3.25 (3H, s, NMe), 3.30 (1H, dt, J=18.5, 8.0 Hz, H-5), 3.48 (2H, m, H-6, H-13), 3.79 (1H, m, H-6), 3.80 (3H, s, 2-OMe), 3.85 (3H, s, 3-OMe), 3.86 (3H, s, 10-OMe), 4.72 (1H, d, J=16.0 Hz, H-8), 4.92 (1H, d, J=16.0 Hz, H-8), 4.97 (1H, ddd, J=11.5, 5.5, 1.5 Hz, H-13a), 6.50 (1H, s, H-4), 6.68 (1H, d, J=8.5 Hz, H-12), 6.95 (1H, d, J=8.5 Hz, H-11). ^{13}C-NMR: see Table 1. Significant NOESY correlations: 3-OMe↔H-4, H-4↔H-5 (δ 3.20), NMe↔H-13a, 10-OMe↔H-11. HMBC correlations: H-4→C-1a, 2, 3, 5, H_2-5→C-4a, H-6 (δ 3.48)→C-4a, H-8 (δ 4.72)→C-6, 8a, 9, 12a, NMe, H-8 (δ 4.92)→C-6, 8a, 9, 12a, 13a, H-11→C-9, 10, 12a, H-12→C-8a, 10, 13, H-13 (δ 2.95)→C-1a, 8a, 12a, 13a, H-13 (δ 3.48)→C-1a, 8a, 12, 12a, H-13a→C-1, 1a, 4a, 6, 13, 2-OMe→C-2, 3-OMe→C-3, 10-OMe→C-10, NMe→C-6, 8, 13a. EI-MS *m/z* (rel. int. %): 371 (M^+−1, 42), 357 (68), 356 (29), 222 (100), 208 (24), 206 (19), 150 (9). HR-EI-MS *m/z*: 371.1744 (Calcd $C_{21}H_{25}NO_5$: 371.1734), 208.1007 (Calcd $C_{11}H_{14}NO_3$: 208.0974), 150.0682 (Calcd $C_9H_{10}O_2$: 150.0681). SI-MS *m/z* (rel. int. %): 372 (M^+, 100), 222 (31). HR-SI-MS *m/z*: 372.1826 (Calcd $C_{21}H_{26}NO_5$: 372.1812).

9-*O*-Methylstecepharine (**7**) Perchlorate: Colorless amorphous powder, $[\alpha]_D^{29}$ −156° (c=0.96, MeOH). CD λ_{max}^{MeOH} nm ($\Delta\varepsilon$): 210 (−23.3), 276 (−0.67). UV λ_{max}^{MeOH} nm (log ε): 233sh (4.24), 280 (3.48). IR λ_{max}^{KBr} cm^{-1}: 3431, 2941, 1618, 1595, 1506, 1464, 1429, 1375, 1294, 1238, 1200, 1082, 1018, 883. ^{1}H-NMR (CD_3OD) δ: 2.97 (1H, dd, J=18.0, 11.5 Hz, H-13), 3.20 (1H, dd, J=18.5, 7.0 Hz, H-5), 3.26 (3H, s, NMe), 3.33 (1H, dt, J=18.5, 8.0 Hz, H-5), 3.50 (1H, m, H-6), 3.52 (1H, dd, J=18.0, 6.0 Hz, H-13), 3.76 (1H, m, H-6), 3.80 (3H, s, 2-OMe), 3.85 (3H, s, 3-OMe), 3.86 (3H, s, 10-OMe), 3.89 (3H, s, 9-OMe), 4.82 (1H, d, J=16.0 Hz, H-8), 4.93 (1H, d, J=16.0 Hz, H-8), 4.98 (1H, ddd, J=11.5, 6.0, 1.5 Hz, H-13a), 6.50 (1H, s, H-4), 6.94 (1H, d, J=8.5 Hz, H-12), 7.06 (1H, d, J=8.5 Hz, H-11). ^{13}C-NMR: see Table 1. Significant NOESY correlations: 3-OMe↔H-4, NMe↔H-13a, 10-OMe↔H-11. HMBC correlations: H-4→C-1a, 2, 3, 5, H_2-5→C-1a, 4, 4a, H-6 (δ 3.50)→C-4a, H-8 (δ 4.82)→C-13a, H-8 (δ 4.93)→C-8a, 9, 12a, 13a, H-11→C-9, 10, 12a, H-12→C-8a, 10, 13, H-13 (δ 2.97)→C-1a, 8a, 12a, 13a, H-13 (δ 3.52)→C-8a, 12a, 13a, H-13a→C-1a, 2-OMe→C-2, 3-OMe→C-3, 9-OMe→C-9, 10-OMe→C-10, NMe→C-6, 8, 13a. EI-MS *m/z* (rel. int. %): 385 (M^+−1, 20), 372 (26), 371 (100), 370 (40), 340 (16), 208 (12), 206 (28), 165 (15), 164 (46), 149 (22). HR-EI-MS *m/z*: 385.1892 (Calcd $C_{22}H_{27}NO_5$: 385.1890), 208.0980 (Calcd $C_{11}H_{14}NO_3$: 208.0974), 164.0868 (Calcd $C_{10}H_{12}O_2$: 164.0838). SI-MS *m/z* (rel. int. %): 386 (M^+, 100), 222 (47). HR-SI-MS *m/z*: 386.1974 (Calcd $C_{22}H_{28}NO_5$: 386.1969).

Tetradehydroreticuline (**8**) Perchlorate: Colorless crystalline solid, mp 231—233 °C (MeOH). UV λ_{max}^{MeOH} nm (log ε): 232 (4.39), 257 (4.59), 280 (4.36), 318 (3.86), 367 (3.49). IR ν_{max}^{KBr} cm^{-1}: 3301, 1631, 1616, 1593, 1543, 1516, 1497, 1297, 1108, 949, 858, 796, 766. ^{1}H-NMR (CD_3OD) δ: 3.80 (3H, s, 4′-OMe), 4.16 (3H, s, 6-OMe), 4.28 (3H, s, NMe), 4.80 (2H, s, H_2-α), 6.46 (1H, dd, J=8.5, 2.0 Hz, H-6′), 6.54 (1H, d, J=2.0 Hz, H-2′), 6.86 (1H, d, J=8.5 Hz, H-5′), 7.64 (1H, s, H-5), 7.75 (1H, s, H-8), 8.10 (1H, d, J=7.0 Hz, H-4), 8.28 (1H, d, J=7.0 Hz, H-3). ^{13}C-NMR (CD_3OD) δ: 34.9 (C-α), 46.3 (NMe), 56.5 (4′-OMe), 57.5 (6-OMe), 107.3 (C-5), 110.3 (C-8), 113.5 (C-5′), 116.1 (C-2′), 120.3 (C-6′), 123.9 (C-4), 126.4 (C-8a), 128.0 (C-1′), 135.9 (C-3), 136.8 (C-4a), 148.6 (C-3′), 148.7 (C-4′), 153.6 (C-7), 156.5 (C-1), 158.8 (C-6). Significant NOESY correlations: NMe↔H-3, H_2-α↔H-8, 6-OMe↔H-5, 4′-OMe↔H-5′. HMBC correlations: H-3→C-1, 4, 4a, NMe, H-4→C-3, 5, 8a, H-5→C-4, 6, 7, 8a, H-8→C-1, 4a, 6, 7, H_2-α→C-1, 1′, 2′, 6′, H-2′→C-3′, 6′, H-5′→C-1′, 3′, H-6′→C-2′, 4′, 6-OMe→C-6, 4′-OMe→C-4′, NMe→C-1, 3. SI-MS *m/z* (rel. int. %): 326 (M^+, 100), 312 (7), 310 (7). HR-SI-MS *m/z*: 326.1399 (Calcd $C_{19}H_{20}NO_4$: 326.1393).

2′-*N*-Methylisotetrandrine (**9**) Perchlorate: Colorless amorphous powder, $[\alpha]_D^{28}$ +12.4° (c=0.95, MeOH). UV λ_{max}^{MeOH} nm (log ε): 232sh (4.46), 284 (3.83). IR ν_{max}^{KBr} cm^{-1}: 2936, 1610, 1585, 1514, 1456, 1417, 1269, 1234, 1221, 1096, 842. ^{1}H-NMR (CD_3OD) δ: 2.51 (3H, s, 2-NMe), 2.89 (1H, m, H-α), 3.10 (1H, m, H-α'), 3.12 (3H, s, 7-OMe), 3.15 (3H, s, 2′-NMe), 3.26 (1H, m, H-α), 3.46 (3H, s, 2′-NMe), 3.60 (3H, s, 6′-OMe), 3.72 (1H, m, H-α'), 3.77 (3H, s, 6-OMe), 3.89 (3H, s, 12-OMe), 4.27 (1H, m, H-1′), 4.34 (1H, br d, J=10.0 Hz, H-1), 6.23 (1H, s, H-8′), 6.42 (1H, br d, J=8.0 Hz, H-10′), 6.54 (1H, dd, J=8.0, 2.0 Hz, H-11′), 6.55 (1H, s, H-5), 6.63 (1H, m, H-10), 6.87 (1H, s, H-5′), 6.93 (1H, dd, J=8.0, 2.0 Hz, H-14), 6.98 (1H, d, J=8.0 Hz, H-13), 7.20 (1H, dd, J=8.0, 2.0 Hz, H-13′), 7.51 (1H, dd, J=8.0, 2.0 Hz, H-14′). ^{13}C-NMR: see Table 2. HMBC correlations: H-5→C-4, 6, 7,

8a, H-α (δ 2.89)→C-1, 10, 14, H-10→C-12, H-13→C-11, 14, H-14→C-α, 10, 12, 6-OMe→C-6, 7-OMe→C-7, 12-OMe→C-12, 2-NMe→C-1, 3, H-5′→C-4′, 6′, 7′, 8a, H-8′→C-4′a, 6′, 7′, H-α′ (δ 3.10)→C-1′, 14′, H-α′ (δ 3.72)→C-1′, 8′a, 14′, H-10′→C-12′, 14′, H-11′→C-9′, 12′, H-13′→C-9′, H-14′→C-α, 10′, 12′, 6′-OMe→C-6′, 2′-NMe_2→C-1′. El-MS *m/z* (rel. int. %): 636 (M^+-1, 2), 622 (49), 395 (13), 223 (23), 149 (100). SI-MS *m/z* (rel. int. %): 637 (M^+, 100), 623 (17), 622 (12), 621 (13), 381 (10), 204 (22), 192 (11), 190 (21), 174 (24). HR-SI-MS *m/z*: 637.3278 (Calcd $C_{39}H_{45}N_2O_6$: 637.3280).

Methylation of 9 and Isotetrandrine (10) To a solution of isotetrandrine (**10**) (21.3 mg) in MeOH (0.2 ml) was added an excess of MeI and the whole was allowed to stand overnight. The reaction mixture was diluted with aq. $NaClO_4$ solution and extracted with $C_2H_4Cl_2$. Evaporation of the solvent gave 2, 2′-*N*-dimethylisotetrandrine (**11**) (28.9 mg). ^{1}H-NMR (CD_3OD) δ: 2.88 (3H, s, 2-NMe), 3.04 (3H, s, 2-NMe), 3.11 (3H, s, 7-OMe), 3.13 (1H, m, H-α′), 3.17 (3H, s, 2′-NMe), 3.23 (1H, m, H-α), 3.46 (3H, s, 2′-NMe), 3.53 (3H, s, 6′-OMe), 3.55 (1H, m, H-α), 3.70 (1H, m, H-α′), 3.79 (3H, s, 6-OMe), 3.86 (3H, s, 12-OMe), 4.13 (1H, m, H-1), 4.27 (1H, m, H-1′), 6.26 (1H, s, H-8′), 6.32 (1H, br d, J=8.5 Hz, H-10′), 6.36 (1H, dd, J=8.5, 2.5 Hz, H-11′), 6.63 (1H, br s, H-5), 6.83 (1H, s, H-5′), 6.86 (1H, m, H-10), 7.00 (1H, dd, J=8.5, 2.0 Hz, H-14), 7.03 (1H, d, J=8.5 Hz, H-13), 7.28 (1H, dd, J=8.5, 2.5 Hz, H-13′), 7.48 (1H, dd, J=8.5, 2.0 Hz, H-14′). ^{13}C-NMR: see Table 2. HMBC correlations: H-5→C-4, 6, 7, 8a, H-α (δ 3.23)→C-1, 9, 10, H-α (δ 3.55)→C-9, H-13→C-9, 11, H-14→C-10, 12, 6-OMe→C-6, 7-OMe→C-7, 12-OMe→C-12, 2-NMe (δ 3.04)→C-1, 3, H-5′→C-4′, 4′a, 6′, 7′, 8a, H-α′ (δ 3.46)→C-1′, 9′, H-α′ (δ 3.70)→C-1′, 8′a, 9′, 10′, H-10′→C-12′, 14′, H-11′→C-9′, H-13′→C-9′, 11′, H-14′→C-α′, 10′, 12′, 6′-OMe→C-6′, 2′-NMe (δ 3.17)→C-1′, 3′, 2′-NMe (δ 52.8), 2′-NMe (δ 3.46)→C-1′, 3′, 2′-NMe (δ 52.4). Compound **9** (6.2 mg) was treated with MeI and worked up in the same way as for **10** to give a methylated compound (5.0 mg), which was identified as 2,2′-*N*-dimethylisotetrandrine (**11**).

Acknowledgements The technical assistance of Misses Y. Takenaka and S. Yamaoka is acknowledged. Thanks are due to Dr. M. Sugiura (Kobe Pharmaceutical University) for ^{1}H- and ^{13}C-NMR spectra, to Dr. K. Saiki (Kobe Pharmaceutical University) for mass spectra measurements.

References and Notes

1) Chiang Su New Medicina College (ed.) "Zhong-yao-dai-ci-dian (Dictionary of Chinese Crude Drugs)," Shanghai Scientific Technologic Publisher, Shanghai, 1978, p. 2141.
2) Kasajima T., Yamakawa M., Maeda K., Matsuda D., Dobashi M., Imai Y., *Jpn. J. Cancer Chemother.*, **10**, 1180—1196 (1973).
3) Makidono R., Makidono A., Matsuura K., *Nippon Acta Radiologica*, **37**, 1153—1167 (1977).
4) *a*) Kashiwaba N., Morooka S., Kimura M., Murakoshi Y., Toda J., Sano T., *Chem. Pharm. Bull.*, **42**, 2452—2454 (1994); *b*) Kashiwaba N., Morooka S., Kimura M., Murakoshi Y., Ono M., Toda J., Suzuki H., Sano T., *ibid.*, **45**, 470—475 (1997).
5) Kamiya T., Sugimito Y., Yamada Y., *Planta Med.*, **59**, 475—476 (1993).
6) Nakaoji K., Nayeshiro H., Tanahashi T., Su Y., Nagakura N., *Planta Med.*, **63**, 389—486 (1997).
7) Xia G., Qiu Y., Yang Q., Zang Y., Liu X., *Zhongcaoyao*, **6**, 266—267 (1985).
8) *a*) Moriyasu M., Ichimaru M., Nishiyama Y., Kato A., *Bunsekikagaku*, **42**, 659—665 (1993); *b*) *Idem*, *Natural Medicines*, **48**, 282—286 (1994).
9) Dwuma-Badu D., Ayim J. S. K., Withers S. F., Agyemang N. O., Ateya A. M., El-Azizi M. M., Knapp J. E., Slatkin D. J., Schiff P. L., *J. Nat. Prod.*, **43**, 123—129 (1980).
10) Marsaioli A. J., Reis F. de A. M., Magalhaes A. F., Ruveda E. A., Kuck A. M., *Phytochemistry*, **18**, 165—169 (1979).
11) Huang Z.-H., Zhu J.-P., Zhou Y.-L., *Org. Mass Spectrom.*, **19**, 605—609 (1984).
12) Martin H.-J., Pachaly P., Zymalkowski F., *Arch. Pharm.*, **310**, 314—319 (1977).
13) Takao N., Iwasa K., Kamigauchi M., Sugiura M., *Chem. Pharm. Bull.*, **25**, 1426—1435 (1977).
14) Singh R. S., Kumar P., Bhakuni D. S., *J. Nat. Prod.*, **44**, 664—667 (1981).
15) Lee S.-S., Lin Y.-J., Chen C.-K., Liu K. C. S., Chen C.-H., *J. Nat. Prod.*, **56**, 1971—1976 (1993).
16) Janssen R. H. A. M., Lousberg R. J. J. Ch, Wijkens P., Kurk C., Theuns H. G., *Phytochemistry*, **28**, 2833—2839 (1989).
17) Karimov A., Lutfullin K. L., *Khim. Phir. Soedin.*, **2**, 249—250 (1986) [*Chem. Abstr.*, **105**, 197034 (1986)].

Structural Studies of C-Amidated Amino Acids and Peptides: Crystal Structures of Z–Gly–Phe–NH_2, Tyr–Lys–NH_2, and Asp–Phe–NH_2

Yasuko In,* Sayuri Tani, and Toshimasa Ishida

Osaka University of Pharmaceutical Sciences, 4–20–1 Nasahara, Takatsuki, Osaka 569–1094, Japan.
Received September 29, 1999; accepted November 15, 1999

As part of the series investigating the structural features of C-terminal amidated amino acids and peptides, three crystal structures of Z–Gly–Phe–NH_2, Tyr–Lys–NH_2, and Asp–Phe–NH_2 were analyzed by the X-ray diffraction method, and their molecular conformations and intermolecular interactions were investigated. Although the respective dipeptides exhibited an energetically allowable torsion angle concerning each backbone or side chain, the observed extended (Z–Gly–Phe–NH_2, Asp–Phe–NH_2) and folded (Tyr–Lys–NH_2) conformations were considerably different from those of the corresponding unamidated peptides, due to the conformational flexibility of the respective dipeptides. The comparison between the crystal packings of the amidated and unamidated dipeptides indicated that the C-terminal amides tend to associate with the same neighboring group through hydrogen bonds, in which both the amide NH and O=C groups participate, while the unamidated peptides prefer a linear molecular connection, where both or either of the two carboxyl oxygens participate in the hydrogen bond formation. The difference in hydrogen bonding ability between the C-terminal amide and carboxyl groups has been considered to be based on the structural data of the related peptides analyzed so far.

Key words Z–Gly–Phe–NH_2; Tyr–Lys–NH_2; Asp–Phe–NH_2; C-terminal α-amidation; crystal structure; molecular conformation

It is well known that a majority of mammalian and insect peptide hormones reveal their biological functions by C-terminal α-amidation,[1] as is exemplified by calcitonin, gastrin, neurokinins, neuropeptides, and substance P. Since the deamination of such peptides leads to a considerable loss of their activity, the amide group could be largely correlated to the bioactivity.[2,3] However, such biological/structural function is not well understood at present, and this is in contrast with the detailed enzymatic analysis for C-terminal α-amidation.[4]

As a clue in considering the biological implication of C-amidation, it appears important to investigate the difference in molecular conformation and intermolecular interaction between the C-amidated and -unamidated peptides, because this information could be expected to reflect certain binding features to the respective receptors. Bearing these in mind, this paper deals with the molecular and crystal structures of Z–Gly–Phe–NH_2, Tyr–Lys–NH_2 and Asp–Phe–NH_2, and comparison with those of the most closely related unamidated dipeptides, *i.e.*, Boc–Gly–Phe–OH,[5] Tyr–Lys–OH,[6] and Asp–Phe–OH.[7] The atomic numberings of C-amidated dipeptides used in this work are given in Fig. 1.

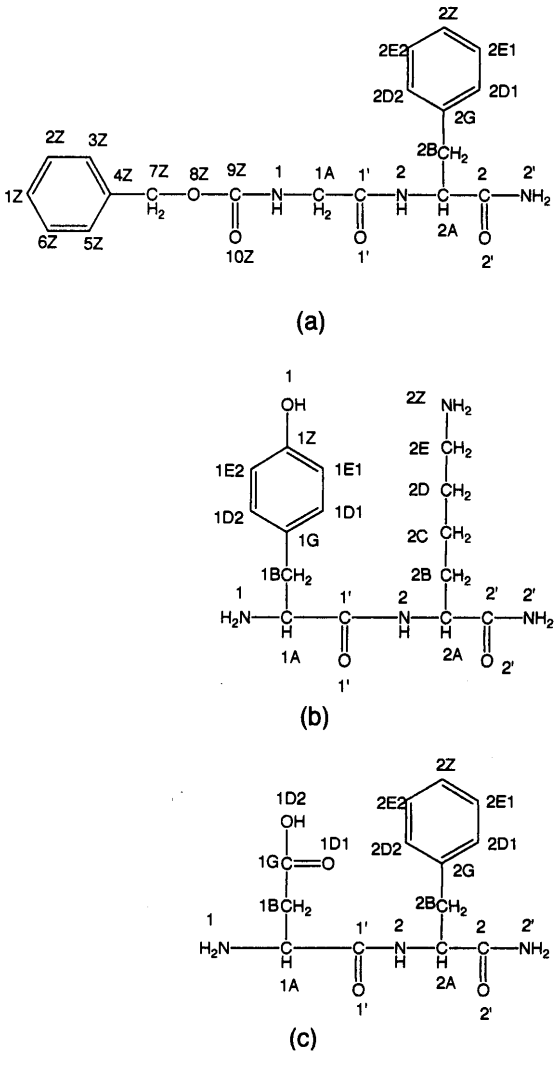

Fig. 1. Chemical Structures of Z–Gly–Phe–NH_2, Tyr–Lys–NH_2, and Asp–Phe–NH_2

The atomic numberings used in this study are also shown.

Experimental

The C-amidated dipeptides used in this work were purchased from Peptide Institute, Inc. (Osaka). Single crystals were obtained from the slow evaporation of aqueous ethanol solution (Z–Gly–Phe–NH_2, Tyr–Lys–NH_2) or isopropanol solution (Asp–Phe–NH_2) at room temperature in the form of transparent needles, respectively. The crystal density was measured by the flotation method using a CCl_4–C_6H_6 mixture.

All X-ray measurements were made on a Rigaku AFC-5 diffractometer with graphite-monochromated Cu$K\alpha$ radiation (λ=1.5418 Å) and a 12 kW rotating anode generator. The crystallographic data and structure refinements are summarized in Table 1. Cell refinements, data collections and data reductions were done using MSC/AFC software.[8] Unit-cell dimensions were determined by a least squares fit of 2θ angles of 25 reflections ranging from $45°<2\theta<55°$. Intensity data less than $2\theta=131°$ were collected at 293 K in an ω–2θ scan mode; the backgrounds were counted for 5 s at both extremes of each reflection peak. The weak intensities ($I<2\sigma(I)$) were rescanned (up to 7 scans) to ensure good counting statistics. The observed intensities were corrected for Lorentz and polarization effects. Empirical absorption corrections were also applied. Four standard reflections were monitored for every

* To whom correspondence should be addressed.

© 2000 Pharmaceutical Society of Japan

Table 1. Summary of Crystal Data, Intensity Collection, and Structure Refinement

	Z–Gly–Phe–NH_2	Tyr–Lys–NH_2	Asp–Phe–NH_2
Crystallographic data			
Empirical formula	$C_{19}H_{21}N_3O_4 \cdot 0.5H_2O$	$C_{15}H_{24}N_4O_3 \cdot 2HCl \cdot H_2O$	$C_{13}H_{17}N_3O_4 \cdot 1.5H_2O$
Molecular weight	364.383	399.31	306.30
Crystal system	Monoclinic	Monoclinic	Monoclinic
Space group	$P2_1$	$P2_1$	$P2_1$
Unit cell dimensions			
a, Å	12.337(2)	10.018(1)	17.443(4)
b, Å	8.485(2)	6.795(1)	4.884(3)
c, Å	18.304(2)	14.588(1)	17.950(2)
β, °	96.76(1)	98.79(1)	100.79(1)
Volume, Å^3	1902.7(4)	981.4(2)	1502.2(9)
Z	4	2	4
F(000)	772	424	652
Crystal size, mm	0.5×0.1×0.9	0.1×0.1×0.8	0.05×0.05×0.6
Density (calculated), g·cm^{-3}	1.272	1.351	1.354
Density (observed), g·cm^{-3}	1.277(5)	1.325(5)	1.322(5)
Absorption coefficient, mm^{-1}	0.791	3.211	0.898
Data collection			
Scan speed in ω, ° min^{-1}	10	10	10
Scan range in ω, °	1.785+0.3 tan θ	1.365+0.3 tan θ	1.155+0.3 tan θ
Index ranges	$0 \leqq h \leqq 14$	$0 \leqq h \leqq 11$	$0 \leqq h \leqq 20$
	$0 \leqq k \leqq 9$	$-7 \leqq k \leqq 0$	$0 \leqq k \leqq 5$
	$-21 \leqq l \leqq 21$	$-17 \leqq l \leqq 16$	$-20 \leqq l \leqq 20$
Max/min transmission	0.9997/0.8552	0.9965/0.6718	0.9992/0.9010
θmax, °	65.07	65.04	64.13
No. of unique data measd.	3491	1819	2832
No. of reflections with $I>2\sigma(I)$	3129	1785	1958
Structure refinement			
No. of variables refined	478	226	387
R (Rw)	0.035 (0.112)	0.037(0.111)	0.060(0.183)
R (Rw) (all data)	0.043 (0.119)	0.038(0.113)	0.112(0.200)
Goodness-of-fit on F^2	1.010	1.100	1.338
Extinction coefficient	0.0025(5)	0.019(2)	——
Largest diff. peak and hole, e Å^{-3}	0.164, −0.166	0.564, −0.357	0.420, −0.387
Max and mean shift/esd	0.277, 0.028	0.356, 0.068	0.170, 0.028

100 reflection intervals throughout the data collection, showing a random variation of $<\pm 2\%$ without significant trends for the respective crystals.

The respective crystal structures were solved by direct methods using the SHELXS97 program.[9] For structural refinement, the reflections with $I>2\sigma(I)$ were used, and the atomic scattering factors and terms of anomalous dispersion corrections were taken from International Tables for Crystallography.[10] The refinement of non-H atoms was carried out using full-matrix least squares calculations with anisotropic thermal parameters using the program SHELXL97.[11] H atoms which participated in hydrogen bonds were located from the difference Fourier map, and the others were geometrically located, and they were treated as riding with fixed isotropic displacement parameters (Uiso=1.2Ueq for the associated C or N atoms, or Uiso=1.5Ueq for methyl C or O atoms). H atomic positions were not included as variables for the refinements. The function of $\Sigma w(Fo^2-Fc^2)^2$ was minimized using the weighting scheme of $w=1/[\sigma^2(Fo^2)+(0.1000P)^2]$, where $P=(Fo^2+2Fc^2)/3$. Final R [$=\Sigma(|Fo|-|Fc|)/\Sigma|Fo|$], Rw [$=(\Sigma w(|Fo|-|Fc|)^2/\Sigma w|Fo|^2)^{1/2}$] and S (goodness-of-fit) [$=(\Sigma w(|Fo|-|Fc|)^2/(M-N))^{1/2}$, where M=no. of reflections and N=no. of variables used for the refinement] are given in Table 1. In the final stage of the refinement, none of the positional parameters of non-H atoms shifted more than one-third from their estimated standard deviations. The averaged estimated standard deviations for the bond lengths and angles of non-H atoms at the final stage were 0.003 Å and 0.3° for both Z–Gly–Phe–NH_2 and Tyr–Lys–NH_2, and 0.01 Å and 0.8° for Asp–Phe–NH_2. The structure analysis of the Asp–Phe–NH_2 crystal was therefore not as accurate as the others; this is largely due to insufficient reflections because of the small sized crystal. However, the bonding parameters obtained were all within an acceptable region, and the uncertainty would not significantly influence the description of the conformational characteristics of the Asp–Phe–NH_2 molecule.

The final atomic coordinates, anisotropic temperature factors, bond lengths, bond angles, torsion angles of non-H atoms, and the atomic coordinates of the H atoms have been deposited in the Cambridge Crystallographic Data Centre, Cambridge University Chemical Laboratory, Cambridge CB21EW, UK. All numerical calculations were carried out at the Computer Center, Osaka University of Pharmaceutical Sciences.

Results

Molecular Conformation The crystal structures of Z–Gly–Phe–NH_2 and Asp–Phe–NH_2 contain two crystallographically independent molecules per asymmetric unit, and they are differentiated as molecules A and B, respectively. The torsion angles defining the conformations of the respective amidated peptides are given in Table 2, together with the corresponding unamidated ones for comparison. To clarify the conformational difference among these molecules, their stereoscopic superimpositions are shown in Figs. 2a—c.

Z–Gly–Phe–NH_2 Two independent molecules take a similar extended conformation, with both the benzene rings of the Phe residue and Z group being extended almost in the opposite direction (Fig. 2a). Although the ϕ ψ, and ω torsion angles of Gly and Phe residues are all in the region acceptable for general peptides,[12,13] ψ_1 and ϕ_2 are significantly different from those of Boc–Gly–Phe–OH, leading to a different open conformation. No notable conformational feature caused by the amidation could be found.

Tyr–Lys–NH_2 By the salt formation with dihydrochloride, the peptide is in a state of two NH_3^+ forms at the N-ter-

Table 2. Torsion Angles (°)[a] of Z-Gly-Phe-NH_2, Tyr-Lys-NH_2, and Asp-Phe-NH_2, Together with the Most Related Unamidated Dipeptides for Comparison

		Z-Gly-Phe-NH_2		Boc-Gly-Phe-OH
		Molecule A	Molecule B	
	ω_0[b]	174.2(2)	170.8(3)	−176.9
Gly	ϕ_1	−68.3(2)	−84.0(3)	−88.0
	ψ_1	172.6(3)	179.2(3)	−14.5
	ω_1	−170.1(3)	172.6(3)	176.4
Phe	ϕ_2	−72.5(2)	−73.0(2)	−164.7
	ψ_2[c]	−23.7(3)	−20.3(2)	−11.0
	χ^1	73.5(3)	78.2(2)	52.0
	$\chi^{2,1}$	98.7(3)	94.5(3)	85.8
	$\chi^{2,2}$	−82.9(3)	−88.9(3)	−96.6
		Tyr-Lys-NH_2		Tyr-Lys-OH
Tyr	ψ_1	139.5(3)		111.3
	ω_1	177.9(3)		−173.7
	χ^1	−179.5(3)		180.0
	$\chi^{2,1}$	54.8(3)		89.4
	$\chi^{2,2}$	−128.4(3)		−91.5
Lys	ϕ_2	−108.6(3)		52.7
	ψ_2	25.7(3)		47.6
	χ^1	−56.4(2)		−61.8
	χ^2	−178.1(3)		178.2
	χ^3	179.5(3)		178.1
	χ^4	−178.4(3)		172.7
		Asp-Phe-NH_2		Asp-Phe-OH
		Molecule A	Molecule B	
Asp	ψ_1	150.7(6)	143.9(6)	154.5
	ω_1	−169.1(6)	−167.1(7)	171.4
	χ^1	−71.6(6)	−66.4(6)	−68.9
	$\chi^{2,1}$	−20.7(6)	−25.1(6)	8.0
	$\chi^{2,2}$	159.8(7)	154.8(7)	−173.1
Phe	ϕ_2	−125.6(7)	−119.8(7)	60.2
	ψ_2	126.1(7)	130.0(7)	28.3
	χ^1	−171.9(7)	−171.8(8)	−54.0
	$\chi^{2,1}$	89.5(8)	92.2(9)	102.2
	$\chi^{2,2}$	−93.1(8)	−91.4(9)	−77.0

a) The estimated standard deviations are given in parentheses. *b*) O8Z-C9Z-N1-C1A; *c*) N2-C2A-C2-N2′.

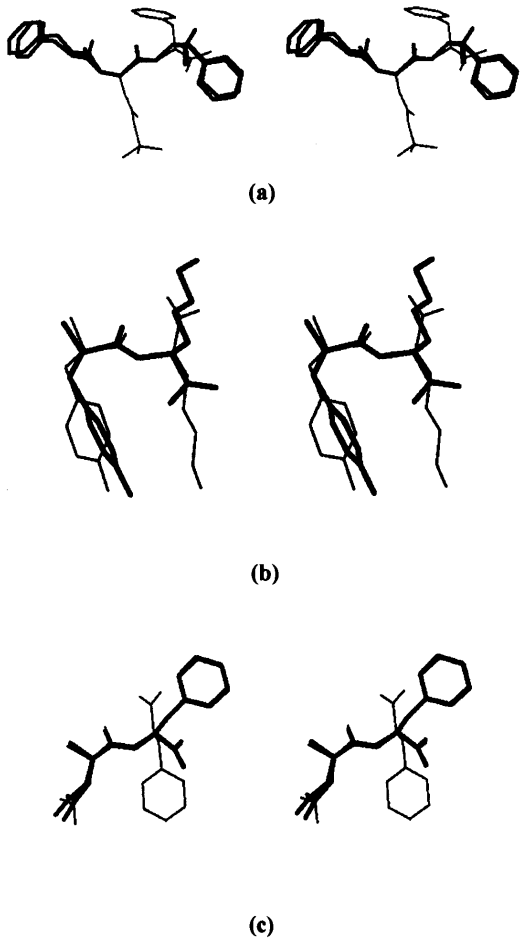

Fig. 2. Stereoscopic Views of Superimpositions of Molecular Conformations of Z-Gly-Phe-NH_2 (Molecules A, B) and Boc-Gly-Phe-OH (a), Tyr-Lys-NH_2 and Tyr-Lys-OH (b), and Asp-Phe-NH_2 (Molecules A, B) and Asp-Phe-OH (c)

Respective figures are shown so as to superimpose the central peptide bond. The amidated and unamidated peptides are shown with thick and thin bonds, respectively. Hydrogen atoms are omitted for clarity.

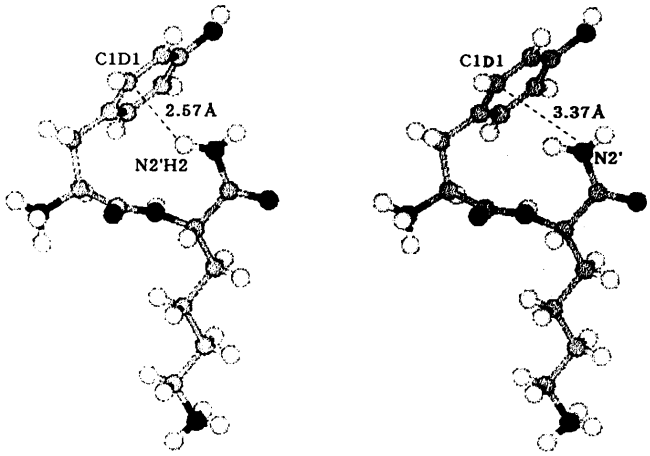

Fig. 3. Stereoscopic View of NH···π Interaction of Tyr-Lys-NH_2

minal and Lys side chain. While the Lys side chain takes the most popular extended conformation [(χ^1, χ^2, χ^3, χ^4)=(*ca.* −60°, *ca.* 180°, *ca.* 180°, *ca.* 180°)], the side chain of Tyr is slightly deviated from the most frequently observed conformation of (χ^1=*ca.* 180°, χ^{21}=*ca.* 90°), probably due to the effects of crystal packing and C-amidation. Although the (ϕ_2, ψ_2) torsion angles are in the 3_{10} helix region, the overall conformation of the peptide is considerably different from that of Tyr-Lys-OH (Fig. 2b), in which these torsion angles are in the α_L region. This obviously resulted from different intramolecular interaction. It is noteworthy that the conformation of the Tyr-Lys-NH_2 molecule is determined by the (C-amide)NH···π (Tyr) interaction, while that of Tyr-Lys-OH is by the hydrophobic interaction between the Lys and Tyr side chains, providing an example of different chemical behavior between C-terminal free acid and α-amide. The C-terminal NH of Tyr-Lys-NH_2 is located almost on the Tyr aromatic C–C bond with a N2′H···C1D1 distance of 2.57 Å (N···C=3.37 Å) (Fig. 3). This value is considerably shorter than the usual separation distance of H···C=2.9 Å, implying that the NH···π interaction is an important force in determining the molecular conformation of this C-amidated peptide.

Asp-Phe-NH_2 Both the independent molecules are in a zwitterionic state of COO^- (Asp side chain) and NH_3^+ (N-terminal), and take a similar extended conformation with the side chains of Asp and Phe being located at the *trans* position with respect to the backbone chain (Fig. 2c). Although the torsion angles around the Asp and Phe side chains are all

within the usual stable region, they are in contrast with the folded conformation of Asp–Phe–OH. A large difference is observed between the (ϕ_2, ψ_2) torsion angles: the β-sheet region of Asp–Phe–NH_2 and the α_L region of Asp–Phe–OH. In analogy with Z–Gly–Phe–NH_2, no conformational feature positively caused by the C-amidation could be observed; the molecular conformation appears to be largely affected by the compact crystal packing (discussed later).

Crystal Packing and Molecular Association The crystal packings of Z–Gly–Phe–NH_2, Tyr–Lys–NH_2, and Asp–Phe–NH_2 molecules are shown in Fig. 4, where filled circles represent water molecules or Cl^- ions, respectively. Hydrogen bonds and short contacts of less than 3.4 Å are given in Table 3.

Table 3. Hydrogen Bonds and Short Contacts (Less Than 3.5 Å)[a]

Possible hydrogen bonds Donor (D–H)	Acceptor (A)	Sym. code of A	D···A (Å)	H···A (Å)	D–H···A (°)
Z–Gly–Phe–NH_2					
N(1)A[b]	O(2′)B	$x, y-1, z$	2.848(3)	1.94	168
N(2)A	O(2′)B	$1-x, y-1/2, 1-z$	2.977(3)	2.13	155
N(2′)A	O(10Z)B	$x, y-1, z$	3.004(3)	2.10	158
N(2′)A	O(1)W	$1-x, y-1/2, 1-z$	2.838(4)	2.11	149
N(1)B	O(2′)A	x, y, z	2.839(3)	2.03	161
N(2)B	O(2′)A	$2-x, y+1/2, 1-z$	2.820(3)	1.89	163
N(2′)B	O(10Z)A	x, y, z	2.980(3)	2.07	170
O(1)W	O(10Z)A	x, y, z	2.865(4)		
O(1)W	O(1′)B	$1-x, y-1/2, 1-z$	2.736(4)		
Tyr–Lys–NH_2					
N(1)	CL(1)	$x-1, y, z$	3.196(2)	2.33	164
N(1)	CL(1)	$2-x, y-1/2, 1-z$	3.233(2)	2.33	157
N(1)	CL(2)	$x-1, y, z$	3.085(2)	2.15	164
N(2)	O(1)W	$2-x, y-1/2, 1-z$	2.875(3)	1.97	161
N(2′)	CL(2)	x, y, z	3.266(3)	2.41	161
N(2Z)	CL(2)	$2-x, y-1/2, 2-z$	3.255(3)	2.28	171
N(2Z)	O(1)	$2-x, y+1/2, 2-z$	2.920(4)	2.16	162
N(2Z)	O(1)W	$x-1, y, z+1$	2.879(4)	1.96	174
O(1)W	O(1′)	$2-x, y-1/2, 1-z$	2.724(3)		
O(1)W	O(2′)	$x, y, z-1$	2.723(3)		
Asp–Phe–NH_2					
N(1)A	O(1D2)A	$x, y-1, z$	2.758(6)	1.90	160
N(1)A	O(1D1)B	$1-x, y+1/2, -z$	2.829(6)	1.88	145
N(1)A	O(1)W	$x+1, y, z$	2.836(7)	2.04	161
N(2)A	O(1′)A	$x, y+1, z$	3.022(8)	2.04	161
N(2′)A	O(2′)A	$x, y-1, z$	2.773(9)	1.92	157
N(2′)A	O(2′)A	$2-x, y-1/2, 1-z$	3.075(9)	2.23	161
N(1)B	O(1D1)B	$x, y-1, z$	2.743(8)	1.88	164
N(1)B	O(1D1)A	$1-x, y-3/2, -z$	2.818(8)	1.81	153
N(1)B	O(3)W	$x, y-2, z$	2.78(1)	1.98	145
N(2)B	O(1′)B	$x, y-1, z$	3.050(9)	2.08	158
N(2′)B	O(2′)B	$x, y-1, z$	2.807(9)	1.87	165
N(2′)B	O(2′)B	$1-x, y-1/2, 1-z$	3.308(9)	2.22	168
O(1)W	N(1)A	$x-1, y, z$	2.836(7)		
O(1)W	O(1D2)B	$x, y+1, z$	2.856(9)		
O(1)W	O(1D2)B	x, y, z	2.927(9)		
O(2)W	O(1D1)A	$1-x, y-1/2, 1-z$	2.75(1)		
O(2)W	O(1D1)A	$1-x, y-3/2, 1-z$	2.80(1)		
O(2)W	O(3)W	$1-x, y+1/2, 2-z$	2.97(1)		
O(3)W	N(1)B	$1-x, y+1/2, 1-z$	2.78(1)		
O(3)W	O(1′)B	$1-x, y+1/2, 1-z$	3.15(1)		
O(3)W	O(2)W	x, y, z	2.71(1)		

Short Contacts

Atom 1	Atom 2	Sym. code of Atom 2	Distance (Å)	Atom 1	Atom 2	Sym. code of Atom 2	Distance (Å)
Tyr–Lys–NH_2							
N(1)	O(1′)	x, y, z	2.759(3)	N(2)	N(2′)	x, y, z	2.756(4)
Asp–Phe–NH_2							
N(1)A	O(1′)A	x, y, z	2.738(7)	N(1)A	O(1)W	$1-x, y+1/2, -z$	3.310(7)
N(1)A	O(1D2)B	$1-x, y+1/2, -z$	3.172(7)	N(2)A	O(2′)A	x, y, z	2.886(8)
N(1)B	O(1D1)B	x, y, z	3.191(8)	N(1)B	O(1D2)A	$1-x, y-3/2, -z$	3.145(8)
N(1)B	O(1′)B	x, y, z	2.722(8)	N(2)B	O(2′)B	x, y, z	2.882(9)
O(1)W	O(1′)A	$x-1, y, z$	3.366(9)	O(3)W	O(1D1)A	$x, y-1, z+1$	3.42(1)

a) The estimated standard deviations (esds) for atomic distances of non-H atoms are given in parentheses. The esds for the distances and angles including H atoms are not given because of the fixed refinement of H atoms. *b*) The suffix letters, A and B, represent the crystallographically independent molecules A and B, respectively.

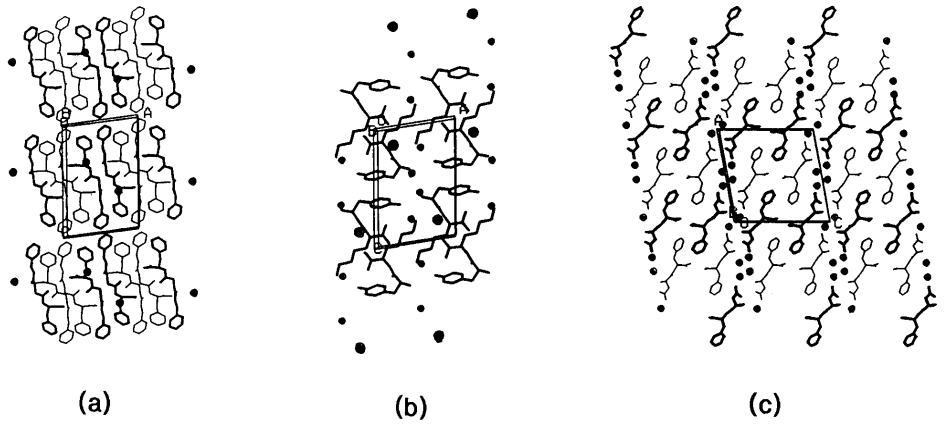

Fig. 4. Overall Molecular Packing Diagrams of Z–Gly–Phe–NH_2 (a), Tyr–Lys–NH_2 (b), and Asp–Phe–NH_2 (c) Crystals

Thick and thin bonds in (a) and (c) show two independent molecules A and B, respectively. The water molecules in (a)—(c) or Cl^- ions (large circle) in (b) are shown with filled circles.

Z–Gly–Phe–NH_2 Respective independent molecules are compactly packed into the crystal lattice, as shown in Fig. 4a. They are antiparallely packed in pairs and form alternative layers running along the *c*-axis. As a molecular packing feature in which the C-amide group participates, the antiparallely-orientated molecular association should be noted (Fig. 5a); a linear arrangement linked by a (Phe) NH···O (amide) hydrogen bond is also formed in the crystal. The amide NH and O of molecule A are hydrogen-bonded to the ester O (10Z) and peptide NH (Gly) of molecule B, respectively; in turn, the amide group of molecule B is hydrogen-bonded to those of molecule A in the same manner. On the other hand, in the crystal structure of Boc–Gly–Phe–OH,[5] the molecular packing in which the C-carboxyl group participates could be characterized as a linear chain arrangement through a (carboxyl)OH···O=C hydrogen bond (Fig. 5b).

Tyr–Lys–NH_2 As is obvious from Fig. 4b, the molecules are much more roughly packed in the crystal. Since the peptide is crystallized as a monohydrate of dihydrochloride salt, the relatively large space is necessary among the neighboring molecules to accommodate these water molecules and chloride ions. This would be a reason why the peptide is able to take a NH···π folded conformation, which is in contrast with the open conformations of Z–Gly–Phe–NH_2 and Asp–Phe–NH_2, and is positively due to the C-amidation. The amino groups of the N-terminal and Lys side chain are protonated and participate in three hydrogen bonds, respectively; this dicationic peptide is neutralized by salt formation with two chloride anions.

A molecular packing feature by the C-amide group is shown in Fig. 6a. For comparison, the arrangement of Tyr–Lys–OH in which the C-carboxyl group participates is shown in Fig. 6b. Tyr–Lys–NH_2 peptides are associated around a diad screw axis along the *b*-direction, where a 12-membered spiral structure per one turn is formed by hydrogen bonds *via* (amide) O···water (W)···NH_3^+(Lys side chain)···Cl^-···NH_2 (amide) (Fig. 6a). In contrast, Tyr–Lys–OH molecules form a sheet structure, where the NH_3^+ of the Lys side chain is bifurcately hydrogen-bonded to two neighboring anionic carboxyl oxygens (Fig. 6b).

Asp–Phe–NH_2 As is shown in Fig. 4c, the respective layers consisting of two crystallographically independent

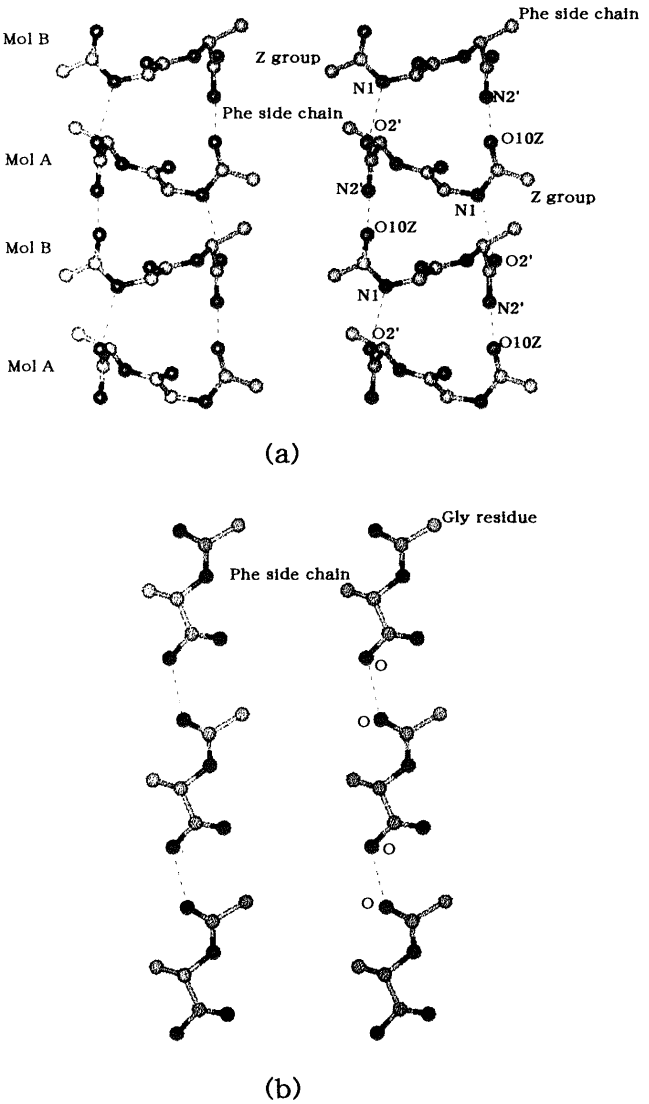

Fig. 5. Stereoscopic Views of Antiparallely-Orientated Ladder-like Molecular Associations Observed in the Z–Gly–Phe–NH_2 Crystal (a), Together with a Linear Chain Arrangement in the Boc–Gly–Phe–OH Crystal (b)

Hydrogen bonds are shown by dotted lines.

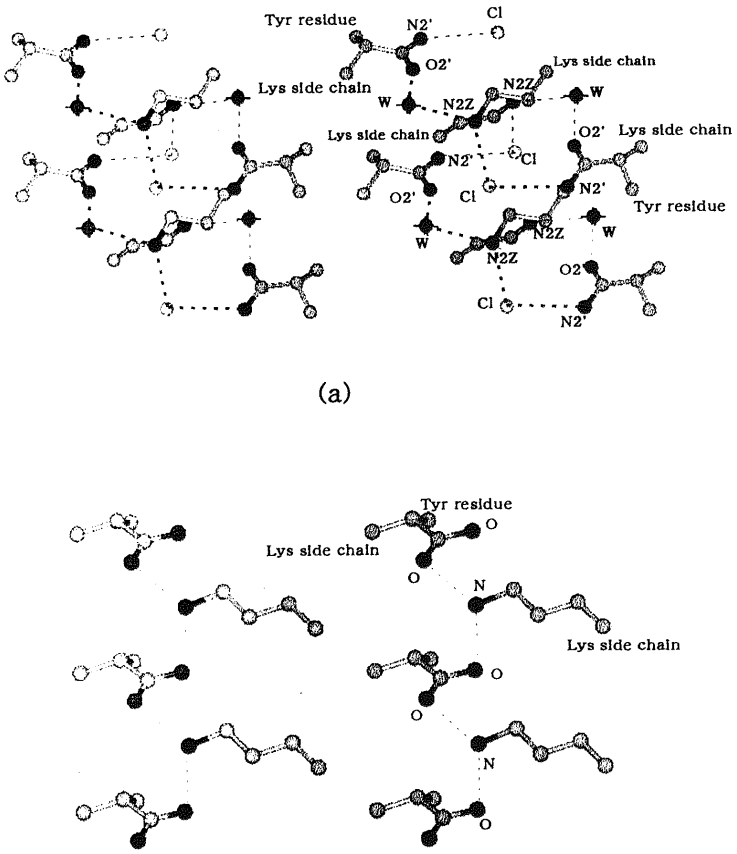

Fig. 6. Stereoscopic Views of Spiral Arrangement of Tyr–Lys–NH_2 Molecules *via* Water Solvents (W), N2Z (Lys), and Chloride Ions (a), Together with Zigzag Arrangement of Tyr–Lys–OH (b)

Hydrogen bonds are shown by dotted lines.

peptides are alternatively arranged along the *c*-direction, and the water molecules are located among these layers and stabilize the structures by hydrogen bonds. As shown in Fig. 7a, the molecular packing feature in which C-amide participates could be described as a ladder-like hydrogen-bonding network; two independent peptides form similar bilayer structures in the crystal, respectively. On the other hand, as shown in Fig. 7b, the molecular packing of Asp–Phe–OH peptides formed a linear connection among the molecules through a (carboxyl) C=O···HN (Phe) hydrogen bond.

Discussion

The present results show that the molecular conformations of C-amidated and unamidated dipeptides are both flexible, depending on the effect of crystal packing, and any common feature which differentiates them was not observed. However, the conformational difference observed between Tyr–Lys–NH_2 and Tyr–Lys–OH molecules (Fig. 2) would be a proper reflection of the different chemical behavior between the carboxyl and amide groups.

Concerning the molecular association in the crystal structure, a definite difference could be observed between the C-terminal free acid and amide peptides. The participation of both the amide O (acceptor) and NH (donor) in the hydrogen bonds leads to a pleated sheet structure as a characteristic association mode of Z–Gly–Phe–NH_2 and Asp–Phe–NH_2 (Figs. 5a, 7a). In the spiral molecular orientation in the Tyr–Lys–NH_2 crystal, also, both the O and NH of the amide group participated in hydrogen bonds (Fig. 6a), although the association pattern is considerably different from the former two crystals. On the other hand, the crystal structures of unamidated peptides showed a linear 'head-to-tail' molecular connection *via* hydrogen bonds in which both or either of the C-carboxyl oxygens participated, as observed in Figs. 5b, 6b, and 7b.

In order to investigate the difference in hydrogen-bonding ability between the C-carboxyl and -amide groups, the spatial distribution of the polar atoms which are hydrogen-bonded to these carboxyl or amide groups was surveyed for the crystal structures of the amidated peptides analyzed so far,[14—21] as well as the corresponding unamidated ones.[22—33] The result is shown in Figs. 8a and 8b, where the upper and lower oxygen atoms of the carboxyl group correspond to the keto O and neutral OH or anionic O^-, respectively. A clear difference could be extracted concerning the spatial disposition of these polar atoms. The amide NH_2 could form two relatively strong hydrogen bonds, because the spatial disposition of its acceptor O atoms is clearly separated into two regions suitable for hydrogen bond formation. In contrast, the amide O forms one to two hydrogen bonds with the donor NH or OH groups, where the number of hydrogen bonds is dependent on the interaction mode with the neighboring molecule.

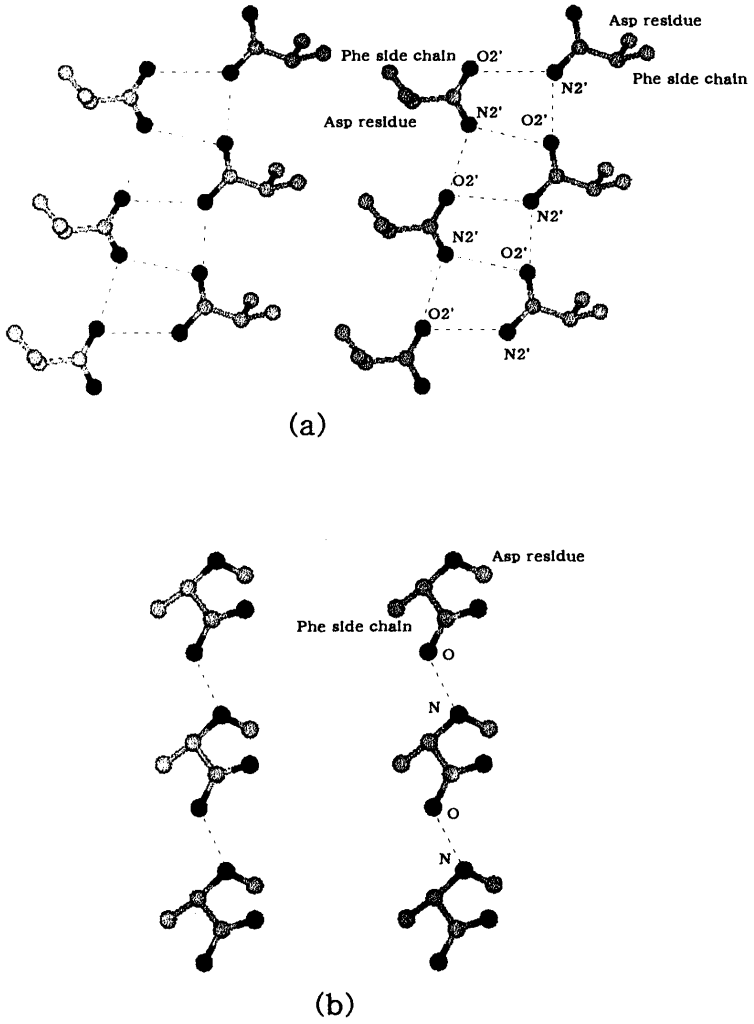

Fig. 7. Stereoscopic Views of Bilayer Arrangement of Molecules A Related by Diad Screw Symmetry Elongating to the *b*-Direction in Asp–Phe–NH_2 Crystal (a), Together with Linear Arrangement in Asp–Phe–OH Crystal (b)

Hydrogen bonds are shown by dotted lines. The same bilayer arrangement as Fig. 7a is also formed for molecules B. Since the crystal structure of Asp–Phe–OH is analyzed as a complex with His–Gly–OH,[7] the molecular packing in which the C-carboxyl group of Asp–Phe–OH interacts with the same peptides is shown is Fig. 7b to compare with the packing pattern (Fig. 7a) of C-amidation.

These donor groups are widely distributed so as to surround the amide O atom, indicating that the hydrogen bonding ability of the amide O is not strong enough to fix the donor group in a definite position.

In the C-carboxyl peptides (Fig. 8b), the spatial distributions of the NH or OH groups which are hydrogen-bonded to the keto O of the carboxyl group are roughly separated into two regions, although its separation is not so clear as that of amide NH. This distribution is considerably different from the case of amide O, and this appears to be an interesting feature which differentiates the hydrogen-bonding behavior between the keto O atoms of the carboxyl and amide groups. On the other hand, in the case of carboxyl O being in OH (lower side), the acceptor O atom (dotted circles in Fig. 8b) is located at a limited region in order to form reasonable O–H···O hydrogen bonds. In the case of an anionic O^-, however, the distribution of a donor NH or OH group is widely scattered, suggesting the wide adaptability of this O^- as a hydrogen-bonding acceptor.

From the comparison of Figs. 8a and 8b, the following discussion would be possible concerning the hydrogen-bonding behavior of carboxyl and amide groups. In the amide group, two hydrogen bonds *via* the NH_2 group are first formed, and then the amide O serves to further stabilize the interaction by the relatively weak hydrogen bonds. On the other hand, in the carboxyl group, the keto O of the carboxyl group serves first as an acceptor to form the tight hydrogen bond with the partner, and then the anionic O^- stabilizes the interaction through additional hydrogen bonding. In the case of the neutral OH group, the interaction appears to be highly specific, because of linear hydrogen bonding with the acceptor atom.

These insights would be useful in understanding why some peptides should be amidated at the C-terminal to reveal their bioactivity. For example, the hydrogen bonding ability and feature of the amide group discussed here may be necessary to fit the binding pocket of the receptor.

References and Notes

1) Eipper B. A., Mains R. E., *Annu. Rev. Physiol.*, **50**, 333—344 (1988).
2) Merkler D. J., *Enzyme Microb. Technol.*, **16**, 450—456 (1994).
3) Suwan S., Isobe M., Yamashita O., Minakata H., Imai K., *Biochem. Mol. Biol.*, **24**, 1001—1007 (1994).
4) Kulathila R., Merkler K. A., Merkler D. J., *Nat. Prod. Rep.*, **16**, 145—

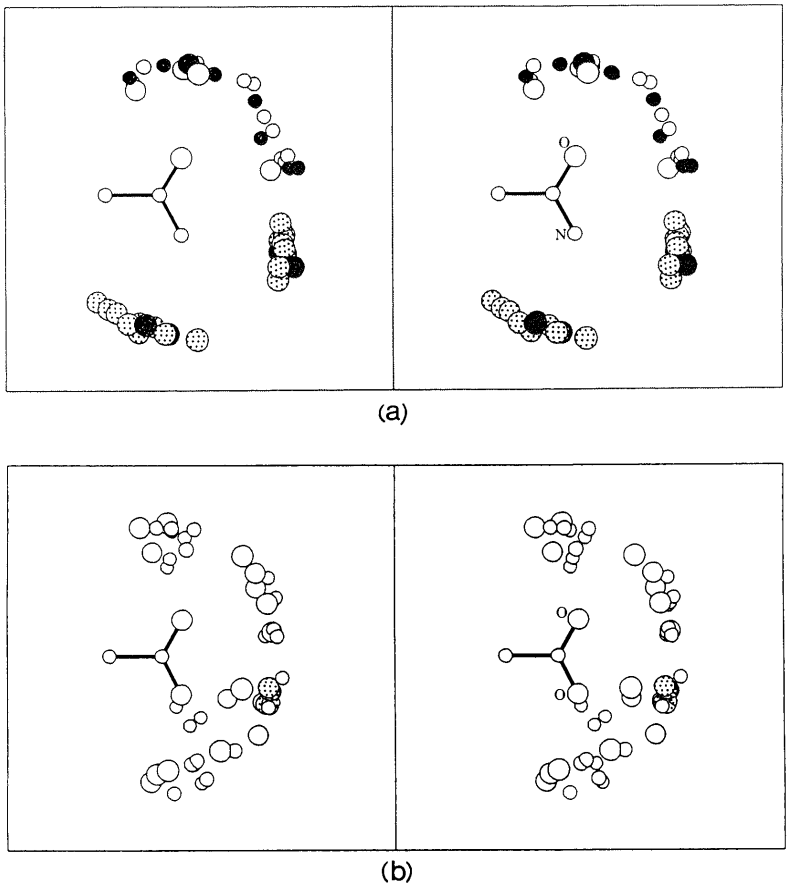

Fig. 8. Stereoscopic View of Spatial Distributions of O Atoms, OH or NH Groups Which Are Hydrogen-Bonded to the C-Terminal α-Amide Group (a) or Carboxyl Group (b)

The donor groups (OH or NH) and acceptor O atoms are shown by open and dotted circles, and the OH and NH groups are distinguished by large and small circles, respectively. The figures were constructed using sixteen amidated peptides and their corresponding unamidated ones; the donor NHs and acceptor Os of the present C-amidated dipeptides are shown by filled circles.

154 (1999).
5) Murali R., Subramanian E., Parthasarathy R., *Int. J. Peptide Protein Res.*, **27**, 478—482 (1986).
6) Urpi L., Coll M., Subirana J. A., *Int. J. Biol. Macromol.*, **10**, 55—59 (1988).
7) Gorbitz C. H., Etter M. C., *Acta Crystallogr.*, **C49**, 1673—1676 (1993).
8) Molecular Structure Corporation. MSC/AFC diffractometer control software. MSC, 3200 Research Forest Drive, The Woodlands, TX 77381, U.S.A, 1991.
9) Sheldrick G. M., SHELXS97. Program for the Solution of Crystal Structure, University of Gottingen, Germany, 1997.
10) "International Tables for X-Ray Crystallography," Vol. C, Kluwer Academic Publishers, 219—222 (1992).
11) Sheldrick G. M., SHELXL97. Program for the Refinement of Crystal Structures, University of Gottingen, Germany, 1997.
12) Bhat T. N., Sasisekharan V., Vijayan M., *Int. J. Peptide Protein Res.*, **13**, 170—184 (1979).
13) Benedetti E., Morelli G., Nemethy G., Sheraga H. A., *Int. J. Peptide Protein Res.*, **22**, 1—15 (1983).
14) Cruse W. B. T., Egert E., Viswamitra M. A., Kennard O., *Acta Crystallogr.*, **B38**, 1758—1764 (1982).
15) Kojima T., Tanaka I., and Ashida T., *Acta Crystallogr.*, **B38**, 221—225 (1982).
16) Valle G., Crisma M., Toniolo C., Yu K. -L., Johnson R. L., *J. Chem. Soc. Perkin Trans.* 2, **1989**, 83—87.
17) Puliti R., Mattia C. A., Lilley T. H., *Acta Crystallogr.*, **C48**, 709—712 (1992).
18) Puliti R., Mattia C. A., Lilley T. H., *Acta Crystallogr.*, **C49**, 2173—2176 (1993).
19) Mlasio B. D., Nastri F., Saviano M., Benedetti E., *Acta Crystallogr.*, **C50**, 250—252 (1994).
20) Puliti R., Mattia C. A., *Acta Crystallogr.*, **C51**, 336—339 (1995).
21) Puliti R., Sena C. D., Mattia C. A., *Acta Crystallogr.*, C52, 1820—1823 (1996).
22) Fletterick R. J., Tsai C., Hughes R. E., *J. Phys. Chem.*, **75**, 918—922 (1971).
23) Naganathan P. S., Venkatesan K., *Acta Crystallogr.*, **B28**, 552—556 (1972).
24) Barrans P. M. C. Y., *Acta Crystallogr.*, **B30**, 1018—1023 (1974).
25) Narasimhan P., Chacko K. K., *Cryst. Struct. Comm.*, **11**, 2051—2056 (1982).
26) Cotrait P. M., Leroy Y. B. F., *Acta Crystallogr.*, **B38**, 1626—1629 (1982).
27) Subramanian E., Lalitha V., Bordner J., *Int. J. Peptide Protein Res.*, **24**, 55—59 (1984).
28) Murali R., Subramanian E., *Int. J. Peptide Protein Res.*, **29**, 187—192 (1987).
29) Ramakrishnan B., Viswamitra M. A., *Acta Crystallogr.*, **C44**, 1957—1959 (1988).
30) Delettre P. J., Lifchitz J. B. A., Jolles P., *Acta Crystallogr.*, **C44**, 905—907 (1988).
31) Ramakrishnan B., Viswamitra M. A., *Acta Crystallogr.*, **C44**, 1959—1961 (1988).
32) Carroll P. J., Stewart P. L., Opella S. J., *Acta Crystallogr.*, **C46**, 243—246 (1990).
33) Krause J. A., Baures P. W., Eggleston D. S., *Acta Crystallogr.*, **B49**, 123—130 (1993).

A Novel Class of Inhibitors for Human Steroid 5α-Reductase: Synthesis and Biological Evaluation of Indole Derivatives. II[1)]

Susumu IGARASHI,* Hiroshi INAMI, Hiromu HARA,[2)] Masahiro FUJII, Hiroshi KOUTOKU, Hiroyuki ORITANI,[3)] and Toshiyasu MASE[4)]

Institute for Drug Discovery Research, Yamanouchi Pharmaceutical Co., Ltd., 21 Miyukigaoka, Tsukuba, Ibaraki 305–8585, Japan. Received September 29, 1999; accepted December 14, 1999

In a search for novel nonsteroidal inhibitors of human prostatic 5α-reductase, we found a new series of indole derivatives that showed potent inhibitory activities for the human enzyme. Among them, 4-[(1-benzyl-1*H*-indol-5-yl)oxy]-3-chlorobenzoic acid (2d, YM-32906) showed more potent inhibitory activity than finasteride with an IC_{50} value of 0.44 nM. 3-Chloro-4-{[1-(4-phenoxybenzyl)-1*H*-indol-5-yl]oxy}benzoic acid (2m) showed inhibitory activities for both human and rat prostatic 5α-reductase with IC_{50} values of 2.1 and 73 nM, respectively. The synthesis and structure–activity relationships of these indole derivatives are presented.

Key words 5α-reductase inhibitor; benign prostatic hypertrophy; indole derivative; YM-32906

5α-Reductase is an NADPH-dependent enzyme responsible for the conversion of testosterone to dihydrotestosterone (DHT), an active agonist for androgen receptors. Benign prostatic hyperplasia (BPH), skin disorders such as acne, male pattern baldness and hirsutism are androgen-related disorders, associated with elevated levels of DHT.[5)] As a consequence, a 5α-reductase inhibitor is expected to provide a potential treatment for various androgen-related disorders. Several 5α-reductase inhibitors have been reported,[6,7)] including both steroidal inhibitors such as finasteride[6a)] and epristeride,[6b)] and nonsteroidal inhibitors such as ONO-3805[7a)] (Fig. 1). Following the discovery of these inhibitors, the existence of two different 5α-reductase isozymes, type 1 and type 2 5α-reductase, has been reported in humans and rats.[8—10)] The type 1 enzyme is normal in men with congenital 5α-reductase deficiency and is expressed in skin tissue throughout the body that has an optimal pH of between 6 and 9. The type 2 enzyme is defective in men with congenital 5α-reductase deficiency and is the dominant form of the enzyme in genital tissue, including prostate that has an optimal pH of about 5.5. However, the exact physiological roles of these isozymes has yet to be fully elucidated. Steroidal inhibitors, for example, finasteride, have been shown to be clinically effective for treatment of BPH, however the possibility of adverse effects due to their steroidal structures remains.[11)] On the other hand, nonsteroidal inhibitors have not shown clinical efficacy for the treatment of BPH. Finasteride showed strong inhibitory activity (IC_{50}=4.1 nM)[12)] for human prostatic 5α-reductase, whereas ONO-3805 showed moderate activity (IC_{50}=538 nM)[12)] which might not be sufficient to show clinical efficacy. We considered that a more potent nonsteroidal inhibitor of human prostatic 5α-reductase than ONO-3805 could show clinical efficacy for the treatment of BPH and reduce the potential for side effects compared to steroidal inhibitors.

In our previous studies on novel human prostatic 5α-reductase inhibitors, we found the biphenyl-4-yloxy benzoic acid derivative, YM-31758 (**1**), which showed potent inhibitory activity with an IC_{50} value of 0.87 nM.[1)] During the course of this study, we found that it is favorable for high potency to have a hydrophobic substituent such as a phenyl group at a position from the carboxyl group in the range of 9—11 Å through the benzene ring juncture. These results suggested that it may be possible to find a more potent inhibitor against human prostatic 5α-reductase through modification of the biphenyl-4-yloxy group in YM-31758. In this

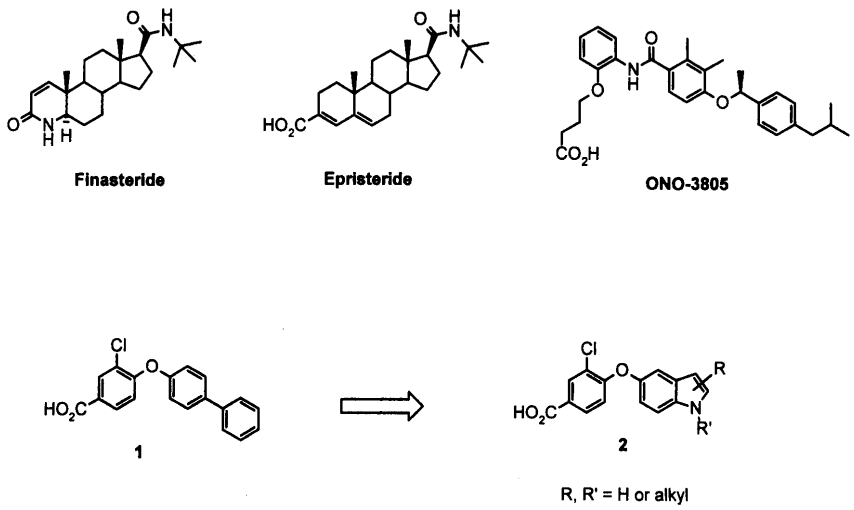

Fig. 1

* To whom correspondence should be addressed.

© 2000 Pharmaceutical Society of Japan

study, we focused on modification of the biphenyl-4-yloxy group. A 1*H*-indole-5-yloxy group as a substituent at the 4-position of the benzoic acid moiety was newly designed as described in Fig. 1. We report here the synthesis and the structure–activity relationships of the indole derivatives **2**.

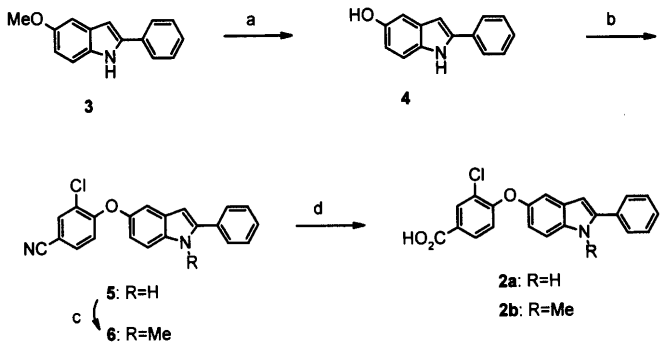

(a) BBr_3, CH_2Cl_2; (b) 3-chloro-4-fluorobenzonitrile, K_2CO_3, DMSO; (c) MeI, KOH, DMSO; (d) 8 N KOH, EtOH

Chart 1

Chemistry

2-Phenyl-1*H*-indole derivatives (**2a**, **2b**) were prepared as shown in Chart 1. The demethylation of compound **3** was performed using BBr_3 to give compound **4**, which was converted to compound **5** by alkylation with 3-chloro-4-fluorobenzonitrile. Compound **2a** was obtained by hydrolysis with KOH. Compound **2b** was prepared by the *N*-methylation of compound **5** in the presence of KOH in dimethyl sulfoxide (DMSO) with methyl iodide[13] and subsequent hydrolysis with KOH. The 3-benzyl-1-methyl-1*H*-indole derivative **2c** was prepared as shown in Chart 2. After methylation of compound **7**, benzoylation was carried out by the Vilsmeier method to give compound **8**. Debenzylation and reduction of the carbonyl group were performed using catalytic hydrogenation in the presence of Pd–C to afford compound **9**, which was converted to the benzoic acid derivative **2c** in two steps. The 1-alkyl-1*H*-indole derivatives (**2d**—**2u**) were prepared from compound **7** by three synthetic methods (Methods A, B and C) as described in Chart 3. Compound **11** was obtained by debenzylation of **7** in the presence of Pd–C and subsequent alkylation with 3-chloro-4-fluorobenzonitrile. *N*-Alkylation of **11** was performed using KOH in DMSO to give compound **13**, which was then hydrolyzed with KOH to

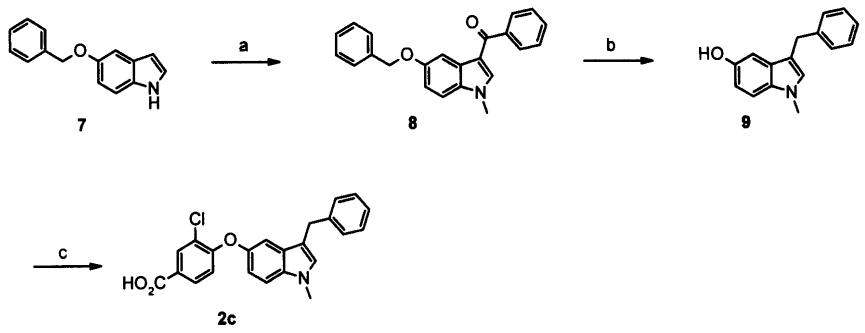

(a) i) MeI, KOH, DMSO, ii) *N*-benzoylpyrrolidine, $POCl_3$, 1,2-dichloroethane; (b) H_2/Pd-C, AcOEt–EtOH–AcOH; (c) i) 3-chloro-4-fluorobenzonitrile, K_2CO_3, DMSO, ii) 8 N KOH, EtOH

Chart 2

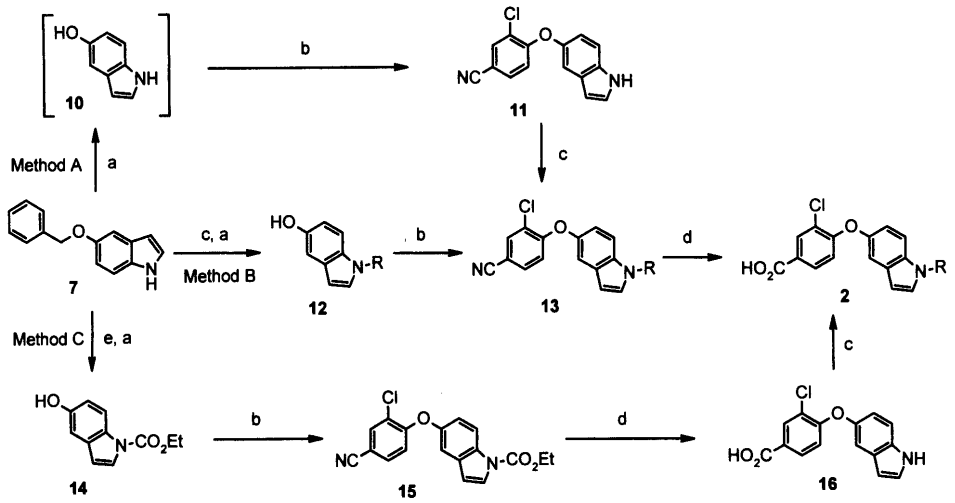

(a) Pd–C, HCO_2NH_4, EtOH; (b) 3-chloro-4-fluorobenzonitrile, K_2CO_3, DMF; (c) R-X (X = Cl, Br or I), KOH, DMSO; (d) 8 N KOH, EtOH; (e) NaH, $ClCO_2Et$, DMF

Chart 3

Table 1. Physicochemical Data and Inhibitory Activities of 5α-Reductase in Human Prostate for Indole Derivatives

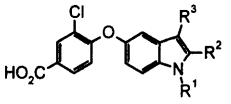

Compd. No.	R^1	R^2	R^3	mp (°C)	Formula	Analysis (%) Calcd (Found)				IC_{50} (nM)
						C	H	N	Cl	
2a	H		H	268—270	$C_{21}H_{14}NO_3Cl$	69.33	3.88	3.85	9.75	0% inhibition
						(69.44	3.91	3.87	9.86)	at 100 nM
2b	Me		H	260—263	$C_{22}H_{16}NO_3Cl$	69.94	4.27	3.71	9.38	3.4
						(69.71	4.35	3.67	9.23)	
2c	Me	H		220—222	$C_{23}H_{18}NO_3Cl$	70.50	4.63	3.57	9.05	12
						(70.28	4.62	3.43	9.06)	
2d[a]		H	H	158—159	$C_{22}H_{16}NO_3Cl$	69.94	4.27	3.71	9.38	0.44
						(69.86	4.29	3.68	9.44)	

a) The compound was prepared by using Method B as shown in Chart 3.

give the benzoic acid derivatives **2f**—**2i** and **2l** (Method A). Compound **12**, prepared by the *N*-alkylation of **7** with an alkyl halide and subsequent debenzylation in the presence of Pd–C, was alkylated with 3-chloro-4-fluorobenzonitrile to afford compound **13**, which was hydrolyzed with KOH to give the benzoic acid derivatives **2d**, **2e** and **2q** (Method B). Compound **7** was acylated with chloroethylformate followed by debenzylation to afford **14**. Alkylation of **14** with 3-chloro-4-fluorobenzonitrile afforded **15**, which was hydrolyzed with KOH to give the benzoic acid derivative **16**. *N*-Alkylation of **16** was also carried out in the presence of KOH in DMSO to afford the benzoic acid derivatives **2j**, **2k**, **2m**—**2p** and **2r**—**2u** (Method C).

Results and Discussion

The inhibitory activities of the indole derivatives were evaluated on the basis of the ability to inhibit 5α-reductase in human prostate at pH 5.5 which is optimal for the activity of the type 2 enzyme. The results are described in Tables 1—4.

In our previous paper, we found that for high potency it is favorable to have a phenyl group at a position from the carboxyl group in the range of 9—11 Å for phenoxy benzoic acid derivatives. Initially, the favorable position for the phenyl group on the indole ring was investigated as shown in Table 1. Compound **2a**, having an acidic proton at the 1-position on the indole ring, showed in a loss of activity, while the 1-methyl-2-phenyl-1*H*-indole derivative **2b** showed potent inhibitory activity with an IC_{50} of 3.4 nM. An acidic proton in this position was found to be incompatible with potent inhibitory activity. The 3-benzyl-1-methyl-1*H*-indole derivative **2c** resulted in decreased activity, while the 1-benzyl-1*H*-indole derivative **2d** showed strong potency with an IC_{50} of 0.44 nM. These findings suggested that the position of the phenyl group is important for high potency. In order to investigate the correlation between distance and inhibitory activity, optimized structures for the indole derivatives **2b**—**2d** were calculated by a systematic search and minimization using the molecular modeling program Sybyl, version 6.3, and the distances between the carbon of the carboxyl group and centroid of the phenyl group (benzene ring A) were calculated from the optimized structures. The calculated data and the optimized structures of **2b**—**2d** are shown in Table 2 and Fig. 2, respectively. The distances for the potent compounds **2b** and **2d** are in the range of 9—11 Å, with values of 11.367 Å and 8.705 Å, respectively.

Table 2. Distances between the Carbon of the Carboxyl Group and the Centroid of the Benzene Ring A for Compounds **2b**—**2d**

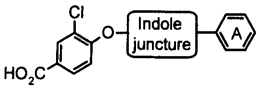

Compd. No.	Indole juncture	C-Centroid distance (Å)	IC_{50} (nM)[a]
2b	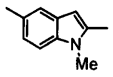	11.367	3.4
2c	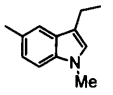	4.657	12
2d	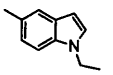	8.705	0.44

a) Inhibitory activities of 5α-reductase in human prostate homogenates.

On the other hand, the reduced potent compound **2c** is a non-linear compound, and the position of the benzene ring A is probably too close to the carboxyl group, with a value of 4.657 Å, to show potent inhibitory activity. The 1-benzyl derivative **2d** showed more potent inhibitory activity compared to **2b** or YM-31758, suggesting that the 1-benzyl-1*H*-indole group of **2d** is more flexible compared to the 1-methyl-2-phenyl-1*H*-indole group of **2b** or the biphenyl group of YM-31758 and the position of the phenyl group in **2d** may be more favorable for hydrophobic interaction with the enzyme compared to the position of the phenyl group in **2b** or YM-31758.

Next, we focused our efforts on modification of the benzyl group of compound **2d**. These results are summarized in Table 3. Concerning the distance between the indole ring and the phenyl group, the 3-phenylpropyl derivative **2e** retained high potency, while the 5-phenylpentyl derivative **2f** showed reduced inhibitory activity. These results suggested that the inhibitory activity is affected by the bulkiness of the substituent, *i.e.*, the 3-phenylpropyl group is tolerant but the 5-phenylpentyl group is too bulky. Concerning the substituent on the benzyl group, the 4-methylbenzyl derivative **2i** re-

Table 3. Physicochemical Data and Inhibitory Activities of 5α-Reductase in Human Prostate Homogenates for Indole Derivatices

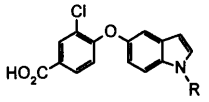

Compd. No.	R	Method[a]	mp (°C)	Formula	Analysis (%) Calcd (Found)					IC_{50} (nM)
					C	H	N	S	Cl	
2e	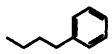	B	Oil	$C_{24}H_{20}NO_3Cl$	71.02 (70.75	4.97 4.95	3.45 3.45		8.73 8.63)	0.61
2f	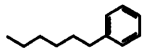	A	144—145	$C_{26}H_{24}NO_3Cl$	71.97 (71.99	5.57 5.54	3.23 3.22		8.17 7.96)	5.0
2g		A	195—197	$C_{23}H_{18}NO_3Cl$	70.50 (70.51	4.63 4.69	3.57 3.54		9.05 9.28)	1.1
2h	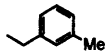	A	182—184	$C_{23}H_{18}NO_3Cl$	70.50 (70.49	4.63 4.68	3.57 3.56		9.05 9.11)	1.3
2i		A	160—162	$C_{21}H_{18}NO_3Cl$	70.50 (70.48	4.63 4.70	3.57 3.54		9.05 9.08)	0.60
2j	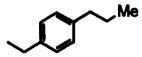	C	168—171	$C_{25}H_{22}NO_3Cl$	71.51 (71.51	5.28 5.33	3.34 3.29		8.44 8.32)	2.3
2k		C	213—217	$C_{23}H_{15}N_2O_3Cl$	68.58 (68.42	3.75 3.84	6.95 6.93		8.80 8.79)	0.93
2l	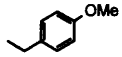	A	173—176	$C_{23}H_{18}NO_4Cl$	67.73 (68.03	4.45 4.43	3.43 3.45		8.69 8.87)	0.47
2m	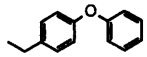	C	213—216	$C_{28}H_{20}NO_4Cl$	71.57 (71.65	4.29 4.28	2.98 2.93		7.54 7.50)	2.1
2n		C	185—188	$C_{20}H_{14}NO_4Cl$	65.31 (65.06	3.84 3.88	3.81 3.79		9.64 9.55)	0.35
2o		C	191—194	$C_{20}H_{14}NO_3SCl$	62.58 (62.25	3.68 3.66	3.65 3.62	8.35 8.48	9.24 9.54)	0.29
2p		C	168—171	$C_{20}H_{14}NO_3SCl$	62.58 (62.37	3.68 3.63	3.65 3.54	8.35 8.35	9.24 9.17)	0.31
2q	Me	B	199—201	$C_{16}H_{12}NO_3Cl$	63.69 (63.62	4.01 4.09	4.64 4.63		11.75 11.65)	11
2r		C	123—126	$C_{19}H_{18}NO_3Cl$	66.38 (66.47	5.28 5.21	4.07 4.13		10.31 10.15)	0.57
2s	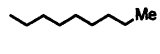	C	oil	$C_{21}H_{26}NO_3Cl$	69.08 (68.97	6.55 6.60	3.50 3.46		8.87 8.83)	5.1
2t		C	185—188	$C_{19}H_{16}NO_3Cl$	66.77 (66.93	4.72 4.78	4.10 4.10		10.37 10.29)	0.64
2u		C	154—157	$C_{20}H_{18}NO_3Cl$	67.51 (67.53	5.10 5.18	3.94 3.92		9.96 9.87)	0.56

a) Synthetic methods as shown in Chart 3.

sulted in a slight increase in activity compared to the 2-methylbenzyl derivative **2g** or 3-methylbenzyl derivative **2h**, suggesting that the 4-position is the favorable position for modification of the benzyl group. Replacement of the methyl group in compound **2i** with a cyano group (**2k**) or methoxy group (**2l**) retained high potency, while replacement with a propyl group (**2j**) or phenoxy group (**2m**) resulted in a slight loss of inhibitory activity, suggesting that the propyl and phenoxy groups are too bulky for high potency. Furthermore, the effect of another aromatic substituent such as a furan ring or thiophene ring instead of the benzene ring in compound **2d** was investigated. The furfuryl derivative **2n**, the 2-thienylmethyl derivative **2o** and the 3-thienylmethyl derivative **2p** showed strong inhibitory activities with IC_{50} values below 0.5 nM, suggesting that these heteroaromatic rings may enhance the inhibitory activity by an interaction with a hydrophobic pocket in the enzyme. Finally, the inhibitory activities of compounds having no aromatic ring at the 1-position of the indole ring was investigated. The methyl derivative **2q** and octyl derivative **2s** showed reduced inhibitory activities, while the butyl derivative **2r**, cyclopropylmethyl derivative **2t** and prenyl derivative **2u** retained high potency with IC_{50} val-

ues below 1 nM. These results demonstrated that the inhibitory activity is affected by the bulkiness of the substituent and an aromatic ring at the 1-position of the indole ring is not essential for high potency.

This new series of indole derivatives **2b**—**2u** was further evaluated for rat prostatic 5α-reductase inhibitory activities in order to investigate *in vivo* inhibitory activity. Compound **1** did not inhibit the rat enzyme, whereas finasteride and (±)-ONO-3805 showed inhibitory activities with IC_{50} values of 13 nM and 2.6 nM, respectively, as shown in Table 4. Except for compound **2m**, none of these indole derivatives showed potent inhibitory activity toward the rat enzyme with an IC_{50} below 100 nM. Compound **2m** showed moderate inhibitory activity against the rat enzyme with an IC_{50} value of 73 nM (Table 4) which may not be sufficient to show inhibitory activity in an *in vivo* model such as the castrated young rat model.[14] These findings suggest that these indole derivatives **2b**—**2u** are selective human prostatic 5α-reductase inhibitors.

Conclusions

In order to prepare a novel potent inhibitor against human prostatic enzymes, we modified the biphenyl-4-yl group of YM-31758 to the 1*H*-indol-5-yl group. Consequently, we have identified a new series of indole derivatives as potent human prostatic 5α-reductase inhibitors. Particularly, compounds **2d** (YM-32906), **2l** and **2n**—**2p** showed potent inhibitory activities with IC_{50} values below 0.5 nM. Replacement of the benzyl group in compound **2d** with a 4-phenoxybenzyl group (**2m**) resulted in an increase in the inhibitory activity against the rat enzyme. Further efforts to discover novel nonsteroidal inhibitors possessing high potency for both human and rat prostatic 5α-reductases are on going.

Table 4. Inhibitory Activities of 5α-Reductase in Human and Rat Prostate Homogenates for Indole Derivatives

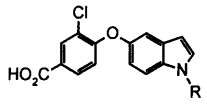

Compound No.	R	IC_{50} (nM)	
		Haman	Rat
1		0.87	>1000
2d		0.44	>300
2m	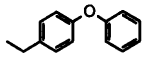	2.1	73
Finasteride		4.1	13
(±)-ONO-3805		538	2.6

Experimental

Melting points were recorded on a Yanaco MP-3 melting point apparatus and are uncorrected. ^{1}H-nuclear magnetic resonance (^{1}H-NMR) spectra were recorded on a JEOL FX-90, JNM-LA 300, JNM-LA 400, JNM-GX 400 or JNM-GX 500 spectrometer with tetramethylsilane as an internal standard. Mass spectra (MS) were recorded on a Hitachi M-80 (electron impact (EI)) or JEOL JMS-DX300 (FAB) mass spectrometer. Elemental analysis was performed with a Yanaco MT-5. Column chromatography was carried out on silica gel (Wakogel C-200). Unless otherwise noted, all reagents and solvents obtained from commercial suppliers were used without further purification. In general, the organic extract was dried over anhydrous Na_2SO_4 or $MgSO_4$, and the organic solvent was evaporated under reduced pressure. All non-aqueous reactions were performed in dry glassware under an atmosphere of dry Ar. The three-dimensional structures of the molecules were constructed using the molecular modeling program Sybyl (version 6.3) on an Indigo Elan workstation (Silicon Graphics Inc., Mountain View, CA). Each structure was energy-minimized using the Tripos force field with the default convergence criteria.

2-Phenyl-1*H*-indole-5-ol (4) To a solution of **3** (670 mg, 3.00 mmol) in 5 ml of CH_2Cl_2, BBr_3 (1.0 M in CH_2Cl_2; 9.0 ml, 9.0 mmol) was added dropwise at −78 °C, and then the mixture was stirred at room temperature for 13 h. The reaction was quenched with ice-water and extracted with AcOEt. The organic layer was washed with water and brine, dried and concentrated. The residue was recrystallized from EtOH to give **4** (459 mg, 73%). ^{1}H-NMR (DMSO-d_6) δ: 6.63 (d, 1H, J=2 Hz), 6.71 (dd, 1H, J=9, 2 Hz), 6.95 (d, 1H, J=2 Hz), 7.2—7.3 (m, 2H), 7.40 (t, 2H, J=8 Hz), 7.76 (d, 2H, J=8 Hz), 8.26 (br s, 1H), 10.55 (br s, 1H); EI-MS *m/z* 209 (M+).

3-Chloro-4-[(2-phenyl-1*H*-indol-5-yl)oxy]benzonitrile (5) A mixture of **4** (450 mg, 2.15 mmol), 3-chloro-4-fluorobenzonitrile (334 mg, 2.15 mmol) and K_2CO_3 (442 mg, 3.20 mmol) in 3 ml of DMSO was stirred at room temperature for 6 h. After dilution with AcOEt, the reaction mixture was washed with water and brine, dried and concentrated. The residue was recrystallized from AcOEt–EtOH to give **5** (595 mg, 80%). ^{1}H-NMR ($CDCl_3$) δ: 6.80—6.82 (m, 2H), 6.93 (dd, 1H, J=9, 2 Hz), 7.3—7.5 (m, 6H), 7.67 (d, 2H, J=8 Hz), 7.74 (d, 1H, J=2 Hz), 8.46 (br s, 1H); EI-MS *m/z* 344 (M^+).

3-Chloro-4-[(2-phenyl-1*H*-indol-5-yl)oxy]benzoic Acid (2a) To a solution of **5** (190 mg, 0.55 mmol) in 5 ml of EtOH, 1.5 ml of 8 N KOH aqueous solution was added, and the mixture was refluxed for 4 h. The reaction mixture was acidified with 3 N HCl aqueous solution and extracted with AcOEt. The extract was washed with water and brine, dried and concentrated, and the residue was recrystallized from AcOEt to give **2a** (150 mg, 75%): mp 268—270 °C. ^{1}H-NMR (DMSO-d_6) δ: 6.84 (d, 1H, J=9 Hz), 6.89—6.92 (m, 2H), 7.3—7.4 (m, 3H), 8.02 (d, 1H, J=2 Hz), 11.72 (s, 1H), 13.07 (br s, 1H); EI-MS *m/z* 363 (M^+).

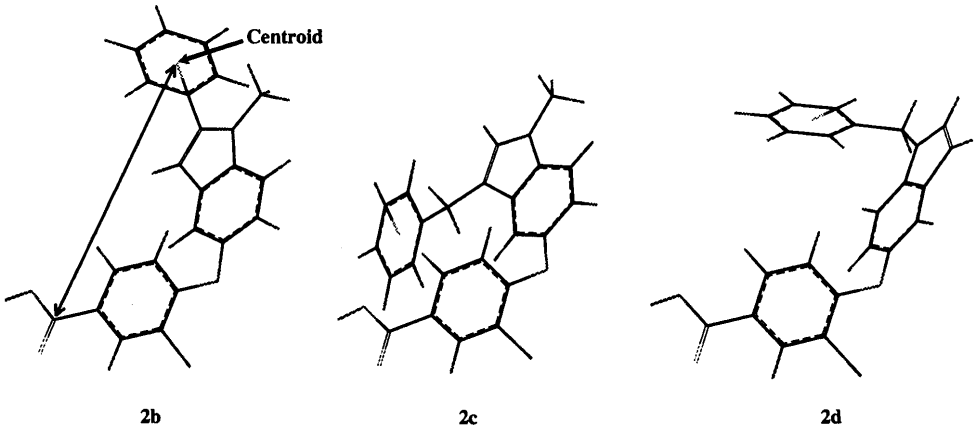

Fig. 2. Optimized Structures of **2b**—**2d** Calculated by the Molecular Modeling Program Sybyl (Version 6.3)

3-Chloro-4-[(1-methyl-2-phenyl-1*H*-indol-5-yl)oxy]benzoic Acid (2b) A mixture of **5** (207 mg, 0.60 mmol), methyl iodide (170 mg, 1.2 mmol) and KOH (67 mg, 1.2 mmol) in 1.0 ml of DMSO was stirred at room temperature for 1.5 h. The reaction was quenched with water and extracted with AcOEt. The organic layer was washed with water and brine, dried and concentrated to give 3-chloro-4-[(1-methyl-2-phenyl-1*H*-indol-5-yl)oxy]benzonitrile (**6**) (211 mg). This crude oil **6** (190 mg) was dissolved in 2.5 ml of EtOH, then 1.0 ml of 8 N KOH aqueous solution was added, and the mixture was refluxed for 5 h. The reaction mixture was acidified with 2 N HCl aqueous solution and extracted with AcOEt. The extract was washed with water and brine, dried and concentrated, and the residue was recrystallized from AcOEt to give **2b** (144 mg, 72%): mp 260—263 °C. ^{1}H-NMR (DMSO-d_6) δ: 3.79 (s, 3H), 6.59 (s, 1H), 6.81 (d, 1H, J=9 Hz), 7.01 (dd, 1H, J=9, 2 Hz), 7.35 (d, 1H, J=2 Hz), 7.4—7.6 (m, 6H), 7.81 (dd, 1H, J=8, 2 Hz), 8.03 (d, 1H, J=2 Hz); EI-MS *m/z* 377 (M^+).

5-Benzyloxy-1-methyl-1*H*-indol-3-yl Phenyl Ketone (8) A mixture of 5-benzyloxy-1*H*-indole (**7**) (4.02 g, 18.0 mmol), methyl iodide (5.11 g, 36.0 mmol) and KOH (2.0 g, 36.0 mmol) in 15 ml of DMSO was stirred at room temperature for 30 min. The reaction was quenched with water and extracted with AcOEt. The organic layer was washed with water and brine, dried and concentrated to give 5-benzyloxy-1-methyl-1*H*-indole (4.06 g). To a solution of 1-benzoylpyrrolidine (1.05 g, 6.0 mmol) in 6 ml of 1,2-dichloroethane, 1.68 ml of $POCl_3$ was added dropwise under refluxing. Stirring was continued for 40 min at this temperature, then the crude 5-benzyloxy-1-methyl-1*H*-indole (1.42 g) in 4 ml of 1,2-dichloroethane was added, and the mixture was refluxed for 6 h. The reaction was quenched with water, then neutralized with 1 N NaOH aqueous solution and extracted with AcOEt. The organic layer was washed with water and a saturated aqueous solution of NaCl, dried and concentrated. The residue was purified by silica gel column chromatography (eluent; hexane : AcOEt=2 : 3) to give **8** (1.33 g, 65%). ^{1}H-NMR ($CDCl_3$) δ: 3.81 (s, 3H), 5.18 (s, 2H), 7.07 (dd, 1H, J=9, 2 Hz), 7.26 (s, 1H), 7.32 (t, 1H, J=7 Hz), 7.40 (dd, 2H, J=8, 7 Hz), 7.5—7.6 (m, 5H), 7.80 (d, 2H, J=8 Hz), 8.08 (d, 1H, J=2 Hz); EI-MS *m/z* 341 (M^+).

3-Benzyl-1-methyl-1*H*-indol-5-ol (9) To a solution of **8** (478 mg, 1.40 mmol) in 16 ml of AcOEt–EtOH–AcOH (10 : 3 : 3), 10% Pd–C (50 mg) was added. The flask was then placed under a hydrogen atmosphere and stirred at room temperature for 2 d. The catalyst was removed by filtration and the filtrate was concentrated. The residue was purified by silica gel column chromatography (eluent; hexane : AcOEt=4 : 1) to give **9** (155 mg, 47%). ^{1}H-NMR ($CDCl_3$) δ: 3.69 (s, 3H), 4.03 (s, 2H), 6.74 (s, 1H), 6.78 (dd, 1H, J=8, 2 Hz), 6.88 (d, 1H, J=2 Hz), 7.1—7.3 (m, 6H); EI-MS *m/z* 237 (M^+).

4-[(3-Benzyl-1-methyl-1*H*-indol-5-yl)oxy]-3-chlorobenzoic Acid (2c) Essentially the same procedure as described above for the preparation of **2a** afforded **2c**: mp 220—222 °C. ^{1}H-NMR (DMSO-d_6) δ: 3.77 (s, 3H), 3.99 (s, 2H), 6.71 (d, 1H, J=9 Hz), 6.93 (dd, 1H, J=9, 2 Hz), 7.15 (m, 1H), 7.2—7.3 (m, 6H), 7.48 (d, 1H, J=9 Hz), 7.77 (dd, 1H, J=9, 2 Hz), 8.00 (d, 1H, J=2 Hz), 13.06 (br s, 1H); EI-MS *m/z* 391 (M^+).

Method A. 3-Chloro-4-(1*H*-indol-5-yloxy)benzonitrile (11) A mixture of 7 (4.47 g, 20.0 mmol), 10% Pd–C (500 mg) and ammonium formate (10.09 g, 160 mmol) in 100 ml of EtOH was stirred at room temperature for 3 h. The catalyst was removed by filtration and the filtrate was concentrated to give 1*H*-indole-5-ol (**10**) (2.89 g). This crude oil **10** (2.89 g) was dissolved in 50 ml of *N*,*N*-dimethylformamide (DMF), then 3-chloro-4-fluorobenzonitrile (3.27 g, 21.2 mmol) and K_2CO_3 (6.91 g, 50.0 mmol) were added, and the mixture was heated at 80 °C for 16 h. The reaction was quenched with water and extracted with AcOEt. The organic layer was washed with water and brine, dried and concentrated. The residue was purified by silica gel column chromatography (eluent; hexane : Et_2O=5 : 1) to give **11** (1.08 g, 29%). ^{1}H-NMR ($CDCl_3$) δ: 6.55 (t, 1H, J=1 Hz), 6.91—6.94 (m, 1H), 7.29 (t, 1H, J=3 Hz), 7.33—7.37 (m, 2H), 7.42 (d, 1H, J=9 Hz), 7.72 (d, 1H, J=2 Hz), 8.37 (br s, 1H); EI-MS *m/z* 268 (M^+).

3-Chloro-4-{[1-(5-phenylpentyl)-1*H*-indol-5-yl]oxy}benzonitrile (13f) To a suspension of KOH (292 mg, 5.21 mmol) in DMSO (3 ml), **11** (350 mg, 1.30 mmol) was added and the mixture stirred at room temperature for 40 min, and 5-phenylpentyl bromide (355 mg, 1.56 mmol) in DMSO (1 ml) was added dropwise at room temperature. Stirring was continued for 2 h at this temperature. The reaction was quenched with water and extracted with AcOEt. The organic layer was washed with water and brine, dried and concentrated. The residue was purified by silica gel column chromatography (eluent; hexane : Et_2O=95 : 5) to give **13f** (337 mg, 62%). ^{1}H-NMR ($CDCl_3$) δ: 1.32—1.43 (m, 2H), 1.61—1.72 (m, 2H), 1.82—1.93 (m, 2H), 2.56—2.63 (m, 2H), 3.43—3.52 (m, 2H), 4.08—4.16 (m, 2H), 6.46 (d, 1H, J=3 Hz), 6.77 (d, 1H, J=9 Hz), 6.92 (dd, 1H, J=9, 2 Hz), 7.11—7.38 (m, 9H), 7.73 (d, 1H, J=2 Hz); EI-MS *m/z* 414 (M^+).

3-Chloro-4-{[1-(5-phenylpentyl)-1*H*-indol-5-yl]oxy}benzoic Acid (2f) Compound **13f** was hydrolyzed in the same manner as described for compound **2a** to give **2f**: mp 144—145 °C. ^{1}H-NMR (DMSO-d_6) δ: 1.33—1.46 (m, 2H), 1.61—1.73 (m, 2H), 1.83—1.95 (m, 2H), 2.60 (t, 2H, J=8 Hz), 4.08—4.17 (m, 2H), 6.46 (d, 1H, J=3 Hz), 6.78 (d, 1H, J=8 Hz), 6.96 (dd, 1H, J=9, 2 Hz), 7.11—7.22 (m, 4H), 7.24—7.38 (m, 4H), 7.83 (dd, 1H, J=9, 2 Hz), 8.20 (d, 1H, J=2 Hz); EI-MS *m/z* 433 (M^+).

Method B. 1-Benzyl-1*H*-indol-5-ol (12d) To a suspension of KOH (13.5 g, 240 mmol) in DMSO (100 ml), 7 (13.4 g, 60.0 mmol) was added and the mixture stirred at room temperature for 50 min, and benzyl bromide (10.8 g, 63.0 mmol) in DMSO (50 ml) was added dropwise at room temperature. Stirring was continued for 3 h at this temperature and the reaction was then quenched with water and extracted with AcOEt. The organic layer was washed with water and brine, dried and concentrated, and the residue recrystallized from EtOH to give 1-benzyl-5-benzyloxy-1*H*-indole (16.0 g, 85%). To a suspension of 1-benzyl-5-benzyloxy-1*H*-indole (16.0 g, 51.0 mmol) in 300 ml of EtOH, 10% Pd–C (1.60 g) and ammonium formate (25.7 g, 408 mmol) was added, and the mixture was stirred at room temperature for 3 h. The catalyst was removed by filtration and the filtrate was concentrated. The residue was extracted with AcOEt and the extract was washed with 1 N HCl aqueous solution, water and brine, then dried and concentrated to give **12d** (10.9 g, 96%). ^{1}H-NMR ($CDCl_3$) δ: 4.61 (s, 1H), 5.25 (s, 2H), 6.41 (d, 1H, J=2 Hz), 6.72 (dd, 1H, J=9, 2 Hz), 7.03 (d, 1H, J=2 Hz), 7.07—7.10 (m, 4H), 7.22—7.30 (m, 3H); EI-MS *m/z* 223 (M^+).

4-[(1-Benzyl-1*H*-indol-5-yl)oxy]-3-chlorobenzonitrile (13d) A mixture of **12d** (3.35 g, 15.0 mmol), 3-chloro-4-fluorobenzonitrile (2.45 g, 15.8 mmol) and K_2CO_3 (3.11 g, 22.5 mmol) in 50 ml of DMF was stirred at 80 °C for 6 h. After dilution with AcOEt, the reaction mixture was washed with 1 N NaOH aqueous solution, water and brine, then dried and concentrated to give **13d** (5.67 g, quant). ^{1}H-NMR ($CDCl_3$) δ: 5.33 (s, 2H), 6.53 (d, J=3 Hz), 6.76 (d, 1H, J=8 Hz), 6.88 (dd, 1H, J=9, 2 Hz), 7.12—7.14 (m, 2H), 7.21 (d, 1H, J=3 Hz), 7.25—7.37 (m, 6H), 7.71 (d, 1H, J=2 Hz); EI-MS *m/z* 358 (M^+).

4-[(1-Benzyl-1*H*-indol-5-yl)oxy]-3-chlorobenzoic Acid (2d) Compound **13d** was hydrolyzed in the same manner as described for compound **2a** to give **2d**: mp 158—159 °C. ^{1}H-NMR ($CDCl_3$) δ: 5.31 (s, 2H), 6.52 (d, 1H, J=3 Hz), 6.76 (d, 1H, J=9 Hz), 6.90 (dd, 1H, J=9, 2 Hz), 7.12 (d, 2H, J=7 Hz), 7.18 (d, 1H, J=3 Hz), 7.22—7.35 (m, 5H), 7.81 (dd, 1H, J=9, 2 Hz), 8.18 (d, 1H, J=2 Hz); EI-MS *m/z* 377 (M^+).

Method C. Ethyl 5-Hydroxy-1*H*-indole-1-carboxylate (14) To a solution of **7** (30.0 g, 134 mmol) in DMF solution, 5.36 g (60% in oil, 134 mmol) of NaH was added at 0 °C and the mixture stirred at 60 °C for 1 h. Ethyl chloroformate (15.2 g, 140 mmol) was added dropwise at 0 °C, and the mixture was stirred at room temperature for 15 h. The reaction was quenched with water and extracted with AcOEt. The organic layer was washed with water and brine, dried and concentrated. The residue was purified by silica gel column chromatography (eluent; hexane : $CHCl_3$=1 : 1) to give ethyl 5-benzyloxy-1*H*-indole-1-carboxylate (28.5 g, 72%). This intermediate (8.98 g, 30.4 mmol) was dissolved in EtOH (180 ml), then 10% Pd–C (0.9 g) and ammonium formate (15.3 g, 243 mmol) were added, and the mixture was stirred at room temperature for 45 min. The catalyst was removed by filtration and the filtrate concentrated, and the residue extracted with AcOEt. The extract was washed with 1 N HCl aqueous solution, water and brine, then dried and concentrated. The residue was purified by silica gel column chromatography (eluent; CH_2Cl_2 : ether=98 : 2) to give **14** (4.90 g, 79%). ^{1}H-NMR ($CDCl_3$) δ: 1.46 (t, 3H, J=7 Hz), 4.42—4.53 (m, 2H), 5.00 (s, 1H), 6.48 (d, 1H, J=4 Hz), 6.86 (dd, 1H, J=9, 2 Hz), 6.99 (d, 1H, J=2 Hz), 7.59 (d, 1H, J=3 Hz), 7.95—8.10 (br s, 1H); EI-MS *m/z* 205 (M^+).

Ethyl 5-(2-Chloro-4-cyanophenoxy)-1*H*-indole-1-carboxylate (15) Essentially the same procedure as described above for the preparation of **13d** afforded **15**. ^{1}H-NMR ($CDCl_3$) δ: 1.44—1.53 (m, 3H), 4.47—4.56 (m, 2H), 6.58 (d, 1H, J=3 Hz), 6.80 (d, 1H, J=9 Hz), 7.06 (dd, 1H, J=9, 2 Hz), 7.26 (d, 1H, J=2 Hz), 7.37—7.43 (m, 1H), 7.69 (d, 1H, J=3 Hz), 7.75 (d, 1H, J=2 Hz), 8.23 (d, 1H, J=9 Hz); EI-MS *m/z* 205 (M^+).

3-Chloro-4-(1*H*-indol-5-yloxy)benzoic Acid (16) Compound **15** was hydrolyzed in the same manner as described for compound **2a** to give **16**. ^{1}H-NMR (DMSO-d_6) δ: 6.45 (s, 1H), 6.80 (d, 1H, J=9 Hz), 6.90 (dd, 1H, J=9, 2 Hz), 7.31 (d, 1H, J=2 Hz), 7.43 (dd, 1H, J=3, 2 Hz), 7.48 (d, 1H, J=9 Hz), 7.80 (dd, 1H, J=9, 2 Hz), 8.02 (d, 1H, J=2 Hz), 11.26 (s, 1H), 13.05 (s, 1H); EI-MS *m/z* 287 (M^+).

3-Chloro-4-{[1-(4-propylbenzyl)-1*H*-indol-5-yl]oxy}benzoic Acid (2j) To a suspension KOH (117 mg, 2.09 mmol) in DMSO (3.5 ml), **16** (150 mg, 0.52 mmol) was added and the mixture stirred at room temperature for 30 min, and 4-propylbenzyl bromide (133 mg, 0.62 mmol) in DMSO (0.5 ml)

was added dropwise at room temperature. Stirring was continued for 2 h at this temperature and the reaction was then quenched with water and extracted with AcOEt. The organic layer was washed with water and brine, dried and concentrated. The residue was purified by silica gel column chromatography (eluent; $CHCl_3$) and recrystallized from EtOH to give **2j** (113 mg, 52%): mp 168—171 °C. ^{1}H-NMR ($CDCl_3$) δ: 0.93 (t, 3H, J=7 Hz), 1.54—1.68 (m, 2H), 2.56 (t, 2H, J=8 Hz), 5.30 (s, 2H), 6.52 (d, 1H, J=3 Hz), 6.79 (d, 1H, J=8 Hz), 6.93 (dd, 1H, J=9, 2 Hz), 7.06 (d, 2H, J=8 Hz), 7.13 (d, 2H, J=8 Hz), 7.19 (d, 1H, J=3 Hz), 7.28—7.37 (m, 2H), 7.79—7.87 (m, 1H), 8.19 (d, 1H, J=2 Hz); EI-MS m/z 419 (M^+).

Authentic Materials The 5α-reductase inhibitors finasteride[6a] and (±)-ONO-3805[7a] were synthesized in our company according to the methods described in the literature.

Biological Methods. Preparation of 5α-Reductases from Rat Prostate and Human Prostate Male Wistar rats 8—12 weeks of age (Charles River Japan Inc. Atsugi, Japan) were sacrificed and the ventral prostates were removed. The prostatic tissues were rinsed with ice-cold saline and minced with scissors. Unless specified, all the following procedures were carried out at 4 °C. The minced tissues were homogenized with a Polytron homogenizer (Kinematica GMBH, Lucerne, Switzerland) in 3 tissue volumes of 20 mM sodium phosphate buffer pH 7.0 containing 0.25 M sucrose and 0.1 mM dithiothreitol (DTT). The homogenate was centrifuged at 10000 ***g*** for 10 min, and the resulting supernatant was centrifuged again at 140000 ***g*** for 60 min. The pellets were resuspended in 40 mM sodium phosphate buffer pH 6.5. The suspension was stored at −80 °C until use.

Human prostatic tissues from BPH patients who received a transurethral prostatectomy were kindly provided by Dr. T. Tahara at Yamato Hospital, Tokyo, Japan, and stored at −80 °C until preparation of the enzyme fractions. The frozen prostatic tissues were minced with scissors and homogenized with a Polytron homogenizer in 3 tissue volumes of 10 mM Tris–HCl buffer pH 7.0 containing 0.33 M sucrose, 1 mM DTT and 1 μM NADPH. The homogenate was centrifuged at 1000 ***g*** for 5 min. The supernatant was centrifuged at 11000 ***g*** for 20 min, and the resulting supernatant was centrifuged again at 140000 ***g*** for 60 min. The resulting pellet was resuspended in 10 mM Tris–HCl buffer pH 7.0 and stored at −80 °C until use.

5α-Reductase Assay *in Vitro* 5α-reductase activities were assayed according to the method described by Liang *et al.*[15] with a minor modification. Briefly, the reaction solutions contained in a final volume of 0.5 ml : 1 μM [4-^{14}C] testosterone, 1 mM DTT, 50 mM NADPH, 50 mM buffer (Tris–HCl pH 6.5, for the rat prostate enzyme; Tris–citrate pH 5.0, for the human prostate enzyme) and the enzyme fractions. To identify the inhibitory effect of the drugs, various concentrations of the test compounds were added in 5 μl DMSO (final conc. 1%). The reaction solutions in duplicate were incubated at 37 °C for 60 min, and the reaction was terminated by addition of 2.0 ml cold AcOEt containing 10 μg testosterone, 5α-DHT, 4-androstene-3,17-dione, 5α-androstan-3α,17β-diol and 5α-androstan-3,17-dione as the standards. The organic phase was separated by centrifugation, evaporated under N_2 gas and resuspended with 40 μl AcOEt. 20 μl of AcOEt was spotted on the TLC plate and separated twice by AcOEt/cyclohexane (1 : 1) as the developing solvent. The steroid standards were located by UV (254 nm) and by spraying with a 1% $CeSO_4$–10% H_2SO_4 solution followed by heating. The regions containing 5α-reduced metabolites (5α-DHT, 5α-androstan-3α, 17β-diol and 5α-androstan-3,17-dione) were cut from the TLC plate, soaked in 5 ml of Aquasol-2 and the radioactivity was counted by a scintillation counter. The IC_{50} values for 5α-reductase activity were obtained from the linear line drawn by least-squares fitting methods.

Acknowledgments We thank Drs. K. Murase, T. Fujikura, H. Shikama and H. Ino for helpful discussions and the staff of the Measurement Division for measurement of NMR and mass spectra and elemental analyses.

References

1) Igarashi S., Kimura T., Naito R., Hara H, Fujii M., Koutoku H., Oritani H., Mase T., *Chem. Pharm. Bull.*, **47**, 1073—1080 (1999).
2) Present address: *Secretariat Dept., Yamanouchi Pharmaceutical Co., Ltd., 2–3–11, Nihonbashi-Honcho, Chuo-ku, Tokyo 103–0023, Japan.*
3) Present address: *Institute for Drug Development Research, Yamanouchi Pharmaceutical Co., Ltd., 1–1–8 Azusawa, Itabashi-ku, Tokyo 174–0051, Japan.*
4) Present address: *Bulk Manufacturing & Technology Division, Yamanouchi Pharmaceutical Co., Ltd., 160–2 Matsukubo, Akahama, Takahagi, Ibaraki 318–0001, Japan.*
5) *a*) Metcalf B. W., Levy M. A., Holt D. A., *Trends Pharmacol. Sci.*, **10**, 491—495 (1989); *b*) Adachi K., Kano M., *Biochem. Biophys. Res. Comm.*, **41**, 884—890 (1970); *c*) Books J. R., *J. Clin. Endocrinol. Metab.*, **74**, 391—405 (1986).
6) Recent studies on steroidal 5α-reductase inhibitors: *a*) Rasmusson G. H., Reynolds G. F., Steinberg N. G., Walton E., Patel G. F., Liang T., Cascieri M. A., Cheung A. H., Brooks J. R., Berman C., *J. Med. Chem.*, **29**, 2298—2315 (1986); *b*) Metcalf B. W., Holt D. A., Levy M. A., Erb J. M., Heaslip J. I., Brandt M, Oh H.-J., *Bioorg. Chem.*, **17**, 372—376 (1989); *c*) Holt D. A., Levy M. A., Ladd D. L., Oh H.-J., Erb J. M., Heaslip J. I., Brandt M., Metcalf B. W., *J. Med. Chem.*, **33**, 937—942 (1990); *d*) Holt D. A., Levy M. A., Oh H.-J., Erb J. M., Heaslip J. I., Brandt M., Lan-Hargest H.-Y., Metcalf B. W., *ibid.*, **33**, 943—950 (1990); *e*) Levy M. A., Metcalf B. W., Brandt M., Erb J. M., Oh H.-J., Heaslip J. I., Yen H.-K., Rozamus L. W., Holt D. A., *Bioorg. Chem.*, **19**, 245—260 (1991); *f*) Bakshi R. K., Patel G. F., Rasmusson G. H., Baginsky W. F., Cimis G., Ellsworth K., Chang B., Bull H., Tolman R. L., Harris G. S., *J. Med. Chem.*, **37**, 3871—3874 (1994); *g*) Li X., Singh S. M., Cote J., Laplante S., Veilleux R., Labrie F., *ibid.*, **38**, 1456—1461 (1995); *h*) Frye S. V., Haffner C. D., Maloney P. R., Hinter R. N., Dorsey G. F., Noe R. A., Unwalla R. J., Batchelor K. W., Bramson H. N., Stuart J. D., Schweiker S. L., Arnold J. V., Bickett D. M., Moss M. L., Tian G., Lee F. W., Tippin T. K., James M. K., Grizzle M. K., Long J. E., Croom D. K., *ibid.*, **38**, 2621—2627 (1995); *i*) Hausler A., Allegrini P. R., Biollaz M., Batzl C., Scheidegger E., Bhatnagar A. S., *J. Steroid Biochem. Mol. Biol.*, **57**, 187—195 (1996).
7) Recent studies on nonsteroidal 5α-reductase inhibitors: *a*) Nakai H., Terajima H., Arai Y., Eur. Patent Appl., EP 291245 [*Chem. Abstr.*, **110**, 212384*t* (1989)]; *b*) Jones C. D., Audia J. E., Lawhorn D. E., McQuaid L. A., Neubauer B. L., Pike A. J., Pennington P. A., Stamm N. B., Toomey R. E., Hirsch K. S., *J. Med. Chem.*, **36**, 421—423 (1993); *c*) Holt D. A., Yamashita D. S., Konialian-Beak A. L., Luengo J. I., Abell A. D., Bergsma D. J., Brandt M., Levy M. A., *ibid.*, **38**, 13—15 (1995); *d*) Blagg J., Ballard S. A., Cooper K., Finn P. W., Johnson P. S., MacIntyre F., Maw G. N., Spargo P. L., *Bioorg. Med. Chem. Lett.*, **6**, 1517—1522 (1996); *e*) Takami H., Koshimura H., Kishibayashi N., Ishii A., Nonaka H., Aoyama S., Kase H., Kumazawa T., *J. Med. Chem.*, **39**, 5047—5052 (1996); *f*) Kato M., Komada K., Namera A., Sakai Y., Okada S., Yamada A., Yokoyama K., Migita E., Minobe Y., Tani T., *Chem. Pharm. Bull.*, **45**, 1767—1776 (1997).
8) Andersson S., Russell D. W., *Proc. Natl. Acad. Sci. U.S.A.*, **87**, 3640—3644 (1990).
9) Moore R. J., Wilson J. D., *J. Biol. Chem.*, **251**, 5895—5900 (1976).
10) Andersson S., Berman D. M., Jenkins E. P., Russell D. W., *Nature* (London), **354**, 159—161 (1991).
11) Rittmaster R.S., *N. Engl. J. Med.*, **330**, 120—125 (1994).
12) The inhibitory activities of finasteride and (±)-ONO-3805 for human prostatic 5α-reductase were evaluated in our company. The results are described in Table 4.
13) Heaney H., Ley S. V., *J. Chem. Soc., Perkin Trans. 1*, **1973**, 499—500.
14) Giudici D., Briatico G., Cominato C., Zaccheo T., Iehle C., Nesi M., Panzeri A., di Salle E., *J. Steroid Biochem. Mol. Biol.*, **58**, 299—305 (1996).
15) Liang T., Cascieri M. A., Cheung A. H., Reynolds G. F., Rasmusson G. H., *Endocrinology*, **117**, 571—579 (1985).

Stereochemistry of *cis*- and *trans*-Hinokiresinol and Their Estrogen-like Activity

Emiko MINAMI,[a] Motohiko TAKI,[b] Sachiko TAKAISHI,[b] Yasuteru IIJIMA,[b] Shinya TSUTSUMI,[c] and Toshiyuki AKIYAMA*,[a]

Exploratory Chemistry Research Laboratories,[a] Pharmacology and Molecular Biology Research Laboratories,[b] and Analytical and Metabolic Research Laboratories,[c] Sankyo Co., Ltd., 2–58 Hiromachi 1-Chome, Shinagawa-ku, Tokyo 140–8710, Japan. Received October 1, 1999; accepted November 19, 1999

Naturally occurring phenylpropanoids, hinokiresinol (*trans*-hinokiresinol) and nyasol (*cis*-hinokiresinol) were found to possess appreciable estrogen receptor binding activity. Strong differences in activity were observed between the geometrical isomers and enantiomers. Among these, (3*S*)-*cis*-hinokiresinol displayed the highest activity, one order of magnitude greater than the activity of genistein. Furthermore, *cis*- and *trans*-hinokiresinol stimulated the proliferation of estrogen-dependent T47D breast cancer cells, and their stimulatory effects were blocked by an estrogen antagonist, indicating that the compounds are estrogen agonists. In addition, the absolute configuration of C-3 in (+)-*cis*-hinokiresinol has been assigned as *S* by comparison with the circular dichroism spectra of the hydrogenated products prepared from *cis* and *trans* ((3*S*)-*trans*-hinokiresinol: previously assigned) isomers. These results incidentally provide us with an unambiguous answer to contradictory reports regarding the assignment of the full stereochemisry of *cis*- and *trans*-hinokiresinol that have existed in the literature for more than two decades.

Key words phytoestrogen; hinokiresinol; stereochemistry; nyasol; *Chamaecyparis obtusa*, *Anemarrhena asphodeloides*

In the past few years there has been broad discussion on a wide variety of man-made chemicals that act as estrogen mimics present in the environment. A reduced fertility rate in addition to the impairment of reproductive function have been hypothesized to be linked to exposure to man-made estrogenic substances.[1] In contrast to the supposed risk of estrogenicity, mounting evidence suggests that estrogen may exert beneficial preventive effects in women against heart attacks and other cardiovascular problems, as well as osteoporosis and possibly Alzheimer's disease.[2] Although there are conflicting findings, phytoestrogens have been postulated to exert a tissue-dependent expression of estrogen agonist and antagonist activity and may promote a significant advancement in the prevention of diseases caused by estrogen deficiency in postmenopausal women compared to conventional hormone replacement therapy: the therapeutic efficacy of soybean phytoestrogens has been well reviewed.[3] Thus, the findings of phytoestrogen occurrence in traditional herbal medicines may open the door to considering the therapeutic value of these herbs.

Appreciable estrogen-like activity has been detected in a number of non-steroidal phytoestrogens such as isoflavones, coumestanes, and several phenolic compounds.[4] In addition, certain prenylflavones have been shown to have estrogen-like activity in *in vitro* and *in vivo* experiments.[5,6] The estrogenicity of phytoestrogens such as isoflavones can be understood in view of the superficial similarity between these compounds and the dihydroxystilbene structure. Previously, we reported that several homoisoflavones and retrodihydrochalcones were found to exhibit appreciable estrogen-like activity.[7] These compounds share two *p*-hydroxy benzene rings connected by a chain of three carbon atoms. On the basis of structural similarity, we examined the estrogen-like activity of hinokiresinol (*trans*-hinokiresinol) (**1**) and nyasol (*cis*-hinokiresinol) (**2**), which each consist of a diphenylpropanoid unit. Both *cis*- and *trans*-hinokiresinol were found to possess appreciable estrogen-like activity, and (3*S*)-*cis*-hinokiresinol (**2b**) displayed the highest activity among its geometrical isomers and enantiomers. In addition, the relative and absolute stereochemistry of these compounds were confirmed to provide an unambiguous answer to contradictory reports regarding the assignment of the full stereochemistry of *cis*- and *trans*-hinokiresinol that have existed in the literature for more than two decades. For the convenience of comparison and discussion, nyasol is referred to as *cis*-hinokiresinol (**2**) and hinokiresinol itself is referred to as *trans*-hinokiresinol (**1**) in this publication.

Results and Discussion

Chemistry In 1965, Hirose *et al.*[8] reported the isolation of hinokiresinol (**1**) from the heartwood of *Chamaecyparis obtusa*, and they proposed the structural formula of **1** as having *trans* geometry at the 1, 2 double bond. The absolute configuration at C-3 in **1** has been assigned as *S* based on the optical rotatory dispersion (ORD) spectrum of its degradation product,[9] and later on the enantioselective synthesis of its di-*O*-methylether.[10] The *cis* isomer (nyasol) (**2**) and

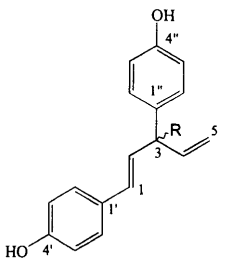

(1) *trans*-hinokiresinol

(1a) 3(*R*): R = —H

(1b) 3(*S*): R = ····H

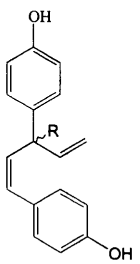

(2) *cis*-hinokiresinol (nyasol)

(2a) 3(*R*): R = —H

(2b) 3(*S*): R = ····H

* To whom correspondence should be addressed.

© 2000 Pharmaceutical Society of Japan

its glycosides have been isolated from various Liliaceous plants,[11—16] although the absolute configuration at C-3 is yet unknown. Subsequent studies on the synthesis[17,18] of **1** and **2** introduced ambiguities in the assignment of the geometry at the 1, 2 double bond. Messana *et al.*[14] pointed out in 1989 that the geometry of several synthetic hinokiresinols have wrongly been assigned and, therefore, erroneously identified.[17,18] In 1996 Tsui and Brown[15] reported that both hinokiresinols seemed likely to share the same *cis* geometry based on comparison with previously published data. Although Oketch-Rabah *et al.*[16] proposed in 1997 that the two isomers are naturally occurring, hinokiresinol is described as an identical compound to nyasol (*cis* geometry), together with a wrong absolute configuration in a widely used compilation of natural products.[19] Moreover, a very recent publication follows the same error.[20]

These ambiguities may have arisen from the limited spectroscopic data presented for natural hinokiresinol (**1**). Thus, we isolated **1** ($[\alpha]_D = -3°$) from a MeOH extract of the heartwood of *C. obtusa*. Assignments of ^{1}H- and ^{13}C-NMR spectra were deduced from the analysis of two dimensional (2D) chemical shift correlations (data not shown), and the results obtained were totally consistent with the structure of **1**. Previously, Nikaido *et al.*[12] reported the isolation of **2** from the Chinese medicinal drug Anemarrhenae Rhizoma (rhizome of *Anemarrhena asphodeloides* BUNGE.). The authors did not document any evidence to assign the isolated compound as **2** nor any spectroscopic data to identify the compound. We obtained the compound ($[\alpha]_D = -67°$) from the same plant source and the compound was identified as **2** by comparisons of its ^{1}H- and ^{13}C-NMR data with those described in the literature.[11,15] Complete ^{1}H- and ^{13}C-NMR spectral assignments for **1** and **2** provided us with unambiguous evidence for the presence of these compounds in nature, and confirmed the geometry of the double bond at C-1,2 in the respective isomers: the *trans*-configured **1** exhibited a ^{1}H–^{1}H coupling constant of 16 Hz, while the *cis* isomer (**2**) showed a value of 12 Hz in its ^{1}H-NMR spectrum.

As was described earlier, the absolute configuration at C-3 in (−)-*trans*-hinokiresinol (**1**) has been assigned as *S*.[9,10] In order to establish the absolute configuration of **2**, we prepared tetrahydro derivatives of **1** and **2**. In the (3*S*)-configured tetrahydro derivative (**3b**) derived from **1**, a positive Cotton effect was observed in the region of 220—250 nm and a negative Cotton effect in the region of 270—290 nm. On the other hand, the tetrahydro derivative (**3a**) prepared from **2** exhibited a circular dichroism (CD) curve which was an antipode to that of **3b**, indicating that the absolute configuration at C-3 in **2** is *R*, as illustrated in the structure of **2a**.

However, the relatively low value of molecular ellipticity of **3a**, compared with that of the (3*S*)-isomer (**3b**), implied that **2** was obtained as a partially racemic mixture. The composition of **2** was then checked using a chiral HPLC column (Chiralpak OD(+)). Two peaks were clearly observed with an approximate ratio of 77 : 23. This composition is consistent with the ratio calculated from the amplitude of the CD spectrum of **3a**, assuming that **1** is optically pure. From the above data we concluded that **2** isolated from *A. asphodeloides* is as illustrated by the structure of **2a**, and is partially racemized at C-3. We then separated the respective enantiomers by preparative HPLC. Both enantiomers (**2a** and **2b**) were obtained and were characterized by their CD spectra: the CD spectrum of the major enantiomer (**2a**) appeared to be the mirror image of that observed for the minor enantiomer (**2b**). The results described here provide unequivocal proof of the structure of (−)-*trans*-hinokiresinol as **1b** and (+)- and (−)-*cis*-hinokiresinol as **2b** and **2a**, respectively.

Table 1. Binding Affinities of Isolates and Other Compounds for the Bovine Uterine Estrogen Receptor

Compound	IC_{50} (nM)		SEM[a]	n[b]
Estradiol	0.40	±	0.01	5
Genistein	480	±	80	5
1	2300	±	100	5
2	350	±	20	5
2a	400			2
2b	60			2

a) SEM: Standard error of mean. *b*) Number of experiments.

Biological Activity The compounds described above were then evaluated for their *in vitro* estrogenic activity by a competitive binding assay using [^{3}H]-17β-estradiol as the tracer and bovine uterine cytosol as the receptor source.[7] Genistein, the best known among naturally occurring non-steroidal estrogens, was used as the reference compound. The semi-logarithmic plot of bound radioactivity *vs.* molar concentration of the compounds exhibited curves parallel to those of 17β-estradiol, suggesting a common binding site for the compounds tested. Concentrations required for 50% displacement of specifically bound radioactivity (IC_{50} values) were calculated from the plotted data and are shown in Table 1. All compounds tested were proven to exhibit binding affinity for the estrogen receptor. (3*S*)-*cis*-Hinokiresinol (**2b**) displayed the highest activity among these compounds, having an IC_{50} of 60 nM. This value indicated that **2b** is one order of magnitude more efficient than genistein.

As far as the tested compounds were concerned, activity appeared to be related to the geometry of the 1,2-double bond in addition to the absolute configuration at C-3: the *cis* isomer (**2**) possesses an activity of about one order of magnitude greater than that of the *trans* isomer (**1**). This is in sharp contrast to previous reports stating that the ability of diethylstilbestrol to act as the functional equivalent of estradiol is due to the particular structural feature of its *trans* geometry. Previously, we reported that 8-isopentenylnaringenin (**4**) exerted estrogenic activity twice as high as that of genistein, as evaluated by a receptor binding assay, and that the (2*S*)- and (2*R*)-enantiomers of **4** did not show significantly different binding affinity for the estrogen receptor.[5] When we studied the receptor binding of the enantiomers of *cis*-hinokiresinol (**2**), we found a major difference between them: the (*S*)-enantiomer (**2b**) displayed activity of about one order of magnitude greater than that of the (*R*)-enantiomer (**2a**). This result was not unexpected because biomolecules are usually able to discriminate between optical isomers. Recently, Kuiper *et al.* discovered the existence of two estrogen receptor subtypes (ERα, ERβ).[21] Although the ligand binding affinity of ERα and ERβ is overall quite similar for the physiological ligands, several phytoestrogens, especially genistein, apigenin and kaempferol, have been reported to have significantly higher affinity for ERβ (20- to 30-fold more).[22] Our experiments have been carried out with a bovine uterine extract

which involves mixtures of ERα and ERβ protein. Additional studies using the respective subtypes of the receptors are critical to understanding the structure–activity relationship and to finding an explanation for the apparently contradictory phenomena described above.

Next, we tested the ability of **1** and **2** to stimulate the growth of estrogen-dependent T47D cells (derived from human breast cancer) in culture to examine if these compounds functioned as an estrogen receptor agonist or antagonist.[23] Test compounds were incubated for 4 d with cells which had been brought into log phase during a 2-d preculture period. The number of cells was assessed by 3-(4,5-dimethyl-2-thiazolyl)-2,5-diphenyl-2*H*-tetrazolium bromide (MTT) assay. As shown in Fig. 1, these compounds stimulated the cell proliferation in a concentration dependent manner and induced T47D proliferation to the same extent as estradiol. The calculated EC_{50} values (concentration of a compound required to increase the cell number to 50% of the plateau level) were 10^{-7} M for **2**, 10^{-6} M for **1** and 10^{-11} M for estradiol. The stimulatory effect was blocked by cotreatment with a pure/complete estrogen antagonist ICI 164 384[24] (Fig. 2). These results clearly indicate that **1** and **2** are estrogen agonists and that **2** possesses the activity of one order of magnitude greater than that of **1**.

cis-Hinokiresinol (**2**) has already been shown to potently inhibit the growth of *Leishmania major* promastigotes, to moderately inhibit *Plasmodium falciparum* schizonts,[16] and has been detected as a potent inhibitor of cAMP phosphodiesterase, having an IC_{50} value of 100 μM.[12] Compound **2** is also reported to be a LTB_4 receptor antagonist having an IC_{50} value of 5.24 μM.[20] We have shown here that **2** possesses noteworthy estrogen-like activity (an EC_{50} value of 100 nM as assessed by the stimulatory effect on the proliferation of estrogen-dependent human breast cancer cells). The rhizome of *A. asphodeloides* is a herbal drug recommended for the treatment of various ailments in Chinese traditional remedies, and **2** is known to be one of the major ingredients of this herbal medicine. Phytoestrogens are known to exert a variety of beneficial effects related to several chronic diseases including osteoporosis and heart diseases, and perhaps hormone-dependent cancer.[25] Although we are far from a satisfactory knowledge of the chemicals responsible for the potent effects of this medicinal plant, the occurrence of an estrogen agonist may contribute to the therapeutic value of this herb.

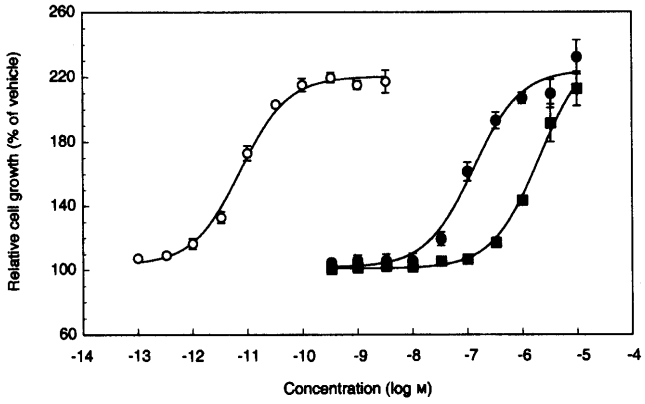

Fig. 1. The Dose-Response Effect of the Compounds on the Proliferation of T47D Cells

Points are mean values, and vertical bars represent standard errors of the mean (n=8). ○: 17β-estradiol, ■: *trans*-hinokiresinol (**1**), ●: *cis*-hinokiresinol (**2**).

Experimental

General Experimental Procedures The ^{1}H-NMR spectra were conducted on a Bruker AMX-360 at 360 and 90.8 MHz for ^{1}H- and ^{13}C-NMR spectra, respectively. Electron ionization mass spectrum (EI-MS) data was obtained on a JEOL JMS-D300 mass spectrometer at 70 eV. IR spectra were measured on a JASCO FT-IR 8300 spectrometer. UV spectra were measured using a Hitachi U-3500 spectrometer. CD measurements were carried out using a JASCO J-500 spectrometer to scan from 420 to 200 nm. Optical rotations were measured at room temperature on a Perkin-Elmer 241 polarimeter.

Plant Materials Powdered heartwood of *Chamaecyparis obtusa* ENDL. (Japanese name, Hinoki) (Cupressaceae) was a generous gift of Dr. M. Yatagai, Forestry and Forest Products Research Institute. The dried rhizome of *Anemarrhena asphodeloides* BUNGE (Japanese name, Chimo) (Liliaceae) was purchased from a Chinese crude drug store in Tokyo.

Origin of Individual Compounds *trans*-Hinokiresinol (**1**)[8]: Isolated from powdered heartwood of *C. obtusa*. Colorless oil, ^{1}H-NMR ($(CD_3)_2C=O$) δ: 4.12 (1H, t, J=6.9 Hz), 5.09 (1H, d, J=10.4 Hz), 5.09 (1H, d, J=17.2 Hz), 6.09 (1H, ddd, J=17.2, 10.4, 6.9 Hz), 6.26 (1H, dd, J=15.9, 6.9 Hz), 6.36 (1H, d, J=15.9 Hz), 6.79 (2H, d, J=8.4 Hz), 6.80 (2H, d, J=8.5 Hz), 7.10 (2H, d, J=8.5 Hz), 7.29 (2H, d, J=8.4 Hz). ^{13}C-NMR ($(CD_3)_2C=O$) δ: 52.7 (d), 114.9 (t), 116.2 (d), 116.3 (d), 128.3 (d), 129.8 (d), 130.2 (s), 130.3 (d), 130.6 (d), 134.9 (s), 142.3 (d), 156.9 (s), 157.8 (s). IR (liquid film) cm^{-1}: 3345, 1610, 1512, 1445, 1368, 1236, 1172, 969, 919, 833, 758. UV λ_{max} (EtOH) nm (ε): 191 (29900), 204 (32500), 265 (22000). EI-MS *m/z*: 252.1151 (M^+) (Calcd for $C_{17}H_{16}O_2$: 252.1150). $[\alpha]_D$ −3° (c=1.0, acetone). CD (EtOH): $[\theta]_{223}$ +11000, $[\theta]_{240}$ +6400, $[\theta]_{261}$ +4000, $[\theta]_{283}$ −4200. Compound **1** provided EI-MS consistent with previous published data.[26]

cis-Hinokiresinol (**2**): Isolated from the rhizome of *A. asphodeloides*.[12,20] Colorless oil, IR (liquid film) cm^{-1}: 3329, 1610, 1510, 1444, 1367, 1236, 1173, 920, 833, 756. UV λ_{max} (EtOH) nm (ε): 202 (37400), 231 (10700), 259 (15700). EI-MS *m/z*: 252.1154 (M^+) (Calcd for $C_{17}H_{16}O_2$: 252.1150).

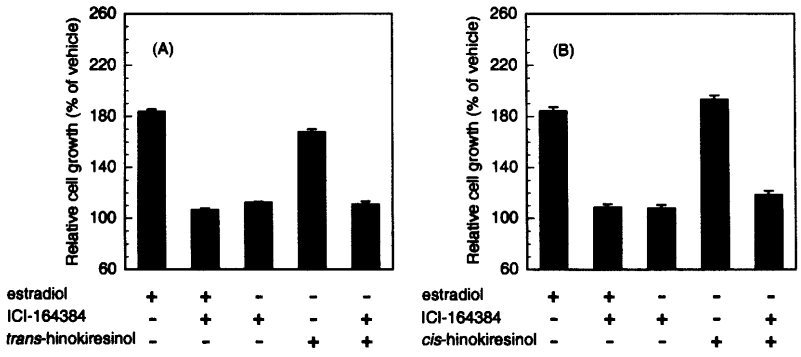

Fig. 2. The Effect of ICI 164 384 on the Ability of **1** and **2** to Stimulate the Growth of T47D Cells

Cells were grown in the presence (+) or absence (−) of (A) 100 pM of estradiol, 1 μM of ICI 164 384 or 10 μM of **1** and (B) 100 pM of estradiol, 1 μM of ICI 164 384 or 3 μM of **2**. Columns are mean values, and vertical bars represent standard errors of the mean (n=8).

$[\alpha]_D$ −67° (c=0.1, acetone). Lit.[11] −147° (c=1.0, acetone). CD (EtOH): $[\theta]_{230}$ +6500, $[\theta]_{254}$ −3300, $[\theta]_{287}$ +2000. ^{1}H- and ^{13}C-NMR data confirmed that the compound was identical to nyasol.[11,15]

Analysis and Separation of the Enantiomers of *cis*-Hinokiresinol, 2a and 2b Chiral HPLC analysis of *cis*-hinokiresinol was performed using a column packed with cellulose carbamate (4.6 mm×25 cm, 10 μm, OD; tris-3,5-dimethylphenylcarbamate, Chiralcel®, Daicel Chemical Industries, Japan). Two peaks were clearly observed at retention times of 26.9 and 29.9 min at an approximate ratio of 77 : 23 with *n*-hexane : 1-propanol (94 : 6) containing 1% trifluoroacetic acid as the mobile phase at a flow rate of 1.0 ml/min. The enantiomers of **2** were separated semi-preparatively by liquid chromatography on a cellulose carbamate column (2×25 cm, 10 μm, OD, Chiralcel®, Daicel Chemical Industries, Japan) using a mixed solvent of *n*-hexane : 1-propanol (94 : 6) +1% trifluoroacetic acid as an eluent (5 ml/min). The chromatogram showed an incomplete separation of the peaks for the two isomers (t_R=38.9 min and t_R=42.0 min). Repeated separation of the racemate (**2**, 20 mg) resulted in optically pure **2a** (2.5 mg) and **2b** (2.9 mg). CD **2a** (EtOH): $[\theta]_{228}$ +11000, $[\theta]_{254}$ −60000, $[\theta]_{287}$ +3000. **2b** (EtOH): $[\theta]_{228}$ −12000, $[\theta]_{254}$ +60000, $[\theta]_{287}$ −3000.

Tetrahydrohinokiresinol, 3a and 3b A mixture of **1** (30 mg), EtOH (5 ml) and PtO_2 (10 mg) was hydrogenated for 1 h. After filtration, the mixture was concentrated to dryness under reduced pressure, and dried to give a colorless solid. The residue was applied to HPLC (ODS column 2×25 cm, 5 μm, Senshu, Japan) eluted with CH_3CN–H_2O (1 : 1) at flow rate of 20 ml/min. The major peak (t_R=12 min) was collected. Evaporation of the solvent gave **3b** (18 mg) as a colorless oil. ^{1}H-NMR ($CDCl_3$) δ: 0.74 (3H, t, J=7.4 Hz), 1.52 (1H, m), 1.63 (1H, m), 1.78 (1H, m), 1.88 (1H, m), 2.36 (3H, m), 6.72 (2H, d, J=6.5 Hz), 6.78 (2H, d, J=6.5 Hz), 7.00 (2H, d, J=6.5 Hz), 7.01 (2H, d, J=6.5 Hz). IR (liquid film) cm^{-1}: 3324, 2928, 1613, 1513, 1452, 1375, 1233, 1174, 830, 758. UV λ_{max} (EtOH) nm (ε) 191 (35000), 202 (21000), 226 (15600), 279 (3400). CD (EtOH): $[\theta]_{203}$ +17000, $[\theta]_{229}$ +11500, $[\theta]_{286}$ −2000.

Compound **2** (72 mg) was hydrogenated in the same way, and its tetrahydro derivative was obtained (16 mg) as a colorless oil. Compound **3a** prepared from **2** was identified as **3b** by comparing ^{1}H- and ^{13}C-NMR spectra. CD (EtOH): $[\theta]_{203}$ −7700, $[\theta]_{229}$ −6200, $[\theta]_{286}$ +950.

Estradiol Receptor Binding Assay The competitive binding assay to measure affinity for the estrogen receptor follows the method described previously.[7]

Effect on T47D Cell Proliferation Hormone-sensitive human T47D breast cancer cells[27] were maintained in Roswell Park Memorial Institute (RPMI) 1640 supplemented with 10% fetal bovine serum. One day after seeding in a 96-well plate at a density of 2.5×10^3 cells/well, the media was changed to RPMI 1640 with 10% charcoal-treated fetal bovine serum. The media was refreshed again the next day. Then, the DMSO solution of the test compounds was added to the cell culture. The final concentrations of compounds were between 10^{-10} and 10^{-4} M. After 4 d in a humidified incubator at 37 °C with 5% CO_2, the number of cells was assessed by MTT assay, as modified by Carmichael *et al.*[28]

Acknowledgements This investigation was carried out as a part of a project conducted by the Physiologically Active Substances of Trees Research Association to which the authors are grateful. Thanks are also due to Dr. M. Yatagai of the Forestry and Forest Products Research Institute for plant identification and collection.

References and Notes

1) Tyler C. R., Jobling S., Sumpter J. P., *Crit. Rev. Toxicol.*, **28**, 319—361 (1998).
2) Ettinger B., *Proc. Soc. Exp. Biol. Med.*, **217**, 2—4 (1998).
3) Clarkson T. B., Anthony M. S., Williams J. K., Honoré E. K., Cline J. M., *Proc. Soc. Exp. Biol. Med.*, **217**, 365—368 (1998).
4) Farnsworth N. R., Bingel A. S., Cordell G. A., Crane F. A., Fong H. H. S., *J. Pharm. Sci.*, **64**, 717—754 (1975).
5) Kitaoka M., Kadokawa H., Sugano M., Ichikawa K., Taki M., Takaishi S., Iijima Y., Tsutsumi S., Boriboon M., Akiyama T., *Planta Med.*, **64**, 511—515 (1998).
6) Miyamoto M., Matsushita Y., Kiyokawa A., Fukuda C., Iijima Y., Sugano M., Akiyama T., *Planta Med.*, **64**, 516—519 (1998).
7) Ichikawa K., Kitaoka M., Taki M., Takaishi S., Iijima Y., Boriboon M., Akiyama T., *Planta Med.*, **63**, 540—543 (1997).
8) Hirose Y., Oishi N., Nagaki H., Nakatsuka T., *Tetrahedron Lett.*, **1965**, 3665—3668.
9) Enzell C. R., Hirose Y., Thomas B. R., *Tetrahedron Lett.*, **1967**, 793—798.
10) Muraoka O., Zheng B.-Z., Fujiwara N., Tanabe G., *J. Chem. Soc., Perkin Trans. 1*, **1996**, 405—411.
11) Marini-Bettolo G. B., Nicoletti M., Messana I., Galeffi C., Msonthi J. D., Chapya W. A., *Tetrahedron*, **41**, 665—670 (1985).
12) Nikaido T., Ohmoto T., Noguchi H., Kinoshita T., Saitoh H., Sankawa U., *Planta Med.*, **43**, 18—23 (1981).
13) Galeffi C., Multari G., Msonthi J. D., Nicoletti M., Marini-Bettolo G. B., *Tetrahedron*, **43**, 3519—3522 (1987).
14) Messana I., Msonthi J. D., De Vicente Y., Multari G., Galeffi C., *Phytochemistry*, **28**, 2807—2809 (1989).
15) Tsui W.-Y., Brown G. D., *Phytochemistry*, **43**, 1413—1415 (1996).
16) Oketch-Rabah H. A., Dossaji S. F., Christensen S. B., Frydenvang K., Lemmich E., Cornett C., Olsen C. E., Chen M., Kharazmi A., Theander T., *J. Nat. Prod.*, **60**, 1017—1022 (1997).
17) Beracierta A. P., Whiting D. A., *J. Chem. Soc., Perkin Trans. 1*, **1978**, 1257—1263.
18) Ameer F., Drewes S. E., Drewes M. W., Roos G. H. P., Watson M. C., *J. Chem. Soc., Perkin Trans. 1*, **1988**, 1425—1430.
19) Dictionary of Natural Products on CD-ROM, Version 7.2 (January 1999). Chapman and Hall, London.
20) Lee H. J., Ryu J.-H., *Planta Med.*, **65**, 391 (1999).
21) Kuiper G. G. J. M., Enmark E., Pelto-Huikko M., Nilsson S., Gustafsson J.-A., *Proc. Natl. Acad. Sci. U.S.A.*, **93**, 5925—5930 (1996).
22) *a*) Kuiper G. G. J. M., Carlsson B., Grandien K., Enmark E., Haggblad J., Nilsson S., Gustafsson J.-A., *Endocrinology*, **138**, 863—870 (1997); *b*) Kuiper G. G. J. M., Lemmen J. G., Carlsson B., Corton J. C., Safe S. H., van der Saag P. T., van der Burg B., Gustafsson J.-A., *ibid.*, **139**, 4252—4263 (1998).
23) Gehm B. D., McAndrews J. M., Chien P.-Y., Jameson J.L., *Proc. Natl. Acad. Sci. U.S.A.*, **94**, 14138—14143 (1997).
24) Katzenellenbogen B. S., Montano M. M., Le Goff P., Schodin D. T., Kraus W. L., Bhardwaj B., Fujimoto N., *J. Steroid Biochem. Molec. Biol.*, **53**, 387—393 (1995).
25) Messina M., Barnes S., Setchell K. D., *Lancet*, **350**, 971—972 (1997).
26) Enzell C. R., Thomas B. R., Wahlberg I., *Tetrahedron Lett.*, **1967**, 2211—2217.
27) *a*) Keydar I., Chen L., Karby S., Weiss F. R., Delarea J., Radu M., Chaitcik S., Brenner H., *Eur. J. Cancer*, **15**, 659—670 (1979); *b*) Reddel R. R., Sutherland R. L., *Eur. J. Cancer Clin. Oncol.*, **20**, 1419—1424 (1984).
28) Carmichael J., DeGraph W. G., Gazdar A. F., Minna J. D., Mitchell J. B., *Cancer Res.*, **47**, 936—942 (1987).

Quantification of the Surface Morphologies of Lactose Carriers and Their Effect on the *in Vitro* Deposition of Salbutamol Sulphate

Paul Wan Sia HENG,* Lai Wah CHAN, and Liang Theng LIM

Department of Pharmacy, National University of Singapore, 10 Kent Ridge Crescent, Singapore 119260.
Received October 4, 1999; accepted November 26, 1999

Application of the scanning probe microscopy technique for quantitative measurement of the surface roughness of lactose carriers was evaluated. The roughness values of four different lactose carriers were related to the *in vitro* deposition results of the drug, salbutamol sulphate. The rugosity values of the lactose carriers were represented by *Ra* values which were in the order of DCL-40>DCL-11>lactose 325M>lactose 200 M. *In vitro* deposition results using a twin impinger showed that rougher carrier surfaces generally allowed more drug particles to be emitted from the capsules and inhaler but the availability of the drug to stage 2 was reduced, as detachment of drug particles from the carrier surfaces was more hindered. There was an optimum *Ra* value for greater delivery of the drug particles to stage 2 of the twin impinger. A balance between adherence and detachment of the drug from the carrier surface was needed in order to optimize the delivery of a drug to the desired target sites using a dry powder inhaler.

Key words surface roughness; lactose carrier; salbutamol sulphate; scanning probe microscopy; twin impinger

Dry powder inhalers are generally formulated by mixing cohesive, micronized drug with larger carrier particles. This is done to improve the dispersion and flow of the drug particles. In such a formulation, the size, shape and surface properties of the carrier and the drug-carrier ratio may affect the respiratory deposition pattern of the inhaled drug-carrier mixture.[1] In more recent years, *in vitro* studies have shown that the addition of ternary components, such as fine lactose particles[2] or magnesium stearate[3] enhanced the detachment of drug from the carrier lactose particles.

The detachment of the drug from the carrier surface is dependent on the adhesive forces between the drug and carrier particles, which are in turn determined by the surface properties of the carrier. This is because adhesion of particles is a surface phenomenon and therefore, the surface morphology of carrier particles will have a significant effect on the adhesion of drug particles to them.[3] The coarser the particles, the higher the proportion of drug adhering to them. The coarser carrier particles apparently have a greater number of active sites which are capable of binding the adherent drug particles more strongly.[4]

There is limited information on the quantification of surface roughness of particles as this is difficult to achieve, especially when the size of the particle approaches micrometer dimensions.[5] Researchers have attempted to characterize the surface roughness of carrier lactose particles and other materials by various means. Iida *et al.*[6] examined the surfaces of glass substrates using the scanning tunneling microscope. Podczeck[7] attempted to assess the surface roughness of lactose particles using a laser profilometer over a 20 μm by 20 μm scan area. The rugosities (surface roughness) of regular, spray-dried and recrystallized lactose were studied by Kassem and Ganderton.[8] The rugosity was assessed by the ratio of the surface area derived from air permeability over that obtained when the particles were considered as spheres. Ganderton[9] reported that decreased rugosity increased the respiratory fraction of salbutamol sulphate. Kawashima *et al.*[10] determined the specific surface area of various lactose grades by air permeametry and Brunauer, Emmett and Teller (BET) adsorption methods.

The scanning probe microscope can be used for evaluating the physical surface features of particles. Unlike the scanning tunneling microscope which is more suitable for conducting materials,[11] the scanning probe microscope can be used for a greater variety of substances since it can be used for both conducting and insulating materials.[12] The scanning probe microscope quantifies directly the surface textures of the particles by the surface parameters, *Ra* (arithmetic mean roughness), *Ry* (maximum height) and *Rz* (10-point mean roughness). For other methods like air permeametry and BET adsorption techniques, the surface characteristics are determined indirectly from surface area measurements. Therefore, the scanning probe microscope was chosen in this study due to the minimal sample preparation required, its suitability in scanning the type of material used in this study and its ability to provide direct quantitative roughness values. The aim of this study was to develop a method to quantify the surface roughness of lactose carrier particles using the scanning probe microscope and to relate this physical parameter to the inhalant performance of salbutamol sulphate and lactose mixtures in the twin impinger. Salbutamol sulphate was selected because it is a commonly used drug in asthma therapy and could be used as a good representative drug for determining the *in vitro* performance of dry powder inhalers.

Experimental

Materials Salbutamol sulphate was obtained from Fine Drugs and Chemicals (India). The geometric mean diameter for the supplied drug was 10.91 μm while that after milling was 2.55 μm. Lactose 325M (Pharmatose® 325M), lactose 200M (Pharmatose® 200M), DCL-11 (spray-dried hydrous lactose) and DCL-40 (mixture of 95% anhydrous lactose and 5% lactitol) were supplied by DMV (The Netherlands). All the lactose and salbutamol sulphate samples were stored in airtight containers at 20 °C.

Preparation of Lactose Carrier and Salbutamol Sulphate Lactose 325M was used as supplied. Lactose 200M, DCL-11, and DCL-40 were sieved to obtain the same mean diameter as lactose 325M (about 40—60 μm). This was carried out using the Micron Air Jet Sieve® (Hosokawa Micron, United States) with sieves of aperture sizes 38 and 63 μm. The sieving time for each sieve was 120 s and the vacuum pressure was 30—35 cm water.

Micronized salbutamol sulphate was prepared by subjecting the supplied drug to a jet mill (Hosokawa, AFG100, Japan) operated at a pressure of 0.4 MPa and a classifying speed of 15000 rpm.

* To whom correspondence should be addressed.

© 2000 Pharmaceutical Society of Japan

Scanning Electron Microscopy The size of the particles used was determined using a scanning electron microscope (JEOL, JSM-5200, Japan). The particles were gold-coated under an argon atmosphere (Bio-Rad, SC502, United Kingdom) and examined under the scanning electron microscope. From the photomicrographs, the diameters of at least four hundred particles were measured using a pair of digital vernier callipers (Mitutoyo, CD-6″BS, Japan) and the actual size calculated by multiplying with the respective magnification factors. For each particle, two diameters, at right angles to each other were measured and the average diameter calculated. The surface morphologies of the lactose particles were assessed qualitatively from the photomicrographs taken.

Scanning Probe Microscopy The lactose carrier particles were first sprinkled on a clean glass slide and the sample holder with double-sided adhesive tape (Scotch® 3M, United States) attached was pressed lightly on the particles to adhere the particles to the tape. The sample holder was inverted and knocked along its side several times to remove any loose particles. It was then placed under the microscope for scanning by the cantilever, using both the contact and dynamic modes.

The lactose particles were scanned over an area of 64 μm by 64 μm to observe the whole lactose particle before zooming down to an area of 8 μm by 8 μm. Other scan areas, for example, 5 μm by 5 μm and 10 μm by 10 μm were also attempted. The depth of scan, Z range, was also varied to obtain the best representative image. Scans of the same image were performed at various frequencies of 1, 2, 3, 5 and 8 Hz. Sample size of ten, fifteen and thirty lactose particles were scanned consecutively. This was repeated and the mean roughness values (*Ra*) obtained for each sample size were compared.

Compression of Lactose 325M Lactose 325M was manually compressed lightly into compacts of about 0.26 g using a single-punch tabletting machine (Manesty, E2, England) with 9 mm flat-faced punches. The surface of the compact was scanned and the roughness values of the constituent lactose particles were determined.

Preparation of Powder Blend Mixtures consisting of about 2% w/w salbutamol sulphate were prepared by weighing 0.10 g drug and 4.90 g lactose into a cylindrical glass container (diameter 4.8 cm, height 4.6 cm) and premixed in a vortex mixer (Ika, VX9/VXR, Germany) for 5 min. The mixture was then passed through a sieve of aperture size 125 μm to break up any large agglomerates. It was returned to the container and mixing continued for another 15 min. Twenty milligrams of each type of lactose-salbutamol sulphate mixture was weighed into three sets of ten gelatin capsules each (size no. 3) and stored in glass bottles in a desiccator at 20 °C.

***In vitro* Deposition of Salbutamol Sulphate** The dispersing behaviour of the different types of lactose-salbutamol sulphate mixtures was assessed in a Rotahaler® (Glaxo, United Kingdom) coupled to a twin impinger (Apparatus A, British Pharmacopoeia 1993, Erweka, Germany). Stages 1 and 2 contained 7 and 30 ml of filtered deionized water respectively to collect the drug deposited in these two stages. After the Rotahaler® was connected to the mouthpiece of the twin impinger, a capsule was placed in the holder of the Rotahaler®, which was twisted to break the capsule. An air stream of 60 l/min was produced throughout the system by attaching the outlet of the twin impinger to a vacuum pump. For each capsule, an actuation time of 30 s was given to allow enough time for complete emptying of the capsule. This test was repeated for 10 capsules. On completion, the drug deposited in the inhaler, mouthpiece, stages 1 and 2 was collected by rinsing with filtered deionized water and made up to 50 ml each in volumetric flasks using the same solvent. The drug content was determined by HPLC using a mobile phase consisting of methanol and acetate buffer pH 5 in the ratio of 55 : 45, a 3.3 cm C18 column (Perkin Elmer, HS-3, United States) and a UV detector (Waters, Lambda-Max 481, United States) at 276 nm. For each type of lactose-drug mixture, three determinations were carried out and the average results calculated. All determinations were carried out under a controlled temperature of 20 °C and humidity of 45% relative humidity.

In this study, the respirable fraction (RF) referred to the fraction (%) of drug deposited in stage 2 of the twin impinger, with regard to the loaded amount of drug. The effective index (EI) proposed by Hino *et al.*[13] to evaluate inhalation behaviour was expressed as :

$$EI=\sqrt{(100-DF)\times RF}$$
$$=\sqrt{Em\times RF} \quad (1)$$

where DF is the fraction (%) of drug remaining in the inhaler and capsules and Em is the fraction (%) of drug emitted from the inhaler and capsules.

Respirable particle percent of emitted particles (RP) was used to express the percentage of drug deposited in stage 2 with regard to the emitted amount.

$$RP=\left(\frac{RF}{Em}\right)\times 100 \quad (2)$$

Results and Discussion

Size Distribution and Surface Morphologies of Lactose Carriers All four lactose batches were prepared by jet-sieving to obtain lactose particles of similar size. Hence, the effects of differences in the size of carrier on the inhalation property, as reported by Steckel and Müller,[14] were likely to be limited in this study.

Under the scanning electron microscope, both lactose 325M and 200M particles appeared to show similar surface textures. On closer examination, very small particles were found to adhere to the surfaces of the larger carrier particles (Fig. 1(a), (b)). The presence of such smaller particles may enhance the detachment of drug particles from the carrier particles.[2] Both DCL-11 and DCL-40 appeared to be rougher (Fig. 1(c), (d)). There were large crevices interspersing with smooth areas for DCL-11 while the whole surface of DCL-40 particles appeared rough with small crevices, suggesting that the DCL-40 particles resembled aggregates of very small agglomerated sub-units. Since the surfaces of DCL-11 and DCL-40 appeared to be quite rough, small drug particles in the formulation of dry powder for inhalation can be embedded into the crevices on the surfaces of these carrier particles, such that their detachment from the carrier particles upon inspiration and subsequent delivery of the drug to the lower reaches of the lungs would be reduced.

Evaluation of the Scanning Probe Microscope Technique to Quantify Surface Morphologies Substrates for Mounting of Lactose Particles on Metal Sample Holder: Different substrates (Table 1) for the mounting of lactose particles for examination using the scanning probe microscope were assessed. All the surfaces appeared similar to that of the lactose particles and could not be easily distinguishable from the lactose surfaces. Only one substrate, Scotch® 3M single-sided adhesive tape showed a different surface texture from the lactose particles when scanned. The adhesive tape surface consisted of very even and regular lines that could be differentiated from images of the surfaces of lactose particles. Therefore, the Scotch® 3M single-sided tape was chosen as the substrate for mounting of the lactose particles on the metal sample holder for scanning probe microscopy.

Mode of Scan: The scanning probe microscope has two operational modes, contact and dynamic modes. In the contact mode, repulsion between the cantilever tip and sample is detected with an optical lever detection method. When this mode of scanning was attemped in this study, the contact made by the cantilever tip with the edges of the particles during the scan made it difficult to scan images without breaking the cantilevers. In the dynamic mode, there is no contact between the cantilever tip and the particle surface. Instead, the cantilever tip vibrates near the resonance frequency of the cantilever. When the vibrating cantilever approaches the sample surface, the resonance frequency of the cantilever shifts due to the force between the cantilever and sample. This shift in the resonance frequency is then detected from a change in the amplitude of the cantilever tip, thus converting to changes in displacement. Both modes were able to pro-

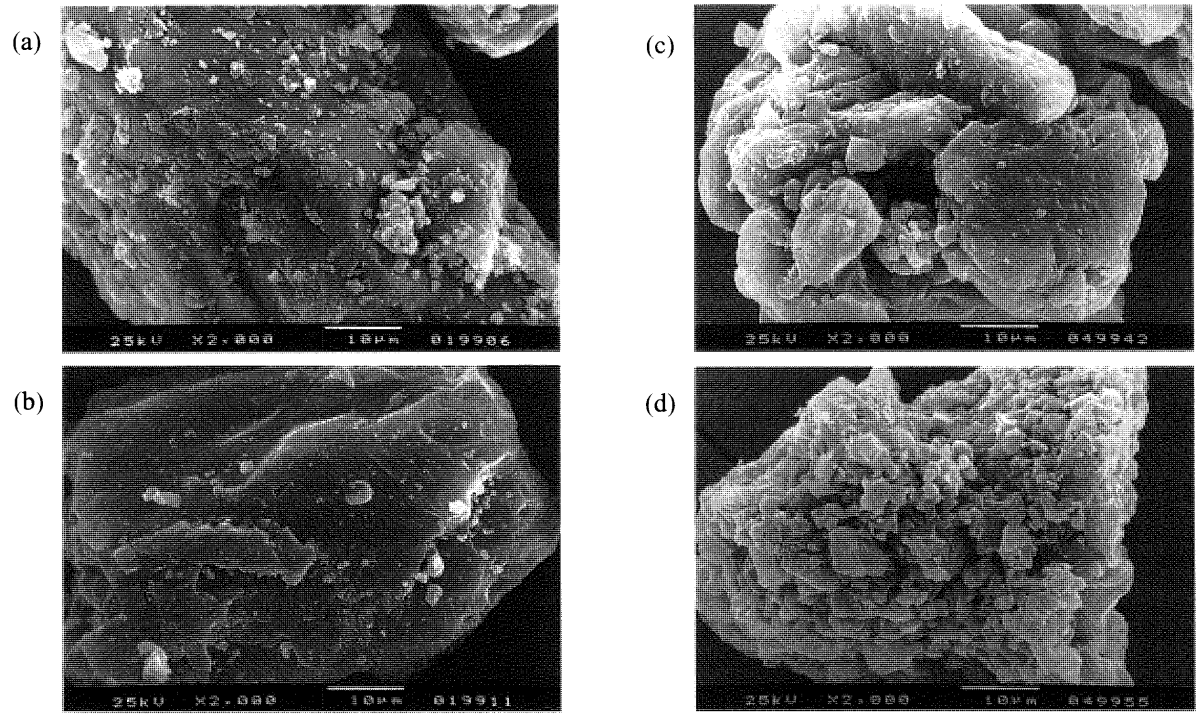

Fig. 1. Scanning Electron Micrographs of (a) Lactose 325M, (b) Lactose 200M (38—63 μm), (c) DCL-11 (38—63 μm) and (d) DCL-40 (38—63 μm)

Table 1. Substrates for Mounting Lactose Particles on Metal Sample Holder

Substrates	Observations
Adhesive glue on metal sample holder Adhesive glue on plastic materials Adhesive glue on paper materials Adhesive glue on glass coverslip Scotch® 3M double-sided stick tape on metal sample holder Itotape® double-sided stick tape on metal sample holder	Surface with irregularities that were similar to lactose surface
Scotch® 3M single-sided stick tape attached to metal sample holder by Scotch® 3M double-sided stick tape	Surface with very regular and even lines

Table 2. Roughness Values of Lactose 325M and Lactose 200M (38—63 μm) at Z Ranges of 2 and 5 μm (n=30)

	Lactose 325M		Lactose 200M (38—63 μm)	
	Z=2 μm	Z=5 μm	Z=2 μm	Z=5 μm
Ra (nm)	199.182	197.473	155.733	158.703
Ry (μm)	1.594	1.582	1.218	1.389
Rz (μm)	1.112	1.006	0.711	0.868

duce reasonably good images. However, the dynamic mode was chosen as the likelihood of damage to the cantilever was lower. In addition, it was felt that using the dynamic mode, the cantilever tip exerts less effect on the sample surface and may provide a higher sensitivity.

Depth of Scan: The depth of scanning, as measured by the Z range, is important for ensuring that the scan can cover a large surface with indentations or undulations that determines the depth of the particle. A Z range with insufficient depth will result in some parts of the images being cut off and thereby causing inaccuracies in the roughness measurements. When the Z range is set too high, there will be a compromise in the clarity and sharpness of the image produced. For this study, thirty images of 8 μm by 8 μm were captured with Z ranges set at 2 and 5 μm. The roughness values obtained for lactose 325M were compared and found to be similar (Table 2). The Ra values for lactose 200M at a Z range of 2 and 5 μm were similar, while the Ry and Rz values differed by 14.0% and 22.1%, respectively. A Z range of 5 μm was chosen in subsequent studies as any unusually large protrusions on the lactose surface could be captured without loss of the image due to insufficient Z range. The Ra value was also chosen to represent surface roughness in the subsequent discussion because it was a calculated average reading based on a reference length across the surface scanned. On the other hand, Ry was a value obtained from the distance between the crest line and trough line and Rz was the average of ten points along the reference length. Ry and Rz would be less representative of the whole surface roughness compared to Ra as they were calculated based on selected points only.

Size of Scan: Although the size of the lactose particles is 40—60 μm, it is not easy for the cantilever to land on a flat surface with sufficient length and width for scanning due to the random orientation of the particles on the adhesive tape. Various scan sizes of 5 μm by 5 μm, 8 μm by 8 μm and 10 μm by 10 μm were attempted. It was generally difficult to locate a particle with the correct orientation to present a surface suitable for a scan size of 10 μm by 10 μm. A scan size of 8 μm by 8 μm was chosen as 5 μm by 5 μm appeared to be too small to adequately represent the whole surface of the lactose particle.

Frequency of Scan: The rate of scan is important as a faster scan rate with an acceptable resolution would be more

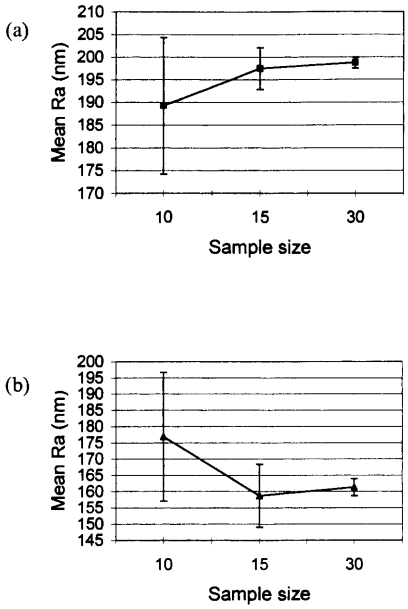

Fig. 2. Effect of Sample Size on the Range of Mean *Ra* values for (a) Lactose 325M and (b) Lactose 200M (38—63 μm)

efficient. Scans at frequencies of 1, 2, 3, 5 and 8 Hz were made. The times needed to scan an image of 8 μm by 8 μm were 256, 128, 86, 52 and 33 s at 1, 2, 3, 5, and 8 Hz respectively. It was found that as the frequency increased, the images were less well resolved and some small features on the surfaces were not captured. Based on the clarity of the image obtained, a slow scan frequency of 1 Hz was chosen as the sharpest image was desired.

Determination of Sample Size: Figures 2(a) and 2(b) show the mean *Ra* values for lactose 325M and lactose 200M respectively with sample sizes of ten, fifteen and thirty particles. Two sets of data were obtained for each sample size and the mean *Ra* values and their range were compared. Since the range for the sample size of 30 was very small, this sample size was used for subsequent roughness determinations.

Comparison of the Surface Characteristics of Lactose 325M, Lactose 200M, DCL-11 and DCL-40 The roughness values obtained for both lactose 325M and 200M showed that the 325M lactose particles had rougher surfaces than 200M lactose particles since the *Ra*, *Ry* and *Rz* values were all higher (Table 3). Roughness values for DCL-11 and DCL-40 were much higher than those for lactose 200M and 325M. From this finding, it could be inferred that the interactive force between the drug and DCL-11 or DCL-40 would be higher than that of lactose 325M and 200M.

Comparison of Surface of Compact with that of Lactose 325M Particles The use of lactose particles mounted on adhesive tape for scanning probe microscopy can pose various problems. Care must be taken to dust just sufficient particles for measurement and to distinguish lactose particles from the tape material. In addition, the particles may shift during measurements, resulting in an unsuccessful scan. The possibility of preparing lactose particles as lightly compacted particles for surface measurements appeared to be an attractive alternative.

The *Ra* value obtained from scanning the surface of compact prepared using lactose 325M was about half of the uncompacted lactose particles (Table 3). This could be due to fragmentation of the protrusions on the particles and surface remoulding under the forces of compaction, thus resulting in smoother surfaces. In one literature study, it was reported that fragmentation of crystalline lactose occurred during compaction even when the mean particle size was small, around 32—45 μm.[15] In another study, it was suggested that surface deformability of the particles occurred due to fragmentation during compaction.[16] Thus, surface roughness values of compacted lactose particles obtained by scanning compacts might not be representative of the actual particle surface.

Table 3. Roughness Values of Lactose 325M, Lactose 200M (38—63 μm), DCL-11 (38—63 μm), DCL-40 (38—63 μm) and Compacted Lactose 325M (n=30)

	Lactose 325M	Compacted lactose 325M	Lactose 200M (38—63 μm)	DCL-11 (38—63 μm)	DCL-40 (38—63 μm)
Ra (nm)	197.473	111.733	158.703	290.907	346.623
Ry (μm)	1.582	1.108	1.389	2.164	2.564
Rz (μm)	1.006	0.642	0.868	1.437	1.732

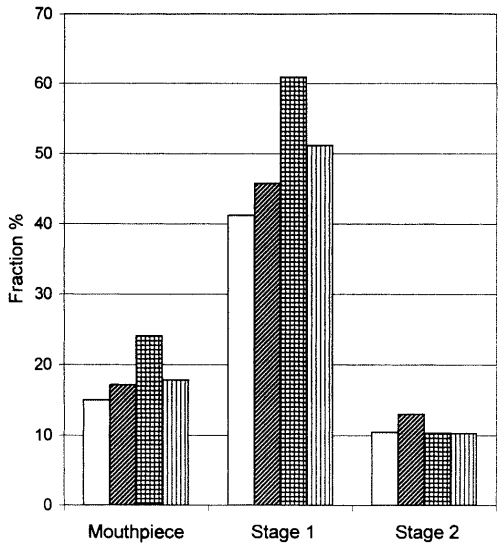

Fig. 3. *In vitro* Deposition of Salbutamol Sulphate in the Twin Impinger with Different Types of Lactose

□, Lactose 200M; ▨, lactose 325M; ▦, DCL-11; ▥, DCL-40.

***In vitro* Deposition of Salbutamol Sulphate** The deposition patterns of salbutamol sulphate by the various types of lactose are shown in Fig. 3 while the calculated inhalation indices are presented in Table 4.

There was a significant difference in the emission of drug particles (% Em) between DCL-11 and the other three lactose carriers (p=0.004, one-way ANOVA at 95% confidence level). DCL-11 was more effective in emitting the drug from the inhaler and capsules, resulting in a large amount of drug deposited in the mouthpiece and stage 1 of the twin impinger (Fig. 3). The % Em for DCL-40 was also significantly higher than that for lactose 200M. This could be due to a higher accommodation of the drug particles in the crevices found on the surfaces of both DCL-11 and DCL-40. However, the fraction (% RF) of drug found in stage 2 of the twin impinger was significantly higher for lactose 325M compared to the

Table 4. *In vitro* Deposition Results for Salbutamol Sulphate with Different Types of Lactose (Represented by Mean±S.D., $n=3$)

	Em (%)	RF (%)	EI (%)	RP
Lactose 200M (38—63 μm)	66.62±6.14	10.43±0.61	26.36±1.92	15.70±0.83
Lactose 325M	75.98±5.91	13.01±1.44[a)]	31.44±2.94	17.10±0.62
DCL-11 (38—63 μm)	95.36±4.13[b)]	10.31±1.06	31.34±2.05	10.81±0.95[c)]
DCL-40 (38—63 μm)	79.29±9.13[d)]	10.25±0.13	28.47±1.57	13.06±1.71[e)]

a) $p<0.05$, significant difference compared to lactose 200M, DCL-11 and DCL-40. *b*) $p<0.05$, significant difference compared to lactose 200M, lactose 325M and DCL-40. *c*) $p<0.05$, significant difference compared to lactose 200M, lactose 325M and DCL-40. *d*) $p<0.05$, significant difference compared to lactose 200M and DCL-11. e) $p<0.05$, significant difference compared to lactose 200M, lactose 325M and DCL-11.

other three lactose carriers ($p=0.019$, one-way ANOVA at 95% confidence level). This was seen even though the amount of drug emitted by lactose 325M was not as high as that compared to DCL-11. This finding indicated that the roughness of the carrier surface can affect drug particle detachment. Although the presence of crevices like those found in DCL-11 and DCL-40 (Fig. 1(c), (d)) allowed more drug particles to be attached and delivered to stage 1 of the twin impinger, they also cause drug particle entrapment. Thus, as the separation of the drug from the carrier in the air stream was more hindered, a relatively smaller amount of drug was deposited in stage 2. There was no significant difference at the 95% confidence level between the EI value of DCL-11 and lactose 325M as the high Em compromised for the drop in RF for DCL-11 (Table 4).

The process of inhalation of a drug-carrier mixture involves the emission of drug on a carrier from the inhaler, the separation of drug from the carrier, the dispersion of the separated drug in the air-stream and the delivery of the dispersed drug to the targeted site of the lung. An effective formulation should consist of a drug and a carrier of a suitable surface morphology such that the adhesion force between the carrier and the drug is strong enough for drug particles on the carrier particles to be emitted from the inhaler, but yet not too strong so that a large proportion of the emitted drug could be detached from the carrier and be deposited in stage 2 of the twin impinger. For *in vitro* studies, a high EI alone may not necessarily represent an effective dry powder formulation. This is because a high EI may be a result of an exceptionally large Em which compromises the low RF. EI is affected by Em and RF. In a reported study,[10] the EI for a formulation without a carrier was significantly lower than that of a formulation with lactose 325M. This was due to the relatively lower Em of the formulation without a carrier. However, the EI of the formulation without a carrier was similar to that of a formulation with fluidized bed granulated lactose. This was because of the relatively higher RF value of the formulation without a carrier. Therefore, in assessing the performance of a dry powder formulation using EI, the RP of a formulation should also be taken into account. A low RP would indicate poor performance in spite of a high EI. In this study, although the EI of DCL-11-drug mixture is equivalent to the EI of lactose 325M-drug mixture, the latter is a more effective formulation because of the much higher RP. The EI of DCL-11 is higher than that of DCL-40 due to the higher Em

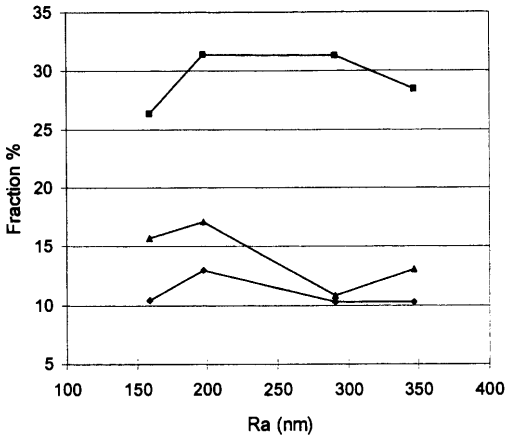

Fig. 4. EI, RP and RF Values of Salbutamol Sulphate with Lactose of Different Roughness Values (*R*a)
■, EI; ▲, RP; ◆, RF.

for DCL-11, suggesting greater drug emission ability of DCL-11. As a result of the higher Em but similar RF for DCL-11 compared to DCL-40, the RP of DCL-11 is lower. This indirectly indicates that the drug releasing property of DCL-11 is lower than that of DCL-40.

When the surface roughness (*R*a) of lactose particles was compared with the RF and RP of the drug-lactose mixture, there was an optimal *R*a value when a RP of 17.10% and a RF of 13.01% drug was delivered to stage 2 (Fig. 4). This could be related to the adhesion force between the drug and carrier as the higher the adhesion force, the less likely for the particle to detach from the lactose surface. From previous work,[10] the rank order of adhesion and interactive force of the lactose with drug particles is shown in Fig. 5 where performance models (i)>(ii)>(iii). The interactive force for (ii) is greater than (iii) because of the larger surface in contact with lactose resulting in higher van der Waals attractive forces. The surface roughness (*R*a) of lactose 200M was smaller than that of lactose 325M, thus resembling (ii) while lactose 325M resembled (iii). Therefore, the interactive force between the drug and lactose 200M would be higher than that between the drug and lactose 325M and a significantly lower RF value was obtained for the lactose 200M–drug mixture when compared to the lactose 325M–drug mixture.

The surface roughness (*R*a) of DCL-11 was found to be higher than lactose 325M and 200M. Deep crevices interspersing with smooth surfaces were observed for DCL-11 and drug-DCL-11 interaction was expected to be resembling performance model (i) in Fig. 5. Drug particles adhered in the deep crevices would become entrapped and become relatively immobile in the clefts and indentations.[3] Thus, the likelihood for overall drug detachment from the lactose particle would be lower, resulting in even lower RP values as compared to the values for lactose 325M and 200M. The *R*a value for DCL-40 was higher compared to that of DCL-11, indicating that the surface of DCL-40 was rougher than that of DCL-11. This could be due to the presence of microscopic projections on the surface of the DCL-40 particle, in addition to some large crevices. A possible representation is shown in Fig. 5 (iv). Therefore, the average surface roughness of DCL-40 was higher than that of DCL-11, on which the presence of smooth areas reduced the average surface roughness of the

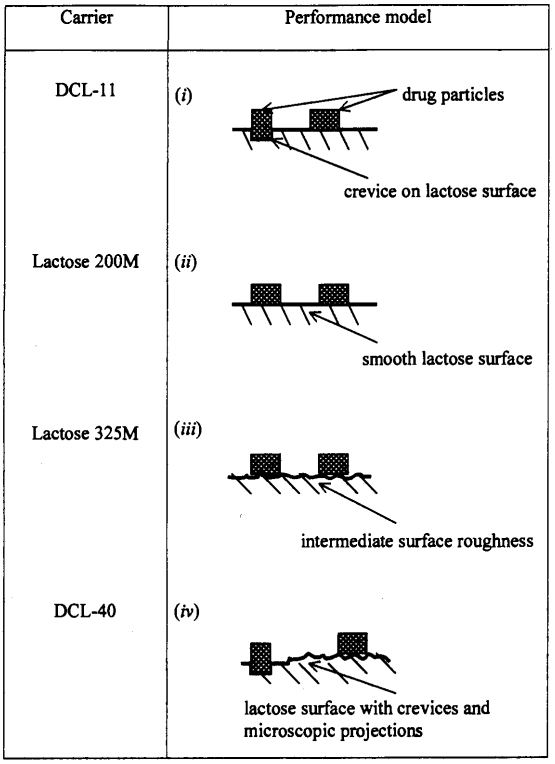

Fig. 5. Performance Model for Different Lactose Carriers

DCL-11 particle. However, although the *Ra* of DCL-40 was higher than that of DCL-11, the RP value was significantly higher than that for DCL-11 while the EI and Em values were lower. A possible reason could be that the microscopic projections reduced the contact areas between the contacting drug and lactose surfaces and increased the distances between them. Due to the smaller areas of actual contact, there may be reduced drug attachment onto DCL-40, resulting in a lower Em and EI. On the other hand, the surface of DCL-11 consists of large crevices interspersing with smooth surfaces. Compared to the microscopic projections on DCL-40, the smooth surfaces allowed a relatively greater area of contact with the drug particles, thus a greater chance of drug adhesion resulting in a higher Em and EI. In addition, for drug particles adhering onto the microscopic projections, van der Waals attractive forces were reduced, resulting in easier separation of deposited drug particles from the surfaces of DCL-40 and a higher RP. Therefore, the drug-releasing property of DCL-40 with respect to the emitted dose would be higher than that of DCL-11.

Conclusion

The scanning probe microscope enabled a quantitative measure of the surface property of the lactose carriers. The ability to measure surface roughness quantitatively provided the means to evaluate carriers for their relative drug delivery efficiencies. There is an optimum roughness (*Ra*) value for increased availability of drug to stage 2 of the twin impinger among the four lactose carriers studied. A balance between adhering to and detachment of the drug particles from the carrier surface is important for optimizing its delivery to the desired sites.

References

1) Timsina M. P., Martin G. P., Marriott C., Ganderton D., Yianneskis M., *Int. J. Pharm.*, **101**, 1—13 (1994).
2) Zeng X. M., Martin G. P., Tee S. K., Marriott C., *Int. J. Pharm.*, **176**, 99—110 (1998).
3) Ganderton D., Kassem N. M., "Advances in Pharmaceutical Sciences," ed. by Ganderton D., Jones T., Academic Press, London, 1992, pp. 165—191.
4) Staniforth J. N., Rees J. E., Lai F. K., Hersey J. A., *J. Pharm. Pharmacol.*, **34**, 141—145 (1982).
5) Schaefer D. M., Carpenter M., Gady B., Reifenberger R., Demejo L. P., Rimai D. S., *J. Adhes. Sci. Technol.*, **9**, 1049—1062 (1995).
6) Iida K., Otsuka A., Danjo K., Sunada H., *Chem. Pharm. Bull.*, **41**, 1621—1625 (1993).
7) Podczeck F., *Int. J. Pharm.*, **160**, 119—130 (1998).
8) Kassem N. M., Ganderton D., *J. Pharm. Pharmacol.*, **42** (Suppl.), 11P (1990).
9) Ganderton D., *J. Biopharm. Sci.*, **3**, 101—105 (1992).
10) Kawashima Y., Serigano T., Hino T., Yamamoto H., Takeuchi H., *Int. J. Pharm.*, **172**, 179—188 (1998).
11) Bennett J. M., Mattsson L., "Introduction to Surface Roughness and Scattering," Optical Society of America, Washington, 1989, p. 11.
12) Jahanmir J., Haggar B. G., Hayes, J. B., *Scanning Microscopy*, **6**, 625—660 (1992).
13) Hino T., Serigano T., Yamamoto H., Takeuchi H., Niwa T., Kawashima Y., *Int. J. Pharm.*, **168**, 59—68 (1998).
14) Steckel H., Müller B. W., *Int. J. Pharm.*, **154**, 31—37 (1997).
15) Riepma K. A., Veenstra J., de Boer A. H., Bolhuis G. K., Zuurman K., Lerk C. F., Vromans H., *Int. J. Pharm.*, **76**, 9—15 (1991).
16) Eriksson M., Alderborn G., *Pharmaceut. Res.*, **12**, 1031—1039 (1995).

Convenient Synthesis of 2,3,9,10-Tetraoxygenated Protoberberine Alkaloids and Their 13-Methyl Alkaloids[1,2)]

Miyoji HANAOKA,* Taeko HIRASAWA, Won Jea CHO, and Shingo YASUDA

Faculty of Pharmaceutical Sciences, Kanazawa University, Takara-machi, Kanazawa 920–0943, Japan.
Received October 12, 1999; accepted November 22, 1999

New and convenient synthesis of 2,3,9,10-tetraoxygenated protoberberine alkaloids and their 13-methyl alkaloids through the same intermediates was developed. Acylation of the brominated benzylphenethylamine (13) with α-chloro-α-(methylthio)acetyl chloride, followed by cyclization with stannic chloride, furnished the key intermediates 4-methylthio-3-phenethylisoquinolin-3-ones (14), which were methylated to provide their methyl derivatives (17). Both isoquinolin-3-ones (14 , 17) were easily transformed into protoberberine alkaloids (16) and their 13-methyl alkaloids (21) in good yield.

Key words protoberberine alkaloid; 13-methylprotoberberine; isoquinolin-3-one; α-(methylthio)acetyl chloride; Bischler–Napieralski reaction

Protoberberine alkaloids (I)[3)] are representative isoquinoline alkaloids which possess physiological activities and have been shown to play important roles as biogenetic precursors of related isoquinoline alkaloids such as benzo[*c*]phenanthridine, spirobenzylisoquinoline, phthalideisoquinoline, protopine, and rhoeadine alkaloids. Therefore, many methods have been developed so far for the synthesis of protoberberine alkaloids.[3)] Among them, a method[4)] *via* the 2-phenethylisoquinolin-3-one (II) can be expected to be promising and practical, especially from a regioselective viewpoint, however, this method has only been applied to limited examples[5)] and lacks generality because the starting materials for II are not easily accessible.

We proposed that the key isoquinolin-3-one (II) might be simply obtained from secondary benzylphenethylamine (V), which could be smoothly derived from commercially or readily available benzaldehyde (VI) and phenethylamine (VII), through acylation and cyclization. Acylation with α-(methylthio)acetyl chloride or its derivative, developed by Tamura *et al.*,[6)] would be the best choice for our purpose, and subsequent cyclization of the intermediate amide (IV) would furnish the six-membered lactam (III) in preference to the seven-membered one.[7)] Desulfurization of III could give rise to II, which has been shown to be converted to protoberberine alkaloids (I) by a standard procedure.

Synthesis of 2,3,9,10-Tetraoxygenated Protoberberine Alkaloids According to our retrosynthesis, we first tried to establish a general synthesis of the abundant but synthetically rather difficult 2,3,9,10-tetraoxygenated protoberberine alkaloids.

Condensation of 3,4-dimethoxyphenethylamine (**1a**) with 2,3-dimethoxybenzaldehyde (**2**), followed by reduction with lithium aluminum hydride (LAH) afforded the secondary amine (**3a**) in 79% yield. Acylation of **3a** with α-(methylthio)acetyl chloride (**4**)[6)] in the presence of triethylamine in dichloromethane at 0 °C gave the amide (**5**, 73%), which was oxidized with *m*-chloroperbenzoic acid (*m*-CPBA) to furnish the sulfoxide (**6**, 74%). Exposure of **6** to *p*-toluenesulfonic acid (*p*-TsOH) in refluxing carbon tetrachloride[6)] effected a Pummerer-type reaction resulting in the desired isoquinolin-3-one (**7a**) and the seven-membered lactam benzazepinone (**8a**) in 24 and 34% yields, respectively. Acidic treatment of **6** with methanesulfonic acid or trifluoroacetic acid instead of *p*-TsOH gave similar results (**7a**: 25 or 17% yield; **8a**: 41 or 47% yield, respectively). Contrary to our expectation, selective formation of the six-membered lactam (**7a**) could not be achieved.[7)]

On the other hand, **3a** was acylated with α-chloro-α-(methylthio)acetyl chloride (**9**)[6)] in the presence of triethylamine and then cyclized with stannic chloride in

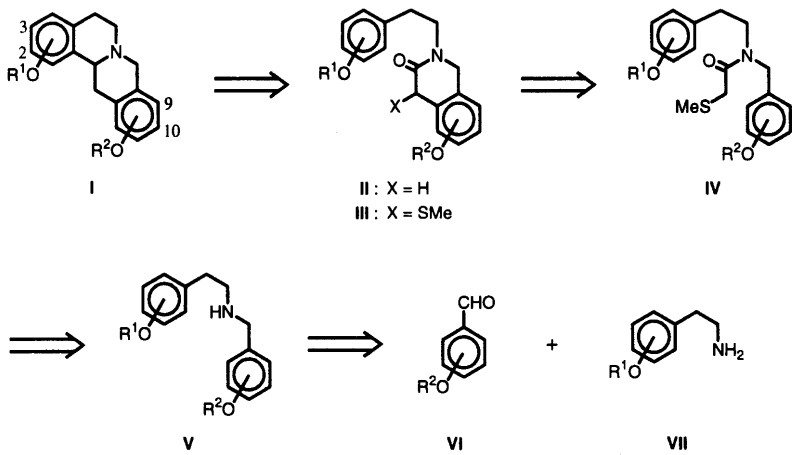

Chart 1

* To whom correspondence should be addressed.

© 2000 Pharmaceutical Society of Japan

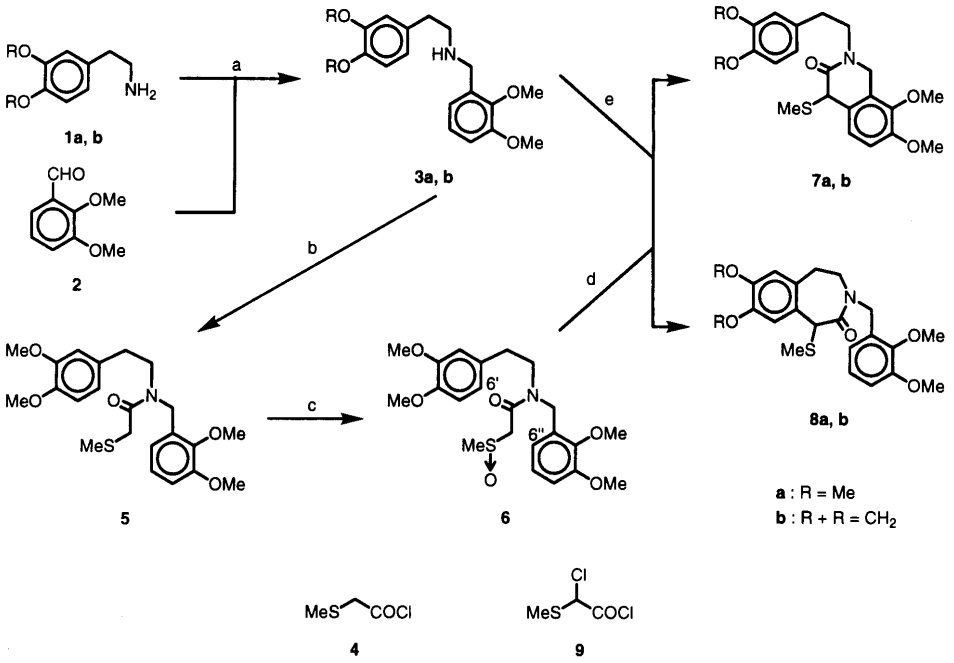

a) 1) CH_2Cl_2, r.t.; 2) LAH, THF, r.t.; b) **4**, Et_3N, CH_2Cl_2, 0 °C; c) *m*CPBA, CH_2Cl_2, 0 °C; d) *p*-TsOH, CCl_4, reflux; e) 1) **9**, Et_3N, CH_2Cl_2, 0 °C; 2) $SnCl_4$, 0 °C.

Chart 2

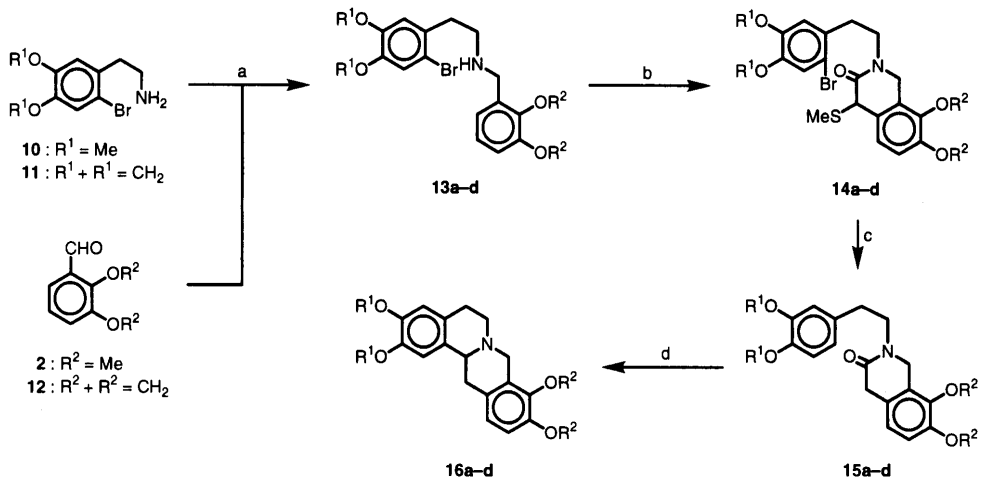

a : $R^1 = R^2$ = Me, **b** : R^1 = Me, $R^2 + R^2 = CH_2$, **c** : $R^1 + R^1 = CH_2$, R^2 = Me, **d** : $R^1 + R^1 = R^2 + R^2 = CH_2$

a) 1) CH_2Cl_2, r.t.; 2) LAH, THF, r.t.; b) 1) **9**, Et_3N, CH_2Cl_2, 0 °C; 2) $SnCl_4$, 0 °C; c) Raney Ni, EtOH, reflux; d) 1) $POCl_3$, K_2CO_3, CH_3CN, 60 °C; 2) $NaBH_4$, MeOH, reflux.

Chart 3

dichloromethane at 0 °C to provide **7a** and **8a** in 29 and 43% yields, respectively. The procedure with **9** was found to be superior to that with **4** in manipulation. Cyclization with $SnCl_4$ under various conditions (temperature: −30—0 °C, solvent: chloroform or benzene) or that with $TiCl_4$ (0 °C, dichloromethane) was not able to affect the product ratio. Changing the oxygenated substituents on the phenethyl part from the dimethoxy to methylenedioxy group again did not alter the cyclization selectivity. Namely, the secondary amine (**3b**, 62%), derived from 3,4-methylenedioxyphenethylamine (**1b**), was acylated with **9** and then cyclized with $SnCl_4$ to afford the isoquinolin-3-one (**7b**) and the benzazepinone (**8b**) in 30 and 41% yields, respectively. Preferential cyclization to the seven-membered lactam in the above electrophilic cyclization reactions would be due to higher electron density at C-6′ on the aromatic ring of phenethyl part in comparison with that at C-6″ on the aromatic ring of benzyl part.[8]

In order to prevent the formation of the seven-membered lactam, benzazepinone, a bromine atom was introduced to the phenethyl part of **3** as a blocking group. Acylation of the brominated amine (**13a**, 85%), prepared from brominated phenethylamine (**10**)[9] and **2**, with acyl chloride (**9**), followed by treatment with $SnCl_4$ afforded the isoquinolin-3-one (**14a**) in 78% yield as a sole product, as expected. Concurrent reductive removal of both the bromine atom and the methylthio group was realized by the exposure of **14a** to Raney Ni in refluxing ethanol, providing the desired isoquinolin-3-one (**15a**, 88%), which was also obtained from **7a** by a similar

procedure in 90% yield. The Bischler–Napieralski reaction of **15a** in acetonitrile with phosphorus oxychloride in the presence of potassium carbonate[10] and subsequent reduction with sodium borohydride provided (±)-tetrahydropalmatine (**16a**), mp 150—152 °C, in 76% yield. Similarly, (±)-sinactine (**16b**), mp 169—171 °C, (±)-canadine (**16c**), mp 172—174 °C, and (±)-stylopine (**16d**), mp 198—200 °C, were synthesized starting from the corresponding phenethylamine (**10** or **11**) and the benzaldehyde (**2** or **12**) *via* the secondary amine (**13**) and the isoquinolin-3-ones (**14** and **15**). The results are summarized in Table 1. The synthetic alkaloids obtained above were proven to be identical with the corresponding authentic samples (see Experimental). Thus, we have developed a convenient, general, and practical synthetic method for 2,3,9,10-tetraoxygenated protoberberine alkaloids.

Synthesis of 13-Methyl-2,3,9,10-tetraoxygenated Protoberberine Alkaloids 13-Methylprotoberberine alkaloids[3] are a small group of protoberberine alkaloids having an extra methyl group at the C-13 position. They have been shown to be biogenetic precursors for 10-methyl-B/C-hexahydrobenzo[*c*]phenanethridine alkaloids.[3] Several synthetic methods for 13-methylprotoberberine alkaloids have been reported so far,[3,11,12] however, they are not necessarily satisfactory in generality. In the previous section, we developed a convenient synthesis of protoberberine alkaloids *via* 4-methylthio-2-phenethylisoquinolin-3-ones (**14**). The latter compounds also seem to be suitable intermediates for the synthesis of 13-methylprotoberberines because the C-4 position of **14** must be doubly activated by the carbonyl and methylthio group to be readily methylated. Our previous synthesis, therefore, should also open a new route to 13-methylprotoberberine alkaloids.

Table 1. Yield in the Synthesis of Protoberberine Alkaloids

Alkaloid	R^1, R^2	Yield (%)			
		16	**15**	**14**	**13**
(±)-Tetrahydropalmatine (**16a**)	$R^1=R^2=Me$	76	88	78	85
(±)-Sinactine (**16b**)	$R^1=Me$, $R^2+R^2=CH_2$	78	80	79	84
(±)-Canadine (**16c**)	$R^1+R^1=CH_2$, $R^2=Me$	68	77	72	88
(±)-Stylopine (**16d**)	$R^1+R^1=R^2+R^2=CH_2$	63	78	88	69

The 4-(methylthio)isoquinolin-3-one (**14a**) was exposed to lithium diisopropylamide at −78 °C and then to methyl iodide, affording the 4-methyl derivative (**17a**) in 80% yield. According to the conversion of **14** to **15**, treatment of **17a** with Raney Ni in refluxing ethanol effected the reductive removal of both the bromine and methylthio group to furnish the 4-methylisoquinolin-3-one (**19a**) in 88% yield. The Bischler–Napieralski reaction[10] of **19a** and subsequent $NaBH_4$ reduction provided (±)-corydaline (**21a**), mp 136—136.5 °C, in 61% yield. Similarly, 4-(methylthio)isoquinolin-3-one (**14b** or **14c**) was transformed into (±)-thalictricavine (**21b**), mp 208—209 °C, or (±)-tetrahydrocorysamine (**21c**), mp 203—204 °C, *via* **17b** or **17c**, and **19b** or **19c**, respectively, as summarized in Table 2. The synthetic alkaloids were proven to be identical with the corresponding authentic samples (see Experimental). Alkylation other than methylation was also possible. Ethylation of **14a** with ethyl iodide afforded the ethyl derivative (**18a**) in 74% yield. Sequential treatment of **18a** with Raney Ni in ethanol, $POCl_3$, and $NaBH_4$ provided (±)-13-ethyltetrahydropalmatine (**22a**, 63%) *via* **20a** (83%).

In conclusion, we developed a practical method for the

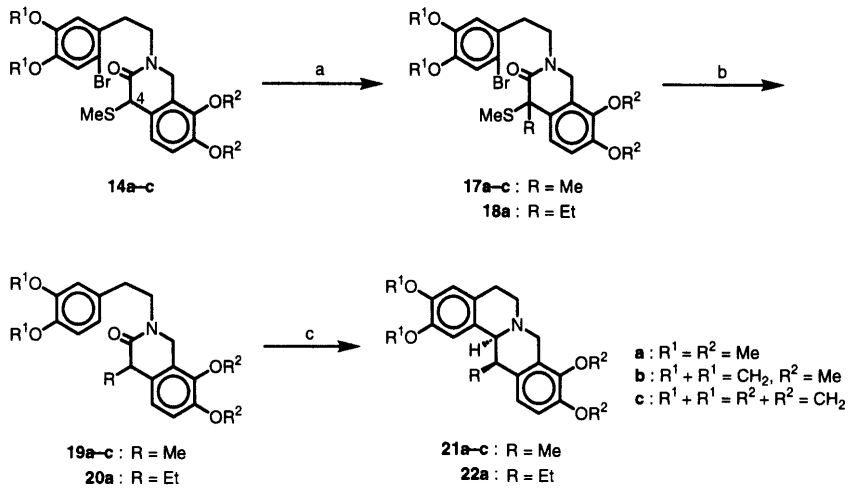

a) 1) LDA, THF, −78 °C; 2) MeI or EtI, r.t.; b) Raney Ni, EtOH, reflux; c) 1) $POCl_3$, K_2CO_3, CH_3CN, 60 °C; 2) $NaBH_4$, MeOH, r.t.

Chart 4

Table 2. Yield in the Synthesis of 13-Methylprotoberberine Alkaloids

Alkaloid	R, R^1, R^2	Yield (%)		
		21	**19**	**17**
(±)-Corydaline (**21a**)	$R=Me$, $R^1=R^2=Me$	61	88	80
(±)-Thalictricavine (**21b**)	$R=Me$, $R^1+R^1=CH_2$, $R^2=Me$	68	91	78
(±)-Tetrahydrocorysamine (**21c**)	$R=Me$, $R^1+R^1=R^2+R^2=CH_2$	55	95	81

synthesis of 2,3,9,10-tetraoxygenated protoberberine alkaloids as well as their 13-methyl alkaloids through the same intermediates, and the present method can be applied to the synthesis of a variety of protoberberine alkaloids.

Experimental

Melting points were determined on a Yanagimoto micro melting point apparatus and are uncorrected. Silica gel (Kieselgel 60, 70—230 mesh, Merck) and alumina (Aluminiumoxid 90, Aktivitätsstufe II—III, 70—230 mesh, Merck) were used for column chromatography. Organic extracts were dried over anhydrous Na_2SO_4. IR spectra were measured with a JASCO A-102 spectrometer in $CHCl_3$, MS with a Hitachi M-80 mass spectrometer, and ^{1}H-NMR spectra with a JEOL FX-100 spectrometer in $CDCl_3$ using tetramethylsilane as an internal standard.

General Procedure for Benzylphenethylamines A molecular sieve 4 Å (3.0 g) was added to a solution of phenethylamine derivative (**1**, **10**, or **11**, 18 mmol) and benzaldehyde derivative (**2** or **12**, 18 mmol) in CH_2Cl_2 (20 ml), and the mixture was stirred at room temperature for 24 h in a stream of nitrogen. The molecular sieve was filtered off and the filtrate was concentrated. A solution of the residue in tetrahydrofuran (THF) (20 ml) was added with stirring to a suspension of $LiAlH_4$ (90 mmol) in THF (100 ml), and the mixture was stirred at room temperature for 2 h. Water was added to the reaction mixture in order to destroy the excess $LiAlH_4$, and the precipitate was filtered off and washed with THF. The filtrate and washings were combined, dried, and concentrated to give the product.

N-(2,3-Dimethoxybenzyl)-3,4-dimethoxyphenethylamine (**3a**): Yield: 79%. Amorphous. IR cm^{-1}: 3300 (NH). ^{1}H-NMR δ: 7.1—6.7 (6H, m, Ar-H), 3.89 (9H, s, OMe×3), 3.82 (2H, s, NCH_2Ar), 3.78 (3H, s, OMe), 2.9—2.7 (4H, m, NCH_2CH_2Ar). MS *m/z* (%): 331 (M^+, 3), 181 (100), 152 (100). High-resolution (HR)-MS: Calcd for $C_{19}H_{25}NO_4$: 331.1860. Found: 331.1844.

N-(2,3-Dimethoxybenzyl)-3,4-methylenedioxyphenethylamine (**3b**): Yield: 62%. Amorphous. ^{1}H-NMR δ: 7.1—6.5 (7H, m, Ar-H×6, NH), 5.91 (2H, s, OCH_2O), 3.85, 3.79 (each 3H, each s, OMe×2), 3.80 (2H, s, NCH_2Ar), 2.80, 2.76 (4H, AB-q, J=4 Hz, NCH_2CH_2Ar). MS *m/z* (%): 315 (M^+, 0.6), 180 (99), 151 (100). HR-MS: Calcd for $C_{18}H_{21}NO_4$: 315.1469. Found: 315.1453.

2-Bromo-4,5-dimethoxy-*N*-(2,3-dimethoxybenzyl)phenethylamine (**13a**): Yield: 85%. Amorphous. ^{1}H-NMR δ: 7.1—6.7 (3H, m, Ar-H×3), 6.98, 6.78 (each 1H, each s, Ar-H), 3.85, 3.84, 3.83. 3.82 (total 14H, each s, OMe×4, NCH_2Ar), 2.87 (4H, s, NCH_2CH_2Ar). MS *m/z* (%): 411, 409 (M^+, 0.11, 0.12), 330 (65), 181 (100), 151 (100). HR-MS: Calcd for $C_{19}H_{24}BrNO_4$: 409.0887. Found: 409.0856.

2-Bromo-4,5-dimethoxy-*N*-(2,3-methylenedioxybenzyl)phenethylamine (**13b**): Yield: 84%. Amorphous. ^{1}H-NMR δ: 6.99, 6.74 (each 1H, each s, Ar-H), 6.76 (3H, s, Ar-H×3), 5.92 (2H, s, OCH_2O), 3.84, 3.83 (total 8H, each s, OMe×2, NCH_2Ar), 2.89 (4H, s, NCH_2CH_2Ar). MS *m/z* (%): 314 (M^+−Br, 40), 231 (7), 164 (100). Picrate: yellow needles, mp 185—187 °C (EtOH–$CHCl_3$). *Anal.* Calcd for $C_{18}H_{20}BrNO_4 \cdot C_6H_3N_3O_7$: C, 46.24; H, 3.72; N, 8.99. Found: C, 46.54; H, 3.78; N, 8.70.

2-Bromo-*N*-(2,3-dimethoxybenzyl)-4,5-methylenedioxyphenethylamine (**13c**): Yield: 88%. Amorphous. ^{1}H-NMR δ: 7.1—6.6 (5H, m, Ar-H×5), 5.92 (2H, s, OCH_2O), 3.86, 3.83, 3.79 (total 8H, each s, OMe×2, NCH_2Ar), 2.84 (4H, s, NCH_2CH_2Ar). MS *m/z* (%): 314 (M^+−Br, 6), 180 (58), 151 (100).

2-Bromo-4,5-methylenedioxy-*N*-(2,3-methylenedioxybenzyl)phenethylamine (**13d**): Yield: 69%. Amorphous. ^{1}H-NMR δ: 6.98, 6.73 (each 1H, each s, Ar-H×2), 6.8—6.5 (3H, m, Ar-H×3), 5.94, 5.93 (each 2H, each s, OCH_2O×2), 3.82 (2H, s, NCH_2Ar), 2.85 (4H, s, NCH_2CH_2Ar). MS *m/z* (%): 298 (M^+−Br, 26), 215 (11), 164 (100), 185 (100).

***N*-(3,4-Dimethoxybenzyl)-*N*-(2,3-dimethoxyphenethyl)-α-(methylthio)acetamide (5)** α-(Methylthio)acetyl chloride (**4**, 250 mg, (2.0 mmol)) was added to a solution of the amine (**2a**, 645.4 mg (1.9 mmol)) in CH_2Cl_2 (10 ml) at 0 °C in the presence of Et_3N (200 mg (2.0 mmol)), and the reaction mixture was stirred for 1.5 h. The mixture was successively washed with dil. HCl, 10% K_2CO_3 aq. and then saturated NaCl aq. and dried. The solvent was evaporated off and the residue was chromatographed on silica gel with C_6H_6 : AcOEt (4 : 1) to give the amide (**5**, 659.5 mg, 81%). Amorphous. IR cm^{-1}: 1630 (NCO). ^{1}H-NMR δ: 7.0—6.7 (6H, m, Ar-H×6), 4.71, 4.49 (each 1H, each s, NCH_2Ar), 3.87 (6H, s, OMe×2), 3.89, 3.79 (each 3H, each s, OMe×2), 3.52 (2H, t, J=6 Hz, $NC\underline{H}_2CH_2Ar$), 3.33, 3.07 (total 2H, each s, SCH_2CO), 2.76 (2H, t, J=6 Hz, $NCH_2C\underline{H}_2Ar$), 2.22 (3H, s, SMe). MS *m/z* (%): 419 (M^+, 5), 268 (3), 180 (8), 164 (100), 151 (59). HR-MS: Calcd for $C_{22}H_{29}NO_5S$: 419.1763. Found: 419.1748.

***N*-(3,4-Dimethoxybenzyl)-*N*-(2,3-dimethoxyphenethyl)-α-(methylsulfinyl)acetamide (6)** *m*-CPBA (80%, 687.5 mg (3.2 mmol)) was added portion-wise to a solution of the amide (**5**, 1.32 g (3.2 mmol)) in CH_2Cl_2 (30 ml). The reaction mixture was stirred under ice-cooling for 1 h, washed with sat. $NaHCO_3$ aq. and then sat. NaCl aq., and dried. The solvent was evaporated off and the residue was chromatographed on alumina with $CHCl_3$ to give the sulfoxide (**6**, 1.25 g, 91%). Amorphous. IR cm^{-1}: 1630 (NCO). ^{1}H-NMR δ: 7.0—6.6 (6H, m, Ar-H×6), 4.71, 4.49 (total 2H, each s, NCH_2Ar), 3.86 (6H, s, OMe×2), 3.9—3.7 (2H, m, SCH_2CO), 3.85, 3.84 (each 3H, each s, OMe×2), 3.6—3.4 (2H, m, $NC\underline{H}_2CH_2Ar$), 2.9—2.6 (2H, m, $NCH_2C\underline{H}_2Ar$), 2.76 (12/7 H), 2.66 (9/7 H) (total 3H, each s, SMe). MS *m/z* (%): 435 (M^+, 1), 372 (1), 164 (100). HR-MS: Calcd for $C_{22}H_{29}NO_6S$: 435.1752. Found: 435.1733.

7,8-Dimethoxy-2-(3,4-dimethoxybenzyl)-4-methylthio-1,2,3,4-tetrahydroisoquinolin-3-one (7a) and 7,8-Dimethoxy-3-(2,3-dimethoxybenzyl)-1-methylthio-1,2,4,5-tetrahydrobenzazepin-2-one (8a) From Sulfoxide (**6**): a) with *p*-TsOH: *p*-TsOH (175 mg (1.0 mmol)) was added to a solution of the sulfoxide (**6**, 219 mg (0.50 mmol)) in CCl_4 (3 ml) and the mixture was refluxed with stirring for 20 min. The mixture was washed with sat. $NaHCO_3$ aq. and sat. NaCl aq., then dried. The solvent was evaporated off and the residue was chromatographed on silica gel with C_6H_6 : AcOEt (10 : 1). The first fraction gave the benzazepinone (**8a**, 70.5 mg, 34%). Colorless plates. mp 112—115 °C (MeOH). IR cm^{-1}: 1630 (NCO). ^{1}H-NMR δ: 7.3—6.7 (3H, m, Ar-H×3), 6.71, 6.48 (each 1H, each s, Ar-H×2), 4.94, 4.59 (each 1H, AB-q, J=15 Hz, NCH_2Ar), 4.72 (1H, s, C_1-H), 4.9—4.5, 3.5—3.1 (each 1H, m, C_4-H), 3.88, 3.87, 3.85, 3.82 (each 3H, each s, OMe×4), 3.0—2.8 (2H, m, C_5-H), 2.53 (3H, s, SMe). MS *m/z* (%): 417 (M^+, 31), 370 (63), 342 (100), 266 (58), 151 (52). *Anal.* Calcd for $C_{22}H_{27}NO_5S$: C, 63.29; H, 6.25; N, 3.35. Found: C, 63.33; H, 6.25; N, 3.15. The second fraction gave the isoquinolinone (**7a**, 50.3 mg, 24%). IR cm^{-1}: 1640 (NCO). ^{1}H-NMR δ: 7.0—6.4 (3H, m, Ar-H×3), 6.83, 6.77 (each 1H, AB-q, J=8 Hz, Ar-H×2), 4.36 (1H, s, C_4-H), 4.51, 4.37 (2H, AB-q, J=17 Hz, C_1-H), 3.86, 3.84 (each 3H, each s, OMe×2), 3.78 (6H, s, OMe×2), 3.16 (2H, t, J=7 Hz, $NC\underline{H}_2CH_2Ar$), 2.89 (2H, t, J=7 Hz, $NCH_2C\underline{H}_2Ar$), 2.19 (3H, s, SMe). MS *m/z* (%): 417 (M^+, 4), 370 (8), 164 (100). HR-MS: Calcd for $C_{22}H_{27}NO_5S$: 417.1608. Found: 417.1595. b) with CH_3SO_3H: **7a** (25%) and **8a** (41%). c) with CF_3CO_2H: **7a** (17%) and **8a** (46%).

From Amine (**3a**) with **9**: According to the general procedure for 4-methylthio-2-phenethylisoquinolin-3-ones, **3a** gave **7a** (29%) and **8a** (43%).

7,8-Dimethoxy-2-(3,4-methylenedioxyphenethyl)-4-methylthio-1,2,3,4-tetrahydroisoquinolin-3-one (7b) and 3-(2,3-Dimethoxybenzyl)-7,8-methylenedioxy-1-methylthio-1,2,4,5-tetrahydrobenzazepin-2-one (8b) According to the general procedure for 4-methylthio-2-phenethylisoquinolin-3-ones, **3b** gave **8b** (41%) and **7b** (30%).

8b: Amorphous. IR cm^{-1}: 1635 (NCO). ^{1}H-NMR δ: 7.0—6.8 (3H, m, Ar-H×3), 6.70, 6.47 (each 1H, each s, Ar-H×2), 5.91 (2H, s, OCH_2O), 4.92, 4.61 (each 1H, AB-q, J=15 Hz, NCH_2Ar), 4.67 (1H, s, C_1-H), 4.8—4.4, 3.5—3.1 (each 1H, m, C_4-H), 3.87, 3.84 (each 3H, each s, OMe×2), 2.9—2.7 (2H, m, C_5-H), 2.33 (3H, s, SMe). MS *m/z* (%): 401 (M^+, 13), 354 (65), 324 (47), 151 (100). HR-MS: Calcd for $C_{21}H_{23}NO_5S$: 401.1295. Found: 401.1295.

7b: Colorless plates. mp 122—123 °C (MeOH). IR cm^{-1}: 1640 (NCO). ^{1}H-NMR δ: 6.99, 6.86 (2H, AB-q, J=8.5 Hz, Ar-H×2), 6.7—6.5 (3H, m, Ar-H×3), 5.90 (2H, s, C_4-H), 3.86, 3.81 (each 3H, each s, OMe×2), 3.7—3.2 (2H, m, $NC\underline{H}_2CH_2Ar$), 2.84 (2H, t, J=7 Hz, $NCH_2C\underline{H}_2Ar$), 2.21 (3H, s, SMe). MS *m/z* (%): 401 (M^+, 4), 355 (21), 206 (84), 148 (100). *Anal.* Calcd for $C_{21}H_{23}NO_5S$: C, 62.83; H, 5.77; N, 3.49. Found: C, 62.68; H, 5.86; N, 3.37.

General Procedure for 4-Methylthio-2-phenethylisoquinolin-3-ones A solution of α-chloro-α-(methylthio)acetyl chloride (**9**, 10 mmol) in CH_2Cl_2 (10 ml) was added dropwise under ice-cooling to a solution of the amine (**3** or **13**, 9 mmol) and Et_3N (10 mmol) in CH_2Cl_2 (30 ml), and the mixture was stirred for 20 min. $SnCl_4$ (11 mmol) was added under ice-cooling to the reaction mixture. The mixture was stirred for 1 h and washed with H_2O, sat. $NaHCO_3$ aq., and sat. NaCl aq., then dried. The solvent was evaporated off and the residue was chromatographed on silica gel with C_6H_6 : AcOEt (10 : 1) to give the product.

2-(2-Bromo-4,5-dimethoxyphenethyl)-7,8-dimethoxy-4-methylthio-1,2,3,4-tetrahydroisoquinolin-3-one (**14a**): Yield: 78%. Pale-yellow needles. mp 131—133 °C (MeOH). IR cm^{-1}: 1640 (NCO). ^{1}H-NMR δ: 7.00, 6.70 (each 1H, each s, Ar-H×2), 6.98, 6.86 (each 1H, AB-q, J=8.5 Hz, Ar-H×2), 4.54, 4.40 (each 1H, AB-q, J=17 Hz, C_1-H), 4.36 (1H, s, C_4-H), 3.86, 3.83, 3.79, 3.68 (each 3H, each s, OMe×4), 3.85—3.75 (2H, m,

NCH_2CH_2Ar), 3.00 (2H, t, J=7 Hz, NCH_2CH_2Ar), 2.21 (3H, s, SMe). MS *m/z* (%): 497, 495 (M^+, 6, 6), 450, 448 (18, 12), 368 (14), 242 (93), 206 (100), 64 (29). *Anal.* Calcd for $C_{22}H_{26}BrNO_5S$: C, 53.22; H, 5.28; N, 2.82. Found: C, 53.04; H, 5.41; N, 2.57.

2-(2-Bromo-4,5-dimethoxyphenethyl)-7,8-methylenedioxy-4-methylthio-1,2,3,4-tetrahydroisoquinolin-3-one (**14b**): Yield: 80%. Colorless needles. mp 121—123 °C (MeOH–Et_2O). IR cm^{-1}: 1640 (NCO). ^{1}H-NMR δ: 7.02, 6.52 (each 1H, each s, Ar-H×2), 6.73 (2H, s, Ar-H×2), 5.95 (2H, s, OCH_2O), 4.48, 3.83 (each 1H, AB-q, J=16 Hz, C_1-H), 4.39 (1H, s, C_4-H), 3.85, 3.50 (each 3H, each s, OMe×2), 4.0—3.5, 3.1—2.8 (each 2H, m, NCH_2CH_2Ar), 2.22 (3H, s, SMe). MS *m/z* (%): 481, 479 (M^+, 8, 6), 435, 433 (16, 19), 352 (7), 242 (100), 189 (36), 164 (23). *Anal.* Calcd for $C_{21}H_{22}BrNO_5S$: C, 52.51; H, 4.62; N, 2.92. Found: C, 52.55; H, 4.61; N, 2.65.

2-(2-Bromo-4,5-methylenedioxyphenethyl)-7,8-dimethoxy-4-methylthio-1,2,3,4-tetrahydroisoquinolin-3-one (**14c**): Yield: 72%. Amorphous. IR cm^{-1}: 1640 (NCO). ^{1}H-NMR δ: 6.99, 6.78 (each 1H, AB-q, J=8.5 Hz, Ar-H×2), 6.99, 6.72 (each 1H, each s, Ar-H×2), 5.91 (2H, s, OCH_2O), 4.55, 4.42 (each 1H, AB-q, J=16 Hz, C_1-H), 4.36 (1H, s, C_4-H), 3.86, 3.82 (each 3H, each s, OMe×2), 3.72 (2H, t, J=7 Hz, NCH_2CH_2Ar), 2.97 (2H, t, J=7 Hz, NCH_2CH_2Ar), 2.24 (3H, s, SMe). MS *m/z* (%): 434, 432 (M^+−47, 4, 3), 400 (8), 352 (14), 206 (100), 151 (51).

2-(2-Bromo-4,5-methylenedioxyphenethyl)-7,8-methylenedioxy-4-methylthio-1,2,3,4-tetrahydroisoquinolin-3-one (**14d**): Yield: 88%. Colorless plates. mp 119—121 °C (MeOH). IR cm^{-1}: 1640 (NCO). ^{1}H-NMR δ: 6.94, 6.66 (each 1H, each s, Ar-H×2), 6.75 (2H, s, Ar-H×2), 5.97, 5.90 (each 2H, each s, OCH_2O×2), 4.55, 4.11 (each 1H, AB-q, J=16 Hz, C_1-H), 4.38 (1H, s, C_4-H), 3.72 (2H, t, J=7 Hz, NCH_2CH_2Ar), 2.97 (2H, t, J=7 Hz, NCH_2CH_2Ar), 2.24 (3H, s, SMe). MS *m/z* (%): 418, 416 (M^+−47, 34, 39), 228 (39), 190 (100), 175 (65), 148 (53). *Anal.* Calcd for $C_{20}H_{18}BrNO_5S$: C, 51.73; H, 3.91; N, 3.02. Found: C, 51.86; H, 3.78; N, 2.80.

General Procedure for Alkylation of Isoquinolin-3-ones A solution of lithium diisopropylamide (LDA) (3.2 ml (0.1 M sol. in THF) (3.2 mmol)) was added to a solution of isoquinolin-3-one (**14**, 2.12 mmol) in THF (20 ml) at −78 °C in a stream of N_2 and stirred for 1 h. Methyl iodide or ethyl iodide (3.2 mmol) was added to the reaction mixture at room temperature and stirred for 1 h. Sat. NH_4Cl aq. (1 ml) was added to the mixture and extracted with $CHCl_3$. The extract was washed with sat. NaCl aq. and dried. The solvent was evaporated off and the residue was chromatographed on silica gel with hexane : AcOEt (4 : 1) to give the product.

2-(2-Bromo-4,5-dimethoxyphenethyl)-7,8-dimethoxy-4-methyl-4-methylthio-1,2,3,4-tetrahydroisoquinolin-3-one (**17a**): Yield: 80%. Colorless needles. mp 131.5—132 °C (MeOH). IR cm^{-1}: 1640 (NCO). ^{1}H-NMR δ: 7.15, 6.88 (each 1H, AB-q, J=8.5 Hz, Ar-H×2), 7.01, 6.71 (each 1H, each s, Ar-H×2), 4.62, 4.45 (each 1H, AB-q, J=16 Hz, C_1-H), 3.87, 3.84, 3.80, 3.70 (each 3H, each s, OMe×4), 3.75—3.65 (2H, br s, NCH_2CH_2Ar), 2.99 (2H, t, J=7 Hz, NCH_2CH_2Ar), 2.03 (3H, s, SMe), 1.95 (3H, s, C_4-Me). MS *m/z* (%): 511, 509 (M^+, 1.1, 1.1),464, 462 (71, 69), 219 (100). *Anal.* Calcd for $C_{23}H_{28}BrNO_5S$: C, 54.12; H, 5.53; N, 2.74. Found: C, 53.86; H, 5.75; N, 2.76.

2-(2-Bromo-4,5-methylenedioxyphenethyl)-7,8-dimethoxy-4-methyl-4-methylthio-1,2,3,4-tetrahydroisoquinolin-3-one (**17b**): Yield: 78%. Colorless needles. mp 134—135 °C (EtOH). IR cm^{-1}: 1640 (NCO). ^{1}H-NMR δ: 7.16, 6.89 (each 1H, AB-q, J=8.8 Hz, Ar-H×2), 6.99, 6.73 (each 1H, each s, Ar-H×2), 5.93, 5.91 (each 1H, AB-q, J=1.5 Hz, OCH_2O), 4.62, 4.47 (each 1H, AB-q, J=16 Hz, C_1-H), 3.87, 3.83 (each 3H, each s, OMe×2), 3.86—2.84 (4H, m, NCH_2CH_2Ar), 2.06 (3H, s, SMe), 1.95 (3H, s, C_4-Me). MS *m/z* (%): 496, 494 (M^++1, 0.4, 0.7), 41 (100). *Anal.* Calcd for $C_{22}H_{24}BrNO_5S$: C, 53.45; H, 4.89; N, 2.83. Found: C, 53.50; H, 5.04; N, 2.82.

2-(2-Bromo-4,5-methylenedioxyphenethyl)-7,8-methylenedioxy-4-methyl-4-methylthio-1,2,3,4-tetrahydroisoquinolin-3-one (**17c**): Yield: 81%. Amorphous. IR cm^{-1}: 1640 (NCO). ^{1}H-NMR δ: 6.98, 6.65 (each 1H, each s, Ar-H×2), 6.93, 6.77 (each 1H, AB-q, J=8.3 Hz, Ar-H×2), 5.98—5.88 (4H, m, OCH_2O×2), 4.63, 4.14 (each 1H, AB-q, J=15.6 Hz, C_1-H), 3.77—2.83 (4H, m, NCH_2CH_2Ar), 2.07 (3H, s, SMe), 1.95 (3H, s, C_4-Me). MS *m/z* (%): 480, 478 (M^++1, 0.2, 0.2), 41 (100). *Anal.* Calcd for $C_{21}H_{20}BrNO_5S$: C, 52.73; H, 4.21; N, 2.93. Found: C, 52.49; H, 4.37; N, 2.79.

2-(2-Bromo-4,5-dimethoxyphenethyl)-4-ethyl-7,8-dimethoxy-4-methylthio-1,2,3,4-tetrahydroisoquinolin-3-one (**18a**): Yield: 74%. Colorless needles. mp 133—134 °C (MeOH). IR cm^{-1}: 1640 (NCO). ^{1}H-NMR δ: 7.14, 6.92 (each 1H AB-q, J=8.8 Hz, Ar-H×2), 7.01, 6.71 (each 1H, each s, Ar-H×2), 4.51, 4.44 (each 1H, AB-q, J=16.6 Hz, C_1-H), 3.88, 3.83, 3.82, 3.69 (each 3H, each s, OMe×4), 3.82—3.01 (4H, m, NCH_2CH_2Ar), 2.17—2.03 (2H, m, CH_2Me), 2.00 (3H, s, SMe), 0.76 (3H, t, J=7.3 Hz, CH_2Me). MS *m/z* (%): 525, 523 (M^+, 1.2, 1.4), 234 (91), 233 (100). *Anal.* Calcd for $C_{24}H_{30}BrNO_5S$: C, 54.95; H, 5.76; N, 2.67. Found: C, 54.94; H, 5.69; N, 2.53.

General Procedure for Desulfurization of Methylthioisoquinolin-3-ones Raney Ni (W-4, 4 g) was added to a solution of methylthioisoquinolin-3-one (**14**, **17**, or **18**, 1.8 mmol) in ethanol (20 ml), and the reaction mixture was refluxed for 2 h. The Raney Ni was filtered off and washed with hot ethanol. The filtrate and washings were combined and concentrated. The residue was chromatographed on alumina with $CHCl_3$ to give the product.

7,8-Dimethoxy-2-(3,4-dimethoxyphenethyl)-1,2,3,4-tetrahydroisoquinolin-3-one (**15a**):Yield: 88% (from **14a**); 90% (from **7a**). Amorphous. IR cm^{-1}: 1640 (NCO). ^{1}H-NMR δ: 6.83 (2H, s, Ar-H×2), 6.79, 6.78, 6.73 (each 1H, each s, Ar-H×3), 4.38 (2H, s, C_1-H), 3.85, 3.84, 3.78, 3.77 (each 3H, each s, OMe×4), 3.74 (each 1H, t, J=8 Hz, NCH_2CH_2Ar), 3.54 (2H, s, C_4-H), 2.88 (each 1H, t, J=8 Hz, NCH_2CH_2Ar). MS *m/z* (%): 371 (M^+, 13), 192 (26), 164 (100). HR-MS: Calcd for $C_{21}H_{25}NO_5$: 371.1730. Found: 371.1725.

2-(3,4-Dimethoxyphenethyl)-7,8-methylenedioxy-1,2,3,4-tetrahydroisoquinolin-3-one (**15b**):Yield: 80%. Amorphous. IR cm^{-1}: 1630 (NCO). ^{1}H-NMR δ: 6.77 (2H, s, Ar-H×2), 6.72, 6.61 (each 1H, AB-q, J=8 Hz, Ar-H×2), 6.63 (1H, s, Ar-H), 5.94 (2H, s, OCH_2O), 4.14 (2H, s, C_1-H), 3.85, 3.67 (each 3H, each s, OMe×2), 3.72 (2H, t, J=7 Hz, NCH_2CH_2Ar), 3.53 (2H, s, C_4-H), 2.85 (2H, t, J=7 Hz, NCH_2CH_2Ar). MS *m/z* (%): 355 (M^+, 6), 220 (3), 176 (13), 164 (100), 151 (6). HR-MS: Calcd for $C_{20}H_{21}NO_5$: 355.1418. Found: 355.1436.

7,8-Dimethoxy-2-(3,4-methylenedioxyphenethyl)-1,2,3,4-tetrahydroisoquinolin-3-one (**15c**):Yield: 77%. Amorphous. IR cm^{-1}: 1635 (NCO). ^{1}H-NMR δ: 6.83 (2H, s, Ar-H×2), 6.70 (1H, s, Ar-H), 6.75—6.65 (2H, m, Ar-H×2), 5.91 (2H, s, OCH_2O), 4.24, 3.54 (each 1H, AB-q, J=16 Hz, C_1-H), 3.85 (6H, s, OMe×2), 3.6—2.5 (6H, m, NCH_2CH_2Ar, C_4-H). MS *m/z* (%): 355 (M^+, 8), 207 (39), 192 (31), 148 (100). HR-MS: Calcd for $C_{20}H_{21}NO_5$: 355.1418. Found: 355.1436.

7,8-Methylenedioxy-2-(3,4-methylenedioxyphenethyl)-1,2,3,4-tetrahydroisoquinolin-3-one (**15d**): Yield: 78%. Amorphous. IR cm^{-1}: 1635 (NCO). ^{1}H-NMR δ: 6.9—6.5 (5H, m, Ar-H×5), 5.95, 5.93 (each 2H, each s, OCH_2O×2), 4.24 (2H, s, C_1-H), 3.69 (2H, t, J=8 Hz, NCH_2CH_2Ar), 3.56, 3.51 (each 1H, AB-q, J=17 Hz, C_4-H), 2.83 (2H, t, J=8 Hz, NCH_2CH_2Ar). MS *m/z* (%): 339 (M^+, 6), 191 (8), 176 (19), 148 (100). HR-MS: Calcd for $C_{19}H_{17}NO_5$: 339.1105. Found: 339.1100.

7,8-Dimethoxy-2-(3,4-dimethoxyphenethyl)-4-methyl-1,2,3,4-tetrahydroisoquinolin-3-one (**19a**): Yield: 88%. Amorphous. IR cm^{-1}: 1640 (NCO). ^{1}H-NMR δ: 6.9—6.7 (5H, m, Ar-H×5), 4.36 (2H, s, C_1-H), 3.85, 3.83, 3.79, 3.78 (each 3H, each s, OMe×4), 3.8—3.65 (2H, m, NCH_2CH_2Ar), 3.48 (1H, q, J=7.3 Hz, C_4-H), 2.87 (2H, t, J=7.5 Hz, NCH_2CH_2Ar), 1.41 (3H, d, J=7.3 Hz, C_4-Me). MS *m/z* (%): 385 (M^+, 6), 219 (7), 206 (9), 164 (100). HR-MS: Calcd for $C_{22}H_{27}NO_5$: 385.1887. Found: 385.1911.

7,8-Dimethoxy-2-(3,4-methylenedioxyphenethyl)-4-methyl-1,2,3,4-tetrahydroisoquinolin-3-one (**19b**): Yield: 91%. Amorphous. IR cm^{-1}: 1640 (NCO). ^{1}H-NMR δ: 6.87, 6.85 (each 1H, AB-q, J=8.8 Hz, Ar-H×2), 6.73—6.67 (3H, m, Ar-H×3), 5.92, 5.91 (each 1H, AB-q, J=2 Hz, OCH_2O), 4.38, 4.35 (each 1H, AB-q, J=16.6 Hz, C_1-H), 3.86, 3.81 (each 3H, each s, OMe×2), 3.8—3.6 (4H, m, NCH_2CH_2Ar), 3.47 (1H, q, J=7.3 Hz, C_4-H), 1.42 (3H, d, J=7.3 Hz, C_4-Me). MS *m/z* (%): 369 (M^+, 13), 221 (63), 206 (46), 148 (100). HR-MS: Calcd for $C_{21}H_{23}NO_5$: 369.1574. Found: 369.1614.

7,8-Methylenedioxy-2-(3,4-methylenedioxyphenethyl)-4-methyl-1,2,3,4-tetrahydroisoquinolin-3-one (**19c**): Yield: 95%. Amorphous. IR cm^{-1}: 1640 (NCO). ^{1}H-NMR δ: 6.8—6.6 (5H, m, Ar-H×5), 5.95, 5.90 (each 2H, each s, OCH_2O×2), 4.25, 4.18 (each 1H, AB-q, J=16 Hz, C_1-H), 3.8—3.53 (2H, m, NCH_2CH_2Ar), 3.09 (1H, q, J=7.3 Hz, C_4-H), 2.9—2.7 (2H, m, NCH_2CH_2Ar), 1.41 (3H, d, J=7.3 Hz, C_4-Me). MS *m/z* (%): 353 (M^+, 9), 205 (27), 190 (33), 148 (100). HR-MS: Calcd for $C_{20}H_{19}NO_5$: 353.1262. Found: 353.1304.

4-Ethyl-7,8-dimethoxy-2-(3,4-dimethoxyphenethyl)-1,2,3,4-tetrahydroisoquinolin-3-one (**20a**):Yield: 83%. Amorphous. IR cm^{-1}: 1640 (NCO). ^{1}H-NMR δ: 6.86—6.7 (5H, m, Ar-H×5), 4.36 (2H, s, C_1-H), 3.86, 3.84, 3.79, 3.78 (each 3H, each s, OMe×4), 3.75—3.6 (2H, m, NCH_2CH_2Ar), 3.40 (1H, t, J=7 Hz, C_4-H), 2.89 (2H, t, J=7.3 Hz, NCH_2CH_2Ar), 1.8—1.67 (2H, m, CH_2Me), 0.83 (3H, t, J=7.3 Hz, CH_2Me). MS *m/z* (%): 399 (M^+, 5), 164 (100). HR-MS: Calcd for $C_{23}H_{29}NO_5$: 399.2044. Found: 399.2106.

General Procedure for Protoberberines A mixture of isoquinolin-3-one (**15**, **19**, or **20**, 0.82 mmol), anhyd. K_2CO_3 (2.2 mmol) and $POCl_3$ (4.2 mmol) in CH_3CN (17 ml) was heated with stirring at 60 °C in a stream

of N_2 for 40 min (2 h for **19** and **20**) and concentrated. MeOH (15 ml) was added to the residue and $NaBH_4$ (13 mmol) was added to the mixture. The reaction mixture was refluxed (or stirred at room temperature for **19** and **20**) for 1 h. The solvent was evaporated off and K_2CO_3 aq. was added to the residue. The mixture was extracted with $CHCl_3$ and the extract was washed with NaCl aq. and dried. The solvent was evaporated off and the residue was chromatographed on silica gel with $CHCl_3$ to give the product. The synthetic alkaloids were identical with the corresponding authentic samples in ^{1}H-NMR spectra and thin-layer chromatographic behavior.

(±)-Tetrahydropalmatine (**16a**): Yield: 76%. Pale-yellow plates. mp 150—152 °C (MeOH) (mp 147 °C[13]). ^{1}H-NMR δ: 6.89, 6.80 (each 1H, AB-q, J=8.5 Hz, Ar-H×2), 6.73, 6.62 (each 1H, each s, Ar-H×2), 4.24, 3.52 (each 1H, AB-q, J=15 Hz, C_8-H), 3.89, 3.87 (each 3H, each s, OMe×2), 3.85 (6H, s, OMe×2), 3.8—2.7 (7H, m, C_5, C_6, C_{13}, C_{13a}-H). MS *m/z* (%): 355 (M^+, 100), 324 (15), 190 (30), 164 (97). *Anal.* Calcd for $C_{21}H_{25}NO_4$: C, 70.96; H, 7.09; N, 3.94. Found: C, 70.97; H, 7.09; N, 3.94.

(±)-Sinactine (**16b**): Yield: 78%. Colorless needles. mp 169—171 °C (MeOH) (mp 167—168 °C[5g]). ^{1}H-NMR δ: 6.73, 6.62 (each 1H, each s, Ar-H×2), 6.67 (2H, s, Ar-H×2), 5.96, 5.93 (each 1H, AB-q, J=1.5 Hz, OCH_2O), 4.10, 3.55 (each 1H, AB-q, J=15 Hz, C_8-H), 3.89, 3.87 (each 3H, each s, OMe×2), 3.7—2.4 (7H, m, C_5, C_6, C_{13}, C_{13a}-H). MS *m/z* (%): 339 (M^+, 59), 190 (28), 148 (100). *Anal.* Calcd for $C_{20}H_{21}NO_4$: C, 70.78; H, 6.24; N, 4.13. Found: C, 70.62; H, 6.24; N, 4.26.

(±)-Canadine (**16c**): Yield: 68%. Pale-yellow plates. mp 172—174 °C (MeOH) (mp 167—168 °C[5g]). ^{1}H-NMR δ: 6.86, 6.79 (each 1H, AB-q, J=8 Hz, Ar-H×2), 6.72, 6.59 (each 1H, each s, Ar-H×2), 5.91 (2H, s, OCH_2O), 4.24, 3.54 (each 1H, AB-q, J=16 Hz, C_8-H), 3.85 (6H, s, OMe×2), 3.6—2.5 (7H, m, C_5, C_6, C_{13}, C_{13a}-H). MS *m/z* (%): 339 (M^+, 60), 174 (18), 164 (100), 149 (67). *Anal.* Calcd for $C_{20}H_{21}NO_4$: C, 70.78; H, 6.24; N, 4.13. Found: C, 70.74; H, 6.36; N, 4.18.

(±)-Stylopine (**16d**): Yield: 63%. Pale-yellow needles. mp 198—200 °C (MeOH–$CHCl_3$) (mp 194—195 °C[5g]). ^{1}H-NMR δ: 6.72, 6.58 (each 1H, each s, Ar-H×2), 6.66 (2H, s, Ar-H×2), 5.96, 5.92 (each 1H, AB-q, J=1 Hz, OCH_2O), 5.91 (2H, s, OCH_2O), 4.09, 3.46 (2H, AB-q, J=15 Hz, C_8-H), 3.6—2.4 (7H, m, C_5, C_6, C_{13}, C_{13a}-H). MS *m/z* (%): 323 (M^+, 27), 174 (12), 148 (100). *Anal.* Calcd for $C_{19}H_{17}NO_4$: C, 70.58; H, 5.30; N, 4.33. Found: C, 70.70; H, 5.23; N, 4.52.

(±)-Corydaline (**21a**): Yield: 61%. Colorless needles. mp 136—136.5 °C (EtOH) (mp 135—136 °C[12,14]). ^{1}H-NMR δ: 6.91, 6.83 (each 1H, AB-q, J=8.5 Hz, Ar-H×2), 6.69, 6.61 (each 1H, each s, Ar-H×2), 4.20, 3.51 (each 1H, AB-q, J=16 Hz, C_8-H), 3.88, 3.86 (each 6H, each s, OMe×4), 3.75—2.45 (6H, m, C_5, C_6, C_{13}, C_{13a}-H), 0.95 (3H, d, J=6.8 Hz, C_{13}-Me). MS *m/z* (%): 369 (M^+, 29), 179 (14), 178 (100). *Anal.* Calcd for $C_{22}H_{27}NO_4$: C, 71.52; H, 7.37; N, 3.79. Found: C, 71.55; H, 7.69; N, 3.80.

(±)-Thalictricavine (**21b**): Yield: 68%. Colorless needles. mp 208—209 °C (MeOH) (mp 211.5—212.5 °C[15], 209—210 °C[12]). ^{1}H-NMR δ: 6.89, 6.82 (each 1H, AB-q, J=8.7 Hz, Ar-H×2), 6.68, 6.58 (each 1H, each s, Ar-H×2), 5.93, 5.91 (each 1H, AB-q, J=1.8 Hz, OCH_2O), 4.19, 3.49 (each 1H, AB-q, J=15.6 Hz, C_8-H), 3.86 (6H, s, OMe×2), 3.65—3.0 (6H, m, C_5, C_6, C_{13}, C_{13a}-H), 0.96 (3H, d, J=6.9 Hz, C_{13}-Me). MS *m/z* (%): 353 (M^+, 30), 178 (100). *Anal.* Calcd for $C_{21}H_{23}NO_4$: C, 71.37; H, 6.56; N, 3.96. Found: C, 71.61; H, 6.60; N, 3.95.

(±)-Tetrahydrocorysamine (**21c**): Yield: 55%. Colorless needles. mp 203—204 °C (MeOH) (mp 210—211 °C[16], 207—209 °C[12]). ^{1}H-NMR δ: 6.71, 6.66 (each 1H, AB-q, J=8 Hz, Ar-H×2), 6.68, 6.58 (each 1H, each s, Ar-H×2), 5.95, 5.91 (each 1H, AB-q, J=1.3 Hz, OCH_2O), 5.93, 5.92 (each 1H, AB-q, J=1.0 Hz, OCH_2O), 4.06, 3.48 (each 1H, AB-q, J=15 Hz, C_8-H), 3.7—2.53 (6H, m, C_5, C_6, C_{13}, C_{13a}-H), 0.95 (3H, d, J=7 Hz, C_{13}-Me). MS *m/z* (%): 337 (M^+, 21), 162 (100). *Anal.* Calcd for $C_{20}H_{19}NO_4$: C, 71.20; H, 5.68; N, 4.15. Found: C, 71.31; H, 5.72; N, 4.13.

(±)-13-Ethyltetrahydropalmatine (**22a**): Yield: 63%. Colorless needles. mp 127—128 °C (MeOH). ^{1}H-NMR δ: 6.90, 6.80 (each 1H, AB-q, J=8.8 Hz, Ar-H×2), 6.70, 6.62 (each 1H, each s, Ar-H×2), 4.23, 3.52 (each 1H, AB-q, J=16 Hz, C_8-H), 3.88, 3.87 (each 3H, each s, OMe×2), 3.86 (6H, s, OMe×2), 3.2—2.9 (6H, m, C_5, C_6, C_{13}, C_{13a}-H), 1.53—1.32 (2H, m, $C\underline{H}_2$Me), 0.79 (3H, t, J=7.3 Hz, $CH_2\underline{Me}$). MS *m/z* (%): 383 (M^+, 42), 193 (19), 192 (100). *Anal.* Calcd for $C_{23}H_{29}NO_4$: C, 72.03; H, 7.62; N, 3.65. Found: C, 72.21; H, 7.69; N, 3.66.

Acknowledgement We are grateful to Professor M. Yamauchi, Faculty of Pharmaceutical Sciences, Josai University, for calculation of electron density of *N*-(2,3-dimethoxybenzyl)-*N*-(3,4-dimethoxyphenethyl)acetamide. Financial support from the Ministry of Education, Science, Sports and Culture of Japan in the form of a Grant-in-Aid for Scientific Research is also gratefully acknowledged.

References and Notes

1) Dedicated to the memory of Professor Yasumitsu Tamura.
2) A part of this work was published as a preliminary communication: Yasuda S., Hirasawa T., Hanaoka M., *Tetrahedron Lett.*, **28**, 2399—2402 (1987).
3) *a*) Bhakuni D. S., Jain S., "The Alkaloids," Vol. 28, ed. by Brossi A., Academic Press, Orlando, 1986, pp. 95—181; *b*) Hanaoka M., "The Alkaloids," Vol. 33, ed. by Brossi A., Academic Press, San Diego, 1988, pp. 141—230; *c*) Iwasa K., "The Alkaloids," Vol. 46, ed. by Cordell G. A., Academic Press, San Diego, 1995, pp. 273—346; *d*) Bentley K. W., *Natural Products Reports*, **5**, 270—272 (1988); **6**, 411—413 (1989); **7**, 249—251 (1990); **8**, 345—346 (1991); **9**, 370—372 (1992); **10**, 454—455 (1993); **11**, 559—561 (1994); **12**, 424—425 (1995); **13**, 131—132 (1996); **14**, 392—393 (1997); **15**, 345—347 (1998); **16**, 371—372 (1999).
4) Battersby A. R., Southgate R., Staunton J., Hirst M., *J. Chem. Soc. (C)*, **1966**, 1052—1057.
5) *a*) Pandey G. D., Tiwari K. P., *Heterocycles*, **16**, 449—485 (1981); *b*) Nagata W., Itazaki H., Okada K., Wakabayashi T., Shibata K., Tokutake N., *Chem. Pharm. Bull.*, **23**, 2867—2877 (1975); *c*) Chatterjee A., Ghosh S., *Synthesis*, **1981**, 818—820; *d*) Patra A., Mukhopadhyay P. K., Ghosh G., *Indian J. Chem.*, **21B**, 173—175 (1982); *e*) Pandey G. D., Tiwari K. P., *ibid.*, **19B**, 66—68 (1980); *f*) *Idem*, *Synth. Comm.*, **10**, 607—610 (1980); *g*) Narasimhan N. S., Mali R. S., Kulkarni B. K., *Tetrahedron*, **39**, 1975—1982 (1983); *h*) Mali R. S., Borse A. U., *Synth. Comm.*, **19**, 2613—2619 (1989); *i*) Mali R. S., Borse A. U., Patil S. D., *Indian J. Chem.*, **28B**, 107—109 (1989); *j*) Mali R. S., Bodkhe Y. T., Gulati N. V., *J. Indian Inst. Sci.*, **74**, 205—211 (1994).
6) Tamura Y., Uenishi J., Maeda H., Choi H., Ishibashi H., *Synthesis*, **1981**, 534—537.
7) Vanderlaan D. G., Schwartz M. H., *J. Org. Chem.*, **50**, 743—747 (1985).
8) Electron density of *N*-(2,3-dimethoxybenzyl)-*N*-(3,4-dimethoxyphenethyl)acetamide, the de(methylthio) derivative of the amide (**5**), in its two most stable conformations was calculated by PM 3. Electron density (−0.202 and −0.198) of C-6′ on the phenethyl aromatic ring is larger than that (−0.189 and −0.187, respectively) of C-6″ on the benzyl aromatic ring.
9) Harley-Mason J., *J. Chem. Soc.*, **1953**, 200—203.
10) Ishii H., Cheu I., Ueki S., Masuda T., Morita K., Ishikawa T., *J. Chem. Soc., Perkin Trans. 1*, **1987**, 2415—2420.
11) *a*) Ninomiya I., Takasugi H., Naito T., *Heterocycles*, **1**, 17—20 (1973); *b*) Pai B. R., Natarajan S., Muikumar G., Rajaraman R., Suguma H., *J. Org. Chem.*, **43**, 1992—1994 (1978); *c*) Dean R. T., Rapoport H., *ibid.*, **43**, 4183—4189 (1978); *d*) Iwasa K., Gupta Y. D., Cushman M., *ibid.*, **46**, 4744—4750 (1981); *e*) Tietze Z. F., Brill G., *Justus Liebigs Ann. Chem.*, **1987**, 311—319; *f*) Mali R. S., Patil S. D., *Indian J. Chem.*, **27B**, 887—890 (1988).
12) Synthesis of 13-methylprotoberberine alkaloids from corresponding protoberberine alkaloids by 13-methylation: Hanaoka M. Yoshida S. Mukai C., *Chem. Pharm. Bull.*, **37**, 3264—3267 (1989) and references cited therein.
13) Hanaoka M., Nagami K., Hirai Y., Sakurai S., Yasuda S., *Chem. Pharm. Bull.*, **33**, 2273—2280 (1985).
14) Tani C., Takao N., Takao S., *Yakugaku Zasshi*, **82**, 748—750 (1962).
15) Iwasa K., Gupta Y. D., Cushman M., *Tetrahedron Lett.*, **22**, 2333—2336 (1981).
16) Kaneko H., Naruto S., Ikeda N., *Yakugaku Zasshi*, **88**, 235—238 (1968).

Studies on Lewis Acid-Mediated Intramolecular Cyclization Reactions of Allene–Ene Systems

Kunio HIROI,* Takashi WATANABE, and Akihiro TSUKUI

Department of Synthetic Organic Chemistry, Tohoku Pharmaceutical University, 4–4–1 Komatsushima, Aoba-ku, Sendai, Miyagi 981–8558, Japan. Received October 12, 1999; accepted November 15, 1999

The Lewis acid-mediated reactions of allene–ene compounds, derived from 3-methylcitronellal or dimethyl malonate, were carried out using various Lewis acids such as ethylaluminum dichloride, diethylaluminum chloride, titanium chloride, zinc chloride etherate, or boron trifluoride etherate, affording unexpectedly intramolecular [2+2]cycloaddition products under some particular reaction conditions without any formation of intramolecular ene reaction products.

Key words allene; [2+2]cycloaddition; Lewis acid; allene–ene system; intramolecular cycloaddition

Allene compounds have received much attention so far in regard to their unique chemical reactivity and specific stereochemical behavior, which arises from the structural characteristics of allenes; thus have been widely employed as a carbon three unit in organic synthesis.[1—11] Currently, much interest is being focused on the transition metal- or Lewis acid-catalyzed reactions of allenes, and our attention is paid to the use of the chirality of allenes in asymmetric synthesis,[12,13] especially with transition metal catalysts.[14,15] We describe in this report our recent works on allene chemistry, in particular, the unprecedented intramolecular [2+2]cycloaddition reactions[16—21] of inactivated allene and ene functionality by the assistance of Lewis acids. A paper concerning Lewis acid-mediated [2+2]cycloaddition reactions of activated allenes (conjugated allenic esters) has appeared,[22] however there has been no intramolecular Lewis acid-mediated [2+2] cycloaddition of simple allenes and enes.[23]

Previously, we reported Lewis acid-catalyzed asymmetric intramolecular ene reactions of 1,7-diene systems bearing a chiral sulfinyl group as a chiral electrophile. Further detailed studies on these reactions reveal that the mode of the cyclization depends on the activity of the electrophilic functional groups in the dienophiles and on the Lewis acid used.[24] Therefore we have taken much interest in the mode of cyclization of allene–ene systems, namely ene, hetero Diels–Alder, and/or [2+2]cycloaddition reactions, by the assistance of Lewis acids.

Allene–ene systems were constructed in the following way. Lithium or magnesium acetylides of **2a**—**c** attacked aldehyde in 3-methylcitronellal (**1**) derived from citral to give propargylic alcohol derivatives **3a**—**c** in excellent yields (83—96%). The corresponding acetates **4a**—**c** of the alcohols were reacted with methyl- or phenylmagnesium bromide in the presence of copper(I) iodide to afford allenyl compounds **5a**—**d** in fairly good yields.

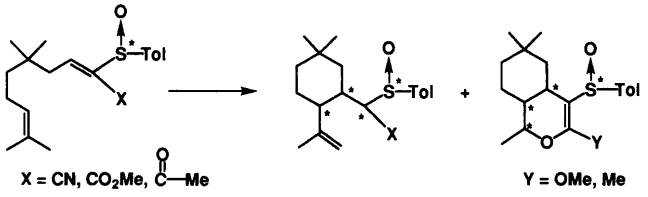

Chart 1

Allenylmalonate was prepared in the usual way. An allenenyl part **14** was prepared starting from 1,3-propanediol (**6**). The selective monosilylation of the diol[25] with *tert*-butyldiphenylchlorosilane (TBDPSCl), followed by Swern oxidation, gave 3-(*tert*-butyldiphenylsilyloxy)propanal (**8**). The addition of 1-propynylmagnesium bromide to the aldehyde in **8** afforded a propargylic alcohol derivative **9** in good yield. The acetate **10** of the alcohol **9** was reacted with methylmagnesium bromide in the presence of copper(I) iodide to furnish allene **11** in 90% yield. Removal of the silyl group in **11** by treatment with tetrabutylammonium fluoride (TBAF), followed by tosylation with TsCl-triethylamine and iodination of the tosylate **13** with NaI, gave 5-methyl-3,4-hexadienyl iodide (**14**).

Alkylation of dimethyl malonate with 3-methyl-2-butenyl bromide was carried out in the presence of sodium hydride to produce dimethyl (3-methyl-2-butenyl)propanedioate (**15**)[26] in 89% yield. The reaction of **15** with allenyl iodide **14** using sodium hydride as a base gave an allene–ene compound, dimethyl (3-methyl-2-butenyl)(5-methyl-3,4-hexadienyl)propanedioate (**16**), in 47% yield.

Studies on Lewis acid-mediated cyclization reactions of the allenyl compounds **5a**—**d** were undertaken under various reaction conditions using typical Lewis acids such as ethylaluminum dichloride ($EtAlCl_2$), diethylaluminum chloride (Et_2AlCl), titanium tetrachloride ($TiCl_4$), boron trifluoride etherate ($BF_3 \cdot OEt_2$), zinc chloride etherate ($ZnCl_2 \cdot OEt_2$), and zinc bromide ($ZnBr_2$). Upon treatment with $EtAlCl_2$ (1.5

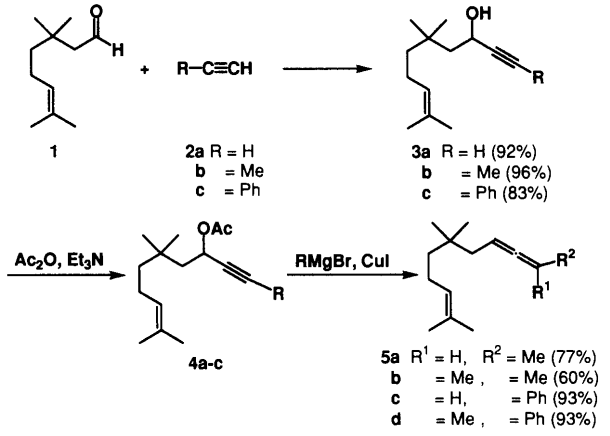

Chart 2

* To whom correspondence should be addressed.

© 2000 Pharmaceutical Society of Japan

or 3.0 eq) at −78 °C, the allenyl compound **5b** unexpectedly underwent a [2+2]cycloaddition reaction to give 8-isopropylidene-3,3,7,7-tetramethylbicyclo[4.2.0] octane (**17**) in a fairly good yield, as listed is Table 1.

However, polymerization occurred upon treatment with $EtAlCl_2$ (1.5 eq) at 0 °C, whereas the reaction using weaker acids, $ZnBr_2$ or $BF_3 \cdot OEt_2$ (3.0 eq), at room temperature recovered the starting material.

Thus, the reactions of **5b** with more acidic Lewis acids under milder reaction conditions gave a [2+2]cyclization product, whereas the reactions under more severe reaction conditions (at a much higher reaction temperature) resulted in polymerization of the starting material, or the reactions with weaker acids provided no cyclization product with recovery of the starting material.

Lewis acid-mediated reactions of other allene–ene compounds **5a**,**c**, and **d** provided no cycloaddition product, presumably due to the high reactivity of the allenyl system **5a** resulting in polymerization, the lability of the allene **5c** leading to decomposition, and the inaccessibility of **5d** by steric hindrance recovering the starting material.

Similarly, the Lewis acid-mediated reactions of another allenyl compound **16** provided the corresponding [2+2]cycloaddition product, dimethyl 8,8-dimethyl-7-isopropylidenebicyclo[4.2.0]octane-3,3-dicarboxylate (**18**) in considerably good yield, as shown in Table 1; however, the reactions were dependent upon the Lewis acids employed, much different from that of **5**.

Upon treatment with more weakly acidic Lewis acids such as $TiCl_4$, $ZnCl_2 \cdot OEt_2$, or $BF_3 \cdot OEt_2$ at room temperature (r.t.), the allene–ene compound **16** was converted into a [2+2]cycloaddition product **18** in 87, 77, and 92% yield, respectively. In contrast to the previous cases mentioned above, upon mediation with more acidic Lewis acids (3.0 eq) such as $EtAlCl_2$ (0 °C), Et_2AlCl (r.t.) or $ZnBr_2$ (r.t.), the allene–ene compound **16** underwent no desired cycloaddition, recovering the starting material. Upon treatment of **16** with stronger Lewis acid ($EtAlCl_2$) at r.t., however, polymerization occurred.

The results thus obtained are rationalized as follows. One of the π-bonds in the allenes **5b** and **16** is activated by the assistance of the Lewis acid used, generating more cationic β-carbon centers, and the intramolecular ene parts in **5b** and **16** attack the cationic β-carbon of the allenes to give [2+2]cycloaddition products **17** and **18**. The existence of a quarternary carbon close to the reaction center (allene) in **5b** makes the activation by the Lewis acid sterically rather inaccessible, compared with the case of **16**. However, in the case of the 1,7-allene–ene system **16** bearing ester groups, the preference of coordination of the ester carbonyl groups to the more acidic Lewis acids provides large steric interference by the two methoxy groups of the esters owing to the conformational fixation resulting from the coordination, thus giving the recovered starting material without any cycloaddition product. With weaker acids, insufficient coordination of the two ester carbonyl groups allows steric access from the allene to the ene part, giving a [2+2]cycloaddition product.

In conclusion, the [2+2]cycloaddition reactions of 1,7-allene–ene systems were largely dependent upon the acidity of the Lewis acid used and the reaction temperature. The simple 1,7-allene–ene compound **5b** without any functional group underwent a [2+2]cycloaddition reaction upon treatment with more acidic Lewis acid ($EtAlCl_2$) at milder reaction conditions (at −78 °C) in dichloromethane, however, poly-

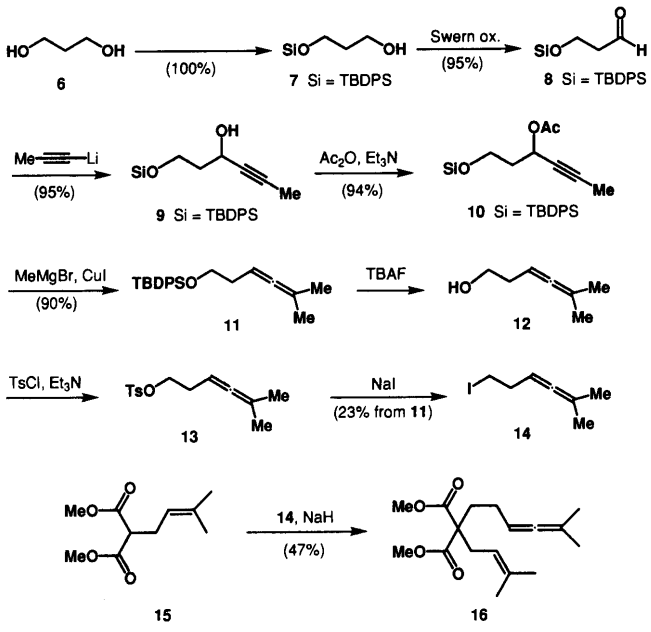

Chart 3

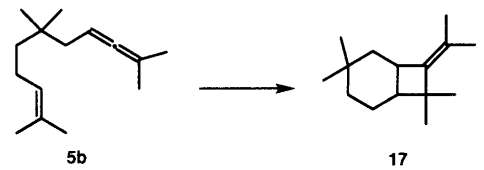

Chart 4

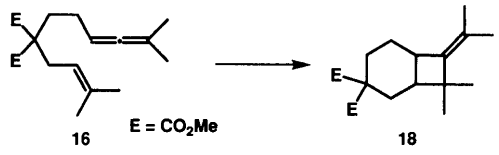

Chart 5

Table 1. Studies on Lewis Acid-Mediated Reactions of Allene–Ene Systems

Substrate	Lewis acid (eq)	Solvent	Reaction temp. (°C)	Reaction time (h)	Product yield (%)
5b	$EtAlCl_2$ (1.5)	CH_2Cl_2	−78	0.5	82 (**17**)
5b	$EtAlCl_2$ (3.0)	CH_2Cl_2	−78	1	93 (**17**)
5b	Et_2AlCl (1.5)	Toluene	−78	1	79 (**17**)
16	$TiCl_4$ (3.0)	CH_2Cl_2	r.t.	22	87 (**18**)
16	$ZnCl_2 \cdot OEt_2$ (3.0)	CH_2Cl_2	r.t.	24	77 (**18**)
16	$BF_3 \cdot OEt_2$ (7.0)	CH_2Cl_2	r.t.	23	92 (**18**)

merization occurred at a higher reaction temperature (0 °C). On the other hand, the 1,7-allene–ene system **16** bearing ester groups gave a [2+2]cycloaddition product upon treatment with rather weaker acids (3.0—7.0 eq) such as $TiCl_4$, $ZnCl_2 \cdot OEt_2$, and $BF_3 \cdot OEt_2$ at r.t., whereas with more acidic Lewis acids (3.0 eq) such as $EtAlCl_2$ (0 °C), Et_2AlCl (r.t.), and $ZnBr_2$ (r.t.), no reaction occurred with recovery of the starting material.

Experimental

Infrared (IR) spectra were obtained in the indicated state with a JASCO DR-81 fourier-transform IR spectrometer. NMR spectra were determined in the indicated solvent with a JEOL EX-270 (^{1}H-NMR; 270 MHz) high-resolution NMR spectrometer; chemical shifts are given in ppm from tetramethylsilane as an internal standard. Splitting patterns are designated as s: singlet, br s: broad singlet, d: doublet, dd: double of doublet, dt: triple of doublet, t: triplet, tt: triple of triplet, tq: quartet of triplet, m: multiplet. Mass spectra were taken on a JEOL JMS-DX 303/JMA-DA 5000 system. Flash column chromatography was performed with Merck Silica gel 60 (230—400 mesh).

5,5,9-Trimethyl-8-decen-1-yn-3-ol (3a) A 0.5 M tetrahydrofuran (THF) solution of ethynylmagnesium bromide (16.4 ml, 8.21 mmol) was added at 0 °C to a solution of 3,3,7-trimethyl-6-octen-1-al (**1**) (920 mg, 5.48 mmol) in THF (10 ml), and the reaction mixture was stirred at the same temperature for 30 min, then at room temperature for 5 h. The reaction mixture was diluted with ether and the solution was washed with 20% aqueous NH_4Cl and saturated aqueous NaCl, dried over anhydrous $MgSO_4$, and concentrated *in vacuo*. The crude product was subjected to flash column chromatography (ether–hexane, 1 : 4) to give **3a** (978 mg, 92% yield).

The reaction of **1** (2.29 g, 13.63 mmol) with 0.5 M THF solution of 1-propynylmagnesium bromide (40.9 ml, 20.45 mmol) was carried out using the same procedure as described above to give 2,6,6-trimethyl-2-undecen-9-yn-8-ol (**3b**) (2.71 g, 96% yield).

3a: IR (neat, cm^{-1}): 3380 (alcohol), 3310 (acetylene), 2260 (acetylene), 1630 (olefin). ^{1}H-NMR ($CDCl_3$) δ: 1.00 (6H, s, $C(CH_3)_2$), 1.08—1.52 (4H, m, $(CH_2)_2$), 1.61, 1.68 (6H, s, s, $C=C(CH_3)_2$), 1.78 (1H, s, C≡CH), 2.38 (1H, br s, OH), 2.65 (2H, d, J=2.0 Hz, $C\underline{H}_2CHOH$), 4.42 (1H, br s, $C\underline{H}OH$), 5.09 (1H, m, CH=C). MS *m/z*: 194 (M^+). Exact mass determination: 194.1671 (Calcd $C_{13}H_{22}O$: 194.1671).

3b: IR (neat, cm^{-1}): 3380 (alcohol), 2230 (acetylene), 1650 (olefin). ^{1}H-NMR ($CDCl_3$) δ: 0.95 (6H, s, $C(CH_3)_2$), 1.05—1.42 (4H, m, $(CH_2)_2$), 1.59, 1.65 (6H, s, s, $C=C(CH_3)_2$), 1.67 (2H, d, J=5.4 Hz, $C\underline{H}_2CHOH$), 1.78 (3H, d, J=2.1 Hz, $C\equiv CCH_3$), 2.11 (1H, br s, OH), 4.31 (1H, br s, $C\underline{H}OH$), 4.96 (1H, m, CH=C). MS *m/z*: 208 (M^+). Exact mass determination: 208.1779 (Calcd $C_{14}H_{24}O$: 208.1827).

1-Phenyl-5,5,9-trimethyl-8-decen-1-yn-3-ol (3c) A 1.54 M hexane solution of *n*-butyllithium (2.1 ml, 3.21 mmol) was added at −78 °C to a solution of phenylacetylene (0.41 ml, 3.75 mmol) in THF (10 ml), and the reaction mixture was stirred at the same temperature for 30 min. A solution of **1** (450 mg, 2.68 mmol) in THF (10 ml) was added to the above solution, and the reaction mixture was stirred at −78 °C for 1 h, quenched by the addition of saturated aqueous NH_4Cl at the same temperature, and then stirred for an additional hour. The reaction mixture was gradually warmed to room temperature and diluted with ether, and the solution was washed with saturated aqueous NH_4Cl and saturated aqueous NaCl, dried over anhydrous $MgSO_4$, and concentrated *in vacuo*. The crude product was subjected to flash column chromatography (ether–hexane, 1 : 8) to give **3c** (598 mg, 83% yield).

3c: IR (neat, cm^{-1}): 3340 (alcohol), 2260 (acetylene), 1650 (olefin), 1590 (aromatic). ^{1}H-NMR ($CDCl_3$) δ: 1.02 (6H, s, $C(CH_3)_2$), 1.12—1.47 (4H, m, $(CH_2)_2$), 1.60, 1.67 (6H, s, s, $C=C(CH_3)_2$), 1.81 (2H, d, J=6.4 Hz, $C\underline{H}_2CHOH$), 2.27 (1H, br s, OH), 4.67 (1H, t, J=6.5 Hz, $C\underline{H}OH$), 5.09 (1H, m, CH=C), 7.03—7.55 (5H, m, C_6H_5). MS *m/z*: 270 (M^+). Exact mass determination: 270.2076 (Calcd $C_{19}H_{26}O$: 270.1984).

3-Acetoxy-5,5,9-trimethyl-8-decen-1-yne (4a) Acetic anhydride (0.71 ml, 7.50 mmol) was added to a solution of **3a** (970 mg, 5.00 mmol) and triethylamine (2.1 ml, 15.00 mmol) in dichloromethane (10 ml) at room temperature. 4-Dimethylaminopyridine (30 mg, 0.25 mmol) was added to the above solution, and the reaction mixture was stirred at room temperature for 12 h. The reaction mixture was diluted with ether and the solution was washed with water and saturated aqueous NaCl, dried over anhydrous $MgSO_4$, and concentrated *in vacuo*. The crude product was subjected to flash column chromatography (ether–hexane, 1 : 9) to give **4a** (1.15 g, 98% yield).

The reaction of **3b** (2.71 g, 13.03 mmol) or **3c** (590 mg, 2.19 mmol) was carried out using the same procedure as described above to give 4-acetoxy-6,6,10-trimethyl-9-undecen-2-yne (**4b**) (3.15 g, 97% yield) or 3-acetoxy-1-phenyl-5,5,9-trimethyl-8-decen-1-yne (**4c**) (626 mg, 92% yield), respectively.

4a: IR (neat, cm^{-1}): 3280 (acetylene), 2250 (acetylene), 1740 (ester), 1660 (olefin). ^{1}H-NMR ($CDCl_3$) δ: 0.97 (6H, s, $C(CH_3)_2$), 1.06—1.44 (4H, m, $(CH_2)_2$), 1.63, 1.68 (6H, s, s, $C=C(CH_3)_2$), 1.81 (2H, d, J=6.3 Hz, $C\underline{H}_2CHO$), 2.05 (3H, s, $COCH_3$), 2.45 (1H, d, J=1.9 Hz, C≡CH), 5.07 (1H, m, CH=C), 5.42 (1H, dt, J=6.5, 2.0 Hz, CHO). MS *m/z*: 236 (M^+). Exact mass determination: 236.1799 (Calcd $C_{15}H_{24}O_2$: 236.1776).

4b: IR (neat, cm^{-1}): 2250 (acetylene), 1740 (ester), 1670 (olefin). ^{1}H-NMR ($CDCl_3$) δ: 0.95 (6H, s, $C(CH_3)_2$), 1.05—1.43 (4H, m, $(CH_2)_2$), 1.62, 1.70 (6H, s, s, $C=(CH_3)_2$), 1.77—1.93 (5H, m, $C\underline{H}_2CHC{\equiv}CC\underline{H}_3$), 2.04 (3H, s, $COCH_3$), 5.08 (1H, m, CH=C), 5.41 (1H, tq, J=6.2, 1.9 Hz, CHO). MS *m/z*: 250 (M^+). Exact mass determination: 250.1967 (Calcd $C_{16}H_{26}O_2$: 250.1933).

4c: IR (neat, cm^{-1}): 2220 (acetylene), 1740 (ester), 1660 (olefin), 1590 (aromatic). ^{1}H-NMR ($CDCl_3$) δ: 1.01 (6H, s, $C(CH_3)_2$), 1.12—1.49 (4H, m, $(CH_2)_2$), 1.62, 1.68 (6H, s, s, $C=C(CH_3)_2$), 1.90 (2H, d, J=6.7 Hz, $C\underline{H}_2CHO$), 2.07 (3H, s, CH_3CO), 5.09 (1H, m, CH=C), 5.70 (1H, t, J=6.6 Hz, CHO), 7.03—7.58 (5H, m, C_6H_5). MS *m/z*: 312 (M^+). Exact mass determination: 312.2122 (Calcd $C_{21}H_{28}O_2$: 312.2090).

2,6,6-Trimethyl-2,8,9-undecatriene (5a) A 3.0 M ether solution of methylmagnesium bromide (9.75 ml, 29.24 mmol) was added at −78 °C to a suspension of copper(I) iodide (2.78 g, 14.62 mmol) and lithium chloride (620 mg, 14.62 mmol) in THF (30 ml), and the reaction mixture was stirred at the same temperature for 1 h. A solution of **4a** (1.15 g, 4.87 mmol) in THF (20 ml) was added to the above solution, and the reaction mixture was stirred at −78 °C for 4 h. The reaction mixture was gradually warmed to −20 °C, quenched by the addition of saturated aqueous NH_4Cl at the same temperature and stirred for an additional hour. The reaction mixture was allowed to warm to room temperature and was diluted with ether, then the solution was washed with saturated aqueous NH_4Cl and saturated aqueous NaCl, dried over anhydrous $MgSO_4$, and concentrated *in vacuo*. The crude product was subjected to flash column chromatography (hexane) to give **5a** (720 mg, 77% yield).

The reaction of **4b** (3.10 g, 12.40 mmol) or **4c** (600 mg, 1.92 mmol) with Me_2CuLi was carried out using the same procedure as described above to give 2,6,6,10-tetramethyl-2,3,9-undecatriene (**5b**) (1.53 g, 60% yield) or 2-phenyl-6,6,10-trimethyl-2,3,9-undecatriene (**5d**) (478 mg, 93% yield), respectively, and the reaction of **4a** (1.35 g, 5.72 mmol) with Ph_2CuLi was carried out using the same procedure as described above to give 1-phenyl-5,5,9-trimethyl-1,2,8-decatriene (**5c**) (1.35 g, 93% yield).

5a: IR (neat, cm^{-1}): 1950 (allene), 1660 (olefin). ^{1}H-NMR ($CDCl_3$) δ: 0.90 (6H, s, $C(CH_3)_2$), 1.05—1.52 (4H, m, $(CH_2)_2$), 1.62, 1.68 (6H, s, s, $C=C(CH_3)_2$), 1.78—2.23 (5H, m, $C\underline{H}_2CH=C=CHC\underline{H}_3$), 4.42—4.75 (1H, m, $C\underline{H}CH_3$), 4.77—5.30 (2H, m, $CH_2C\underline{H}=C\times2$). MS *m/z*: 192 ($M^+$). Exact mass determination: 192.1801 (Calcd $C_{14}H_{24}$: 192.1878).

5b: IR (neat, cm^{-1}): 1970 (allene), 1650 (olefin). ^{1}H-NMR ($CDCl_3$) δ: 0.88 (6H, s, $C(CH_3)_2$), 1.02—1.42 (4H, m, $(CH_2)_2$), 1.53—1.77 (12H, m, $C=C(CH_3)_2\times2$), 1.86 (2H, d, J=7.9 Hz, $CH_2C=C=C$), 4.63—5.27 (2H, m, $CH=C\times2$). MS *m/z*: 206 (M^+). Exact mass determination: 206.2030 (Calcd $C_{15}H_{26}$: 206.2034).

5c: IR (neat, cm^{-1}): 1950 (allene), 1660 (olefin), 1600 (aromatic). ^{1}H-NMR ($CDCl_3$) δ: 0.97 (6H, s, $C(CH_3)_2$), 1.08—1.45 (4H, m, $(CH_2)_2$), 1.58, 1.68 (6H, s, s, $C=C(CH_3)_2$), 2.05 (2H, dd, J=7.7, 2.3 Hz, $CC\underline{H}_2CH$), 5.08 (1H, m, $C\underline{H}=C(CH_3)_2$), 5.47 (1H, dt, J=7.8, 3.7 Hz, $CH_2C\underline{H}=C=CH$), 5.93—6.17 (1H, m, $C\underline{H}C_6H_5$), 7.00—7.67 (5H, m, C_6H_5). MS *m/z*: 254 (M^+). Exact mass determination: 254.1939 (Calcd $C_{19}H_{26}$: 254.2034).

5d: IR (neat, cm^{-1}): 1950 (allene), 1670 (olefin), 1600 (aromatic). ^{1}H-NMR ($CDCl_3$) δ: 0.94 (6H, s, $C(CH_3)_2$), 1.07—1.52 (4H, m, $(CH_2)_2$), 1.59, 1.67 (6H, s, s, $CH=C(C\underline{H}_3)_2$), 2.00 (2H, d, J=5.5 Hz, $C\underline{H}_2CH=C=C$), 2.08 (3H, s, $C=C=CCH_3$), 4.91—5.70 (2H, m, $CH=C\times2$), 7.03—7.58 (5H, m, C_6H_5). MS *m/z*: 268 (M^+). Exact mass determination: 268.2139 (Calcd $C_{20}H_{28}$: 268.2191).

3-(*tert*-Butyldiphenylsilyloxy)-1-propanol (7) A 50 ml two-necked flask equipped with a septum inlet and a magnetic stirring bar, and containing sodium hydride (50% oil dispersion; 630 mg, 13.14 mmol) was flushed with argon, and maintained under a positive pressure of argon. THF (10 ml) and a solution of 1,3-propandiol (**6**) (1.00 g, 13.14 mmol) in THF (10 ml) were added to the above flask. The reaction mixture was stirred at room temperature for 1 h. A solution of TBDPSCl (3.68 g, 13.14 mmol) in THF (10 ml)

was added to the above solution at 0 °C, and the mixture was stirred at 0 °C for 2 h. The reaction mixture was allowed to warm to room temperature, was diluted with ether, then the solution was washed with saturated aqueous $NaHCO_3$ and saturated aqueous NaCl, dried over anhydrous $MgSO_4$, and concentrated *in vacuo*. The crude product was subjected to flash column chromatography (ether–hexane, 1 : 1) to give **7** (4.13 g, 100% yield).

7: IR (neat, cm^{-1}): 3260 (alcohol), 1580 (aromatic). ^{1}H-NMR ($CDCl_3$) δ: 1.03 (9H, s, $C(CH_3)_3$), 1.77 (2H, tt, J=5.7, 5.7 Hz, $CH_2C\underline{H}_2CH_2$), 2.33 (1H, m, OH), 3.58—3.92 (4H, m, $C\underline{H}_2CH_2C\underline{H}_2$), 7.04—7.65 (10H, m, $C_6H_5\times2$). MS *m/z*: 314 (M^+). Exact mass determination: 314.1731 (Calcd $C_{19}H_{26}O_2Si$: 314.1702).

3-(*tert*-Butyldiphenylsilyloxy)-1-propanal (8) A solution of dimethyl sulfoxide (0.68 ml, 9.54 mmol) in dichloromethane (10 ml) was added to a solution of oxalyl chloride (0.42 ml, 4.77 mmol) in dichloromethane (10 ml) at −78 °C. After the mixture was stirred for 30 min, a solution of **7** (1.00 g, 3.18 mmol) in dichloromethane (10 ml) was added to the above solution at −78 °C, and the mixture was stirred at the same temperature for 1 h. Triethylamine (4.0 ml, 28.62 mmol) was then added to the reaction mixture, which was gradually warmed to room temperature. The reaction mixture was washed with water and saturated aqueous NaCl, dried over anhydrous $MgSO_4$, and concentrated *in vacuo*. The crude product was subjected to flash column chromatography (ether–hexane, 1 : 4) to give **8** (948 mg, 95% yield).

8: IR (neat, cm^{-1}): 1720 (aldehyde), 1580 (aromatic). ^{1}H-NMR ($CDCl_3$) δ: 1.04 (9H, s, $C(CH_3)_3$), 2.57 (2H, dt, J=5.8, 1.8 Hz, CH_2CO), 4.00 (2H, t, J=5.8 Hz, CH_2O), 7.16—7.81 (10H, m, $C_6H_5\times2$), 9.75 (1H, t, J=1.8 Hz, CHO). MS *m/z*: 312 (M^+). Exact mass determination: 312.1499 (Calcd $C_{19}H_{24}O_2Si$: 312.1546).

1-(*tert*-Butyldiphenylsilyloxy)-4-hexyn-3-ol (9) A 0.5 M THF solution of 1-propynylmagnesium bromide (19.2 ml, 9.60 mmol) was added at 0 °C to a solution of **8** (2.00 g, 6.40 mmol) in THF (19.2 ml), and the reaction mixture was stirred at room temperature for 3.5 h. The reaction mixture was diluted with ether, and the solution was washed with 20% aqueous NH_4Cl and saturated aqueous NaCl, dried over anhydrous $MgSO_4$, and concentrated *in vacuo*. The crude product was subjected to flash column chromatography (ether–hexane, 1 : 2) to give **9** (2.14 g, 95% yield).

9: IR (neat, cm^{-1}): 3400 (alcohol), 2240 (acetylene), 1590 (aromatic). ^{1}H-NMR ($CDCl_3$) δ: 1.07 (9H, s, $C(CH_3)_3$), 1.62—2.17 (5H, m, $C\underline{H}_2CHC{\equiv}CC\underline{H}_3$), 3.05 (1H, d, J=5.6 Hz, OH), 3.87 (2H, t, J=5.2 Hz, CH_2O), 4.65 (1H, br s, $C\underline{H}OH$), 7.12—7.82 (10H, m, $C_6H_5\times2$). MS *m/z*: 352 (M^+). Exact mass determination: 352.1812 (Calcd $C_{22}H_{28}O_2Si$: 352.1859).

3-Acetoxy-1-(*tert*-butyldiphenylsilyloxy)-4-hexyne (10) Acetic anhydride (0.63 ml, 6.70 mmol) was added to a solution of **9** (1.57 g, 4.47 mmol) and triethylamine (1.87 ml, 13.40 mmol) in dichloromethane (15 ml) at room temperature. 4-Dimethylaminopyridine (27 mg, 0.22 mmol) was added to the above solution, and the reaction mixture was stirred at room temperature for 6 h. The reaction mixture was diluted with ether and the solution was washed with saturated aqueous NaCl, dried over anhydrous $MgSO_4$, and concentrated *in vacuo*. The crude product was subjected to flash column chromatography (ether–hexane, 1 : 9) to give **10** (1.66 g, 94% yield).

10: IR (neat, cm^{-1}): 2250 (acetylene), 1740 (ester), 1590 (aromatic). ^{1}H-NMR ($CDCl_3$) δ: 1.07 (9H, s, $C(CH_3)_3$), 1.79 (3H, d, J=1.9 Hz, $CH_3C{\equiv}C$), 1.88—2.21 (5H, m, $C\underline{H}_2CHOCOC\underline{H}_3$), 3.77 (2H, t, J=6.0 Hz, OCH_2), 5.56 (1H, tq, J=6.8, 2.2 Hz, CHOCO), 7.12—7.81 (5H, m, C_6H_5). MS *m/z*: 394 (M^+). Exact mass determination: 394.1959 (Calcd $C_{24}H_{30}O_3Si$: 394.1964).

1-(*tert*-Butyldiphenylsilyloxy)-5-methyl-3,4-hexadiene (11) A 3.0 M ether solution of methylmagnesium bromide (4.20 ml, 12.62 mmol) was added at −78 °C to a suspension of copper(I) iodide (1.2 g, 6.31 mmol) in THF (43 ml), and the reaction mixture was stirred at −78 °C for 1 h. A solution of **10** (1.66 g, 4.21 mmol) in THF (20 ml) was added to the above solution, and the reaction mixture was stirred at −78 °C for 2 h. The reaction mixture was gradually warmed to −10 °C, and quenched by the addition of 20% aqueous NH_4Cl at the same temperature and stirred for an additional hour. The reaction mixture was allowed to warm to room temperature and was diluted with ether, then the solution was washed with 20% aqueous NH_4Cl and saturated aqueous NaCl, dried over anhydrous $MgSO_4$, and concentrated *in vacuo*. The crude product was subjected to flash column chromatography (ether–hexane, 1 : 9) to give **11** (1.32 g, 90% yield).

11: IR (neat, cm^{-1}): 1970 (allene), 1590 (aromatic). ^{1}H-NMR ($CDCl_3$) δ: 1.07 (9H, s, $C(CH_3)_3$), 1.63 (6H, d, J=2.7 Hz, $C{=}C(CH_3)_2$), 2.21 (2H, dt, J=7.1, 6.8 Hz, $C\underline{H}_2CH{=}C$), 3.70 (2H, t, J=6.7 Hz, OCH_2), 4.70—5.15 (1H, m, CH=C), 7.07—7.82 (10H, m, $C_6H_5\times2$). MS *m/z*: 350 (M^+). Exact mass determination: 350.2017 (Calcd $C_{23}H_{30}OSi$: 350.2066).

1-Iodo-5-methyl-3,4-hexadiene (14) A 1.0 M THF solution of TBAF (6.9 ml, 6.90 mmol) was added at room temperature to a solution of **11** (1.21 g, 3.451 mmol) in THF (10 ml) and the reaction mixture was stirred at the same temperature for 2 h. The reaction mixture was diluted with ether, then the solution was washed with water and saturated aqueous NaCl, dried over anhydrous $MgSO_4$, and concentrated *in vacuo*. The crude product of 5-methy-3,4-hexadien-1-ol (**12**) was used in the next step without further purification. TsCl (990 mg, 5.18 mmol) was added to a solution of the crude alcohol **12** obtained above and triethylamine (1.4 ml, 10.04 mmol) in dichloromethane (10 ml) at 0 °C. 4-Dimethylaminopyridine (21 mg, 0.17 mmol) was added to the above solution, and the reaction mixture was stirred at 0 °C for 1 h and then at room temperature for 12 h. The reaction mixture was diluted with ether, and the solution was washed with water and saturated aqueous NaCl, dried over anhydrous $MgSO_4$, and concentrated *in vacuo*. The crude product of 2-methy-6-(*p*-toluenesulfonyloxy)-2,3-hexadiene (**13**) was used in the next step without further purification. A crude product **13** obtained above was dissolved in acetone (30 ml), then NaI (1.4 ml, 34.51 mmol) was added at room temperature. The reaction mixture was stirred at room temperature for 21 h, then filtered. The filtrate was concentrated *in vacuo*. The crude product was subjected to flash column chromatography (hexane) to give **14** (174 mg, 23% yield from **11**).

14: IR (neat, cm^{-1}): 1970 (allene). ^{1}H-NMR ($CDCl_3$) δ: 1.68 (6H, d, J=2.3 Hz, $C(CH_3)_2$), 2.45 (2H, dt, J=7.5, 6.9 Hz, $C\underline{H}_2CH_2I$), 3.15 (2H, t, J=7.0 Hz, CH_2I), 4.62—5.18 (1H, m, CH=C=C). MS *m/z*: 222 (M^+). Exact mass determination: 221.9961 (Calcd $C_7H_{11}I$: 221.9906).

Dimethyl (3-Methyl-2-butenyl)(5-methyl-3,4-hexadienyl)propanedioate (16) A 50 ml two-necked flask equipped with a septum inlet and a magnetic stirring bar, and containing sodium hydride (50% oil dispersion; 49 mg, 1.03 mmol) was flushed with argon, and maintained under a positive pressure of argon. THF (5 ml) and a solution of dimethyl (3-methyl-2-butenyl)propanedioate (**15**) (206 mg, 1.03 mmol) in THF (10 ml) were added to the above solution at 0 °C, and the reaction mixture was stirred at room temperature for 30 min. A solution of **14** (190 mg, 0.86 mmol) in THF (10 ml) was added to the above solution at 0 °C, and the mixture was stirred at room temperature for 48 h. The reaction mixture was diluted with ether, then the solution was washed with water and saturated aqueous NaCl, dried over anhydrous $MgSO_4$, and concentrated *in vacuo*. The crude product was subjected to flash column chromatography (ether–hexane, 1 : 9) to give **16** (118 g, 47% yield).

16: IR (neat, cm^{-1}): 1970 (allene), 1740 (ester), 1670 (olefin). ^{1}H-NMR ($CDCl_3$) δ: 0.87—1.24 (12H, m, $C{=}C(CH_3)_2\times2$), 1.80—1.99 (4H, m, $(CH_2)_2$), 2.60 (2H, d, J=7.1 Hz, $C\underline{H}_2CH$), 3.78 (6H, s, $C(CO_2CH_3)_2$), 4.71—5.14 (2H, m, CH=C×2). MS *m/z*: 294 (M^+). Exact mass determination: 294.1876 (Calcd $C_{17}H_{26}O_4$: 294.1831).

Lewis Acid–Mediated Intramolecular Cyclization Reactions of 5b. General Procedure A dry 25 ml two-necked flask equipped with a septum inlet and a magnetic stirring bar was flushed with argon and maintained under a positive pressure of argon. A 1.0 M hexane solution of Lewis acid was added at −78 °C to a solution of **5b** (100 mg, 0.49 mmol) in solvent (10 ml). The reaction mixture was stirred under the conditions listed in Table 1, then diluted with ether; the solution was then washed with saturated aqueous $NaHCO_3$ and saturated aqueous NaCl, dried over anhydrous $MgSO_4$, and concentrated *in vacuo*. The crude product was subjected to flash column chromatography (hexane) to give 8-(1-methylethylidene)-3,3,7,7-tetramethylbicyclo[4.2.0]octane (**17**). The yields of the product are summarized in Table 1.

17: IR (neat, cm^{-1}): 1680 (olefin). ^{1}H-NMR ($CDCl_3$) δ: 0.87—1.00 (12H, m, $C(CH_3)_2\times2$), 1.07—1.27 (6H, m, $CH_2\times3$), 1.29—1.46 (2H, m, CH×2), 1.54 (6H, s, $C{=}C(CH_3)_2$). MS *m/z*: 206 (M^+). Exact mass determination: 206.2055 (Calcd $C_{15}H_{26}$: 206.2034).

Lewis Acid–Mediated Intramolecular Cyclization Reactions of 16. General Procedure A dry 15 ml two-necked flask equipped with a septum inlet and a magnetic stirring bar was flushed with argon and maintained under a positive pressure of argon. A solution of Lewis acid in dichloromethane (1 ml) was added at 0 °C to a solution of **16** (30 mg, 0.10 mmol) in dichloromethane (2 ml). The reaction mixture was stirred under the conditions listed in Table 1, then diluted with ether; the solution was then washed with saturated aqueous $NaHCO_3$ and saturated aqueous NaCl, dried over anhydrous $MgSO_4$, and concentrated *in vacuo*. The crude product was subjected to flash column chromatography (ether–hexane, 1 : 9) to give dimethyl [8,8-dimethyl-7-(1-methylethylidene)bicyclo[4.2.0]octane] 3,3-dicarboxylate (**18**). The yields of the product are summarized in Table 1.

18: IR (neat, cm^{-1}): 1740 (ester), 1680 (olefin). ^{1}H-NMR ($CDCl_3$) δ: 0.92—1.05 (8H, m, $C(CH_3)_2$, $CH_2C\underline{H}_2CH$), 1.13—1.40 (2H, m, CH×2),

1.58 (6H, s, $C=C(CH_3)_2$), 1.80—2.55 (4H, m, $C(CH_2)_2$), 3.73 (6H, s, $C(CO_2CH_3)_2$). MS *m/z*: 294 (M^+). Exact mass determination: 294.1863 (Calcd $C_{17}H_{26}O_4$: 294.1831).

References

1) Taylor D. R., *Chem. Rev.*, **67**, 317—359 (1967).
2) Rossi R., Diversi P., *Synthesis*, **1973**, 25—36.
3) Smadija W., *Chem. Rev.*, **83**, 263—320 (1983).
4) Okamura W. H., *Acc. Chem. Res.*, **16**, 81—88 (1983).
5) Pasto D. J., *Tetrahedron*, **40**, 2805—2827 (1984).
6) Hayakawa K., *Yuki Gosei Kagaku Kyokai Shi*, **45**, 60—70 (1987).
7) Okamura W. H., Curtin M. L., *Synlett*, **1990**, 1—9.
8) Dzhemilev U. M., Khusnutdinov R. I., Tolstikov G. A., *J. Organomet. Chem.*, **409**, 15—65 (1991).
9) Kanematsu K., *Yakugaku Zasshi*, **112**, 693—711 (1992).
10) Nagashima S., Kanematsu K., *Yuki Gosei Kagaku Kyokai Shi*, **51**, 608—619 (1993).
11) Zimmer R., *Synthesis*, **1993**, 165—178.
12) Hiroi K., Kato F., Yamagata A., *Chem. Lett.*, **1998**, 397—398.
13) Hiroi K., Kato F., Nakasato H., *Chem. Lett.*, **1998**, 553—554.
14) Hiroi K., Kato F., *Annual Report of Tohoku College of Pharmacy*, **43**, 1—33 (1996).
15) Tsuji J., Mandai T., *Angew. Chem., Int. Ed. Engl.*, **34**, 2589—2612 (1995).
16) Schreiber S. L., *Science*, **227**, 857—863 (1985).
17) Bellus D., Ernst B., *Angew. Chem., Int. Ed. Engl.*, **27**, 797—827 (1988).
18) Demuth M., Mikhail G., *Synthesis*, **1989**, 145—162 .
19) Inoue Y., *Chem. Rev.*, **92**, 741—770 (1992).
20) De Keukeleire D., He S. -L., *Chem. Rev.*, **93**, 359—380 (1993).
21) Bach T., *Synthesis*, **1998**, 683—701.
22) Hiroi K., Watanabe T., to be published in due course.
23) Snider B. B., Ron E., *J. Org. Chem.*, **51**, 3643—3652 (1986).
24) Lukas J. H., Kouwenhoven A. P., Baardman F., *Angew. Chem.*, **87**, 740—741 (1975).
25) McDougal P. G., Rico J. G., Oh Y.-I., Condon B. D., *J. Org. Chem.*, **51**, 3388—3390 (1986).
26) Mook R., Jr., Sher P. M., *Org. Synth. Collect. Vol. VIII*, **1993**, 381—386.

Convenient Synthesis of 5-Trifluoroacetylated Imidazoles by Ring Transformation of Mesoionic 1,3-Oxazolium-5-olates

Masami KAWASE* and Setsuo SAITO

Faculty of Pharmaceutical Sciences, Josai University, 1–1 Keyakidai, Sakado, Saitama 350–0295, Japan.
Received October 14, 1999; accepted November 15, 1999

Mesoionic 4-trifluoroacetyl-1,3-oxazolium-5-olates (1), obtained from the reaction of *N*-acyl-*N*-alkylglycines (2) with trifluoroacetic anhydride, react with amidines to give 5-trifluoroacetylimidazoles (3) in moderate yield. The novel ring transformations of 1 into 3 occur *via* an initial attack of amidines on the C-2 position of the ring.

Key words: imidazole; 1,3-oxazolium-5-olate; trifluoroacetyl compound; ring transformation; trifluoroacetic anhydride

Trifluoromethyl ketones are interesting compounds in the design of enzyme inhibitors.[1] The concept of mimicking tetrahedral transition states of enzyme-mediated peptide bond hydrolysis previously led to the successful design and synthesis of trifluoroacetyl compounds as a promising class of proteinase inhibitors.[1] Recently, we have reported that heteroaromatic and aromatic trifluoromethyl ketones show interesting biological activities such as bactericidal activity[2a] and apoptosis-induced cytotoxic activity.[2b] However, there appear to be few practical procedures available for the synthesis of trifluoroacetyl substituted heterocycles, such as imidazoles and pyridines.[3] Generally, heterocycles, which are electron deficient, are resistant to electrophilic substitution reactions, such as Friedel–Crafts acylation.[4] Hence, an effective method for the synthesis of trifluoroacetylated heteroaromatic compounds is required.

Although the imidazole ring is an important residue and fluorinated systems are much sought after by medicinal and agricultural chemists,[5] trifluoroacetyl substituted imidazoles remain rare compounds.

In the course of our studies on the reactivities of mesoionic 1,3-oxazolium-5-olates,[6] we have focused on 4-trifluoroacetyl-1,3-oxazolium-5-olates (**1**) as useful synthons for trifluoromethyl-substituted heterocycles.[7] Compound **1** could easily be prepared from *N*-acyl-*N*-alkylglycines **2** with trifluoroacetic anhydride (TFAA).[8] In general, the mesoionic 1,3-oxazolium-5-olates are too unstable to be isolated and are utilized *in situ*.[6] However, compound **1** with 4-trifluoroacetyl group can be isolated and stored for several months. It is reported that compound **1** showed high reactivity towards nucleophilic reagents such as H_2O, EtOH, and AcOH, bringing about ring-opening reactions.[8] These reactions occur *via* an initial attack of a nucleophile on the C-5 position of the ring.[7d] We have been interested in the reactions of **1** with *N*-nucleophiles such as amidines,[7a] ammonia,[7b] hydrazines,[7c] and aminomalonate.[7e] In principle, nucleophilic reagents can be expected to be added to one of the three electrophilic centers at C-2, C-5, and $COCF_3$ in **1**. We now present a full account of the reactions of **1** with amidines[7a] and the new synthesis of 5-trifluoroacetylimidazoles **3**.

Results and Discussion

The 4-trifluoroacetyl-1,3-oxazolium-5-olates (**1a—d**) required for this study have been prepared by the reaction of *N*-acyl-*N*-alkylglycines (**2a—d**) with TFAA. The derivatives employed in this study, along with the products (**3a—h**, **4a—f**, **5a—b**), are summarized in Chart 1. Table 1 shows the results when 4-trifluoroacetyl-1,3-oxazolium-5-olate (**1a**) was allowed to react with formamidine under various conditions. The best result was obtained by the reaction of **1a** (1 mmol) with formamidine hydrochloride (1.5 mmol) in *N*,*N*-dimethylformamide (DMF) (5 ml) in the presence of potassium carbonate (1.5 mmol) at 70 °C for 2 h: 5-trifluoroacetylimidazole **3a** and dihydroimidazole **4a** were isolated in 63% and 19% yields, respectively (Table 1, run 5). Various substituted 4-trifluoroacetyl-1,3-oxazolium-5-olates **1a—d** were subjected to a reaction under the optimum conditions and the results are listed in Table 2. In all reactions examined, 4,5-dihydroimidazoles **4a—f** were isolated as side products, whose mechanism of formation is discussed later. In runs 7 and 8, **5a** and **5b** were also isolated, possibly formed *via* hydrolysis of the mesoionic 1,3-oxazolium-5-olates **1**.

A one-pot conversion of **2** to **3** also proceeded successfully. Thus, **2a** reacted with TFAA in CH_2Cl_2 to give **1a**, which was directly subjected to the ring transformation reaction to yield **3a** in 68% yield (Table 2, run 2). The one-pot procedure gave slightly higher yield. When acetamidine or benzamidine was used instead of formamidine, 4-methyl- and 4-phenylimidazole derivatives (**3e**, **3f**) were obtained in good yield, respectively (Table 2, runs 6, 7). Pentafluoropropionic and heptafluorobutyric anhydride also reacted readily with *N*-benzoyl-*N*-methylglycine **2a** to yield 5-pentafluoropropionyl- (**3g**) and 5-heptafluorobutyrylimidazole (**3h**) by the one-pot procedure in good yield, respectively (Table 2, runs 8, 9, Chart 1).

The structure of **3a—f** is supported by spectral and analytical data. The presence of the $COCF_3$ group in **3a—f** was determined on the basis of long-range ^{13}C–^{19}F coupling. Thus, the carbons of the $COCF_3$ group appear at around δ 116 ppm (quartet, $^1J_{C\text{-}F}$=280—290 Hz) and δ 170 ppm (quartet, $^2J_{C\text{-}F}$= 37—38 Hz). The ultimate proof of the structure of **3a** rests upon its conversion into the known[9] 5-formyl-1-methyl-2-phenylimidazole (**8**), as shown in Chart 2. Thus, treatment of **3a** with NaH followed by ethyl iodide afforded an ethyl ester (**6**).[10] In this reaction, compound **7** of formula $C_{15}H_{14}F_6N_2O$ was also isolated as a side product. The ^{1}H-NMR spectrum of **7** contained a signal of ethoxy protons, whereas the IR spectrum of **7** showed no carbonyl group. MS and analytical data indicated the existence of two trifluoromethyl groups, while the ^{13}C-NMR spectrum indicated only one trifluoromethyl group at δ 122 ppm (quartet, $^1J_{C\text{-}F}$=293 Hz). The reduction with $LiAlH_4$ of the ester **6**, followed by oxidation

* To whom correspondence should be addressed.

© 2000 Pharmaceutical Society of Japan

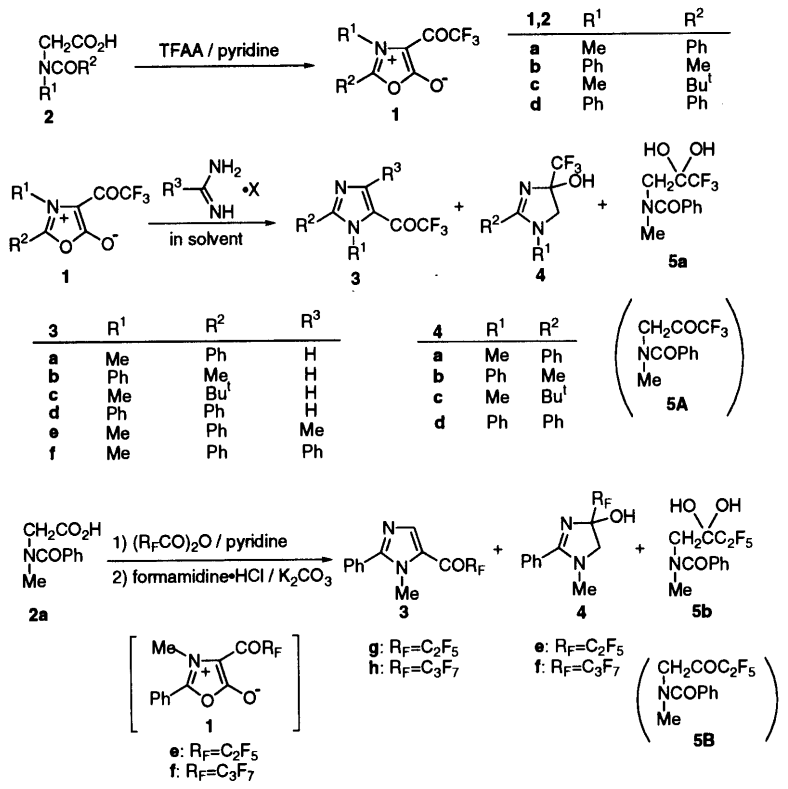

Chart 1

Table 1. Reactions of **1a** with Formamidine·X[a]

Run	X	Base (eq)[b]	Solvent	Product (%)		
				3a	**4a**	**5a**
1	HCl	None	Dioxane	5	9	74
2	HCl	Et_3N (3)	Dioxane	43	7	3
3	HCl	Pyridine (3)	Dioxane	9	—	81
4	HCl	K_2CO_3 (1.5)	Dioxane	42	10	3
5	HCl	K_2CO_3 (1.5)	DMF	63	19	—
6	HCl	K_2CO_3 (1.5)	$CHCl_3$	31	6	19
7	AcOH	K_2CO_3 (1.5)	DMF	55	38	—
8	AcOH	None	Dioxane	40	18	—

a) The reactions were carried out on a 1 mmol scale at 70 °C for 2 h. *b*) Eq refers to molar equivalents with respect to **1a**.

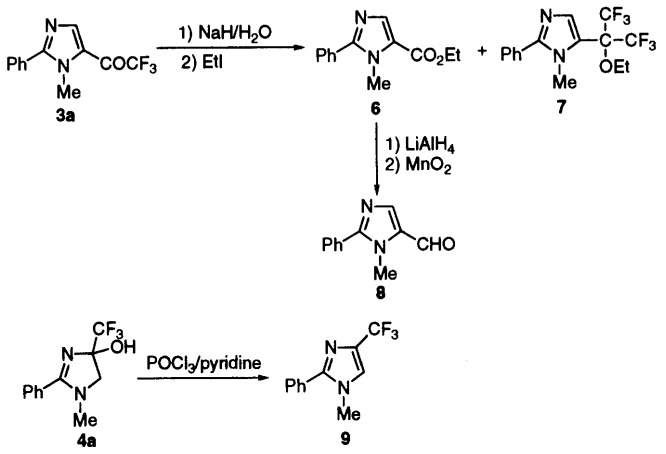

Chart 2

Table 2. Reactions of Mesoionic Compounds (**1**) or *N*-Acyl-*N*-alkylglycine (**2**) with Formamidine·HCl

Run	Starting material	Product (yield, %)
1	**1a**	**3a** (63), **4a** (19)
2	**2a**[a]	**3a** (68), **4a** (15)
3	**1b**	**3b** (55), **4b** (14)
4	**1c**	**3c** (49), **4c** (15)
5	**1d**	**3d** (54), **4d** (11)
6[b]	**1a**	**3e** (46), **4a** (16)
7[c]	**1a**	**3f** (55), **4a** (25), **5a** (4)
8[d]	**2a**[a]	**3g** (60), **4e** (14), **5b** (11)
9[e]	**2a**[a]	**3h** (56), **4f** (20)

a) Yields refer to the one-pot procedure using **2a**. *b*) Acetamidine·HCl was used instead of formamidine. *c*) Benzamidine·HCl was used instead of formamidine. *d*) Pentafluoropropionic anhydride was used instead of TFAA in a one-pot conversion procedure. *e*) Heptafluorobutyric anhydride was used instead of TFAA in a one-pot conversion procedure.

of the resulting alcohol with MnO_2, leads the known[9] 5-formyl-1-methyl-2-phenylimidazole **8** in a high overall yield.

The structure of **4a—f** was also deduced from spectroscopic data, and dehydration of **4a** with $POCl_3$ and pyridine[11] gave the known[12] 4-trifluoromethyl-1-methyl-2-phenylimidazole (**9**) in 88% yield (Chart 2).

The IR spectra of **5** did not exhibit an absorption band due to the trifluoroacetyl form (**5A** and **5B**), but a band represented the hydrated form. The ^{13}C-NMR spectra of **5a** and **5b** contained hydrated carbon signals appearing at 94.42 ($^2J_{C\text{-}F}$=32 Hz) and 95.50 ($^2J_{C\text{-}F}$=27 Hz), respectively.

Mechanistic Consideration The novel ring transformation of **1** into imidazoles **3** may proceed through an initial attack of amidines on the C-2 position of the ring. This involves direct displacement of the O(1)–C(5) portion by a N–C fragment of the amidines, which corresponds with 1,3-

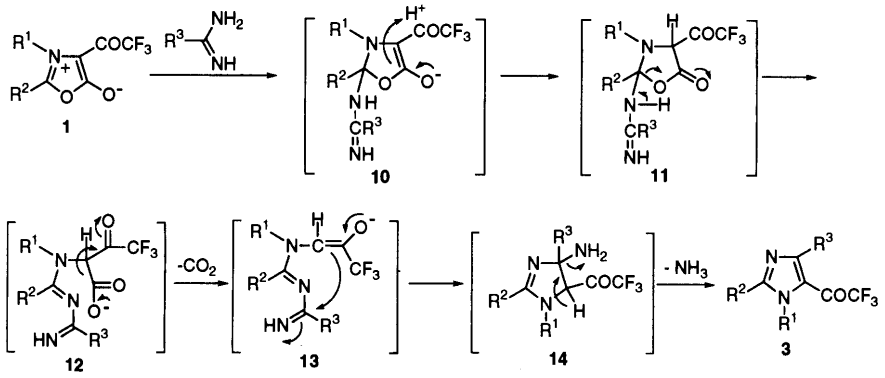

Chart 3

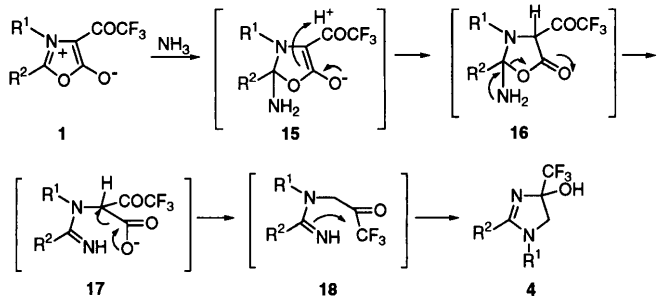

Chart 4

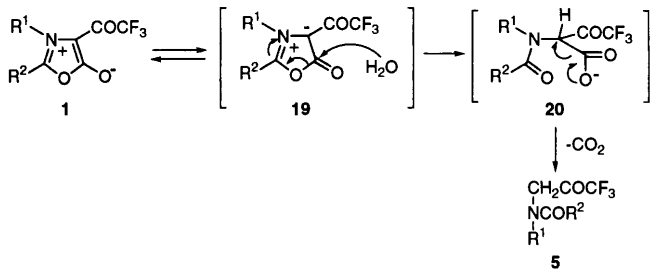

Chart 5

dipolar cycloaddition of munchnones with nitriles to afford imidazoles.[13] However, the cycloaddition has limited synthetic applicability, for only electron-deficient nitriles can react as dipolarophiles, and only one case using 2,4-diphenyl-1,3-oxazolium-5-olates as a dipole has been recorded.[13] On the other hand, the analogous reaction of a munchnone with a tosylimine to provide an imidazole has been also reported.[14]

As shown in Chart 3, a nucleophilic attack of amidines on the C-2 position of **1** affords an adduct (**10**) which is converted to **11**. The intermediate **11** gives an open-chain intermediate **12**, which is then decarboxylated to afford an enolate anion (**13**). The intermediate **13** can undergo cyclization to give **14**, which loses ammonia leading to the imidazoles **3**. A similar reactivity of amidines which extrudes ammonia has been postulated in their reactions with benzoins[15] or cyanohydrins[16] to give oxazoles.

A plausible mechanism of the formation of **4** and **5** is suggested in Charts 4 and 5, respectively. Compound **4** is not formed by the reaction of **5** with ammonia, because the reaction of **5a** with ammonium acetate did not afford the expected **4a**. However, the same reaction of **2a** with ammonium acetate gave **4a** in a high yield. Thus, a nucleophilic attack of ammonia, which was generated during the reaction, on C-2 of **1** gives rise to the adduct **15**. The scission of the O(1)–C(2) bond of **16** gives an open-chain intermediate **17**, which extrudes carbon dioxide to provide the ketone **18**. Finally, intramolecular cyclization of **18** affords dihydroimidazoles **4**. The formation of **5** might be formed through the hydrolysis of the keto form **19**, which is probably in equilibium with **1**.

In summary, we devised an easy method of accessing 5-trifluoroacetylimidazole derivatives which are otherwise difficult to obtain. The principle advantage of using mesoionic oxazoles **1** is the great variety of substituents available for R^1 and R^2. This flexibility in the type of substituents in the mesoionic ring will be reflected in the corresponding substitution of the resulting imidazole. The trifluoroacetyl group at the 5-position serves as a handle for further elaborations, therefore making a variety of functionalized imidazoles accessible.

Experimental

General Methods All melting points were determined using a Yanagimoto hot-stage melting point apparatus and are uncorrected. ^{1}H-NMR spectra were measured on either a JEOL JNM-PMX60SI, JNM-FX270, or JNM-GSX500 spectrometer with tetramethylsilane (Me_4Si) as an internal reference and $CDCl_3$ as the solvent. ^{13}C-NMR spectra were obtained on a JEOL JNM-FX270 or JNM-GSX500 spectrometer (at 68 or 127 MHz). Both ^{1}H- and ^{13}C-NMR spectral data are reported in parts per million (δ) relative to Me_4Si. Infrared (IR) spectra were recorded on a JASCO IR810 spectrometer. Low- and high-resolution MS were obtained with a JEOL JMS-DX300 spectrometer with a direct inlet system at 70 eV. Elemental analyses were carried out in the microanalytical laboratory of this university. Standard workup means that the organic layers were finally dried over Na_2SO_4, filtered, and concentrated *in vacuo* below 45 °C using a rotary evaporator.

Materials The following compounds were prepared by reported procedures: *N*-Benzoyl-*N*-methylglycine (**2a**): mp 101—104 °C (mp[17] 102—104 °C). *N*-Acetyl-*N*-phenylglycine (**2b**): mp 196—198 °C (mp[17] 193—195 °C). *N*-Methyl-*N*-pivaloylglycine (**2c**): Yield 91%. mp 75—76 °C (benzene–hexane). ^{1}H-NMR (60 MHz) δ: 1.30 (9H, s), 3.18 (3H, s), 4.25 (2H, s), 10.13 (1H, br s). IR (Nujol) cm^{-1}: 2500—300, 1680, 1620. MS *m/z*: 173 (M^+, 3%), 57 (100). High-resolution MS: Calcd for $C_8H_{15}NO_3$: 173.1053. Found: 173.1045. *N*-Benzoyl-*N*-phenylglycine (**2d**): mp 190—193 °C (mp[17] 193—195 °C).

General Procedure for the Preparation of 4-Trifluoroacetyl-1,3-oxazolium-5-olates (1) TFAA (11 ml, 78 mmol) was added to a stirred solution of *N*-acyl-*N*-alkylglycine (26 mmol) in CH_2Cl_2 (50 ml) at 0 °C for 10 min. The mixture was stirred at 25 °C for 3 h and then extracted with CH_2Cl_2 (80 ml×2). The extract was washed successively with 3% HCl, H_2O, 1% Na_2CO_3, and H_2O. After the standard workup, the residue was recrystallized from CH_2Cl_2–hexane to give the 4-trifluoroacetyl-1,3-oxazolium-5-olates (**1**).

3-Methyl-2-phenyl-4-trifluoroacetyl-1,3-oxazolium-5-olate (**1a**): Yield 92%. mp 161—163 °C (mp[8b] 162—163 °C). 2-Methyl-3-phenyl-4-trifluoroacetyl-1,3-oxazolium-5-olate (**1b**): Yield 78%. mp 200—203 °C (mp[8b] 211—212 °C). 2-*tert*-Butyl-3-methyl-4-trifluoroacetyl-1,3-oxazolium-5-olate (**1c**): Yield 94%. mp 120—121 °C (benzene–hexane). IR (Nujol) cm^{-1}: 1800, 1630. ^{1}H-NMR (270 MHz) δ: 1.52 (9H, s), 4.08 (3H, s). ^{13}C-NMR ($CDCl_3$, 68 MHz) δ: 27.43 (CH_3), 35.26 (C), 36.26 (C), 36.27 (CH_3), 96.69 (C), 116.84 (CF_3, $^1J_{C\text{-}F}$=289.0 Hz), 157.82 (C), 162.69 (C), 167.15 (C, $^2J_{C\text{-}F}$=37.4 Hz). MS *m/z*: 251 (M^+, 22%), 105 (100%). *Anal.* Calcd for $C_{10}H_{12}F_3NO_3$: C, 47.81; H, 4.81; N, 5.58. Found: C, 47.87; H, 4.76; N, 5.63. 2,3-Diphenyl-4-trifluoroacetyl-1,3-oxazolium-5-olate (**1d**): Yield 81%. mp 194—196 °C (mp[8b] 194—196 °C).

General Procedure for the Reactions of 4-Trifluoroacetyl-1,3-oxazolium-5-olates (1) with Amidines A solution of **1** (1.5 mmol), an amidine (2.2 mmol), and potassium carbonate (207 mg, 2.2 mmol) in dry DMF (5 ml) was stirred at 70 °C for 2 h. The mixture was diluted with AcOEt (40 ml) and H_2O (30 ml). After the standard workup, the residue was purified by column chromatography on silica gel with EtOAc–hexane to give the products (**3**, **4**, and/or **5**).

1-Methyl-2-phenyl-5-trifluoroacetylimidazole (**3a**) and 4-Hydroxy-1-methyl-2-phenyl-4-trifluoromethyl-4,5-dihydroimidazole (**4a**): **3a**; 63% yield from the less polar fraction (EtOAc : hexane=1 : 1), mp 107—108 °C (hexane). IR (Nujol) cm^{-1}: 1680. ^{1}H-NMR (500 MHz) δ: 4.00 (3H, s), 7.51—7.54 (3H, br s), 7.61—7.66 (2H, br s), 8.15 (1H, s). ^{13}C-NMR (127 MHz) δ: 35.23 (CH_3), 116.56 (CF_3, $^1J_{C\text{-}F}$=291 Hz), 126.34 (C), 128.31 (C), 128.94 (CH), 129.45 (CH), 130.66 (CH), 143.31 (CH, $^3J_{C\text{-}F}$=5.2 Hz), 156.16 (C), 170.79 (C, $^2J_{C\text{-}F}$=37 Hz). MS *m/z*: 254 (M^+, 100%). *Anal.* Calcd for $C_{12}H_9F_3N_2O$: C, 56.70; H, 3.57; N, 11.02. Found: C, 56.75; H, 3.55; N, 11.11. **4a**; 19% yield from the more polar fraction (EtOAc : hexane=1 : 1), mp 196—198 °C (Et_2O). IR (Nujol) cm^{-1}: 2400—3300 (br). ^{1}H-NMR (500 MHz) δ: 2.91 (3H, s), 3.56 (1H, d, *J*=11.7 Hz), 3.70 (1H, d, *J*=11.7 Hz), 7.41—7.48 (3H, m), 7.53—7.56 (2H, m). ^{13}C-NMR (127 MHz) δ: 34.60 (CH_3), 59.73 (CH_2), 94.01 (C, $^2J_{C\text{-}F}$=31 Hz), 124.24 (CF_3, $^1J_{C\text{-}F}$=286 Hz), 128.44 (CH), 128.52 (CH), 128.59 (C), 130.81 (CH), 169.71 (C). MS *m/z*: 244 (M^+, 10%), 91 (100%). *Anal.* Calcd for $C_{11}H_{11}F_3N_2O$: C, 54.10; H, 4.54; N, 11.47. Found: C, 53.98; H, 4.65; N, 11.27.

2-Methyl-1-phenyl-5-trifluoroacetylimidazole (**3b**) and 4-Hydroxy-2-methyl-1-phenyl-4-trifluoromethyl-4,5-dihydroimidazole (**4b**): **3b**; 55% yield from the less polar fraction (EtOAc : hexane=1 : 1), oil. IR (oil) cm^{-1}: 1700. ^{1}H-NMR (500 MHz) δ: 2.30 (3H, s), 7.19—7.22 (2H, m), 7.51—7.56 (3H, m), 8.06 (1H, q, *J*=1.8 Hz). ^{13}C-NMR (127 MHz) δ: 13.89 (CH_3), 116.39 (CF_3, $^1J_{C\text{-}F}$=291 Hz), 126.41 (CH), 126.77 (CH), 129.67 (CH), 129.70 (CH), 136.01 (C), 142.48 (C, $^3J_{C\text{-}F}$=5.2 Hz), 154.92 (C), 169.11 (C, $^2J_{C\text{-}F}$=37 Hz). MS *m/z*: 254 (M^+, 58%), 185 (100%). High-resolution MS: Calcd for $C_{12}H_9F_3N_2O$: 254.0667. Found: 254.0661. **4b**; 14% yield from the more polar fraction (EtOAc : hexane=1 : 1), mp 201—202 °C (Et_2O). IR (Nujol) cm^{-1}: 2400—3300. ^{1}H-NMR (500 MHz) δ: 2.05 (3H, s), 3.92 (1H, d, *J*=11.0 Hz), 4.09 (1H, d, *J*=11.0 Hz), 7.17 (2H, d, *J*=8.5 Hz), 7.27 (1H, t, *J*=7.6 Hz), 7.41 (2H, t, *J*=7.6 Hz). ^{13}C-NMR (127 MHz) δ: 14.69 (CH_3), 59.55 (CH_2), 93.49 (C, $^2J_{C\text{-}F}$=32 Hz), 124.37 (CF_3, $^1J_{C\text{-}F}$=285 Hz), 124.69 (CH), 126.77 (CH), 129.61 (CH), 138.79 (C), 166.03 (C). MS *m/z*: 244 (M^+, 17%), 106 (100%). *Anal.* Calcd for $C_{11}H_{11}F_3N_2O$: C, 54.10; H, 4.54; N, 11.47. Found: C, 54.20; H, 4.61; N, 11.48.

2-*tert*-Butyl-1-methyl-5-trifluoroacetylimidazole (**3c**) and 2-*tert*-Butyl-4-hydroxy-1-methyl-4-trifluoromethyl-4,5-dihydroimidazole (**4c**): **3c**; 49% yield from the less polar fraction (EtOAc : hexane=1 : 2), mp 38—40 °C (hexane). IR (Nujol) cm^{-1}: 1685. ^{1}H-NMR (500 MHz) δ: 1.51 (9H, s), 4.07 (3H, s), 7.94 (1H, q, *J*=2.1 Hz). ^{13}C-NMR (127 MHz) δ: 28.94 (CH_3×3), 33.97 (C), 35.09 (CH_3), 116.57 (CF_3, $^1J_{C\text{-}F}$=291 Hz), 126.29 (CH), 142.16 (C, $^3J_{C\text{-}F}$=5.2 Hz), 163.34 (C), 170.56 (C, $^2J_{C\text{-}F}$=37 Hz). MS *m/z*: 234 (M^+, 20%), 219 (100%). High-resolution MS: Calcd for $C_{10}H_{13}F_3N_2O$: 234.0980. Found: 234.0964. **4c**; 15% yield from the more polar fraction (EtOAc : hexane=1 : 1), mp 155—157 °C (Et_2O). IR (Nujol) cm^{-1}: 2400—3400. ^{1}H-NMR (500 MHz) δ: 1.30 (9H, s), 3.07 (3H, s), 3.43 (1H, dq, *J*=1.2, 11.6 Hz), 3.64 (1H, d, *J*=11.6 Hz). ^{13}C-NMR (127 MHz) δ: 28.04 (CH_3×3), 33.69 (C), 34.93 (CH_3), 60.55 (CH_2), 92.75 (C, $^2J_{C\text{-}F}$=31 Hz), 124.48 (CF_3, $^1J_{C\text{-}F}$=286 Hz), 175.58 (C). MS *m/z*: 224 (M^+, 3%), 191 (100%). *Anal.* Calcd for $C_9H_{15}F_3N_2O$: C, 48.21; H, 6.74; N, 12.49. Found: C, 48.23; H, 6.64; N, 12.52.

1,2-Diphenyl-5-trifluoroacetylimidazole (**3d**) and 1,2-Diphenyl-4-hydroxy-4-trifluoromethyl-4,5-dihydroimidazole (**4d**): **3d**; 54% yield from the less polar fraction (EtOAc : hexane=1 : 2), mp 134—136 °C (Et_2O). IR (Nujol) cm^{-1}: 1680. ^{1}H-NMR (500 MHz) δ: 7.24—7.27 (4H, m), 7.33—7.36 (1H, m), 7.40—7.45 (2H, m), 7.46—7.51 (3H, m), 8.24 (1H, q, *J*=1.8 Hz). ^{13}C-NMR (127 MHz) δ: 116.40 (CF_3, $^1J_{C\text{-}F}$=291 Hz), 127.04 (C), 127.62 (CH), 128.23 (C), 128.44 (CH), 129.29 (CH), 129.51 (CH), 129.69 (CH), 130.26 (CH), 136.48 (C), 143.09 (C, $^3J_{C\text{-}F}$=4.1 Hz), 154.77 (C), 169.41 (C, $^2J_{C\text{-}F}$=37 Hz). MS *m/z*: 316 (M^+, 100%). *Anal.* Calcd for $C_{17}H_{11}F_3N_2O$: C, 64.56; H, 3.51; N, 8.86. Found: C, 64.65; H, 3.57; N, 8.88. **4d**; 11% yield from the more polar fraction (EtOAc : hexane=1 : 1), mp 174—175 °C (Et_2O). IR (Nujol) cm^{-1}: 2500—3300. ^{1}H-NMR (500 MHz) δ: 4.09 (1H, d, *J*=11.6 Hz), 4.13 (1H, d, *J*=11.6 Hz), 6.85 (2H, d, *J*=7.9 Hz), 7.10 (1H, t, *J*=7.6 Hz), 7.20 (2H, t, *J*=7.9 Hz), 7.30 (2H, t, *J*=7.6 Hz), 7.40 (1H, t, *J*=7.6 Hz), 7.49 (2H, d, *J*=7.6 Hz), 8.08 (1H, br s). ^{13}C-NMR (127 MHz) δ: 60.68 (CH_2), 93.98 (C, $^2J_{C\text{-}F}$=31 Hz), 124.04 (CF_3, $^1J_{C\text{-}F}$=285 Hz), 124.39 (CH), 125.71 (CH), 128.28 (CH), 128.82 (C), 129.14 (CH), 129.17 (CH), 131.05 (CH), 140.66 (C), 166.49 (C). MS *m/z*: 306 (M^+, 15%), 106 (100%). *Anal.* Calcd for $C_{16}H_{13}F_3N_2O$: C, 62.74; H, 4.28; N, 9.15. Found: C, 62.88; H, 4.40; N 9.08.

1,4-Dimethyl-2-phenyl-5-trifluoroacetylimidazole (**3e**) and **4a**: **3e**; 55% yield from the less polar fraction (EtOAc : hexane=1 : 2), mp 88—89 °C (hexane). IR (Nujol) cm^{-1}: 1660. ^{1}H-NMR (500 MHz) δ: 2.61 (3H, q, *J*=1.8 Hz), 3.89 (s, 3H), 7.51—7.54 (m, 3H), 7.62—7.64 (m, 2H). ^{13}C-NMR (127 MHz) δ: 16.39 (C, $^3J_{C\text{-}F}$=5.1 Hz), 36.14 (CH_3), 116.40 (CF_3, $^1J_{C\text{-}F}$=289 Hz), 124.45 (C), 128.52 (C), 128.87 (CH), 129.48 (CH), 130.48 (CH), 151.93 (C), 154.59 (C), 171.12 (C, $^2J_{C\text{-}F}$=37 Hz). MS *m/z*: 268 (M^+, 79%), 199 (100%). *Anal.* Calcd for $C_{13}H_{11}F_3N_2O$: C, 58.21; H, 4.13; N, 10.44. Found: C, 57.95; H, 4.28; N, 10.56. **4a**; 16% yield from the more polar fraction (EtOAc : hexane=1 : 1).

2,4-Diphenyl-1-methyl-5-trifluoroacetylimidazole (**3f**), **4a** and *N*-Methyl-*N*-[1-(3,3,3-trifluoro-2,2-dihydroxy)propyl]benzamide (**5a**): **3f**; 55% yield from the less polar fraction (EtOAc : hexane=1 : 1), oil. IR (Nujol) cm^{-1}: 1670. ^{1}H-NMR (500 MHz) δ: 3.91 (3H, s), 7.41—7.44 (3H, m), 7.51—7.53 (5H, m), 7.68—7.72 (2H, m). ^{13}C-NMR (127 MHz) δ: 35.55 (CH_3), 115.75 (CF_3, $^1J_{C\text{-}F}$=290 Hz), 124.17 (C), 128.00 (CH), 128.56 (C), 128.84 (CH), 129.13 (CH), 129.48 (CH), 129.66 (CH), 130.48 (CH), 133.95 (C), 153.70 (C), 154.21 (C), 174.35 (C, $^2J_{C\text{-}F}$=38 Hz). MS *m/z*: 330 (M^+, 78%), 261 (100%). High-resolution MS: Calcd for $C_{18}H_{13}F_3N_2O$: 330.0980. Found: 330.0982. **5a**; 4% yield from the more polar fraction (EtOAc : hexane=1 : 1), mp 90—92 °C (Et_2O–hexane). IR (Nujol) cm^{-1}: 3280, 1600. ^{1}H-NMR (500 MHz) δ: 3.18 (3H, s), 3.88 (2H, s), 5.96 (2H, br s), 7.42—7.46 (2H, m), 7.4—7.51 (3H, m). ^{13}C-NMR (127 MHz) δ: 41.26 (CH_2), 52.92 (CH_3), 94.42 (C, $^2J_{C\text{-}F}$=32 Hz), 122.87 (CF_3, $^1J_{C\text{-}F}$=288 Hz), 127.46 (CH), 128.53 (CH), 130.80 (CH), 133.86 (C), 175.72 (C). CI-MS *m/z*: 246 (M^+-H_2O+1, 100%). *Anal.* Calcd for $C_{11}H_{12}F_3NO_3$: C, 50.20; H, 4.60; N, 5.32. Found: C, 50.40; H, 4.66; N, 5.37. **4a**; 25% yield from the most polar fraction (EtOAc : hexane=1 : 1).

One-Pot Procedure for the Conversion of *N*-Acyl-*N*-alkylglycine (2) to Imidazoles (3) TFAA (0.64 ml, 4.5 mmol) was added to a stirred solution of *N*-acyl-*N*-alkylglycine (1.5 mmol) in dry CH_2Cl_2 (4 ml) at 0 °C. The mixture was stirred at 25 °C for 3 h and the solvents were evaporated to dryness. The residue was dissolved in dry DMF (6 ml), and K_2CO_3 (304 mg, 2.2 mmol) and formamidine·HCl (182 mg, 2.2 mmol) were added to the DMF solution at 0 °C. The mixture was stirred at 70 °C for 2 h. After the standard workup, the residue was purified by column chromatography on silica gel with EtOAc–hexane to give the products (**3**, **4** and/or **5**).

1-Methyl-5-pentafluoropropionyl-2-phenylimidazole (**3g**), 4-Hydroxy-1-methyl-4-pentafluoroethyl-2-phenyl-4,5-dihydroimidazole (**4e**), and *N*-Methyl-*N*-[1-(2,2-dihydroxy-3,3,4,4,4-pentafluoro)butyl]benzamide (**5b**): **3g**; 60% yield from the less polar fraction (EtOAc : hexane=1 : 2), mp 95—96 °C (Et_2O–hexane). IR (Nujol) cm^{-1}: 1670. ^{1}H-NMR (500 MHz) δ: 4.00 (3H, s), 7.53—7.55 (3H, m), 7.65—7.67 (2H, m), 8.19 (1H, t, *J*=2.6 Hz). ^{13}C-NMR (127 MHz) δ: 35.46 (CH_3), 108—120 (CF_2CF_3), 127.39 (CH), 128.25 (CH), 128.96 (CH), 129.51 (CH), 130.73 (C), 143.66 (C, $^3J_{C\text{-}F}$=8.3 Hz), 156.18 (C), 172.96 (C, $^2J_{C\text{-}F}$=27 Hz). MS *m/z*: 304 (M^+, 71%), 185 (100%). *Anal.* Calcd for $C_{13}H_9F_5N_2O$: C, 51.33; H, 2.98; N, 9.21. Found: C, 51.33; H, 3.04; N, 9.34. **4e**; 14% yield from the more polar fraction (EtOAc : hexane=1 : 1), mp 183—186 °C (Et_2O). IR (Nujol) cm^{-1}: 2400—3200. ^{1}H-NMR (500 MHz) δ: 2.93 (3H, s), 3.64 (1H, d, *J*=11.9 Hz), 3.69 (1H, d, *J*=11.9 Hz), 7.44 (2H, t, *J*=7.3 Hz), 7.49 (1H, t, *J*=7.3 Hz), 7.55 (2H, d, *J*=7.3 Hz). ^{13}C-NMR (127 MHz) δ: 34.56 (CH_3), 60.19 (CH_2), 94.00 (C, $^2J_{C\text{-}F}$=27 Hz), 105—115 (CF_2CF_3), 128.50 (CH), 128.58 (CH), 129.00 (C), 130.96 (CH), 169.57 (C). MS *m/z*: 294 (M^+, 0.4%), 276 (100%). *Anal.* Calcd for $C_{12}H_{11}F_5N_2O$: C, 48.99; H, 3.77; N, 9.52. Found: C, 48.81; H, 3.86; N, 9.66. **5b**; 11% yield from the most polar fraction (EtOAc : hexane=1 : 1), oil. IR (oil) cm^{-1}: 3360, 1600. ^{1}H-NMR (500 MHz) δ: 3.05 (3H, s), 3.19+3.90 (1H, s), 4.69 (2H, s), 7.26—7.50 (3H, m), 8.08—8.10 (2H, m). ^{13}C-NMR (127 MHz) δ: 38.65 (CH_3), 53.28 (CH_2), 95.50 (C, $^2J_{C\text{-}F}$=

27 Hz), 110—120 (CF_2CF_3), 127.25 (CH), 128.39 (CH), 130.06 (CH), 133.49 (C), 171.08 (C). MS *m/z*: 276 (M^+-H_2O-F, 100%).

5-Heptafluorobutyryl-1-methyl-2-phenylimidazole (**3h**) and 4-Heptafluoropropyl-4-hydroxy-1-methyl-2-phenyl-4,5-dihydroimidazole (**4f**): **3h**; 56% yield from the less polar fraction (EtOAc : hexane = 1 : 2), mp 72—73 °C (hexane). IR (Nujol) cm^{-1}: 1660. ^{1}H-NMR (500 MHz) δ: 4.00 (3H, s), 7.52—7.55 (3H, m), 7.65—7.68 (2H, m), 8.16 (1H, br s). ^{13}C-NMR (127 MHz) δ: 35.53 (CH_3), 105—120 ($CF_2CF_2CF_3$), 128.17 (CH), 128.24 (CH), 128.96 (CH), 129.53 (CH), 130.75 (C), 143.85 (C, $^3J_{C\text{-}F}$=8.3 Hz), 156.20 (C), 172.66 (C, $^2J_{C\text{-}F}$=27 Hz). MS *m/z*: 354 (M^+, 61%), 185 (100%). *Anal.* Calcd for $C_{14}H_9F_7N_2O$: C, 47.47; H, 2.56; N, 7.91. Found: C, 47.20; H, 2.67; N, 8.15. **4f**; 20% yield from the more polar fraction (EtOAc : hexane = 1 : 1), mp 188—189 °C (Et_2O). IR (Nujol) cm^{-1}: 2450—3100. ^{1}H-NMR (500 MHz) δ: 2.91 (3H, s), 3.60—3.66 (2H, m), 7.43 (2H, t, *J*=7.3 Hz), 7.48 (1H, t, *J*=7.3 Hz), 7.53 (2H, d, *J*=7.0 Hz). ^{13}C-NMR (127 MHz) δ: 34.54 (CH_3), 60.26 (CH_2), 95.10 (C, $^2J_{C\text{-}F}$=28 Hz), 110—120 ($CF_2CF_2CF_3$), 128.46 (CH), 128.56 (CH), 128.71 (C), 130.85 (CH), 169.65 (C). CI-MS *m/z*: 345 (M^++1, 20%), 327 (100%). *Anal.* Calcd for $C_{13}H_{11}F_7N_2O$: C, 45.36; H, 3.22; N, 8.14. Found: C, 45.16; H, 3.31; N, 8.30.

Ethyl 1-Methyl-2-phenyl-1*H*-imidazole-5-carboxylate (6) and 5-[2′-(2-Ethoxy-1,1,1,3,3,3-heptafluoropropyl)]-1-methyl-2-phenylimidazole (7) A solution of **3a** (196 mg, 0.77 mmol) in DMF (1 ml) was added to a stirred mixture of NaH (60%) (124 mg, 3.1 mmol) in DMF (2 ml) at 0 °C, and the mixture was stirred at 60 °C for 0.5 h. After the reaction, a solution of EtI (0.25 ml, 3.1 mmol) in DMF (2 ml) was added to the reaction mixture and the mixture was stirred at 80 °C for 0.5 h. After the standard workup, the residue was purified by column chromatography on silica gel with EtOAc–hexane (1 : 2) to give **6** (110 mg, 62%) and **7** (11 mg, 4%). **6**: The less polar fraction, mp 83—84 °C (Et_2O–hexane). IR (Nujol) cm^{-1}: 1705. ^{1}H-NMR (500 MHz) δ: 1.39 (3H, t, *J*=7.2 Hz), 3.95 (3H, s), 4.35 (2H, q, *J*=7.2 Hz), 7.46—7.50 (3H, m), 7.60—7.63 (2H, m), 7.84 (1H, s). ^{13}C-NMR (127 MHz) δ: 14.39 (CH_3), 34.19 (CH_3), 60.41 (CH_2), 124.22 (C), 128.65 (CH), 129.31 (CH), 129.59 (CH), 129.74 (C), 137.18 (CH), 152.63 (C), 160.76 (C). MS *m/z*: 230 (M^+, 100%). *Anal.* Calcd for $C_{13}H_{14}N_2O_2$: C, 67.81; H, 6.13; N, 12.17. Found: C, 67.72; H, 6.32; N, 12.06. **7**: The more polar fraction, mp 79—80 °C (hexane). IR (Nujol) cm^{-1}: 1660. ^{1}H-NMR (500 MHz) δ: 1.35 (3H, dt, *J*=1.8, 7.0 Hz), 3.74 (2H, q, *J*=6.7 Hz), 3.79 (3H, s), 7.39 (1H, s), 7.46—7.49 (3H, m), 7.61—7.62 (2H, m). ^{13}C-NMR (127 MHz) δ: 15.04 (CH_3), 34.14 (CH_3), 62.98 (CH_2), 80.63 (C), 119.05 (CH), 122.20 (CF_3, $^1J_{C\text{-}F}$=293 Hz), 128.64 (CH), 129.44 (CH), 129.51 (CH), 130.01 (C), 133.58 (C), 152.13 (C). MS *m/z*: 352 (M^+, 57%), 255 (100%). *Anal.* Calcd for $C_{15}H_{14}F_6N_2O$: C, 51.14; H, 4.01; N, 7.95. Found: C, 51.13; H, 4.08; N, 8.05.

1-Methyl-2-phenyl-1*H*-imidazole-5-carboxaldehyde (8) A solution of ethyl ester (**6**) (196 mg, 0.85 mmol) in dry tetrahydrofuran (THF) (5 ml) was added to a suspension of lithium aluminum hydride (LAH) (65 mg, 1.7 mmol) in dry THF (3 ml) at 0 °C and the mixture was stirred at 25 °C for 3 h. The reaction was quenched with $Na_2SO_4 \cdot 10H_2O$ (5 g) and filtrated through a Celite pad and washed with AcOEt (30 ml). The filtrate was evaporated to dryness and the residue was dissolved in dry CH_2Cl_2 (6 ml). MnO_2 (739 mg, 8.5 mmol) was added to the solution and the mixture was stirred at 25 °C for 3 h. The mixture was filtered through a Celite pad and the filtrate was evaporated *in vacuo*. The residue was purified by column chromatography on silica gel with EtOAc–hexane (1 : 1) to give **8** (140 mg, 88%). **8**: mp 92—94 °C (Et_2O–hexane) (mp[9] 94—95 °C). IR (Nujol) cm^{-1}: 1665. ^{1}H-NMR (500 MHz) δ: 4.01 (3H, s), 7.50—7.53 (3H, m), 7.65—7.68 (2H, m), 7.88 (1H, s), 9.78 (1H, s). ^{13}C-NMR (127 MHz) δ: 34.46 (CH_3), 128.74 (C), 128.80 (CH), 129.27 (CH), 130.16 (CH), 132.79 (C), 143.63 (CH), 154.39 (C), 179.36 (C). MS *m/z*: 186 (M^+, 100%).

1-Methyl-2-phenyl-4-trifluoromethylimidazole (9) $POCl_3$ (0.23 ml, 2.5 mmol) was added to a stirred solution of **4a** (251 mg, 1.0 mmol) in pyridine (0.73 ml, 9.0 mmol) at 0 °C and the mixture was heated at 90 °C for 2 h. The solvent was evaporated to dryness and the residue was extracted with AcOEt (40 ml×2). After the standard workup, the residue was purified by column chromatography on silica gel with EtOAc–hexane (1 : 5) to give **9** (198 mg, 88%). **9**: mp 59—60 °C (hexane) (mp[12] 61.5—62.5 °C). IR (Nujol) cm^{-1}: 1585. ^{1}H-NMR (500 MHz) δ: 3.76 (3H, s), 7.31 (1H, s), 7.45—7.48 (3H, m), 7.61—7.63 (2H, m). ^{13}C-NMR (127 MHz) δ: 34.82 (CH_3), 121.74 (CH, $^3J_{C\text{-}F}$=4.1 Hz), 121.77 (CF_3, $^1J_{C\text{-}F}$=267 Hz), 128.69 (CH), 128.95 (CH), 129.27 (C), 129.54 (CH), 131.56 (C, $^2J_{C\text{-}F}$=39 Hz), 149.06 (s). MS *m/z*: 226 (M^+, 100%).

References and Notes

1) Begue J. P., Bonnet-Delpon D., *Tetrahedron*, **47**, 3207—3258 (1991).
2) *a*) Kawase M., Harada H., Saito S., Cui J., Tani S., *Bioorg. Med. Chem. Lett.*, **9**, 193—194 (1999); *b*) Kawase M., Sakagami H., Kusama K., Motohashi N., Saito S., *ibid.*, **9**, 3113—3118 (1999).
3) Kawase M., Koyanagi J., Saito S., *Chem. Pharm. Bull.*, **47**, 718—719 (1999).
4) Comins D. L., O'Connor S., "Advances in Heterocyclic Chemistry," Vol. 44, ed. by Katritzky A. R., Academic Press, New York, 1988, pp. 199—267; Reiter L. A., *J. Org. Chem.*, **52**, 2714—2726 (1987); Chatani N., Fukuyama T., Kakiuchi F., Murai S., *J. Am. Chem. Soc.*, **118**, 493—494 (1996).
5) Grimmett M. R., "Advances in Heterocyclic Chemistry," Vol. 27, ed. by Katritzky A. R., Academic Press, New York, 1970, pp. 241—326; *idem*., "Comprehensive Heterocyclic Chemistry," Vol. 5, ed. by Potts K. T., Pergamon, Oxford, 1984, pp. 345—498; Elguero J., Fruchier A., Jagerovic N., Werner A., *Org. Prep. Proced. Int.*, **27**, 33—74 (1995).
6) Kawase M., Miyamae H., Kurihara T., *Chem. Pharm. Bull.*, **46**, 749—756 (1998); Kawase M., Hirabayashi M., Kumakura H., Saito S., Yamamoto K., *ibid.*, **48**, 114—119 (2000).
7) *a*) Kawase M., *J. Chem. Soc., Chem. Commun.*, **1994**, 2101—2102; *b*) Kawase M., Saito S., Kurihara T., *Heterocycles*, **41**, 1617—1620 (1995); *c*) Kawase M., Koiwai H., Yamano A., Miyamae H., *Tetrahedron Lett.*, **39**, 663—666 (1998); *d*) Kawase M., Koiwai H., Saito S., Kurihara T., *ibid.*, **39**, 6189—6190 (1998); *e*) Kawase M., Miyamae H., Saito S., *Heterocycles*, **50**, 71—74 (1999).
8) *a*) Singh G., Singh S., *Tetrahedron Lett.*, **1964**, 3789—3792; *b*) Greco C. V., Gray R. P., Grosso V. G., *J. Org. Chem.*, **32**, 4101—4103 (1967).
9) Sircar I., Bobowski G., Bristol J. A., Weishaar R. E., Evans D. B., *J. Med. Chem.*, **29**, 261—267 (1986).
10) Delgado A., Clardy J., *Tetrahedron Lett.*, **33**, 2789—2790 (1992).
11) Kamitori Y., Hojo M., Masuda R., Wada M., Takahashi T., *Heterocycles*, **37**, 153—156 (1994).
12) Baldwin J. J., Novello F. C., U.S. Pat., 4125530 [*Chem. Abst.*, **90**, P121593*n* (1979)].
13) Brunn E., Funke E., Gotthardt H., Huisgen R., *Chem. Ber.*, **104**, 1562—1572 (1971).
14) Consonni R., Croca P. D., Ferraccioli R., La Rosa C., *J. Chem. Res., Synop.*, **1991**, 188—189; Bilodeau M. T., Cunningham A. M., *J. Org. Chem.*, **63**, 2800—2801 (1998).
15) Bredereck H., Gompper R., Schuh H. G., Theiling G., *Angew. Chem.*, **71**, 753—774 (1959).
16) Haruki H., Imanaka H., Imoto E., *Bull. Chem. Soc. Jpn.*, **41**, 1368—1371 (1968).
17) Deruiter J., Swearingen B. E., Wandreker V., Mayfield C. A., *J. Med. Chem.*, **34**, 2120—2126 (1991).

A Tetrahydroisoquinoline-monoterpene Glucoside and an Iridoid Glucoside from *Alangium kurzii*

Takao TANAHASHI,*[,a] Chizu KOBAYASHI,[a] Atsuko ITOH,[a] Naotaka NAGAKURA,[a] Kenichiro INOUE,[b] Hiroshi KUWAJIMA,[c] and Hua-Xin WU[d]

Kobe Pharmaceutical University,[a] 4–19–1 Motoyamakita-machi, Higashinada-ku, Kobe 658–8558, Japan, Gifu Pharmaceutical University,[b] Mitahora-higashi, Gifu 502–8585, Japan, Faculty of Pharmaceutical Sciences, Kinki University,[c] Kowakae, Higashiosaka 577–8502, Japan and Yunnan Pharmaceutical Group Corporation Technical Center,[d] 547 Beijing Road, Kunming, Yunnan, People's Republic of China.

Received October 18, 1999; accepted November 23, 1999

From the leaves of *Alangium kurzii*, a new tetrahydroisoquinoline-monoterpene glucoside, 6-*O*-methyl-*N*-deacetylipecosidic acid and a new iridoid glucoside, 10-*O*-benzoyladoxosidic acid, were isolated along with alangiside, demethylalangiside, 6″-*O*-β-D-glucosylhenryoside, uridine and four known flavonoid glycosides. The structures of new glucosides were determined on the basis of spectroscopic and chemical methods.

Key words *Alangium kurzii*; Alangiaceae; 6-*O*-methyl-*N*-deacetylipecosidic acid; 10-*O*-benzoyladoxosidic acid

Alangium kurzii CRAIB. (Alangiaceae) is a deciduous shrub distributed in South China and Malaya. Previous phytochemical investigation demonstrated that the plant contained a pyridine alkaloid, anabasine, and a benzoquinolizine alkaloid, ankorine.[1] The glycosidal fraction, in contrast, however, remained to be investigated. In the course of our chemical studies on the plants of Alangiaceae,[2] we have investigated the constituents of the leaves of *A. kurzii*, and isolated a tetrahydroisoquinoline-monoterpene glucoside **1** and an iridoid glucoside **2** as well as eight known compounds, alangiside (**3**),[3] demethylalangiside (**4**),[4] kaempferol-3-*O*-[2,6-di-*O*-(α-L-rhamnopyranosyl)-β-D-galactopyranoside] (**5**),[5] kaempferol-3-*O*-[2-*O*-(β-D-glucopyranosyl)-β-D-galactopyranoside] (**6**),[6] kaempferol-3-*O*-[2-*O*-(β-D-xylopyranosyl)-β-D-galactopyranoside] (**7**),[7] quercetin-3-*O*-[2-*O*-(β-D-xylopyranosyl)-β-D-galactopyranoside] (**8**),[7] 6″-*O*-β-D-glucosylhenryoside (**9**)[8] and uridine (**10**).[9] Compounds **3**—**10** were isolated for the first time from this species. We report here the structural elucidation of two new glucosides, **1** and **2**.

Compound **1** was isolated as a colorless crystalline solid, mp 203—205 °C. It showed UV maxima at 207, 228, 286 and 291sh nm, and IR bands at 3340, 1645 and 1539 cm^{-1}. ^{1}H-NMR spectrum of **1** showed a singlet for a methoxyl at δ 3.82, two singlets for aromatic protons at δ 6.68 and 6.71, a singlet for an olefinic proton at δ 7.27, signals for a terminal vinyl group at δ 5.45 (dt, J=10.5, 1.0 Hz), 5.48 (dt, J=18.0, 1.0 Hz) and 6.05 (ddd, J=18.0, 10.5, 7.5 Hz), and two acetal proton signals at δ 5.47 (d, J=8.0 Hz) and 4.75 (d, J=8.0 Hz). These spectral features as well as ^{13}C-NMR spectral data of **1** demonstrated its structural similarity to alangiside (**3**), which was also isolated from this plant material. The high resolution secondary ion mass spectrum (HR-SI-MS) of **1**, however, exhibited a strong peak at m/z 524.2125 ($[M+H]^+$) indicating a molecular formula of $C_{25}H_{33}NO_{11}$ for **1**, H_2O more than that of **3**. All these results, together with its chromatographic behavior, suggested **1** to be a hydrolysate of alangiside, *i.e.* 6-*O*-methyl-*N*-deacetylipecosidic acid. The placement of the methoxyl group at C-6 was deduced from a nuclear Overhauser enhancement and exchange spectroscopy (NOESY) interaction between a methoxyl signal at δ 3.82 and an aromatic proton at δ 6.71, which was assignable to H-5 by a cross-peak with H-4.

Final structural confirmation was obtained from the chemical correlation of **1** with alangiside (**3**) and 6-*O*-methylipecoside (**11**).[10] Conventional acetylation of **1** gave alangiside pentaacetate (**12**) and **13**, the latter of which was methylated with CH_2N_2–Et_2O to yield 6-*O*-methylipecoside pentaacetate (**14**).[10] Accordingly, the structure of **1** was elucidated as 6-*O*-methyl-*N*-deacetylipecosidic acid.

Compound **2** was isolated as a colorless amorphous powder, and was analyzed for $C_{23}H_{28}O_{11}$ from its HR-SI-MS. This revealed UV absorptions at 229 and 279sh nm and IR bands at 3413, 1702, 1637 and 1508 cm^{-1}. The ^{1}H-NMR spectrum of **2** showed a doublet at δ 7.46 (J=1.5 Hz) charac-

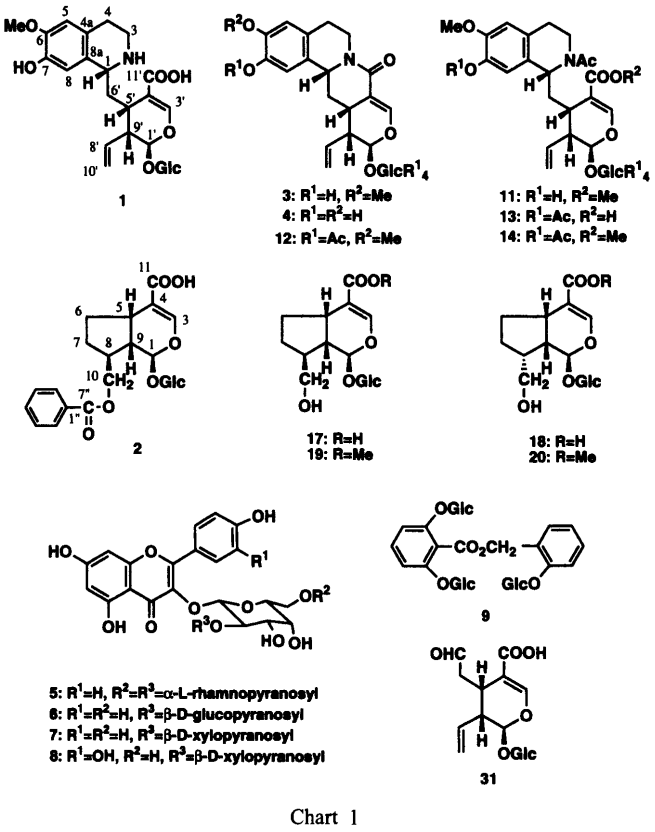

Chart 1

* To whom correspondence should be addressed.

© 2000 Pharmaceutical Society of Japan

Table 1. ^{13}C-NMR Spectral Data for Compounds **2**, **15**, **16**, **19**, **20**, **22**, **23**, **27** and **28**

C	**2** [a,c]	**15** [b,c]	**16** [a,d,f]	**19** [e]	**20** [e]	**22** [b,d,g]	**23** [b,d,g]	**27** [a,d,f]	**28** [a,d,f]
1	98.8	98.9	95.8	98.6	96.3	96.8	97.5	96.5	94.5
3	152.9	153.5	150.6	153.2	152.9	151.5	151.7	150.8	150.5
4	112.7	111.8	111.8	111.8	112.7	111.8	111.7	111.7	112.0
5	37.0	36.8	33.8	35.0	34.4	34.3	35.8	34.5	35.1
6	33.8	33.7	31.0	32.4	31.1	38.7	39.0	31.8	31.0
7	28.9	28.8	27.2	27.8	27.0	128.5	129.6	27.4	24.9
8	41.3	41.2	39.2	43.1	44.4	140.1	142.8	42.9	45.1
9	44.5	44.9	44.1	43.7	42.2	46.6	45.0	43.7	41.0
10	69.1	69.0	67.5	65.9	63.4	62.5	61.0	66.3	62.6
11	171.5	169.5	167.2	170.7	171.1	167.8	167.6	167.4	167.4
OMe	—	51.7	51.2	52.6	52.6	51.3	51.3	51.2	51.3
1′	100.9	100.9	96.4	99.9	99.4	98.8	98.4	96.3	96.3
2′	74.6	74.6	70.6	73.6	73.5	73.1	73.3	70.8	70.8
3′	78.0	78.0	72.5	76.6	76.5	75.5	75.1	72.4	72.0
4′	71.4	71.4	68.2	70.4	70.3	69.6	70.9	68.3	68.4
5′	78.3	78.3	72.1	77.1	77.1	76.0	76.3	72.1	72.3
6′	62.7	62.7	61.7	61.5	61.5	61.7	63.0	61.7	61.4
1″	131.5	131.5	130.1						
2″, 6″	130.6	130.6	129.6						
3″, 5″	129.7	129.7	128.4						
4″	134.3	134.4	133.1						
7″	168.3	168.7	166.5						

a—*d*) Measured at *a*) 125 MHz or *b*) 75 MHz in *c*) CD_3OD or *d*) $CDCl_3$. *e*) Data taken from ref. 12. *f*) Compounds **16**, **27** and **28** showed signals of acetyl groups at δ 20.6—20.7 (CH_3) and 169.4—170.6 (CO). *g*) Compounds **22** and **23** showed signals of the trityl group at δ 113.3 (C), 143.4 (3×C) and 127.0—128.6 (15×CH) or close to those values.

teristic of an olefinic proton of the enol ether system conjugated with a carbonyl group, and signals for two acetal protons at δ 5.18 (d, J=7.5 Hz) and 4.66 (d, J=8.0 Hz), implying an iridoidic skeleton for **2**. Furthermore, it showed signals for H_2-6 and H_2-7 at δ 1.48—2.26, and acyloxy methylene signals at δ 4.29 (dd, J=11.0, 6.5 Hz) and 4.37 (dd, J=11.0, 6.5 Hz), which were assigned to H_2-10 by a sequence of correlations of H_2-10, H-8 (δ 2.52), H-9 (δ 2.09) and H-1 (δ 5.18) in the ^{1}H–^{1}H chemical shift correlation spectroscopy (COSY) spectrum, and aromatic proton signals (5H) assignable to a benzoyl group. The ^{13}C-NMR spectrum of **2** exhibited, besides the signals corresponding to a benzoyl group and a β-D-glucosyl unit, ten carbon signals including a carboxyl carbon (δ 171.5) and an oxymethylene (δ 69.1). In the ^{1}H-detected heteronuclear multiple-bond connectivity (HMBC) spectrum, interactions from H_2-10 to a carbonyl carbon (δ 168.3) were observed. The presence of a carboxyl group was confirmed by the fact that the methylation of **2** with CH_2N_2–Et_2O gave a methyl ester, **15**, which was further acetylated to a tetraacetate, **16**. These findings suggest that compound **2** possesses adoxosidic acid (**17**)[11] or its 8-epimer (**18**) as a basic skeleton, whose hydroxyl group at C-10 is benzoylated. Inspection of the chemical shifts of C-8 and C-9 in the ^{13}C-NMR spectra of **15**, adoxoside (**19**), and **20** implied the β-orientation of the oxymethylene group in **2**.[12] The configuration of C-8 was further supported by a NOESY interaction between H-8 and H-1. All these findings allowed us to formulate the structure of **2** as 10-*O*-benzoyladoxosidic acid.

In order to confirm the proposed structure, 10-*O*-benzoyladoxoside tetraacetate was chemically prepared from geniposide (**21**), as follows. Geniposide (**21**) was treated with 1 eq mol of trityl chloride (TrCl) in pyridine, giving two trityl ethers, **22** and **23**, in the ratio of 3 : 1. The attachment of a trityl group to the hydroxyl at C-10 in **22** and at C-6′ in **23** was determined by comparison of their ^{13}C-NMR data, where a downfield shift was observed for C-10 in **22** and for C-6′ in **23**. This was further supported by downfield shifts due to the acetylation of H_2-10 in **25** (**24**: δ 3.63, 3.78; **25**: δ 4.74, 4.88) and H_2-6′ in **24** (**24**: δ 3.88, 4.12; **25**: δ 3.10, 3.25), when **22** and **23** were acetylated to **24** and **25**, respectively. Compound **24** was heated at 80 °C in 80% AcOH to remove a trityl group, giving rise to 10-ol (**26**). Hydrogenation of **26** over Adams' catalyst afforded two stereoisomers, **27** and **28** (1 : 2). Comparative studies of their ^{13}C-NMR spectra, in which carbon signals for C-9 and C-10 of **28** were observed in a higher region than those of **27**, whereas the C-8 of **28** resonated at a lower field than that of **27**, suggested that **27** has a β-oriented substituent at C-8.[12] This assumption was supported by the fact that a NOESY correlation between H-1 and H-8 was observed in **27** but not in **28**. The stereochemistry of **27** and **28** was further confirmed by acetylation of each compound to the two known acetates **29** and **30**, respectively.[13] Finally, compound **27** was benzoylated to give 10-*O*-benzoyladoxoside tetraacetate, which was completely identical with **16** derived from **2**. Thus, the new glucoside was unequivocally assigned as 10-*O*-benzoyladoxosidic acid (**2**).

Tetrahydroisoquinoline-monoterpene glycosides such as 6-*O*-methyl-*N*-deacetylipecosidic acid (**1**) and alangiside (**3**), have so far been isolated only in species of the genera *Alangium* (Alangiaceae) and *Cephaelis* (Rubiaceae). The present work gives an additional example of the isolation of this type of glucoside from the *Alangium* species. It is also noteworthy that **1** possesses amino and carboxy groups in its structure. This is the first instance of a tetrahydroisoquinoline-monoterpene glucoside with an amino group, implying the possibility of biogenetic condensation of secologanic acid (**31**) with dopamine.

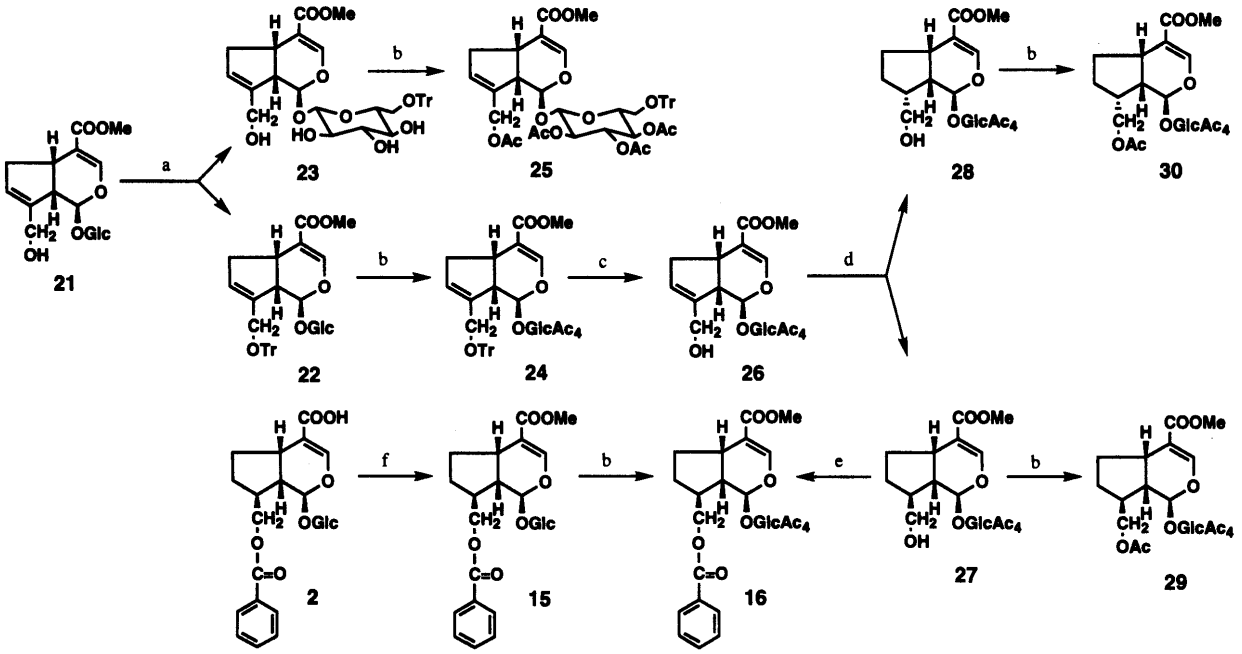

(a) TrCl, Py; (b) Ac_2O, Py; (c) 80% AcOH, 80°C; (d) H_2/PtO_2, EtOH; (e) Benzoyl chloride, Py; (f) CH_2N_2–Et_2O, MeOH.

Chart 2

Experimental

Melting points were measured on Yanagimoto microapparatus and are uncorrected. The UV spectra were recorded on a Shimadzu UV-240 spectrophotometer and the IR spectra on a Shimadzu FT-IR-8200 spectrophotometer. The optical rotations were measured on a Jasco DIP-370 digital polarimeter. SI-MS, electron impact (EI)-MS, HR-SI-MS and HR-EI-MS were obtained with a Hitachi M-4100 mass spectrometer. Glycerol or 3-nitrobenzyl alcohol (3-NOBA) was used for SI-MS as the matrix. The NMR experiments were performed with Varian VXR-500, Varian Gemini-300 and Varian Gemini-200 spectrometers, with tetramethylsilane as an internal standard. HPLC was performed using a Waters system (510 HPLC pump, 486 Tunable absorbance detector). Thin-layer chromatography was performed on precoated Kieselgel $60F_{254}$ plates (Merck) and spots were visualized under UV light.

Isolation of Glucosides *Alangium kurzii* Craib. was collected in Xishuangbanna, Yunnan Province, People's Republic of China. A voucher specimen (KPFY-942) was deposited in the laboratory of Kobe Pharmaceutical University. The dried leaves (173 g) were extracted with hot MeOH. The MeOH extract (34.5 g) was suspended in H_2O and successively partitioned with $CHCl_3$ and *n*-BuOH, to give three fractions weighing 0.91 g ($CHCl_3$), 7.8 g (*n*-BuOH) and 16.2 g (H_2O). An aliquot (3.6 g) of the *n*-BuOH-soluble fraction was chromatographed on a Diaion HP-20 (Nippon Rensui Co., Japan) column. Elution with MeOH–H_2O mixtures with increasing MeOH content (0—50%) gave 8 fractions, B-I (H_2O), B-II (5% MeOH–H_2O), B-III (10% MeOH–H_2O), B-IV (15% MeOH–H_2O), B-V (20% MeOH–H_2O), B-VI (40% MeOH–H_2O), B-VII (45% MeOH–H_2O), and B-VIII (50% MeOH–H_2O). Fraction B-II (135 mg) was further purified by a combination of prep. TLC ($CHCl_3$–MeOH, 7:3) and prep. HPLC (μBondasphere 5 μC18-100 Å, MeOH–H_2O, 1:9), giving **10** (9.2 mg). The following fractions were also purified by prep. HPLC (μBondasphere 5 μC18-100 Å, MeOH–H_2O, 1:4, 3:17, 3:7, 2:3, 11:9 or MeCN–H_2O, 13:87) and prep. TLC ($CHCl_3$–MeOH, 7:3 or 6:4 or acetone–$CHCl_3$–H_2O, 8:2:1). Fraction B-IV (207 mg) yielded **9** (6.0 mg); fraction B-V (183 mg): **1** (31.7 mg); fraction B-VI (752 mg): **3** (13.8 mg), **4** (23.9 mg), **5** (188 mg), **6** (27.4 mg), **7** (127 mg), and **8** (13.1 mg); fraction B-VII (187 mg): **3** (64.4 mg); and fraction B-VIII (122 mg): **2** (24.5 mg). An aliquot (7.8 g) of the H_2O-soluble fraction was chromatographed on a Wakogel LP-40 C18 (Wako Pure Chemical Industries, Ltd., Osaka, Japan) column. Elution with MeOH–H_2O mixtures with increasing MeOH content (0—50%) gave 4 fractions, W-I (H_2O), W-II (10% MeOH–H_2O), W-III (30% MeOH–H_2O), and W-IV (50% MeOH–H_2O). Fractions W-II (870 mg) and W-III (618 mg) were purified by prep. HPLC (μBondasphere 5 μC18-100 Å, MeOH–H_2O, 3:7 and MeCN–H_2O, 13:87) to yield **1** (231 mg and 146 mg, respectively). Fraction W-IV was purified by prep. HPLC (μBondasphere 5 μC18-100 Å, MeOH–H_2O, 1:1) to yield **3** (37.3 mg).

6-*O*-Methyl-*N*-deacetylipecosidic Acid (**1**): Colorless crystalline solid, mp 203—205 °C (MeOH); $[\alpha]_D^{26}$ −144° (*c*=0.2, pyridine); $[\alpha]_D^{21}$ −124° (*c*=0.34, MeOH). UV λ_{max}^{MeOH} nm (log ε): 207 (4.51), 228 (4.18), 286 (3.56), 291sh (3.52). IR ν_{max}^{KBr} cm^{-1}: 3340, 1645, 1539. ^{1}H-NMR (500 MHz, CD_3OD) δ: 1.93 (1H, ddd, *J*=15.5, 12.0, 3.5 Hz, H-6′), 2.21 (1H, ddd, *J*=15.5, 5.0, 2.0 Hz, H-6′), 2.76 (1H, dddt, *J*=8.0, 7.5, 5.0, 1.0 Hz, H-9′), 2.84 (1H, td, *J*=5.0, 3.5 Hz, H-5′), 2.89 (1H, dt, *J*=17.0, 4.5 Hz, H-4), 2.96 (1H, dt, *J*=17.0, 8.0 Hz, H-4), 3.22 (1H, dd, *J*=9.0, 8.0 Hz, H-2″), 3.26 (1H, dd, *J*=10.0, 9.0 Hz, H-4″), 3.28—3.33 (2H, m, H_2-3), 3.31 (1H, ddd, *J*=10.0, 6.0, 2.0 Hz, H-5″), 3.39 (1H, t, *J*=9.0 Hz, H-3″), 3.65 (1H, dd, *J*=12.0, 6.0 Hz, H-6″), 3.82 (3H, s, OMe), 3.91 (1H, dd, *J*=12.0, 2.0 Hz, H-6″), 4.30 (1H, dd, *J*=12.0, 2.0 Hz, H-1), 4.75 (1H, d, *J*=8.0 Hz, H-1″), 5.45 (1H, dt, *J*=10.5, 1.0 Hz, H-10′), 5.47 (1H, d, *J*=8.0 Hz, H-1′), 5.48 (1H, dt, *J*=18.0, 1.0 Hz, H-10′), 6.05 (1H, ddd, *J*=18.0, 10.5, 7.5 Hz, H-8′), 6.68 (1H, s, H-8), 6.71 (1H, s, H-5), 7.27 (1H, s, H-3′). ^{13}C-NMR (125 MHz, CD_3OD) δ: 26.0 (C-4), 35.2 (C-5′), 38.8 (C-6′), 39.1 (C-3), 46.0 (C-9′), 56.4 (OMe), 57.6 (C-1), 62.9 (C-6″), 71.7 (C-4″), 74.8 (C-2″), 78.0 (C-3″), 78.5 (C-5″), 96.9 (C-1′), 100.2 (C-1″), 112.5 (C-5), 114.1 (C-8), 116.4 (C-4′), 120.2 (C-10′), 123.9 (C-4a), 126.0 (C-8a), 136.3 (C-8′), 147.0 (C-7), 149.1 (C-6), 150.1 (C-3′), 175.2 (C-11′). NOESY: H-1/H-8, H-1/H-5′, H-4 (δ 2.89)/H-5, H-5/OMe, H-8/H-6′ (δ 2.21), H-1′/H-9′, H-1′/H-1″. HMBC: H-1→C-3, 4a, 8, 8a, 5′, 6′, H_2-3→C-1, 4, 4a, H_2-4→C-3, 4a, 5, 8a, H-5→C-4, 4a, 6, 7, 8a, H-8→C-1, 4a, 6, 7, 8a, H-1′→C-3′, 5′, 9′, 1″, H-3′→C-1′, 4′, 5′, 11′, H-5′→C-1′, 9′, H-6′ (δ 1.93)→C-1, H-6′ (δ 2.21)→C-8a, 5′, 9′, H-8′→C-1′, H-9′→C-1′, 5′, 6′, 8′, 10′, H_2-10→C-8′, 9′, OMe→C-6. Positive ion SI-MS *m/z*: 524 $[M+H]^+$, 344, 178. Positive ion HR-SI-MS Calcd for $C_{25}H_{34}NO_{11}$: 524.2133. Found: 524.2125.

10-*O*-Benzoyladoxosidic Acid (**2**): Colorless amorphous powder, $[\alpha]_D^{24}$ −46° (*c*=1.11, MeOH). UV λ_{max}^{MeOH} nm (log ε): 229 (4.29), 279sh (3.03). IR ν_{max}^{KBr} cm^{-1}: 3413, 1702, 1637, 1508. ^{1}H-NMR (500 MHz, CD_3OD) δ: 1.48 (2H, m, H-6, 7), 1.95 (1H, m, H-7), 2.09 (1H, td, *J*=7.5, 5.0 Hz, H-9), 2.26 (1H, m, H-6), 2.52 (1H, m, H-8), 2.90 (1H, br q, *J*=7.5 Hz, H-5), 3.07 (1H, dd, *J*=9.0, 8.0 Hz, H-2′), 3.25 (1H, dd, *J*=9.5, 9.0 Hz, H-4′), 3.28 (1H, ddd, *J*=9.5, 5.5, 2.0 Hz, H-5′), 3.35 (1H, t, *J*=9.0 Hz, H-3′), 3.65 (1H, dd, *J*=12.0, 5.5 Hz, H-6′), 3.84 (1H, dd, *J*=12.0, 2.0 Hz, H-6″), 4.29 (1H, dd, *J*=11.0, 6.5 Hz, H-10), 4.37 (1H, dd, *J*=11.0, 6.5 Hz, H-10), 4.66 (1H, d, *J*=8.0 Hz, H-1′), 5.18 (1H, d, *J*=7.5 Hz, H-1), 7.46 (1H, d, *J*=1.5 Hz, H-3), 7.49 (2H, td, *J*=7.5, 1.5 Hz, H-3″, 5″), 7.61 (1H, tt, *J*=7.5, 1.5 Hz, H-4″), 8.04 (2H, dt, *J*=7.5, 1.5 Hz, H-2″, 6″). ^{13}C-NMR: Table 1. NOESY: H-1/H-

8, H-5/H-6 (δ 2.26), H-5/H-9, H-6 (δ 1.48)/ H-7 (δ 1.95), H-6 (δ 2.26)/H-7 (δ 1.48), H-7 (δ 1.95)/H-8. HMBC: H-1→C-1′, H-3→C-4, 11, H-5→C-3, 4, 6, H_2-6→C-5, 7, H_2-7→C-5, H-8→C-1, 5, 6, 7, 9, 10, H-9→C-1, 4, 5, 7, 8, 10, H_2-10→C-7, 8, 9, 7″, H-2″, 6″→C-1″, 7″, H-3″, 5″→C-1″. Negative ion SI-MS *m/z*: 479 $[M-H]^-$. Negative ion HR-SI-MS Calcd for $C_{23}H_{27}O_{11}$: 479.1554. Found: 479.1557.

Acetylation of 1 Compound **1** (10.8 mg) was acetylated with Ac_2O–pyridine, and the crude acetate (14.6 mg) was purified by prep. TLC ($CHCl_3$–MeOH, 19 : 1) to yield **12** (1.0 mg) and **13** (12.5 mg). Compound **12** was identified with authentic alangiside pentaacetate. **13** (6-*O*-Methylipecosidic acid pentaacetate): ^{1}H-NMR (200 MHz, $CDCl_3$) δ: 1.46 (1H, ddd, *J*=14.0, 13.0, 4.0 Hz, H-6′), 1.86, 2.00, 2.02, 2.13, 2.24, 2.27 (18H, each s, 6×Ac), 2.42—2.63 (2H, m, H-5′, 6′), 2.74 (1H, dd, *J*=17.0, 3.6 Hz, H-4), 2.93 (1H, ddd, *J*=17.0, 12.0, 6.0 Hz, H-4), 3.32 (1H, m, H-9′), 3.56—3.80 (2H, m, H-3, 5″), 3.77 (3H, s, OMe), 3.89 (1H, dd, *J*=14.0, 6.0 Hz, H-3), 4.14 (1H, dd, *J*=12.5, 2.2 Hz, H-6″), 4.27 (1H, dd, *J*=12.5, 4.0 Hz, H-6″), 4.78 (1H, d, *J*=8.0 Hz, H-1″), 5.00 (1H, dd, *J*=9.0, 8.0 Hz, H-2″), 5.10 (1H, t, *J*=9.0 Hz, H-4″), 5.20 (1H, t, *J*=9.0 Hz, H-3″), 5.42 (1H, d, *J*=2.0 Hz, H-1′), 5.42 (1H, dd, *J*=6.5, 5.0 Hz, H-10′), 5.57—5.70 (3H, m, H-1, 8′, 10′), 6.59 (1H, s, H-8), 6.63 (1H, s, H-5), 7.44 (1H, d, *J*=1.5 Hz, H-3′).

Compound **13** (5.8 mg) was dissolved in MeOH (1 ml) and treated with CH_2N_2–Et_2O in the usual way. Purification of the crude product (6.6 mg) by prep. TLC ($CHCl_3$–MeOH, 19 : 1) gave **14** (5.9 mg) as a colorless amorphous powder, $[\alpha]_D^{26}$ −163° (*c*=0.35, $CHCl_3$). HR-EI-MS Calcd for $C_{38}H_{47}NO_{17}$: 789.2846. Found: 789.2865. The ^{1}H-NMR, IR, UV and EI mass spectral data for the compound were completely identical with those of authentic 6-*O*-methylipecoside pentaacetate.

Methylation of 2 Compound **2** (10.3 mg) was dissolved in MeOH and treated with CH_2N_2–Et_2O in the usual way to afford **15** (10.0 mg). **15**: Colorless amorphous powder. ^{1}H-NMR (300 MHz, CD_3OD) δ: 1.47 (2H, m, H-6, 7), 1.94 (1H, m, H-7), 2.10 (1H, td, *J*=7.5, 5.0 Hz, H-9), 2.25 (1H, m, H-6), 2.51 (1H, m, H-8), 2.91 (1H, br q, *J*=7.5 Hz, H-5), 3.07 (1H, dd, *J*=9.0, 8.0 Hz, H-2′), 3.26 (1H, t, *J*=9.0 Hz, H-4′), 3.31 (1H, m, H-5′), 3.35 (1H, t, *J*=9.0 Hz, H-3′), 3.65 (1H, dd, *J*=12.0, 5.5 Hz, H-6′), 3.71 (3H, s, COOMe), 3.84 (1H, dd, *J*=12.0, 2.0 Hz, H-6′), 4.28 (1H, dd, *J*=11.0, 6.5 Hz, H-10), 4.37 (1H, dd, *J*=11.0, 6.0 Hz, H-10), 4.66 (1H, d, *J*=8.0 Hz, H-1′), 5.19 (1H, d, *J*=7.5 Hz, H-1), 7.49 (1H, br s, H-3), 7.49 (2H, td, *J*=7.5, 1.5 Hz, H-3″, 5″), 7.61 (1H, tt, *J*=7.5, 1.5 Hz, H-4″), 8.04 (2H, dt, *J*=7.5, 1.5 Hz, H-2″, 6″). ^{13}C-NMR: Table 1.

Acetylation of 15 Conventional acetylation of **15** (10.0 mg) and subsequent purification of the crude acetate (13.2 mg) by prep. TLC (Et_2O) yielded **16** (8.4 mg). **16**: Colorless needles, mp 180—182 °C (MeOH). $[\alpha]_D^{22}$ −52° (*c*=0.70, $CHCl_3$). UV λ_{max}^{EtOH} nm (log ε): 230 (4.36). IR ν_{max}^{KBr} cm^{-1}: 1742, 1700, 1641, 1367. ^{1}H-NMR (500 MHz, $CDCl_3$) δ: 1.49 (1H, m, H-7), 1.65 (1H, m, H-6), 1.89 (1H, m, H-7), 1.97, 2.00, 2.02, 2.05 (12H, each s, 4×Ac), 2.13 (1H, m, H-6), 2.20 (1H, td, *J*=7.5, 4.5 Hz, H-9), 2.34 (1H, m, H-8), 2.95 (1H, br q, *J*=7.5 Hz, H-5), 3.69 (1H, ddd, *J*=9.5, 4.5, 2.5 Hz, H-5′), 3.72 (3H, s, COOMe), 4.04 (1H, dd, *J*=12.0, 2.5 Hz, H-6′), 4.26 (1H, dd, *J*=12.0, 4.5 Hz, H-6′), 4.27 (1H, dd, *J*=11.0, 7.0 Hz, H-10), 4.33 (1H, dd, *J*=11.0, 7.0 Hz, H-10), 4.85 (1H, d, *J*=8.5 Hz, H-1′), 4.96 (1H, dd, *J*=9.5, 8.5 Hz, H-2′), 5.07 (1H, t, *J*=9.5 Hz, H-4′), 5.21 (1H, t, *J*=9.5 Hz, H-3′), 5.23 (1H, d, *J*=4.5 Hz, H-1), 7.39 (1H, d, *J*=1.0 Hz, H-3), 7.46 (2H, td, *J*=7.5, 1.5 Hz, H-3″, 5″), 7.57 (1H, tt, *J*=7.5, 1.5 Hz, H-4″), 8.03 (2H, dt, *J*=7.5, 1.5 Hz, H-2″, 6″). ^{13}C-NMR: Table 1. NOESY: H-1/H-8, H-5/H-9. HMBC: H-1→C-3, 9, 1′, H-3→C-1, 4, 5, 11, H-5→C-1, 4, 8, 9, H_2-6→C-4, 5, 7, 8, H-7 (δ 1.49)→C-5, 6, 8, 10, H-7 (δ 1.89)→C-5, 8, 9, H-8→C-1, 5, 7, 10, H-9→C-1, 5, 7, 8, H_2-10→C-7, 8, 9, 7″, H-2″, 6″→C-1″, 4″, 7″, H-3″, 5″→C-1″, 2″, 4″, 6″, H-4″→C-2″, 6″. Positive ion SI-MS *m/z*: 663 $[M+H]^+$. Positive ion HR-SI-MS Calcd for $C_{32}H_{39}O_{15}$: 663.2290. Found: 663.2280.

Tritylation of Geniposide (21) To a solution of geniposide (**21**) (502 mg) in pyridine (3 ml) was added TrCl (360 mg), and the mixture was stirred at room temperature overnight. After concentration, the residue was purified by column chromatography on silica gel ($CHCl_3$–MeOH), giving rise to **22** (303 mg, 37%) and **23** (117 mg, 14%). **22**: IR ν_{max}^{KBr} cm^{-1}: 3419, 1713, 1634, 1491. ^{1}H-NMR (300 MHz, $CDCl_3$) δ: 2.14 (1H, m, H-6), 2.74 (1H, m, H-5), 2.89 (1H, m, H-6), 3.02 (1H, m, H-9), 3.16—3.27 (4H, m, H-2′, 3′, 4′, 5′), 3.57—3.67 (2H, m, H_2-6′), 3.58 (1H, m, H-10), 3.67 (3H, s, COOMe), 3.78 (1H, d, *J*=13.5 Hz, H-10), 4.53 (1H, d, *J*=8.0 Hz, H-1′), 4.96 (1H, d, *J*=6.5 Hz, H-1), 5.99 (1H, m, H-7), 7.15—7.43 (15H, m, ArH), 7.44 (1H, d, *J*=1.0 Hz, H-3). ^{13}C-NMR: Table 1. Negative ion SI-MS *m/z*: 629 $[M-H]^-$. Negative ion HR-SI-MS Calcd for $C_{36}H_{37}O_{10}$: 629.2388. Found: 629.2373. **23**: IR ν_{max}^{KBr} cm^{-1}: 3363, 1711, 1634, 1491. ^{1}H-NMR (300 MHz, $CDCl_3$) δ: 1.96 (1H, m, H-6), 2.74—2.87 (2H, m, H-5, 6), 3.13 (1H, m, H-9), 3.10—3.47 (3H, m, H-2′, 3′, 4′), 3.24 (1H, dd, *J*=10.0, 5.0 Hz, H-6′), 3.27—3.32 (1H, m, H-5′), 3.32 (1H, m, H-6′), 3.70 (3H, s, COOMe), 4.17 (1H, d, *J*=13.5 Hz, H-10), 4.31 (1H, d, *J*=13.5 Hz, H-10), 4.74 (1H, d, *J*=8.0 Hz, H-1′), 5.71 (1H, m, H-7), 7.15—7.44 (15H, m, ArH), 7.46 (1H, br s, H-3). ^{13}C-NMR: Table 1.

Acetylation of 22 and 23 Compound **22** (303 mg) was acetylated with Ac_2O–pyridine, and an aliquot (21.8 mg) of the crude acetate (403 mg) was purified by prep. TLC ($CHCl_3$–MeOH, 19 : 1) to yield **24** (16.0 mg). Compound **23** was acetylated by the same procedure as described for **22** to give **25**. **24**: IR ν_{max}^{KBr} cm^{-1}: 1761, 1636, 1367. ^{1}H-NMR (300 MHz, $CDCl_3$) δ: 1.93, 1.96 (6H, each s, 2×Ac), 2.02 (6H, s, 2×Ac), 2.16 (1H, m, H-6), 2.83—2.88 (2H, m, H-5, 6), 3.19 (1H, m, H-9), 3.58 (1H, m, H-5′), 3.63 (1H, d, *J*=13.5 Hz, H-10), 3.71 (3H, s, COOMe), 3.78 (1H, d, *J*=13.5 Hz, H-10), 3.88 (1H, dd, *J*=12.0, 2.5 Hz, H-6′), 4.12 (1H, dd, *J*=12.0, 4.5 Hz, H-6′), 4.73 (1H, d, *J*=8.0 Hz, H-1′), 4.75 (1H, m, H-2′), 5.00 (1H, t, *J*=9.0 Hz, H-4′), 5.13 (1H, d, *J*=5.4 Hz, H-1), 5.15 (1H, t, *J*=9.0 Hz, H-3′), 5.88 (1H, m, H-7), 7.16—7.43 (15H, m, ArH), 7.47 (1H, d, *J*=1.0 Hz, H-3). Positive ion HR-SI-MS Calcd for $C_{44}H_{47}O_{14}$: 799.2968. Found: 799.2954. **25**: IR ν_{max}^{KBr} cm^{-1}: 1761, 1636, 1375. ^{1}H-NMR (300 MHz, $CDCl_3$) δ: 1.70, 1.92, 1.99, 2.02 (12H, each s, 4×Ac), 2.16 (1H, m, H-6), 2.89 (2H, m, H-5, 6), 2.90 (1H, m, H-9), 3.10 (1H, dd, *J*=12.0, 4.5 Hz, H-6′), 3.25 (1H, m, H-6′), 3.58 (1H, m, H-5′), 3.73 (3H, s, COOMe), 4.74 (1H, d, *J*=13.5 Hz, H-10), 4.88 (1H, d, *J*=13.5 Hz, H-10), 4.91 (1H, d, *J*=8.0 Hz, H-1′), 5.08 (1H, t, *J*=8.0 Hz, H-2′), 5.12 (1H, t, *J*=8.0 Hz, H-4′), 5.17 (1H, d, *J*=7.0 Hz, H-1), 5.17 (1H, t, *J*=8.0 Hz, H-3′), 5.88 (1H, m, H-7), 7.22—7.42 (15H, m, ArH), 7.48 (1H, br s, H-3).

Removal of the Trityl Group of 24 A solution of **24** (403 mg) in 80% HOAc (26 ml) was heated at 80 °C for 40 min. The reaction mixture was diluted with ice-water and extracted with $CHCl_3$. The $CHCl_3$ layer was washed successively with 5% $NaHCO_3$ aq. solution and brine, dried and concentrated *in vacuo*. The residue (288 mg) was subjected to prep. TLC ($CHCl_3$–MeOH, 19 : 1), giving **26** (211 mg, 76%). **26**: IR ν_{max}^{KBr} cm^{-1}: 3566, 1766, 1636, 1373. ^{1}H-NMR (300 MHz, $CDCl_3$) δ: 2.02 (6H, s, 2×Ac), 2.03, 2.08 (6H, each s, 2×Ac), 2.28 (2H, m, H-6, 9), 2.78 (1H, br q, *J*=7.5 Hz, H-5), 2.69—3.78 (1H, m, H-6), 3.69—3.78 (1H, m, H-5′), 3.73 (3H, s, COOMe), 4.15 (1H, dd, *J*=12.0, 2.0 Hz, H-6′), 4.25 (2H, s-like, H_2-10), 4.31 (1H, dd, *J*=12.0, 4.5 Hz, H-6′), 4.91 (1H, d, *J*=8.0 Hz, H-1′), 5.02 (1H, d, *J*=6.6 Hz, H-1), 5.03 (1H, dd, *J*=9.0, 8.0 Hz, H-2′), 5.11 (1H, t, *J*=9.0 Hz, H-4′), 5.26 (1H, t, *J*=9.0 Hz, H-3′), 5.82 (1H, m, H-7), 7.44 (1H, br s, H-3). Positive ion SI-MS *m/z*: 557 $[M+H]^+$. Positive ion HR-SI-MS Calcd for $C_{25}H_{33}O_{14}$: 557.1871. Found: 557.1876.

Catalytic Hydrogenation of 26 A solution of compound **26** (211 mg) in EtOH (7.0 ml) was hydrogenated at room temperature over PtO_2 (40 mg). After completion of the H_2 uptake, the catalyst was filtered off and the filtrate was concentrated *in vacuo*. The residue (231 mg) was purified by prep. HPLC (MeOH–H_2O, 47 : 53) to give **27** (48.9 mg, 23%) and **28** (105 mg, 50%). **27**: IR ν_{max}^{KBr} cm^{-1}: 3480, 1759, 1636. ^{1}H-NMR (500 MHz, $CDCl_3$) δ: 1.32 (1H, m, H-7), 1.47 (1H, m, H-6), 1.81 (1H, m, H-7), 1.98, 2.01, 2.03, 2.10 (12H, each s, 4×Ac), 2.00 (1H, m, H-9), 2.06 (1H, m, H-8), 2.13 (1H, m, H-6), 2.84 (1H, br q, *J*=7.5 Hz, H-5), 3.56 (1H, dd, *J*=10.5, 7.5 Hz, H-10), 3.63 (1H, dd, *J*=10.5, 7.5 Hz, H-10), 3.71 (3H, s, COOMe), 3.74 (1H, ddd, *J*=10.0, 4.5, 2.0 Hz, H-5′), 4.17 (1H, dd, *J*=12.0, 2.0 Hz, H-6′), 4.28 (1H, dd, *J*=12.0, 4.5 Hz, H-6′), 4.90 (1H, d, *J*=8.0 Hz, H-1′), 5.01 (1H, dd, *J*=9.5, 8.0 Hz, H-2′), 5.09 (1H, d, *J*=6.0 Hz, H-1), 5.12 (1H, dd, *J*=10.0, 9.5 Hz, H-4′), 5.24 (1H, t, *J*=9.5 Hz, H-3′), 7.39 (1H, d, *J*=1.5 Hz, H-3). ^{13}C-NMR: Table 1. NOESY: H-1/H-8, H-5/H-6 (δ 2.13), H-5/H-9, H-6 (δ 2.13)/H-7 (δ 1.81), H-7 (δ 1.81)/H-8. HMBC: H-1→C-3, 5, 1′, H-3→C-1, 4, 5, H-5→C-1, 3, 4, 6, 7, 8, 9, H_2-6→C-4, 5, 7, 8, 9, H-7 (δ 1.32)→C-8, 9, 10, H-7 (δ 1.81)→C-8, H-8→C-1, 7, 9, 10, H-9→C-1, 4, 5, 6, 8, 10, H_2-10→C-7, 8, 9, OMe→C-11. Positive ion SI-MS *m/z*: 559 $[M+H]^+$. Positive ion HR-SI-MS Calcd for $C_{25}H_{35}O_{14}$: 559.2028. Found: 559.2026. **28**: IR ν_{max}^{KBr} cm^{-1}: 3566, 1759, 1639. ^{1}H-NMR (500 MHz, $CDCl_3$) δ: 1.41 (1H, m, H-7), 1.43 (1H, m, H-6), 1.78 (1H, m, H-7), 2.02, 2.03, 2.04, 2.09 (12H, each s, 4×Ac), 2.20—2.28 (1H, m, H-6), 2.20 (1H, m, H-9), 2.46 (1H, m, H-8), 2.89 (1H, br q, *J*=7.5 Hz, H-5), 3.64 (1H, dd, *J*=11.0, 5.0 Hz, H-10), 3.72 (3H, s, COOMe), 3.72 (1H, dd, *J*=11.0, 4.0 Hz, H-10), 3.75 (1H, ddd, *J*=9.5, 4.0, 3.0 Hz, H-5′), 4.22 (1H, dd, *J*=12.0, 4.0 Hz, H-6′), 4.25 (1H, dd, *J*=12.0, 3.0 Hz, H-6′), 5.00 (1H, d, *J*=8.0 Hz, H-1′), 5.04 (1H, dd, *J*=9.5, 8.0 Hz, H-2′), 5.12 (1H, t, *J*=9.5 Hz, H-4′), 5.21 (1H, d, *J*=7.5 Hz, H-1), 5.29 (1H, t, *J*=9.5 Hz, H-3′), 7.38 (1H, d, *J*=1.0 Hz, H-3). ^{13}C-NMR: Table 1. NOESY: H-5/H-6 (δ 1.43), H-5/H-8, H-5/H-9, H-7 (δ 1.78)/H-8, H-8/H-9. HMBC: H-1→C-3, 5, 1′, H-3→C-1, 4, 11, H-5→C-1, 4, 6, 9, H-6 (δ 2.20—2.28)→C-5, 9, H-7 (δ 1.78)→C-5, 9, H-8→C-1, H-9→C-1, 5, 6, 7, 8, H_2-10→C-7, 8, 9, OMe→C-11. Positive ion SI-MS *m/z*: 559 $[M+H]^+$.

Positive ion HR-SI-MS Calcd for $C_{25}H_{35}O_{14}$: 559.2028. Found: 559.2024.

Acetylation of 27 Compound **27** (7.7 mg) was acetylated in the usual way and the resulting crude product (8.2 mg) was purified by prep. TLC (Et_2O) to yield **29** (6.7 mg, 80%) as colorless needles, mp 141—142 °C (EtOH). $[\alpha]_D^{26}$ −58° (c=0.34, $CHCl_3$). IR ν_{max}^{KBr} cm^{-1}: 1751, 1705, 1636. ^{1}H-NMR (500 MHz, $CDCl_3$) δ: 1.37 (1H, m, H-7), 1.61 (1H, m, H-6), 1.80 (1H, m , H-7), 1.94, 2.01, 2.03, 2.06, 2.09 (15H, each s, 5×Ac), 2.06—2.09 (2H, m, H-6, 9), 2.19 (1H, m, H-8), 2.89 (1H, br q, J=7.5 Hz, H-5), 3.71 (3H, s, COOMe), 3.73 (1H, ddd, J=9.5, 4.5, 2.5 Hz, H-5′), 4.02 (1H, dd, J=11.5, 6.5 Hz, H-10), 4.06 (1H, dd, J=11.5, 6.5 Hz, H-10), 4.16 (1H, dd, J=12.0, 2.5 Hz, H-6′), 4.26 (1H, dd, J=12.0, 4.5 Hz, H-6′), 4.86 (1H, d, J=8.0 Hz, H-1′), 4.99 (1H, dd, J=9.5, 8.0 Hz, H-2′), 5.10 (1H, t, J=9.5 Hz, H-4′), 5.18 (1H, d, J=4.0 Hz, H-1), 5.23 (1H, t, J=9.5 Hz, H-3′), 7.37 (1H, d, J=1.5 Hz, H-3). ^{13}C-NMR (125 MHz, $CDCl_3$) δ: 20.3, 20.6 (×2), 20.7, 20.9 (5×COMe), 27.1 (C-7), 31.0 (C-6), 33.7 (C-5), 38.9 (C-8), 44.1 (C-9), 51.2 (OMe), 61.7 (C-6′), 67.1 (C-10), 68.3 (C-4′), 70.7 (C-2′), 72.2 (C-3′), 72.5 (C-5′), 95.6 (C-1), 96.2 (C-1′), 111.8 (C-4), 150.5 (C-3), 167.2 (C-11), 169.1, 169.4, 170.2, 170.6, 171.1 (5×COMe). Positive ion SI-MS m/z: 601 $[M+H]^+$, 331. Positive ion HR-SI-MS Calcd for $C_{27}H_{37}O_{15}$: 601.2134. Found: 601.2139.

Acetylation of 28 Compound **28** (10.2 mg) was acetylated as usual and the resulting crude product (10.1 mg) was purified by prep. TLC (Et_2O) to yield **30** (9.5 mg, 88%) as colorless needles, mp 113—115 °C (EtOH). $[\alpha]_D^{29}$ −55° (c=0.55, $CHCl_3$). IR ν_{max}^{KBr} cm^{-1}: 1759, 1709, 1638. ^{1}H-NMR (500 MHz, $CDCl_3$) δ: 1.40 (1H, m, H-7), 1.63 (1H, m, H-6), 1.83 (1H, m, H-7), 1.95, 2.01, 2.03, 2.06, 2.10 (15H, each s, 5×Ac), 2.08 (1H, m, H-6), 2.40 (1H, m, H-9), 2.48 (1H, m, H-8), 2.92 (1H, br td, J=8.0, 5.0 Hz, H-5), 3.71 (3H, s, COOMe), 3.71 (1H, ddd, J=9.5, 4.0, 3.0 Hz, H-5′), 4.02 (1H, dd, J=11.0, 7.5 Hz, H-10), 4.21 (1H, dd, J=12.0, 3.0 Hz, H-6′), 4.22 (1H, dd, J=11.0, 7.5 Hz, H-10), 4.23 (1H, dd, J=12.0, 4.0 Hz, H-6′), 4.87 (1H, d, J=8.5 Hz, H-1′), 4.98 (1H, dd, J=9.5, 8.5 Hz, H-2′), 5.11 (1H, t, J=9.5 Hz, H-4′), 5.22 (1H, t, J=9.5 Hz, H-3′), 5.31 (1H, d, J=5.0 Hz, H-1), 7.37 (1H, d, J=1.0 Hz, H-3). ^{13}C-NMR (125 MHz, $CDCl_3$) δ: 20.3, 20.6 (×2), 20.7, 21.0 (5×COMe), 27.2 (C-7), 30.6 (C-6), 33.3 (C-5), 40.3 (C-8), 41.6 (C-9), 51.2 (OMe), 61.6 (C-6′), 65.1 (C-10), 68.3 (C-4′), 70.7 (C-2′), 72.2 (C-3′), 72.5 (C-5′), 93.9 (C-1), 95.9 (C-1′), 112.5 (C-4), 150.5 (C-3), 167.1 (C-11), 169.1, 169.4, 170.2, 170.6, 170.9 (5×COMe). Positive ion SI-MS m/z: 601 $[M+H]^+$, 331. Positive ion HR-SI-MS Calcd for $C_{27}H_{37}O_{15}$: 601.2134. Found: 601.2136.

Benzoylation of 27 A mixture of **27** (3.5 mg), benzoyl chloride (0.1 ml) and pyridine (0.3 ml) was allowed to stand at room temperature overnight. The conventional workup of the reaction mixture afforded a crude residue, which was subjected to prep. TLC (Et_2O) to yield **16** (4.4 mg, 100%) as colorless needles, mp 180—182 °C (MeOH). $[\alpha]_D^{26}$ −51° (c=0.25, $CHCl_3$). Positive ion HR-SI-MS Calcd for $C_{32}H_{39}O_{15}$: 663.2290. Found: 663.2297. The ^{1}H-NMR, IR and SI-MS data for the compound were completely identical with those of **16** derived from **2**.

Acknowledgements The technical assistance of Misses K. Sonobe and N. Takemura is acknowledged. Thanks are also due to Dr. M. Sugiura (Kobe Pharmaceutical University) for ^{1}H- and ^{13}C-NMR spectra, and to Dr. K. Saiki (Kobe Pharmaceutical University) for mass spectra measurements.

References and Notes

1) Hou L., Chen M., Zhu H., *Zhongcaoyao*, **12**, 352—353 (1981) [*Chem. Abstr.*, **96**, 139646*r* (1982)].
2) Itoh A., Tanahashi T., Nagakura N., *Heterocycles*, **48**, 499—505 (1998) and references cited therein.
3) Itoh A., Tanahashi T., Nagakura N., Nayeshiro H., *Phytochemistry*, **36**, 383—387 (1994).
4) Itoh A., Tanahashi T., Nagakura N., *Phytochemistry*, **31**, 1037—1040 (1992).
5) Simone F. D., Dini A., Pizza C., Saturnino P., Schettino O., *Phytochemistry*, **29**, 3690—3692 (1990).
6) Zerback R., Bokel M., Geiger H., Hess D., *Phytochemistry*, **28**, 897—899 (1989).
7) Larsen L. M., Nielsen J. K., Sørensen H., *Phytochemistry*, **21**, 1029—1033 (1982).
8) Kijima H., Ide T., Otsuka H., Ogimi C., Hirata E., Takushi A., Takeda Y., *Phytochemistry*, **44**, 1551—1557 (1997).
9) Yaoita Y., Kikuchi M., *Nat. Med.*, **50**, 49—53 (1996).
10) Itoh A., Tanahashi T., Nagakura N., *Phytochemistry*, **30**, 3117—3123 (1991).
11) Gardner D. R., Narum J., Zook D., Stermitz F. R., *J. Nat. Prod.*, **50**, 485—489 (1987).
12) Damtoft S., Jensen S. R., Nielsen B. J., *Phytochemistry*, **20**, 2717—2732 (1981).
13) Inouye H., Nishioka T., *Chem. Pharm. Bull.*, **21**, 497—502 (1973).

Influence of Production Variables on the Sphericity of Melt Pellets

Paul Wan Sia HENG,* Tin Wui WONG, and Lai Wah CHAN

Department of Pharmacy, National University of Singapore, 10 Kent Ridge Crescent, Singapore 119260.
Received October 25, 1999; accepted November 26, 1999

This paper reports the influence of post-melt impeller speed, post-melt processing time, binder concentration and particle size of bulk material on the sphericity of pellets produced by melt pelletization in a high shear mixer. Lactose was used as the bulk material with polyethylene glycol 3000 as a meltable binder. The sphericity of pellets was found to be affected by post-melt impeller speed and post-melt processing time. Binder concentration and particle size of bulk material had a lesser effect on pellet sphericity. The melt pelletization process can be divided into two spheronization phases (a fast initial rate, followed by a slower rate). The change in the spheronization rate was associated with the pellet size, porosity and flow pattern of the processing material. The present study established a bi-exponential mathematical model to relate the pellet sphericity with post-melt specific energy consumption. The relationship of pellet sphericity with post-melt specific energy consumption was independent of the effects of the production variables.

Key words energy; high shear mixer; melt pelletization; sphericity

Melt pelletization is an agglomeration process involving the melting of a solid binder by frictional heat generated from material agitation and shear forces generated by impeller rotation. The agitation impact forces from the impeller increase the plastic deformability of the melt agglomerates and promote coalescence growth. The level of agitation impact forces is dependent on the impeller speed. At higher impeller speeds, the agitation impact forces are stronger and pellet growth rate increases. The mean pellet size is an important variable to be monitored in the production of melt pellets. The control of mean pellet size has been carried out by monitoring the power consumption of the process.[1—3] In a recent study by Heng *et al.*,[4] energy consumption was found to be more suitable for use as a tool for control of mean size of melt pellets. Prediction of pellet growth rate using energy consumption was more accurate than that using power consumption. A more descriptive profile of pellet growth can also be obtained with energy consumption as it indicates the workload expended to consolidate a powder mass into pellets.

Another important measure of the quality of pellets is sphericity. Highly spherical pellets are desirable as such pellets flow well and have minimum surface area to volume ratio, which is ideal for the design of a sustained-release product. This paper describes the effects of processing time, impeller speed, binder concentration and property of bulk material on the sphericity of melt pellets produced. It also examines the relationship of pellet sphericity and post-melt specific energy consumption.

Experimental

Materials Lactose (α-monohydrate lactose, Pharmatose, DMV, The Netherlands) 200, 350 and 450 M with mean particle sizes of 40.32, 35.58 and 21.11 μm respectively were used as the bulk material with polyethylene glycol 3000 (PEG 3000, Hoechst, Germany) as the meltable binder.

Equipment A laboratory scale vertical high shear mixer (Pellmix PL 1/8, Niro, Denmark), not fitted with a chopper, was used for preparation of the pellets.[5] The mixer bowl was water-jacketed for cooling and heating. The inner wall of the mixer bowl was polytetrafluoroethylene (PTFE) -lined. The mixer was fitted with a conical PTFE lid with a viewing glass port at the truncated apex.

A two-bladed, bottom-driven impeller with speeds adjustable up to 1500 rpm was used. The tips of the impeller blades were curved. The bowl was equipped with a thermoresistance probe (PT 100), allowing the temperature of the product to be recorded. The probe was placed through the side wall of the bowl, 50 mm from the floor of the mixer.

Preparation of Pellets A load of lactose 450 M (1 kg) and PEG 3000 at concentration levels of 22, 23 and 24% (w/w), expressed as the percentage of lactose, was used for pelletization. The amount of PEG 3000 was reduced to 17% (w/w) when different lactose grades, 200, 350 and 450 M, were used to compare their effects on the properties of the pellets produced. The lactose and binder were first manually pre-mixed for 5 min. The mixture was then transferred to the high shear mixer and processed at an impeller speed of 1300 rpm. Outputs for power consumption, product temperature and impeller speed were recorded using a 3-pen recorder (LR92620, Linear, U.S.A.). During the dry-processing phase, the impeller produced shear friction that increased the product temperature to the melting point of the binder within a reasonably short time. The onset of melting was read at the inflection point on the product temperature-processing time profile of the recorder tracing.[5] The pre-melt processing time was taken from the start of high shear processing in the melt pelletizer to the onset of binder melting. The post-melt processing time was the additional process time taken from the onset of binder melting to the end of the run. At 2 min after onset of melting, the impeller speed was reduced to 1150 rpm, unless otherwise stated.[4]

At the start of each run, the water jacket was maintained at 30 °C. One minute into the post-melt processing, the jacket set temperature was increased to 80 °C to prevent material adhesion on the mixer wall. On completion of a run, the pellets were immediately collected, weighed and then spread out in thin layers on trays to cool. For each variable studied, preparation of pellets was carried out with different post-melt processing times.

Image Analysis At least 50 pellets were randomly selected for image analysis. These pellets were taken from the modal fraction obtained by sieving. The aperture sizes of the nest of sieves used were 0.075, 0.125, 0.25, 0.355, 0.5, 0.71, 1, 1.4, 2, 2.8 and 4 mm. The image analyser (PC Image 2.2, Foster Findlay Associates, U.K.) consisted of a computer system connected to a video camera (SSC-M370CE, Sony, Japan) mounted on a stereomicroscope (SZH, Olympus, Japan). The average projected area and perimeter of the pellets were determined from the digitized images of the pellets. By transformation of these basic parameters, pellet sphericity was calculated. Sphericity values gave a measure of pellet roundness. A value of unity describes a perfect circle. Sphericity is determined as:

$$\text{pellet sphericity} = \frac{4\pi[\text{area}]}{[\text{perimeter}]^2} \quad (1)$$

Size Analysis The pellets from each batch were divided into random samples using a spinning riffler (PT, Retsch, Germany). A sample of about 100 g was sized using a nest of sieves of aperture sizes 1, 1.4, 2, 2.8 and 4 mm, vibrated at an amplitude of 1 mm (EVS1, Endecotts, U.K.) for 10 min. The sample collected in the receiving pan was subsequently transferred to another set of sieves of aperture sizes 0.075, 0.125, 0.25, 0.355, 0.5 and 0.71 mm and vibrated for 20 min. The mean pellet size was calculated as reported by Heng *et al.*[4]

* To whom correspondence should be addressed.

© 2000 Pharmaceutical Society of Japan

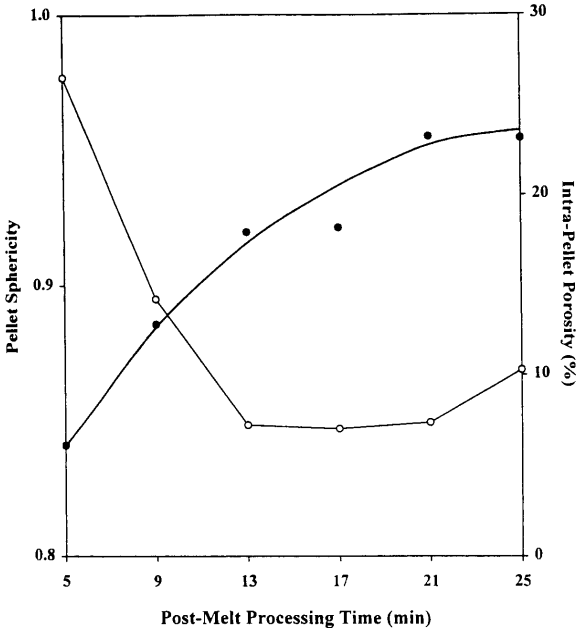

Fig. 1. Profiles of Sphericity and Intra-Pellet Porosity of Pellets Formed at Different Post-Melt Processing Time

Material: lactose 450 M; PEG 3000 concentration: 23% (w/w); post-melt impeller speed: 1150 rpm. Pellet sphericity, ●; intra-pellet porosity, ○.

Porosity Analysis The intra-pellet porosity was determined by a mercury intrusion method (Poresizer 9320, Micromeritics, U.S.A.). The sample size for porosity measurement was about 1.5 g. Triple distilled mercury (Instrument grade, D.F. Goldsmith Chemical and Metal Corporation, U.S.A.) was used. An average intra-pellet porosity was calculated from two determinations for each batch of pellets.

Scanning Electron Microscopy The pellets were fixed with a carbon paste onto studs. The prepared studs were viewed under a scanning electron microscope (JSM 5200, Jeol, Japan). Representative sections were photographed to show the surface morphology of the pellets.

Results and Discussion

Under the influence of centrifugal force generated by the rotation of the impeller, the materials at the bottom of the mixer bowl were observed to move outwards and upwards from the central axis of the impeller and circulated along the wall of the bowl. As they reached the top, they moved inwards and downwards. During the pre-melt processing phase, the lactose and PEG particles were intimately mixed but the binding forces present were insufficient to produce permanent entities. The clusters of adhering particles were constantly fragmenting due to the impact forces of the rotating impeller.

In the post-melt processing phase, the PEG particles were melted when the frictional heat raised the product temperature beyond the melting point of PEG. The molten PEG then acted as a liquid binder responsible for strong liquid bonds between the solid bulk particles and contributed to the formation of more permanent agglomerates. With improved binding strength, the agglomerates could withstand impact shattering forces caused by the impeller. The agglomerates existed as larger unit entities where further growth, consolidation and spheronization could be sustained. At the initial period of the post-melt processing phase, the agglomerates formed were irregular in shape and had lower sphericity values (Fig. 1). Photomicrographs of these agglomerates showed

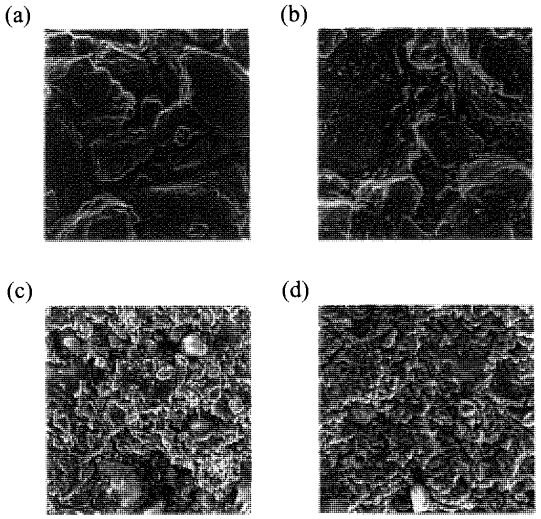

Fig. 2. Scanning Electron Photomicrographs Showing Surface of Agglomerates Formed at (a) 5, (b) 13, (c) 21 and (d) 25 min of Post-Melt Processing Time

Magnification factor: 500×. Material: lactose 450 M; PEG 3000 concentration: 23% (w/w); post-melt impeller speed: 1150 rpm.

that their surfaces were generally rough (Fig. 2(a)). The agglomerates were porous (Fig. 1). The agglomerate surfaces were made up of loose clusters of lactose particles bound by molten PEG and the lactose particles were easily identified on the photomicrographs. By further post-melt processing (Figs. 2(b)—(d)), the agglomerate surfaces appeared denser as the molten PEG was squeezed out towards the surface by impact. The agglomerates were spheronized mainly by spirally rolling against the wall of the mixer bowl. The rolling action reduced the irregular protrusions of the agglomerate surfaces by the rearrangement of particles, accompanied by protrusions being sloughed off or impacted towards the center of the core as interpreted from the reduction in the porosity of the pellets formed (Fig. 1).

After prolonged post-melt processing, the sphericity values of the agglomerates approached unity (Fig. 1). The distance for pellets to roll on the wall of the mixer bowl was time dependent. Keeping all the other processing parameters constant, a longer processing time improved the sphericity of pellets by increasing the total wall rolling distance made by the agglomerates. A longer processing time also increased the level of coalescence and densification of agglomerates (Fig. 1). The resultant pellets would be stronger and became less liable to breakdown.[6] The pellet spheronization process would also be facilitated and more spherical products obtained.

The change in pellet sphericity with post-melt processing time was found to be generally independent of both the binder concentration (Fig. 3(a)) and particle size of the bulk material (Fig. 3(b)). In the study using bulk materials of different particle sizes (Fig. 3(b)), the sphericity values of pellets formed, using lactose 450 M and 17% (w/w) of PEG 3000, at post-melt processing times of 5 and 9 min were not measured. The very small pellets produced were found to have fine powders adhering to their surfaces which made it difficult to determine the sphericity.

The sphericity of pellets was affected by the post-melt impeller speed employed, particularly in the early phase of post-

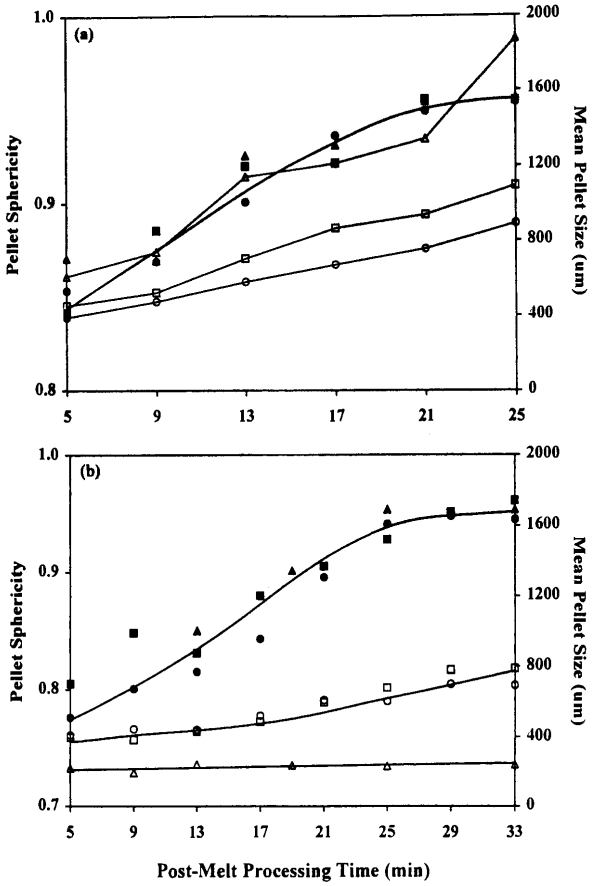

Fig. 3. Profiles of Sphericity and Mean Size of Pellets Formed at Different Post-Melt Processing Time with Respect to the Effect of (a) Binder Concentration and (b) Particle Size of Bulk Material

(a) Material: lactose 450 M; post-melt impeller speed: 1150 rpm. PEG 3000 concentration: 22% (w/w), (●, ○); 23% (w/w), (■, □); 24% (w/w), (▲, △).

(b) PEG 3000 concentration: 17% (w/w); post-melt impeller speed: 1150 rpm. Material: lactose 200 M, (●, ○); 350 M, (■, □); 450 M, (▲, △). Pellet sphericity, (●, ■, ▲); mean pellet size, (○, □, △).

melt processing. At an impeller speed of 1150 rpm, the kinetic impact forces produced by impeller rotation were rather low. The spheronization process was correspondingly much slower (Fig. 4). With a higher impeller speed, the rate of spheronization of the agglomerates was faster and highly spherical pellets were produced with a relatively shorter post-melt processing time. The strong kinetic forces associated with higher impeller speeds augmented the rounding of agglomerates into highly spherical pellets. The high post-melt impeller speed provided high kinetic energy to the agglomerating mass and this enabled the agglomerates to remain suspended above the impeller for longer periods and to roll against the mixer wall at higher speeds, covering longer wall rolling distances.

The actual rolling distances of the agglomerates were difficult to determine. However, it was expected that the number of revolutions made by the impeller would reflect the rolling distance covered by the agglomerates. This assumption takes into account that the kinetic energy imparted to the agglomerates was directly derived from the impact forces of the rotating impeller blades. The number of impeller revolutions was a product of post-melt impeller speed and processing time. The plot of the number of impeller revolutions against pellet sphericity showed that the pellet spheronization process was related to the number of impeller revolutions

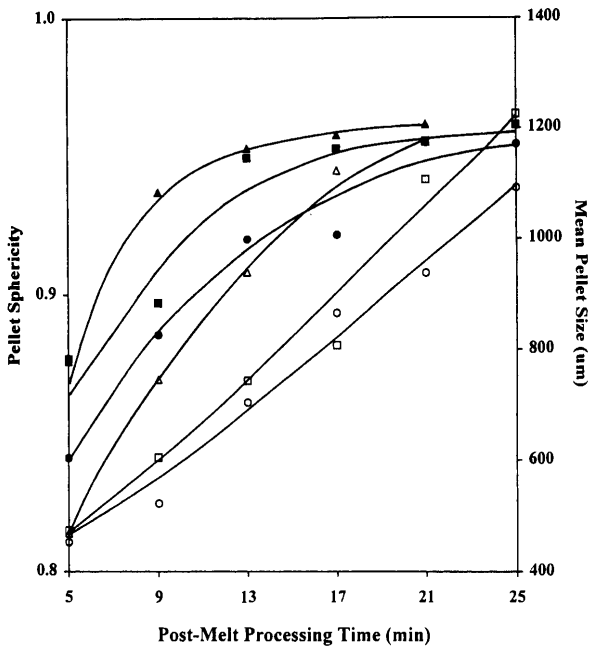

Fig. 4. Profiles of Sphericity and Mean Size of Pellets Formed at Different Post-Melt Processing Time with Respect to the Effect of Post-Melt Impeller Speed

Material: lactose 450 M; PEG 3000 concentration: 23% (w/w). Post-melt impeller speed: 1150 rpm, (●, ○); 1300 rpm, (■, □); 1450 rpm, (▲, △). Pellet sphericity, (●, ■, ▲); mean pellet size, (○, □, △).

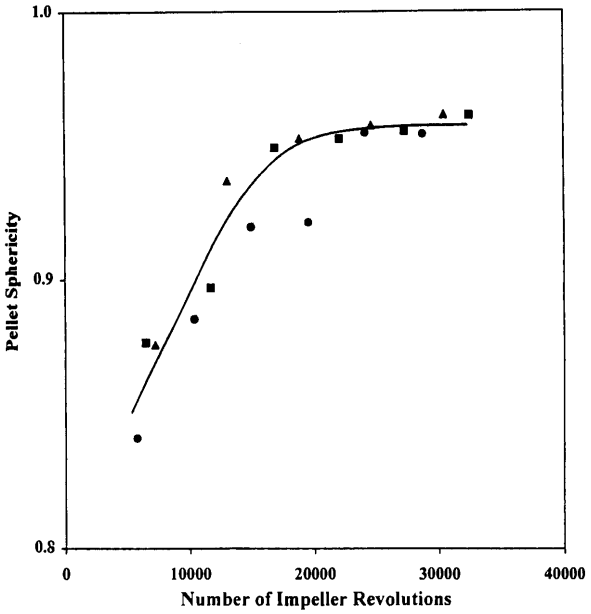

Fig. 5. Relationship between Number of Impeller Revolutions and Sphericity of Pellets Formed Using Varying Post-Melt Impeller Speeds

Material: lactose 450 M; PEG 3000 concentration: 23% (w/w). Post-melt impeller speed: 1150 rpm, ●; 1300 rpm, ■; 1450 rpm, ▲.

(Fig. 5). The relationship of pellet sphericity with number of impeller revolutions was independent of the actual post-melt impeller speed. At a higher post-melt impeller speed, a shorter post-melt processing time was required to produce pellets of equivalent sphericity when compared with that when a lower post-melt impeller speed was used (Fig. 4).

A two-phase spheronization process can be observed from the plot of the pellet sphericity against number of impeller revolutions (Fig. 5). The post-melt processing time was an

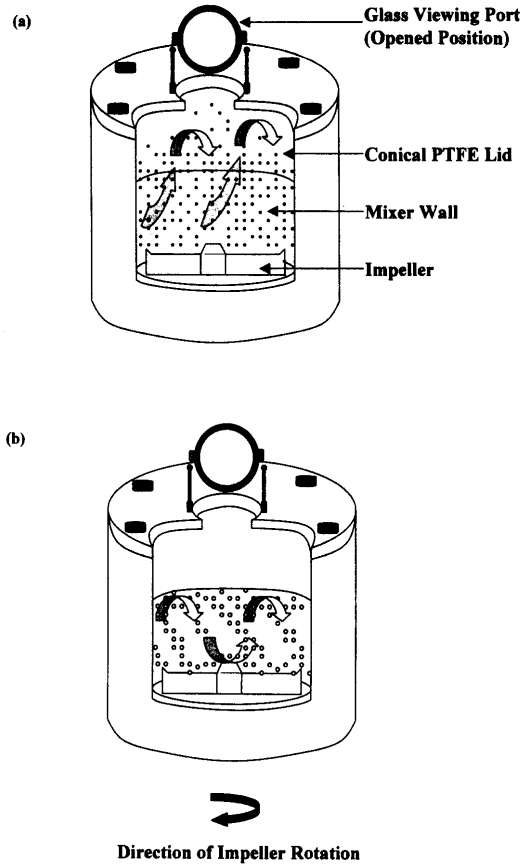

Fig. 6. Material Circulation Profiles in the High Shear Mixer at the (a) Initial and (b) Later Post-Melt Processing Phases

The Lower End of the Conical PTFE Lid Served as a Demarcation for Judgement of Material Circulation Height.

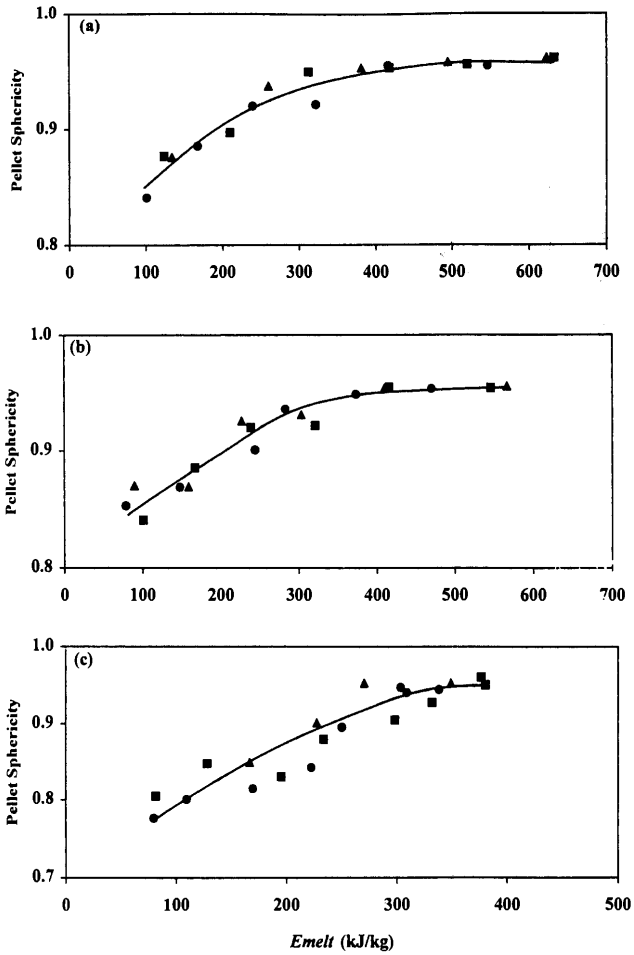

Fig. 7. Relationship between Post-Melt Specific Energy Consumption, *E*melt, and Sphericity of Pellets Formed at Different Post-Melt Processing Time with Respect to the Effect of (a) Post-Melt Impeller Speed, (b) Binder Concentration and (c) Particle Size of Bulk Material

(a) Material: lactose 450 M; PEG 3000 concentration: 23% (w/w). Post-melt impeller speed: 1150 rpm, ●; 1300 rpm, ■; 1450 rpm, ▲.

(b) Material: lactose 450 M; post-melt impeller speed: 1150 rpm. PEG 3000 concentration: 22% (w/w), ●; 23% (w/w), ■; 24% (w/w), ▲.

(c) PEG 3000 concentration: 17% (w/w); post-melt impeller speed: 1150 rpm. Material: lactose 200 M, ●; 350 M, ■; 450 M, ▲.

indicator of the number of impeller revolutions when the same impeller speed was used. The rate of spheronization appeared to be faster at the initial post-melt processing phase and slower at the later phase when different binder concentrations and bulk materials of different particle sizes were used (Fig. 3). It was likely that there were changes in the pelletization process with time and these divided the agglomerate spheronization process into two phases.

The two-phase spheronization process may be explained by the events occurring during the pelletization process. During the initial post-melt processing phase, the agglomerates were made up of loose clusters of solid lactose particles bound by the molten PEG. These agglomerates were highly porous. For each agglomerate, the particles could rearrange themselves easily into the voids within the agglomerate. A greater degree of particle rearrangement can be effected, which in turn, was translated to a more marked increase in the pellet sphericity with time.

In addition, the initial agglomerates formed were smaller and irregularly shaped. The contact surface areas of these agglomerates with the impeller blades and mixer wall surface were large. Observation through the glass viewing port of the high shear mixer showed that the agglomerates rebound upon impact by impeller in a less orderly manner (Fig. 6(a)). The random agglomerate distribution and flow in the mixer bowl allowed opportunity for particle rearrangement and a higher rate of spheronization.

In the later phase of post-melt processing, the agglomerates were larger and denser. The resulting agglomerates became heavier. The agglomerates gradually became more spherical and impacts by impeller were translated to a more directional flow pattern, moving in a regular twisted rope-like manner (Fig. 6(b)). The height to which the agglomerates travelled was lower, covering a lesser area of mixer wall surface. The fraction of the agglomerates in contact with the mixer wall became smaller and this may partially contribute to the observation of the second phase of the spheronization process. In this phase, there were also less intra-agglomerate voids available for particles to rearrange within to achieve a higher degree of sphericity.

Energy was consumed for the circulation of material and for overcoming the resistance of the viscous molten binder during the agglomerate growth process. The post-melt specific energy consumption of the pelletization process was found to be related to the sphericity changes of the pellets during pelletization (Fig. 7). Post-melt specific energy consumption was calculated from the records of post-melt specific power consumption–processing time tracings as described by Heng *et al.*[4] The post-melt specific energy con-

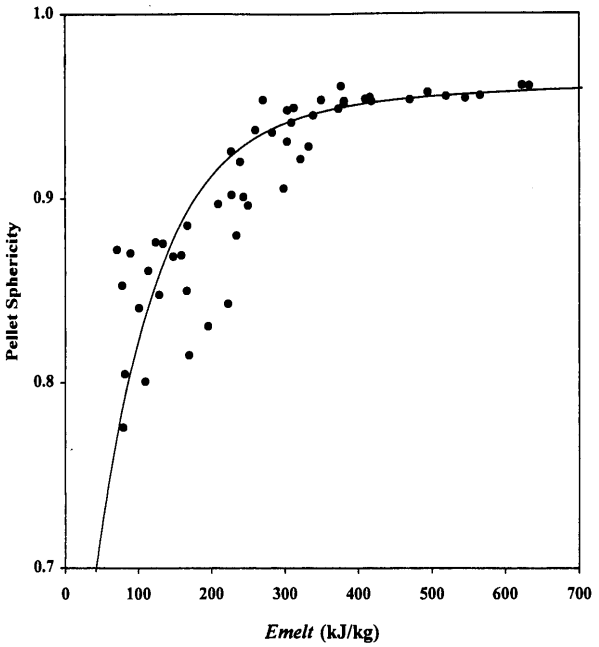

Fig. 8. Profiles of Post-Melt Specific Energy Consumption, *E*melt, with Experimental and Predicted Sphericity Values of the Pellets Formed at Different Post-Melt Processing Time Using Different Post-Melt Impeller Speeds, Binder Concentrations and Bulk Material of Different Particle Sizes

Experimental, ●; predicted, —.

sumption was more useful than post-melt processing time for relating to pellet sphericity when post-melt impeller speed was varied. The relationship of post-melt specific energy consumption with the sphericity of the pellets formed at different post-melt processing times was independent of the effects of post-melt impeller speed (Fig. 7(a)). Pellets of similar sphericity could be obtained with comparable post-melt specific energy consumption in processes where different post-melt impeller speeds were used. As the impeller speed affected the post-melt specific energy consumption, it would have, in turn, affected the pellet sphericity.

In the case where binder concentration and particle size of bulk material were varied, there were no marked differences in both the post-melt specific energy consumption, as reported in the previous paper,[4] and the sphericity of the pellets (Fig. 3) produced at different post-melt processing times. The relationship of post-melt specific energy consumption with pellet sphericity was found to be independent of the variation of formulation parameters under investigation (Figs. 7(b)—(c)).

Figure 8 indicates that the relationship of pellet sphericity and post-melt specific energy consumption can be described using a simple mathematical model. Pellet sphericity was related to the post-melt specific energy consumption and this relationship was independent of the magnitude of post-melt impeller speed, binder concentration and particle size of the bulk material. The two-phase spheronization process was seen when post-melt specific energy consumption was used to relate to the pellet sphericity. The post-melt specific energy consumption data and pellet sphericity values could be fitted with a bi-exponential equation model where the spheronization process was rapid initially and becoming slower at the later phase:

$$\text{1-pellet sphericity} = [0.4107\exp(-0.0118E\text{melt})] + [0.0533\exp(-0.0004E\text{melt})] \quad (2)$$

where *E*melt was the post-melt specific energy consumption (kJ/kg).

Figure 8 shows that the results predicted by Eq. 2 could describe the relationship between the pellet sphericity and post-melt specific energy consumption determined experimentally ($r=0.82$, $p<0.001$).

Conclusion

The sphericity of melt pellets was mainly affected by post-melt impeller speed and post-melt processing time. There were two phases in the melt spheronization process: a high spheronization rate, followed by a slow one. The two-phase melt spheronization process was associated with the changes of size, porosity and flow pattern of the processing material. A bi-exponential mathematical model was established to relate the sphericity of the pellets produced at both phases of the spheronization process with post-melt specific energy consumption. Pellet sphericity was directly related to post-melt specific energy consumption and the relationship was independent of the production variables.

References

1) Schaefer T., Holm P., Kristensen H. G., *Acta Pharm. Nord.*, **4**, 141—148 (1992).
2) Schaefer T., Holm P., Kristensen H. G., *Acta Pharm. Nord.*, **4**, 245—252 (1992).
3) Royce A., Suryawanshi J., Shah U., Vishnupad K., *Drug Dev. Ind. Pharm.*, **22**, 917—924 (1996).
4) Heng P. W. S., Wong T. W., Shu J. J., Wan L. S. C., *Chem. Pharm. Bull.*, **47**, 633—638 (1999).
5) Heng P. W. S., Wan L. S. C., Wong T. W., *Pharm. Dev. Technol.*, **4**, 27—33 (1999).
6) Wong T. W., Wan L. S. C., Heng P. W. S., *Pharm. Dev. Technol.*, **4**, 449—456 (1999).

Cimiracemoside A: A New Cyclolanostanol Xyloside from the Rhizome of *Cimicifuga racemosa*

Erdal BEDIR[a,b] and Ikhlas A. KHAN*[,a,c]

National Center for Natural Products Research, Research Institute of Pharmaceutical Sciences,[a] and Department of Pharmacognosy, School of Pharmacy,[b] The University of Mississippi,[c] University, MS 38677, U.S.A., and Department of Pharmacognosy, Faculty of Pharmacy, Hacettepe University,[c] 06100-Ankara, Turkey.

Received September 6, 1999; accepted November 15, 1999

A new 9,19-cyclolanostane-type triterpene xyloside (1), from the rhizomes of *Cimicifuga racemosa*, has been isolated together with four known saponins; cimiaceroside A, 25-*O*-methylcimigenol-3-*O*-β-D-xylopyranoside, 27-deoxyactein and 23-*O*-acetylshengmanol-3-*O*-β-D-xylopyranoside. The structure of the new compound was established as 16β,23 : 22β,25-diepoxy-12-acetoxy-3β,23,24β-trihydroxy-9,19-cyclolanost-7-ene-3-*O*-β-D-xylopyranoside. For the structure elucidation, 1D- and 2D-NMR experiments and high resolution electrospray ionization Fourier transformation mass spectrometry (HRESIFTMS) were used.

Key words *Cimicifuga racemosa*; 9,19-cyclolanostanol; Ranunculaceae

Cimicifuga (*C.*), one of the smallest genus in the family Ranunculaceae, comprises about 25 species distributed throughout North America, Europe and East Asia. This genus is represented by 6 species in the flora of North America. *Cimicifuga racemosa*, best known as black cohosh (formerly black snakeroot), is the most common American species.[1,2] The rhizomes of *C. racemosa* have been used in European phytotherapy for the treatment of menopausal symptoms for over 50 years. Pharmacological and controlled clinical studies have confirmed that *C. racemosa* preparations are a safe and effective alternative for hormone replacement therapies in the treatment of menopause.[2] The rhizomes of Asian species, *C. simplex*, *C. dahurica*, *C. foetida* and *C. heracleifolia*, have been used as anti-inflammatory, antipyretic and analgesic agents in traditional Japanese and Chinese medicine. Generally, Asian species of *Cimicifuga* are chemically much better characterized than North American species, including *C. racemosa*. During a series of chemical investigations of *Cimicifuga* species, 9,19-cyclolanostane-type triterpenoids, fukiic acid esters, piscidic acid esters, caffeic acid derivatives, phenolic acid derivatives and chromones have been isolated.[3—8]

In this study, *C. racemosa* was investigated for its triterpene glycoside content, and here we describe the isolation and structure elucidation of a new 9,19-cyclolanostane-type triterpene xyloside (**1**). The related known xylosides, cimiaceroside A,[9] 25-*O*-methylcimigenol-3-*O*-β-D-xylopyranoside,[4] 27-deoxyactein[11] and 23-*O*-acetylshengmanol-3-*O*-β-D-xylopyranoside[10] were also isolated.

The IR spectrum of **1** exhibited a hydroxyl absorption band (3413 cm^{-1}), and an ester carbonyl absorption band (1729 cm^{-1}).

High resolution electrospray ionization Fourier transformation mass spectrometry (HRESIFTMS) of **1** showed an ion peak for $[M+Na]^+$ at *m/z* 699.2665, in agreement with the molecular formula $C_{37}H_{56}O_{11}$.

The ^{1}H-NMR spectrum of **1** (Table 1) displayed signals characteristic of cyclopropane-methylene protons as an AX system (δ 0.48, 1.02, J=3.8 Hz), an acetyl group [δ 2.10 ($COCH_3$)], and six tertiary (1.77, 1.69, 1.40, 1.33, 1.06 and 1.02) and a secondary methyl (δ 1.31, d, J=6.6 Hz) group. Additionally, an anomeric proton signal was observed at δ 4.80 (d, J=7.3 Hz). Thus, compound **1** was considered to be

Table 1. ^{1}H- and ^{13}C- Assignments of **1**,[a] (in Pyridine, at 500 and 125 MHz, respectively)

C/H	δ_C	δ_H (J Hz)
1	31.36 t	1.22 m, 1.55 m
2	30.50 t	1.84 m, 2.27 m
3	89.03 d	3.44 dd (4.0, 11.7)
4	41.54 s	
5	43.58 d	1.26[b]
6	22.97 t	1.56 m, 1.84 m
7	115.04 d	5.11 d (8.0)
8	149.80 s	
9	22.33 s	
10	29.40 s	
11	37.83 t	1.26[b], 2.62 dd (16.0, 9.1)
12	77.82 d	5.25 d (8.7)
13	49.88 s	
14	52.10 s	
15	43.09 t	2.05 dd (13.1, 7.5), 2.15 dd (12.7, 8.0)
16	73.40 d	5.05 dd (13.1, 7.8)
17	54.42 d	1.77[b]
18	16.18 q	1.40 s
19	29.86 t	0.48 (3.8), 1.00 (3.8)
20	35.37 d	2.29 m
21	18.68 q	1.31 d (6.6)
22	87.80 d	3.90 d (10.5)
23	106.84 s	
24	84.40 d	4.23 s
25	84.80 s	
26	29.11 q	1.77 s
27	26.03 q	1.69 s
28	27.86 q	1.06 s
29	26.03 q	1.33 s
30	15.38 q	1.02 s
1′	108.57 d	4.80 d (7.3)
2′	76.72 d	4.01 dd (7.3, 7.6)
3′	79.73 d	4.14 dd (7.6, 8.2)
4′	72.37 d	4.23[b]
5′	68.24 t	3.70 dd (10.0, 11.3), 4.31 dd (5.1, 11.3)
$COCH_3$	171.78 s	2.10 s

a) Assignments confirmed by COSY, HMQC and HMBC experiments. *b*) Signal pattern was unclear due to overlapping.

* To whom correspondence should be addressed.

© 2000 Pharmaceutical Society of Japan

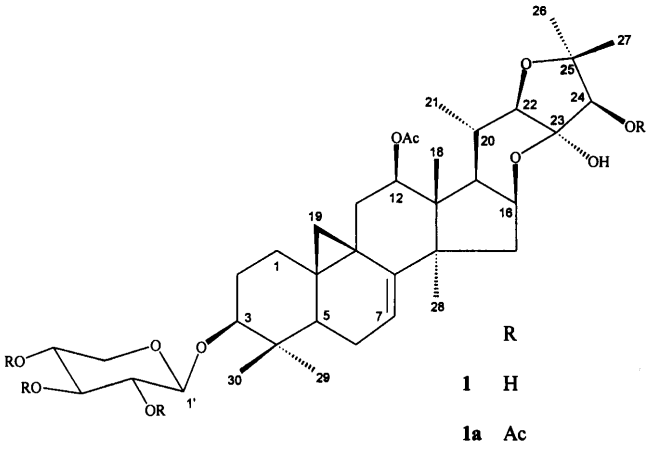

Chart 1. Structures of **1** and **1a**

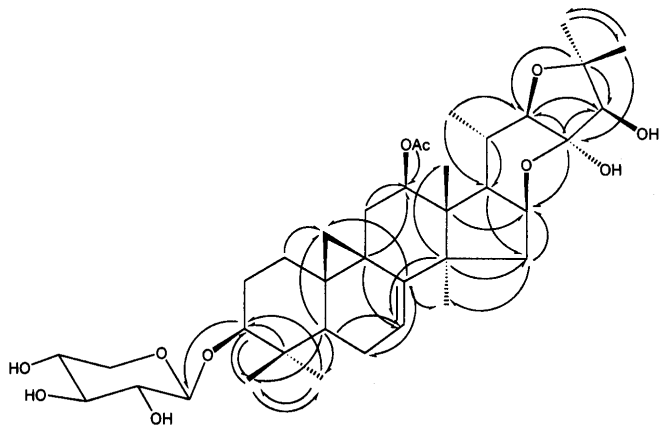

Chart 3. Structure and HMBC For **1**

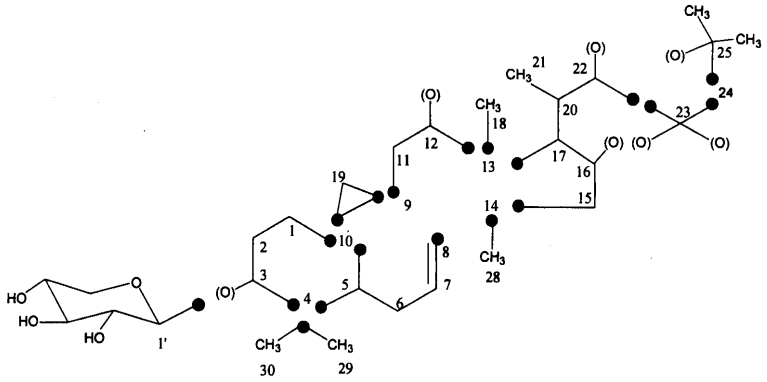

Chart 2. Partial Structures of **1** Deduced from 2D-NMR Measurements

a 9,19-cyclolanostane-type triterpene monoglycoside.

The ^{13}C-NMR spectrum of **1** exhibited 37 signals. Thirty signals were accounted for by the aglycone moiety. The remaining signals were in accord with the presence of one pentose and an acetyl unit. The ^{1}H- and ^{13}C-NMR data (Table 1) supported the assignment of the sugar moiety in **1** as β-D-xylopyranose.[3—5]

Beside glycosidic carbons, the remaining downfield signals displayed nine signals due to five oxymethine carbon atoms (δ 89.03, d, C-3; δ 87.80, d, C-22; δ 84.40, d, C-24; δ 77.82, d, C-12; δ 73.40, d, C-16), two quaternary carbon atoms, one of which is a ketal (δ 106.84, s, C-23; δ 84.80, s, C-25), as well as one endocyclic double bond (δ 115.04, d, C-7; δ 149.8, s, C-8). Taking into account the results from our comprehensive 1D and 2D-NMR studies and previous knowledge derived from metabolites isolated from the genus *Astragalus*,[12—14] it suggests that **1** possesses a highly oxidized triterpene nucleus. These data, together with the information from the ^{1}H–^{1}H-correlation spectroscopy (COSY) and ^{1}H–^{13}C-correlation spectroscopy (HMQC) experiments indicated the presence of the partial structures shown in Chart 2. In order to establish the interfragment relationship, a heteronuclear multiple bond correlation experiment (HMBC) was performed (Chart 3).

Acetylation of **1** yielded a tetraacetate, **1a**. From the HRESIFTMS of **1a**, which displayed an $[M+Na]^+$ ion at *m/z* 867.3791, a molecular formula of $C_{45}H_{64}O_{15}$ was proposed. The IR spectrum of **1a** still displayed a free hydroxyl absorption band after acetylation (3433 cm^{-1}), indicating the presence of the tertiary hydroxyl group at C-23. In the ^{1}H-NMR spectrum of **1a**, H-24 was observed at δ 5.60 (s), showing the expected downfield shift in comparison to **1**.

The relative stereochemistry of **1** was resolved by a combination of two dimensional nuclear Overhouser enhancement spectroscopy (2D-NOESY) data, an analysis of the coupling constants, and comparison with analogous compounds. The cross peaks observed in the NOESY spectrum between H-16, H-12 and CH_3-26; H-12, CH_3-21, CH_3-28 and H-22; H-24 and H-17, implied that these protons were cofacial (α). Based on these findings and a comparison of ^{1}H- and ^{13}C-NMR data with those of cimiaceroside A,[9] the orientation of O(H)-groups were determined to be 3β, 12β, 16β, 22β, 24β.

Consequently, the structure of **1** was elucidated as 16β,23;22β,25-diepoxy-12β-acetoxy-3β,23,24β-trihydroxy-9,19-cyclolanost-7-ene-3-*O*-β-D-xylopyranoside.

Cimiaceroside A,[9] 25-*O*-methylcimigenol-3-*O*-β-D-xylopyranoside,[4] 23-*O*-acetylshengmanol-3-*O*-β-D-xylopyranoside[10] and 27-deoxyactein[11] were also isolated from the rhizomes of *C. racemosa* and identified on the basis of their NMR (^{1}H- and ^{13}C-) data, in comparison with literature values.

As far as could be ascertained, this is the first report of cimiaceroside A,[9] 25-*O*-methylcimigenol-3-*O*-β-D-xylopyranoside,[4] and 23-*O*-acetylshengmanol-3-*O*-β-D-xylopyranoside[10] from *C. racemosa*.

Experimental

General Experimental The IR spectra were recorded with an ATI Mattson Genesis Series Fourier transform (FT)-IR spectrophotometer. The 1D- and 2D-NMR spectra were obtained on a Bruker® Avance DRX 500 FT spectrometer operating at 500 and 125 MHz, respectively. The chemical shift values are reported as parts per million (ppm) units relative to tetramethylsilane (TMS) for ^{1}H- and ^{13}C-; and the coupling constants are in Hz (in parentheses). For the ^{13}C-NMR spectra, multiplicities were determined by a distortionless enhancement by polarization transfer (DEPT) experiment. HRESIFTMS were obtained using a Bruker BioApex FT-MS in ESI mode.

Chromatographic Conditions TLC, precoated Si 250F plates (Baker); developing system, ethyl formate–toluene–formic acid (50 : 50 : 15); visualization, 50% H_2SO_4. Column chromatography, silica gel 230—400 mesh (Merck).

Plant Material The powdered rhizome material of *C. racemosa* was purchased from Frontier Natural Products Co., 3021 78th Street, Norway, IA 52318, product code/lot number: 957.9012.

Extraction and Isolation Plant material (900 g) was extracted with dichloromethane (600 ml) for 8 h and the extract was filtered. The filtrate was concentrated to dryness *in vacuo* (12.08 g). An aliquot of the extract (10.80 g) was chromatographed on a silica gel column (500 g). Elution with increasing amounts of EtOAc in hexane (15—60% EtOAc) yielded 23 fractions (frs. 1—23). Fraction 22 (1.34 g), rich in saponins, was subjected to flash column chromatography using reversed-phase material (C-18, 150 g). H_2O–MeOH mixtures (40 : 60, 30 : 70 and 20 : 80) and MeOH were used as the eluents, to yield **1** (fr. A, 43.5 mg) and frs. B—K. Further purification of the frs. B—K by normal, and reversed-phase column chromatography led to the isolation of four compounds (Cimiaceroside A, 23.0 mg; 25-*O*-methylcimigenol-3-*O*-β-D-xylopyranoside, 101.0 mg; 23-*O*-acetylshengmanol-3-*O*-β-D-xylopyranoside, 88.6 mg; and 27-deoxyactein, 57 mg).

Compound **1**: 16β,23;22β,25-diepoxy-12-β-acetoxy-3β,23,24β-trihydroxy-9,19-cyclolanost-7-ene-3-*O*-β-D-xylopyranoside: IR (KBr) ν_{max}: 3413, 2968, 2359, 1729, 1461 cm^{-1}. ^{1}H- and ^{13}C-NMR: see Table 1. HRESIFTMS *m/z* : 699.2665 $[M+Na]^+$.

Acetylation of **1**: Treatment of compound **1** (5 mg), with Ac_2O (1 ml) and pyridine (1 ml) at room temperature overnight followed by the usual workup yielded compound **1a** (4 mg).

Cimiracemoside A tetraacetate (**1a**): IR (KBr) ν_{max}: 3433, 2961, 2359, 1726, 1624, 1458 cm^{-1}. ^{1}H- NMR: ($CDCl_3$) δ 5.60 (1H, s, H-24), 5.15 (1H, t, J=9.0 Hz, H-3′), 5.08 (1H, d, J=8.9 Hz, H-12), 4.95 (3H, H-16, H-7 and H-2′, overlapped), 4.49 (1H, d, J=7.1 Hz, H-1′), 4.47 (1H, overlapped, H-4′), 4.08 (1H, dd, J=10.2, 5.1 Hz, H-5′a), 3.70 (1H, d, J=11.1 Hz, H-22), 3.29 (1H, dd, J=9.9, 9.5 Hz, H-5′b), 3.12 (1H, dd, J=11.2, 4.0 Hz, H-3), HRESIFTMS *m/z* 867.3791 $[M+Na]^+$.

Acknowledgments We are grateful to Dr. Chuck Dunbar for conducting the HRESIFTMS analysis. We also thank Mr. Frank Wiggers for his assistance in obtaining the 2D-NMR spectra of **1**.

References

1) Gleason H. A., Cronquist A., "Manual of Vascular Plants of the Northeastern United States and Adjajent Canada", 2nd ed., Bronx, New York Botanical Garden, 1991.
2) Foster S., *Herbal Gram*, **45**, 35—49 (1999).
3) Kusano A., Shibano M., Kusano G., Miyase T., *Chem. Pharm. Bull.*, **44**, 2078—2085 (1977).
4) Kusano A., Hojyo S., Kondo Y., Takemoto T., *Chem. Pharm. Bull.*, **25**, 3182—3189 (1996).
5) Kusano A., Takahira M., Shibano M., Miyase T., Kusano G., *Chem. Pharm. Bull.*, **46**, 467—472 (1998).
6) Matsumoto T., Hidaka K., Nakayama T., Fukui K., *Chem. Lett.*, **1**—4 (1972).
7) Takahira M., Kusano A., Shibano M., Kusano G., *Phytochemistry*, **49**, 2115—2119 (1998).
8) Takahira M., Yanagi Y., Kusano A., Shibano M., Baba K., Kusano G., Sakurai N., Nagai M., *Nat. Med.*, **52**, 330—338 (1998).
9) Kusano A., Takahira M., Shibano M., Miyase T., Okuyama T., Kusano G., *Heterocycles*, **48**, 1003—1013 (1998).
10) Sakurai N., Inoue T., Nagai M., *Chem. Pharm. Bull.*, **27**, 158—165 (1979).
11) Berger S., Junior P., Kopanski L., *Planta Med.*, **54**, 579—580 (1988).
12) Bedir E., Calis I., Zerbe O., Sticher O., *J. Nat. Prod.*, **61**, 503—505 (1998).
13) Bedir E., Calis I., Aquino R., Piacente S., Pizza C., *J. Nat. Prod.*, **61**, 1469—1472 (1998).
14) Bedir E., Calis I., Aquino R., Piacente S., Pizza C., *J. Nat. Prod.*, **62**, 563—568 (1999).

Novel Potassium Channel Activators. III.[1] Synthesis and Pharmacological Evaluation of 3,4-Dihydro-2*H*-1,4-benzoxazine Derivatives: Modification at the 2 Position

Yuzo MATSUMOTO,*[,a,b] Wataru UCHIDA,[a] Hideaki NAKAHARA,[a] Isao YANAGISAWA,[a] Tadao SHIBANUMA,[a] and Hiroyuki NOHIRA[b]

Institute for Drug Discovery Research, Yamanouchi Pharmaceutical Co., Ltd.,[a] 21, Miyukigaoka, Tsukuba, Ibaraki 305–8585, Japan, and Graduate School of Science and Engineering, Saitama University,[b] Shimo-Ohkubo, Urawa, Saitama 338–8570, Japan. Received September 8, 1999; accepted November 8, 1999

A new series of 3,4-dihydro-2*H*-1,4-benzoxazine derivatives, where various substituents were introduced into one of the geminal dimethyl groups at the 2 position, were synthesized and their potassium channel-activating activity was evaluated. Introduction of a hydroxyl group, as in compound 5, resulted in good solubility in water and a long duration of action compared with the parent compound 1. Introduction of a nitrato group, as in compound 8, produced typical nitrate activity such as exhibited by nitroglycerine in addition to potassium channel-activating activity. X-ray structural analysis of compound 5 showed that the sum of the bond angles around the N atom at the 4 position was 357.8°, suggesting that the N atom had an approximately sp^2-like planar bond configuration.

Key words potassium channel activator; 1,4-benzoxazine; antihypertensive; cromakalim; nitroglycerine; nitrate activity

Potassium channels regulated by changes in the intracellular level of adenosine triphosphate (ATP) are called ATP-sensitive K^+ channels or K_{ATP} channels and are an important class of ionic channels. These channels are closed when intracellular ATP levels are elevated and opened when intracellular ATP levels decline, linking the membrane potential directly to the metabolic state of the cell.[2] Activation of these channels in the membrane of cells, such as smooth muscle cells, allows K^+ ions to move out, causing transmembrane hyperpolarization and repolarization. These effects reduce the intracellular calcium concentration by blocking voltage-dependent calcium channels and inhibiting intracellular calcium release, producing smooth muscle relaxation and antispasmodic action.[3] The use of potassium channel activators or openers[4] may, therefore, be valuable in the treatment of diseases caused by smooth muscle contraction, such as hypertension, angina pectoris, asthma,[5] and urinary incontinence,[6] as well as baldness.[7] Additionally, these agents are expected to afford cellular protection against ischemic attacks, independent of their vasodilating actions,[8] and exhibit antilipemic effects, lowering low density lipoprotein (LDL) cholesterol and triglycerides, while increasing high density lipoprotein (HDL) cholesterol.[9]

There are several prototypes of this class of compound, represented by cromakalim,[10] pinacidil,[11] nicorandil,[12] and aprikalim.[13] A great deal of research on structural modifications based on cromakalim, a benzopyran derivative, has been reported. As part of our chemical program based on cromakalim, we previously reported[1] the synthesis and biological activity of a new series of 3,4-dihydro-2*H*-1,4-benzoxazine derivatives, represented by compound **1**, which have potent ATP-sensitive K^+ channel-activating activity. Recently, several modifications of the 2 position of the benzopyran skeleton have been reported, such as JTV-506[14] with selective coronary vasorelaxant activity, KC-399[15] which reduces reflux tachycardia, SKP-450[16] with a more potent hypotensive activity than levcromakalim, and KP-30818[17] with an equivalent vasorelaxant activity to levcromakalim in the rat aorta, as shown in Chart 1. As an example of the benzoxazine skeleton, ZM-260384[18] has also been reported, where the geminal dimethyl group at the 2 position of compound **1** was changed to the bis-difluoromethyl group, resulting in more potent vasorelaxant activity than compound **1** in detrusor tissue. Thus, our attention has focused on further modifications of the 2 position of benzoxazine. We tried to introduce various substituents into one of the geminal dimethyl groups at the 2 position of compound **1** and obtained two characteristic potassium channel activators. Firstly, introduction of a hydroxyl group, as in compound **5**, was found to result in good solubility and a long duration of action compared with the parent compound **1**. Secondly, introduction of a nitrato group, as in compound **8**, produced typical nitrate activity such as exhibited by nitroglycerine in addition to potassium channel-activating activity.

Chemistry Preparation of the 1,4-benzoxazine derivatives modified at the 2 position followed the route outlined in Chart 2. Treatment of 2-amino-4-nitrophenol (**2**) with diethyl 2-bromo-2-methylmalonate and potassium fluoride in dimethylformamide (DMF) gave 2-ethoxycarbonyl-2-methyl-3-oxo-1,4-benzoxazine **3**, which was reduced with borane-tetrahydrofuran (BH_3-THF) complex to yield 2-hydroxymethyl-1,4-benzoxazine **4**. Pyridine *N*-oxide derivative **5** was prepared easily without heating by nucleophilic substitution of **4** with 2-bromopyridine *N*-oxide in the presence of sodium hydride (NaH) in DMF. In this case, selective substitution on the N atom at the 4 position occurred and substitution on the O atom at the 2 position did not. *O*-alkylation or acetylation of **5** with several alkyl halides or acetylchloride in the presence of NaH gave **6a**—**e** or **6f** respectively. Treatment of **5** with methylisocyanate yielded the carbamoyl derivative **7**. Selective nitration at the 2 position of compound **5** could be achieved with nitronium tetrafluoroborate at −35—−40 °C to give compound **8**, while nitration at −10—0 °C gave 2-nitratomethyl-6,7-dinitro-1,4-benzoxazine derivative **9**.

* To whom correspondence should be addressed.

© 2000 Pharmaceutical Society of Japan

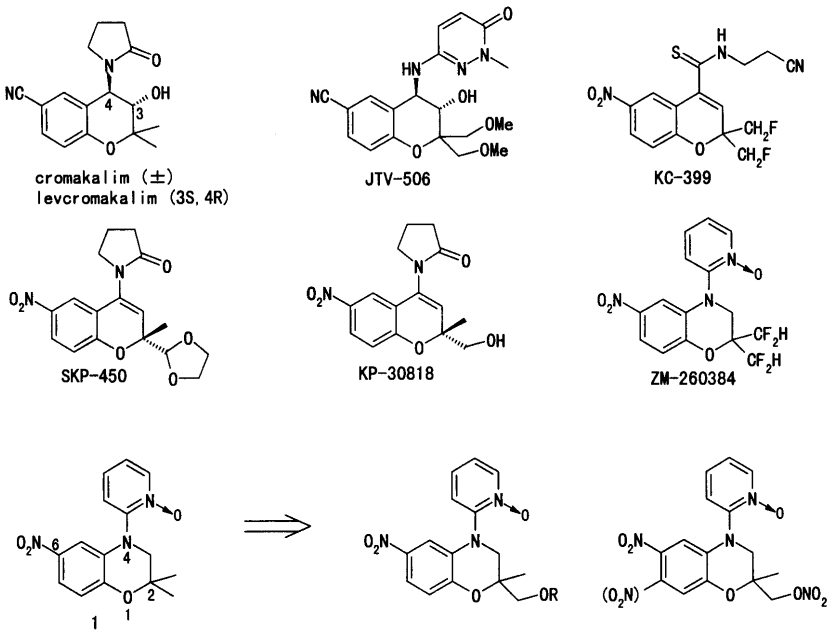

Chart 1

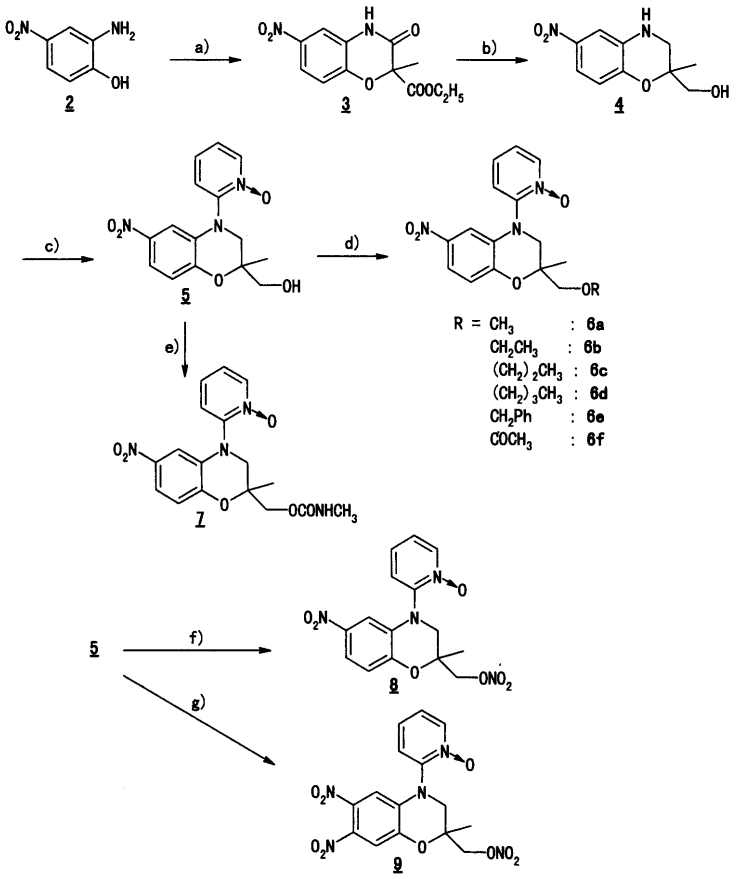

a) $BrCCH_3(COOC_2H_5)_2$, KF, DMF b) BH_3-THF c) 2-bromopyridine *N*-oxide hydrochloride, NaH, DMF d) R-X, NaH, DMF e) CH_3NCO, Et_3N, CH_2Cl_2 f) NO_2BF_4, CH_3CN, -40℃—-35℃ g) NO_2BF_4, CH_3CN, -10℃—0℃

Chart 2

Results and Discussion

The potassium channel-activating effects of the compounds were evaluated *in vitro* in terms of their inhibitory effect (IC_{50}) on 3,4-diaminopyridine-induced rhythmic contraction[19] in isolated dog coronary artery (Table 1). Introduction of a hydroxyl group into one of the geminal methyl groups at the 2 position of the 1,4-benzoxazine derivative **1** afforded **5** which retained potent activity. Alkylation of the hydroxyl

Table 1. Modification at the 2 Position

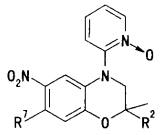

Comp.	R^2	R^7	*In vitro* IC_{50}[a] (μM)
1	CH_3	H	0.014
5	CH_2OH	H	0.057
6a	CH_2OCH_3	H	0.083
6b	$CH_2OCH_2CH_3$	H	0.17
6c	$CH_2O(CH_2)_2CH_3$	H	0.55
6d	$CH_2O(CH_2)_3CH_3$	H	>10
6e	CH_2OCH_2Ph	H	>10
6f	CH_2OCOCH_3	H	0.069
7	$CH_2OCONHCH_3$	H	0.51
8	CH_2ONO_2	H	0.025
9	CH_2ONO_2	NO_2	1.4
Nicorandil			7.2
Cromakalim			0.39

a) Drug concentration required to inhibit 3,4-diaminopyridine-induced rhythmic contractions in dog coronary artery by 50% (n=3—6).

Table 2. Hemodynamic Effect in Dogs

Comp.	μg/kg i.v.	MBP[a]	CBF[a]	
		Δ%	Δ%	Duration (min)
1	3	−16	155	30
5	3	−24	204	>60

a) Measured in groups of 4—5 dogs.

group of **5** with a methyl group, as in **6a**, caused a slight reduction in potency. Alkylation with an ethyl group, as in **6b**, caused a further reduction and alkylation with a propyl group, as in compound **6c**, caused a much greater reduction. In the case of alkylation with *n*-butyl and benzyl groups, as in compound **6d** and **6e**, there was a loss of activity at 10 μM. From the above data, it was concluded that as the alkyl substituent introduced into the hydroxymethyl group at the 2 position of compound **5** became more bulky, the activity became weaker. Acetylation of **5** afforded **6f** with restored high activity, while the carbamate derivative **7** showed reduced activity. Surprisingly, the nitrato derivative **8** was found to be approximately 10 times more potent than cromakalim. Further introduction of a nitro group into the 7 position of **8** afforded 6,7-dinitro derivative **9** with reduced activity. Although the compounds mentioned above have a chiral center at the 2 position, we prepared them as racemic mixtures. So, the relationship between activity and chirality remains unknown.

Among these compounds, compound **5** possessing a hydroxyl group, was readily soluble in water compared with compound **1**. Its pharmacological properties were investigated, because we thought that high solubility might change the physicochemical properties of the parent compound **1** to produce a unique pharmacological profile. In anesthetized dogs, compound **5** exhibited a more potent mean blood pressure (MBP)-lowering effect and coronary artery blood flow

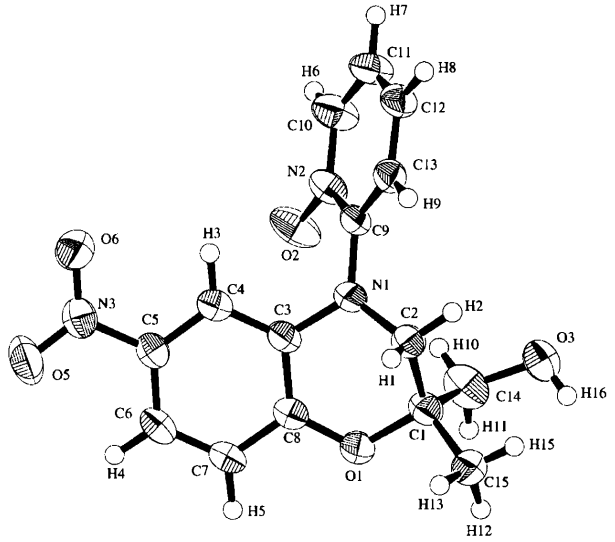

Fig. 1. X-Ray Structure of Compound **5**

Table 3. Vasodilating Effect in Rabbit Isolated Coronary Artery

Comp.	IC_{50} (nM)[a]	
	No treatment methylene blue	Pretreated with methylene blue
8	7	45

a) Drug concentration to inhibit phenylephrine-induced contraction by 50% (n=2).

(CBF)-increasing effect than compound **1** (Table 2). Surprisingly, there was a remarked difference between compound **1** and **5** in the duration of action on CBF. In the case of compound **1**, the CBF returned to baseline after 30 min, but in the case of compound **5**, there was no return to baseline even after 1 h, and the CBF-increasing effect persisted. Differences in the physicochemical properties and affinity for coronary artery tissue would account for the different duration of action. It has also been reported that N–K hybrids,[20] which have a dual vasodilatory mechanism of a nitrate and a K^+ channel activator, such as nicorandil and KRN2391,[21] are beneficial compared with the pure K^+ channel activators in the treatment of angina pectoris and hypertension. This is because N–K hybrids relax not only small coronary arteries by the K^+ channel activation but also large coronary arteries by the nitrate action, without causing a "coronary steal" phenomenon.[22] Thus, we investigated whether compound **8**, possessing a nitrato group at the 2 position, exhibited nitrate activity or not. In isolated rabbit coronary artery, compound **8** relaxed the phenylephrine-induced contraction in a dose-dependent manner, and the effect was clearly inhibited by pre-treatment with methylene blue, a c-GMP synthetase inhibitor (Table 3). This indicates that compound **8** exhibits nitrate activity, like nitroglycerine, in addition to potassium channel-activating activity. Details of the pharmacological profile of compound **8** are currently under investigation.

The X-ray crystal structure of compound **5** is shown in Fig. 1. The torsion angle formed from the four centers, C3/N1/C9/N2, amounted to 53.6°, indicating that the pyridine *N*-oxide ring was roughly orthogonal to the pseudoplane of 1,4-benzoxazine, like the relationship between the γ lactam

ring and the benzopyran skeleton of cromakalim.[23] The bond angle around N1 was 123.3° (C3/N1/C9), 112.7° (C3/N1/C2), 121.8° (C2/N1/C9) and the sum of the angles was 357.8°, suggesting that N1 had approximately an sp^2-like planar bond configuration, while the atom at the 4 position of the benzopyran in cromakalim had an sp^3 tetrahedral bond configuration. This result was similar to the result of our previous work[1b] and a feature of 1,4-benzoxazine derivatives. However, the relationship between activity and the bond angles is not yet clear.

In conclusion, we synthesized and evaluated pharmacologically a new series of 1,4-benzoxazine derivatives where one of the geminal dimethyl groups at the 2 position of compound **1** was modified. Among these compounds, compound **5** with a hydroxyl group exhibited potent hypotensive and coronary vasodilating effects in dogs, characterized by a long duration of action. Compound **8**, with a nitrato group, exhibited nitrate activity, like nitroglycerine, in addition to potassium channel-activating activity, suggesting a unique profile as a drug for the treatment of cardiovascular diseases.

Experimental

All melting points were determined on a Yanaco MP-500D micro melting point apparatus without correction. Nuclear magnetic resonance (NMR) spectra were recorded on a JEOL FX90Q, FX100, FX270 or FX400 spectrometer using tetramethylsilane as an internal standard. The following abbreviations are used: s=singlet, d=doublet, t=triplet, q=quartet, m=multiplet, dd=double doublet, br s=broad singlet. Mass spectra (MS) were recorded with a Hitachi M-80, JEOL JMS-DX300, or JMS-700T spectrometer. Infrared (IR) spectra were measured with a Hitachi 270-30 spectrophotometer. Elemental analyses were performed using Yanaco MT-5 equipment. HPLC was carried out using a Hitachi L-6000 pump, L-4000 UV-detector and D-2500 recorder. Thin-layer chromatography (TLC) plates were performed on silica-gel F_{254} (Merck), and column chromatography was performed on 100—200 mesh silica-gel from Wako. Anhydrous $MgSO_4$ or Na_2SO_4 was used as the drying agent for organic extraction. All solvent evaporation was performed under vacuum. Yields were not optimized.

Ethyl (3,4-Dihydro-2-methyl-6-nitro-3-oxo-2*H*-1,4-benzoxazin-2-yl)-carboxylate (3) A mixture of KF (6.0 g, 100 mmol), DMF (30 ml), diethyl 2-bromo-2-methylmalonate (10 g, 40 mmol), and 4-nitro-2-aminophenol (6.1 g, 40 mmol) was stirred for 16 h, and then, poured into water, and extracted with AcOEt. The extract was washed with brine, dried, and concentrated to give **3**, which was recrystallized from EtOH (8.7 g, 79%), mp 170—172 °C. ^{1}H-NMR ($CDCl_3$) δ: 1.21 (3H, t, J=7 Hz), 1.95 (3H, s), 4.21 (2H, q, J=7 Hz), 7.17 (1H, d, J=9 Hz), 7.85 (1H, d, J=3 Hz), 7.96 (1H, dd, J=3, 9 Hz), 9.66 (1H, br s). *Anal.* Calcd for $C_{12}H_{12}N_2O_6$: C, 51.43; H, 4.32; N, 10.00. Found: C, 51.41; H,4.39; N, 10.04.

3,4-Dihydro-2-hydroxymethyl-2-methyl-6-nitro-2*H*-1,4-benzoxazine (4) Compound **3** (2.8 g, 10 mmol) was added to a solution of borane–THF complex in THF (1.0 M, 100 ml) and the mixture was refluxed for 4 h and then carefully diluted with MeOH (24 ml). After adding conc. HCl (24 ml), it was refluxed for 0.5 h. After concentration, the residue was made alkaline with NaOH solution to give **4** as a precipitate, which was recrystallized from EtOH–ether (1.7 g, 76%), mp 125—127 °C (dec.). ^{1}H-NMR (DMSO-d_6) δ: 1.23 (3H, s), 3.01 (2H, ABq, J=12 Hz), 3.35—3.39 (1H, m), 3.42—3.46 (1H, m), 6.50 (1H, br s), 6.81 (1H, d, J=9 Hz), 7.41 (1H, dd, J=3, 9 Hz), 7.48 (1H, d, J=3 Hz). *Anal.* Calcd for $C_{10}H_{12}N_2O_4$: C, 53.57; H, 5.39; N, 12.49. Found: C, 53.45; H,5.34; N, 12.42.

2-(3,4-Dihydro-2-hydroxymethyl-2-methyl-6-nitro-2*H*-1,4-benzoxazin-4-yl)pyridine 1-Oxide (5) To a mixture of **4** (1.7 g, 7.4 mmol) and 2-bromopyridine 1-oxide hydrochloride (1.6 g, 7.4 mmol) in DMF 10 ml, NaH (60% in oil, 0.74 g, 18.5 mmol) was slowly added under ice-cooling, followed by stirring at r.t. for 1 h. The whole was poured into ice water and concentrated to give **5** as a precipitate, which was collected and washed with ether and then recrystallized from MeOH–EtOH (1.3 g, 88%), mp 189—191 °C. ^{1}H-NMR (DMSO-d_6) δ: 1.33 (3H, s), 3.46—3.81 (4H, m), 6.91 (1H, d, J=3 Hz), 7.03 (1H, d, J=9 Hz), 7.33—7.38 (1H, m), 7.45—7.49 (1H, m), 7.64 (1H, m), 7.71 (1H, dd, J=3, 9 Hz), 8.39 (1H, m). *Anal.* Calcd for $C_{15}H_{15}N_3O_5$: C, 56.78; H, 4.76; N, 13.24. Found: C, 56.55; H,4.72; N, 13.05.

2-(3,4-Dihydro-2-methoxymethyl-2-methyl-6-nitro-2*H*-1,4-benzoxazin-4-yl)pyridine 1-Oxide Monohydrochloride (6a) To a solution of **5** (0.2 g, 0.63 mmol) in DMF (2 ml), NaH (60% in oil, 0.05 g, 1.3 mmol) was added, followed by methyl iodide (0.27 g, 1.9 mmol). The whole was stirred for 15 min, poured into ice water, and extracted with AcOEt. The extract was washed with brine, dried, and concentrated. The residue was subjected to column chromatography with AcOEt–MeOH (20 : 1, v/v) and treated with HCl in EtOH to give **6a**, which was crystallized from EtOH–ether (0.22 g, 96%), mp 140—143 °C. ^{1}H-NMR (DMSO-d_6) δ: 1.35 (3H, s), 3.24 (3H, s), 3.37—4.00 (4H, m), 7.08 (1H, d, J=9 Hz), 7.37—7.40 (1H, m), 7.53—7.56 (1H, m), 7.69—7.75 (2H, m), 8.44—8.45 (1H, m). *Anal.* Calcd for $C_{16}H_{17}N_3O_5 \cdot HCl$: C, 52.25; H, 4.93; N, 11.43; Cl, 9.64. Found: C, 52.25; H,4.88; N, 11.42; Cl, 9.73.

Compounds **6b—f** were prepared in the same way.

2-(3,4-Dihydro-2-ethoxymethyl-2-methyl-6-nitro-2*H*-1,4-benzoxazin-4-yl)pyridine 1-Oxide (**6b**): An amorphous powder. ^{1}H-NMR ($CDCl_3$) δ: 1.05 (3H, t, J=7 Hz), 1.43 (3H, s), 3.32—4.10 (6H, m), 6.98 (1H, d, J=9 Hz), 7.2—7.4 (3H, m), 7.51 (1H, d, J=2 Hz), 7.80 (1H, dd, J=2, 9 Hz), 8.37 (1H, m). *Anal.* Calcd for $C_{17}H_{19}N_3O_5 \cdot 0.75H_2O$: C, 56.90; H, 5.76; N, 11.71. Found: C, 56.90; H, 5.83; N, 11.71.

2-(3,4-Dihydro-2-methyl-6-nitro-2-propoxymethyl-2*H*-1,4-benzoxazin-4-yl)pyridine 1-Oxide (**6c**): An amorphous powder. ^{1}H-NMR ($CDCl_3$) δ: 0.78 (3H, t, J=7 Hz), 1.25—1.58 (5H, m), 3.2—3.6 (4H, m), 3.81 (2H, ABq, J=14 Hz), 6.96 (1H, d, J=9 Hz), 7.12—7.36 (3H, m), 7.45 (1H, d, J=3 Hz), 7.79 (1H, dd, J=3, 9 Hz), 8.33 (1H, m). *Anal.* Calcd for $C_{18}H_{21}N_3O_5 \cdot 0.25H_2O$: C, 59.41; H, 5.96; N, 11.55. Found: C, 59.28; H, 5.94; N, 11.54.

2-(2-Butoxymethyl-3,4-dihydro-2-methyl-6-nitro-2*H*-1,4-benzoxazin-4-yl)pyridine 1-Oxide Monohydrochloride (**6d**): An amorphous powder. ^{1}H-NMR (DMSO-d_6) δ: 0.79 (3H, t, J=7 Hz), 1.1—1.4 (7H, m), 3.2—3.9 (6H, m), 7.0—7.1 (2H, m), 7.3—7.8 (4H, m), 8.4—8.5 (1H, m). *Anal.* Calcd for $C_{19}H_{23}N_3O_5 \cdot HCl$: C, 55.68; H, 5.90; N, 10.25; Cl, 8.65. Found: C, 55.63; H, 5.86; N, 10.25; Cl, 8.41.

2-(2-Benzyloxymethyl-3,4-dihydro-2-methyl-6-nitro-2*H*-1,4-benzoxazin-4-yl)pyridine 1-Oxide (**6e**): An amorphous powder. ^{1}H-NMR ($CDCl_3$) δ: 1.45 (3H, s), 3.50—4.01 (4H, m), 4.45—4.47 (2H, m), 6.97 (1H, d, J=9 Hz), 7.12—7.31 (8H, m), 7.44 (1H, s), 7.78 (1H, dd, J=3, 9 Hz), 8.30—8.31 (1H, m). *Anal.* Calcd for $C_{22}H_{21}N_3O_5 \cdot 0.25H_2O$: C, 64.15; H, 5.26; N, 10.20. Found: C, 63.99; H, 5.33; N, 10.16.

2-(2-Acetyloxymethyl-3,4-dihydro-2-methyl-6-nitro-2*H*-1,4-benzoxazin-4-yl)pyridine 1-Oxide (**6f**): An amorphous powder. ^{1}H-NMR ($CDCl_3$) δ: 1.45 (3H, s), 2.03 (3H, s), 3.81 (2H, ABq, J=14 Hz), 4.20 (2H, ABq, J=12 Hz), 6.99 (1H, d, J=9 Hz), 7.17—7.40 (3H, m), 7.48 (1H, d, J=3 Hz), 7.79 (1H, dd, J=3, 9 Hz), 8.30—8.36 (1H, m). *Anal.* Calcd for $C_{17}H_{17}N_3O_6 \cdot H_2O$: C, 54.11; H, 5.08; N, 11.14. Found: C, 54.02; H, 4.72; N, 10.97.

2-[3,4-Dihydro-2-methyl-2-(*N*-methylcarbamoyloxymethyl)-6-nitro-2*H*-1,4-benzoxazin-4-yl]pyridine 1-Oxide (7) To a solution of **5** (0.2 g, 0.63 mmol) and triethylamine (0.19 g, 1.9 mmol) in 4 ml CH_2Cl_2, methyl isocyanate (0.11 g, 1.9 mmol) was added. The mixture was stirred for 22 h and then poured into ice water, and extracted with $CHCl_3$. The extract was washed with brine, dried, and concentrated. The residue was subjected to column chromatography with $CHCl_3$–MeOH (50 : 1, v/v) to give **7** (0.14 g, 61%), as an amorphous powder. ^{1}H-NMR ($CDCl_3$) δ: 1.44 (3H, s), 2.73 (3H, s), 3.69—4.18 (4H, m), 7.00 (1H, d, J=9 Hz), 7.20—7.49 (4H, m), 7.81 (1H, d, J=9 Hz), 8.33 (1H, m). *Anal.* Calcd for $C_{17}H_{18}N_4O_6 \cdot 0.5H_2O$: C, 53.26; H, 5.00; N, 14.61. Found: C, 53.22; H, 5.05; N, 14.27.

2-(3,4-Dihydro-2-methyl-6-nitro-2-nitrooxymethyl-2*H*-1,4-benzoxazin-4-yl)pyridine 1-Oxide (8) To a solution of **5** (2.0 g, 6.3 mmol) in acetonitrile (50 ml), nitronium tetrafluoroborate (1.26 g, 7.6 mmol) was slowly added at −35—−40 °C and then the mixture was poured into ice water, made alkaline with $NaHCO_3$ solution, and extracted with $CHCl_3$. The extract was washed with brine, dried, and concentrated. The residue was subjected to column chromatography with $CHCl_3$ to give **8**, which was recrystallized from ether (0.74 g, 32%), 156—158 °C. ^{1}H-NMR ($CDCl_3$) δ: 1.52 (3H, s), 3.83 (2H, ABq, J=13 Hz), 4.67 (2H, ABq, J=12 Hz), 7.01 (1H, d, J=9 Hz), 7.24—7.27 (1H, m), 7.38—7.43 (3H, m), 7.79 (1H, dd, J=3, 9 Hz), 8.33—8.34 (1H, m). *Anal.* Calcd for $C_{15}H_{14}N_4O_7$: C, 49.73; H, 3.89; N, 15.46. Found: C, 49.61; H, 3.83; N, 15.31.

2-(3,4-Dihydro-6,7-dinitro-2-methyl-2-nitrooxymethyl-2*H*-1,4-benzoxazin-4-yl)pyridine 1-Oxide (9) To a solution of **5** (0.4 g, 1.3 mmol) in acetonitrile (10 ml), nitronium tetrafluoroborate (0.45 g, 3.4 mmol) was slowly added at −10—0 °C. The mixture was poured into ice water, made alkaline with $NaHCO_3$ solution, and extracted with $CHCl_3$. The extract was washed with brine, dried, and concentrated to give **9**, which was recrystallized from

AcOEt–EtOH (0.16 g, 31%), 156—159 °C. ^{1}H-NMR (DMSO-d_6) δ: 1.45 (3H, s), 3.90 (2H, ABq, J=13 Hz), 4.77—4.87 (2H, m), 6.93 (1H, s), 7.41—7.52 (2H, m), 7.71—7.74 (2H, m), 8.40—8.42 (1H, m). *Anal.* Calcd for $C_{15}H_{13}N_5O_9$: C, 44.23; H, 3.22; N, 17.19. Found: C, 44.09; H, 3.23; N, 17.19.

Single-Crystal X-Ray Analysis of 5 Crystals of compound **5** were grown from AcOEt as yellow prisms. Data was collected from a crystal of dimensions 0.28×0.10×0.10 mm^3 on a Rigaku AFC5R diffractometer and corrected for Lorentz and polarization factors. The structure was solved by a direct method using the program SIR92 and refined using the program teXsan.[24] The final refinement was achieved by the full-matrix least-squares method with anisotropic thermal parameters for all non-hydrogen atoms and fixed isotropic thermal parameters for all hydrogen atoms. Crystal data: $C_{15}H_{15}N_3O_5$, M.W.=317.30, monoclinic, space group $P2_1/n$(#14), a=13.092 (1) Å, b=11.027 (1) Å, c=10.274 (1) Å, β=101.977 (7)°, V=1450.9 (3) Å^3, Z=4, Dc=1.452 g/cm^3, F_{000}=664.00, temperature 25.0 °C, Cu$K\alpha$ (λ=1.54178 Å), 2610 observed reflections (I>3.00σ (I)), 218 variable parameters, R=0.047, R_w=0.070.

Biological Testing i) Effects on 3,4-Diaminopyridine-Induced Rhythmic Contractions[19]: The left coronary circumflex branch or the anterior-descending branch of mongrel dogs of either sex was isolated in Krebs–Henseleit solution and cut into rings about 2 mm wide. A ring segment was fixed to a stainless-steel hook and suspended in a Krebs–Henseleit bath (37 °C) aerated with 95%O_2–5%CO_2 under a tension load of 1.0 g, and isometric contractions were recorded. The specimen was allowed to stabilize for 30 min, then rhythmic contractions were induced by the addition of 3,4-diaminopyridine (10 mM). When the amplitude and frequency of the rhythmic contractions stabilized, cumulative addition of the test compound to the organ bath was started. Concentration–response curves for the amplitude and frequency of contractions were constructed and efficacy was evaluated. The inhibitory effect (IC_{50}) on the frequency of contractions is shown in Table 1.

ii) Hemodynamic Effect in Dogs (i.v.): Mongrel dogs of either sex were anesthetized with pentobarbital (30 mg/kg, i.v.). The experiment was performed under artificial respiration after tracheal intubation. After a thoracotomy, blood pressure was measured with a pressure transducer and CBF was measured directly with an electromagnetic flowmeter *via* a probe. The test compound was administered through a cannula in the femoral vein. The MBP-lowering effect (Δ%), the CBF-increasing effect (Δ%) and the duration are shown in Table 2.

iii) Vasodilating Effect on Rabbit Isolated Artery: The aorta of rabbits of either sex was isolated and cut into rings about 3 mm wide. After removal of the endothelium, each ring was suspended on wire hooks in an organ bath containing Krebs–Henseleit solution maintained at 37 °C and aerated with 95%O_2–5%CO_2, under a tension of 1.0 g, and isometric contractions were measured. Contraction was induced by the addition of phenylephrine (10^{-7} M) and the contractile response was allowed to reach a plateau. The test compound was then added to the preparation cumulatively. As far as antagonism by methlene blue was concerned, after adding methylene blue (3×10^{-6} g/ml) and allowing the contractile response to reach a plateau, the test compound was added cumulatively. As an indicator of the vasodilative effect, the inhibitory effect (IC_{50}) on the response to papaverine (10^{-4} M) was taken as 100%, and is shown in Table 3.

Acknowledgements We wish to thank Associate Professor T. Hirose of Saitama University and Drs. T. Takenaka, T. Tamura, T. Fujikura, T. Mase, S. Tsukamoto, S. Sakamoto, and S. Fujita of Yamonouchi Pharmaceutical Co., Ltd., for their encouragement and helpful discussions. We also thank the staff of the Structure Analysis Research Group for elemental analyses and spectral measurements.

References and Notes

1) For previous papers in this series see: *a*) Part I: Matsumoto Y., Tsuzuki R., Matsuhisa A., Takayama K., Yoden T., Uchida W., Asano M., Fujita S., Yanagisawa I., Fujikura T., *Chem. Pharm. Bull.*, **44**, 103—114 (1996); *b*) Part II: Matsumoto Y., Tsuzuki R., Matsuhisa A., Masuda N., Yamagiwa Y., Yanagisawa I., Shibanuma T., Nohira H., *ibid.*, **47**, 971—979 (1999).
2) Gopalakrishnan M., Janis R. A., Triggle D. J., *Drug Devel. Res.*, **28**, 95—127 (1993).
3) Ulrich Q., *Trens Pharmacol Sci.* **14**, 332—337 (1993).
4) For reviews of potassium channel activators, see: *a*) Cook N. S., *Trends Pharmacol. Sci.*, **9**, 21—28 (1988); *b*) Robertson D. W., Steinberg M. I., *Ann. Reports Med. Chem.*, **1989**, 91—100; *c*) Quast U., Cook N. S., *Trends Pharmacol. Sci.*, **10**, 431—435 (1989); *d*) Robertson D. W., Steinberg M. I., *J. Med. Chem.*, **33**, 1529—1541 (1990); *e*) Edwards G., Weston A. H., *Trends Pharmacol. Sci.*, **11**, 417—422 (1990); *f*) Evans J. M., Longman S. D., *Ann. Reports Med. Chem.*, **1991**, 73—82; *g*) Longman S. D., Hamilton T. C., *Med. Res. Rev.*, **12**, 73—148 (1992); *h*) Atwal K. S., *Drug Devel. Res.*, **33**, 250—262 (1994); *i*) Evans J. M., Taylor S. G., *Prog. Med. Chem.*, **31**, 411—446 (1994); *j*) Pirotte B., Fontaine J., Lebrun P., *Cur. Med. Chem.*, **2**, 573—582 (1995).
5) Raeburn D., Karlson J.-A., *Prog. Drug. Res.*, **37**, 161—180 (1991).
6) Edwards G., Henshaw M., Miller M., Weston A. H., *Br. J. Pharmacol.*, **102**, 679—686 (1991).
7) Buhl A. E., Waldon D. J., Conrad S. J., Mulholland M. J., Shull K. L., Kubicek M. F., Johnson G. A., Brunden M. N., Stefanski K. J., Stehle R. G., Gadwood R. C., Kamdar B. V., Thomasco L. M., Schostarez H. J., Schwartz T. M., Diani A. R., *J. Invest. Dermatol.*, **98**, 315—319 (1992).
8) Escande D., Cavero I., *Trnds Pharmacol. Sci.*, **13**, 269—272 (1992).
9) Hamilton T. C., Beerahee A., Moen J. S., Price P. K., Ramji J. V., Clapham J. C., *Cardiovascular Drug Rev.*, **11**, 199—222 (1993).
10) Ashwood V. A., Buckingham R. E., Cassidy F., Evans J. M., Faruk E. A., Hamilton T. C., Nash D. J., Stemp G., Willcocks K., *J. Med. Chem.*, **29**, 2194—2201 (1986);
11) Peterson H. J., Nielsen C. K., Martelli E. A., *J. Med. Chem.*, **21**, 773—781 (1978).
12) Sakai K., *Jpn. J. Pharmacol.*, **30**, 881—890 (1980).
13) Brown T. J., Chapman R. F., Cook D. C., Hart T. W., Mclay I. M., Jordan R., Mason J. S., Palfreyman M. N., Walsh R. J. A., Withnall M. T., Aloup J. C., Cavero I., Farge D., James C., Mondot S., *J. Med. Chem.*, **35**, 3613—3624 (1992).
14) Cho H., Katoh S., Sayama S., Murakami K., Nakanishi H., Kajimoto Y., Ueno H., Kawasaki H., Aisaka K., Uchida I., *J. Med. Chem.*, **39**, 3797—3805 (1996).
15) Koga H., Sato H., Imagawa J., Ishizawa T., Yoshida S., Sugo I., Taka N., Takahashi T., Nabata H., *Bioorg. Med. Chem. Lett.*, **3**, 2005—2010 (1993).
16) Lee B. H., Yoo S. E., Shin H. S., *J. Cardiovasc. Pharmacol.*, **31**, 85—94 (1998).
17) Shin H. S., Seo H. W., Yoo S. E., Lee B. H., *Pharmacology*, **56**,111—124 (1998).
18) Russell K., Brown F. J., Warwick P., Forst J., Grant T., Howe B., Kau S. T., Li J. H., McLaren F. M., Shapiro H. S., Trivedi S., *Bioorg. Med. Chem. Lett.*, **3**, 2727—2728 (1993).
19) Uchida Y., Sugimoto T., *Myakkangaku.*, **24**, 133—143 (1984).
20) Yanagisawa T., Okada Y., *Cardiovasc. Drug Rev.*, **11**, 94—115 (1993).
21) Nakajima T., Izawa T., Kashiwabara T., Nakajima S., Munezuka Y., *Chem. Pharm. Bull.*, **42**, 2475—2482 (1994).
22) Hashimoto K., Kinoshita M., Ohbayashi Y., *Cardiovasc. Drugs Ther.*, **5**, 131—138 (1991).
23) Cassidy F., Evans J. M., Smith D. M., Stemp G., Edge C., Williams D. J., *J. Chem. Soc., Chem. Commun.*, **1989**, 377—378.
24) Crystal structure analysis package, Molecular Structure Corporation (1985 & 1992).

Indonesian Medicinal Plants. XXIII.[1] Chemical Structures of Two New Migrated Pimarane-type Diterpenes, Neoorthosiphols A and B, and Suppressive Effects on Rat Thoracic Aorta of Chemical Constituents Isolated from the Leaves of *Orthosiphon aristatus* (Lamiaceae)

Kazuyoshi OHASHI,[a] Takako BOHGAKI,[a] Toshiyuki MATSUBARA,[b] and Hirotaka SHIBUYA*,[a]

Faculty of Pharmacy and Pharmaceutical Sciences, Fukuyama University,[a] Sanzo, 1 Gakuen-cho, Fukuyama, Hiroshima 729–0292, Japan and Toyama Prefectural Institute for Pharmaceutical Research,[b] 17–1, Nakataikouyama, Kosugi-machi, Imizu-gun, Toyama 939–0363, Japan. Received September 27, 1999; accepted November 23, 1999

Two novel migrated pimarane-type diterpenes named neoorthosiphols A (1) and B (2) were isolated from the water decoction of the leaves of *Orthosiphon aristatus* (Lamiaceae), which has been prescribed in Javanese traditional medicine (jamu) for the treatment of hypertension, *etc.* The absolute chemical structures have been elucidated on the basis of physicochemical properties.

It has been found that two migrated pimarane-type diterpenes (1, 2), four isopimarane-type diterpenes (3, 4, 5, 6), three benzochromenes (7, 8, 9) and two flavones (12, 13) exhibit a suppressive effect on contractile responses in rat thoracic aorta, among thirteen chemical constituents (1—13) isolated from the leaves.

Key words Indonesian medicinal plant; *Orthosiphon aristatus*; Lamiaceae; migrated pimarane; neoorthosiphol; circular dichroism

A lamiaceaous plant *Orthosiphon aristatus* (BL.) MIQ. is a popular medicinal plant in Southeast Asia and is well known by the name of kumis kucing. The leaves have been prescribed in Javanese traditional medicine (jamu)[2] for the treatment of hypertension, *etc.* The water decoction of the leaves was partitioned into a mixture of chloroform and water. The chloroform-soluble portion of the water decoction shows an inhibitory effect on the contractile responses in rat thoracic aorta smooth muscle stimulated with K^+, an activity which is thought to be closely related with antihypertensive activity.

In our previous papers, we reported the isolation of four isopimarane-type diterpenes [orthosiphols A (**3**)[3] and B (**4**),[3] orthosiphonones A (**5**) and B (**6**)[1]] and three benzochromenes [methylripariochromene A (**7**),[4] acetovanillochromene (**8**),[5] and orthochromene A (**9**)[1]] from the chloroform-soluble portion of the water decoction. In a continuing study of the portion, we have isolated two novel migrated pimarane-type diterpenes designated neoorthosiphols A (**1**) and B (**2**),[6] as well as four flavones [5-hydroxy-6,7,3′,4′-tetramethoxyflavone (**10**), eupatorin (**11**), tetramethylscutellarein (**12**) and sinensetin (**13**)].[7] This paper describes the elucidation of the absolute chemical structures of **1** and **2**, and the suppressive effects of the chemical constituents of the leaves on the contraction induced by K^+ in rat thoracic aorta.[8]

Neoorthosiphol A (1) Neoorthosiphol A (**1**) showed a quasi-molecular ion peak at *m/z* 693 $[M+H]^+$, $C_{38}H_{45}O_{12}$, in the FAB-MS, and the IR spectrum showed the presence of a hydroxyl (3420 cm^{-1}) group, a vinyl (3080, 712 cm^{-1}) group and an ester (1720, 1267 cm^{-1}) group. The UV spectrum showed absorption bands at 230 nm (ε 24000) and 274 nm (ε

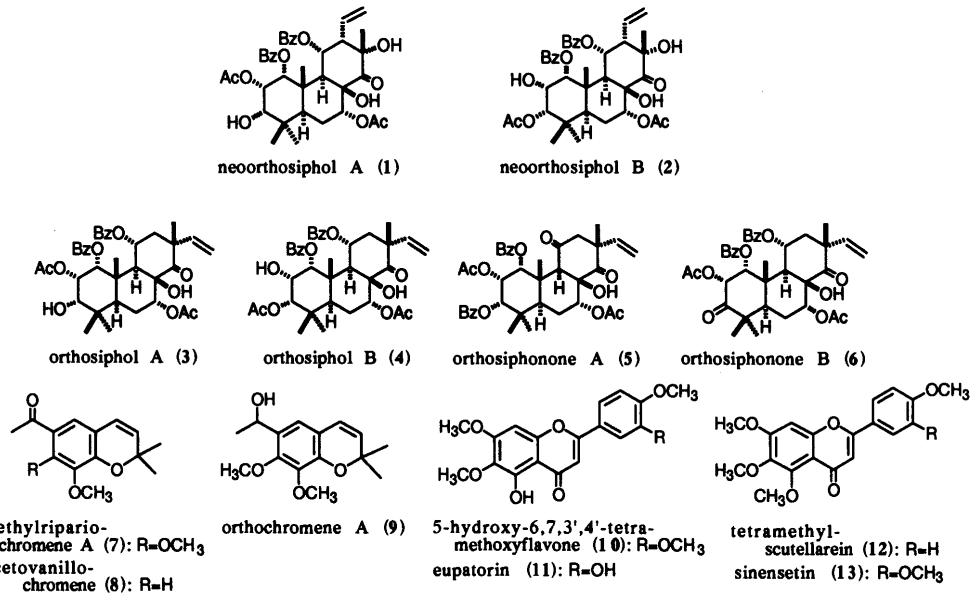

Fig. 1

* To whom correspondence should be addressed.

© 2000 Pharmaceutical Society of Japan

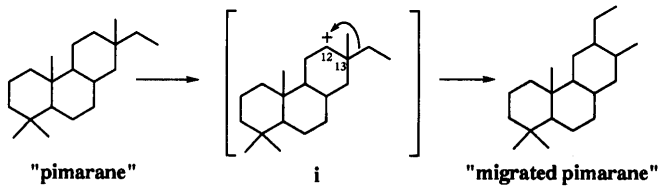

Fig. 2. Plausible Biosynthetic Route for "Migrated Pimarane" from "Pimarane"

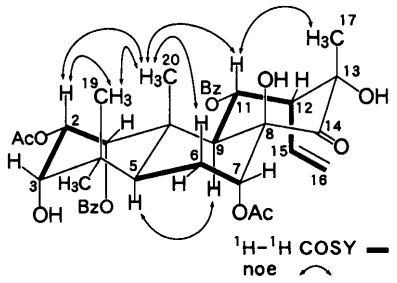

Fig. 3. ^{1}H–^{1}H COSY and ROESY Correlations of **1**

2000).

The ^{1}H-NMR spectrum showed signals due to four tertiary methyls, two acetoxymethyls, one hydroxymethine proton, four methine protons attached to an ester function, three olefinic protons and ten aromatic protons. The ^{13}C-NMR and the distortionless enhancement by polarization transfer (DEPT) spectra revealed the presence of six methyl carbons, two methylene carbons, nine methine carbons, one ketonic carbonyl carbon, four ester carbonyl carbons, twelve aromatic carbons and four quaternary carbons, including two carbons bearing a hydroxyl function (δ_C 76.6, 8-C; δ_C 76.9, 13-C).

The ^{1}H–^{1}H correlated spectroscopy (COSY) spectrum of **1** showed correlation peaks revealing sequences from 1-C to 3-C *via* 2-C, from 5-C to 7-C *via* 6-C, and from 9-C to 16-C *via* 11-C, 12-C and 15-C (Fig. 3). From these findings and from analysis of the heteronuclear multiple bond correlation (HMBC) spectrum, it has been deduced that **1** possesses a novel diterpene skeleton, which may be biosynthetically produced through a 1,2-shift of a C2-unit into C-12 from the C-13 position in a pimarane-type diterpene.

The rotating frame nuclear Overhauser effect spectroscopy (ROESY) spectrum of **1** showed correlation peaks between 19-H_3 and 20-H_3, 2-H and 19-H_3, 2-H and 20-H_3, 6β-H and 20-H_3, and 5-H and 9-H, which suggested that the relative configuration and conformation of the A and B rings in **1** were the same as those in orthosiphol A (**3**).[3] The orientations of 11-H and 17-H_3 were both determined to be β-axial based on the coupling constants of $J_{9,11}$ (11.0 Hz) and the correlations with 11-H and 17-H_3, and 11-H and 20-H_3 in the ROESY spectrum. The signals due to 20-H_3 and 17-H_3 were observed at a lower field than expected, which was assumed to be due to an anisotropic effect of the 8β-axial hydroxyl group. This assumption was supported by the pyridine-induced solvent shifts[9] ($\delta_{CDCl_3}-\delta_{C_5D_5N}$)$\Delta=-0.43$ ppm for 20-CH_3 and $\Delta=-0.30$ ppm for 17-CH_3. Furthermore, the coupling constant $J_{11,12}$ (3.5 Hz) indicated that the vinyl group at C-12 was oriented to be an α-axial configuration.

In the HMBC experiment, **1** showed the presence of four characteristic cross-peaks between two hydroxymethine protons (1-, 11-H) and two benzoyl carbonyl carbons, and between two hydroxymethine protons (2-, 7-H) and two acetyl carbonyl carbons, respectively. In addition, the presence of cross-peaks between the protons at C-12 and C-17 and the ketonic carbonyl carbon, indicated that the ketonic function was oriented at C-14.

Table 1. Suppressive Effects on the Contraction Induced by K^+ in Endothelium-Denuded Rat Thoracic Aorta

Compound	IC_{50} (μmol/ml)
Neoorthosiphol A (**1**)	1.52×10^{-2}
Neoorthosiphol B (**2**)	6.01×10^{-2}
Orthosiphol A (**3**)	4.93×10^{-3}
Orthosiphol B (**4**)	4.23×10^{-3}
Orthosiphonone A (**5**)	3.69×10^{-3}
Orthosiphonone B (**6**)	3.89×10^{-3}
Methylripariochromene A (**7**)	8.32×10^{-2}
Acetovanillochromene (**8**)	1.01×10^{-1}
Orthochromene A (**9**)	1.31×10^{-1}
5-Hydroxy-6,7,3′,4′-tetramethoxyflavone (**10**)	No suppression
Eupatorin (**11**)	No suppression
Tetramethylscutellarein (**12**)	8.08×10^{-3}
Sinensetin (**13**)	4.92×10^{-2}
Nifedipine[a]	1.79×10^{-5}

a) Positive control.

The absolute configuration of **1** was established by application of the exciton chirality method.[10] Positive maximum ($[\theta]_{236}$ +63000), which was caused by two chromophoric benzoates at C-1 and C-11, was observed in the circular dichroism (CD) spectrum. Consequently, it has been clarified that the absolute chemical structure of **1** is as shown.

Neoorthosiphol B (2) Neoorthosiphol B (**2**) showed a quasi-molecular ion peak at *m/z* 693 $[M+H]^+$, $C_{38}H_{45}LiO_{12}$, in the FAB-MS.

The ^{1}H- and ^{13}C-NMR spectra of **2**, including ^{1}H–^{1}H COSY, ROESY and HMBC correlations, were quite similar to those of neoorthosiphol A (**1**), except for the chemical shifts for 2-H and 3-H. Furthermore, a cross peak between 3-H and 3-$\underline{C}OCH_3$ was observed in the HMBC spectrum, instead of that between 2-H and 2-$\underline{C}OCH_3$ in **1**. From the evidence, the chemical structure of **2** was deduced as shown. The absolute configuration was clarified by application of the exciton chirality method[10] in the CD spectrum ($[\theta]_{237}$ +47000).

So far, thirteen chemical components (**1**—**13**) have been isolated from the chloroform-soluble portion in the water decoction of the leaves of *Orthosiphon aristatus* (kumis kucing). It should be mentioned that two migrated pimarane-type diterpenes (**1**, **2**), the four isopimarane-type diterpenes (**3**, **4**, **5**, **6**), the three benzochromenes (**7**, **8**, **9**) and the two flavones (**12**, **13**) exhibit concentration-dependent suppression of contractions induced by K^+ in endothelium-denuded rat thoracic aorta (Table 1).[8] This finding may be related to the use of kumis kucing for the treatment of hypertension in Javanese traditional medicine (jamu).

Experimental

Melting points were determined on a Yanagimoto micromelting point apparatus and are uncorrected. Optical rotations were measured with a JASCO DIP-360 digital polarimeter. FAB-MS were recorded on a JEOL SX-102A spectrometer. IR spectra were recorded on a Shimadzu FT-IR 8500 spectrometer. UV spectra were recorded on a Hitachi U-3500 spectrometer. CD

spectra were recorded on a JASCO J-500A spectrometer. ^{1}H- and ^{13}C-NMR spectra were obtained with a JEOL JNM-Lambda 500 spectrometer operating at 500 and 125 MHz for ^{1}H and ^{13}C nuclei, respectively; chemical shifts are reported in ppm relative to that of tetramethylsilane (δ=0) as an internal standard, and coupling constants are given in hertz. HPLC was carried out with a Shimadzu LC-10A. Column chromatography was carried out on Silica gel 60 (70—230 mesh, Merck). Thin-layer chromatography on Silica gel 60F_{254} (Merck) was used to ascertain the purity of the compounds. The spots were visualized by spraying the plates with 1% $Ce(SO_4)_2$ in 10% aqueous sulfuric acid, followed by heating.

Plant Material *Orthosiphon ariatatus* (Bl.) Miq. was collected in Yogyakarta, Java Island, Indonesia, in December, 1995, and identified at the Herbarium Bogoriense, Research and Development Centre for Biology-LIPI, Indonesia.

Extraction and Isolation Procedure The leaves (800 g) of *Orthosiphon aristatus* (Bl.) Miq. (Lamiaceae) were extracted four times with boiled water. The combined solution was evaporated under reduced pressure to give the H_2O extract (220 g, 27.5% from the leaves). The H_2O extract (23 g) was partitioned into a chloroform and water mixture (1:1). The chloroform phase was concentrated under reduced pressure to give a $CHCl_3$ extract (1.9 g, 2.3%) and a H_2O extract (21.1 g, 25%). The $CHCl_3$ extract (1.2 g) was subjected to silica gel column chromatography (SiO_2 40 g, *n*-hexane : EtOAc = 2 : 1→EtOAc→$CHCl_3$: MeOH = 10 : 1→MeOH) to give fraction 1 (820 mg, 1.5%), fraction 2 (80 mg, 0.15%), fraction 3 (110 mg, 0.21%), fraction 4 (130 mg, 0.25%). Fraction 1 (600 mg) was again purified by HPLC (YMC-Pack SIL, 250×20 mm; *n*-hexane : EtOAc = 2 : 1) to afford neoorthosiphol A (**1**, 15 mg, 0.039%), neoorthosiphol B (**2**, 1.9 mg, 0.005%), orthosiphol A (**3**, 15 mg, 0.039%), orthosiphol B (**4**, 14 mg, 0.035%), orthosiphonone A (**5**, 8.9 mg, 0.023%) and orthosiphonone B (**6**, 1.2 mg, 0.003%), methylripariochromene A (**7**, 244 mg, 0.63%), acetovanillochromene (**8**, 11 mg, 0.030%), orthochromene A (**9**, 12 mg, 0.024%), 5-hydroxy-6,7,3′,4′-tetramethoxyflavone (**10**, 4.6 mg, 0.012%), and eupatorin (**11**, 2.7 mg, 0.007%). Fraction 2 (40 mg) was purified by HPLC (YMC-Pack SIL, 250×10 mm; *n*-hexane : EtOAc = 2 : 3) tetramethylscutellarein (**12**, 4.1 mg, 0.011%) and sinensetin (**13**, 3.2 mg, 0.009%).

Neoorthosiphol A (**1**): Colorless plates from ether, mp 148—149 °C, $[\alpha]_D$ −28.7° ($CHCl_3$, at 20 °C). IR (KBr) cm^{-1}: 3420, 3080, 1720, 1267, 712. UV (MeOH) nm (ε): 230 (24000), 274 (2000). CD (MeOH) nm ([θ]): 204 (+60000), 235 (+63000). ^{1}H-NMR (500 MHz, $CDCl_3$) δ: 1.02 (3H, s, 19-H_3), 1.08 (3H, s, 18-H_3), 1.39 (3H, s, 20-H_3), 1.66 (3H, s, 17-H_3), 1.87 (1H, br d, *J*=13.5 Hz, 6-Hα), 2.02 (3H, s, 2-$COCH_3$), 2.09 (1H, dd, *J*=13.5, 13.5 Hz, 6-Hβ), 2.18 (3H, s, 7-$COCH_3$), 2.61 (1H, d, *J*=13.5 Hz, 5-H), 2.94 (1H, dd, *J*=3.5, 9.8 Hz, 12-H), 2.98 (1H, d, *J*=11.0 Hz, 9-H), 3.52 (1H, d, *J*=3.1 Hz, 3-H), 4.45 (1H, d, *J*=9.8 Hz, 16-Ha), 4.81 (1H, d, *J*=16.8 Hz, 16-Hb), 5.07 (1H, ddd, *J*=9.8, 9.8, 16.8 Hz, 15-H), 5.32 (1H, dd, *J*=3.1, 3.1 Hz, 2-H), 5.40 (1H, br s, 7-H), 5.82 (1H, d, *J*=3.1 Hz, 1-H), 6.30 (1H, dd, *J*=3.5, 11.0 Hz, 11-H), 7.48 (2H, dd, *J*=7.9, 7.9 Hz), 7.61 (1H, dd, *J*=7.9, 7.9 Hz), 8.24 (2H, d, *J*=7.9 Hz) (11-COPh), 7.42 (2H, dd, *J*=7.9, 7.9 Hz), 7.57 (1H, dd, *J*=7.9, 7.9 Hz), 8.05 (2H, d, *J*=7.9 Hz) (1-COPh). ^{13}C-NMR (125 MHz, $CDCl_3$) δ_C: 15.5 (20-C), 20.9 (2C, 6-C, 2-$COCH_3$), 21.2 (7-$COCH_3$), 22.4 (19-C), 29.0 (17-C), 29.3 (18-C), 34.4 (5-C), 38.2 (4-C), 40.7 (9-C), 43.5 (10-C), 54.4 (12-C), 67.8 (2-C), 70.1 (7-C), 70.3 (11-C), 75.9 (1-C), 76.6 (13-C), 76.8 (8-C), 77.0 (3-C), 121.1 (16-C), 128.2, 129.3, 130.6, 133.3 (11-COPh), 128.5, 129.5, 130.5, 133.2 (1-COPh), 131.2 (15-C), 164.1 (1-COPh), 166.9 (11-COPh), 169.9 (7-$COCH_3$), 170.0 (2-$COCH_3$), 208.9 (14-C). FAB-MS *m/z*: 693 $(M+H)^+$. High-resolution FAB-MS *m/z*: Calcd for $C_{38}H_{45}O_{12}$: 693.2911. Found: 693.2924 $(M+H)^+$.

Neoorthosiphol B (**2**): Colorless plates from ether, mp 194—195 °C, $[\alpha]_D$ +18.1° ($CHCl_3$, at 21 °C). IR (KBr) cm^{-1}: 3410, 3080, 1720, 1250, 712. UV (MeOH) nm (ε): 230 (24000), 274 (2000). CD (MeOH) nm ([θ]): 203 (+65000), 237 (+47000). ^{1}H-NMR (500 MHz, $CDCl_3$) δ: 0.89 (3H, s, 18-H_3), 1.07 (3H, s, 19-H_3), 1.46 (3H, s, 20-H_3), 1.54 (3H, s, 3-$COCH_3$), 1.65 (3H, s, 17-H_3), 1.87 (1H, br d, *J*=13.7 Hz, 6-Hα), 2.08 (1H, dd, *J*=13.7, 13.7 Hz, 6-Hβ), 2.24 (3H, s, 7-$COCH_3$), 2.52 (1H, d, *J*=13.7 Hz, 5-H), 2.99 (1H, dd, *J*=3.9, 9.8 Hz, 12-H), 3.24 (1H, d, *J*=10.3 Hz, 9-H), 4.40 (1H, br s, 2-H), 4.47 (1H, d, *J*=11.6 Hz, 16-Ha), 4.87 (1H, d, *J*=16.8 Hz, 16-Hb), 5.03 (1H, d, *J*=2.7 Hz, 3-H), 5.28 (1H, ddd, *J*=9.8, 11.6, 16.8 Hz, 15-H), 5.43 (1H, br s, 7-H), 5.49 (1H, br s, 1-H), 6.27 (1H, dd, *J*=3.9, 10.3 Hz, 11-H), 7.42 (2H, dd, *J*=7.9, 7.9 Hz), 7.43 (2H, dd, *J*=7.9, 7.9 Hz), 7.59 (1H, dd, *J*=7.9, 7.9 Hz), 7.60 (1H, dd, *J*=7.9, 7.9 Hz), 7.98 (2H, d, *J*=7.9 Hz), 8.06 (2H, d, *J*=7.9 Hz) (1-, 11-COPh). ^{13}C-NMR (125 MHz, $CDCl_3$) δ_C: 16.0 (20-C), 20.5 (2-$COCH_3$), 21.2 (7-$COCH_3$), 21.3 (6-C), 22.2 (19-C), 28.0 (18-C), 28.2 (17-C), 36.3 (5-C), 37.2 (4-C), 41.4 (9-C), 44.4 (10-C), 54.0 (12-C), 66.0 (2-C), 70.2 (7-C), 70.5 (11-C), 76.1 (13-C), 76.7 (8-C), 78.5 (3-C), 80.0 (1-C), 121.0 (16-C), 128.4, 128.5, 129.3, 129.6, 130.1, 130.2, 133.5, 133.6 (1-, 11-COPh), 131.6 (15-C), 166.2 (11-COPh), 167.3 (1-COPh), 169.3 (7-$COCH_3$), 170.7 (2-$COCH_3$), 208.3 (14-C). FAB-MS *m/z*: 693 $(M+H)^+$. High-resolution FAB-MS *m/z*: Calcd for $C_{38}H_{45}O_{12}$: 693.2911. Found: 693.2894 $(M+H)^+$.

Effects of Thirteen Constituents from the Leaves of *Orthosiphon aristatus* on Contractile Responses Induced by K^+ in Endothelium-Denuded Rat Thoracic Aorta Male Wistar rats were sacrificed and their thoracic aorta were isolated. Each aortaspiral strip (approx. 2.5 mm×20 mm) was prepared following a removement of connective tissues, and suspended in a 30 ml organ bath filled with Krebs–Henseleit solution (118 mM NaCl, 4.7 mM KCl, 2.55 mM $CaCl_2 \cdot 2H_2O$, 1.18 mM $MgSO_4 \cdot 7H_2O$, 1.18 mM KH_2PO_4, 11.1 mM $NaHCO_3$, 11.1 mM glucose) maintained at 37 °C. The solution was continuously aerated with a gas mixture of 95% O_2 and 5% CO_2. A resting tension of 1.0 g was initially applied to each preparation, and it was then allowed to equilibrate for 90 min before the start of the experiment. The endothelium was removed by gently rubbing the internal surface of the aorta with filter paper, and the functional loss of endothelial cell was confirmed pharmacologically by the absence of a 10^{-6} M ACh-induced relaxing response in *l*-phenylephrine-induced contractions. The muscle responses were measured isometrically by means of a force displacement transducer (TB-652T, Nihon Kohden, Tokyo) coupled to an amplifer (EF-601G, Nihon Kohden), and were described on a pen recorder. After the contractions by 60 mM K^+ reached a plateau, a sample was applied cumulatively. The relaxing response was expressed in terms of a percentage of the maximal relaxation developed by 10^{-4} M papaverine. IC_{50} values were determined from the dose–response curves using computer software (Delta Graph TM, Polaroid Computing, Tokyo).

Acknowledgments This work was supported by a Grant-in-Aid (No. 0641071, 08041186) for Scientific Research from the Ministry of Education, Science, Sports and Culture, Japan.

References

1) Part XXII: Shibuya H., Bohgaki T., Matsubara T., Watarai M., Ohashi K., Kitagawa I., *Chem. Pharm. Bull.*, **47**, 695—698 (1999).
2) Riswan S., Sangat H. M., "Jamu as a Javanese Traditional Medicine in Indonesia," The Bioresources-Diversity, Ethnobiology Development and Sustainability International Centenary Conference, Sydney, July 1991.
3) Masuda T., Masuda K., Shiragami S., Jitoe A., Nakatani N., *Tetrahedron*, **48**, 6787—6793 (1992).
4) Guerin J. C., Reveillere H. P., Ducrey P., Toupet L., *J. Nat. Prod.*, **52**, 171—175 (1989).
5) Tailor D. R., Wright J. A., *Phytochemistry*, **10**, 1665—1669 (1971).
6) The preliminary report: Shibuya H., Bohgaki T., Ohashi K., *Chem. Pharm. Bull.*, **47**, 911—912 (1999).
7) Lyckander I. M., Malterud K. E., *Acta Pharm. Nord.*, **4**, 159—166 (1992).
8) *a*) Abe A., Karaki H., *Jpn. J. Pharmacol.*, **60**, 389—392 (1992); *b*) Matsubara T., Bohgaki T., Watarai M., Suzuki H., Ohashi K., Shibuya H., *Biol. Pharm. Bull.*, **22**, 1083—1088 (1999).
9) Demarco P. V., Farkas E., Doddrell D., Mylari B. L., Wenkert E., *J. Am. Chem. Soc.*, **90**, 5480—5486 (1968).
10) *a*) Harada N., Chen Sow-Mei L., Nakanishi K., *J. Am. Chem. Soc.*, **97**, 5345—5352 (1975); *b*) Harada N., Iwabuchi J., Yokota Y., Uda H., Nakanishi K., *ibid*, **103**, 5590—5591 (1981).

Synthesis of 2-Substituted 3-Nitro-1,2-dihydropyridines by Heterocyclic Annulation Reactions of a *sec*-Nitrodienamine with Aldehyde Compounds

Takeshi KOIKE,* Yoshifumi SHINOHARA, Noriko ISHIBASHI, Naoki TAKEUCHI, and Seisho TOBINAGA

Showa Pharmaceutical University, Higashitamagawagakuen 3–3165, Machida, Tokyo 194–8543, Japan.
Received September 27, 1999; accepted December 16, 1999

The reaction of a *sec*-nitrodienamine 3 with aldehyde compounds afforded 2-substituted 3-nitro-1,2-dihydropyridines 5, providing a heterocyclic annulation reaction.

Key words nitrodienamine; aldehyde; 2-substituted 3-nitro-1,2-dihydropyridine; heterocyclic annulation reaction

We are interested in the reactivities of *tert*-nitrodienamines [*ex.* 1-(*N*,*N*-dimethylamino)-4-nitro-1,3-butadiene **1**] and *sec*-nitrodienamines [*ex.* 4-nitro-1-(2-phenethylamino)-1,3-butadiene **3**] as potentially useful synthons in organic synthesis. The chemistry of nitrodienamines exploits in the enaminic, dienic, and electronic "push pull" character of these molecules, and leads to interesting cycloaddition reactions as well as aminodienyl esters and aminoacrylate synthons.[1—4] The reactions of a *sec*-nitrodienamine, 4-nitro-1-(2-phenethylamino)-1,3-butadiene **3**, with aldehyde compounds **4** afforded 2-substituted 3-nitro-1-(2-phenethyl)-1,2-dihydropyridines **5**, which provide a heterocyclic annulation reaction.

Dihydropyridine chemistry is of interest from the point of view of pure research on heterocyclic compounds and also from a biological point of view.[5] Regarding studies on dihydropyridines, we recently reported the synthesis of 1-substituted 2-methyl-3-nitro-1,2-dihydropyridines by the reaction of *sec*-nitrodienamines with acetaldehyde (**4a**) in good yield.[1d] Here, we describe full details of the heterocyclic annulation reactions of **3** with aldehydes **4** to prepare 2-substituted 3-nitro-1-(2-phenethyl)-1,2-dihydropyridines **5** (Chart 1). The *sec*-nitrodienamine **3** was prepared by the reaction of *tert*-nitrodienamine **1** with 2-phenethylamine in benzene at room temperature in 95% yield.[1d]

The reaction of **3** with propionaldehyde (**4b**) under neat refluxing conditions provided 2-ethyl-3-nitro-1-(2-phenethyl)-1,2-dihydropyridine (**5b**) in 82% yield. The structure of the product **5b** was confirmed on the basis of the following spectroscopic analyses. The molecular formula of **5b** was found to be $C_{15}H_{18}N_2O_2$. The ^{1}H-NMR spectrum indicated the presence of two methylene protons at δ 2.92 (2H, t, J=6.8 Hz), 3.58 (1H, dt, J=13.6, 6.8 Hz), 3.64 (1H, dt, J=13.6, 6.8 Hz), and aromatic protons at δ 7.09—7.26 (5H, m) due to a phenethyl group, ethyl protons at δ 0.91 (3H, t, J=7.7 Hz, Me) and 1.38—1.92 (2H, m), a methine proton at δ 5.05 (1H, t, J=4.6 Hz), and three olefinic protons at δ 4.83 (1H, dd, J=7.5, 6.4 Hz), 6.53 (1H, d, J=6.4 Hz) and 7.65 (1H, d, J=7.5 Hz) due to a 1,2-dihydropyridine ring. The IR spectrum of **5b** showed absorption bands at 1624, 1541, 1516, 1474, 1456, and 1360 cm^{-1} due to nitro, two olefinic, and phenethyl groups.

In a similar manner, several other 2-substituted 3-nitro-1-(2-phenethyl)-1,2-dihydropyridines **5c—g** listed in Table 1 were prepared from the corresponding **4c—g** (Chart 1, Table 1).

Unexpectedly, treatment of the *sec*-nitrodienamine **3** with 35% formaldehyde solution (**4h**) in tetrahydrofuran (THF) afforded 2-methyl-3-nitro-1-(2-phenethyl)-1,2-dihydropyridine (**5a**) and 3-nitro-2-(3-nitrophenyl)-1-(2-phenethyl)-1,2-dihydropyridine (**5i**) in 2% and 8% yields, respectively. The heterocyclic annulation reactions of **3** with aldehydes may be explained as follows. Initially, the hydrolysis reaction of **3** may generate acetaldehyde (**4a**) *via* intermediate **6a**, and self-condensation reaction of **3** may generate 3-nitrobenzaldehyde (**4i**) *via* intermediate **6i**. Then, the condensation reactions of **3** with **4a** and **4i**, followed by intramolecular ring closure with dehydration could lead to 1,2-dihydropyridines **5a** and **5i**, respectively, as shown in Chart 2.

These results provide a method of synthesizing 2-substituted 3-nitro-1,2-dihydropyridines **5** by utilizing *sec*-nitrodienamine **3** with aldehyde compounds **4**.

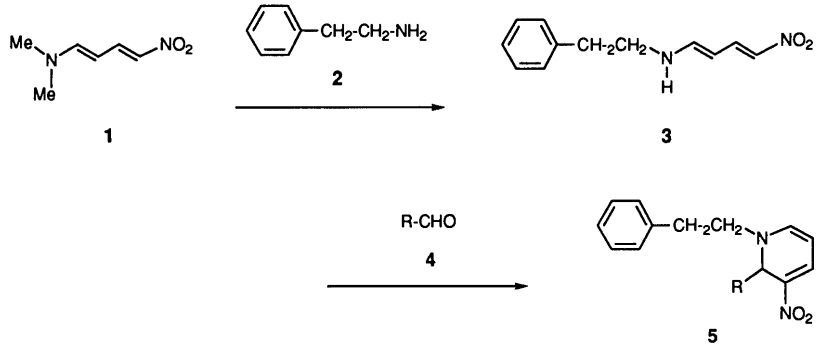

Chart 1

* To whom correspondence should be addressed.

© 2000 Pharmaceutical Society of Japan

Table 1. The Heterocyclic Annulation Reactions of *sec*-Nitrodienamine **3** with Aldehyde Compounds **4**

R–CHO

4

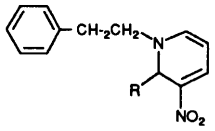

5

Starting amine	R	Reaction temp. (°C)	Reaction time (h)	Reaction product	Yield (%)	^{1}H-NMR ($CDCl_3$), δ (ppm)	IR (cm^{-1})
4a	Me–	25	1.2	**5a**	92	1.19 (3H, d, J=6.2 Hz, Me), 2.94 (2H, t, J=6.9 Hz, methylene H), 3.46 (1H, dt, J=13.9, 6.9 Hz, methylene H), 3.68 (1H, dt, J=13.9, 6.9 Hz, methylene H), 4.85 (1H, dd, J=7.4, 6.2 Hz, olefinic H), 5,12 (1H, q, J=6.2 Hz, methine H), 6.46 (1H, d, J=6.2 Hz, olefinic H), 7.05—7.33 (5H, m, aromatic H), 7.58 (1H, d, J=7.4 Hz, olefinic H)	1616, 1514, 1481, 1435, 1358, 1325, (neat)
4b	Me–CH_2–	Reflux	39	**5b**	82	0.91 (3H, t, J=7.7 Hz, Me), 1.38—1.92 (2H, m, methylene H), 2.92 (2H, t, J=6.8 Hz, methylene H), 3.58 (1H, dt, J=13.6, 6.8 Hz, methylene H), 3.64 (1H, dt, J=13.6, 6.8 Hz, methylene H), 4.83 (1H, dd, J=7.5, 6.4 Hz, olefinic H), 5.05 (1H, t, J=4.6 Hz, methine H), 6.53 (1H, d, J=6.4 Hz, olefinic H), 7.09—7.26 (5H, m, aromatic H), 7.65 (1H, d, J=7.5 Hz, olefinic H)	1624, 1541, 1516, 1474, 1456, 1360, (neat)
4c		25	7	**5c**	59	2.89 (2H, t, J=6.8 Hz, methylene H), 3.35 (1H, dt, J=13.6, 6.8 Hz, methylene H), 3.60 (1H, dt, J=13.6, 6.8 Hz, methylene H), 4.82 (1H, dd, J=7.5, 6.7 Hz, olefinic H), 6.01 (1H, s, methine H), 6.59 (1H, d, J=6.7 Hz, olefinic H), 7.10 (2H, d, J=6.9 Hz, aromatic H), 7.23—7.35 (6H, m, aromatic H), 7.45 (2H, d, J=6.9 Hz, aromatic H), 7.75 (1H, d, J=7.5 Hz, olefinic H)	1620, 1505, 1495, 1460, 1420, 1590, (neat)
4d	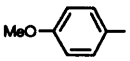	25	26	**5d**	53	2.88 (2H, t, J=6.8 Hz, methylene H), 3.31 (1H, dt, J=13.6, 6.8 Hz, methylene H), 3.55 (1H, dt, J=13.6, 6.8 Hz, methylene H), 3.78 (3H, s, OMe), 4.80 (1H, dd, J=7.5, 6.3 Hz, olefinic H), 5.95 (1H, s, methine H), 6.57 (1H, d, J=6.3 Hz, olefinic H), 6.84 (2H, d, J=8.8 Hz, aromatic H), 7.06—7.30 (5H, m, aromatic H), 7.38 (2H, d, J=8.8 Hz, aromatic H), 7.74 (1H, d, J=7.5 Hz, olefinic H)	1605, 1585, 1515, 1500, 1495, 1485, (neat)
4e	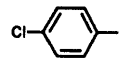	25	15	**5e**	44	2.88 (2H, t, J=6.8 Hz, methylene H), 3.34 (1H, dt, J=13.6, 6.8 Hz, methylene H), 3.59 (1H, dt, J=13.6, 6.8 Hz, methylene H), 4.82 (1H, dd, J=7.5, 6.4 Hz, olefinic H), 5.97 (1H, s, methine H), 6.60 (1H, d, J=6.4 Hz, olefinic H), 7.08—7.43 (9H, m, aromatic H), 7.72 (1H, d, J=7.5 Hz, olefinic H)	1615, 1510, 1490, 1460, 1450, 1440, (neat)
4f	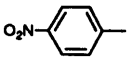	25	15	**5f**	57	2.91 (2H, t, J=6.8 Hz, methylene H), 3.43 (2H, dt, J=13.6, 6.8 Hz, methylene H), 4.90 (1H, dd, J=7.5, 6.4 Hz, olefinic H), 6.09 (1H, s, methine H), 6.69 (1H, d, J=6.4 Hz, olefinic H), 7.03—7.32 (5H, m, aromatic H), 7.60 (2H, d, J=8.8 Hz, aromatic H), 7.72 (1H, d, J=7.5 Hz, olefinic H), 8.17 (2H, d, J=8.8 Hz, aromatic H)	1620, 1520, 1485, 1455, 1445, 1395, (neat)
4g	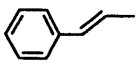	25	39	**5g**	5	2.98 (2H, t, J=6.8 Hz, methylene H), 3.50 (1H, dt, J=13.6, 6.8 Hz, methylene H), 3.74 (1H, dt, J=13.6, 6.8 Hz, methylene H), 4.85 (1H, dd, J=7.3, 6.7 Hz, olefinic H), 5.65 (1H, d, J=7.0 Hz, methine H), 6.19 (1H, dd, J=15.9, 7.0 Hz, olefinic H), 6.62 (1H, d, J=6.7 Hz, olefinic H), 7.03—7.37 (11H, m, aromatic and olefinic H), 7.64 (1H, d, J=7.3 Hz, olefinic H)	1615, 1545, 1510, 1495, 1480, 1460, (neat)
4h	H–	25	1	**5a** R=Me–	2	1.19 (3H, d, J=6.2 Hz, Me), 2.94 (2H, t, J=6.9 Hz, methylene H), 3.46 (1H, dt, J=13.9, 6.9 Hz, methylene H), 3.68 (1H, dt, J=13.9, 6.9 Hz, methylene H), 4.85 (1H, dd, J=7.4, 6.2 Hz, olefinic H), 5.12 (1H, q, J=6.2 Hz, methine H), 6.46 (1H, d, J=6.2 Hz, olefinic H), 7.05—7.33 (5H, m, aromatic H), 7.58 (1H, d, J=7.4 Hz, olefinic H)	1616, 1514, 1481, 1435, 1358, 1325, (neat)
				5i 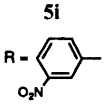	8	2.91 (2H, t, J=6.8 Hz, methylene H), 3.43 (1H, dt, J=13.6, 6.8 Hz, methylene H), 3.57 (1H, dt, J=13.6, 6.8 Hz, methylene H), 5.04 (1H, t, J=6.7 Hz, olefinic H), 6.05 (1H, s, methine H), 7.00 (1H, d, J=6.7 Hz, olefinic H), 7.22 (2H, d, J=7.9 Hz, aromatic H), 7.37—7.43 (3H, m, aromatic H), 7.53 (1H, t, J=7.9 Hz, aromatic H), 7.77 (1H, d, J=7.9 Hz, aromatic H), 7.81 (1H, d, J=6.7 Hz, olefinic H), 8.18 (1H, d, J=7.9 Hz, aromatic H), 8.30 (1H, s, aromatic H)	1668, 1620, 1529, 1454, 1392, 1352, (neat)

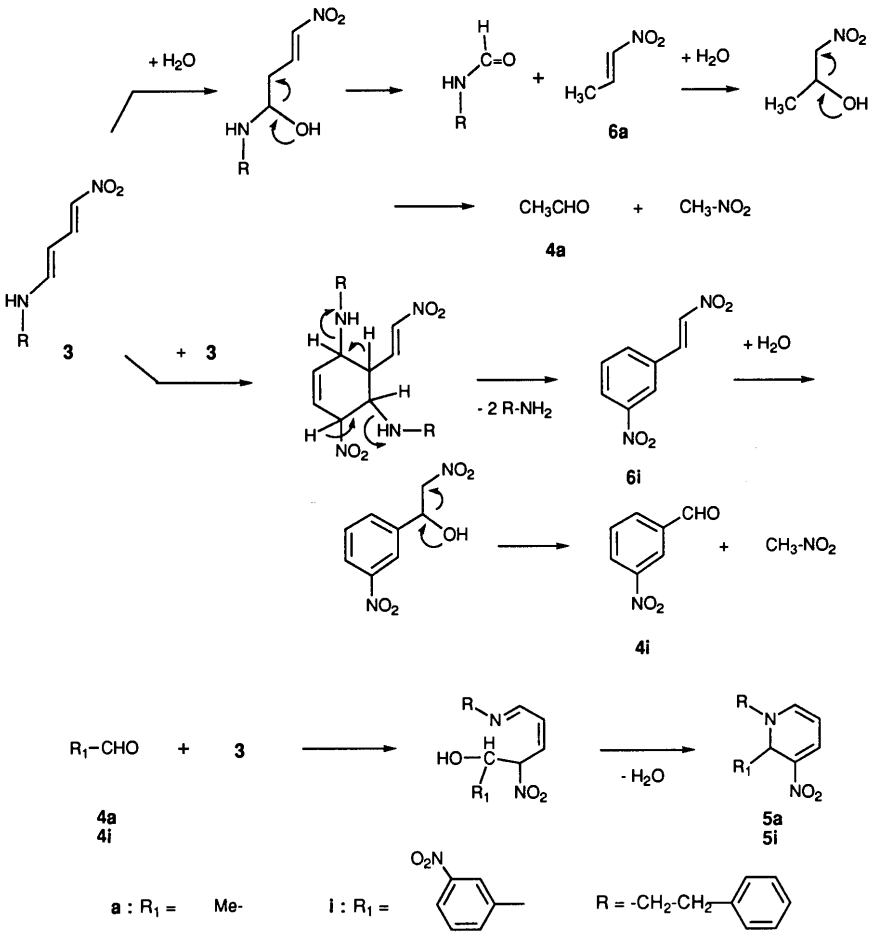

Chart 2

Experimental

All melting points were determined on a Yanagimoto melting point apparatus and are uncorrected. IR spectra were recorded on a JASCO FT/IR-200 or JASCO FT/IR-8000 spectrometer, and ^{1}H-NMR spectra on a JEOL EX-90 or JEOL JNM-α500 spectrometer with tetramethylsilane as internal standard. MS were recorded on a JEOL JMS-D 300 spectrometer. Silica gel 60 (Cica-Merck) and NH-DM 1020 (basic 100 Å type silica gel, Fuji Silysia Chemical, Ltd.) were used for column chromatography and thin layer chromatography (TLC), respectively. All reactions were carried out under an argon atmosphere.

General Procedure for Reactions of 4-Nitro-1-(2-phenethylamino)-1,3-butadiene (3) with Aldehyde Compounds 4 A solution of *sec*-nitrodienamine **3** (40 mg, 0.183 mmol) with the aldehyde compound **4** and 2-phenethylamine (2 drops) in a liquid reaction mixture (no solvent) or THF (3 ml) in a sealed tube was stirred at room temperature or refluxed for an appropriate period until the disappearance of **3** (checked by TLC). The reaction mixture was concentrated under vacuum, and the residue subjected to silica gel column chromatography. The isolated yield of **5** is based on **3**. The reaction conditions and properties of the prepared compounds **5** are shown in Table 1.

2-Methyl-3-nitro-1-(2-phenethyl)-1,2-dihydropyridine (**5a**):[1d] Aldehyde **4a**: 0.4 ml (7.16 mmol). Reaction solvent: THF. Solvent for chromatography: 20% ethyl acetate in hexane. Product **5a**: 41 mg, dark red oil. ^{13}C-NMR (125 MHz, $CDCl_3$) δ: 15.4, 35.9, 52.5, 56.4, 93.5, 126.7, 127.1, 128.7, 128.8, 133.2, 137.1, 146.6. This product was identical with an authentic sample on the basis of IR, MS and NMR spectral comparisons.

2-Ethyl-3-nitro-1-(2-phenethyl)-1,2-dihydropyridine (**5b**): Aldehyde **4b**: 1063 mg (18.3 mmol). Reaction solvent: no solvent. Solvent for chromatography: 15% ethyl acetate in hexane. Product **5b**: 39 mg, dark red oil. High-resolution EI MS *m/z*: Calcd for $C_{15}H_{18}N_2O_2$ (M^+): 258.1367. Found: 258.1357.

3-Nitro-1-(2-phenethyl)-2-phenyl-1,2-dihydropyridine (**5c**): Aldehyde **4c**: 1942 mg (18.3 mmol). Reaction solvent: no solvent. Solvent for chromatography: 20% ethyl acetate in hexane. Product **5c**: 33 mg, dark red oil. High-resolution EI MS *m/z*: Calcd for $C_{19}H_{18}N_2O_2$ (M^+): 306.1368. Found: 306.1371.

2-(4-Methoxyphenyl)-3-nitro-1-(2-phenethyl)-1,2-dihydropyridine (**5d**): Aldehyde **4d**: 2492 mg (18.3 mmol). Reaction solvent: no solvent. Solvent for chromatography: 15% ethyl acetate in hexane. Product **5d**: 32 mg, dark red oil. High-resolution EI MS *m/z*: Calcd for $C_{20}H_{20}N_2O_3$ (M^+): 336.1471. Found: 336.1453.

2-(4-Chlorophenyl)-3-nitro-1-(2-phenethyl)-1,2-dihydropyridine (**5e**): Aldehyde **4e**: 515 mg (3.66 mmol). Reaction solvent: THF. Solvent for chromatography: 40% hexane in chloroform. Product **5e**: 28 mg, dark red oil. High-resolution EI MS *m/z*: Calcd for $C_{19}H_{17}N_2O_2Cl_1$ (M^+): 340.0979. Found: 340.0986.

3-Nitro-2-(4-nitrophenyl)-1-(2-phenethyl)-1,2-dihydropyridine (**5f**): Aldehyde **4f**: 24 mg (0.16 mmol). Reaction solvent: THF. Solvent for chromatography: 40% hexane in chloroform. Product **5f**: 37 mg, dark red oil. High-resolution EI MS *m/z*: Calcd for $C_{19}H_{17}N_3O_4$ (M^+): 351.1218. Found: 351.1248.

3-Nitro-1-(2-phenethyl)-2-(*trans*-2-phenylvinyl)-1,2-dihydropyridine (**5g**): Aldehyde **4g**: 484 mg (3.66 mmol). Reaction solvent: THF. Solvent for chromatography: 40% hexane in chloroform. Product **5g**: 3 mg, dark red oil. CI-MS *m/z*: 333 ($M^+ + 1$).

2-Methyl-3-nitro-1-(2-phenethyl)-1,2-dihydropyridine (**5a**)[1d] and 3-Nitro-2-(3-nitrophenyl)-1-(2-phenethyl)-1,2-dihydropyridine (**5i**): Aldehyde **4h**: 47.2 μl (35% formaldehyde, 0.60 mmol). Reaction solvent: THF. Solvent for chromatography: 20% ethyl acetate in hexane. First eluated product **5a**: 1 mg, dark red oil. This product was identical with an authentic sample on the basis of IR, MS and NMR spectral comparisons. Second eluated product **5i**: 2 mg, dark red oil. CI-MS *m/z*: 352 ($M^+ + 1$). (The *sec*-nitrodienamine **3** was almost completely decomposed under these conditions.)

References

1) *a*) Takeuchi N., Ohki J., Tobinaga S., *Chem. Pharm. Bull.*, **36**, 481—487 (1988); *b*) Takeuchi N., Tanabe M., Hagiwara M., Goto K., Koike T., Tobinaga S., *Heterocycles*, **38**, 613—627 (1994); *c*) Koike T., Hagi-

wara M., Takeuchi N., Tobinaga S., *ibid.*, **45**, 1271—1280 (1997); *d*) Koike T., Shinohara Y., Tanabe M., Takeuchi N., Tobinaga S., *Chem. Pharm. Bull.*, **47**, 1246—1248 (1999); *e*) Koike T., Takeuchi N., Hagiwara M., Yamazaki K., Tobinaga S., *Heterocycles*, **51**, 2687—2695 (1999).

2) Rajappa S., *Tetrahedron*, **37**, 1453—1480 (1981).

3) *a*) Severin T., Ipach I., *Chem. Ber.*, **109**, 3541—3546 (1976); *b*) *Idem*, *ibid.*, **111**, 692—697 (1978).

4) *a*) Koike T., Tanabe M., Takeuchi N., Tobinaga S., *Chem. Pharm. Bull.*, **45**, 243—248 (1997); *b*) *Idem*, *ibid.*, **45**, 27—31 (1997); *c*) *Idem*, *ibid.*, **45**, 1117—1119 (1997); *d*) Koike T., Takeuchi N., Tobinaga S., *ibid.*, **46**, 1497—1500 (1998); *e*) *Idem*, *ibid.*, **47**, 128—130 (1999).

5) *a*) Hantzsch A., *Justus Liebigs Ann. Chem.*, **215**, 1—82 (1882); *b*) Eisner U., Kuthan J., *Chem. Rev.*, **72**, 1—42 (1972); *c*) Kuthan J., Kurfürst A., *Ind. Eng. Chem. Prod. Res. Dev.*, **1982**, 191—261; *d*) Stout D. M., Meyers A. I., *Chem. Rev.*, **82**, 223—243 (1982).

A Novel Cytotoxic *C*-Methylated Biflavone from the Stem of *Cephalotaxus wilsoniana*

Yao-Haur KUO,*[a,b] Chin-Hou LIN,[a,b] Shy-Yuan HWANG,[c] Ya-Ching SHEN,[d] Yi-Ling LEE,[a,b] and Shyh-Yuan LI*[a,b]

National Research Institute of Chinese Medicine,[a] Shih-Pai, Taipei, 112, Taiwan, R.O.C., Department of Applied Chemistry, Chinese Culture University,[b] Taipei,113, Taiwan, R.O.C., Department of Agriculture and Forestry, Taiwan Endemic Species Research Institute,[c] Nantou County, 552, Taiwan, R.O.C., and Institute of Marine Resources, National Sun Yat-Sen University,[d] Kaohsiung, 804, Taiwan, R.O.C. Received October 12, 1999; accepted November 12, 1999

Bioassay-directed fractionation of an ethanolic extract of *Cephalotaxus wilsoniana* has resulted in the isolation of a novel *C*-methylated biflavone, taiwanhomoflavone-A (1). Its structure was elucidated on the basis of spectroscopic analysis. Taiwanhomoflavone-A is cytotoxic with ED_{50} values of 3.4, 1.0, 2.0 and 2.5 μg/ml, respectively, against KB epidermoid carcinoma of nasopharynx, COLO-205 colon carcinoma, Hepa-3B hepatoma, and Hela cervix tumor cells.

Key words *Cephalotaxus wilsoniana*; cytotoxicity; taiwanhomoflavone-A; 6-*C*-methyl-7, 4′-*O*-dimethylamentoflavone

Several antitumor alkaloids[1—6] have been reported from *Cephalotaxus* spp. *Cephalotaxus wilsoniana* HAYATA (Cephalotaxaceae) is an evergreen tree distributed over the middle mountain of Taiwan. During a search for antitumor agents from the terrestrial plants of Taiwan,[8—11] we found a crude extract from *C. wilsoniana* which possesses inhibitory effect against KB, Hepa-3B, and Hela cancer cell lines. Bioassay-guided fractionation of an EtOH extract led to the isolation of a novel *C*-methylated biflavone (**1**) in addition to the known compounds, harringtonolide (=hainanolide), *epi*-wilsonine, sugiol, isopimaric acid and kayaflavone. In this paper we describe the structural elucidation of **1** using H–H correlation spectroscope (COSY), ^{13}C–^{1}H heteronuclear multiple quantum coherence (HMQC) and ^{13}C–^{1}H heteronuclear multiple bonds coherence (HMBC) experiments.

The molecular formula of taiwanhomoflavone (**1**) ($C_{33}H_{24}O_{10}$) was indicated by a molecular ion (*m/z* 579 $[M-H]^+$) in the FAB-MS spectra. The IR spectrum suggested that **1** contained hydroxyl, conjugated carbonyl and aromatic functions.

Observing the ^{1}H-NMR spectrum of **1**, an AMX coupling system with signals at δ 8.49 (H-2′), 8.08 (H-6′), and 7.29 (H-5′) revealed a 1,3, 4-trisubstituted benzene ring. The signals at δ_H 7.76 (H-2‴, 6‴, d, J=8.5 Hz) and δ_H 7.15 (H-3‴, 5‴, d, J=8.5 Hz), together with the signals of δ_C 128.56 (C-2‴, 6‴), and 116.81 (3‴, 5‴) in the ^{13}C-NMR spectrum indicated another aromatic moiety in an A_2B_2 coupling system. In addition, four aromatic protons in each singlet, two aromatic methoxyls in singlet, and a unique methyl group in singlet were observed in the ^{1}H-NMR spectrum. This evidence revealed that **1** has a biflavone skeleton with a *C*-methyl group and excluded the possibility of linkage between the two flavone moieties at C-2‴, -6‴, -3‴ and -5‴ in the B-ring.

In the HMBC spectrum, the correlations between C-8″ and H-6″ and H-2′ revealed the connective positions to be at C-3′

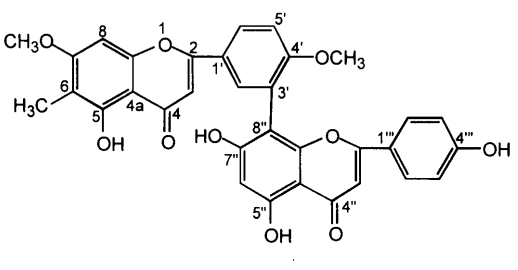

1

Table 1. ^{1}H- and ^{13}C-NMR Data[a] (Pyridine-d_5) for Compound **1**

Carbon	^{13}C (ppm)	^{1}H (ppm)	^{13}C–^{1}H connectivities[b]
2	164.14 s	—	H-3
3	104.76 d	7.12 (s)	—
4	182.73 s	—	H-3
4a	105.54 s	—	H-3
5	158.83 s	—	6-Me
6	108.67 s	—	H-8, 6-Me
7	163.64 s	—	H-8, OMe
8	90.31 d	6.71 (s)	—
8a	156.31 s	—	H-8
1′	123.25 s	—	H-5′
2′	131.87 d	8.49 (d, 2.0)	H-6′
3′	104.93 s	—	H-5′
4′	161.44 s	—	H-2′, 6′, OMe
5′	111.82 d	7.29 (d, 8.5)	—
6′	128.40 d	8.08 (dd, 2.0,8.5)	H-2′
2″	164.36 s	—	H-3″
3″	103.44 d	6.95 (s)	—
4″	183.02 s	—	H-3″
4″a	104.85 s	—	H-3″, 6″
5″	162.40 s	—	H-3″, 6″
6″	99.31 d	6.93 (s)	—
7″	163.64 s	—	—
8″	104.76 s	—	H-2′, 6″
8″a	155.53 s	—	—
1‴	122.18 s	—	H-3‴, 5‴
2‴	128.56 d	7.76 (d, 8.5)	H-6‴
3‴	116.81 d	7.15 (d, 8.5)	H-5‴
4‴	162.67 s	—	H-3‴, 5‴, 2‴, 6‴
5‴	116.81 d	7.15 (d, 8.5)	H-3‴
6‴	128.56 d	7.76 (d, 8.5)	H-2‴
6-Me	7.60 q	2.22 (s)	—[c]
7-*O*-Me	56.02 q	3.74 (s)	—[c]
4′-*O*-Me	55.98 q	3.77 (s)	—[c]

a) All assignments (^{13}C;75.5 MHz, multiplicity; ^{1}H; 300 MHz) are based on one dimensional (1D) and two dimensional (2D) NMR experiments, including COSY 90, HETCOR, and HMBC spectra. *b*) HMBC corresponded to two or three bonds connectivities. *c*) These assignments were explained in the text.

* To whom correspondence should be addressed.

© 2000 Pharmaceutical Society of Japan

and C-8″ between the flavones. Generally, the carbonyl carbon signal (C-4 or -4″) observed near δ_C 183 for biflavones such as ginkgetin[12] would permit the assignment of a peri-OH at C-5 or -5″. The signal for C-8 at δ_C 90.3 in **1** was consistent with the carbon bearing a methoxyl group at the C-7 position; otherwise, a chemical shift for C-8 would appear around δ_C 94.0 suggesting a hydroxyl group at C-7.[12] After detailed examination of the HMBC spectrum of **1**, a methyl group was assigned at C-6 due to the correlation between the methyl group and C-5 and C-6, respectively. Together with the above evidence, the structure of **1** was deduced to be an analogue of 6-*C*-methyl-7-*O*-methylamentoflavone (**2**)[13] except for a methoxyl group in **1** and a hydroxyl group in **2**. The remaining methoxyl group in **1** was assigned at C-4′ due to the HMBC spectrum. Then, the structure of **1** was confirmed unambiguously, and was tentatively named taiwanhomoflavone-A.

Furthermore, bioassays showed that taiwanhomoflavone-A (**1**) exhibited cytotoxic effects against four cancer cell lines: KB, COLO-205, Hepa-3B and Hela with ED_{50} of 3.45, 1.06, 2.03 and 2.53 μg/ml, respectively. To our knowledge, this is the first report that 6-*C*-methyl biflavone as compound **1** has cytotoxic activity.

Experimental

General Experimental Procedures ^{1}H- and ^{13}C-NMR spectra were recorded at 300.13 and 75.46 MHz, respectively, on a Bruker 300 AC spectrometer. The spectra of heteronuclear correlation, HMBC was established by the coupling of 8 Hz. Electron impact (EI)-MS and FAB-MS were performed on a JEOL SX-102A instrument. Si gel (Merck 70—230 mesh) was used for column chromatograph, and precoated Si gel (Merck 60F-254) plates were used for TLC. HPLC was accomplished on an SPD-6AV liquid chromatography using a preparative C_{18} column. Melting points were determined on a Fisher-Johns apparatus and are uncorrected.

Plant Material The stems of *Cephalotaxus wilsoniana* were collected in Septemper 1995 on Taipei, Taiwan. A voucher specimen is deposited at the National Research Institute of Chinese Medicine, Shih-Pai, Taipei, Taiwan, R.O.C.

Extraction and Isolation The dried stems of *C. wilsoniana* (6.3 kg) were extracted exhaustively with ethanol . An EtOH extract (200 g) of dried stems of *Cephalotaxus wilsoniana* was extracted successively with *n*-hexane and $CHCl_3$. The $CHCl_3$ extract was chromatographed by column chromatography over Si gel and eluted with *n*-hexane–EtOAc and EtOAc to give 8 fractions. The bioactive fr. 5 (*n*-hexane : EtOAc=2 : 1) was further separated by HPLC ($5C_{18}$, 250×10 mm) with MeOH–H_2O (9 : 1) to furnish taiwanhomoflavone-A (**1**) (11 mg).

Taiwanhomoflavone-A (**1**): Pale yellow crystal, mp 245—248 °C; IR ν_{max} (KBr) 3400 (OH), 1660 (conjugated CO), 1620 (aromatic rings) cm^{-1}; ^{1}H- and ^{13}C-NMR, see Table 1; FAB-MS *m/z* 579 $[M-H]^+$; HR-EI-MS *m/z* 580.1379 $[M]^+$ (Calcd for $C_{33}H_{24}O_{10}$, 580.1369).

Cytotoxicity Assay An *in vitro* cytotoxicity assay was performed as previously described.[11]

Acknowledgments The authors thank the National Science Council, R.O.C. (NSC 88-2314-B-077-007) for financial support to Y. H. Kuo. We also thank Mr. Shih-Jen Wang, NSC Regional Instrument Center of HSIN-CHU, for measuring the FABMS data.

References

1) Powell R. G., Weisleder D., Smith C. R., Jr., Wolff I. A., *Tetradron Lett.*, **1969**, 4081—4084.
2) Powell R. G., Weisleder D., Smith C. R., Jr., Rohwedder W. K., *Tetradron Lett.*, **1970**, 815—818.
3) Khan N. U., Ilyas M., Rahman W., Okigawa M., Kawano N., *Phytochemistry*, **10**, 2541—2545 (1971).
4) Powell R. G., Mikolajczak K. L., Weisleder D., Smith C. R., Jr., *Phytochemistry*, **11**, 3317—3320 (1972).
5) Sun N., Xue Z., Liang S., Huang L., *Acta Pharmaceut. Sinica*, **1**, 39—43 (1979).
6) Qiu M., Lu B. M. X., Nie R., *Acta Botanica Yunnanica*, **1**, 97—99 (1997).
7) Furukawa H., Itoigawa M., Haruna M., Jinno Y., Ito K., Lu S. T., *Yakugaku Zasshi*, **96**, 1373—1377 (1976).
8) Kuo Y. H., Kuo Yang L. M., Chen C. F., *J. Org. Chem.*, **62**, 3242—3245 (1997).
9) Kuo Y. H., Chang Chi. I., Li S. Y., Chou C. J., Chen C. F., Kuo Y. H., Lee K. H., *Planta Med.*, **63**, 363—365 (1997).
10) Kuo Y. H., Kuo Yang L. M., *Phytochemistry*, **44**, 1275—1281 (1997).
11) Kuo Y. H., Huang H. C., Kuo Yang L. M., Chen C. F., *J. Org. Chem.*, **64**, 7023—7027 (1999).
12) Markham K. R., Sheppard C., Geiger H., *Phytochemistry*, **26**, 3335—3337 (1987).
13) Aqil M., Rahman W., Hasaka N., Okigawa M., Kawano N., *J. Chem. Soc., Perkin Trans. 1*, **1981**, 1389—1392.

O-(*N*-Succinimidyl)-1,1,3,3-tetramethyluronium Tetrafluoroborate–*N*-Hydroxysuccinimide–$CuCl_2$: A Facile and Reliable System for Racemization-Free Coupling of Peptides Having a Carboxy-terminal *N*-Methylamino Acid[1)]

Yasuhiro NISHIYAMA,* Sou ISHIZUKA, Tomonori MORI,[2)] and Keisuke KURITA

Department of Industrial Chemistry, Faculty of Engineering, Seikei University, Musashino-shi, Tokyo 180–8633, Japan.
Received October 27, 1999; accepted November 24, 1999

Simultaneous use of *N*-hydroxysuccinimide (HOSu) and $CuCl_2$ with a HOSu-based uronium coupling reagent, *O*-(*N*-succinimidyl)-1,1,3,3-tetramethyluronium tetrafluoroborate, has been found to eliminate the racemization of the carboxy-terminal *N*-methylamino acid residue during the segment condensation.

Key words *N*-methylamino acid; racemization-free coupling; copper(II) chloride; racemization; segment condensation; peptide synthesis

In peptide synthesis by the convergent strategy the carboxy-terminal amino acid residue of the peptide segment is exposed to the risk of racemization.[3)] Extensive studies on the prevention of racemization have thus been continued, and some compounds, *e.g.*, *N*-hydroxysuccinimide (HOSu),[4)] 1-hydroxybenzotriazole (HOBt),[5)] *N*-hydroxy-5-norbornene-2,3-dicarboximide,[6)] 1-hydroxy-7-azabenzotriazole (HOAt),[7)] and $CuCl_2$,[8,9)] were found to reduce the racemization in the carbodiimide-mediated coupling effectively. However, the situation is quite different when the carboxy-terminal residue is an *N*-methylamino acid, which is considerably more susceptible to racemization than a common amino acid. For instance, McDermott and Benoiton reported that the dicyclohexylcarbodiimide (DCC)–HOSu coupling of (*N*-benzyloxycarbonyl-alanyl)-*N*-methylleucine and H–Gly–OBzl (Bzl, benzyl) in tetrahydrofran at room temperature was accompanied by 11% racemization of the *N*-methylleucine residue.[10)] Though the racemization decreased to an undetectable level on cooling to −5 °C,[11)] more convenient and reliable methods are desirable.

Recently, we have reported that $CuCl_2$ could eliminate the racemization of the carboxy-terminal *N*-methylamino acid residue in the 1-ethyl-3-(3-dimethylaminopropyl)carbodiimide hydrochloride (WSCI)-mediated segment coupling at room temperature,[12)] but could not sufficiently suppress the racemization in the coupling with onium-based reagents including benzotriazolyl-*N*-oxytris(dimethylamino)phosphonium hexafluorophosphate (BOP)[13)] and *O*-(7-azabenzotriazol-1-yl)-1,1,3,3-tetramethyluronium hexafluorophosphate (HATU).[7)] This class of coupling reagents is popularly used in peptide synthesis because of its advantages over carbodiimides; compared to carbodiimides, onium reagents usually complete couplings in a short time without any serious side reactions, give no troublesome by-products such as urea derivatives, and are safe to use from the standpoint of allergenicity. If racemization can be suppressed sufficiently, therefore, onium-based reagents would be convenient for use in the segment coupling of peptides having the carboxy-terminal *N*-methylamino acid and could facilitate efficient synthesis of *N*-methylamino acid-containing peptides by the convergent strategy. We have thus directed our study to the development of a racemization-free coupling system using an onium-based coupling reagent.

Leading studies by McDermott and Benoiton[10)] and Davies and Mohammed[11)] suggested that racemization of the carboxy-terminal *N*-methylamino acid in the DCC–HOBt coupling occurs by two major routes as outlined in Fig. 1. Elimination of the racemization by $CuCl_2$ in the carbodiimide-mediated coupling[12)] reveals that $CuCl_2$ inhibits almost completely the oxazolonium pathway (Fig. 1a). On the contrary, insufficient suppression of the racemization by $CuCl_2$ in the BOP-mediated coupling[12)] implies that $CuCl_2$ cannot inhibit the active ester pathway (Fig. 1b). Racemization by pathway b, however, is known not to appear in the HOSu ester coupling.[11)] This suggests that pathway b can possibly be omitted when a HOSu-based onium salt is used as a coupling reagent. Taking this knowledge of racemization-mechanisms into consideration, we have designed a novel coupling system consisting of *O*-(*N*-succinimidyl)-1,1,3,3-tetramethyluronium tetrafluoroborate (TSTU)[14)] and $CuCl_2$ to achieve racemization-free segment coupling at the *N*-methylamino-acyl bond, and evaluated it in a simple model reaction between Boc–Phe–MeAla–OH (Boc, *tert*-butoxycarbonyl; MeAla, *N*-methylalanine) and H–Phe–OBzl.

Boc–Phe–MeAla–OH[12,15)] was coupled with H–Phe–OBzl in *N*,*N*-dimethylformamide (DMF) by TSTU in the presence or absence of additives, HOSu, HOBt, and $CuCl_2$. After storage of each reaction mixture at room temperature for >24 h, a portion was subjected to HPLC analysis, and % L–D–L isomer was determined as (peak area of the L–D–L isomer)×100/[(peak area of the L–L–L isomer)+(peak area of the L–D–L isomer)]. Coupling yields were determined from the sum of peak areas of diastereomers in comparison with a standard solution of the L–L–L authentic sample. Partial HPLC profiles of samples from coupling with TSTU, TSTU–$CuCl_2$, and TSTU–HOSu–$CuCl_2$ are shown in Fig. 2.

The results are listed in Table 1 with some data selected from our previous report[12)] for comparison. A significant amount of the L–D–L product was detected in the coupling with TSTU alone, and also in the presence of HOSu and HOBt. However, $CuCl_2$ could reduce the amount of the L–D–L product in the TSTU coupling, whereas it was not sufficiently effective in the BOP- and HATU-mediated couplings. These results indicate that the racemization by both pathways

* To whom correspondence should be addressed.

© 2000 Pharmaceutical Society of Japan

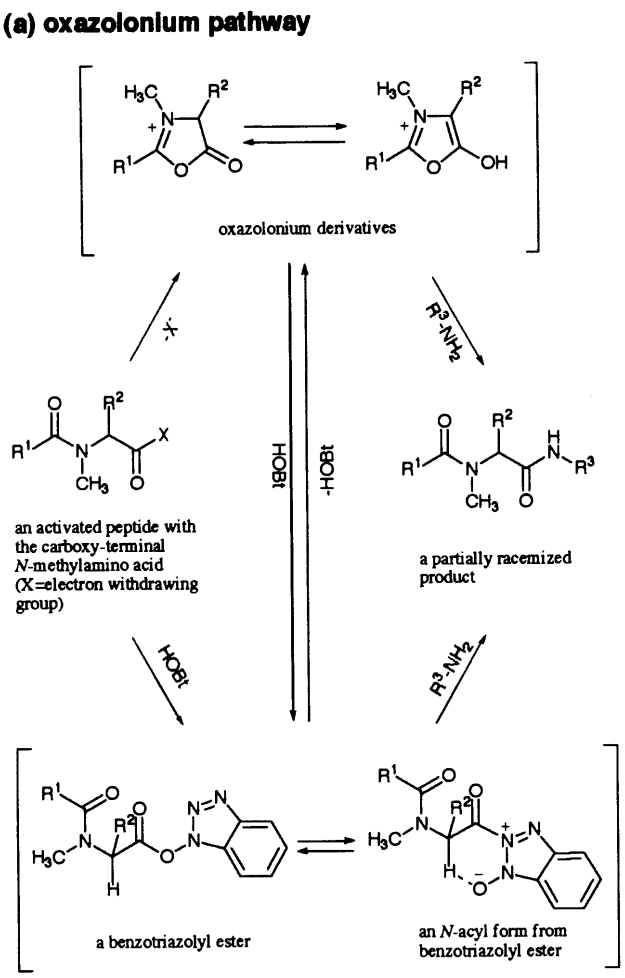

Fig. 1. Two Major Pathways for Racemization of the Carboxy-Terminal *N*-Methylamino Acids in Segment Condensation

Table 1. Extents of Racemization during the Coupling of Boc–Phe–MeAla–OH with H–Phe–OBzl

Additive[a]	% L–D–L[b]			% yield[b]		
	TSTU[c]	Bop[c,d]	HATU[c,d]	TSTU[c]	Bop[c,d]	HATU[c,d]
—	18.1	13.6	9.5	80	95	103
HOSu	14.0	14.5	11.1	73	95	97
HOBt	18.9	15.9	20.9	92	97	102
$CuCl_2$	0.4	2.7	4.7	47	35	52
HOSu–$CuCl_2$	<0.2	3.5	8.1	45[e]	27	46

a) One eq. *b*) Average of two independent experiments. *c*) Coupling reagents, 1.25 eq.; diisopropylethylamine, 2 eq. *d*) Ref. 12. *e*) 60% with 2.5 eq. of TSTU.

a and b can be suppressed effectively by a combination of TSTU and $CuCl_2$. A small amount of the L–D–L product was, however, detected even in the presence of $CuCl_2$. In the segment condensation of common peptides, BOP–HOBt was reported to result in a lower racemization level than BOP alone.[16] We thus examined the simultaneous use of HOSu and $CuCl_2$ in the TSTU coupling. No appreciable racemization was detected by HPLC at an identification limit of 0.2%, and TSTU–HOSu–$CuCl_2$ proved to be an appropriate combination to suppress the racemization in the coupling of peptide segments having a carboxy-terminal *N*-methylamino

Fig. 2. Partial HPLC Profiles of Samples from Coupling with (a) TSTU, (b) TSTU–$CuCl_2$, and (c) TSTU–HOSu–$CuCl_2$

acid. In the WSCI–$CuCl_2$ coupling of Boc–Phe–MeAla–OH and H–Phe–OBzl, a small amount of the L–D–L product (0.2%) was detected, and the yield was similar (46%) to that of TSTU–HOSu–$CuCl_2$.[12] When HOSu and $CuCl_2$ were simultaneously used in the WSCI-coupling, racemization was not detected, but the yield decreased to 33%.[12] Thus the TSTU–HOSu–$CuCl_2$ system would be more favorable than WSCI–$CuCl_2$ or WSCI–HOSu–$CuCl_2$ systems.

In conclusion, a novel coupling system consisting of TSTU, HOSu, and $CuCl_2$ has proved to completely eliminate the racemization of the carboxy-terminal *N*-methylamino acid residue during segment condensation. This is the first example of an onium-based coupling system which enables the racemization-free segment condensation at the *N*-methylaminoacyl bond. Optimization of the reaction conditions is now under way,[17] facilitating the efficient convergent synthesis or head-to-tail cyclization of *N*-methylamino acid-containing peptides.

Experimental

In the HPLC analysis, elution profiles were monitored at 220 nm by a Waters 480 UV/VIS tunable absorbance detecter and recorded with a SIC Chromatocoder-21.

Boc–Phe–MeAla–OH, Boc–Phe–MeAla–Phe–OBzl, and Boc–Phe–D–MeAla–Phe–OBzl were prepared as previously reported.[12] TSTU was purchased from Novabiochem (U.S.A.). DMF was of peptide synthesis grade, and used without purification. $CuCl_2$ used in this study was its dihydrate.

Racemization Test The coupling reactions were conducted using the following stock solutions: A, 0.04 M Boc–Phe–MeAla–OH in DMF; B, 0.04 M H–Phe–OBzl (prepared from H–Phe–OBzl·HCl in the usual manner) in DMF; C, 0.25 M TSTU in DMF; D, 0.1 M diisopropylethylamine in DMF; E, 0.4 M HOSu in DMF; F, 0.4 M $CuCl_2$ in DMF.

TSTU Method: To a mixture of A (50 μl, 2 μmol), B (50 μl, 2 μmol), C (10 μl, 2.5 μmol), and DMF (10 μl) was added D (40 μl, 4 μmol).

TSTU–HOSu Method: To a mixture of A (50 μl, 2 μmol), B (50 μl,

2 μmol), C (10 μl, 2.5 μmol), E (5 μl, 2 μmol), and DMF (5 μl) was added D (40 μl, 4 μmol).

TSTU–$CuCl_2$ Method: To a mixture of A (50 μl, 2 μmol), B (50 μl, 2 μmol), C (10 μl, 2.5 μmol), F (5 μl, 2 μmol), and DMF (5 μl) was added D (40 μl, 4 μmol).

TSTU–HOSu–$CuCl_2$ Method: To a mixture of A (50 μl, 2 μmol), B (50 μl 2 μmol), C (10 μl, 2.5 μmol), E (5 μl, 2 μmol), and F (5 μl, 2 μmol) was added D (40 μl, 4 μmol).

Determination of % L–D–L: After >24 h reaction at room temperature, each reaction mixture was diluted with DMF (640 μl), and a portion (10 μl) of the resultant solution was analyzed by HPLC [column, Waters μBondasphere $5C_{18}$ 100 Å (3.9×150 mm); solvent system, 0.05% trifluoroacetic acid (TFA) in water : 0.05% TFA in MeCN 60 : 40 to 20 : 80 in 40 min at a flow rate of 1.0 ml/min. Boc–Phe–MeAla–Phe–OBzl, t_R 24.26 min; Boc–Phe–D-MeAla–Phe–OBzl, t_R 25.44 min]. % L–D–L and % yield were determined as follows: % L–D–L=(peak area of the Boc–Phe–D-MeAla–Phe–OBzl)×100/[(peak area of the Boc–Phe–MeAla–Phe–OBzl)+(peak area of the Boc–Phe–D-MeAla–Phe–OBzl)]; % yield=[(peak area of the Boc–Phe–MeAla–Phe–OBzl)+(peak area of the Boc–Phe–D-MeAla–Phe–OBzl)]×100/[peak area of standard solution of Boc–Phe–MeAla–Phe–OBzl (2 μmol/800 μl DMF, 10 μl injection)]. The results are summarized in Table 1.

References and Notes

1) Amino acids used in this study are of L-configuration, unless otherwise noted. Abbreviations used in this report for amino acids, peptides and their derivatives are those recommended by the IUPAC–IUB Commission on Biochemical Nomenclature: *Biochem. J.*, **219**, 345—373 (1984).
2) Present address: *Faculty of Engineering, Towa University, Minami-ku, Fukuoka 815—8510, Japan.*
3) For review; Kemp D. S., "The Peptides–Analysis, Synthesis, Biology," Vol. 1, ed. by Gross E., Meienhofer J., Academic Press, New York, 1979, pp. 315—383.
4) Weygand F., Hoffmann D., Wünsch E., *Z. Naturforsch*, **21B**, 426—428 (1966).
5) König W., Geiger R., *Chem. Ber.*, **103**, 788—798 (1970).
6) Fujino M., Kobayashi S., Obayashi M., Fukuda T., Shinagawa S., Nishimura O., *Chem. Pharm. Bull.*, **22**, 1857 (1974).
7) Carpino L. A., *J. Am. Chem. Soc.*, **115**, 4397—4398 (1993).
8) Miyazawa T., Otomatsu T., Yamada T., Kuwata S., *Tetrahedron Lett.*, **25**, 771—772 (1984); Miyazawa T., Otomatsu T., Fukui Y., Yamada T., Kuwata S., *Int. J. Peptide Protein Res.*, **39**, 237—244 (1992).
9) Miyazawa T., Otomatsu T., Fukui Y., Yamada T., Kuwata S., *J. Chem. Soc., Chem. Commun.*, **1988**, 419—420; *idem, Int. J. Peptide Protein Res.*, **39**, 308—314 (1992).
10) McDermott J. R., Benoiton N. L., *Can. J. Chem.*, **51**, 2562 (1973).
11) Davies J. S., Mohammed A. K., *J. Chem. Soc., Perkin Trans. 1*, **1981**, 2982—2990.
12) Nishiyama Y., Tanaka M., Saito S., Ishizuka S., Mori T., Kurita K., *Chem. Pharm. Bull.*, **47**, 576—578 (1999).
13) Castro B., Dormoy J.-R., Evin G., Selve C., *Tetrahedron Lett.*, **1975**, 1219.
14) Knorr R., Trzeciak A., Bannwarth W., *Tetrahedron Lett.*, **30**, 1927—1930 (1989).
15) Spencer J. R., Antonenko V. V., Delaet N. G. J., *Int. J. Peptide Protein Res.*, **40**, 282—293 (1992).
16) Steinauer R., Chen F. M. F., Benoiton N. L., *Int. J. Peptide Protein Res.*, **34**, 295—298 (1989).
17) Preliminarily, the coupling yield could be improved to 60% by using 2.5 eq. TSTU without detectable racemization. At present, the reason for the incomplete coupling is unclear; no side products but only Boc–Phe–MeAla–Phe–OBzl and Boc–Phe–MeAla–OH were detected on the HPLC analaysis of the crude product after extraction with ethyl acetate and washing with 1 N HCl.

Novel Catalytic Asymmetric Sulfoxidation in Water Using the Hypervalent Iodine Reagent Iodoxybenzene

Hirofumi TOHMA, Shinobu TAKIZAWA, Hironori MORIOKA, Tomohiro MAEGAWA, and Yasuyuki KITA*

Graduate School of Pharmaceutical Sciences, Osaka University, 1–6 Yamada-oka, Suita, Osaka 565–0871, Japan.
Received December 14, 1999; accepted January 14, 2000

A new catalytic asymmetric oxidation of sulfides to sulfoxides in water using the hypervalent iodine(V) reagent iodoxybenzene ($PhIO_2$) has been developed. This methodology is distinctly different from the previously reported use of cyclodextrins or biological catalysts and provides a new route to asymmetric sulfoxidation in water.

Key words: asymmetric oxidation; hypervalent iodine reagent; sulfoxide; water

The recent demand for eco-friendly chemical processes has fueled the development of several clean and practical oxidation reactions and encourages further development of high-yielding, clean, safe, economical, and highly stereoselective oxidation methods. As a reaction medium, water is both economical and environmentally benign and has been applied to a variety of oxidation reactions.[1] With regard to asymmetric oxidation of sulfides to sulfoxides in water, only a limited number of examples including the use of cyclodextrin derivatives,[2] chiral micelles,[3] or biological catalysts[4] exist. Although both biological catalysts and the use of cyclodextrins sometimes give sulfoxides with high enantioselectivities in water, these methods lack practicality and generality due to their low to moderate optical yields and high substrate specificity. Therefore we attempted to develop an alternative chemical method with higher versatility compared with the previous methods for asymmetric sulfoxidation. As a continuation of our studies on hypervalent iodine reagents which have mild reactivity, low toxicity, and high versatility,[5,6] we recently achieved a novel catalytic asymmetric oxidation of sulfides to sulfoxides *via* cetyltrimethylammonium bromide (CTAB)-reversed micelles[7] (toluene–H_2O) using iodoxybenzene ($PhIO_2$).[8] Here we report a new and efficient catalytic activation of $PhIO_2$ in water using catalytic amounts of both $MgBr_2$ and (+)-dibenzoyl-D-tartaric acid **3** to yield chiral sulfoxides quantitatively with moderate optical yields.

In this study, we first examined the asymmetric oxidation of *p*-tolyl methylsulfide **1a** using our reported micellar conditions ($PhIO_2$–CTAB–**3**) in water. However, only low optical yield (18% ee [enantiomeric excess]) of *p*-tolyl methylsulfoxide **2a** was obtained, while the reaction proceeded quantitatively. Since we have recently found that the addition of a catalytic amount of KBr significantly activates hypervalent iodine reagents in water,[9] we tested other water-soluble additives such as alkali metal, alkali earth metal, and other metal salts in the presence of 10 mol% of **3** as a chiral source. Consequently, the addition of bromide salts effectively catalyzed the hypervalent iodine(V) sulfoxidation regardless of the type of metal cation. Therefore we chose $MgBr_2$, the most economical and safest metal bromide, for further studies, since it also showed a slightly enhanced ee value among the bromides tested (LiBr [43% ee], NaBr [42% ee], $MgBr_2$ [47% ee], $CaBr_2$ [46% ee], $BaBr_2$ [45% ee], $ZnBr_2$ [33% ee], $YbBr_3$ [38% ee], MgX_2 [X: Cl, OAc, ClO_4 {0—19 % yields, <15% ee}]).

In order to enhance the optical yield of **2a**, we examined the reaction using a variety of oxidants, chiral sources, and reaction conditions. In the presence of $MgBr_2$ (20 mol%) and **3** (10 mol%), common water-soluble oxidants such as H_2O_2 and cumene hydroperoxide completed the reaction immediately with no asymmetric induction, and sodium hypochrolite (NaOCl) only yielded *p*-tolyl methylsulfone. On the other

Table 1

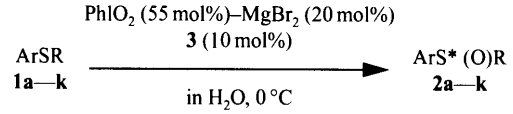

Entry	Substrate		Time (h)	Yield (%)	% ee[a] (config.)[b]	$[\alpha]_D^{24}$ (°)
	Ar	R				
1	4-MePh	Me (**1a**)	24	quant.	59 [*R*]	+101.7 (*c*=0.47, $CHCl_3$)
2	3-MePh	Me (**1b**)	24	quant.	63 [*R*]	+74.8 (*c*=0.76, MeOH)
3	2-MePh	Me (**1c**)	48	95	60 [*R*]	+146.8 (*c*=1.03, acetone)
4	4-NO_2Ph	Me (**1d**)	48	quant.	60 [*R*]	+77.7 (*c*=1.67, $CHCl_3$)
5	3-NO_2Ph	Me (**1e**)	64	quant.	61 [*R*]	+58.0 (*c*=0.21, $CHCl_3$)
6	4-MeOPh	Me (**1f**)	64	84	63 [*R*]	+83.8 (*c*=0.98, $CHCl_3$)
7	4-CNPh	Me (**1g**)	30	97	56 [*R*]	+66.1 (*c*=1.09, EtOH)
8	Ph	Me (**1h**)	36	quant.	60 [*R*]	+102.0 (*c*=0.64, $CHCl_3$)
9	Ph	Et (**1i**)	48	quant.	51 [*R*]	+107.8 (*c*=0.44, acetone)
10	Ph	$(CH_2)_2OH$ (**1j**)	72	quant.	43 [*R*]	+91.2 (*c*=1.07, acetone)
11	(**1k**)		48	quant.	52 [*R*]	−129.6 (*c*=0.53, acetone)

a) Determined by HPLC analysis employing a Daicel Chiralcel OD, OJ, or Chiralpak AD. *b*) Absolute configurations were established by comparison of the sign of $[\alpha]_D$ to values reported in the literature.

* To whom correspondence should be addressed.

© 2000 Pharmaceutical Society of Japan

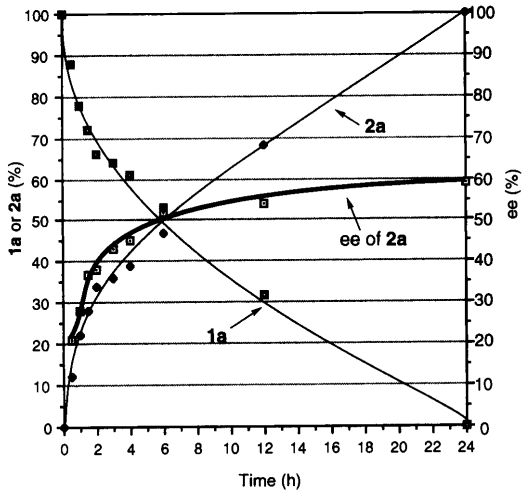

Fig. 1

hand, the best optical yield (47% ee) was observed using the normally unreactive $PhIO_2$ which is nearly insoluble in water in the absence of chiral activator **3**, while only low ee values were observed using the more reactive iodine reagents such as PhI=O (9% ee), (diacetoxyiodo)benzene (5% ee), and iodosobenzoic acid (38% ee), which could be activated by $MgBr_2$ even in the absence of **3**. Next, we optimized the chiral sources in the reaction. So far, the best chemical and optical yields have been obtained using 10 mol% of commercially available (+)-dibenzoyl-D-tartaric acid **3**. The use of other tartaric acids or chiral sources such as various carboxylic acids, a sulfonic acid, an *N*-protected amino acid, and a phosphonic acid did not improve the ee of **2a**.[10] Interestingly, the reaction temperature affects the ee of **2a**. That is, the ee value of **2a** was enhanced up to 59% ee at 0 °C although the reaction took longer to complete. Under these reaction conditions, we performed asymmetric oxidation of various sulfides.[11] The results are listed in Table 1. Table 1 shows that the reaction proceeds quantitatively with moderate optical yields, regardless of the substrate used.

A time profile of the oxidation of **1a** with 0.55 equivalent of $PhIO_2$ is depicted in Fig. 1. The remarkable enhancement of the ee value of **2a** observed at the initial step is surprising since there is no kinetic resolution derived from overoxidation to the sulfone and also because PhI=O(III),which was formed during the course of the reaction, only gave a low optical yield as described above. Probably the hydrophobic effect brings the reactants together to promote the *in situ* formation of the stereo-controlled reactive intermediates from $PhIO_2$(V), PhI=O(III), and the chiral tartaric acid **3**. However, the mechanism of asymmetric induction is still unclear. Although the optical yields of sulfoxides are not excellent so far, we have opened up a new and facile route for asymmetric sulfoxidation in water. The optimization of optical yields and further application of this system are now underway.

Acknowledgments This research was financially supported in part by a Grant-in-Aid for Scientific Research (B) (No. 10470469) and a Grant-in-Aid for Encouragement of Young Scientists (No. 09771907) from the Ministry of Education, Science, Sports and Culture, Japan.

References and Notes

1) *a*) Grieco P. A. (ed.), "Organic Synthesis in Water," Blackie Academic, London, 1998; *b*) Cornils B., Herrmann W. A. (eds.), "Aqueous-Phase Organometallic Catalysis," Wiley-VCH, Weinheim, 1998; *c*) Li C. J., Chan T. H. (eds.), "Organic Reactions in Aqueous Media," John Wiley, New York, 1997.
2) *a*) Mikolajczyk M., Drabowicz J., *J. Am. Chem. Soc.*, **100**, 2510—2515 (1978); *b*) Czarnik A. W., *J. Org. Chem.*, **49**, 924—927 (1984); *c*) Sakuraba H., Natori K., Tanaka Y., *J. Org. Chem.*, **56**, 4124—4129 (1991); *d*) Bonchio M., Carofiglio T., Furia F. D., Fornasier R., *J. Org. Chem.*, **60**, 5986—5988 (1995).
3) Zhang Y. M., Fu C. L., Fan W. Q., *Chin. J. Chem.*, **1**, 89—96 (1990).
4) *a*) Kagan H. B., "Catalytic Asymmetric Synthesis," ed. by Ojima, I., VCH, New York, 1993, pp. 203—226; *b*) Mata E. G., *Phosphorus, Sulfur, and Silicon*, **117**, 231—286 (1996) and references cited therein.
5) For recent reviews see: *a*) Stang P. J., Zhdankin V. V., *Chem. Rev.*, **96**, 1123—1178 (1996); *b*) Varvoglis A., "Hypervalent Iodine in Organic Synthesis," San Diego, Academic Press, 1997; *c*) Kitamura T., Fujiwara Y., *Org. Prep. Proc. Int.* **29**, 409—458 (1997); *d*) Wirth T., Hirt U. H., *Synthesis*, **1999**, 1271—1287.
6) Our recent work: *a*) Kita Y., Arisawa M., Gyoten M., Nakajima M., Hamada R., Tohma H., Takada T., *J. Org. Chem.*, **63**, 6625—6633 (1998); *b*) Kita Y., Egi M., Takada T., Tohma H., *Synthesis*, **1999**, 885—897; *d*) Arisawa M., Utsumi S., Nakajima M., Ramesh N. G., Tohma H., Kita Y., *Chem. Commun.*, **1999**, 469—470 and references cited therein.
7) Tohma H., Takizawa S., Watanabe H., Kita Y., *Tetrahedron Lett.*, **39**, 4547—4550 (1998).
8) Tohma H., Takizawa S., Watanabe H., Fukuoka Y., Maegawa T., Kita Y., *J. Org. Chem.*, **64**, 3519—3523 (1999).
9) Tohma H., Takizawa S., Maegawa T., Kita Y., *Angew Chem. Int. Ed. Engl.*, in press.
10) The ee values when using other chiral sources are as follows: di(2-MeO)benzoyl-L-tartaric acid (34% ee), di(2-toluoyl)-L-tartaric acid (14% ee), dipivaloyl-L-tartaric acid (13% ee), di(2-naphthoyl)-D-tartaric acid (24% ee), (*S*)-(+)-α-methoxyphenylacetic acid (14% ee), (+)-10-camphorsulfonic acid (0% ee), *N*-phthaloyl-L-glutamic acid (16% ee), and (*S*)-(+)-1,1′-binaphthyl-2,2′-diyl hydrogenphosphate (0% ee).
11) Typical experimental procedure: A mixture of (+)-dibenzoyl-D-tartaric acid **3** (7.2 mg, 0.02 mmol), $MgBr_2$ (7.4 mg, 0.04 mmol), and $PhIO_2$ (26.0 mg, 0.11 mmol) in water (5.0 ml) was stirred for 5 min at room temperature. To the stirred mixture, sulfide (**1**) (0.20 mmol) was added dropwise at 0 °C and then stirred until completion of the reaction at 0 °C. The reaction mixture was extracted with AcOEt, dried over Na_2SO_4, filtered, and evaporated. The residue was purified by column chromatography (SiO_2/CH_2Cl_2–acetone=4 : 1) to give pure sulfoxide (**2**), the ee of which was determined by HPLC. Absolute configurations were assigned by comparison of the sign of the specific rotation with data in the literature.[4,8]